

Springer Geography

Aznarul Islam · Pravat Kumar Shit ·  
Dilip Kumar Datta · M. Shahidul Islam ·  
Suwendu Roy · Sandipan Ghosh ·  
Balai Chandra Das *Editors*

# Floods in the Ganga— Brahmaputra— Meghna Delta

 Springer

# Springer Geography

## Advisory Editors

Mitja Brilly, Faculty of Civil and Geodetic Engineering, University of Ljubljana, Ljubljana, Slovenia

Richard A. Davis, Department of Geology, School of Geosciences, University of South Florida, Tampa, FL, USA

Nancy Hoalst-Pullen, Department of Geography and Anthropology, Kennesaw State University, Kennesaw, GA, USA

Michael Leitner, Department of Geography and Anthropology, Louisiana State University, Baton Rouge, LA, USA

Mark W. Patterson, Department of Geography and Anthropology, Kennesaw State University, Kennesaw, GA, USA

Márton Veress, Department of Physical Geography, University of West Hungary, Szombathely, Hungary

The Springer Geography series seeks to publish a broad portfolio of scientific books, aiming at researchers, students, and everyone interested in geographical research.

The series includes peer-reviewed monographs, edited volumes, textbooks, and conference proceedings. It covers the major topics in geography and geographical sciences including, but not limited to; Economic Geography, Landscape and Urban Planning, Urban Geography, Physical Geography and Environmental Geography.

**Springer Geography — now indexed in Scopus**

\* \* \*


Aznarul Islam • Pravat Kumar Shit  
Dilip Kumar Datta • M. Shahidul Islam  
Suvendu Roy • Sandipan Ghosh  
Balai Chandra Das  
Editors

# Floods in the Ganga–Brahmaputra– Meghna Delta

 Springer


*Editors*


Aznarul Islam   
Department of Geography  
Aliah University  
Kolkata, India


Pravat Kumar Shit   
Post-Graduate Department of Geography  
Raja N.L.Khan Women's College (Autonomous)  
Midnapore, West Bengal, India

Dilip Kumar Datta   
Environmental Science Discipline  
Khulna University  
Khulna, Bangladesh

M. Shahidul Islam  
Department of Geography and Environment  
University of Dhaka  
Dhaka, Bangladesh

Suvendu Roy   
Department of Geography  
Kalipada Ghosh Tarai Mahavidyalaya  
Darjeeling, West Bengal, India

Sandipan Ghosh   
Department of Geography  
Chandrapur College  
Purba Bardhaman, India

Balai Chandra Das   
Department of Geography  
Krishnagar Government College  
Krishnanagar, India

ISSN 2194-315X

ISSN 2194-3168 (electronic)

Springer Geography

ISBN 978-3-031-21085-3

ISBN 978-3-031-21086-0 (eBook)

<https://doi.org/10.1007/978-3-031-21086-0>

© The Editor(s) (if applicable) and The Author(s), under exclusive license to Springer Nature Switzerland AG 2023

This work is subject to copyright. All rights are solely and exclusively licensed by the Publisher, whether the whole or part of the material is concerned, specifically the rights of translation, reprinting, reuse of illustrations, recitation, broadcasting, reproduction on microfilms or in any other physical way, and transmission or information storage and retrieval, electronic adaptation, computer software, or by similar or dissimilar methodology now known or hereafter developed.

The use of general descriptive names, registered names, trademarks, service marks, etc. in this publication does not imply, even in the absence of a specific statement, that such names are exempt from the relevant protective laws and regulations and therefore free for general use.

The publisher, the authors, and the editors are safe to assume that the advice and information in this book are believed to be true and accurate at the date of publication. Neither the publisher nor the authors or the editors give a warranty, expressed or implied, with respect to the material contained herein or for any errors or omissions that may have been made. The publisher remains neutral with regard to jurisdictional claims in published maps and institutional affiliations.

This Springer imprint is published by the registered company Springer Nature Switzerland AG  
The registered company address is: Gewerbestrasse 11, 6330 Cham, Switzerland

# Foreword

The famous American geographer, Gilbert F. White (1911–2006), observed that, while floods may well be “acts of God,” flood damages result from “acts of man.” The rivers that ultimately feed to the great Ganga-Brahmaputra-Meghna (GBM) delta are indeed part of the natural world, and that world has traditionally been viewed as a sacred creation, held in reverence through religions practiced by the inhabitants of the river basins. However, with its very high population density (about 200 persons per square kilometer) plus the infrastructure associated with perhaps 150 million total inhabitants, this region is obviously at very high vulnerability for immense flood damages.

The rivers that drain to the GBM delta derive their flow from five different modern nations. The Ganga has tributaries that drain the Himalaya Mountains of India and Nepal, extending into parts of Tibet (China). Brahmaputra tributaries extend from India to Bhutan, and the main course traverses the Himalaya Range through the Tsangpo Gorge, draining much of southern Tibet (China), where the mainstem is known as the Yarlung Tsangpo. Along with the Meghna, these rivers converge in Bangladesh and break into the distributary components of the delta. Of these, the Padma and Hooghly are especially noteworthy, lying near the megacities of Kolkata and Dhaka, with respective populations of about 15 million and nearly 23 million.

This present book deals the floods and the associated hazards posed to the GBM delta, the world’s largest, covering an area of more than 100,000 km<sup>2</sup>. Deltas develop where rivers come to rest as they enter bodies of standing water, in this case the Bay of Bengal of the Indian Ocean. Deltas occur where river gradients are at their lowest, and their entrained sediments get deposited in channel bars (alluvial islands), or when the rivers leave their banks and spill into adjacent land that is built up by the sediment accumulations of successive inundations. Given that these low-lying lands are naturally inundated, they are really portions of their associated rivers. Thus, human habitation of such lands is literally “in the river,” even though the flood-prone land is not continuously inundated.

The GBM rivers are laden with sediment derived from the intense erosion of the world's greatest mountain range, the Himalaya. This circumstance is the result of special geological history. About 35 million years ago, the northward-migrating subcontinental plate of peninsular India collided with the southern margin of the Asian continental plate. The compression zone of this collision created the Tibetan Plateau and the great Himalayan Mountain Range. Sediments derived from these mountains filled a trough that was created to the south of collision zone, and the modern Ganges River flows eastward along the axis of this trough. The combination of very high mountains with south Asian Monsoon, bringing extremely heavy seasonal precipitation, produces the immensely high rates of erosion, water runoff, and sediment yields that characterize this region.

Though it is fed by some of the world's greatest rivers, the GBM becomes a tidally dominated delta at its mouth. The lower tidal reaches of the rivers are at high risk from the occasional tropical cyclones and from progressive impact of rising sea level. The great cyclone of November 1970 was one of the world's worst disasters for the loss of life, resulting in over a half million deaths. Progressively rising sea level associated with global warming is exacerbating the hazard for future tropical cyclones.

The tidally dominated lower reaches of the delta are spread across an east-west distance of about 300 km, with the nation of Bangladesh to the east and the Indian state of West Bengal to the west. The coastal margins of the delta comprise the world's largest mangrove forest. Unfortunately, the progressive destruction of this forest is limiting its positive role in moderating the impacts of tropical cyclones, further exacerbation their potential hazard.

The many flood-related problems described in this book contrast with the great reverence for the region's rivers. It can be hoped that the religious tradition of that reverence can inspire the kind of stewardship that will both mitigate the flooding hazard and produce a sustainable relationship between the rivers and the humans that inhabit them.

Victor R. Baker  
Regents Professor of Hydrology  
and Atmospheric Sciences  
The University of Arizona  
Tucson, AZ, USA

# Preface

A few years back, when travelling flooded Bengal, a graduate student from Ahmed Draia University said, ‘You have too many water resources to manage, but we die from dehydration’. He uttered the serious truth of the Earth’s extreme contrast of climate. Rather, extreme contrast of all – the soil, the water, the air, the life and the living. In India, better all over the world, the threat of water scarcity is increasing day by day. It is reported that even the Bengal basin will come under the threat of permanent drought in near future. The lowering of groundwater level in the Bengal basin is ringing the alarm. Discharges of rivers are diminishing rapidly. Some rivers have dried out and got lost. Many lakes and swamps have ceased to exist.

Yet our fellows get killed under flood water! Our cattle and poultry get washed away. Each year, either here or there, floods toll our lands, our properties. We, from the Ganga-Brahmaputra-Meghna delta, suffer the pains of floods. It goes beyond our capacity for utilization and management. The flood erases all differences in terrain. Even barriers of international border crossings disappear under flood water and make the landscape uniform. People of different nations feel the pain and suffering of floods the same way. Regarding floods, India and Bangladesh have fellow feelings. Moreover, during the Covid-19 situation, we became accustomed to online communication to come closer.

In 2020, when the Covid-19 pandemic locked down the entire world, Dr Aznarul Islam took the initiative to introduce ourselves to each other, and eventually, we came closer to thinking on a single point with multi-dimensions – the flood. We felt the urge to work and invited articles on ‘Floods in the Ganga-Brahmaputra-Meghna Delta’ and did pile huge responses from worldwide contributors, which offered us the opportunity to be selective. We are very much thankful to our authors who contributed to this volume. Their thought-provoking contributions made this volume knowledgeable. We are also equally thankful to our compadre authors, whose articles do not appear as chapters in this volume but who made us feel blessed with their articles rich in noesis.



We are grateful to Dr Guido Zosimo-Landolfo, Editorial Director/Asset Manager of Springer Nature Switzerland AG, for signing the agreement on this project and providing the opportunity of using their prestigious pages for manuscripts of our eminent authors.

We hope, the outcomes of this volume will flood the thoughts of scholars, faculties, planners and stakeholders returning us the apt worth.

Kolkata, West Bengal, India  
Midnapore, West Bengal, India  
Khulna, Bangladesh  
Dhaka, Bangladesh  
Darjeeling, West Bengal, India  
Purba Bardhaman, West Bengal, India  
Krishnanagar, West Bengal, India

Aznarul Islam  
Pravat Kumar Shit  
Dilip Kumar Datta  
M. Shahidul Islam  
Suvendu Roy  
Sandipan Ghosh  
Balai Chandra Das

# Contents

<b>1</b>	<b>Floods of Ganga-Brahmaputra-Meghna Delta in Context</b> . . . . .	<b>1</b>
	Sandipan Ghosh, Suvendu Roy, Aznarul Islam, Pravat Kumar Shit, Dilip K. Datta, M. Shahidul Islam, and Balai Chandra Das	
<b>2</b>	<b>Flood Inundation Modelling in Data-Sparse Flatlands: Challenges and Prospects</b> . . . . .	<b>19</b>
	Joy Sanyal	
<b>3</b>	<b>Nature of Flood and Channel Sedimentation in the Torsa River: A Hydro-Geomorphic Study</b> . . . . .	<b>37</b>
	Ujwal Deep Saha, Md Juber Alam, Soma Bhattacharya, and Arijit Majumder	
<b>4</b>	<b>Flood Risk Assessment of Himalayan Foothill Rivers: A Study of Jaldhaka River, India</b> . . . . .	<b>63</b>
	Adrija Raha, Suraj Gupta, and Mery Biswas	
<b>5</b>	<b>Flood Dynamics, River Erosion, and Vulnerability in the Catchment of Dharla and Dudhkumar Rivers in Bangladesh</b> . . . . .	<b>91</b>
	Md Rejaur Rahman, Sabbir Ahmed Sweet, and A. H. M. Hedayutul Islam	
<b>6</b>	<b>Assessing Human Control on Planform Modification over Floods: A Study of Lower Mahananda–Balason River System, India</b> . . . . .	<b>127</b>
	Suman Mitra, Meheub Mondal, Khusbu Khatoon, Susmita Oraon, and Lakpa Tamang	

<b>7</b>	<b>Exploring the Flooding Under Damming Condition in Punarbhaba River of India and Bangladesh . . . . .</b>	<b>161</b>
	Swapan Talukdar, Swades Pal, Mohd Waseem Naikoo, and Atiqur Rahman	
<b>8</b>	<b>Morphometric Analysis and Prioritization of Watersheds for Flood Susceptibility Mapping in the Eastern Himalayan Foothills, India . . . . .</b>	<b>183</b>
	Md Hasanuzzaman, Biswajit Bera, Aznarul Islam, and Pravat Kumar Shit	
<b>9</b>	<b>Application of Multi-Criteria Decision-Making Approach for Assessing Flood Susceptibility of the Tal-Diara and Barind Region in Malda District, India . . . . .</b>	<b>203</b>
	Kunal Chakraborty, Mantu Das, and Snehasish Saha	
<b>10</b>	<b>Agrarian and Socio-Infrastructural Vulnerability in the Wake of Flood: An Example from the Mayurakshi River Basin, India . . . . .</b>	<b>231</b>
	Aznarul Islam, Susmita Ghosh, Mohan Sarkar, Suman Deb Barman, Pravat Kumar Shit, and Abdur Rahman	
<b>11</b>	<b>Contemporary and Future Flood Characteristics and Associated Environmental Impact: A Study of Ajay River Basin, India . . . . .</b>	<b>267</b>
	Suwendu Roy	
<b>12</b>	<b>Nature of Floods in the Khari River Basin, Eastern India . . . . .</b>	<b>285</b>
	Subhankar Bera and Abhay Sankar Sahu	
<b>13</b>	<b>Flood Risk Assessment and Numerical Modelling of Flood Simulation in the Damodar River Basin, Eastern India . . . . .</b>	<b>303</b>
	Sandipan Ghosh and Soumya Kundu	
<b>14</b>	<b>An Account of the Flood History in the Ghatal Region of West Bengal, India . . . . .</b>	<b>351</b>
	Sayoni Mondal and Priyank Pravin Patel	
<b>15</b>	<b>A Baseline Study on Silaboti River Shifting, Flood, and Its Impact on Livelihood at Ghatal, Paschim Medinipur District, West Bengal . . . . .</b>	<b>365</b>
	Sudip Bera, Riya Samanta, and Nilanjana Das Chatterjee	
<b>16</b>	<b>Future Floods in the Brahmaputra River Basin Based on Multi-model Ensemble of CMIP6 Projections . . . . .</b>	<b>385</b>
	Md. Khalequzzaman, Badrul Masud, Zahidul Islam, Sarfaraz Alam, and Md. Mostafa Ali	

**17 Assessment of Flood Risk in the Brahmaputra-Jamuna Floodplain, Bangladesh . . . . . 403**  
 Md. Serajul Islam and Nazmun Nahar

**18 Characteristics of Flood in the Meghna River Basin Within Bangladesh . . . . . 423**  
 M. Shahidul Islam and Afrin Sharabony

**19 Flooding and Floodplain Management Around Dhaka City: A Case of Buriganga and Shitalakhya Rivers . . . . . 449**  
 Asib Ahmed and Md. Shamim Hossain

**20 Floods of Jalangi and Mathabhanga-Churni Rivers, Indo-Bangladesh . . . . . 465**  
 Balai Chandra Das, Sanat Das, and Biplab Sarkar

**21 Geospatial Assessment of Fluvial Dynamics and Associated Flood Vulnerability in the Bhagirathi-Hugli Sub-basin in West Bengal, India . . . . . 491**  
 Biraj Kanti Mondal, Tanmoy Basu, Rima Das, Sanjib Mahata, and Ming-An Lee

**22 Floods of Gorai-Madhumati and Arial Khan Rivers, Bangladesh . . . . . 529**  
 Al Artat Bin Ali, Nazmoon Nahar Sumiya, and M. Shahidul Islam

**Index . . . . . 551**

# Contributors

**Asib Ahmed** Department of Geography and Environment, University of Dhaka, Dhaka, Bangladesh

**Md Juber Alam** Department of Geography, Jadavpur University, Kolkata, West Bengal, India

**Sarfaraz Alam** Department of Geophysics, Stanford University, Stanford, CA, USA

**Al Artat Bin Ali** Department of Geography and Environment, University of Dhaka, Dhaka, Bangladesh

**Suman Deb Barman** Independent Researcher, Barasat, Kolkata, India

**Tanmoy Basu** Department of Geography, Katwa College, Katwa, West Bengal, India

**Biswajit Bera** Department of Geography, Sidho Kanho Birsha University, Purulia, West Bengal, India

**Subhankar Bera** Department of Geography, University of Kalyani, Kalyani, West Bengal, India

**Sudip Bera** Department of Geography, Vidyasagar University, Midnapore, West Bengal, India

**Soma Bhattacharya** Post Graduate Department of Geography, Vivekananda College for Women, Kolkata, West Bengal, India

**Mery Biswas** Department of Geography, Presidency University, Kolkata, West Bengal, India

**Kunal Chakraborty** Department of Geography & Applied Geography, University of North Bengal, Siliguri, India

**Balai Chandra Das** Department of Geography, Krishnagar Government College, Krishnanagar, West Bengal, India

**Mantu Das** Department of Geography & Applied Geography, University of North Bengal, Siliguri, India

**Rima Das** Department of Geography, Bhangar Mahavidyalaya, Bhangar, West Bengal, India

**Sanat Das** Department of Geography, Adamas University, Kolkata, India

**Nilanjana Das Chatterjee** Department of Geography, Vidyasagar University, Midnapore, West Bengal, India

**Dilip K. Datta** Environmental Science Discipline, Khulna University, Khulna, Bangladesh

**Sandipan Ghosh** Department of Geography, Chandrapur College, Purba Bardhaman, West Bengal, India

**Susmita Ghosh** Department of Geography, Aliah University, Kolkata, West Bengal, India

**Suraj Gupta** Department of Geography, Presidency University, Kolkata, West Bengal, India

**Md Hasanuzzaman** PG Department of Geography, Raja N. L. Khan Women's College (Autonomous), Midnapore, West Bengal, India

**Md. Shamim Hossain** Department of Geography and Environmental Science, Begum Rokeya University, Rangpur, Bangladesh

**A. H. M. Hedayutul Islam** Department of Geography and Environmental Studies, University of Rajshahi, Rajshahi, Bangladesh

**Aznarul Islam** Department of Geography, Aliah University, Kolkata, West Bengal, India

**M. Shahidul Islam** Department of Geography and Environment, University of Dhaka, Dhaka, Bangladesh

**Zahidul Islam** Department of Environment and Protected Areas, Government of Alberta, Edmonton, AB, Canada

**Md. Khalequzzaman** Department of Environmental, Geographical, and Geological Sciences, Commonwealth University of Pennsylvania, Lock Haven, PA, USA

**Khusbu Khatoon** Department of Geography, University of Calcutta, Kolkata, India

**Soumya Kundu** Department of Geography, Chandrapur College, Purba Bardhaman, West Bengal, India

**Ming-An Lee** Department of Environmental Biology Fisheries Science, National Taiwan Ocean University, Keelung, Taiwan

**Sanjib Mahata** Department of Geography, Netaji Subhas Open University, Kolkata, West Bengal, India

**Arijit Majumder** Department of Geography, Jadavpur University, Kolkata, West Bengal, India

**Badrul Masud** Ministry of Environment, Government of Saskatchewan, Regina, SK, Canada

**Suman Mitra** Department of Geography, University of Calcutta, Kolkata, India

**Biraj Kanti Mondal** Department of Geography, Netaji Subhas Open University, Kolkata, West Bengal, India

**Meheub Mondal** Department of Geography, University of Calcutta, Kolkata, India

**Sayoni Mondal** Department of Geography, Presidency University, Kolkata, India

**Md. Mostafa Ali** Department of Water Resources Engineering, Bangladesh University of Engineering and Technology, Dhaka, Bangladesh

**Nazmun Nahar** Department of Geography and Environment, University of Dhaka, Dhaka, Bangladesh

**Mohd Waseem Naikoo** Department of Geography, Faculty of Natural science, Jamia Millia Islamia, New Delhi, India

**Susmita Oraon** Department of Geography, University of Calcutta, Kolkata, India

**Swades Pal** Department of Geography, University of Gour Banga, Englishbazar, India

**Priyank Pravin Patel** Department of Geography, Presidency University, Kolkata, India

**Adrija Raha** Department of Geography, Presidency University, Kolkata, West Bengal, India

**Abdur Rahman** Department of Geography, Dr. Kanailal Bhattacharyya College, Howrah, West Bengal, India

**Atiqur Rahman** Department of Geography, Faculty of Natural science, Jamia Millia Islamia, New Delhi, India

**Md Rejaur Rahman** Department of Geography and Environmental Studies, University of Rajshahi, Rajshahi, Bangladesh

**Suwendu Roy** Department of Geography, Kalipada Ghosh Tarai Mahavidyalaya, Bagdogra, Darjeeling, India

**Snehasish Saha** Department of Geography & Applied Geography, University of North Bengal, Siliguri, India

**Ujwal Deep Saha** Post Graduate Department of Geography, Vivekananda College for Women, Kolkata, West Bengal, India

**Abhay Sankar Sahu** Department of Geography, University of Kalyani, Kalyani, West Bengal, India

**Riya Samanta** Department of Geography, Vidyasagar University, Midnapore, West Bengal, India

**Joy Sanyal** Department of Geography, Presidency University, Kolkata, India

**Biplab Sarkar** Department of Geography, Aliah University, Kolkata, India

**Mohan Sarkar** Department of Geography, Visva-Bharati, Santiniketan, West Bengal, India

**Md. Serajul Islam** Department of Geography and Environment, University of Dhaka, Dhaka, Bangladesh

**Afrin Sharabony** Research Intern, Coastal Research Unit (CRU), Department of Geography and Environment, University of Dhaka, Dhaka, Bangladesh

**Pravat Kumar Shit** PG Department of Geography, Raja N. L. Khan Women's College (Autonomous), Midnapore, West Bengal, India

**Nazmoon Nahar Sumiya** Department of Geography and Environment, University of Dhaka, Dhaka, Bangladesh

**Sabbir Ahmed Sweet** Department of Geography and Environmental Studies, University of Rajshahi, Rajshahi, Bangladesh

**Swapan Talukdar** Department of Geography, Faculty of Natural science, Jamia Millia Islamia, New Delhi, India

**Lakpa Tamang** Department of Geography, University of Calcutta, Kolkata, India



## About the Editors



**Aznarul Islam** Dr Aznarul Islam is currently an assistant professor in the Department of Geography, Aliah University, Kolkata. Previously, he was engaged in teaching and research in the Department of Geography, Barasat Government College, West Bengal, under West Bengal Education Service (WBES). He did MSc (2010) in geography from Kalyani University, India, and MPhil (2013) and PhD (2016) in geography from the University of Burdwan, India. He has already published more than 40 research papers including 20 SCI(E) papers in different journals of national and international repute and contributed more than 15 book chapters in edited volumes and conference proceedings. Dr Islam has already published 8 books (Springer – 5, CRC Press – 1, RK publication – 1, FPG – 1). He has presented papers in more than 20 national and international seminars and conferences. He has completed one major research project funded by the Indian Council of Social Science Research (ICSSR), Ministry of Human Resource Development, Government of India. Dr Islam delivered several invited lectures and special lectures in different national and regional programmes. He has been performing the role of a reviewer in more than 20 international journals including that of Springer, Elsevier and Taylor & Francis. He is a life member of the Foundation of Practising Geographers (FPG), Kolkata, and the National Association of Geographers, India (NAGI), New Delhi. He has to date successfully supervised 1 PhD thesis and more than 50 dissertations on various topics of geomorphology at the master's level. His principal area of research includes hydro-

geomorphological issues of the Bengal Delta, including channel shifting riverbank erosion, flood, ecological stress of the riverine tract and environmental flow.



**Pravat Kumar Shit** Pravat Kumar Shit (PhD) is an assistant professor in the PG Department of Geography, Raja N. L. Khan Women's College (Autonomous), West Bengal, India. He received his MSc and PhD degrees in geography from Vidyasagar University and PG diploma in remote sensing and GIS from Sambalpur University. His research interests include applied geomorphology, soil erosion, groundwater, forest resources, wetland ecosystem, environmental contaminants and pollution, and natural resources mapping and modelling. He has published 20 books (Springer – 15, Elsevier – 3, CRC Press – 1), more than 80 research articles in peer-reviewed journals and 75 book chapters. His research work has been funded by the University Grants Commission (UGC), Govt. of India, and Department of Science and Technology and Biotechnology (DSTBT), Govt. of West Bengal. He is also guest editor of *Environmental Science and Pollution Research* (Springer) and *Applied Water Science* (Springer). He is currently editor of the GIScience and Geo-environmental Modelling (GGM) book series, Springer Nature.



**Dilip Kumar Datta** Dr Dilip Kumar Datta is Professor of Environmental Science, Khulna University, Bangladesh, where he has been a faculty member since October, 1997. He was Head of the Discipline between 2009 and 2012 and from 1999 to 2001. Dilip was also engaged as the director of the *Centre for Integrated Studies on the Sundarbans*(CISS) between 2016 and 2020 that has been upgraded to *Institute of Integrated Studies on the Sundarbans and the Coastal Ecosystem* (ISSCS) during his tenure. He has also served the Headship of Development Studies Discipline of Khulna University during 2017, and was executive editor of *KU-Studies* (Khulna University Journal) – a multidisciplinary peer-reviewed journal – between 2009 and 2020. However, Dr Datta has begun his professional career as a museologist at Bangladesh National

Museum, where he has spent approximately 7 years in the position of assistant keeper in the Department of Natural History. Dilip Kumar Datta also has contributed on policy issues of many universities as a member of the relevant committees.

Dilip Kumar Datta has completed his MPhil and PhD from the School of Environmental Sciences, Jawaharlal Nehru University, New Delhi, India. He has completed BSc and MSc from the Department of Geology, Dhaka University, Bangladesh. His research interest encompasses a wide range of environmental science of the Bengal Drainage Basin with particular emphasis to the Lower Bengal Delta. His research areas include hydrogeochemistry and water resource management in deltaic environment. He also looks into women's security under stressed environmental conditions as well as the requirements for ICT in managing water resources under the realm of rapid climate change.

Dilip Kumar Datta has published many journal articles and book chapters in the area of sediment geochemistry, hydrochemistry, water resource management, and in application of ICT in agriculture. He has collaborated widely with researchers from allied disciplines from home and abroad, in research projects supported by both national and transnational organizations such as NWO and APN. He has supervised numerous undergraduate and graduate students for their research work leading to academic degree programmes.



**M. Shahidul Islam** Dr M Shahidul Islam is Professor of Physical Geography in the [Department of Geography and Environment](#) at Dhaka University. He completed his BSc (Hons) and MS in geography from the University of Dhaka in 1983 and 1984, respectively, and stood first class first in both the examinations. Dr Islam completed his PhD in 1996 from the [University of St. Andrews](#), UK, under the Commonwealth Scholarship Programme. Currently, he is the general secretary of Bangladesh Association of Commonwealth Scholars and Fellows (BACSAF), the alumni association in Bangladesh supported by the Commonwealth Commission. He is also the secretary of Bangladesh Geographical Society (BGS). He was the secretary and president of INQUA (International Union for Quaternary

Research) SLCCE: Indian Ocean Sub-commission, during 1995–1999 and 2000–2004, respectively. He was also the Coleader of IGCP-495, UNESCO. He participated in a month-long international expedition in the Indian Ocean (Maldives) in 2000.

He started his career as Lecturer in Geography and Environment at Rajshahi University in 1990 and then moved to Chittagong University in 1998 as founding chairman of the Department of Geography and Environmental Studies of that university. He was promoted to professor in 2005. In 2008, Dr Islam moved to Jagannath University and became the dean of its Faculty of Sciences. He finally moved to Dhaka University as Professor of Physical Geography in 2010. He was also a visiting professor at Nagoya University, Japan, in 2006. He has more than 30 years' experience on various issues of natural environment, including geomorphology, coastal environment and dynamics, sea-level changes, physical oceanography, paleo-environment, hydro-meteorological hazards, and disaster management. Dr Islam has more than 75 research publications in peer-reviewed national and international journals and books, and he has published 7 books. He has been teaching oceanography and marine environment, and research methodology – field techniques and lab techniques – at undergraduate levels, and paleogeomorphology, climate change and disaster management at postgraduate level at Dhaka University.



**Suvendu Roy** Dr Suvendu Roy focuses his research interest on the interface between anthropogenic activities and changing channel geomorphology, especially on the effect of transportation infrastructure on tropical rivers. This includes field-based studies to identify micro-level alteration of geomorphological processes and landforms. He is also interested in the application of GIS and remote sensing to insight into the impact of human activities on landscapes. He earned a BA in geography from Burdwan Raj College, University of Burdwan, and an MA in geography (specialized in advanced geomorphology) from the University of Burdwan (India). He earned a PhD in geography (anthropogeomorphology) from the University of Kalyani (India). Dr Roy has more than 20 research

publications in various journals of international and national repute. Since 2013, he is deeply involved in his research on human-induced changes in river systems and edited an international book on the anthropogeomorphology of Bhagirathi-Hooghly river system in India published by CRC Press. Dr Roy is the life member of the International Association of Hydrological Sciences (IAHS, UK), the Foundation of Practising Geographer (Kolkata, India) and the Indian Institute of Geomorphologists (Allahabad, India). He is an invited reviewer of different Scopus and SCI-indexed journals by Springer, Elsevier, Taylor & Francis, Willy, and Science Domain groups of publication. His main areas of innovative research include forest river geomorphology, anthropogeomorphology and transport-geomorphology. Dr Roy is an assistant professor in the Department of Geography, Kalipada Ghosh Tarai Mahavidyalaya, Siliguri, West Bengal, India. He is also the former vice president of the Young Geomorphologists Forum – 2021 of the Indian Institute of Geomorphologists affiliated with the International Association of Geomorphologists (IAG).



**Sandipan Ghosh** Dr Sandipan Ghosh is an applied geographer with a postgraduate, MPhil and PhD in geography from the University of Burdwan. He has published more than 40 book chapters, and international and national research articles in various renowned journals of geography and geo-sciences. He is the author of two books, *Flood Hydrology and Risk Assessment: Flood Study in a Dam-Controlled River of India* (ISBN 978-3-659-50098-5) and *Laterites of the Bengal Basin: Characterization, Geochronology and Evolution* (ISBN 978-3-030-22937-5). He is also co-editor of (1) *Neo-Thinking on Ganges – Brahmaputra Basin Geomorphology* (ISBN 978-3-319-26442-4), (2) *Quaternary Geomorphology in India: Case Studies from the Lower Ganga Basin* (ISBN 978-3-319-90426-9), (3) *Anthropogeomorphology of Bhagirathi-Hooghly River System in India* (ISBN 978-0-367-86102-5) and (4) *Drainage Basin Dynamics: An Introduction to Morphology, Landscape and Modelling* (ISBN: 978-3-030-79634-1). Dr Ghosh has worked as one of editors in the *Asian Journal of Spatial Science* and *Journal of*

*Geography and Cartography*. Simultaneously he has worked as a reviewer in many international geo-science journals by Taylor & Francis (*Geo-Carto International*), Springer (*Environment Development and Sustainability*, *Arabian Journal of Geosciences and Geosciences*, *Spatial Information Research*, *Journal of Earth System Sciences* and *Journal of Geological Society of India*), Frontiers (*Frontiers in Earth Science* and *Frontiers in Research Metrics and Analytics*), the International Water Association (*Water International*), and Indian Academy of Sciences (*Current Science*). Dr Ghosh is a lifetime member of The International Association of Hydrological Sciences (IAHS), Eastern Geographical Society (EGS) and Indian Geographical Foundation (IGF). His principal research fields are various dimensions of fluvial geomorphology, flood geomorphology, quaternary geology, soil erosion and laterite study. Currently, he has worked on (a) the gully morphology and soil erosion on the lateritic terrain of West Bengal and (b) quaternary geomorphology and active tectonics in the Eastern Himalayas and the Bengal Basin, West Bengal. At present, he is an assistant professor in the Department of Geography, Chandrapur College, Purba Bardhaman, West Bengal.



**Balai Chandra Das** Dr Balai Chandra Das is Associate Professor of Geography, Krishnagar Government College, Nadia, West Bengal. He earned a postgraduate degree in geography from the University of Burdwan and a PhD in geography from the University of Calcutta. He has published more than 40 research articles in reputed national and international journals, proceedings and edited volumes. Dr Das has served as an editorial board member for two international journals and as a reviewer for five more. He is the first editor of three books (1) *Neo-thinking on Ganges–Brahmaputra Basin Geomorphology*, ISBN 978-3-319-26442-4, <https://www.springer.com/gp/book/9783319264424> (2) *Quaternary Geomorphology in India: Case Studies from the Lower Ganga Basin*, ISBN 978- 3-319-90426-9, <https://link.springer.com/book/10.1007/978-3-319-90427-6> published by Springer International Publishing,

Switzerland and (3) *Anthropogeomorphology of Bhagirathi-Hooghly River System in India*. ISBN 9780367557270 published by Taylor & Francis Group. <https://doi.org/10.1201/9781003032373>. He was one of the members of the *Scientific Committee* of *IWC-2016* and *WRAA-2020 Oman*. His current research interest is on the fundamental geomorphology of rivers and lakes.

# Chapter 1

## Floods of Ganga-Brahmaputra-Meghna Delta in Context



Sandipan Ghosh , Suwendu Roy , Aznarul Islam , Pravat Kumar Shit, Dilip K. Datta , M. Shahidul Islam, and Balai Chandra Das 

**Abstract** The Ganga-Brahmaputra-Meghna (GBM) delta is the world's one of the most populated regions and has the highest concentration of population affected by floods. Millions of people become displaced, and tens to hundreds die each year of the flood incidents. Principally, the heavy rainfall and cyclonic storm are the key drivers of floods in the GBM delta. Although the GBM system covers a vast area of varying topography, diversified lithology, heterogeneous soils, and varying vegetations, the delta formed by the rivers is one and unique geomorphic unit. In this chapter, we focused broadly on the geology, relief, and river systems of this geomorphic unit. We also discussed the nature of floods in the region and their causes – natural and anthropogenic. The seasonality of floods in the GBM delta is also addressed in this chapter. This is not the age of combating floods, but rather the age of coexistence of man with floods. We illuminated this issue of living with floods. Finally, we outlined the prime theme of all other chapters.

---

S. Ghosh

Department of Geography, Chandrapur College, Purba Bardhaman, West Bengal, India

S. Roy

Department of Geography, Kalipada Ghosh Tarai Mahavidyalaya, Bagdogra, West Bengal, India

A. Islam (✉)

Department of Geography, Aliah University, Kolkata, West Bengal, India

P. K. Shit

PG Department of Geography, Raja N. L. Khan Women's College (Autonomous), Midnapore, West Bengal, India

D. K. Datta

Environmental Science Discipline, Khulna University, Khulna, Bangladesh

M. S. Islam

Department of Geography and Environment, University of Dhaka, Dhaka, Bangladesh  
e-mail: [shahidul.geoenv@du.ac.bd](mailto:shahidul.geoenv@du.ac.bd)

B. C. Das

Department of Geography, Krishnagar Government College, Krishnanagar, West Bengal, India



**Keywords** Riverine floods · Tidal floods · Monsoon regime · Dams · Embankments · Flood management · Living with flood

## 1 Backdrop

The Global Flood Database (Tellman et al., 2021) has reported about 3054 flood events worldwide during the 2000–2018 period only from different sources (mostly from news reports); however, the organization has successfully mapped 913 flood events in 169 countries using satellite imageries, which were cumulatively inundated about 2.23 million km<sup>2</sup> of land with a major concentration in Southeast Asia (Fig. 1.1). During this time period, the most severe rain-induced flood event has been noticed in the adjoining area of the Ganga-Brahmaputra-Meghna (GBM) delta on 21 July 2007, when about 27 million human population were directly affected by flooding over an area of 78.8 thousand km<sup>2</sup> and about 5 million population were displaced with 1071 causality (Global Flood Database (cloudtostreet.ai) (Fig. 1.1). The table of the top 15 flood events over the GBM basin, including some parts of Myanmar, shows, except one, all the 14 events occurred mainly due to intensive rainfall during the monsoon period (July–October), only with an average exposure of 19 million population (Table 1.1). The region holds over 10% population of the world from the two most populated countries, India and Bangladesh (Rasul, 2014). Although the GBM basin spatially covers about 174.5 million hectares and comprises five countries, i.e., India, Bangladesh, Bhutan, Nepal, and Tibetan China (Rasul, 2014), however, the major concentration of severe and devastating flood events have been frequently observed only in the north and eastern India and over

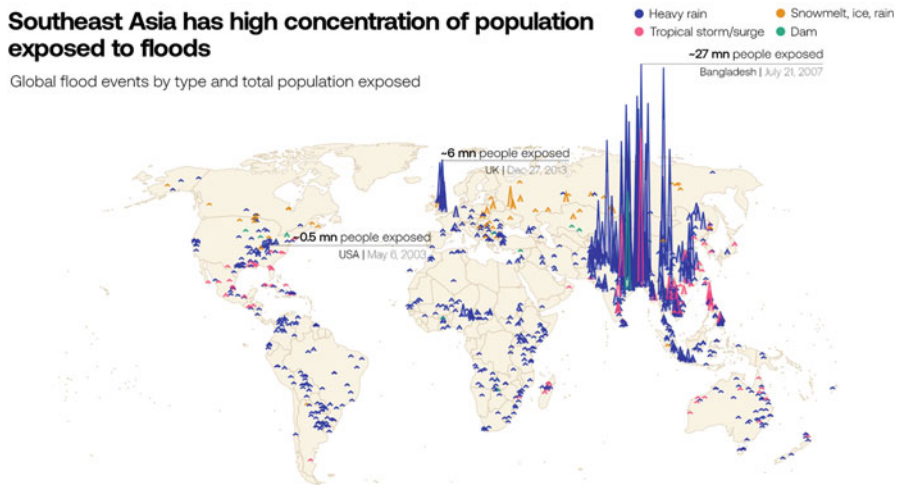


**Fig. 1.1** Exposer of the global population to the flood events during 2000–2018. (Source: after The Global Flood Database, Global Flood Database (cloudtostreet.ai) accessed on December 2021)

**Table 1.1** List of top 15 flood events over the GBM basin including some parts of Myanmar as per data provided by Global Flood Database (cloudtostreet.ai)

Date	Population exposed	Population displaced	Causality	Duration (Days)	Cause
7/21/2007	2,77,12,991	50,00,000	1071	86	Heavy rain
09/09/2010	2,31,37,894	1,40,000	0	21	Heavy rain
8/30/2008	2,16,31,628	6,00,000	0	9	Heavy rain
8/18/2008	2,15,29,060	1,00,00,000	400	37	Heavy rain
07/12/2007	2,14,88,636	1,11,00,000	96	90	Heavy rain
6/20/2004	1,98,55,086	4,00,00,000	3000	109	Heavy rain
10/01/2010	1,93,62,985	5,00,000	15	11	Tropical storm, surge
7/25/2016	1,84,56,496	25,000	42	32	Heavy rain
09/01/2018	1,72,13,562	1000	20	6	Heavy rain
06/11/2003	1,68,22,143	95,00,000	600	121	Heavy rain
7/21/2002	1,65,41,422	2,50,000	380	25	Heavy rain
07/03/2007	1,64,86,188	30,00,000	958	81	Heavy rain
08/02/2018	1,64,24,780	25,000	0	8	Heavy rain
9/16/2012	1,55,26,445	200	45	2	Heavy rain
8/15/2011	1,48,30,495	70,000	158	48	Heavy rain

entire Bangladesh, in particular the delta region of GBM (Fig. 1.2). The area of the GBD delta is approximately 1,00,000 km<sup>2</sup> and is also a habitat for over 170 million people (Edmonds et al., 2020; Auerbach et al., 2015; Paszkowski et al., 2021).

The GBM delta is a unique example of multilateral interaction between water (fresh and saline), land (including livelihood), and forest, which consists of distinguished features like the world's largest and most populated delta (Paszkowski et al., 2021); about 75% of the Himalayan water (~1200 km<sup>3</sup>) drains here with containing about 1 billion tonnes (BT) of sediment annually (Reitz et al., 2015; Allison, 1998; Wilson & Goodbred Jr., 2015; Paszkowski et al., 2021); the interplay between higher sediment input and tidal forces makes this region an active zone of land formation and degradation by accretion – erosion and aggradation – and progradation processes (Sarker et al., 2011), holding largest mangrove system of the world (Sundarbans) (Spalding & Leal, 2021) and facing significant changes in the processes of geomorphology naturally and anthropogenically (Paszkowski et al., 2021). The period of formations is still active since the early Holocene (~12,000 years) as a part of the Bengal Basin, which is a result of about 8500 km<sup>3</sup> of sediment deposited from the Ganga, Brahmaputra, and Meghna Rivers (Goodbred Jr. et al., 2014). The GBM delta is also experiencing active tidal action ranging from 3 m to 6 m high with an influence up to 100 km inland (Haque & Nicholls, 2017).

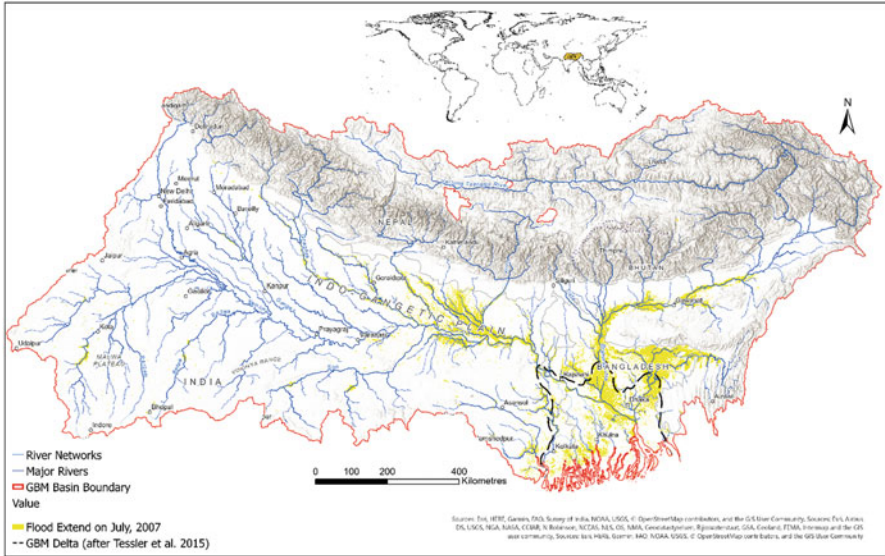


**Fig. 1.2** The outline of the Ganga-Brahmaputra-Meghna (GBM) basin marked with its deltaic zone (in black dashed line) after Tessler et al. (2015) and showing the extension of the most severe flood during July 2007 as per mapped by Dartmouth Flood Observatory (DFO). (Sources: Esri, HERE, Garmin, FAO, Survey of India, NOAA, USGS, © OpenStreetMap contributors, and the GIS User Community. Sources: Esri, Airious DS, USGS, NGA, NASA, CGIAR, N Robinson, NCEAS, NLS, OS, NMA, Geodatastyrelsen, Rijkswaterstat, GSA, GEoland, FEMA, Intermap and the GIS, user community. Sources: Esri, HERE, Garmin, FAO, NOAA, USGS, © OpenStreetMap contributors, and the GIS User Community)

## 2 The Ganga-Brahmaputra-Meghna Delta: A Geomorphic Unit

The cradle of the GBM delta is the tectonically active Bengal Basin (Fig. 1.3), which spans the western margin of the Indian Shield or Craton, getting maximum sediments from the Himalayan Rivers. The basin is situated at a plate boundary of the Indian Plate, Burma Plate, and Eurasian Plate, as a continent–continent collision (forming the Himalayan Arc). Flexural subsidence over a broad area, in addition to faulting, folding and localized compaction, allows the subaerial portion of the GBM delta to trap and store ~30% of the 1.1 billion tonnes of sediment delivered to the fluvial system by the rivers (Reitz et al., 2015). The important studies (Bandyopadhyay, 2007; Auerback et al., 2015; Reitz et al., 2015; Akter et al., 2016; Rudra, 2018; Wilson & Goodbred Jr., 2015; Becker et al., 2020; Paszkowski et al., 2021) revealed that the GBM delta is fed by the combined sediment load of ~1 billion tonnes by the fluvial system of Ganga, Brahmaputra and Meghna and most of the delta lies within 20–25 m from present mean sea level. The course of the Ganga, Bhagirathi, Jamuna, Meghna, and other rivers divides the Bengal Basin or

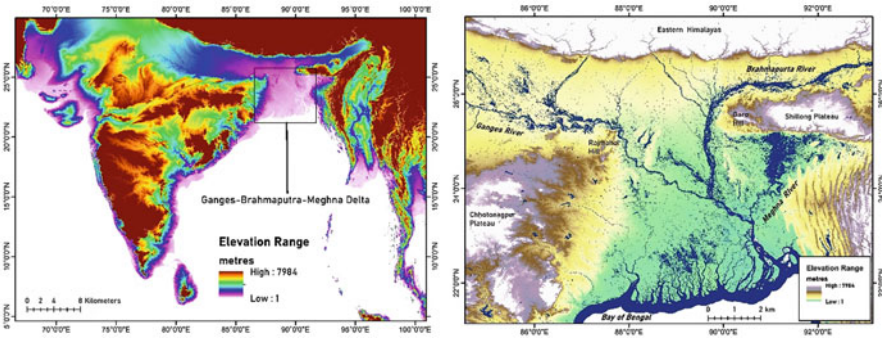


**Fig. 1.3** Location of Ganga-Brahmaputra Delta at the eastern part of Indian Craton, showing the fluvial system and seasonally inundated region

undivided Bengal into six geological regions. These regions are: (1) the plains adjoining the Himalayas of North Bengal, (2) the Barind region between the Ganga and the Jamuna, (3) the Rarh region west of the Bhagirathi, (4) the delta east of the Bhagirathi and south of the Ganga, (5) the Meghna Basin, and (6) numerous coastal areas consisting of numerous river creeks and islands.

The GBM delta has morphologic and stratigraphic attributes of an upland fluvial fan, a lowland fluvial delta plain below the backwater transition, a tide-dominated portion amalgamated to its seaward edge, and a large, actively prograding subaqueous-delta cliniform. It is, therefore, best characterized as a composite delta system. Although much of the GBM delta is robust in terms of its construction and maintenance through the Holocene, there are some portions of the delta where sediment supply is insufficient to offset subsidence rates or erosion. These areas are considered most at risk of flooding (e.g., from monsoons, cyclonic storm surges, and high astronomical tides) or erosion (from tidal action). The three regions undergoing this type of decline in the landscape are located in the Sylhet basin, along the Indian tidal delta plain, and at the fluvial-tidal transition in the western and central areas of the delta.

The main geomorphic characteristics of this delta are mentioned as follows (Steckler et al., 2022).

- The GBM delta originated with the opening of the Rajmahal-Garo Gap in the Plio – Pleistocene while it acquired its present form during the Late Holocene after the sea level near its present position following the mid-Holocene transgression.
- The entry of the Ganga (at the Rajmahal Hills of Chotanagpur Plateau) and the Brahmaputra (at the Garo Hills of Shillong Massif) form the apex of the GBM delta, with maximum inputs of water and sediments since Palaeocene. The upper part of this delta exhibits fan-like behaviours of rivers and the apex serves as a principal node of river avulsion. Similarly, the peninsular rivers of India also have formed the vast span of fan-delta at the west (10–40 m elevation range), as a part

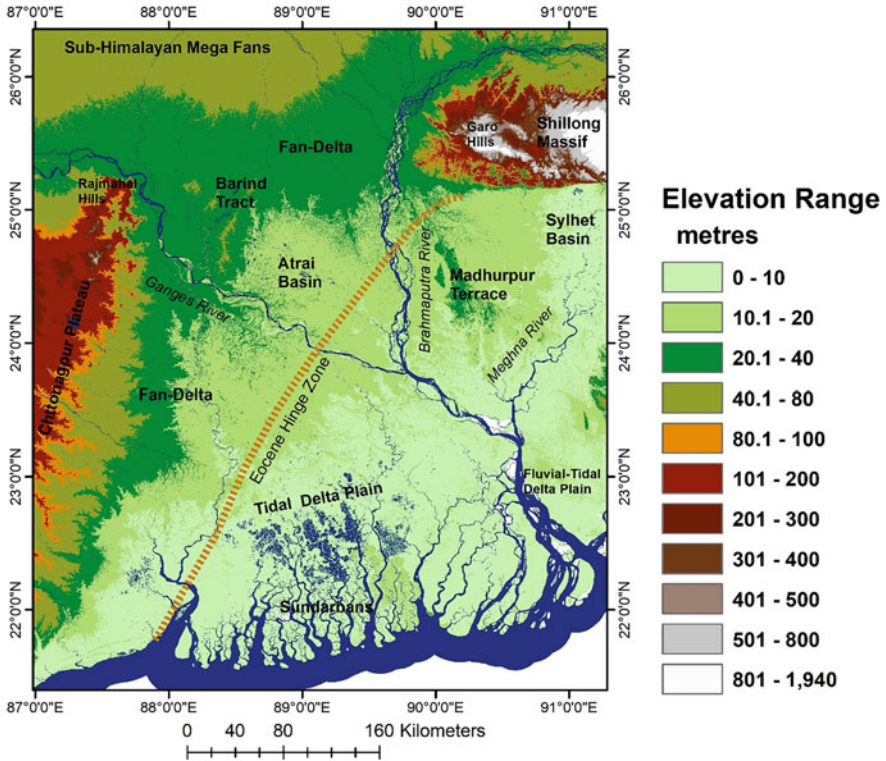
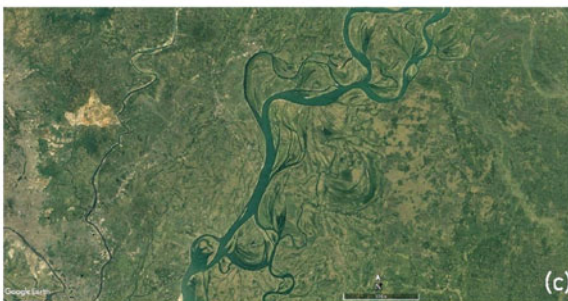


**Fig. 1.4** Topographic variation of GBM delta and its important geomorphic units

of Bengal Basin's shelf deposits (Fig. 1.4). Downstream of fan deltas the relief becomes less and the topography is very flat, defining the low-lying tidal or fluvial-tidal delta plain and coastal swamps (Sundarbans).

- In the northern part of the GBM delta, mega-fans of Himalayan Rivers (viz., Teesta, Torsa, Mahananda, Jaldhaka, etc.) are observed. Downstream of the rivers, the dominance of fan deltas, and bed-load alluvial channels are the major landforms. Braided rivers of the Brahmaputra fluvial system undergo rapid channel aggradation, lateral migration, and avulsion.
- The fluvial delta parts of the region also exhibit braided pattern with intensive bank erosion, and some alluvial reaches shows anastomosing pattern where channel braids are reconnected again downstream with mature islands. Many rivers (like Bhagirathi-Hooghly and Meghna) show active meander belts where the channel shows increasing lateral migration and bank-line shifting with the development of oxbow lakes, abandoned channels, and meander scars (Fig. 1.5). The active river-mouth distributaries, in between Padma and Bhagirathi-Hooghly, have developed  $\sim 5000$  km<sup>2</sup> of large coalescing islands toward the Bay of Bengal. This tidal mud-flat region of more than 100 islands is recognized

**Fig. 1.5** Aerial views of river morphology and pattern: **(a)** Braided Brahmaputra River with its tributary confluences, **(b)** mature fan-delta of Ganga River at downstream of Farakka Barrage with its bifurcated western branch Bhagirathi-Hooghly River, **(c)** anastomosing pattern of Meghna River, and **(d)** active deltas of tidal mud-flats at the river mouth of Padma. (Image collected from Google Earth Pro)



as a UNESCO World Heritage Site (World's largest mangrove ecosystem; an area of about 10,000 km<sup>2</sup>).

- Development of bars and channel migration (braided channel) force bank erosion rates up to 1 km year<sup>-1</sup> along the Brahmaputra River. Sediment accretion rates in the floodplains or fan deltas vary from 1 to 4 cm year<sup>-1</sup> near the Brahmaputra. The observed periodicity of major avulsions varies from 1500 to 2500 years in the Ganga and Brahmaputra. With the decrease in sediment load and monsoon discharge, many rivers of the GBM delta display a phenomenon of metamorphosis, i.e., the transformation of braided to meander pattern in two parts – (a) Ganga fluvial fan in the south-west and (b) Old Brahmaputra fluvial fan near the Sylhet Basin in the north-east. In the last five decades, the GBM has prograded at a rate of 17 km<sup>2</sup> year<sup>-1</sup> (Akter et al., 2016).
- Near the tidal mud-flat region (i.e., Sundarbans), the monsoon river discharge varies from 50,000 to 1,00,000 m<sup>3</sup> s<sup>-1</sup> and the suspended sediment load of the estuary ranges from 0.5 to 9.0 gm l<sup>-1</sup>. About 11,200 km<sup>2</sup> of the lower tidal delta plain is densely inhabited (population density of 500–1000 person km<sup>-2</sup>) and embanked for settlements and agriculture. This part is extremely vulnerable to natural hazards, like cyclones, storm surges, coastal floods, tsunamis, and sea-level change.
- Due to natural and anthropogenic processes at different spatial scales, the subsidence of unconsolidated deltaic sediments is a natural process in the deltas (Akter et al., 2016). Subsidence of the Bengal Basin is a relevant issue, though the Madhupur Terrace and Barind Tract show regional upliftment. The estimated short-term subsidence rate varies over the delta from 0 to 12 mm year<sup>-1</sup>. The Sylhet Basin shows a very high subsidence rate of 7–12 mm year<sup>-1</sup>, and the coastal belt shows a moderate rate, i.e., 3–8 mm year<sup>-1</sup>. The maximum tilting rate is  $1.4 \times 10^{-7}$  radians year<sup>-1</sup>. The regions of greater subsidence and tilting show increased river avulsion and channel migration.
- The evidence of climate change is that the probable maximum change in precipitation in the Ganga Basin and the Brahmaputra Basin might be 13.1% and 10.2%, respectively, for a temperature increase of 2 °C (Akter et al., 2016). Between 1968 and 2012, the mean sea level raised at a rate of ~2 mm year<sup>-1</sup>. The sea level observed from the data collected by three different stations showed rises in sea level by 1.0 mm year<sup>-1</sup> (Khepupara), 2.7 mm year<sup>-1</sup> (Haldia), and 3.9 mm year<sup>-1</sup> (Diamond Harbour), respectively (Jabir et al., 2021). By 2100, even under global warming and greenhouse gas emission mitigation scenario, the subsidence could double the projected sea level rise, mounting it 85–150 cm across the delta (Becker et al., 2020). In addition, in the previous years, tropical cyclones such as *Aila*, *Fani*, *Bulbul*, *Amphan*, and *Yass* devastated the coastal region to a great extent, making the region more vulnerable to floods and biodiversity loss.

### 3 Living with Monsoon Floods

The Ganga-Brahmaputra-Meghna and their numerous tributaries and distributaries carry a giant volume of sediments, through floods, in the monsoon months, and the deltaic floodplains have been formed by the accumulation of sand, silt, and clay in the Bengal Basin to develop it as world's largest delta. Three river systems drain a catchment of about 1.72 million km<sup>2</sup>, from the Himalayas to the Bay of Bengal. Rivers of the GBM delta, like the pendulum of a wall clock, are constantly moving and shifting within a certain range. The range within which the river is constantly moving is called the "Meander Belt" (Islam et al., 2020). The river "Meander Belt" can be called its playground where the river is always active with recurrent floods, changing landforms, and bank-line shifting. Although this area can be used for agriculture, it is not suitable for the construction of railways or roads, but now with the pace of economic development, the natural floodplains are delinked (horizontal disconnectivity) from the rivers, and the lands are utilized for settlements and communicating network. The danger is bound to come when people enter the river playground without realizing it. Ten or twenty years later, the river will return to its old course. With this dynamic character of the river in mind, floodplains can be used scientifically to protect people from erosion damage (Islam, 2011). But as the country's population has grown, settlements have moved to the riverbanks, increasing the risk of erosion (e.g. Islam & Guchhait, 2017, 2018) and flooding (e.g. Islam & Ghosh, 2021). The land use – land cover map (Fig. 1.6) – shows the dominance of the population in the river valleys of the Bengal Basin, showing the maximum area of cropland and patches of settlements. With some 130 million inhabitants, the GBM delta belongs to the most densely populated areas in the world (1300 persons/km<sup>2</sup>).

In the GBM delta, the average rainfall is 1474 mm year<sup>-1</sup>, with maximum rainfall of 2269 mm year<sup>-1</sup> and minimum rainfall of 341 mm year<sup>-1</sup>. From the maps (Fig. 1.7), it is observed that the eastern and south-eastern part receives a maximum annual rainfall of greater than 2800 mm, and the western and north-western part receives rainfall of less than 1600 mm. The annual average discharge of the Padma River is 29,692 m<sup>3</sup>s<sup>-1</sup>, with a maximum discharge of 80,984 m<sup>3</sup>s<sup>-1</sup> and a minimum discharge of 6041 m<sup>3</sup>s<sup>-1</sup>. With high monsoon discharge, flood is a normal occurrence and recurrent hazard in the GBM delta. There are two types of flooding: (a) first, strong cyclones occasionally flood coastal areas and (b) second, in case of low-pressure rainfall. The Himalayan-adjacent plains of North Bengal; the flood plains of North and South Dinajpur, Malda, and Murshidabad; the entire Rarh plain; and Brahmaputra floodplains of Bangladesh are prone to monsoon floods due to their location, topography, type of rainfall, variability of water flow in rivers, etc. Carrying a huge volume of sediment-laden flood water, the Ganga and the Brahmaputra, between the Garo and Rajmahal Gap, have entered into the Bengal Basin Bengal through the two ends of the plain between Meghalaya/Shillong Plateau and Eastern Chotanagpur Plateau. The other four tributaries that flow in the same direction are Mahananda, Teesta, Jaldhaka, and Torsa. The main tributary of the Meghna enters Bengal through the Barak Shrihat or Sylhet Basin. The Ganga, Brahmaputra, and



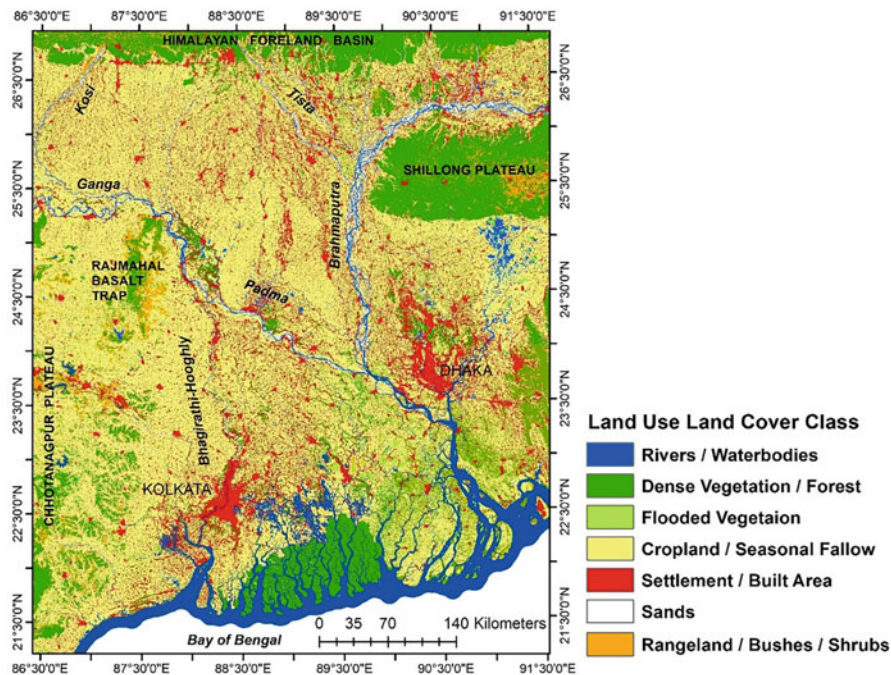


**Fig. 1.6** Major land use and land cover classes in the GBM delta

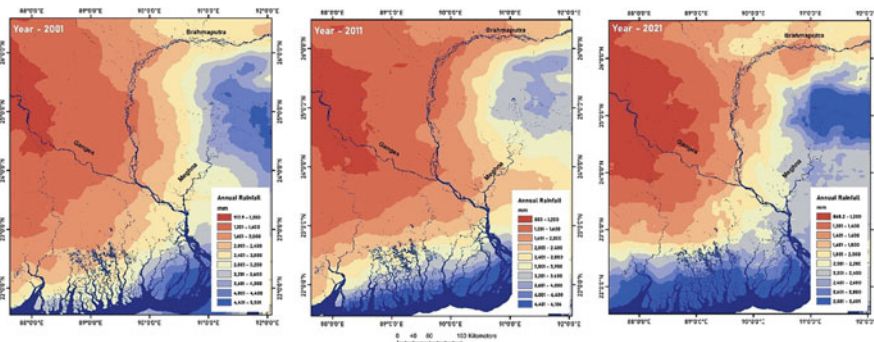


**Fig. 1.7** Pattern of mean annual rainfall distribution in the GBM Delta: 2001 (a), 2011 (b), and 2021 (c)

Meghna carry about  $1375 \text{ km}^3$  of water per year from a basin of about 16.21 lakh  $\text{km}^2$ , and the Padma reaches the Bay of Bengal through Bangladesh. The annual flow of these three rivers is unequal, during the monsoon season  $69,000 \text{ m}^3 \text{ s}^{-1}$  of water flows and at other times it decreases to  $5714 \text{ m}^3 \text{ s}^{-1}$ .

The severity and extent of floods depend on the amount of water flowing across the border, the intensity of rainfall, the slope of the land, the carrying capacity of the

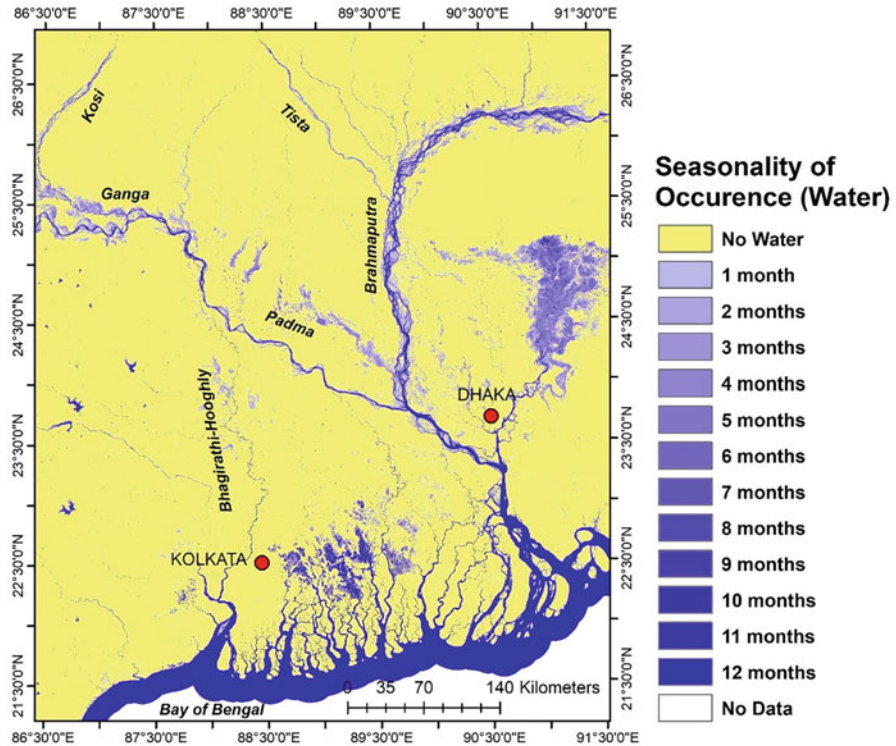


**Fig. 1.8** The regions of seasonal inundation and recurrent floods in the GBM Delta (1984–2020)

river, and so on. The major floods in the GBM delta (including other parts of the Bengal Basin) are usually in the last part of the monsoon season, i.e., August or September (Fig. 1.8). The rains in the first part of the monsoon saturate the soils, filling the shallow groundwater table, which goes down a lot in the summer, and the wetlands fill up with the water including the reservoirs and rivers. In the second phase, i.e., in August or September, heavy rains due to depression bring floods. Therefore, September is a “black month” in the history of floods in the GBM delta. Exceptions to this rule have sometimes caused floods in June, July, or even October. The basins of Teesta, Torsa, and Jaldhaka of North Bengal, adjacent to the Himalayas, are prone to more floods in July–August as the south-west monsoon hits the foothills about a month ago. Floods are usually caused by low pressure and heavy rains during the monsoons but have sometimes occurred twice in a row. Due to the heavy rainfall of the late monsoon, the water level of the river rises in such a way that the shallow channels cannot hold so much water, flooding the villages and towns on both sides. Approximately 42% of West Bengal, India, and about 80% of Bangladesh are prone to annual floods (Fig. 1.8). Areas of the Bengal Basin, which are frequently flooded, are:

- (A) The Himalayan-adjacent plains of North Bengal where the rivers like Teesta, Jaldhaka, Torsa, Raydak, etc. are flooded.
- (B) The Srihatta Basin and the Meghna Basin are flooded – burning down from the southern slope of the Meghalaya Plateau– and this low-lying area remains submerged for about six months.
- (C) Floodplain of Jamuna and Atrayee located to the south-east of Barind land.
- (D) Rarh plain of West Bengal, especially the lower basins of Damodar, Ajay, Mayurakshi, and Kangsabati.
- (E) Floodplains on both banks of Ganga, Jamuna, and Bhagirathi.
- (F) The coastal area is submerged by the tidal wave and storm surges.

The rainfall distribution of this region is not even, and the extremity of weather events is now enhanced due to global climate change. Darjeeling, Jalpaiguri, Alipurduar, and Cooch Behar in North Bengal (West Bengal) receive 2500–3000 mm of rainfall annually, whereas the Rarh region (western part of the Bengal Basin) receives an average of 1500 mm of rainfall per year, while the plains of South 24 Parganas receive 1600–1600 mm of rainfall from Murshidabad. Although the average annual rainfall in Bangladesh is 2300 mm, the rainfall is 1200 mm in the Barind region and 5000 mm in the north-eastern part of the country. The trend of heavy rains has been increasing in recent times. Renowned Indian scientist Dr. Meghnad Saha said that surplus water and its unequal distribution is the problem of West Bengal and Bangladesh. Till today, the problem has not changed much; floods and river erosion in the rainy season and severe waterlogging and drainage congestion during the monsoon season are the innate problems. Crying for relief in case of floods, the government trying its best, and mutual blame are all familiar to us. Attempts to control flooding have not diminished since the seven decades of independence from that colonial period, but not much success has been achieved; Many studies reveal that people are largely responsible for this flood. If there was a proper drainage system under the railway line, the damage to crops and property would be much less.

Alongside, the reservoirs and floods are other key issues that deal with downstream changes in flood dynamics due to anthropogenic interventions. The capacity of reservoirs is limited, and the accumulation of sediment is decreasing every year. For example, the Massanjore Dam lost about 474.82 mcm of live storage capacity with a 0.295% annual loss rate, and the annual siltation rate is 1.617 mcm/ year (World Commission on Dams, 2000). Not all upstream waters can be caught in this limited capacity. If it rains heavily at the upper catchment, the water has to be released; otherwise, the dam could break and cause more catastrophes. As a result, the reservoirs built for flood control increase the flooding (evidenced in the Damodar River Basin). Bangladesh has not tried to control floods by trapping water in large reservoirs because of the type of hilly valleys required for reservoir construction. There is no such topography anywhere except Chittagong. As a result, attempts have been made to control the flood only through embankments and polders. In a nutshell, the flood dynamics of the GBM delta can be categorized in the following points:

- The Ganga carries the highest streamflow about one month earlier than the Brahmaputra or Jamuna Ganga, i.e., at the end of July or the beginning of August. On the other hand, the highest currents of the Ganga and its tributaries enter West Bengal and Bangladesh at the end of August or September. When the Ganga water reaches Goalanda, the Jamuna swells and blocks the south-easterly flow of the Ganga, causing the Ganga to overflow its banks.
- Many scholars believe that the erosion and landslides in the Himalayan region have resulted in huge amounts of gravel–sand–silt coming down and blocking the river basin of Bengal and consequently increasing the extent of floods,
- The extent of floods in West Bengal is increasing. Normal floods in the 1950s flooded areas up to 16.764 m high from the mean sea level. In the late 1970s, the reach of flooded areas increased to 19.812 m. The area was submerged up to 20 m during the 1986 floods. During the floods of 2000, the current rose to a height of 68.58 m and crossed the railway line near the Subarnamrigi station in Murshidabad. The same thing is happening in Bangladesh; natural reservoirs, such as Chalonbil or Hurasagar, have become increasingly shallow, causing floodwaters to spread further.
- Floods often disrupt the normal life and livelihood almost year. The agrarian economy is paralyzed by floods during the monsoon period, and rural livelihood becomes at stake. However, sometimes flood blesses the agriculture with fertile silt producing bumper crops. For example, the Panskura region in Medinipur, West Bengal, India, produces good floriculture and vegetables after the monsoon flood enriches the soil with fertile silt.
- Flood pushes the local people to migrate to stabilize the economy. The labour migration in turn earns good remuneration and remittances are sent by the economic migrants to the source region, thus elevating the economic profile by creating an economic multiplier. For example, there has been observed an uplift in the economic profile of the flood-inundated areas of the Mayurakshi River basin, India, i.e., the higher the flood propensity, the higher the labour migration and the higher the receipt of the remittance to rebuild the rural economy (Islam & Ghosh, 2022).
- That huge body of flood water cannot be contained in the rivers or reservoirs; it is inevitable to spread in the floodplains. Technology does not check floods totally, but it can manage to an extent only. The simple fact is that there is research that needs to adapt strategies for living with floods, not to be controlled low-magnitude floods in the fertile floodplains. Thus, instead of controlling floods and living with floods, social various social side management measures like in situ and ex situ livelihood strategies may be encouraged (Islam et al., 2022).

## 4 The Present Volume and Its Focus

Having this context in mind, the present volume of floods in the GBM delta was conceived. There are 22 chapters in this volume including this chapter. The chapters of this volume are primarily concerned with the floods; their nature, drivers, impacts, and management. The book is arranged systematically with a beginning introducing the general nature of floods in the GBM delta and various issues and challenges for future modeling. This introduction is completed considering two chapters (Chaps. 1 and 2). Therefore, the rest 20 chapters are primarily concerned with floods at the regional scale (basin scale) in regions of both India and Bangladesh. Thus, the book presents a good blend of a systematic and regional approach. The first chapter is mainly focused on the existing nature of floods in the GBM delta, living with monsoon floods and briefing on other chapters included in this volume. The second chapter deals with flood inundation modeling in a data-sparse environment like flatland in the lower Ganga region. This chapter has clearly uttered the main problems, challenges, and prospects while dealing with the floods in a systematic way. The Chap. 3 is concerned with the nature of floods and channel sedimentation in the Torsa River Basin of North Bengal. The fourth chapter is a clear manifesting of similar issues of floods in the Teesta River Basin in India and Bangladesh. Flood Risk Assessment has been done on the Himalayan foothill basin of Jaldhaka river in Chap. 4. Similarly, Chap. 5 is concerned with the flood dynamics and problems of river erosion and channel oscillation with their impacts on the life and livelihood patterns of the people in the Dudhkumar and Dharala Rivers in Bangladesh. Chapter 6 is focused on another investing problem of channel platform development in response to the flood dynamics and anthropogenic interventions in the Mahananda Balason River Basin in the Northern part of West Bengal. Chapter 7 deals with the flood intensity and propensity in the context of dam construction in the Punarbha River Basin of Indo-Bangladesh. Moreover, Chap. 8 explores the morphometry of a small river basin in the Himalayan foothill and relates to the floods based on the prioritization of the subbasins using GIS tools. Chapter 9 is concerned with the flood dynamics of the lower Ganga River in Malda district, India, using multi-criteria analysis. Chapter 10 is focused on the socio-infrastructure vulnerability in the wake of floods in the Mayurakshi River Basin, India, based on the empirical field survey. Moreover, Chap. 11 is focused on the characteristics of floods and their future condition in the Ajay River basin, India. Similarly, Chap. 12 is a clear manifestation of the present flood characteristics and vulnerability of the people in the Khari River Basin, a small basin in the Lower Ganga system. Floods of the Damodar River are very popular among flood geomorphologists because it has a long history of floods that devastated the then Bengal and hence the once sorrow of the Bengal. Thus, Chap. 13 is deals with the floods of the Damodar River and risk assessment using numerical modeling of flood simulation in the Damodar River Basin, Eastern India. Furthermore, the floods and associated changes in the channel shifting of the Shilabati River, the western part of Bengal, are discussed in Chap. 14 of this volume. Chapter 15 is concerned with the flood history of the Ghatal region, India. Similarly,

the next chapter (Chap. 16) portrays the future flood scenario of the Brahmaputra River using the multi-model ensemble of CMIP6 projections. This would help the planners and stakeholders for future preparations. Chapter 17 explores the various dimensions of the floods in the Old Brahmaputra River Basin with implications for the sustainable management of the flood. Thus, Chap. 18 deals with the major characteristics of floods of the Meghna River in Bangladesh. Problems of Buriganga and Shitalakhya Rivers with special reference to floods in and around Dhaka City in Bangladesh are discussed in Chap. 19. It would help the various stakeholders how to manage the floods of an urban river. Furthermore, Chap. 20 deals with other fluvial floods mainly triggered by the monsoon rainfall in the context of the Jalangi–Churni River system, which was once active and now decayed. Geospatial assessment of the fluvial dynamics and flood vulnerability is assessed in the Bhagirathi–Hooghly River, India, in Chap. 21. Finally, Chap. 22 is mainly concerned with tidal floods of the Madhumati–Arial Khan Rivers in Bangladesh.

## 5 Concluding Remarks

Flood in the GBM delta is inevitable because of its hydrogeomorphic, climatic, and anthropic set-up. On the one hand, every year flood takes a toll on thousands of humans and assets, and on the other hand, agriculture gets benefitted through the receipt of the fertile silts derived from the floods. To protect the social and economic infrastructure from the wrecks of the floods, mainly structural interventions are popularly undertaken by the Govt. and other organizations in the form of constructing concrete embankments, dams, barrages, and weirs across the major rivers of the GBM Delta. However, breaching of the embankment and dam failure is commonly observed in these regions, especially during the heavy monsoon downpours. Therefore, it is true that instead of controlling the floods, understanding flood behaviour and social side management measures would be embraced to better live with the floods. In brief, the focused attention on the floods in the context of the GBM delta is really vital for the management of future floods. Thus, this book will cater to the need of the diverse communities from land to laboratory.

## References

- Akter, J., Sarker, M. H., Popesca, I., & Roelvink, D. (2016). Evolution of the Bengal Delta and its prevailing processes. *Journal of Coastal Research*, 32(5), 1212–1226.
- Allison, M. (1998). Historical changes in the Ganges–Brahmaputra delta front. *Journal of Coastal Research*, 14, 1269–1275.
- Auerbach, L. W., et al. (2015). Flood risk of natural and embanked landscapes on the Ganges–Brahmaputra tidal delta plain. *Nature Climate Change*, 5, 153–157.

- Auerback, L. W., Goodbred, S. L., Mondal, D. R., Wilson, C. A., Ahmed, K. R., Roy, K., Steckler, M. S., Small, C., Gilligan, J. M., & Ackerly, B. A. (2015). Flood risk of natural and embanked landscapes on the Ganges-Brahmaputra tidal delta plain. *Nature Climate Change*, *5*, 153–157.
- Bandyopadhyay, S. (2007). Evolution of the Ganga Brahmaputra Delta: A review. *Geographical Review of India*, *69*(3), 235–268.
- Becker, M., Papa, F., Karpytchev, M., Delebecque, C., Krien, Y., Khan, J. U., Ballu, V., Durand, F., Cozannet, S. L., Islam, A. K. M. S., Calmant, S., & Shum, C. K. (2020). Water level changes, subsidence and sea level rise in the Ganges-Brahmaputra-Meghna Delta. *PNAS Earth, Atmospheric and Planetary Sciences*, *117*(4), 1867–1876.
- Edmonds, D. A., Caldwell, R. L., Brondizio, E. S., & Siani, S. M. O. (2020). Coastal flooding will disproportionately impact people on river deltas. *Nature Communications*, *11*, 4741.
- Goodbred, S. L., Jr., et al. (2014). Piecing together the Ganges–Brahmaputra–Meghna River delta: Use of sediment provenance to reconstruct the history and interaction of multiple fluvial systems during Holocene delta evolution. *Geological Society of America Bulletin*, *126*, 1495–1510.
- Haque, A., & Nicholls, R. J. (2017). Floods and the Ganges Brahmaputra-Meghna Delta. In R. J. Nicholls, C. W. Hutton, W. N. Adger, S. E. Hanson, M. M. Rahman, & M. Salehin (Eds.), *Ecosystem services for well-being in deltas: Integrated assessment for policy analysis*. Palgrave Macmillan.
- Islam, A. (2011). Variability of stream discharge and bank erosion—A case study on the river Bhagirathi. *Journal of River Research Institute River Behaviour and Control*, *31*(1), 55–66.
- Islam, A., & Ghosh, S. (2021). Economic transformation in the wake of flood: A case of the lower stretch of the Mayurakshi River Basin, India. *Environment, Development and Sustainability*, *23*(10), 15550–15590.
- Islam, A., & Ghosh, S. (2022). Community-based riverine flood risk assessment and evaluating its drivers: Evidence from Rarh Plains of India. *Applied Spatial Analysis and Policy*, *15*(1), 1–47.
- Islam, A., & Guchhait, S. K. (2017). Search for social justice for the victims of erosion hazard along the banks of river Bhagirathi by hydraulic control: A case study of West Bengal, India. *Environment, Development and Sustainability*, *19*(2), 433–459.
- Islam, A., & Guchhait, S. K. (2018). Analysis of social and psychological terrain of bank erosion victims: A study along the Bhagirathi river, West Bengal, India. *Chinese Geographical Science*, *28*(6), 1009–1026.
- Islam, A., et al. (2020). Assessing meander belt width of Bhagirathi-Jalangi river system in lower Ganga delta, India. *European Journal of Geography*, *11*(1), 140–162. <https://doi.org/10.48088/ejg.a.isl.11.1.140.162>
- Islam, A., Ghosh, S., Barman, S. D., Nandy, S., & Sarkar, B. (2022). Role of in-situ and ex-situ livelihood strategies for flood risk reduction: Evidence from the Mayurakshi River basin, India. *International Journal of Disaster Risk Reduction*, *70*, 102775.
- Jabir, A., Hasan, G. M. J., & Anan, M. M. (2021). Correlation between temperature, sea level rise and land loss: An assessment along the Sundarbans coast. *Journal of King Saud University – Engineering Sciences*. <https://doi.org/10.1016/j.jksues.2021.07.012>
- Paszowski, A., Goodbred, S., Borgomeo, E., et al. (2021). Geomorphic change in the Ganges–Brahmaputra–Meghna delta. *Nature Reviews Earth & Environment*, *2*, 763–780. <https://doi.org/10.1038/s43017-021-00213-4>
- Rasul, G. (2014). Why Eastern Himalayan countries should cooperate in transboundary water resource management. *Water Policy*, *16*, 19–38.
- Reitz, M. D., Pickening, J. L., Goodbred, S. L., Paola, C., Steckler, M. S., Seeber, L., & Akhter, S. A. (2015). Effects of tectonic deformation and sea level on river path selection: Theory and application to the Ganges-Brahmaputra-Meghna River Delta. *Journal of Geophysical Research: Earth Surface*, *120*(4), 671–689.
- Rudra, K. (2018). *Rivers of the Ganga-Brahmaputra-Meghna Delta: A fluvial account of Bengal*. Springer Nature.

- Sarker, M. H., Akter, J., Ferdous, M. R., & Noor, F. (2011). Sediment dispersal processes and management in coping with climate change in the Meghna Estuary, Bangladesh. In D. E. Walling (Ed.), *Sediment problems and sediment management in Asian River Basins* (pp. 203–217). IAHS.
- Spalding, M. D., & Leal, M. (2021). *The state of the World's mangroves 2021*. Global Mangrove Alliance. Accessed 15 Jan 2022. <https://www.mangrovealliance.org/wp-content/uploads/2021/07/The-State-of-the-Worlds-Mangroves-2021-FINAL.pdf>
- Steckler, M. S., Cryan, B., Wilson, C. A., Gralll, C., Nooner, S. L., Mondal, D. R., Akter, S. H., Dewolf, S., & Goodbred, S. L. (2022). Synthesis of the distribution of subsidence of the lower Rivers of the Ganga-Brahmaputra Delta, Bangladesh. *Earth Science Reviews*, 224, 103887. <https://doi.org/10.1016/j.earscirev.2021.103887>
- Tellman, B., Sullivan, J. A., Kuhn, C., et al. (2021). Satellite imaging reveals increased proportion of population exposed to floods. *Nature*, 596, 80–86. <https://doi.org/10.1038/s41586-021-03695-w>
- Tessler, Z. D., et al. (2015). Profiling risk and sustainability in coastal deltas of the world. *Science*, 7, 638–643.
- Wilson, C. A., & Goodbred, S. L., Jr. (2015). Construction and maintenance of the Ganges-Brahmaputra-Meghna Delta: Linking process, morphology and stratigraphy. *Annual Review of Marine Science*, 7, 67–88. <https://doi.org/10.1146/annurev-marine-010213-135032>
- World Commission on Dams. (2000). *Dams and development: A new framework for decision-making: The report of the world commission on dams*. Earthscan. <https://pubs.iied.org/sites/default/files/pdfs/migrate/9126IIED.pdf>



# Chapter 2

## Flood Inundation Modelling in Data-Sparse Flatlands: Challenges and Prospects



Joy Sanyal

**Abstract** In the last three decades, many sophisticated tools have been developed that can accurately predict the dynamics of flooding. However, due to the paucity of adequate and immediate infrastructure, this technological advancement did not benefit the vast ungauged flood-prone regions in the developing countries in a major way. This chapter explores the improvement in methodology that is essential for utilising recently developed flood prediction and management tools, particularly in the flat deltaic landscapes in the developing world, where ideal model inputs and validation datasets do not exist. The issue of appropriate model selection assumes greater significance when modelling is carried out without the availability of ideal inputs and validation datasets in the largely ungauged river basins. This discussion include key considerations for undertaking flood inundation modelling in data-sparse environments and can be valuable for flood managers and hydrologists engaged in tackling this problem with limited resources.

**Keywords** Hydrodynamic modelling · Coarse model inputs · DEM selection · The Ganga delta

### 1 Flood as a Global Natural Hazard

Floods account for approximately one-third of global natural hazards, and more people are adversely affected by flooding than any other geophysical phenomenon (Smith & Ward, 1998). On average, 20,000 people lose their lives due to flooding each year, and it affects 75 million people globally, most of whom become homeless (Smith, 2001). These global figures mask much regional variation in the occurrence of floods, the causes and the consequences on the populations. Adhikari et al. (2010) compiled a digitised global flood inventory for the period of 1998–2008 that reveals some important facts about different causes of flooding, the spatial variation and

---

J. Sanyal (✉)

Department of Geography, Presidency University, Kolkata, India

e-mail: [joy.geog@presiuniv.ac.in](mailto:joy.geog@presiuniv.ac.in)

frequency of occurrences. According to this database, heavy rain, monsoon rain and tropical cyclones were reported as the causative factors for 64%, 11% and 6% floods, respectively. These types of meteorological phenomena occur only in the tropical and subtropical regions where most of the developing countries are located. This database further reported that seven of the top ten countries with most flooding events reported between 1998 and 2008 were outside the industrialised world and that Asia and Africa have the highest percentage of reported flood events each year. Jonkman (2005) pointed out that the floods caused by Asian rivers claim the most lives and affect more people than any other region in the world. Flood-affected population in the developed world have the means to combat the extreme natural events through better infrastructure, health care, and functional flood warning systems (Allenby & Fink, 2005) while in the developing countries vulnerable populations lack the capital resource to develop sustainable protection mechanisms or rebuilt their damaged infrastructure after a major flood event.

The deltas of large rivers in the tropical regions are particularly flood prone. Such landscape is characterised by very low gradient of land, numerous branches and sub-branches of the main channel and a near absence of local-level hydrological and terrain-related information that are crucial for predicting the extent and depth of fluvial inundation. The Ganga delta, spreading across the Indian state of West Bengal and the southern part of Bangladesh, offers a typical example of such terrain. This region urgently need to develop a flood-prediction capability at an affordable cost for creating an early warning system and adopting structural (such as building embankments) and nonstructural (such as floodplain zoning) measures for flood management.

## **2 The Issue of Limited Data in Flood-Prone Regions**

### ***2.1 Prevailing Mismatch in Scientific Advancement and Global Availability of Suitable Datasets***

Hydrodynamic models are the standard tools for predicting fluvial inundation. Streamflow data and topography of channels and floodplains are the two most significant model inputs that influence the flow hydraulics and modelled flood extents. The science of inundation modelling has transformed rapidly in recent years from a 'data-poor' to a 'data-rich' discipline with a gradual shift from developing more physically based models to simple ones that can effectively harness the increasing availability of high-resolution earth observation data to improve on their predictions (Bates, 2012). Constant improvement of very high-resolution terrain data form of LiDAR survey and all-weather capable synthetic-aperture radar (SAR) images for calibrating and validating distributed performances of flood-inundation models has advanced the flood prediction capability in the developed world significantly.

The study by Bates et al. (2006) in a 16 km reach of the River Severn in the United Kingdom is a typical example of the data-intensive inundation modelling approach. This study used LiDAR-generated DEMs in combination with a series of airborne synthetic-aperture radar (ASAR) images captured opportunistically during the peak and recession limb of the flood hydrograph in order to calibrate and validate flood models. The LiDAR DEM used was of <1 m horizontal resolution with a vertical root mean square error (RMSE) of 0.079 m. Elevation is measured by differential GPS points of approximately 0.01 m vertical accuracy that was used as reference spot heights for obtaining the RMSE value of the DEM while the ASAR images were of 1.2 m resolution. This dataset was further supplemented with spaceborne RADARSAT images, upstream and downstream gauging records at 15 min intervals and extensive field data collected during the actual flood event.

The quality of LiDAR data has improved further in recent years. Inundation modelling has been performed successfully at 10 cm grid size for a small piece of urban land by using very high-resolution LiDAR data captured with vehicle-mounted terrestrial laser scanner (Sampson et al., 2012). High-resolution SAR data are typically available at ~25 m ground resolution, but Mason et al. (2009) utilised TerraSAR-X images with 3 m resolution for detecting flood water in the urban environment. The availability of fine resolution inputs, particularly the fine-resolution validation data from SAR imageries help reduce the equifinality arising from the difficulty in differentiating between different model physics and parameters and provided a more controlled environment for comparing the effect of including individual hydraulic process in the code (Bates, 2012). Thus, it is clear that a steady trend of advancement in the quality and coverage of the required data has led to marked improvement in the science of inundation modelling. Nevertheless, the major flood-prone areas in the world are not able to benefit much from this development of state-of-the-art inundation models given that LiDAR-derived terrain data are almost always unavailable in the developing countries due to the prohibitive cost of acquiring them (Sanyal & Lu, 2004). This scenario leaves us with the option of using freely available DEMs such as the Shuttle Radar Topography Mission (SRTM) DEM or the Advanced Spaceborne Thermal Emission and Reflection Radiometer (ASTER) Global Digital Elevation Model (GDEM) for defining the model geometry.

## ***2.2 Applicability of SRTM DEMs for Flood Inundation Modelling***

Although Sanders (2007) demonstrated the potential of employing the SRTM DEM in inundation modelling and Manfreda et al. (2011) highlighted the reliability of this data to identify flood-prone regions with a modified topographic index, it is well known that these terrain data contains considerable noise (Bhang et al., 2006). Such noise nullifies the hydrodynamic exchange during the coupling of 1-D and 2-D flow

in the recent improved models (Mohanty et al., 2020). A global performance assessment study of the SRTM data by Rodriguez et al. (2006) revealed an absolute height error of 6.2 m, 5.6 m and 6.2 m for Eurasia, Africa and South America, respectively. The SRTM DEM is also dated (acquired in the year 2000) and creates problem in areas where previous events have known to have modified the floodplain considerably (Schumann & Bates, 2018).

The ASTER GDEM is reported to have significant anomalies and much higher RMSE than the SRTM DEM when compared with LiDAR-derived elevation data derived from ICESat (Reuter et al., 2009) and is not suitable for inundation modelling in any manner. Due to their overall vertical inaccuracies, global DEMs are not deemed suitable for detailed flood inundation modelling in local and regional scale (Yan et al., 2015). Having said that, it is worth noting that in the flat floodplain areas, SRTM DEM was reported to have a vertical accuracy of better than 2 m (Schumann et al., 2013). However, modelling flood inundation in large rivers flowing over extremely gentle gradient with commonly anabranching channel patterns and slow-moving flood waves are particularly sensitive to the vertical accuracy of the terrain data (Jarihani et al., 2015).

In spite of all the constraints mentioned above, there is an increasing trend of utilising freely available terrain data for hydraulic modelling of streamflow. Due to the coarse nature of the available terrain data (e.g., SRTM DEM), the majority of these studies has been undertaken at continental scale. For example, Yamazaki et al. (2012a) applied a global river model, CaMa-Flood (Yamazaki et al., 2011), to model the seasonal cycles of water level elevations in the Amazon River using the SRTM DEM as the terrain input and the simulated water surface elevations were compared with Envisat altimetry. Development and application of flow routing and inundation models in the data-sparse regions of the world is mostly confined to the very large continental river basins such as the Amazon (da Paz et al., 2011), Congo (Jung et al., 2010), Niger (Neal et al., 2012a) and Ob (Biancamaria et al., 2009). The abovementioned studies are primarily engaged in simulating seasonal or annual cycle of river discharge and water level or even water budget and flooding pattern of large wetlands of the Niger River (Zahera et al., 2011) and the Nile Basin (Petersen & Fohrer, 2010).

A number of novel attempts have been reported to deal with the low resolution of the freely available DEMs that were used in these investigations. Paiva et al. (2011) developed a GIS-based algorithm that includes extraction of river cross-sections, delineation of river networks and catchments from the SRTM DEM and used geomorphic principles to estimate the river width and depth. Yamazaki et al. (2012b) proposed a pit removal strategy to reduce the anomalies in the SRTM data arising from vegetation canopy and sub-pixel structure and reported an improvement in the simulated water surface elevation with the adjusted DEM in terms of agreement with the observed records. Neal et al. (2012a) demonstrated how a sub-grid scale representation of a channelised portion of the flow can help to simulate streamflow in narrow channels that cannot be captured in the low-resolution global DEMs. However, this model still needs measurements about channel depth and width to derive the empirical relationship for estimating channel-bed elevation

from bank elevation and channel width. The slope break approach was employed in estimating channel bathymetry in a stretch of the Po River in Italy, which led to tangible improvement in the performance of a hydrodynamic model (Domeneghetti, 2016).

Since the X and C band radars used in the SRTM instrument do not penetrate the canopy, the SRTM DEM captured the tree top elevation rather than the surface at any place with dense foliage. Recently, global percentage vegetation map is derived from MODIS satellite images, global vegetation height map and sparse, but very accurate elevation points obtained from IceSat laser altimeter have been used to remove the vegetation artefacts from the 90 m version of SRTM DEM for producing a 'bare-earth' variant of the dataset (O'Loughlin et al., 2016). The global vertical RMSE of this product was reported to have gone down from 14 m to 6 m. Yamazaki et al. (2017) created Multi-Error-Removed Improved Terrain DEM (MERIT DEM) from the SRTM dataset by removing absolute bias, stripe noise, speckle noise and tree height bias. Such improved DEM was used to create a global river topography database, known as the MERIT Hydro (Yamazaki et al., 2019).

### ***2.3 Applicability of Other Low-Cost Sources of DEMs in Inundation Modelling***

Few attempts were made to generate terrain data from relatively affordable stereo satellite imagery sources for reach scale inundation modelling in the developing world where generally the SRTM DEM is the best available option. For example, Tarekegn et al. (2010) generated a DEM of 15 m resolution from ASTER imagery using ERDAS LPS digital photogrammetry software for 2-D hydrodynamic simulation of flooding in the Ribb River in Ethiopia but reported only 30.5% match between the simulated flooded extent and observed flood extent derived from a MODIS image. Considering the previous studies regarding the accuracy of the ASTER DEM data, this result is not surprising.

Low-cost Cartosat-1 stereo satellite imageries (2.5 m spatial resolution) from Indian Remote Sensing Satellites (IRS) were found to produce more accurate DEMs than the SRTM or ASTER data when compared with surveyed ground control points (Rawat et al., 2013). Sarhadi et al. (2012) used Cartosat-1 images to create high-resolution DEM of 2.5 m grid spacing in order to perform inundation modelling in the mountainous region of Iran and reported a high accuracy in the modelled flood extent. Cartosat-1 imageries were used in conjunction with 42 differential GPS (DGPS) ground control points (GCPs) to create a DEM of 30 m resolution for modelling floods in wide valleys (width > 500 m) of the Mahanadi River, India, and the model performed reasonably well when compared with the results derived from surveyed cross-sections (Jena et al., 2016). In a similar set-up in the Damodar River, India Sanyal et al. (2013) reported that only seven surveyed cross-sections for a 100 km reach were sufficient to supplement SRTM DEM for accurately predict

downstream water stages during high magnitude flow events provided the water remain confined within the banks/embankments. However, for slightly narrower channels (width ~ 300 m), the DEM created from IRS Cartosat-1 stereo images with 10 GCPs were not found to be accurate enough for simulating widespread floodplain flow and had to be supplemented with a series of surveyed cross-sections for the detailed representation of the channel (Sanyal et al., 2014a).

It is worth noting that a mass-produced DEM derived from Cartosat-1 imageries has been generated by National Remote Sensing Centre (NRSC), India, covering the entire India, which are available for download free of cost. The vertical accuracy of CartoDEM was reported to be 5.2 m and 7.9 m for plain and hilly terrain, respectively, when compared with ICESat Glass data (Muralikrishnan et al., 2013). The bias in the SRTM DEM was found to be more systematic than CartoDEM. Kumar et al. (2019) noted that a corrected version of the SRTM data improved the accuracy of a 1-D hydrodynamic model while similar effort to modify the CartoDEM resulted in degraded prediction. In spite of these limitations, it is encouraging to note that Mohanty et al. (2020) found the performance of CartoDEM in hydrodynamic modelling almost at par with LiDAR DEMs and highly recommended its use for India.

## ***2.4 Creating Accurate River Terrain Model from Sparse Data***

The most significant determinant of the performance of a hydraulic model is the accuracy in the representation of the channel geometry (French & Clifford, 2000; Pappenberger et al., 2005). Creating a continuous and detailed terrain data for the channel is a requirement for 2-D hydrodynamic models. Even for the 1-D models, a continuous DEM including the channel is often required to derive the extent of inundation where the terrain height is subtracted from the simulated water level at each cross-section to identify the wet cells. Creating a reasonably accurate river terrain model in data-sparse regions can be quite challenging because of the narrow width of the channel in comparison to the coarse resolution of the freely available DEMs. Particularly, for the SRTM DEM, the problem is aggravated by voids in the wet part of the channel arising from specular reflection of radar backscatter from calm water. In the 'finished' versions of the SRTM DEM, which have less void and noise, any river with more than 183 m of width was monotonically stepped down at the direction of flow (Slater et al., 2006). This processing led to step-like appearance in channels along their longitudinal profiles and made them difficult to use, at least in the reach scale.

Merwade et al. (2008a) pointed out that linear interpolation of the available surveyed cross-sections for creating a continuous river terrain model is not straightforward due to various facts including bends in the river and imperfect location of the cross-sections. In addition, the existence of channel islands not captured by enough number of cross-sections and inadequate representation of channel thalwegs by the bathymetric surveys also make the interpolation a challenging task. Merwade

et al. (2006) reported that in a flow-oriented coordinate system, the performance of anisotropic spatial interpolation techniques resulted in significant reduction in RMSE as compared with the conventional interpolation techniques such as nearest neighbour or kriging. This study proposed elliptical inverse distance weighting, a modified version of conventional inverse distance weighting (IDW), to take advantage of the flow oriented coordinate system as the channel bed morphology is essentially anisotropic due to greater variability of bed elevation perpendicular to the flow direction than along it. However, the investigation used spatially irregular bathymetry data collected by boat-mounted acoustic depth sounders rather than linear channel cross-sections. Even the isotropic techniques of interpolation were reported to perform well if the surveyed bathymetry data are de-trended and transformed into a flow-oriented coordinate system (Merwade, 2009). However, after experimenting with various interpolation techniques in a flow-oriented coordinate system, Legleiter and Kyriakidis (2008) commented that the density of surveyed points exerts primary control over the accuracy of interpolated surface and the RMSE of the interpolated surface has a strong relation with the spacing of the cross-sections.

All the interpolation techniques mentioned above are likely to create accurate interpolated surfaces of the channel if there is adequate data in the form of irregular elevation points or linear surveyed cross-sections. In the case of anabranching and anastomosing rivers with a number of flow bifurcations and large river islands, the abovementioned methods may not perform well (Merwade et al., 2008a). For a successful implementation of the aforesaid interpolation techniques to capture the flow diversion near the river bifurcations, very high density of surveyed points will be required, and therefore these methods may not be suitable for use in a complex fluvial system, especially in the flat deltaic environments of the developing countries.

### **3 Inundation Modelling at Regional and Reach Scales with Limited Data**

In general, there is a lack of focus on flooding as a natural hazard when it comes to hydraulic modelling in data-sparse regions. When we develop a tool for a flood prediction and warning system, it is conventionally focussed on modelling extreme flow events with an accuracy that is acceptable in flood management and planning practices. There are very few case studies at regional scales outside the industrialised countries for river basins that are fairly large (length > 500 km) but not of continental scale such as the Amazon and of cases that regularly inundate densely populated floodplains. Use of the global DEMs for routing high-magnitude floods at a regional scale is likely to require some additional reference data in order to correct the systematic bias and noise present in them and increase the details of topographic representations where it is absolutely necessary. Due to this reason, there is almost

no scientific literature on hydrodynamic predictions of inundation that are of fluvial origin in the Ganga Delta. Storm surge modelling in the Bay of Bengal Coast of Bangladesh was carried out (Deb & Ferreira, 2018; Islam et al., 2019) including prediction of the probable impacts of climate change (Rahman et al., 2019). However, lack of accurate terrain data and information on the tidal influence led to a challenging environment to develop a functional hydrodynamic model for the Ganga Delta.

Few attempts were made to simulate river flows in regional scales by correcting the vertical errors in SRTM DEM using spot heights from topographic maps of 1:50,000 scale in sparsely gauged parts of the Mahanadi (Patro et al., 2009) and the Brahmani Rivers (Pramanik et al., 2010) in India. Casas et al. (2006) evaluated the effect of quality of input terrain data on the accuracy of predicted water surfaces using HEC-RAS model. Although this study reported poor performance of contour maps with 5 m intervals in comparison with high-resolution LiDAR DEMs, it is interesting that the observed error in predicted water surface reduced quite dramatically as the flow crosses the bank limit and lack of river channel bathymetry becomes less significant. Adding GPS control points to the less accurate contour-derived TIN model improved the predicted water-surface elevation by 4.5 m. This finding is particularly encouraging with a view to employing relatively low-resolution DEMs for large flood prediction, which can be supplemented with GPS surveyed control data to improve accuracy.

The majority of the inundation modelling that is focussed on analysing flood risk is conducted at the reach scale (<20 km). Generally, a major flood is considered for which detailed topographic data for the flood-prone reach is available. There is an acute lack of literature that deals with this kind of study outside the industrialised countries because the globally available DEMs are normally too noisy to accurately simulate floodplain flow at this scale. One such attempt has been made by Masood and Takeuchi (2012) for creating a flood risk map for part of Dhaka City in Bangladesh where the SRTM data was resampled into 30 m resolution. The areas which experienced significant landfilling since the time of the SRTM mission were identified, and the corresponding grid cells were raised to match the current topography. The nature of the reach scale studies performed with no access to LiDAR DEMs or other comparable sources in developing countries such as Bangladesh (Masood & Takeuchi, 2012), Iran (Sarhadi et al., 2012) or Thailand (Keokhumcheng et al., 2012) was probabilistic. The flood events considered were only designed events with a high return period, not the actual ones, and the modelled flood extents were compared with the observed flood extent of a typically large event rather than the actual satellite overpass.

A more rigorous validation of the results in the reach scale derived from freely available DEMs is necessary. It is evident that the SRTM or ASTER DEMs in their available form are not suitable for modelling widespread floodplain flow at reach scale. Even for applications in regional scale such as Patro et al. (2009) or Pramanik et al. (2010), the SRTM DEM was modified with reference ground control points before employing in 1-D hydraulic models. For undertaking hydraulic modelling at the reach scale without access to very high-resolution terrain data, some researchers



have tried to combine elevation information from a variety of sources to increase the detail of channel and floodplain representation. For example, Tate et al. (2002) exported the ground surveyed XYZ data from HEC-RAS model into real-world coordinates and merged them with a relatively low-resolution DEM to get more detailed representation of the channel and embankments. The assumption of straight-line cross-sections is one of the limitations of this approach as the cross-sections are generally doglegged in shape. Shapiro and Nelson (2004) edited and merged terrain data from various sources and created a TIN with higher density of elevation points at or near the channel and less resolution further away. Sanyal et al. (2014a) created a suitable DEM by combining accurate elevation information from SRTM DEM, Cartosat-1 stereo imagery and DGPS-aided surveys of channel cross-sections for flood inundation modelling at reach scale.

#### **4 Choice of the Model and the Required Level of Complexity**

A number of benchmarking studies depending on the 1-D versus 2-D code (Horritt & Bates, 2001), scale of the model domain (Fewtrell et al., 2008), the nature of the numerical solution of 2-D hydrodynamic models (Horritt et al., 2007) and ways of setting up the parallel computing environment (Neal et al., 2010) were carried out in the past. One-dimensional hydrodynamic models are computationally efficient and can produce accurate water surface elevations without very high-resolution terrain data. However, high-resolution terrain data are required for modelling extensive floodplain inundation. Although 1-D models were found to perform equally well as the 2-D models in certain cases (Horritt & Bates, 2002; Alho & Aaltonen, 2008), generally 1-D models are less efficient in simulating the lateral diffusion of flood waves in the floodplain because of the discrete representation of the topography in the form of cross-sections (Hunter et al., 2008). It is also not technically sound for modelling backflow in floodplains (Merwade et al., 2008b). In addition, the roughness coefficients, which are required to account for the energy loss from a variety of sources, depend on the dimensionality of coding and level of process representation (Lane & Hardy, 2002). The roughness parameters estimated from field data are more likely to work well in physically consistent 2-D models than simpler models (Hunter et al., 2007).

Physically-based more complex finite element codes were also found to be less sensitive to the resolution of the terrain model and therefore are effective in containing the uncertainty in the model outcomes (Cook & Merwade, 2009). There is an element of non-stationarity of the friction parameter arising from the variation in the magnitude of the flood under consideration and physically-based fully 2-D models can keep the effect of this factor low (Horritt et al., 2007). Hunter et al. (2008) compared the performance of a number of diffusive and shallow water codes in an urban setting in Glasgow and noticed variations in the modelled depth

and flooded extent depending on the hydraulic process representations and types of numeric solvers in use. Process representation was not always found to influence the model outcome decisively. Sanyal et al. (2014a) compared the performance of a reduced complexity approach-based 1-D and 2-D-coupled LISFLOOD-FP model with a fully 2-D finite element TELEMAC2D in an anabranching river system. Results show that the latter was less sensitive to the limited accuracies of the terrain data and fared better than the former in handling the flow-splits in the channels.

Often the subtle modelling decision such as methods of downgrading the resolution of a DEM from 10 to 50 m can have more effect on model outputs than selecting models with different degree of complexity (Neal et al., 2012b). However, while working with low-gradient river systems using global DEMs, Jarihani et al. (2015) reported that the performance enhancement with finer DEM grid size was nonlinear and  $< 120$  m grid size did not provide additional benefit when the associated increase in the computational cost was taken into account.

The most important parameter after topography in influencing the flow in natural channels and overland inundation is the roughness of the terrain (Straatsma, 2009). Manning's roughness coefficient ( $n$ ) is the most common form of roughness parameter used in modelling hydrological studies. Although  $n$  is primarily used to account for the energy loss due to friction at the boundary of the flowing water and terrain surfaces, it is often used for compensating for the physical processes that are not considered by the governing equations of a hydrological/hydraulic model (Morvan et al., 2008). Various studies have used measured flow velocity, depth and cross-sectional area to determine bottom friction with numerical modelling (Stephen & Gutknecht, 2002; Mailapalli et al., 2008; Aricò et al., 2009). In most of these studies, terrain was used as inputs, measured flow data as boundary conditions, and the value of  $n$  was calibrated to achieve a best-fit to measure water surface data.

The extent to which a hydrodynamic model is sensitive to roughness and geometry uncertainty partially depends on the dimensionality of the model structure as this factor represents the geometry in different manners (Lane et al., 1999). However, Lane (2005) argued that roughness is strictly a component of topography, and better parameterisation of topography would ultimately reduce the sensitivity of hydrodynamic models to  $n$  values. This view has been further put forward by Medeiros et al. (2012) who concluded that parameterising floodplain roughness on the basis of the detailed terrain configurations and the presence of obstruction would be more effective than relying on remotely sensed LULC information for inundation modelling. We often change the description of roughness with changes in scales to compensate the effect of topography on processes influencing interaction between the surface and the terrain, hence implicitly recognising that roughness is scale dependant (Lane, 2005). The published sources for recommended values of  $n$  were commonly derived from plot scale experimental set-ups or small controlled experimental catchments, which makes it unreliable to use in numerical modelling involving large rivers.

## 5 Treatment of Uncertainties

A systematic estimation of the predictive uncertainty in a hydrodynamic modelling experiment is an essential component of any flood prediction mechanism. Uncertainty analysis in inundation modelling and flood risk analysis is important because it improves the evaluation of risk by identifying the sources of variation in model predictions, and even can influence decision-making on flood mitigation (Merz et al., 2008). It can also result in serious error in hazard assessment (Di Baldassarre et al., 2010). Merz et al. (2008) further pointed out that if the uncertainty component of a particular prediction is found to be too large for a reasonable decision-making process, it may highlight the necessity of further research to understand the physical process of inundation in that study area. Uncertainty assessment is more essential in the context of data-sparse situations in order to know the level of confidence we can attach to a particular prediction that was derived from model inputs of coarse quality and approximate measurements. The proportion of area in a model domain affected by the uncertain flood prediction increases with increasing uncertainties in the model inputs and choice of techniques and vice versa (Merwade et al., 2008b). Particular forms of channel configuration in a flood-prone reach, such as an anabranching pattern, sometimes require special attention for uncertainty assessment (Sanyal et al., 2014b). An uncertainty assessment is important in order to know the extent to which the modelled flood extents are affected by (1) each of the uncertain inputs and modelling considerations, (2) the spatial dimension of the effect of changes in each of the uncertain variables and (3) the nature of propagation of each uncertain variable in the inundation process and its effect over the combined state of uncertainty of a prediction (Jung & Merwade, 2012).

The generalised uncertainty likelihood estimation (GLUE) (Beven & Binley, 1992) methodology has been widely used in inundation modelling by using time series of river stages from gauging sites (Hunter et al., 2005) as well as distributed observed inundation patterns derived from satellite images (Horritt & Bates, 2001) and aerial photographs (Romanowicz & Beven, 2003). Uncertainty in the topographic data, especially a continuous surface interpolated from spot heights and contours, can have significant impact over hydraulic variables such as velocity and depth of inundation in small scale (Wilson & Atkinson, 2005a, b). The inundation boundaries depicted in flood hazard maps have inherent uncertainties related to the grid size of DEMs and the steepness of the gradient of the land perpendicular to the streamflow direction (Brandt, 2016). Channel cross-sections are sometimes difficult to measure in some locations (Sefe, 1996); sometimes they are not stationary (Callede et al., 2000) and particularly prone to modification after major floods.

Uncertainty in the measurements of observed data such as time series of stage/discharge records or flood-extent maps derived from airborne or spaceborne platforms may affect the computation of predictive uncertainty. Such error may also add a significant amount of uncertainty in estimating design flood events (Di Baldassarre et al., 2012). As the reference vertical datum for the river gauges are often based on local datum and not related to a global geoid model, it is difficult to make a direct

comparison between simulated river stages and an observed one (Hall et al., 2011, 2012). For data-sparse regions, we commonly use freely available global DEMs such as SRTM or ASTER GDEM that are generated from global geoid models such as EGM96. Survey authorities in developing countries featuring large flood-prone deltaic tracts generally do not follow a geoid model for preparing large-scale topographic maps and geodetic control networks. For example, in India, no geoid model is used for determining the vertical datum, and there is no straightforward way of converting the local mean sea-level information into an established geoid (Agrawal, 2005). This factor introduces uncertainty in the observed river-stage information when global DEMs and surveyed data collected through differential GPS is used in models to predict water-surface elevations.

## 6 Conclusion

The overall message from this discussion is that when the general goal is to predict the dynamics of riverine floods in the deltaic flatlands with limited data, particular attention should be paid to the choice of the model in relation to the available data and hydraulic characteristics of the event. Adaptations are necessary to create inputs for the models that have been primarily designed for areas with better availability of data. Freely available geospatial information of moderate resolution can often meet the minimum data requirements of hydrological and hydrodynamic models if they are supplemented carefully with limited surveyed/measured information. The amount of uncertainty in these types of prediction setups for extreme streamflow events was not found so great that it would discourage scientific community from using them under severe data constraint. The need of the hour is to develop highly skilled human resource for tackling this challenge. It is also crucial for the governments of respective countries to take an initiative towards establishing a hydrologic monitoring infrastructure and a framework of surveying channel bathymetry of the major flood-prone rivers.

## References

- Adhikari, P., Hong, Y., Douglas, K. R., Kirschbaum, D. B., Gourley, J., Adler, R., & Brakenridge, G. R. (2010). A digitized global flood inventory (1998–2008): Compilation and preliminary results. *Natural Hazards*, 55(2), 405–422.
- Agrawal, N. K. (2005). Geodetic infrastructure in India. *Coordinates*, 1(7). <http://mycoordinates.org/geodetic-infrastructure-in-india/>. Accessed online on 30 Sept 2021.
- Alho, P., & Aaltonen, J. (2008). Comparing a 1D hydraulic model with a 2D hydraulic model for the simulation of extreme glacial outburst floods. *Hydrological Processes: An International Journal*, 22(10), 1537–1547.
- Allenby, B., & Fink, J. (2005). Toward inherently secure and resilient societies. *Science*, 309(5737), 1034–1036.

- Aricò, C., Nasello, C., & Tucciarelli, T. (2009). Using unsteady-state water level data to estimate channel roughness and discharge hydrograph. *Advances in Water Resources*, 32(8), 1223–1240.
- Bates, P. D., Wilson, M. D., Horritt, M. S., Mason, D. C., Holden, N., & Currie, A. (2006). Reach scale floodplain inundation dynamics observed using airborne synthetic aperture radar imagery: Data analysis and modelling. *Journal of Hydrology*, 328(1–2), 306–318.
- Bates, P. D. (2012). Integrating remote sensing data with flood inundation models: how far have we got? *Hydrological Processes*, 26, 2515–2521.
- Beven, K., & Binley, A. (1992). The future of distributed models: Model calibration and uncertainty prediction. *Hydrological Processes*, 6(3), 279–298.
- Bhang, K. J., Schwartz, F. W., & Braun, A. (2006). Verification of the vertical error in C-band SRTM DEM using ICESat and Landsat-7, Otter Tail County, MN. *IEEE Transactions on Geoscience and Remote Sensing*, 45(1), 36–44.
- Biancamaria, S., Bates, P. D., Boone, A., & Mognard, N. M. (2009). Large-scale coupled hydrologic and hydraulic modelling of the Ob river in Siberia. *Journal of Hydrology*, 379(1–2), 136–150.
- Brandt, S. A. (2016). Modeling and visualizing uncertainties of flood boundary delineation: Algorithm for slope and DEM resolution dependencies of 1D hydraulic models. *Stochastic Environmental Research and Risk Assessment*, 30(6), 1677–1690.
- Casas, A., Benito, G., Thorndycraft, V., & Rico, M. (2006). The topographic data source of digital terrain models as a key element in the accuracy of hydraulic flood modelling. *Earth Surface Processes and Landforms*, 31, 444–456.
- Callede, J., Kosuth, P., LOUP, J. L., & Guimarães, V. S. (2000). Discharge determination by Acoustic Doppler Current Profilers (ADCP): A moving bottom error correction method and its application on the River Amazon at Obidos. *Hydrological Sciences Journal*, 45(6), 911–924.
- Cook, A., & Merwade, V. (2009). Effect of topographic data, geometric configuration and modeling approach on flood inundation mapping. *Journal of Hydrology*, 377(1–2), 131–142.
- Da Paz, A. R. D., Collischonn, W., Tucci, C. E., & Padovani, C. R. (2011). Large-scale modelling of channel flow and floodplain inundation dynamics and its application to the Pantanal (Brazil). *Hydrological Processes*, 25(9), 1498–1516.
- Deb, M., & Ferreira, C. M. (2018). Simulation of cyclone-induced storm surges in the low-lying delta of Bangladesh using coupled hydrodynamic and wave model (SWAN+ ADCIRC). *Journal of Flood Risk Management*, 11, S750–S765.
- Di Baldassarre, G., Schumann, G., Bates, P. D., Freer, J. E., & Beven, K. J. (2010). Flood-plain mapping: A critical discussion of deterministic and probabilistic approaches. *Hydrological Sciences Journal—Journal des Sciences Hydrologiques*, 55(3), 364–376.
- Di Baldassarre, G., Laio, F., & Montanari, A. (2012). Effect of observation errors on the uncertainty of design floods. *Physics and Chemistry of the Earth*, 42–44, 85–90.
- Domeneghetti, A. (2016). On the use of SRTM and altimetry data for flood modeling in data-sparse regions. *Water Resources Research*, 52(4), 2901–2918.
- Fewtrell, T. J., Bates, P. D., Horritt, M., & Hunter, N. M. (2008). Evaluating the effect of scale in flood inundation modelling in urban environments. *Hydrological Processes: An International Journal*, 22(26), 5107–5118.
- French, J. R., & Clifford, N. J. (2000). Hydrodynamic modelling as a basis for explaining estuarine environmental dynamics: Some computational and methodological issues. *Hydrological Processes*, 14(11–12), 2089–2108.
- Hall, A. C., Schumann, G. J. P., Bamber, J. L., & Bates, P. D. (2011). Tracking water level changes of the Amazon Basin with space-borne remote sensing and integration with large scale hydrodynamic modelling: A review. *Physics and Chemistry of the Earth, Parts A/B/C*, 36(7–8), 223–231.
- Hall, A. C., Schumann, G. J.-P., Bamber, J. L., Bates, P. D., & Trigg, M. A. (2012). Geodetic corrections to Amazon River water level gauges using ICESat altimetry. *Water Resources Research*, 48(6), W06602. <https://doi.org/10.1029/2011WR010895>

- Horritt, M. S., & Bates, P. D. (2001). Predicting floodplain inundation: Raster-based modelling versus the finite-element approach. *Hydrological Processes*, 15(5), 825–842.
- Horritt, M. S., & Bates, P. D. (2002). Evaluation of 1D and 2D numerical models for predicting river flood inundation. *Journal of Hydrology*, 268(1–4), 87–99.
- Horritt, M. S., Di Baldassarre, G., Bates, P. D., & Brath, A. (2007). Comparing the performance of a 2-D finite element and a 2-D finite volume model of floodplain inundation using airborne SAR imagery. *Hydrological Processes: An International Journal*, 21(20), 2745–2759.
- Hunter, N. M., Bates, P. D., Horritt, M. S., De Roo, A. P. J., & Werner, M. G. (2005). Utility of different data types for calibrating flood inundation models within a GLUE framework. *Hydrology and Earth System Sciences*, 9(4), 412–430.
- Hunter, N. M., Bates, P. D., Horritt, M. S., & Wilson, M. D. (2007). Simple spatially-distributed models for predicting flood inundation: A review. *Geomorphology*, 90(3–4), 208–225.
- Hunter, N. M., Bates, P. D., Neelz, S., Pender, G., Villanueva, I., Wright, N. G., et al. (2008, February). Benchmarking 2D hydraulic models for urban flooding. In *Proceedings of the Institution of Civil Engineers-Water Management* (Vol. 161, No. 1, pp. 13–30). Thomas Telford Ltd.
- Islam, M. F., Bhattacharya, B., & Popescu, I. (2019). Flood risk assessment due to cyclone-induced dike breaching in coastal areas of Bangladesh. *Natural Hazards and Earth System Sciences*, 19(2), 353–368.
- Jarihani, A. A., Callow, J. N., McVicar, T. R., Van Niel, T. G., & Larsen, J. R. (2015). Satellite-derived Digital Elevation Model (DEM) selection, preparation and correction for hydrodynamic modelling in large, low-gradient and data-sparse catchments. *Journal of Hydrology*, 524, 489–506.
- Jena, P. P., Panigrahi, B., & Chatterjee, C. (2016). Assessment of Cartosat-1 DEM for modeling floods in data scarce regions. *Water Resources Management*, 30(3), 1293–1309.
- Jonkman, S. N. (2005). Global perspectives on loss of human life caused by floods. *Natural Hazards*, 34(2), 151–175.
- Jung, Y., & Merwade, V. (2012). Uncertainty quantification in flood inundation mapping using generalized likelihood uncertainty estimate and sensitivity analysis. *Journal of Hydrologic Engineering*, 17(4), 507–520.
- Jung, H. C., Hamski, J., Durand, M., Alsdorf, D., Hossain, F., Lee, H., et al. (2010). Characterization of complex fluvial systems using remote sensing of spatial and temporal water level variations in the Amazon, Congo, and Brahmaputra Rivers. *Earth Surface Processes and Landforms: The Journal of the British Geomorphological Research Group*, 35(3), 294–304.
- Keokhumcheng, Y., Tingsanchali, T., & Clemente, R. S. (2012). Flood risk assessment in the region surrounding the Bangkok Suvarnabhumi Airport. *Water International*, 37(3), 201–217.
- Kumar, A., Dasgupta, A., Lokhande, S., & Ramsankaran, R. A. A. J. (2019). Benchmarking the Indian National CartoDEM against SRTM for 1D hydraulic modelling. *International Journal of River Basin Management*, 17(4), 479–488.
- Lane, S. N. (2005). Roughness-time for a re-evaluation? *Earth Surface Processes and Landforms*, 30(2), 251–253.
- Lane, S. N., & Hardy, R. J. (2002). Porous rivers: A new way of conceptualising and modelling river and floodplain flows?. In *Transport phenomena in porous media II* (pp. 425–449). Pergamon.
- Lane, S. N., Bradbrook, K. F., Richards, K. S., Biron, P. A., & Roy, A. G. (1999). The application of computational fluid dynamics to natural river channels: Three-dimensional versus two-dimensional approaches. *Geomorphology*, 29(1–2), 1–20.
- Legleiter, C. J., & Kyriakidis, P. C. (2008). Spatial prediction of river channel topography by kriging. *Earth Surface Processes and Landforms: The Journal of the British Geomorphological Research Group*, 33(6), 841–867.
- Mailapalli, D. R., Raghuwanshi, N. S., Singh, R., Schmitz, G. H., & Lennartz, F. (2008). Spatial and temporal variation of Manning's roughness coefficient in furrow irrigation. *Journal of Irrigation and Drainage Engineering*, 134(2), 185–192.

- Manfreda, S., Di Leo, M., & Sole, A. (2011). Detection of flood-prone areas using digital elevation models. *Journal of Hydrologic Engineering*, 16(10), 781–790.
- Mason, D. C., Speck, R., Devereux, B., Schumann, G. J. P., Neal, J. C., & Bates, P. D. (2009). Flood detection in urban areas using TerraSAR-X. *IEEE Transactions on Geoscience and Remote Sensing*, 48(2), 882–894.
- Masood, M., & Takeuchi, K. (2012). Assessment of flood hazard, vulnerability and risk of mid-eastern Dhaka using DEM and 1D hydrodynamic model. *Natural Hazards*, 61(2), 757–770.
- Medeiros, S. C., Hagen, S. C., & Weishampel, J. F. (2012). Comparison of floodplain surface roughness parameters derived from land cover data and field measurements. *Journal of Hydrology*, 452, 139–149.
- Merwade, V. (2009). Effect of spatial trends on interpolation of river bathymetry. *Journal of Hydrology*, 371(1–4), 169–181.
- Merwade, V. M., Maidment, D. R., & Goff, J. A. (2006). Anisotropic considerations while interpolating river channel bathymetry. *Journal of Hydrology*, 331(3–4), 731–741.
- Merwade, V., Cook, A., & Coonrod, J. (2008a). GIS techniques for creating river terrain models for hydrodynamic modeling and flood inundation mapping. *Environmental Modelling & Software*, 23(10–11), 1300–1311.
- Merwade, V., Olivera, F., Arabi, M., & Edleman, S. (2008b). Uncertainty in flood inundation mapping: Current issues and future directions. *Journal of Hydrologic Engineering*, 13(7), 608–620.
- Merz, B., Kreibich, H., & Apel, H. (2008). Flood risk analysis: Uncertainties and validation. *Österreichische Wasser-und Abfallwirtschaft*, 60(5), 89–94.
- Mohanty, M. P., Nithya, S., Nair, A. S., Indu, J., Ghosh, S., Bhatt, C. M., et al. (2020). Sensitivity of various topographic data in flood management: Implications on inundation mapping over large data-scarce regions. *Journal of Hydrology*, 590, 125523.
- Morvan, H., Knight, D., Wright, N., Tang, X., & Crossley, A. (2008). The concept of roughness in fluvial hydraulics and its formulation in 1D, 2D and 3D numerical simulation models. *Journal of Hydraulic Research*, 46(2), 191–208.
- Muralikrishnan, S., Pillai, A., Narendar, B., Reddy, S., Venkataraman, V. R., & Dadhwal, V. K. (2013). Validation of Indian national DEM from Cartosat-1 data. *Journal of the Indian Society of Remote Sensing*, 41(1), 1–13.
- Neal, J. C., Fewtrell, T. J., Bates, P. D., & Wright, N. G. (2010). A comparison of three parallelisation methods for 2D flood inundation models. *Environmental Modelling & Software*, 25(4), 398–411.
- Neal, J., Schumann, G., & Bates, P. (2012a). A subgrid channel model for simulating river hydraulics and floodplain inundation over large and data sparse areas. *Water Resources Research*, 48(11), W11506. <https://doi.org/10.1029/2012WR012514>
- Neal, J., Villanueva, I., Wright, N., Willis, T., Fewtrell, T., & Bates, P. (2012b). How much physical complexity is needed to model flood inundation? *Hydrological Processes*, 26(15), 2264–2282.
- O’Loughlin, F. E., Paiva, R. C., Durand, M., Alsdorf, D. E., & Bates, P. D. (2016). A multi-sensor approach towards a global vegetation corrected SRTM DEM product. *Remote Sensing of Environment*, 182, 49–59.
- Paiva, R. C., Collischonn, W., & Tucci, C. E. (2011). Large scale hydrologic and hydrodynamic modeling using limited data and a GIS based approach. *Journal of Hydrology*, 406(3–4), 170–181.
- Pappenberger, F., Beven, K., Horritt, M., & Blazkova, S. (2005). Uncertainty in the calibration of effective roughness parameters in HEC-RAS using inundation and downstream level observations. *Journal of Hydrology*, 302(1–4), 46–69.
- Patro, S., Chatterjee, C., Singh, R., & Raghuvanshi, N. S. (2009). Hydrodynamic modelling of a large flood-prone river system in India with limited data. *Hydrological Processes: An International Journal*, 23(19), 2774–2791.

- Petersen, G., & Fohrer, N. (2010). Two-dimensional numerical assessment of the hydrodynamics of the Nile swamps in southern Sudan. *Hydrological Sciences Journal–Journal des Sciences Hydrologiques*, 55(1), 17–26.
- Pramanik, N., Panda, R. K., & Sen, D. (2010). One dimensional hydrodynamic modeling of river flow using DEM extracted river cross-sections. *Water Resources Management*, 24(5), 835–852.
- Rahman, S., Islam, A. S., Saha, P., Tazkia, A. R., Krien, Y., Durand, F., et al. (2019). Projected changes of inundation of cyclonic storms in the Ganges–Brahmaputra–Meghna delta of Bangladesh due to SLR by 2100. *Journal of Earth System Science*, 128(6), 1–11.
- Rawat, K. S., Mishra, A. K., Sehgal, V. K., Ahmed, N., & Tripathi, V. K. (2013). Comparative evaluation of horizontal accuracy of elevations of selected ground control points from ASTER and SRTM DEM with respect to CARTOSAT-1 DEM: A case study of Shahjahanpur district, Uttar Pradesh, India. *Geocarto International*, 28(5), 439–452.
- Reuter, H. I., Neison, A., Strobl, P., Mehl, W., & Jarvis, A. (2009). A first assessment of ASTER GDEM tiles for absolute accuracy, relative accuracy and terrain parameters. In *2009 IEEE international geoscience and remote sensing symposium* (Vol. 5, pp. V-240). IEEE.
- Rodriguez, E., Morris, C. S., & Belz, J. E. (2006). A global assessment of the SRTM performance. *Photogrammetric Engineering & Remote Sensing*, 72(3), 249–260.
- Romanowicz, R., & Beven, K. (2003). Estimation of flood inundation probabilities as conditioned on event inundation maps. *Water Resources Research*, 39(3), 1073. <https://doi.org/10.1029/2001WR001056>
- Sampson, C. C., Fewtrell, T. J., Duncan, A., Shaad, K., Horritt, M. S., & Bates, P. D. (2012). Use of terrestrial laser scanning data to drive decimetric resolution urban inundation models. *Advances in Water Resources*, 41, 1–17.
- Sanders, B. F. (2007). Evaluation of on-line DEMs for flood inundation modeling. *Advances in Water Resources*, 30(8), 1831–1843.
- Sanyal, J., & Lu, X. X. (2004). Application of remote sensing in flood management with special reference to monsoon Asia: A review. *Natural Hazards*, 33(2), 283–301.
- Sanyal, J., Carbonneau, P., & Densmore, A. L. (2013). Hydraulic routing of extreme floods in a large ungauged river and the estimation of associated uncertainties: A case study of the Damodar River, India. *Natural Hazards*, 66(2), 1153–1177.
- Sanyal, J., Carbonneau, P., & Densmore, A. L. (2014a). Low-cost inundation modelling at the reach scale with sparse data in the Lower Damodar River basin, India. *Hydrological Sciences Journal*, 59(12), 2086–2102.
- Sanyal, J., Densmore, A. L., & Carbonneau, P. (2014b). 2D finite element inundation modelling in anabranching channels with sparse data: Examination of uncertainties. *Water Resources Management*, 28(8), 2351–2366.
- Sarhadi, A., Soltani, S., & Modarres, R. (2012). Probabilistic flood inundation mapping of ungauged rivers: Linking GIS techniques and frequency analysis. *Journal of Hydrology*, 458, 68–86.
- Schumann, G. J., & Bates, P. D. (2018). The need for a high-accuracy, open-access global DEM. *Frontiers in Earth Science*, 6, 225.
- Schumann, G. P., Neal, J. C., Voisin, N., Andreadis, K. M., Pappenberger, F., Phanthuwongpakdee, N., et al. (2013). A first large-scale flood inundation forecasting model. *Water Resources Research*, 49(10), 6248–6257.
- Sefe, F. T. K. (1996). A study of the stage-discharge relationship of the Okavaiigo River at Mohembo, Botswana. *Hydrological Sciences Journal*, 41(1), 97–116.
- Shapiro, M. G., & Nelson, E. J. (2004). Digital terrain model processing for integrated hydraulic analysis and floodplain mapping. In *Critical Transitions in Water and Environmental Resources Management* (pp. 1–9). ASCE Press.
- Slater, J. A., Garvey, G., Johnston, C., Haase, J., Heady, B., Kroenung, G., & Little, J. (2006). The SRTM data “finishing” process and products. *Photogrammetric Engineering & Remote Sensing*, 72(3), 237–247.
- Smith, K., & Ward, R. (1998). *Floods: Physical Processes and Human Impacts*. Wiley, New York.




- Smith, K. (2001). *Environmental hazards: Assessing risk and reducing disaster*. Routledge.
- Stephan, U., & Gutknecht, D. (2002). Hydraulic resistance of submerged flexible vegetation. *Journal of Hydrology*, 269(1), 27–43.
- Straatsma, M. (2009). 3D float tracking: In situ floodplain roughness estimation. *Hydrological Processes: An International Journal*, 23(2), 201–212.
- Tarekegn, T. H., Haile, A. T., Rientjes, T., Reggiani, P., & Alkema, D. (2010). Assessment of an ASTER-generated DEM for 2D hydrodynamic flood modeling. *International Journal of Applied Earth Observation and Geoinformation*, 12(6), 457–465.
- Tate, E. C., Maidment, D. R., Olivera, F., & Anderson, D. J. (2002). Creating a terrain model for floodplain mapping. *Journal of Hydrologic Engineering*, 7(2), 100–108.
- Wilson, M. D., & Atkinson, P. M. (2005a). The use of elevation data in flood inundation modelling: A comparison of ERS interferometric SAR and combined contour and differential GPS data. *International Journal of River Basin Management*, 3(1), 3–20.
- Wilson, M. D., & Atkinson, P. M. (2005b). Prediction uncertainty in elevation and its effect on flood inundation modelling. In P. M. Atkinson, G. M. Foody, S. Darby, & F. Wu (Eds.), *GeoDynamics* (pp. 185–202). Wiley.
- Yamazaki, D., Kanae, S., Kim, H., & Oki, T. (2011). A physically based description of floodplain inundation dynamics in a global river routing model. *Water Resources Research*, 47(4), W04501. <https://doi.org/10.1029/2010WR009726>
- Yamazaki, D., Lee, H., Alsdorf, D. E., Dutra, E., Kim, H., Kanae, S., & Oki, T. (2012a). Analysis of the water level dynamics simulated by a global river model: A case study in the Amazon River. *Water Resources Research*, 48(9), W09508. <https://doi.org/10.1029/2012WR011869>
- Yamazaki, D., Baugh, C. A., Bates, P. D., Kanae, S., Alsdorf, D. E., & Oki, T. (2012b). Adjustment of a spaceborne DEM for use in floodplain hydrodynamic modeling. *Journal of Hydrology*, 436, 81–91.
- Yamazaki, D., Ikeshima, D., Tawatari, R., Yamaguchi, T., O’Loughlin, F., Neal, J. C., et al. (2017). A high-accuracy map of global terrain elevations. *Geophysical Research Letters*, 44(11), 5844–5853.
- Yamazaki, D., Ikeshima, D., Sosa, J., Bates, P. D., Allen, G. H., & Pavelsky, T. M. (2019). MERIT Hydro: A high-resolution global hydrography map based on latest topography dataset. *Water Resources Research*, 55(6), 5053–5073.
- Yan, K., Di Baldassarre, G., Solomatine, D. P., & Schumann, G. J. P. (2015). A review of low-cost space-borne data for flood modelling: Topography, flood extent and water level. *Hydrological Processes*, 29(15), 3368–3387.
- Zahera, S. S., Di Baldassarre, G., & Balekelay, C. N. (2011). Modelling seasonally flooded wetlands in the semi-arid Sahelian Zone. *Nile Basin Water Science and Engineering Journal*, 4(2), 83–93.

## Chapter 3

# Nature of Flood and Channel Sedimentation in the Torsa River: A Hydro-Geomorphic Study



Ujwal Deep Saha , Md Juber Alam, Soma Bhattacharya, and Arijit Majumder

**Abstract** This scientific venture to understand the nature and impact of channel hydrological fluctuations on channel sedimentation of the Torsa River has utilised daily discharge, water level and periodic channel cross-sections provided by the Central Water Commission of Govt. of India. The flood-frequency analysis and prediction of extreme flood discharge of the Torsa River was conducted using the Gumbel's extreme value, log-Pearson's III and log-normal method. Higher flood volume and greater flashiness of flood discharge with lower channel water residence time is evident on the piedmont surface compared with the northern plains in the Torsa River catchment located on the Himalayan foothills of West Bengal, India. The Peak Over Threshold (PoT) or the vulnerable river discharge at Hasimara is measured  $2856 \text{ m}^3 \text{ s}^{-1}$ , and at Ghughumari, it is  $2954 \text{ m}^3 \text{ s}^{-1}$ . The mean flash flood magnitude between 1990 and 2015 was found 1.60 and 1.38 at Hasimara (representative of Piedmont surface) and Ghughumari (representative of the Northern plains), respectively. The higher accumulation of sediment during any flood period is evident throughout the course, but the intensity of channel aggradation decreases downstream as the piedmont surface acts as the depo-centre of channel deposits brought down from the Himalayan terrain. The correlation coefficient between the channel bar width and ratio of peak discharge and long-term mean peak discharge was found 0.45 and 0.34 at Reach I (roughly covering the Piedmont) and Reach II (covering the Northern plains), respectively. The sensitiveness of channel bed modification to annual flood discharges is found higher at Hasimara in comparison with Ghughumari. The correlation coefficient between channel Bed Roughness Index and ratio of peak discharge and long-term mean peak discharge was measured 0.54 and 0.46 at Hasimara and Ghughumari, respectively. Even the temporal difference in channel mean elevation during the pre-monsoon and post-monsoon period and

---

U. D. Saha (✉) · S. Bhattacharya

Post Graduate Department of Geography, Vivekananda College for Women, Kolkata, West Bengal, India

M. J. Alam · A. Majumder

Department of Geography, Jadavpur University, Kolkata, West Bengal, India

corresponding annual peak discharge was measured at 0.80 and 0.46 at Hasimara and Ghughumari, respectively. This study carries a concerned level of significance to regional planners and institutes responsible for flood forecasting and framing flood protection measures.

**Keywords** Flood · Flood-frequency analysis (FFA) · Channel aggradation · Himalayan foothill channel · Bed elevation

## 1 Introduction

Rivers flowing through the Himalayan terrain bring huge debris, and the associated frontal plains are the major depo-centre of it (Saha & Bhattacharya, 2019). Rivers in the Himalayan frontal basin (HFB) have higher sediment yield compared with the global average (Gupta, 2008). The in-channel sedimentation aggravates the perilous impact of the riverine hazards, i.e., flood and avulsion. The change in the rainfall gradient in the eastern Himalayas brings heavy rainfall and often its torrential character results in flood havoc. The perennial rivers flowing through the Bhutan and Darjeeling Himalayas are highly responsive to rainfall effects where rainfall-discharge correlation is highly positive (Soja & Sarkar, 2008). The geomorphology and surface forms of the Himalayan foothill regions often contribute to the hazardous effects of floods both on the socio-economic domain and in floodplain geomorphology (Sinha, 2009). Thus, as a “soft” domain of flood management, measuring the flood frequency and flood simulation is required for the Himalayan foothill rivers at least for the gauged ones. Apart from this, since the flood flows are responsible for bringing down heavy sediment load, understanding the direct impact of hydrological components on channel sedimentation becomes essential as it helps in gauging the future trajectory of channel evolution. For measuring the flood frequency, peak discharge of at least 30 years without any break is desired (Islam & Sarkar, 2020), but for data-sparse environment like the Indian foothills, specifically for the transboundary rivers, it often becomes a huge challenge to get peak discharge for such a considerable span. It has been a huge challenge in computing flood forecasting and flood simulation in this part of the world.

Globally, several techniques have been used to simulate the magnitude of a flood, viz., Gumbel, normal, log-Pearson type III and log-normal. However, several authors have commonly used the log-Pearson type III method to estimate and study flood extremities in Indian rivers (Lakshmi Kumar et al., 2014; Ghosh, 2013; Bandyopadhyay et al., 2016; Islam & Sarkar, 2020). In a couple of studies conducted on the HFB, Bhat et al. (2019) and Kumar (2019) found better suitability of the log-Pearson type III method compared with Gumbel’s extreme value 1. Studies have also been done on the Himalayan foothills part of West Bengal where complex structural attributes, geomorphic complexities and anthropogenic structures are responsible for the flood havoc (Kormokar & De, 2020). The flashiness like channel

flood is of high concern in the Himalayan foothills part of West Bengal as the rivers carry a huge amount of debris downstream (Ghosh & Ghosal, 2021). It often plugs channel flow and helps in developing alluvial ridges within the channel beds (Starkel et al., 2008; Kormokar & De, 2020; Saha & Bhattacharya, 2021).

This study aims to study the nature of flood in the perennial Torsa River, which flows in the HFB region of the eastern Himalayas, i.e., the foothills region in West Bengal. Alongside, the direct impact of the flood and annual hydrological fluctuations on channel sedimentation of the Torsa River is also a major thrust of this study. This is the pioneer attempt on the Torsa River to understand its flood extremities and its impact on channel morphological alterations.

## 2 Study Area

The study is concentrated on a selected stretch of river Torsa, approximately 98 km that comes under the Indian Territory within its entire flow path of 295 km. Torsa River emerges at Chumbi valley in Tibet and flows through Bhutan and India up to its mouth near Nageshwari in Bangladesh. The northern limit of the concerned stretch of the Torsa in this study is Jaigaon ( $26^{\circ}51'54.88''\text{N}$  and  $89^{\circ}22'16.67''\text{E}$ ) in the Alipurduar District of West Bengal, and the southernmost limit is Balabhut ( $26^{\circ}11'26.77''\text{N}$  and  $89^{\circ}42'13.88''\text{E}$ ) in Cooch Behar district of West Bengal (Fig. 3.1). A drop in surface gradient of 75 m/km from the mountainous catchment to 4.53 m/km immediately on the foredeep plain (Mukhopadhyay & Dasgupta, 2010) provides a favourable ground for the Torsa River to develop an elongated fan deposit perched between its course and that of the Kaljani River in the east. Broadly, on the eastern part of the Teesta River, three different physiographic zones are associated consecutively from north to south: the Bhabar, the Terai region and the low-lying northern plains (Das, 2012). Sediment sorting and decreasing diameter of the mean sediment compositions differentiate all these regions from one another (Das & Chattopadhyay, 1993). The bed material of the Torsa varies from gravel bed with occasional boulders to mixed sediment of gravel and sand and finally a mixture of sand and silt in these three physiographic regions, respectively, from north to south (Saha & Bhattacharya, 2016). The overall channel gradient changes from 2.70 m/km in the piedmont region to 0.30 m/km on the northern plain. This tropic humid part of the world receives an average rainfall of nearly 300–600 cm and the intensity decreases southward.

Daily discharge and gauge height of the Torsa River between 1990 and 2015, measured at Hasimara and Ghughumari by CWC (Fig. 3.1), are used in this work. The rainfall-discharge relation of the Torsa River is very much intense where the response is very certain rather than gradual. A sudden increase in discharge after a couple of days of rainfall is well associated with a rapid drop in the underline character of the Torsa River (Soja & Sarkar, 2008). The highest measured discharge of the Torsa River at Hasimara was 4067.4 cumec on 13.10.1973, and at

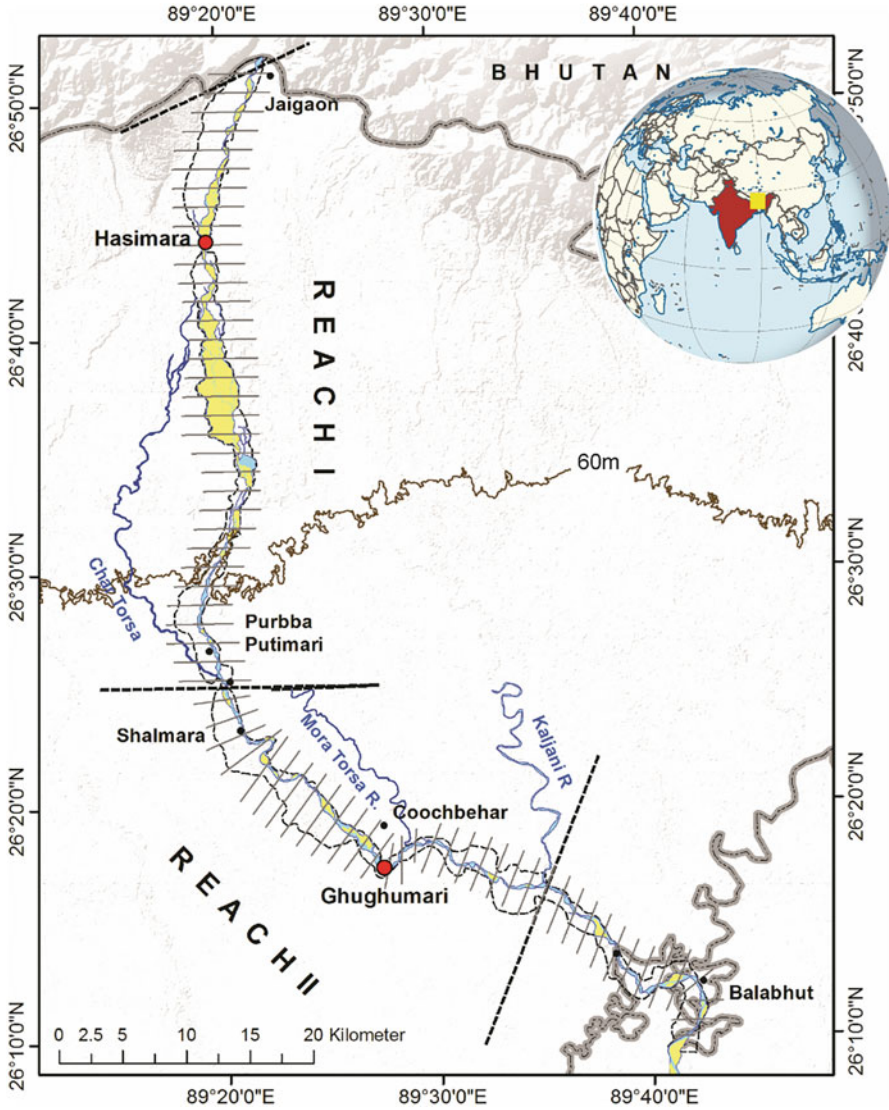


**Fig. 3.1** Location of the selected stretch of the Torsa River; the demarcated channel reaches are marked using black dashed lines and the cross-sections used in measuring channel bar width are in grey continuous lines

Ghughumari, it was 3375.2 cumec measured on 06.10.1968, whereas the highest gauge height measured at Hasimara was 119.10 m on 05.10.1968 and at Ghughumari it was 41.08 m measured on 06.10.1968 (Mukhopadhyay, 2014). The highest discharge observed at Hasimara and Ghughumari between 1990 and 2015 was 3800 m<sup>3</sup>/s and 3300 m<sup>3</sup>/s on 03.08.2000, respectively (Fig. 3.2).

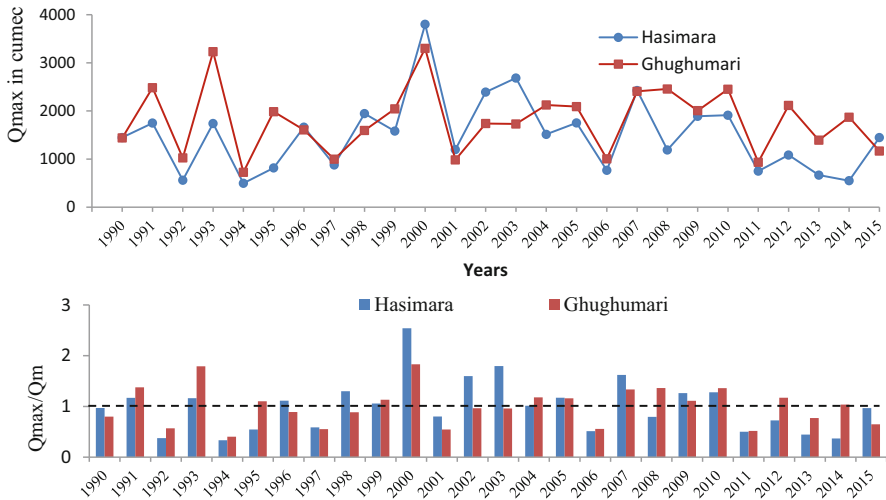


**Fig. 3.2** (Top) Temporal distribution of maximum discharge ( $Q_{max}$ ) of the Torsa River measured at Hasimara and Ghughumari. (Bottom) Distribution of  $Q_{max}/Q_m$  during 1990–2015 measured at Hasimara and Ghughumari. The black dashed line denotes the level of  $Q_m$  as 1

### 3 Methodology

#### 3.1 Data Used

Satellite datasets of multiple years acquired during the pre-monsoon period (February–April) have been used to measure the morphological parameters. Daily discharge, gauge height and river cross-sections measured by the CWC of the Torsa River at Hasimara and Ghughumari were provided by B&BB Organisation, Shilong, Govt. of India. The Landsat images were downloaded free of cost from <https://earthexplorer.usgs.gov/>, and the Resourcesat data was from <https://bhuvan.nrsc.gov.in/>. To avoid the error lines found in Landsat 7 (ETM+) data of 2013, LISS III data has been considered (Table 3.1).

#### 3.2 Channel Hydrological Components

Multiple temporal components of the river discharge measured at the two hydrological observation centres of CWC from 1989 to 2015 have been calculated for specific reasons. The ratio of peak discharge ( $Q_{max}$ ) and long-term average peak discharge ( $Q_m$ ) is calculated for measuring the relative strength of floods. Distributional variability of annual daily discharge ( $Q_d$ ) is measured to denote annual fluctuations of discharge that are likely to point out the relative weightage of flood volume, while the average monsoon discharges (June–September) denote the relative strength of

**Table 3.1** Satellite data inventory used in this study

Date of acquisition	Satellite and sensor	P/R	Resolution (m)
08.03.1987	Landsat 5; TM	138/42 and 138/41	30
06.03.1991	Landsat 5; TM	138/42 and 138/41	30
28.01.1995	Landsat 5; TM	138/42 and 138/41	30
18.02.1997	Landsat 5; TM	138/42	30
19.02.2000	Landsat 7; ETM+	138/42	30
24.02.2005	Landsat 5; TM	138/42 and 138/41	30
10.03.2008	Landsat 5; TM	138/42 and 138/41	30
06.02.2010	Landsat 5; TM	138/42 and 138/41	30
06.01.2013	Resourcesat1; LISS III	G45L05, G45L06, G45L07, G45L11, G45L12	24
08.03.2015	Landsat 8; OLI	138/42	30
09.02.2017	Landsat 8; OLI	138/42	30

**Table 3.2** Different discharge and water level components used in this study

Hydrological components (temporal)	Significance	Remarks
Annual maximum discharge ( $Q_{max}$ )	Modal property of the yearly discharge; the magnitude of flood	
Ratio of annual maximum discharge and long-term mean of annual maximum discharge ( $Q_{max}/Q_m$ )	Proxy to flood power	
Mean daily discharge ( $Q_d$ )	Mean properties of the flow regime	
Mean monsoon discharge ( $Q_{mon}$ )	Monsoonal strength of river flow (effective discharge)	Except for the monsoon period, streamflow remains very low throughout the year
Relative fluctuation in monsoon discharge ( $CV Q_{mon}$ )	Relative strength and fall of monsoon discharge	
Relative fluctuation in monsoon water level ( $CV W_{mon}$ )	Relative strength and fall of monsoon water level	
Mean monsoon discharge of previous year ( $Q_{mon\ prev}$ )	Last effective discharge	Since satellite images of the pre-monsoon period have been taken, discharge and water level of the previous year is the last effective flow for any concerned year
Mean monsoon water level of the previous year ( $W_{mon\ prev}$ )	Last effective water level	

the high flow period. Table 3.2 elaborates on different channel hydrological components (temporal) used in this study to showcase the direct hydrological impact on channel morphological characteristics.

### 3.2.1 Flood Frequency

Floods are extremely complicated natural processes that are the result of a variety of component characteristics, making them extremely challenging to predict analytically. The frequency and magnitude of floods can be determined using a variety of probability distribution function techniques (Raghunath, 2006). In this study, for calculating flood peaks of different return periods and probability of occurrence, Gumbel’s method, log-Pearson’s III and log-normal distribution functions have been used. Apart from that, multiple statistical analyses have been done to understand the nature of the distribution of flood discharges, both actual and measured. All these tests were performed using XLSTAT except the ADF test as it was prepared using Python (Table 3.3).

The annual maximum discharge data was first organized in a descending order, and then, the following equation (Eq. 3.1) was used to compute the probability ( $P$ ) of occurrence (percent):

$$P = \frac{m}{(N + 1)} \tag{3.1}$$

where  $m$  represents the order of the event and  $N$  represents the total number of events. The returns periods,  $T_r$  (Years), have been computed using Eq. 3.2 (Weibull, 1939):

$$T_r = \frac{1}{P} \tag{3.2}$$

**Table 3.3** Statistical tests performed

Statistical test	Significance	Used module and language
Probability density function	Distribution of the flood peaks	Distribution fitting
Homogeneity test	Whether data sets are from same location or not	Time series module
U test	Degree of similarity between the datasets	Non-parametric test module
Cochrane–Orcutt model	Autocorrelation of the dataset	Time series module
Augmented dickey–fuller test (ADF)	Data stationarity	Python
Shapiro–Wilk test	Normality test	Normality test
Anderson–Darling test	Normality test	Normality test



### Gumbel's Method

Gumbel's approach for predicting flood peak is one of the most extensively used probability distribution functions for extreme values in hydrology (Chow, 1964). This technique uses the following algorithm to determine the expected maximum discharge ( $X_T$ ) and the chance of exceeding ( $P$ ) for each return period ( $T$ ):

$$x_T = \bar{x} + K\sigma_{n-1} \quad (3.3)$$

where  $x_T$  stands for the maximum amount of expected discharge,  $\bar{x}$  for mean rainfall,  $\sigma_{n-1}$  for standard deviation and  $K$  stands for the frequency factor, which is determined using the formula below:

$$k = \frac{(y_T - \bar{y}_n)}{s_n} \quad (3.4)$$

where  $y_T$  represents reduced variate,  $\bar{y}_n$  represents mean of the reduced variate and  $s_n$  represents standard deviation of reduced variate. The following equation is used to determine the reduced variate:

$$y_T = - \left[ \ln \cdot \ln \frac{T}{T-1} \right] \quad (3.5)$$

To determine whether the observed discharge data fits the Gumbel distribution or not, the reduced variate is employed. The Gumbel distribution accurately reflects the data where the plot of the reduced variate and flood peak displays a linear trend (Gumbel, 1958).

### Log-Pearson Type III

This method entails a series of calculations that determine the maximum expected discharge ( $X_T$ ) for each return period ( $T$ ) and also the likelihood of exceeding that value ( $P$ ). In this technique, the discharge data is first converted into logarithmic form (base 10), and then, it is used for further analysis. The observed discharge value has been converted into logarithmic form by:

$$Z = \log(X) \quad (3.6)$$

where  $Z$  represents the logarithmic value of the observed discharge value ( $X$ ). Then, the mean ( $\bar{Z}$ ), standard deviation ( $\sigma_z$ ) and the skewness coefficient ( $C_s$ ) of the  $Z$  series have been estimated using the following equations:

$$k = \frac{(y_T - \bar{y}_n)}{s_n} \quad (3.7)$$

$$\sigma_z = \sqrt{\frac{\sum (z - \bar{z})^2}{N - 1}} \quad (3.8)$$

$$C_s = \frac{N \cdot \sum (z - \bar{z})^3}{(N - 1)(N - 2) \cdot (\sigma_z)_3} \quad (3.9)$$

The value of the frequency factor ( $K_z$ ) has been obtained from the computed  $C_s$  table value for a particular return period ( $T_r$ ), and  $Z_T$  is required to be computed using the following formula:

$$z_T = \bar{z} + k_z \cdot \sigma_z \quad (3.10)$$

where  $Z_T$  is the logarithmic discharge value,  $\bar{z}$  represent the mean of  $Z$ ,  $k_z$  represent frequency factors and  $\sigma_z$  is the standard deviation. Finally, the predicted discharge is determined using the following function to convert the log value ( $Z_T$ ) to a normal value:

$$X_T = \text{Antilog}(Z_T) \quad (3.11)$$

where  $X_T$  represents the maximum value of expected discharge ( $\text{m}^3/\text{s}$ ).

### Log Normal

Log-normal distribution is another important method to compute the discharge at particular return periods. This method of computation is virtually identical to that of the log-Pearson's type III distribution, except that the coefficient of skewness ( $C_s$ ) is assumed to be zero (0) during all the returns periods and the frequency factor depends on that.

### 3.2.2 Flash Flood Magnitude Index (FFMI)

Flash Flood Magnitude Index is regarded as the suddenness of flood discharge. Flash Flood Magnitude Index (FFMI) is calculated from the standard deviation of the logarithms of annual maximum discharge (Kochel, 1988; Ghosh & Guchhait, 2014). The equation is as follows:

$$\text{FFMI} = \chi^2 / (N - 1) \quad (3.12)$$

$X$  is  $X_m - M$ ,  $X_m$  is the log of annual maximum discharge,  $M$  is the log of mean annual discharge and  $N$  is the number of years in the selected interval. FFMI value, close to 1 or above, signifies the higher intensity of flashiness of flood discharge.

### 3.3 Channel Morphology Parameters

#### 3.3.1 Demarcation of Channel Reach

The compartmentalisation of any river course while studying its fluvial dynamics requires a fluvial or physiographic base. Following the works of Leopold and Wolman (1960) and Dallaire et al. (2019), the discharge was considered the standard criteria for dividing the studied stretch of the Torsa River into three separate segments. The delineation of the segments has been based on the change of discharge, which is manifested by considering the basic assumption of ‘at a station’ hydraulics that if any tributary joins the trunk stream it will help to increase the channel discharge downstream (Knighton, 1998). The confluence of the Sil Torsa and Char Torsa has been considered as the lowermost limit of the reach I (R I), while the confluence of Kaljani and Torsa was considered the lowermost part of the reach II (R II). Since the temporal relative variability of the morphological parameters has been judged in response to discharge variability, segment R III has been excluded from the analysis due to the location of the hydrological observation station, which is not included within the study area. The downstream hydrological observation station of Torsa is at Ghughumari, which is located upstream of the Torsa-Kaljani confluence. Thus, the discharge downstream of the confluence is naturally greater than the measured discharge at Ghughumari.

#### 3.3.2 Measurements of Channel Bar Width and Channel Bar Area

Digitization of the river boundary has been done based on the Modified Normalized Difference Water Index (MNDWI) prepared for each of the selected years. Channel width has been measured at an interval of 1.5 km, which is logical enough since the total length of the course is approximately 100 km and the bank material condition does not vary too much. Moreover, a total of six guide bunds are present within the concerned length of the Torsa River course (5 within R I and R II). If the interval of the sections was considered less than 1.5 km, multiple sections were seen falling on the structurally constrained part of the channel. Width properties measured at each of the sections are averaged to compute the width of R I and R II. Non-channel width (sand and gravel bars and sheets) ( $W_b$ ) is measured by accumulating the non-water pixels landed on the section line within the extent of channel width, and similarly, the total pixel area of non-channel properties was considered to measure the channel bar area ( $Ab$ ). Channel braiding was computed using Eq. 3.13 as formulated by Brice (1964):

$$\frac{2 \sum L_b}{L_r} \quad (3.13)$$

where  $L_b$  is the length of bars and islands and  $L_r$  is the length of the concerned reach.

### 3.3.3 Bed Elevation Change

In this study, the temporal nature of changes in channel bed elevation ( $Z$ ) has been analysed to portray the location-specific sedimentation magnitude. Here, point data source of river cross-sections measured by CWC between 2005 and 2015 at Hasimara and Ghughumari has been used. Although the temporal changes within a period of 11 years cannot be considered as the general trend of the channel form adjustment at two certain locations, it can help to understand the associated role of hydrological attributes through the adjustment of the cross-sectional form. In this data, sparse environment elevation measurements at these two locations have been used as proxy representatives of two different physiographic domain: Hasimara for the piedmont surface and Ghughumari for the Northern plains. The Torsa is a Transboundary River and thus comes under the restricted river category of CWC, Govt. of India, and this creates certain obligations for getting hydrological and channel bed topographic data for a considerably larger timespan. Apart from that in this region, CWC is the only organisation that measures channel cross-section, and since there are only two hydro-meteorological stations on the Torsa River, it restricts researchers from getting more downstream spatial variations in channel cross-sectional character. Mean elevation of the river bed and thalweg along with their deviations from the long-term mean and annual net changes has been measured to ascertain the temporal changes. Apart from that, the inter-annual changes (pre- and post-monsoon) of mean channel elevation are also measured to correlate the relative importance of monsoon discharge in modifying channel bed characteristics. The topographic roughness of the river bed at Hasimara and Ghughumari is measured using the Bed Relief Index (BRI). It is an indication of the magnitude of the river bed elevation relative to the mean channel bed elevation. BRI increases with the degradation of the channel bed and increases with the aggradation of the river bed. It can also help to put an insight into the relative incision or sedimentation within the primary channel (Hoey & Sutherland, 1991). It is calculated using Eq. 3.14:

$$\text{BRI} = \frac{\sum_{i=1}^{n-1} \left[ \left\{ \frac{Z_i^2 + Z_{i+1}^2}{2} \right\}^{0.5} \times \{(X_{i+1}) - (X_i)\} \right]}{L} \quad (3.14)$$

where  $Z_i$  is the difference between bed elevation at  $i$ th point and the mean cross-sectional elevation in metre,  $\{(X_{i+1}) - (X_i)\}$  is the length between  $i$ th point and its next point in metre and  $L$  is the total cross-sectional length in  $m$ . Since the roughness of the channel bed is concerned in this formula, the embankments were deducted from the cross-sections, and bankfull width was taken into consideration.

## 4 Results and Discussion

### 4.1 Flood Discharge

The relationship between discharge and gauge height of any river measured at a particular location denotes the dependency on the volume of water. It's a good indicator of bankfull discharge and possible flood discharge. The correlation between the daily gauge height and discharge of the Torsa River both at the Hasimara and Ghughumari observation stations was positive for obvious reasons. The correlation coefficient of daily discharge and gauge height (1990–2015) was 0.713 and 0.837 at Hasimara and Ghughumari, respectively, and was significant at 99% ( $p = 0.01$ ). The best fit model for both the instances was power regression model, where  $Y = 111.74x^{0.0048}$  at  $R^2 = 0.558$  and  $Y = 35.229x^{0.0166}$  at  $R^2 = 0.8386$  (Fig. 3.3). The stage-discharge relationship was used to measure the flood discharge and bankfull discharge. Since the motive was to predict the discharge,  $Q$  was considered on Y-axis, and  $W_L$  was placed on X-axis. The best-fit equation (Exponential) at Hasimara is  $4E - 238e^{1.0186x}$ , and at Ghughumari, it was  $2E - 78x^{50.526}$  (power regression). The DL (danger level) denoted by the CWC for flood forecasting of Torsa level is 117.50 m and 40.41 m at Hasimara and Ghughumari, respectively. The WL (warning level) denoted by CWC for flood forecasting is 116.30 m and 39.80 m at Hasimara and Ghughumari, respectively. Both the elevations were calculated at WGS 84 datum. The scheme of flood forecasting by CWC defines that if the gauge height is between WL and DL, the flood situation will be defined as

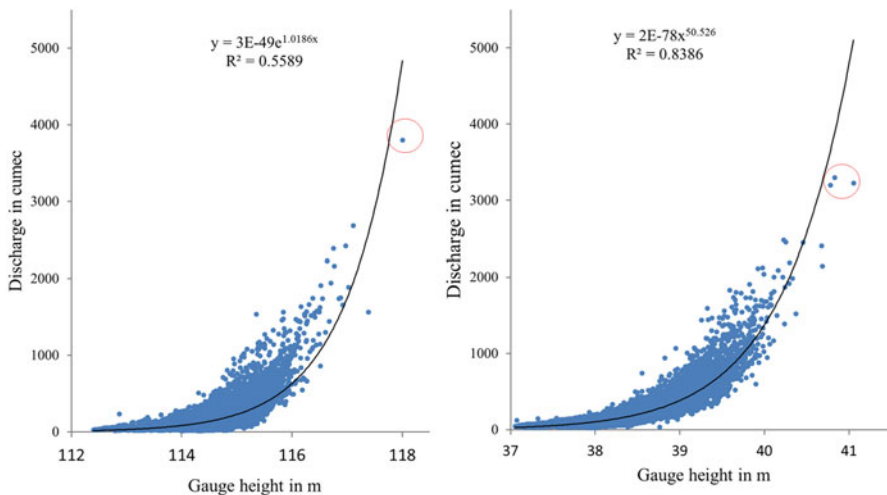


**Fig. 3.3** Discharge-gauge height relationship of the Torsa River (1990–2015); (left) Hasimara and (right) Ghughumari. Red circles depict extreme discharge events between 1990 and 2015

‘LOW FLOOD’. If the water level of the river touches or crosses its danger level but remains 0.50 m below the highest flood level of the site (commonly known as “HFL”), then the flood situation is called the ‘MODERATE FLOOD’, and if the water level of the river at the forecasting site is below the highest flood level (HFL) of the forecasting site but still within 0.50 m of the HFL, then the flood situation is called ‘HIGH FLOOD’. These predefined values were used to depict the Peak Over Threshold (PoT) using the best-fit equation of the stage–discharge curve. The DL was used to calculate the flood discharge ( $Q_f$ ) of Torsa at the respective gauge stations. The flood discharge at Hasimara was found to be  $2856 \text{ m}^3 \text{ s}^{-1}$ , and at Ghughumari, it was  $2954 \text{ m}^3 \text{ s}^{-1}$ . Any discharge above that will be vulnerable to the Torsa River.

## 4.2 Nature of Flood

The peak discharge condition in the Torsa River has been observed occurring in the monsoon months where its dominance was seen to be concentrated in the month of July. Flood incidents are common environmental hazards experienced by the local inhabitants residing on either side of the Torsa River. The floods of 1978 and 2000 were the most catastrophic flood incidents in the Torsa River basin. However, almost every year, both CWC and I&WD issue flood danger warning for the Torsa River where agricultural practices and houses located immediately to the bank lines face a considerable amount of damage. Apart from the flood inundation problem, the direct impact of the flood is often found in the form of bank erosion. Since the riverbank on the alluvial plain is composed of unconsolidated sands, the post-monsoon seasons bring perils to the nearby settlement and anthropogenic structures when the water level starts receding. The surface gradient is quite high on the piedmont, which leads to a lower residence time for the river water but often embankment breaching causes inundation in the nearby agricultural regions. The intensity of the flood impact often worsens on the alluvial plains since the drainage arteries (active course, tributaries and the abandoned courses) are closely spaced (Saha & Bhattacharya, 2016). The downstream region of the Torsa River near its confluence with Kaljani and the Cooch Behar town has been documented as flood prone (Chakraborty & Dutta, 2013). The sediment yield of the river increases during any flooding period and since the nature of the flood is flashy due to lower channel residence time and sudden inflow from the mountain catchment; it often helps in clogging a significant part of the active channel. The low-intensity annual flood is often responsible for the bifurcation of the active channel mostly on the piedmont surface of the Torsa River (Saha & Bhattacharya, 2021).

The magnitude of the flashiness is measured higher at Hasimara as compared with Ghughumari. Since the channel slope is higher on the piedmont, the flashiness of flood flow increases due to lower residence time. The higher flashiness often becomes a significant control of channel morphological changes within the channel bed (Ghosh, 2013). Saha and Bhattacharya (2021) have mentioned a greater

**Table 3.4** Flash Flood Magnitude Index and proxy flood power of the Torsa River computed at Hasimara and Ghughumari

Years	FFMI (at Hasimara)	FFMI (at Ghughumari)	Qmax/Qm (at Hasimara)	Qmax/Qm (at Ghughumari)
1990–1995	0.197	0.220	1.540	1.780
1996–2000	0.308	0.276	1.925	1.729
2001–2005	0.288	0.232	1.407	1.225
2006–2010	0.266	0.245	1.481	1.189
2011–2015	0.231	0.229	1.608	1.413

sensitiveness of the avulsion activities within the channel belt to annual fluctuation in river discharge on the piedmont plains as compared with the flat terrain of the northern plains. Similarly, the Qmax and Qm ratio, which are used as the proxy to flood strength, have been found to be much higher at Hasimara as compared with Ghughumari (Table 3.4). Thus, the high strength of flood discharge with a relatively higher flashiness is the relative nature of the flood discharge for the Torsa River on the piedmont plain compared with the northern plains.

### 4.3 Distribution of Peak Discharge

The overall concentration of the peak discharge both at Hasimara and Ghughumari has a skewed distribution. At Hasimara, the maximum concentration of the peak discharges is found within  $1500\text{--}2000\text{ m}^3\text{ s}^{-1}$  while at Ghughumari, the maximum concentration of the peak discharges is found within  $2000\text{--}2500\text{ m}^3\text{ s}^{-1}$ . Both these distributions differ from the normal distribution (Fig. 3.4). The two-sample homogeneity test suggests that the distribution of the peak discharge is homogeneous since the p-value is 0.2444 (at  $\alpha = 0.05$ ) while the Man-Whitney U test suggests no difference in locational attributes or the nature of the data since the p-value is 0.084 (at  $\alpha = 0.05$ ). Although the flooding strength and flashiness decrease downstream, the overall nature of the peak discharge is the same at both the hydrological stations. Since all the distributary systems of the Torsa are presently beheaded and abandoned, hence diffusion of floodwater does not occur. The mean of long-term peak discharge is comparatively higher at Ghughumari  $1803.87\text{ m}^3\text{ s}^{-1}$  than at Hasimara  $1495.933\text{ m}^3\text{ s}^{-1}$ . It suggests a contribution of the catchment run-off and input of water being provided by different small tributaries during the monsoon period. The distribution of the peak discharge is quite discrete at both the locations as the monsoon's uncertainty is responsible. The distribution at both the locations is very much non-stationary as the ADF test shows a value of 1.32 and 0.899 for Hasimara and Ghughumari, respectively, (at  $\alpha = 0.05$ ).

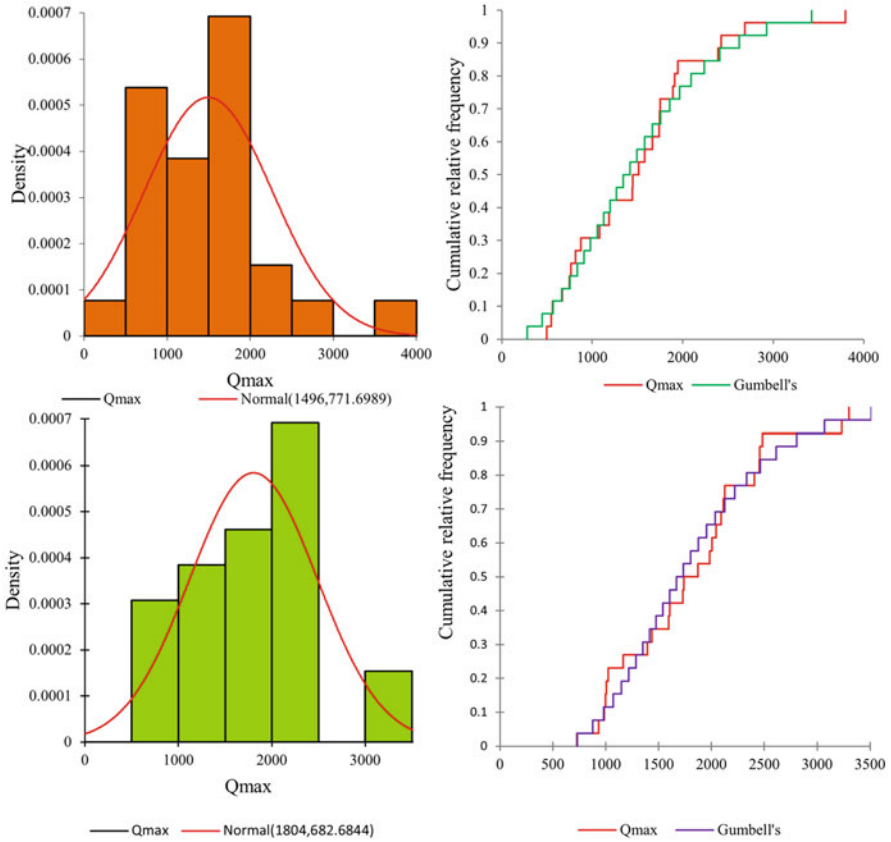


**Fig. 3.4** (Left) Probability density of Qmax of the Torsa River at Hasimara (top) and Ghughumari (bottom); (right) cumulative frequency plot of Qmax of the Torsa River at Hasimara (top) and Ghughumari (bottom)

### 4.4 Simulation of the Flood Discharge

The flood extremities of the Torsa at Hasimara and Ghughumari have been measured by calculating the flood-frequency analysis (FFA) and by simulating and predicting the extreme discharge values for high magnitude floods using log-normal (LN), log-Pearson type III (LP III) and Gumbel's extreme value 1 (Fig. 3.5). The maximum discharge at Hasimara and Ghughumari between 1990 and 2015 is found in 2000 where the Qmax was  $3800 \text{ m}^3 \text{ s}^{-1}$  and  $3300 \text{ m}^3 \text{ s}^{-1}$ , respectively. The downstream flood discharge was lower because of flood occurrences in many parts of the Jalpaiguri district (now Alipurduar) due to embankment breaching. At Hasimara, the annual flood discharge (at 1.04 years return period) is measured to be  $497 \text{ m}^3 \text{ s}^{-1}$  while at Ghughumari, it is  $725.80 \text{ m}^3 \text{ s}^{-1}$ . Using the Gumbel's extreme value the



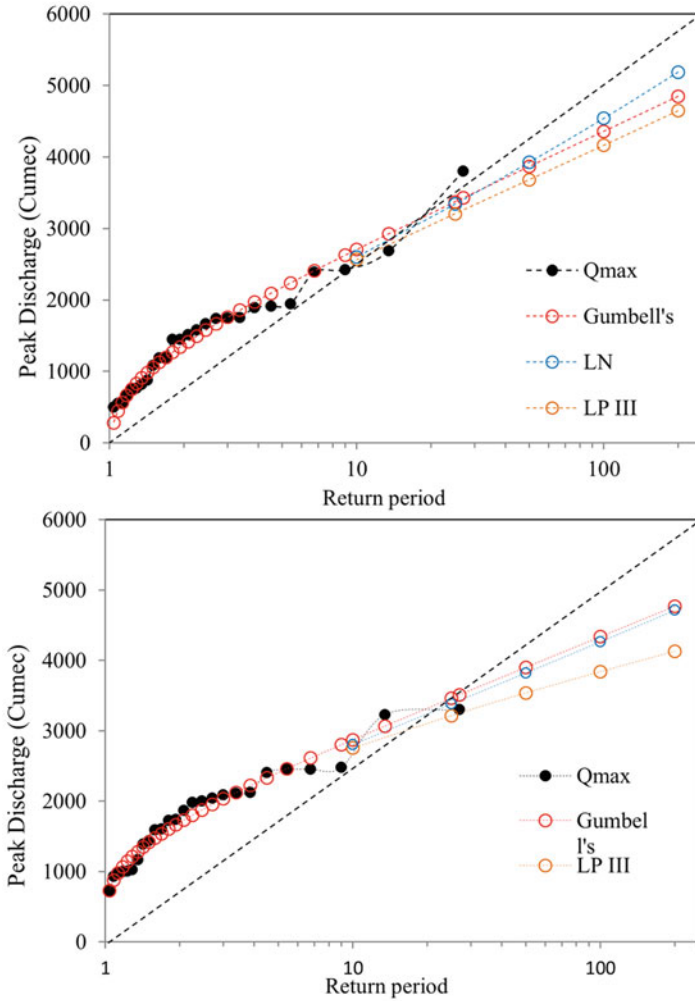


**Fig. 3.5** Semi-logarithmic distribution of the peak discharge and simulated flood discharge using Gumbell's, LP III and log-normal method

100 years flood discharge at Hasimara is predicted to be  $4360.8 \text{ m}^3 \text{ s}^{-1}$ . Similarly, using the LP III and LN method, it was found to be  $4162.9 \text{ m}^3 \text{ s}^{-1}$  and  $4540.78 \text{ m}^3 \text{ s}^{-1}$ , respectively. However, at Ghughumari in all the instances, the predicted discharge values are quite low. It was measured to be  $4337.64 \text{ m}^3 \text{ s}^{-1}$ ,  $3842.3 \text{ m}^3 \text{ s}^{-1}$  and  $4264.3 \text{ m}^3 \text{ s}^{-1}$  using the Gumbell's extreme value 1, LP III and LN methods, respectively (Table 3.5). Since the highest flood discharge at Ghughumari is lower as compared with the value measured at Hasimara due to upstream loss of the water in the catchment, the predicted values have taken that phenomenon into account. Thus, the predicted extreme flood discharge at Ghughumari is not bias-free at all.

**Table 3.5** Predicted extreme flood values as calculated by the authors

Location	Return period (Rt) (years)	Extreme discharge (cumec)		
		Gumbel's	LP III	LN
Hasimara	10	2705.73	2565.37	2602.02
	25	3373.28	3204.60	3341.42
	50	3868.51	3683.95	3927.41
	100	4360.08	4162.91	4540.47
	200	4849.85	4646.29	5188.02
Ghughumari	10	2874.12	2754.90	2804.01
	25	3464.67	3217.45	3385.12
	50	3902.77	3539.42	3823.11
	100	4337.64	3842.35	4264.36
	200	4770.92	4132.03	4714.70

#### 4.4.1 Goodness of Fit

The goodness of fit is required to be tested while simulating flood discharge data. In this study since the LP III method was calculated using the  $K_T$  table, it was not possible to calculate the discharge volume at all the return periods measured for the actual data. Thus, only the dataset obtained using Gumbel's method has been tested for its normality using the Shapiro–Wilk test and Anderson–Darling test along with the actual data after making a descending sequence based on the return periods (from 27 to 1.04 years). The semi-logarithmic distribution of the actual data depicts almost no deviation from the normal plot at both the hydrological stations. Still, the deviation of the actual data from the 1:1 line is comparatively lower at Ghughumari. At both the hydrological stations, the mean of measured discharge is slightly on the upper side with no outliers as compared with the actual discharge volume (Fig. 3.6). At Hasimara, the Shapiro–Wilk and Anderson–Darling test reveal that the Gumbel's distribution of the measured discharge follows a normal distribution while the actual discharge volume does not. Similarly, at Ghughumari, both the tests suggest a normal distribution for the measured flood discharges, and interestingly, the actual data is also very less skewed and tends to be normally distributed (Table 3.6).

### 4.5 Channel Morphology and Hydrological Control

The absolute morphological properties that have been used to portray the channel sedimentation characteristics are hardly correlated with any of the discharge and channel water level components in the Reach I. Here,  $W_b$  was found negatively correlated ( $r = -0.27$ ) with the  $W_{mon\ prev}$  possibly due to inundation of the braid bars during the high-stage period. However, the channel  $Ab$  was found positively correlated ( $r = +0.24$ ) with the  $CV\ W_{mon\ prev}$  because greater variability means greater lean patches, which expose most of the mid-channel bar surface. A similar

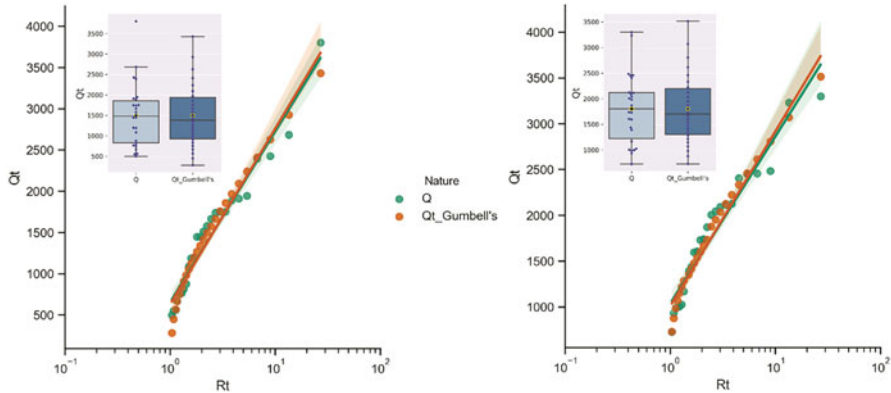


**Fig. 3.6** The goodness of fit of the natural peak discharge ( $Q_{max}$ ) and simulated peak discharge ( $Q_t$ ) using Gumbell's method

**Table 3.6** Normality test of the actual and measured discharge using Gumbel's method

Location	Nature	Shapiro-Wilk test (p-value) $\alpha = 0.05$	Remarks	Anderson-Darling test (p-value) $\alpha = 0.05$	Remarks
Hasimara	Actual	0.0499	Null hypothesis should be rejected	0.2059	Null hypothesis cannot be rejected
	Gumbel's	0.5170	Null hypothesis cannot be rejected	0.6654	Null hypothesis cannot be rejected
Ghughumari	Actual	0.2665	Null hypothesis cannot be rejected	0.3990	Null hypothesis cannot be rejected
	Gumbel's	0.5170	Null hypothesis cannot be rejected	0.6654	Null hypothesis cannot be rejected

scenario also exists in correlation between certain morphological changes and channel hydrological parameters. The changes in the channel bar area and channel bar width were found positively correlated with FFMI and  $Q_{max}/Q_m$ . Although the association was not significant at all, the coefficient values infer certain understandings (Table 3.7). With higher flood power, the net volume of sedimentation increases heading to the net change in the mid-channel bar area and its increase in width. However, in Reach II, the association is quite different. Most of the morphological properties were found negatively correlated (significant at  $\alpha = 0.10$ ). The Ab, Wb and BI were all found negatively correlated with  $Q_{max}/Q_m$  where the coefficient values were  $-0.42$ ,  $-0.59$  and  $-0.45$ , respectively. Similarly, these three factors were also found negatively correlated with the mean monsoon discharge ( $Q_{mon}$ )

**Table 3.7** Correlation coefficients of temporal changes in channel morphological properties and hydrological components

Hydrological parameters	Reach I		Reach II	
	Change in Ab	Change in Wb	Change in Ab	Change in Wb
Qd	0.1351	-0.0979	-0.2654	-0.2769
CV Qd	-0.2054	-0.2639	-0.1616	-0.2827
Qmon	0.0759	-0.0671	-0.5179	-0.3731
Qmax	0.2011	0.1861	0.5261	0.5212
Qmax prev	-0.1721	-0.1978	<b>-0.9301</b>	<b>-0.7893</b>
Qmon prev	-0.2744	-0.1573	<b>-0.7135</b>	<b>-0.6876</b>
FEMI	0.2875	0.3214	0.4462	0.5813
Qmax/Qm	0.0996	0.4509	0.4239	0.3471

(Fig. 3.7). Since the flow residence time on the northern plain is higher compared with the piedmont slope, higher flood flow obviously submerges a greater bar area, and thereby, the width and braiding also decrease. These three parameters are significantly correlated with the previous year's mean monsoon water level in a negative manner where the coefficients of Ab, Wb and BI are  $-0.668$ ,  $-0.73$  and  $-0.59$ , respectively. These observations somehow strengthen the previous inference being made. On the other hand, the association between the temporal changes of the morphological parameters and  $Q_{max}/Q_m$  and FFMI were found to be positive, which portrays in-channel deposition brought down by flood flows.

#### 4.6 Channel Bed Elevation and Discharge Characteristics

Coming down from the reach scale to point observations, channel bed level changes have been measured at the two hydrological stations, i.e., Hasimara and Ghughumari (Fig. 3.8). At Hasimara, channel aggradation is evident after any high discharge. The correlation between the Z and BRI with  $Q_{max}/Q_m$  and  $Q_{mon}$  is significantly positive (Fig. 3.9). The correlation coefficient between Z and  $Q_{max}/Q_m$  is found 0.675 while between Z and  $Q_{mon}$ , it is +0.533. Similarly, the correlation coefficient between BRI and  $Q_{max}/Q_m$  is +0.54, and between BRI and  $Q_{mon}$ , it is +0.778 at Hasimara. Although the correlation coefficients between channel thalweg depth (T) and the concerned hydrological parameters are not significant enough, the negative nature of 'r' also signifies the relative bed aggradation after flood flow at Hasimara located on the piedmont surface. On the other hand, at Ghughumari, the nature of bed level changes is not that intensely correlated with hydrological parameters. Saha and Bhattacharya (2021) also found in their studies that the bed elevation properties on the northern plain are not as sensitive to hydrological function as it is on the piedmont surface. A similar scenario is also found here while studying the statistical association between the pre-monsoon and post-monsoon bed level changes with  $Q_{max}$ . At both the hydrological stations, the

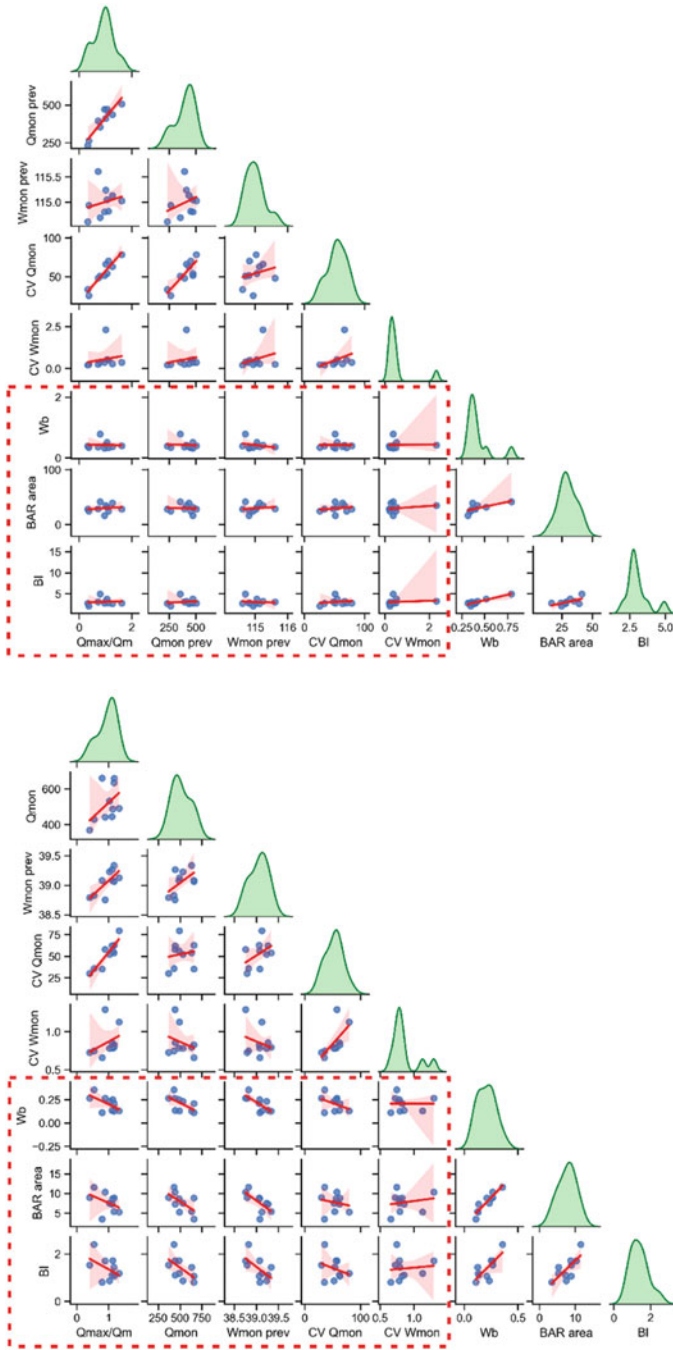


**Fig. 3.7** Correlation plot of the channel morphological properties and different channel hydrological attributes

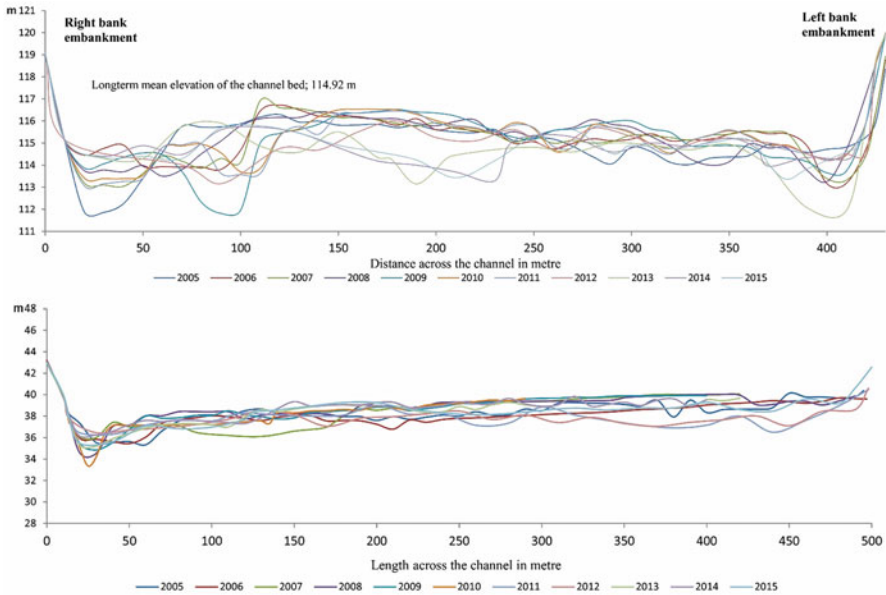


**Fig. 3.8** Cross-sections measured at Hasimara (top) and Ghughumari (bottom) between 2005 and 2015

correlation is positive, but the magnitude is comparatively higher on the piedmont slope (Fig. 3.10). The rate of sedimentation is much higher on the piedmont slope in comparison with the northern plains as the major break in slope occurs at the mountain front and the piedmont surface becomes the major depo-centre of the channel aggradations. Still, this generalisation may differ at the reach scale because certain structural effects may be seen at certain pockets, which is also a major controlling factor of channel morphological evolution. Alongside, the anthropogenic interventions within the fluvial often disturb the sedimentation pattern of the channel too (Islam et al., 2021).

## 5 Conclusion

This study portrays the significant impact of hydrological components especially the flood flow on in-channel sedimentation spatially along with an understanding of the nature of channel flood. The major findings of this study are listed below:

- (a) The flood power and magnitude are greater on the piedmont surface with a lower residence time. Thus, the flashiness of flood increases on the piedmont surface as compared to the northern plains. The greater flood power and a higher degree of flood flashiness significantly control the channel morphological development within the river course.

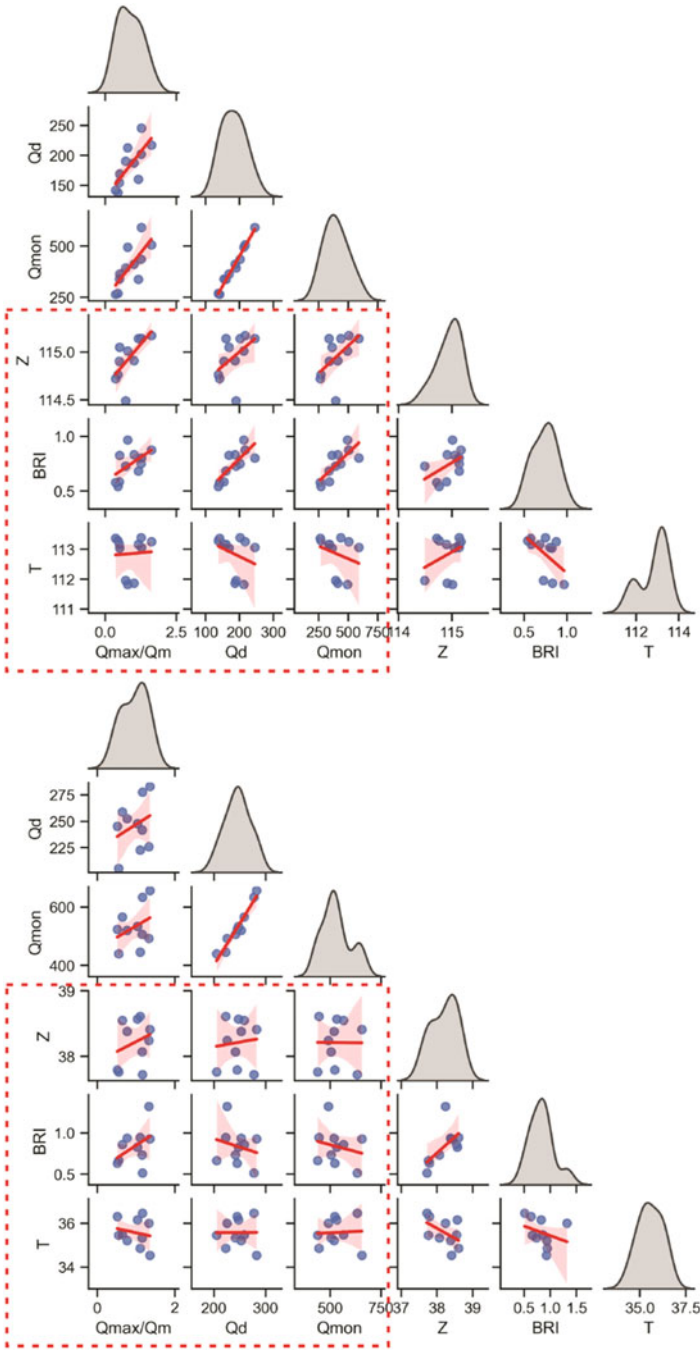


**Fig. 3.9** Correlation plot of the channel bed properties and different channel hydrological attributes

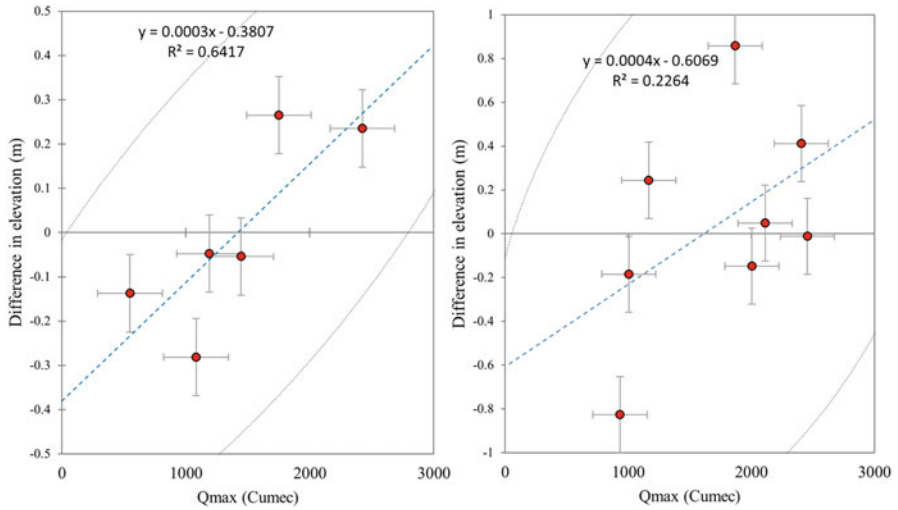


**Fig. 3.10** Temporal change in net bed elevation and its association with Qmax at Hasimara (left) and Ghughumari (right)

- (b) The intensity of controls on channel morphology and channel aggradation decreases downstream.
- (c) Since the flood residence time is greater on the northern plains, it significantly submerges a greater extent of the bar surface. However, as most of the sediment load gets deposited on the piedmont slope, the downstream channel segments experience a lower degree of sedimentation at least at the point of hydrological observation (Ghughumari).

This study carries a significant understanding of the sole impact of the flood on channel sedimentation. Making any generalisation on the nature of channel morphological evolution based on the hydrological impact could not be apt enough since other catchment variables are playing a significant role in channel morphology and sedimentation too. The nature of the flood is of significant help for planners and institutions whoever is involved in flood forecasting of the Torsa River as this river is often considered as ‘sorrow of Cooch Behar’.

**Acknowledgement** We thank the Central Water Commission (CWC) for proving us with some important hydrological data on the Torsa River. We also thank Nilanjana Biswas, UGC-Research Fellow at the Vivekananda College for Women, for her valuable efforts.

**Declaration** No conflict of interest.



## References

- Bandyopadhyay, S., Ghosh, P. K., Jana, N. C., & Sinha, S. (2016). Probability of flooding and vulnerability assessment in the Ajay River, Eastern India: implications for mitigation. *Environmental Earth Science*. <https://doi.org/10.1007/s12665-016-5297-y>
- Bhat, M. S., Alam, A., Ahmad, B., Kotlia, B. S., Farooq, H., Taloor, A. K., & Ahmad, S. (2019). Flood frequency analysis of river Jhelum in Kashmir basin. *Quaternary International*, 507, 288–294. <https://doi.org/10.1016/j.quaint.2018.09.039>
- Brice, J. C. (1964). Channel patterns and terraces of the Loup Rivers in Nebraska. US Government Printing Office.
- Chakraborty, S., & Dutta, K. (2013). Causes and consequences of fluvial hazard – A hydrogeomorphic analysis in duars region, India. *Indian Stream Research Journal*, 2(12), 1–10.
- Chow, V. T. (1964). Statistical and probability analysis of hydrologic data. In V. T. Chow (Ed.), *Handbook of applied hydrology* (pp. 81–97). McGraw Hill.
- Dallaire, C. O., Lehner, B., Sayre, R., & Thieme, M. (2019). A multidisciplinary framework to derive global river reach classifications at high spatial resolution. *Environmental Research Letters*, 14(2). <https://doi.org/10.1088/1748-9326/aad8e9>
- Das, A. (2012). The quaternary geological map of North Bengal. *Indian Cartographer*, 32, 312–321.
- Das, A., & Chattopadhyay, G. S. (1993). Neotectonics in the Tista, Jalldhaka and Torsa interfluvial belt of North Bengal. *Geological Survey of India Records*, 121(2–8), 101–109.
- Ghosh, S. (2013). Estimation of flash flood magnitude and flood risk in the lower segment of Damodar River basin, India. *International Journal of Geology, Earth & Environmental Sciences*, 3(2), 97–114.
- Ghosh, M., & Ghosal, S. (2021). Climate change vulnerability of rural households in flood-prone areas of Himalayan foothills, West Bengal, India. *Environment, Development and Sustainability*, 23(2), 2570–2595. <https://doi.org/10.1007/s10668-020-00687-0>
- Ghosh, S., & Guchhait, S. K. (2014). Hydrogeomorphic variability due to dam constructions and emerging problems: A case study of Damodar River, West Bengal, India. *Environment, Development and Sustainability*, 16(3), 769–796. <https://doi.org/10.1007/s10668-013-9494-5>
- Gumbel, E. J. (1958). *Statistics of extremes*. Columbia University Press. <https://doi.org/10.7312/gumb92958>
- Gupta, N. (2008). Geoinformatics for inter-basin water transfer assessment – a study in part of Ganga-Brahmaputra basin, Eastern India. Unpublished M.Sc Dissertation. Retrieved from [https://webapps.itic.utwente.nl/librarywww/papers\\_2008/msc/gem/niladri.pdf](https://webapps.itic.utwente.nl/librarywww/papers_2008/msc/gem/niladri.pdf)
- Hoey, T. B., & Sutherland, A. J. (1991). Channel morphology and bedload pulses in braided rivers: A laboratory study. *Earth Surface Processes and Landforms*, 16(5), 447–462. <https://doi.org/10.1002/esp.3290160506>
- Islam, A., & Sarkar, B. (2020). Analysing flood history and simulating the nature of future floods using Gumbel method and log-Pearson Type III: The case of the Mayurakshi River Basin, India. *Bulletin of Geography. Physical Geography Series*, 19(1), 43–69. <https://doi.org/10.2478/bgeog-2020-0009>
- Islam, A., Sarkar, B., Saha, U.D., Islam, M., & Ghosh, S. (2021). Can an annual flood induce changes in channel geomorphology? *Natural Hazards*. <https://doi.org/10.1007/s11069-021-05089-7>
- Knighton, D. (1998). *Fluvial forms and processes: A new perspective*. Edward Arnold.
- Kochel, R. C. (1988). Geomorphic impact of large floods: Review and new perspectives on magnitude and frequency. In V. Baker, R. Kochel, & P. Patton (Eds.), *Flood geomorphology* (pp. 169–187). Wiley.
- Kormokar, S., & De, M. (2020). Flash flood risk assessment for drainage basins in the Himalayan foreland of Jalpaiguri and Darjeeling Districts, West Bengal. *Modeling Earth Systems and Environment*. <https://doi.org/10.1007/s40808-020-00807-9>

- Kumar, R. (2019). Flood frequency analysis of the Rapti river basin using log pearson type-III and Gumbel Extreme Value-1 methods. *Journal of the Geological Society of India*, 94(5), 480–484. <https://doi.org/10.1007/s12594-019-1344-0>
- Lakshmi Kumar, T. V., Koteswara Rao, K., Barbosa, H., & Uma, R. (2014). Trends and extreme value analysis of rainfall pattern over homogeneous monsoon regions of India. *Natural Hazards*, 73(2), 1003–1017. <https://doi.org/10.1007/s11069-014-1127-2>
- Leopold, L. B., & Wolman, M. G. (1960). River meanders. *Geological Society of America Bulletin*, 71(6), 769–793. [https://doi.org/10.1130/0016-7606\(1960\)71\[769:RM\]2.0.CO;2](https://doi.org/10.1130/0016-7606(1960)71[769:RM]2.0.CO;2)
- Mukhopadhyay, S. C. (2014). Aspects of hydro-geomorphology of North Bengal drainage, India and surroundings with emphasis on the Torsa basin. *Indian Journal of Landscape Systems and Ecological Studies*, 37(2), 163–176.
- Mukhopadhyay, S. C., & Dasgupta, A. (2010). *River dynamic of West Bengal: Physical aspects*. Prayash.
- Raghunath, H. M. (2006). *Hydrology: Principles, analysis and design*. New Age International.
- Saha, U. D., & Bhattacharya, S. (2016). A study of river induced major hydrogeomorphic issues and associated problems in Torsa basin, West Bengal. *Geographical Review of India*, 78(2), 132–145.
- Saha, U. D., & Bhattacharya, S. (2019). Reconstructing the channel shifting pattern of the Torsa River on the Himalayan Foreland Basin over the last 250 years. *Bulletin of Geography. Physical Geography Series*, 16(1), 99–114. <https://doi.org/10.2478/bgeo-2019-0007>
- Saha, U. D., & Bhattacharya, S. (2021). Channel avulsion in the Torsa River course and its response to topographic and hydrological controls on the Himalayan Foreland Basin. *Journal of Earth System Science*, 130(4), 1–29.
- Sinha, R. (2009). The great avulsion of Kosi on 18 August 2008. *Current Science*, 429–433.
- Soja, R., & Sarkar, S. (2008). Characteristics of hydrological regimes. In L. Starkel, S. Sarkar, R. Soja, & P. Prokop (Eds.), *Present-day evolution of Sikkimese–Bhutanese Himalayan Piedmont* (pp. 37–46). Institute of Geography and Spatial Organization.
- Starkel, L., Soja, R., & Sarkar, S. (2008). Rainfall at the margin of the Himalayan foothills and in the piedmont zone. In: Starkel, L., Sarkar, S., Soja, R., Prokop, P. (Eds.), *Present-day evolution of Sikkimese Bhutanese Himalayan Piedmont*. Stanisława Leszczyckiego, Warszawa, pp. 29–36.
- Weibull, W. (1939). The Phenomenon of Rupture in Solids. Ingeniors Vetenskaps Akademiens Handlingar, Royal Swedish Institute for Engineering Research, Stockholm, Sweden, No. 153.

# Chapter 4

## Flood Risk Assessment of Himalayan Foothill Rivers: A Study of Jaldhaka River, India



Adrija Raha, Suraj Gupta, and Mery Biswas

**Abstract** Flood is an annual recurrent event in the Himalayan foothill province of West Bengal. The middle course of Jaldhaka River basin experiences flood occasionally. The main river with its tributaries carries huge discharge during monsoon periods, resulting floods that affect the entire landscape. The study is an assessment of flood susceptibility using analytical hierarchy process (AHP) where elevation (m), slope (degree), mean rainfall (cm), normalized difference vegetation index (NDVI), bare soil index (BSI), topographic wetness index (TWI), and distance from rivers (km) have been considered. Five classes have been assessed where very high and high flood susceptibility areas are concentrated in the lower flood plain section of Rothikhola, Sukti, and Jaldhaka itself. There is remarkable changes from 2000–2020 in land utilization also where settlement and agricultural land have increased enormously in moderate to low flood-risk sections of near-foothill area and settlement has shifted from the flood plains to the northern section. Natural vegetation has decreased, and there is a remarkable increase of agricultural land over both banks of river channels. The outcome of the study portrays a change in the land utilization pattern affected by recurrent flood events.

**Keywords** Himalayan foothill · AHP · Flood susceptibility · LU/LC change

### 1 Introduction

Flood is one of the destructive natural hazards, which causes huge loss to human life, property, infrastructure, agricultural lands, and much irreversible damages (Swain et al., 2020). It causes overall disruption to the development activity and the daily economic practice of people (Zhong et al., 2018; Yésou et al., 2013; Patrikaki et al., 2018; Birkholz et al., 2014; Mouratidis & Sarti, 2012; Astaras et al., 2011; Domakinis et al., 2020). Among the hydrometeorological disasters, flood is

---

A. Raha · S. Gupta · M. Biswas (✉)

Department of Geography, Presidency University, Kolkata, West Bengal, India

e-mail: [mery.geog@presiuniv.ac.in](mailto:mery.geog@presiuniv.ac.in)

considered as the most destructive natural hazard, accounting for 43.5% of death (Ahmed et al., 2021; CRED, 2015; Hu et al., 2018; Li et al., 2016). It has been surveyed that 170 million people get affected annually by this natural hazard (Kowalzig, 2008). The economic challenges are much greater for developing and underdeveloped countries (Quesada Román, 2021). Therefore, it is of utmost importance to focus on flood risk management programs and to overcome national boundaries, socioeconomic limitations, and geographical locations (Degiorgis et al., 2012; Kazakis et al., 2015). Due to rapid urbanization and developmental activity as well as other human interventions like deforestations, natural hazards like floods are becoming frequent and devastating as well. Deforestation, unplanned urbanization, change in land use and land cover, faulty agricultural practices, and climate change are some of the important factors responsible for the increasing frequency of flood occurrence (Quesada Román, 2021; Jarrett & Tomilson, 2000; Chang & Franczyk, 2008). Along with these factors, the characteristics of river basins can also play a major part in the occurrence of floods (Mohamed & El-Raey, 2019; Bhat et al., 2019; Ahmed et al., 2021). With the evolution of different methodologies, the approach to flood management has been changed (Das & Sahu, 2017). The nonstructural methods for flood risk management are gaining popularity, which encompasses forecasting of floods, flood susceptibility mapping, and flood inundation mapping. The application of remote sensing and geographical information system have provided updated tools, which are helpful for preparing flood susceptibility maps and for assessing the flood hazard risk more accurately (Sankhua et al., 2015; Rai & Mohan, 2014; Ahmad, 2018; Sahu, 2014), and have provided a reliable decision-making tool for the management of flood risk (Dewan, 2013; Ahmed et al., 2021; El Bastawesy et al., 2019; Mohamed & El-Raey, 2019; Shehata & Mizunaga, 2018; Youssef et al., 2015). The incorporation of certain factors like meteorology, geomorphology, topography, lithology, geology, and land use pattern with the help of geographic information system can provide a detailed account of the flood risk zonation (Das & Sahu, 2017, Biswas & Dhara, 2019). The global coverage of remote sensing data and its accessibility have helped to monitor the flood hazard more accurately (Baez-Villanueva et al., 2018; Zhao et al., 2014; Paul et al., 2019). The approach of integration of remote sensing and geographic information system along with morphological and meteorological analysis is being used significantly for the assessment of flood hazard zonation (Kabenge et al., 2017; Mahmood & Rahman, 2019; Rastogi et al., 2018). It has also become a helpful management tool to delineate flood susceptibility zones (Adnan et al., 2019; Dawod et al., 2012; Mahmood & Rahman, 2019; Sarkar & Mondal, 2019; Youssef et al., 2010). Analytical hierarchy process (AHP) (Chakraborty & Joshi, 2014; Dandapat & Panda, 2017; Kazakis et al., 2015), frequency ratio (FR) model (Sarkar & Mondal, 2019), machine learning, multi-criteria decision model (MCDM) (Costache et al., 2019; Khosravi et al., 2016; Rahman et al., 2019), and flow model (FM) simulation (Baky et al., 2019) are some popular and cost-effective approaches to prepare flood susceptibility maps.

In the case of India, due to the unpredictable and uncertain activity of summer monsoon, numerous events of catastrophic flood are witnessed (Roy et al., 2021; Dhar & Nandagri, 2003). In the areas where much of the rainfall happens between June and September, during the summer monsoon, floods are considered to be a perpetual natural disaster (Roy et al., 2021). Therefore, this season is a matter of concern, as around 32 million citizens of India are vulnerable to flood risk (Kale, 2004).

The Himalayan foreland in West Bengal is drained by numerous rivers with a general flow direction toward the south and southeast (Raha & Biswas, 2022a, b). These rivers have largely shaped the foreland portion with its huge sediment deposition, which is associated with monsoonal rainfall and discharge fluctuations. The rise in the river water level is dependent upon the spatial distribution of rainfall, its duration, and intensity (Roy, 2011; Paul & Biswas, 2019; Biswas & Banerjee, 2018). In the upper catchment areas of the rivers, occasional landslide events perpetuate into sudden bursting of water, which eventually makes the river channels release massive volumes of water, as it happened in the case of Teesta River in 1968 (Roy, 2011). Teesta, Leesh, Gheesh, Chel, Neora, Muri, Jaldhaka, Diana, Rohtikhola, and Sukti are some of the major rivers that flow through Jalpaiguri and Alipurduar. The Jaldhaka River's middle course, as well as its tributaries, experience extensive flooding, particularly in the lower course. It is associated with excessive rainfall, slope, flow behavior, etc., which makes the rivers unpredictable (Ghosh, 2018). Therefore, the objectives of the study are to analyze the flood susceptibility zones considering certain parameters and to understand the effects of flood inundation on different land use and land cover and its consequential changes.

## 2 Study Area

One of the main rivers of the Himalayan Foothill region in West Bengal is River Jaldhaka. A report provided by the North Bengal Flood Control Commission, North Bengal (NBFCC) (1965) based on the Gauge Height of various rivers at various time periods indicated the flood-prone nature of the rivers (Table 4.1). The Himalayan foreland region in West Bengal (Fig. 4.1) is endowed with River Jaldhaka and its tributaries like Murti, Jiti, Khuji Diana, Diana, Rohtikhola, and Sukti, which are considered to be flood prone. The area under consideration has an area of 1745.4 km<sup>2</sup> extending from River Murti in the West to River Sukti in the East, from the Himalayan Mountain front in the north to the confluence of Jaldhaka and Sukti in the South. The focus on flood risk zonation of the considered study area is of utmost importance as the area forms the riparian parts of the sub-Himalayas where maximum number of rivers have a common source (Chakraborty & Mukhopadhyay, 2019; Ghosh & Kar, 2018). In the varying nature of climatic components, high amount of annual rainfall has contributed to the flood susceptibility of the area (Table 4.2) (Mandal & Sarkar, 2016; Shrestha et al., 2012; Roy, 2011). Though

**Table 4.1** Flood and nonflood event in different rivers in the district (Das et al. 2017)

Rivers	Floods	Nonfloods	Observation year
Teesta	14	9	23
Jaldhaka	18	8	26
Diana	7	8	15
Torsa	14	1	15
Raidak I	11	4	15
Raidak II	6	9	15
Kaljani	9	6	15
Sankosh	5	10	15
Mujnai	8	7	15
Jainti	12	3	15
Dharala	11	4	15
Neora	7	9	16

Source: NBFCC (North Bengal Flood Control Commission)

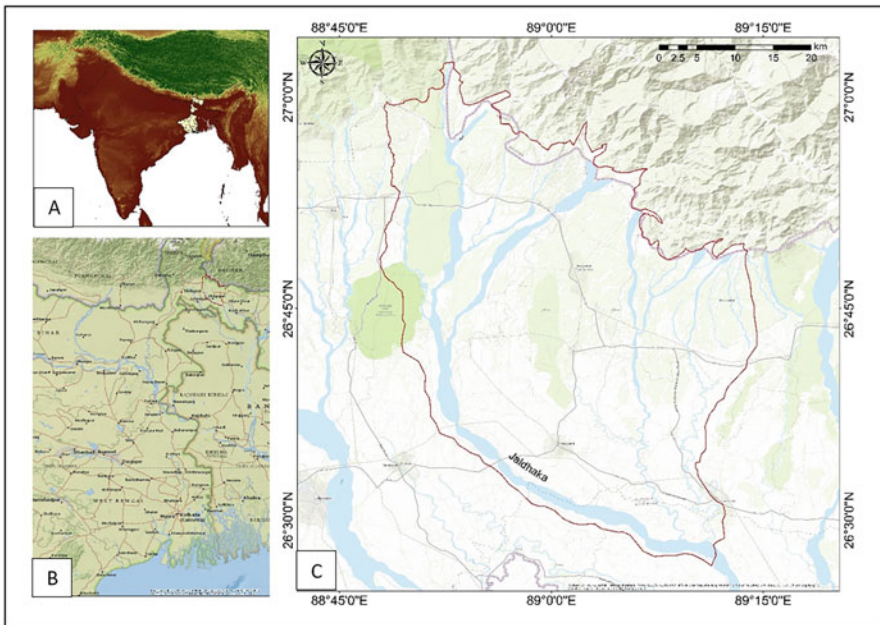


**Fig. 4.1** (a-c) Location of the considered study area with Jaldhaka and its tributaries

inundation is a very common and frequent phenomenon, the intensity and damage potentials vary spatially depending upon the areal extent of inundation, the total number of population affected, loss of life, livelihood, properties, and damages to the infrastructures (Das et al., 2017).

**Table 4.2** Previous records of rise in gauge height of River Jaldhaka (Gauge station: NH-31 Crossing)

Year	Maximum water level/flood peak		One day maximum rainfall (mm)
	On	Remarks	
2020	11.07.2020	0.13 M above DL	222.0
2018	10.09.2018	0.15 m. above DL	300.0
2017	12.08.2017	0.11 m above DL	216.00
2015	07.06.2015	0.10 m above DL	Data not available
	23.06.2015	0.11 m above DL	
	02.09.2014	0.85 m above DL	
2012	17.06.2012	0.05 m above DL	
	16.07.2012	0.25 m above DL	
2009	20.08.2009	0.28 m above DL	
2008	06.07.2008	0.09 m above DL	
2007	04.09.2007	0.11 m above DL	
	07.09.2007	0.30 m above DL	
2005	20.07.2005	0.23 m above DL	
2004	20.07.2004	0.20 m above DL	
2003	01.07.2003	0.13 m above DL	
	08.07.2003	0.14 m above DL	
2000	04.08.2000	0.10 m above EDL	
1998	26.08.1998	0.35 m above DL	
1996	13.07.1996	0.42 m above DL	

Annual Flood Report from 1991 to 2020, Irrigation and Waterways Directorate, Government of West Bengal

*DL* danger level, *EDL* extreme danger level

### 3 Data Used and Methodology

To execute the flood susceptibility zone, mapping of total seven parameters has been taken into consideration (Table 4.3). After literature review and thorough field investigations, these parameters have been considered to be applicable in the region. Authors have considered these parameters to be suitable for susceptibility mapping. Other parameters could have been applied if the study area was larger.

#### 3.1 Elevation

The altitudinal attribute of any region plays an important role to understand the probability of flooding in that region. It is important to note that flat lands and low-lying regions are more prone to flood hazards as the water flows down from high altitudinal zone to lowland areas causing stagnation of water for a significantly long period of time, which ultimately leads to flood-like situation, that is inundation of the land (Tehrany et al., 2014).

**Table 4.3** Parameters selected for preparing flood susceptibility map

Parameters	Elevation (meter)	Slope (degree)	Normalized Difference Vegetation Index (NDVI)	Topographic Wetness Index (TWI)	Bare Soil Index (BSI)	Mean rainfall (cm)	Distance from rivers (km)
Formula and details	Classified into five classes based on Digital Elevation Model in ArcGIS 10.4.1	Processed from DEM in ArcGIS 10.4.1 following the steps: <b>3D Analyst Tool</b> → <b>Raster Sur-face</b> → <b>Slope</b> <b>(Degree)</b>	$\frac{NIR-R}{NIR+R}$ Where, NIR = Near Infrared R = Red	$\ln \left( \frac{As}{\tan \beta} \right)$ Where, As = Flow Accumulation Tan $\beta$ = Sur-face slope gradient	$\frac{(SWIR-R) - (NIR-B)}{(SWIR+R) + (NIR+B)}$ Where, NIR = Near Infrared R = Red B = Blue SWIR = Short Wave Infrared	Gridded data process in ArcGIS 10.4.1 to prepare mean rainfall map	Map has been prepared based on line density tool of ArcGIS 10.4.1
Data type	ASTER GDEM Version 3, 30m $\times$ 30m	ASTER GDEM Version 3, 30m $\times$ 30m	Landsat 8 OLI/TIRS USGS, 30m $\times$ 30-m	ASTER GDEM Version 3, 30 m $\times$ 30 m	Landsat 8 OLI/TIR USGS, 30m $\times$ 30-m	High-resolution gridded data, 0.5 $^{\circ}$ $\times$ 0.5 $^{\circ}$ CRU TS v. 4.04 (Climatic Research Unit gridded Time Series) version 4	Geological survey of India (GSI) data, 1:50,000
Source of data	<a href="https://search.earthdata.nasa.gov">https://search.earthdata.nasa.gov</a>	<a href="https://search.earthdata.nasa.gov">https://search.earthdata.nasa.gov</a>	<a href="https://search.earthdata.nasa.gov">https://search.earthdata.nasa.gov</a>	<a href="https://search.earthdata.nasa.gov">https://search.earthdata.nasa.gov</a>	<a href="https://search.earthdata.nasa.gov">https://search.earthdata.nasa.gov</a>	<a href="https://sites.uea.ac.uk/cru/data">https://sites.uea.ac.uk/cru/data</a>	<a href="https://www.gsi.gov.in">https://www.gsi.gov.in</a>



### **3.2 Slope**

Slope is a significant factor of flood susceptibility mapping as it determines the flow of river water and runoff. It is noted that areas of flat slope disrupt the natural flow of water, which perpetuates into the stagnation of water, thus leading to flood-hazard risk (Bui et al., 2019). The infiltration rate is directly related to the topographic slope (Das, 2019). The steep gradient of land hinders infiltration of rainwater.

### **3.3 Rainfall**

The flood hazard risk is largely dependent upon the duration and intensity of rainfall of a particular region. The rainfall characteristics of the study area is influenced by the south-west monsoon wind. The location of the study area as a Himalayan foreland makes it receive heavy rain as the Himalayan orogenic belt acts as a barrier, which intercepts the monsoon wind and causes huge rainfall between the month of June to September (Roy et al., 2021). The duration and intensity of rainfall directly influence the flood susceptibility of an area. With the increasing intensity of rainfall, the flood hazard risk also increases (Rozalis et al., 2010; Mirzaei et al., 2020).

### **3.4 Distance from Rivers**

Previous researchers (Tien Bui et al., 2019) have considered distance from rivers to be a significant factor determining the risk of flood hazard. The heavy rainfall increases the discharge amount of the rivers exceeding their carrying capacity. Thus, the areas near the rivers are more prone to flood hazards. Numerous researches have provided the threshold distance from the rivers, which are more susceptible to flooding. Samanta et al. 2016 has considered less than 100 m from the rivers to be most susceptible to flooding. Pradhan 2009 has observed that a distance less 90 m from the rivers is prone to flood hazard risk.

### **3.5 Normalized Difference Vegetation Index (NDVI)**

NDVI is a dimensionless index, which ranges between +1 and - 1 where the dense vegetation represents values near +1. Vegetation cover largely affects flood susceptibility and intensity of flood risk hazard as there is a negative correlation between vegetation density and flood hazards (Mojaddadi et al., 2017; Rahman et al., 2019; Kaur et al., 2017).

### 3.6 Bare Soil Index (BSI)

The bare soil index indicates the bare regions, which have nearly no vegetation cover and thus are susceptible to flood risk. The bare soil cover facilitates runoff decreasing the infiltration rate, therefore increasing the flood risk.

### 3.7 Topographic Wetness Index (TWI)

Topographic wetness index is a useful parameter to understand the extent of flood susceptible zone. Previous researches have analyzed the fact that if the value of TWI exceeds a threshold for a part of the watershed, the area is supposed to be saturated (Woods & Sivapalan, 1997; Alam et al., 2021). The index helps to delineate the extent of the watershed, which is likely to get inundated after heavy rainfall.

Each parameter has been classified into five classes. Analytical hierarchy process (AHP) has been adopted to give (Table 4.4) the parameters weightage. AHP is a significant tool that takes into account multiple variables in GIS platform for decision-making (Şener et al., 2010). This technique was introduced by Saaty (1980, 1990) to assign weightage to the parameters based on some indicators to make a structure, which is hierarchical in nature. Consistency Index (CI) is calculated:

$$CI = \frac{\lambda_{Max} - n}{n - 1} \tag{4.1}$$

$$CR = CI - RI \tag{4.2}$$

**Table 4.4** Pairwise comparison matrix and weightages of the parameters assigned using AHP

	Rainfall	Elevation	Slope	NDVI	BSI	SAVI	Distance from river	Weightage
Rainfall	1	2	2	3	3	4	5	0.285499
Elevation		1	2	3	3	4	5	0.234821
Slope			1	3	3	4	4	0.189104
NDVI				1	2	3	4	0.111195
BSI					1	3	4	0.0914571
TWI						1	3	0.0538256
Distance from River							1	0.0340976
Maximum eigen value = 7.45045								
Consistency index = 0.0750754								
Consistency ratio (consistency index/random consistency index) = 0.0750754/1.35 = 0.055611407								

**Table 4.5** Accuracy Assessment for LULC, 2000 using kappa coefficient, where overall accuracy is 95.62%

	River	Agriculture	Vegetation	Built-up	Barren land	Water body	Total (user)
River	21	0	0	0	0	0	21
Agriculture	0	32	1	1	0	0	34
Vegetation	0	1	59	0	0	0	60
Built-up	0	0	1	19	2	0	22
Barren land	0	0	0	0	9	0	9
Water body	0	0	0	1	0	13	14
Total (producer)	21	33	61	21	11	13	<b>160</b>

$$\begin{aligned}
 \text{Overall accuracy} &= \frac{\text{Total Number of Correctly Classified Pixels (Diagonal Elements)}}{\text{Total Number of Reference Pixels}} \times 100 \\
 &= \frac{153}{160} \times 100 \\
 &= 95.625\%
 \end{aligned}$$

$$\begin{aligned}
 \text{Kappa coefficient (K)} &= \frac{(TS \times TCS) - \sum (\text{Column Total} \times \text{Row Total})}{(TS)^2 - \sum (\text{Column Total} \times \text{Row Total})} \times 100 \\
 &= \frac{[(160 \times 153) - \{(21 \times 21) + (33 \times 34) + (61 \times 60) + (21 \times 22) + (9 \times 11) + (14 \times 13)\}]}{[(160)^2 - \{(21 \times 21) + (33 \times 34) + (61 \times 60) + (21 \times 22) + (9 \times 11) + (14 \times 13)\}]} \times 100 \\
 &= \frac{[24480 - 5966]}{[25600 - 5966]} \times 100 \\
 &= \frac{18514}{19634} \times 100 \\
 &= 94.29\%
 \end{aligned}$$

Here CI is consistency index, CR is consistency ratio, RI is random consistency index,  $\gamma_{Max}$  is computed average value of weight, and  $n$  is the number of parameters. There is a randomly generated comparison matrix according to Satty scale. CR has been computed to check the consistency of the judgment matrix. As per the Satty scale, for  $CR \leq 0.10$ , the matrix can be marked with satisfactory consistency.

Land use/land cover maps for 2000 and 2020 have been prepared to understand the impact of flood hazard on different land use patterns. The land use maps have been prepared based on Landsat 4–5 and Landsat 8 data. Landsat 4–5 Thematic Mapper (TM) images consist of seven spectral bands with a spatial resolution of 30 meters for Bands 1–5 and 7. Spatial resolution for Band 6 (thermal infrared) is 120 meters but is resampled to 30-meter pixels. The approximate scene size is 170 km north-south by 183 km east-west (106 mi by 114 mi). The used Landsat 8 data is 30 m spatial resolution having 11 bands. It is under UTM projection system of zone 45 and WGS84 ellipsoid. Accuracy assessment (Tables 4.5 and 4.6) has been performed to verify the reliability of the classification using Kappa coefficient. According to the kappa coefficient in 2000, over all accuracy is 95.26% and kappa coefficient (#x049A) is 94.29%. It has also calculated in 2020 LUSC map where 98.12% is overall and 97.64% is kappa coefficient (K).

**Table 4.6** Accuracy assessment for LULC, 2020 using kappa coefficient, where overall accuracy is 98.12%

	River	Agriculture	Vegetation	Built-up	Barren land	Water body	Total (user)
River	18	0	0	0	0	0	18
Agriculture	0	41	1	0	0	0	42
Vegetation	0	1	46	0	0	0	47
Built up	0	0	1	24	0	0	25
Barren land	0	0	0	0	15	0	15
Water body	0	0	0	0	0	13	13
Total (producer)	18	42	48	24	15	13	<b>160</b>

$$\text{Overall accuracy} = \frac{\text{Total Number of Correctly Classified Pixels (Diagonal Elements)}}{\text{Total Number of Reference Pixels}} \times 100$$

$$= \frac{157}{160} \times 100$$

$$= 98.125\%$$

$$\text{Kappa coefficient (K)} = \frac{(\text{TS} \times \text{TCS}) - \sum (\text{Column Total} \times \text{Row Total})}{(\text{TS})^2 - \sum (\text{Column Total} \times \text{Row Total})} \times 100$$

$$= \frac{[(160 \times 157) - \{(18 \times 18) + (42 \times 42) + (48 \times 47) + (24 \times 25) + (15 \times 15) + (9 \times 9)\}]}{[(160)^2 - \{(18 \times 18) + (42 \times 42) + (48 \times 47) + (24 \times 25) + (15 \times 15) + (9 \times 9)\}]} \times 100$$

$$= \frac{[25120 - 5250]}{[25600 - 5250]} \times 100$$

$$= \frac{19870}{20350} \times 100$$

$$= 97.64\%$$

## 4 Results

### 4.1 Elevation

The overall altitudinal pattern of the region is important to understand the areal extent of flood susceptible zones. The elevation of the considered study area has been classified under five classes – very high altitude (427–536 m), high altitude (317–426 m), moderate (207–316 m), gentle (97–206 m), and flat (50–96 m) (Fig. 4.2). The moderate altitudinal zone corresponds to the alluvial fan area of the foothill region whereas the gentle altitudinal zone corresponds with distal fan portions. The flat land in the southern-most part of the study area has been marked with several meandering rivers.

### 4.2 Slope

The slope of the entire region has been mapped categorizing into five classes – very steep slope (12.22–55.14 degree), steep slope (3.71–12.21 degree), moderate slope (2.03–3.7 degree), gentle slope (1.69–2.02 degree), and flat land (0–1.68 degree) (Fig. 4.3). It is noticed that the southern part of the study area is characterized by flat

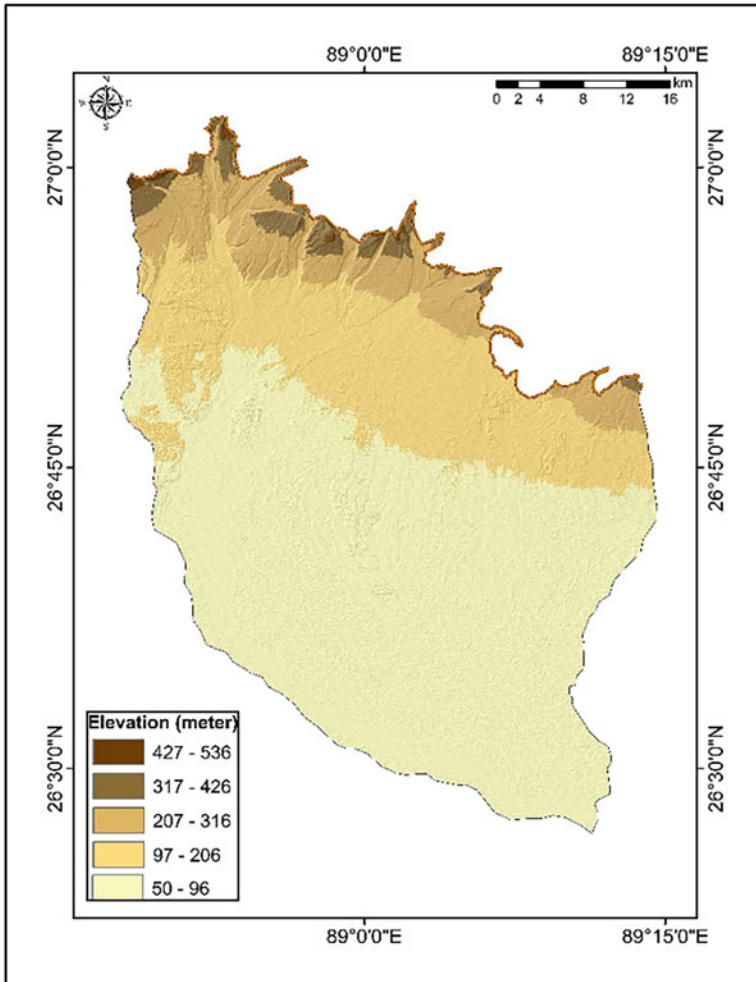


Fig. 4.2 Elevation map showing the altitudinal variation of the entire study area

land topography with very gentle slopes where the rivers have been characterized as meandering. On the other hand, in the frontal zone of the Himalayas, forested areas (Chapramari Reserve Forest, Maraghat Forest) have steep slopes.

### 4.3 Rainfall (Cm)

The mean rainfall map has been prepared based on five classes: class 1 (285.9–288.3 cm), class 2 (283.5–285.8 cm), class 3 (281.0–283.4 cm), class

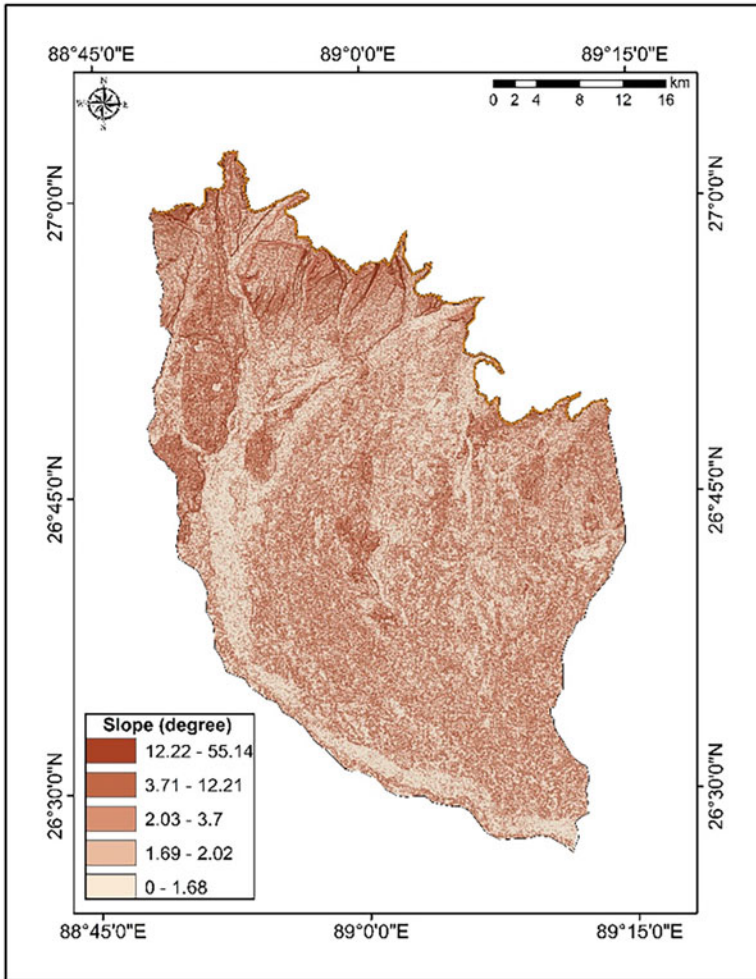


Fig. 4.3 Five classes of slope differentiation

4 (278.4–280.9), and class 5 (273.4–278.3 cm). It is to be noted that the eastern part of the map, which is drained by rivers Rohtikhola and Sukti, is receiving maximum amount of rainfall (285.9 cm). The amount of rainfall is decreasing from the eastern part of the area to the western part, which is drained by river Murti (Fig. 4.4).

### 5 Distance from Rivers (Meter)

The distance from rivers has been classified into five classes: class 1 (0–223.68 m), class 2 (223.69–306.84 m), class 3 (306.85–530.51 m), class 4 (530.52–1132.11 m), and class 5 (1132.12–2750.16 m) (Fig. 4.5).

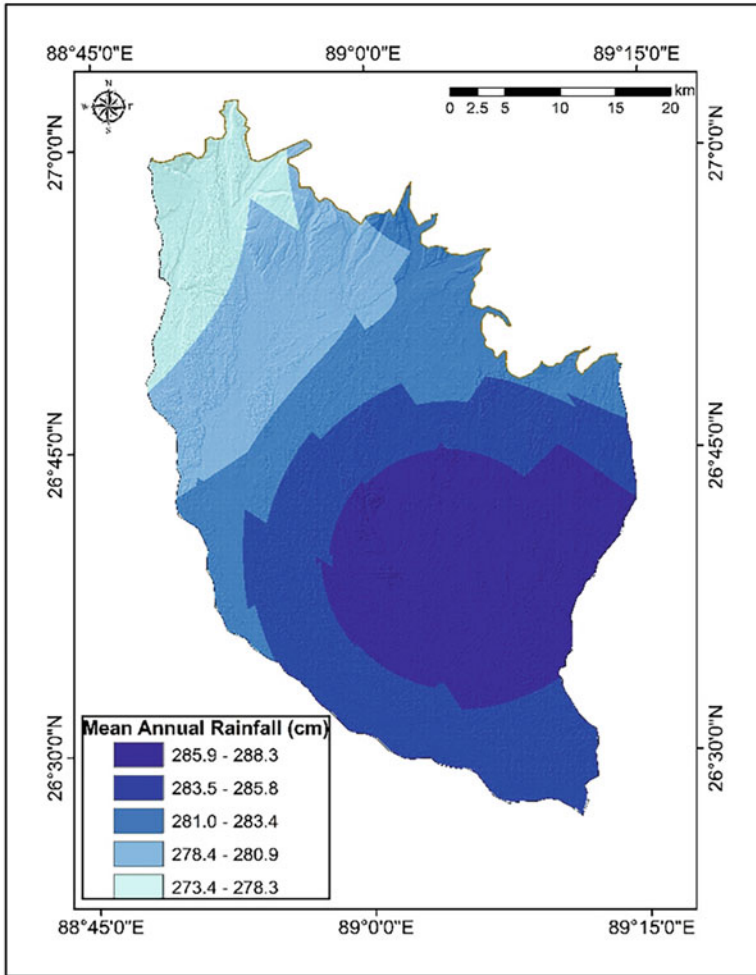


Fig. 4.4 Isohyet map of mean Rainfall of the study area

## 6 Normalized Difference Vegetation Index (NDVI)

In the considered study area, the maximum range of NDVI is 0.29–0.52, which corresponds to the dense forest region (part of Gorumara forest, Gairkata forest, Maraghat forest, and Chapramari.

Reserve forest) (Fig. 4.6). The agricultural plots of the alluvial fans including the tea gardens, which are on an elevated land, also represent higher values of NDVI (0.26–0.28). The southernmost part of the rivers represents very low value of NDVI, which indicates the bare land and less vegetation cover in that part.

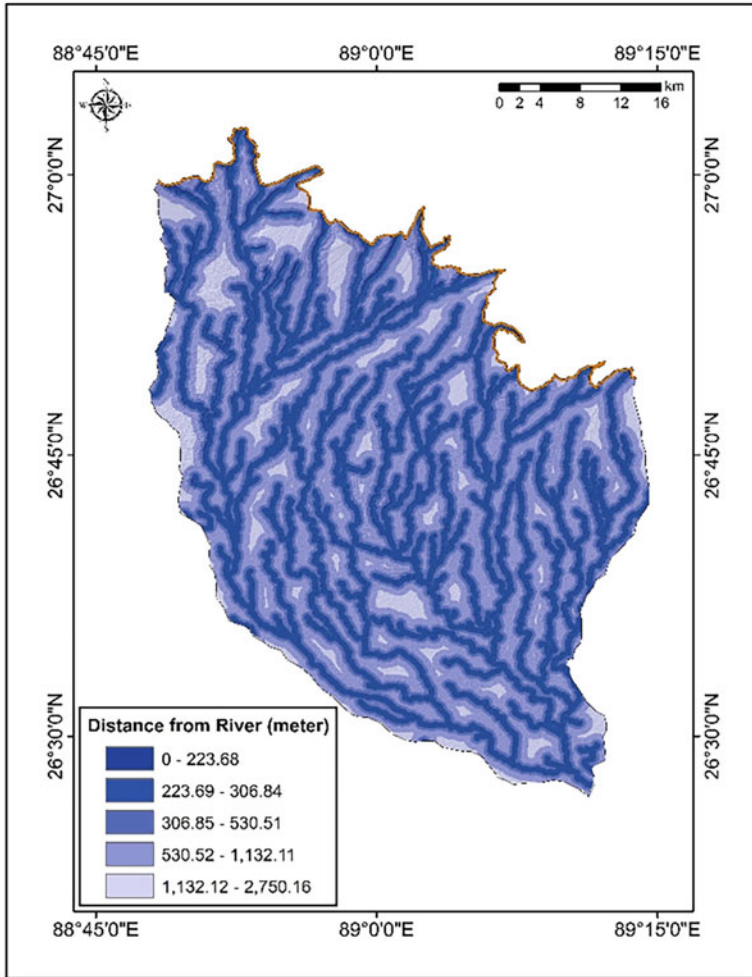
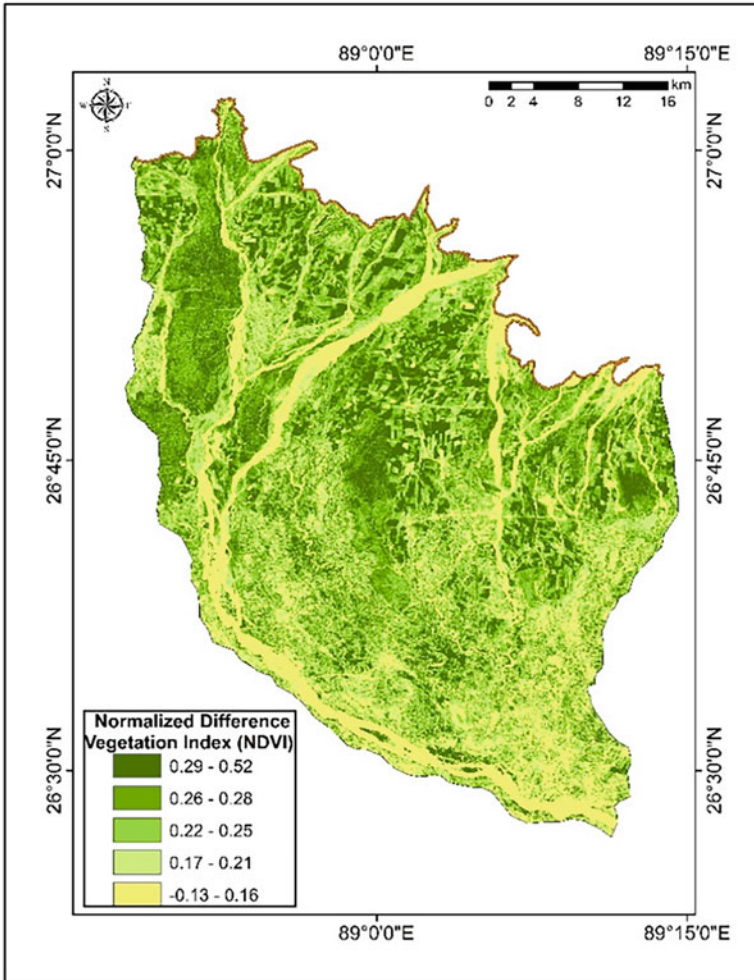


Fig. 4.5 Distance from River map showing five classes

## 7 Bare Soil Index (BSI)

Bare soil index has been classified into five classes: class 1 (0.01–0.14), class 2 (–0.04–0), class 3 (from –0.08 to –0.05), class 4 (from –0.12 to –0.09), and class 5 (from –0.28 to –0.13) (Fig. 4.7). The densely vegetated regions of the study area (part of Gorumara forest, Gaikata forest, Maraghat forest, and Chapramari Reserve forest correspond to lower values of BSI (from –0.28 to –0.13). The southern and western regions of the study area correspond to higher values of BSI (0.01–0.14), indicating less vegetation in the region.





**Fig. 4.6** Normalized Difference Vegetation Index (NDVI) map for visualizing 5 different classes of spatial distribution

### 8 Topographic Wetness Index (TWI)

TWI for the region has been classified into five classes: very high (12.55–18.06), high (9.03–12.54), moderate (6.78–9.02), low (5.35–6.77), and very low (3.09–5.34) (Fig. 4.8). It is to be noted that the areas in close proximity with the rivers portray higher values (12.55–9.03) of TWI.

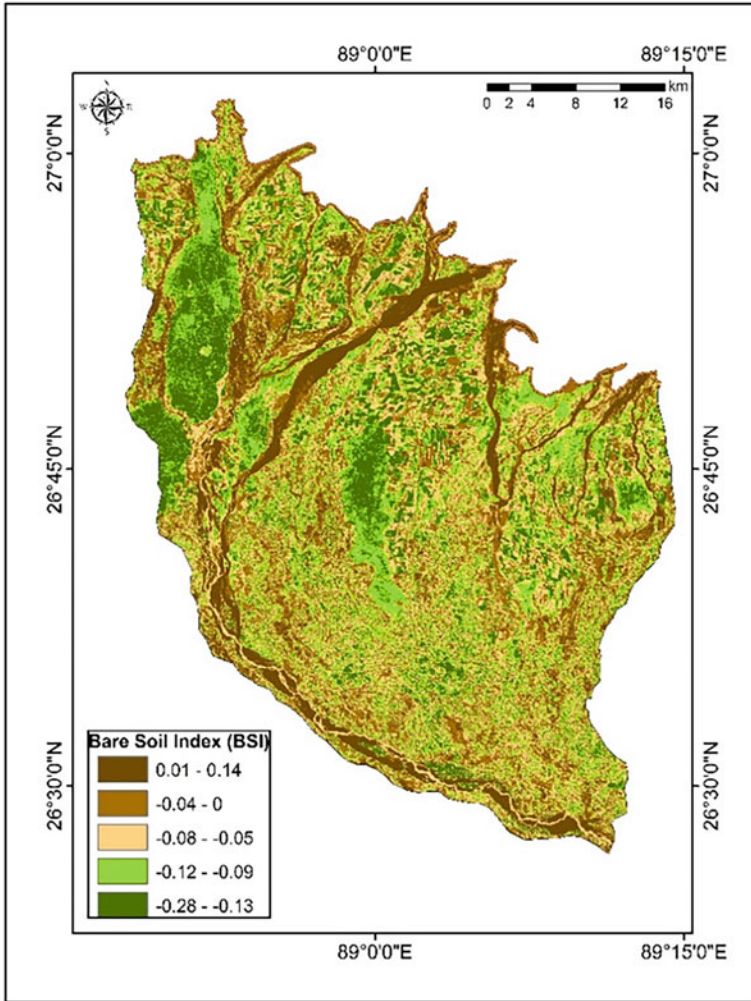
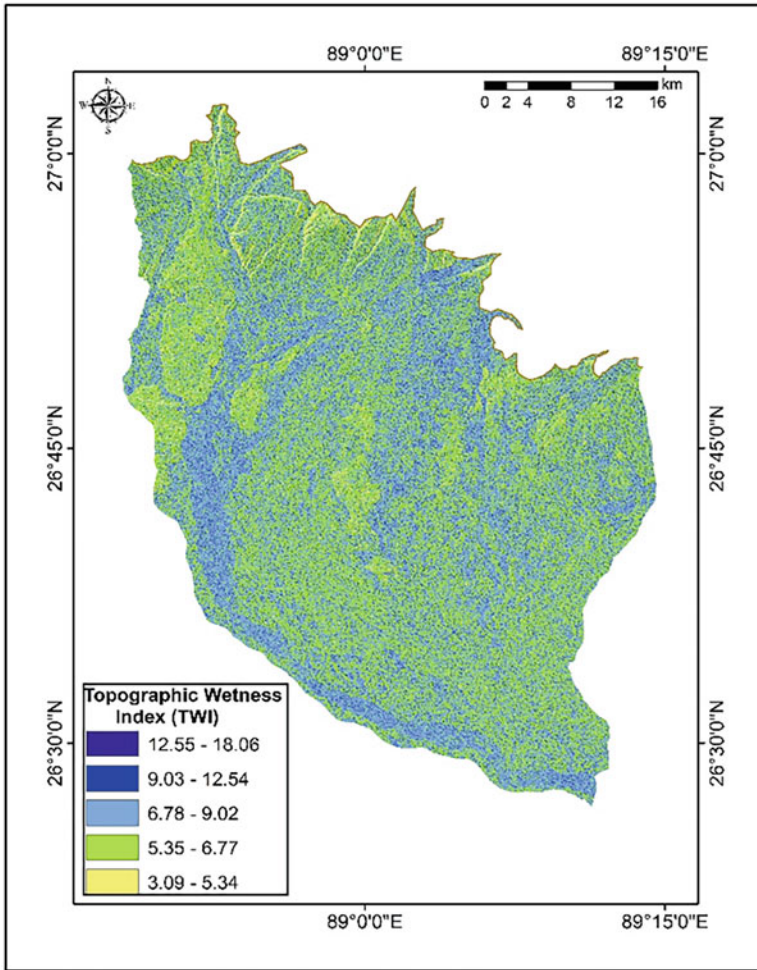


Fig. 4.7 Bare Soil Index (BSI) map of the study area

## 9 Flood Susceptibility Mapping

On the basis of the selected parameters, flood susceptibility map has been prepared, which has categorized the whole study area into five flood-susceptible classes (very high, high, moderate, low, and very low). Figure 4.9 portrays that the southern and western parts of the region specifically the region drained by rivers Rohtikhola and Sukti are very much susceptible to flood hazard risk. The narrow belt encircling the lower reaches of river Jaldhaka also seems to be susceptible to flood hazards. The region close to the higher reaches of the rivers is very less susceptible to flooding.



**Fig. 4.8** Map of soil-adjusted vegetation index (SAVI)

### 9.1 Validation

It is of utmost importance to validate any model and to verify the outcome of the study. In spatial earth science, the multi-criteria decision making model can best be validated with the help of area under curve (AUC) as it verifies the outcome of the model with comprehensiveness and simplicity (Malik et al., 2020; Darabi et al., 2019).

To verify the present model regarding flood susceptibility, several flood inventory points have been used from the AUC analysis. Previous research works, official documents from the Irrigation and Waterways Department, Govt. of West Bengal

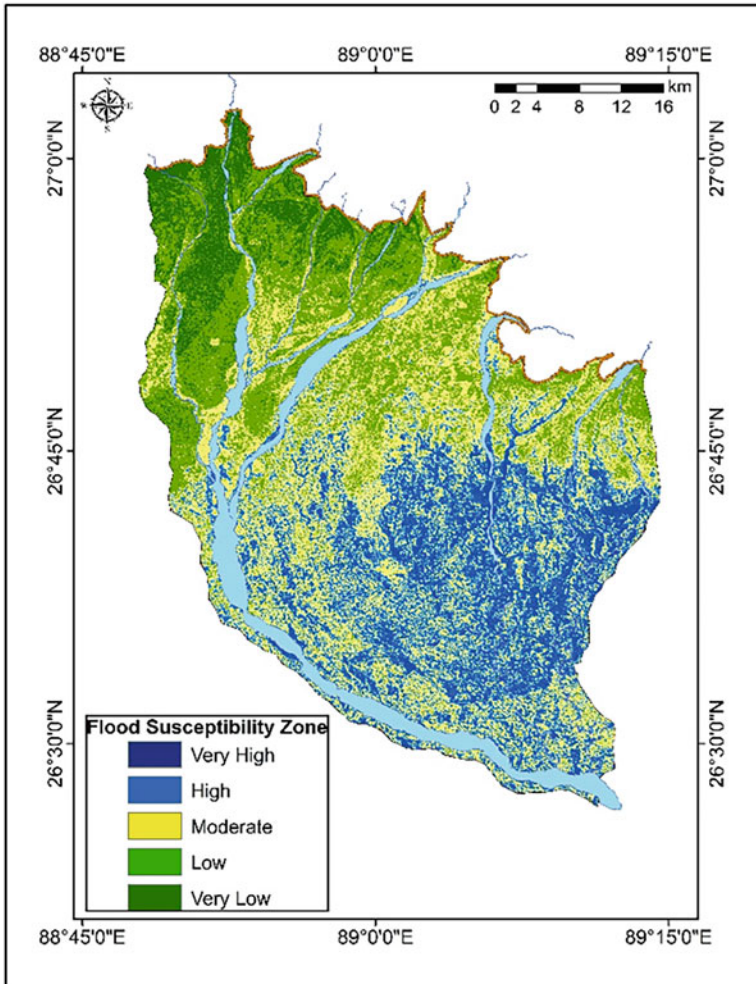
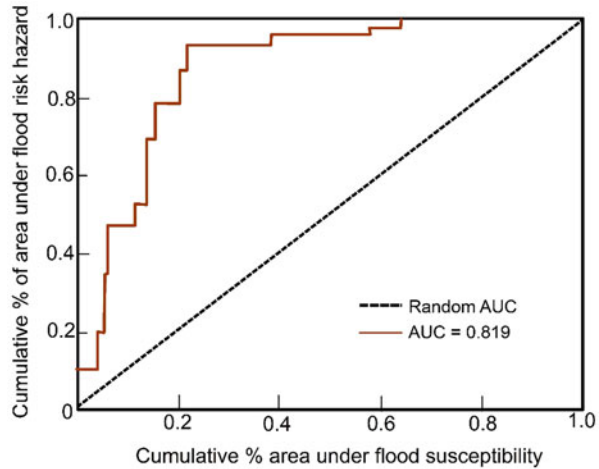


**Fig. 4.9** Flood susceptibility map based on analytic hierarchic process (AHP)

([www.wbiwb.gov.in/](http://www.wbiwb.gov.in/)), have been analyzed for the verification of the model with AUC.

Arabameri et al. (2019) and Rimba et al. (2017) have provided a classification of the accuracy of AUC curve as excellent (0.9–1.0), very good (0.80–0.90), good (0.70–0.80), poor (0.60–0.70), and weak (0.50–0.60). The computation of AUC has provided a value of 0.819 or 81.9%, which can be considered very good for the outcome of the model (Fig. 4.10).

**Fig. 4.10** Validation of the flood susceptibility model using area under curve (AUC)



## 10 Discussion

The present study evaluates the flood susceptibility zonation by applying the multi-criteria decision method based on a combination of hydrological and geomorphic indices. The altitudinal zonation of the study area reveals the fact that the low elevated land in the southern part is mostly prone to flood risk hazard as the flat land creates stagnation of the rainwater during monsoon season.

The apex and distal part of alluvial fans having higher altitudes propagate easy flow of the rainwater (Raha & Biswas, 2022a, b). The gradient of the land portrays the probability of easy flow of river discharge and heavy monsoonal rainwater. The region in close proximity to the Himalayan Mountain front having steeper slope (12.22–55.14 degree) initiates easy and quick flow of river water, which in turn reduces the risk of flood hazard in the upper reaches of the rivers and adjoining areas. The very gentle sloping rolling topography encircling the middle and lower reaches of rivers Jaldhaka, Rohtikhola, and Sukti is vulnerable to flood hazard as the flood water during peak discharge of the rivers gets accumulated for a longer period of time. Moreover, the rivers Rohtikhola, Sukti, and their tributaries flow in a meandering pattern over the gently sloped land, which helps to propagate flood in this region as the velocity of river discharge decrease. The catastrophic rainfall in the region can be attributed as a major flood-controlling factor. The eastern part of the region drained by rivers Rohtikhola and Sukti is highly susceptible to flooding. Distance from rivers is also playing a significant role determining flood susceptibility. However, it is important to note that this parameter is playing crucial role in the lower and middle course of the rivers where the flood risk is dependent upon the higher order streams having greater volume of discharge.

The first-order and second-order streams that join the main Jaldhaka in foothill section have little or no significance in propagating flood-like situation as the volume of discharge is much less. But the main Jaldhaka river is fifth-order stream, and the

huge water during monsoon is carried by the catchment tributaries that cover ~1745.4 km<sup>2</sup>. The vegetation cover seems to be a significant factor in controlling flood hazards. Vegetation cover helps in the infiltration of water, and it is strongly related with soil texture. The study area is mainly composed of sandy, sandy loamy and clay soil, which has infiltration rate of 20–30 mm/hour, 10–20 mm/year and 1–5 mm/year, respectively (<https://www.fao.org/3/s8684e/s8684e0a.htm>) (Fig. 4.11). The most flood susceptible zone is covered by sandy loam soil with bare surface, where bare soil index value ranges from -0.04 to -0.08 and the fluctuation of groundwater level (both rise and fall) is from 2–5 to 5–10 mbgl

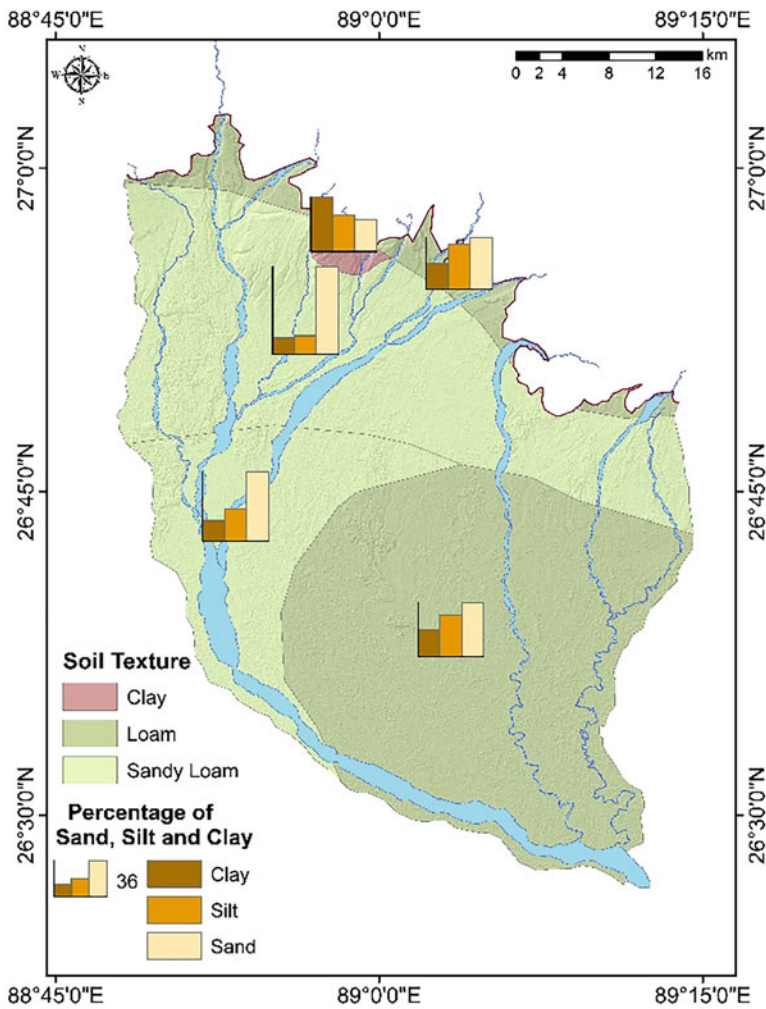


**Fig. 4.11** Soil texture map and % of sand, silt and clay (based on Food and Agriculture Organization (FAO))

(central groundwater board, ministry of Jal Shakti, department of water resources, river development, and ganga rejuvenation government of India). Therefore, due to the infiltration, groundwater gets recharged seasonally. The dense vegetated areas are thus not susceptible to flooding (Kaur et al., 2017).

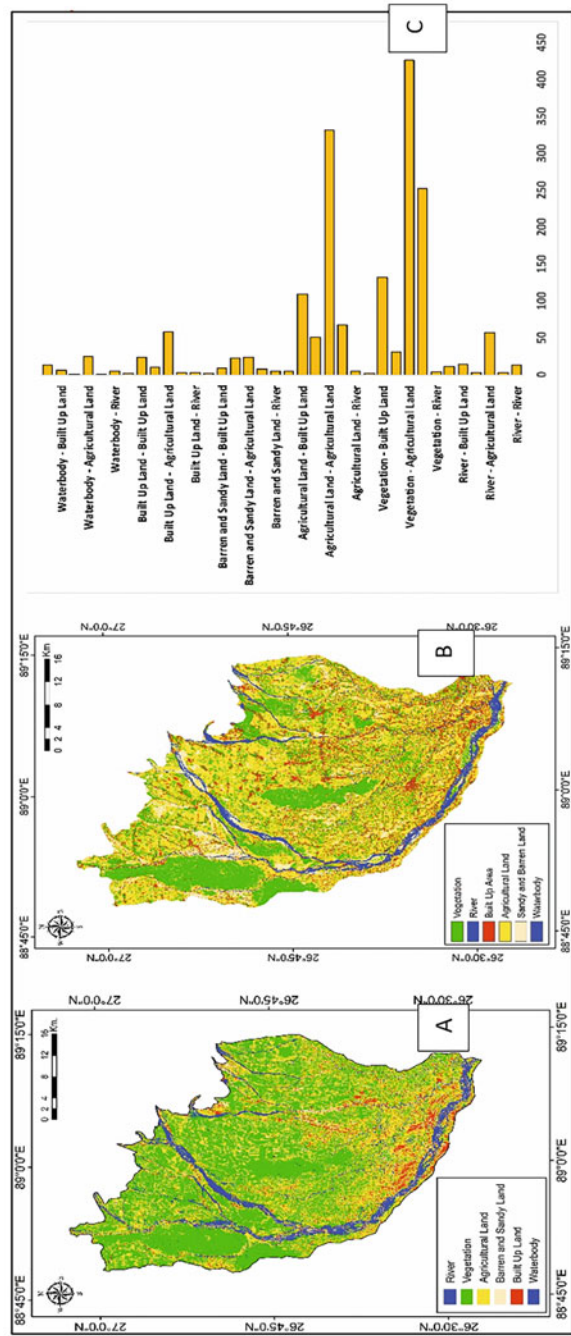
The bare surface of the southern part of the study area has lesser vegetation cover, which propagates flood hazard. It is interesting to note that among the different land use patterns (Fig. 4.12a–c), agricultural land and settlement are mostly affected by flood hazards. From 2000 to 2020 highest changes are found from vegetation to agricultural land (425.84 km<sup>2</sup>) and vegetation to settlement (132.52 km<sup>2</sup>). It specifies that vegetation has decreased and mostly been converted to agricultural land and settlement. These converted lands have increased the probability of flood as 40% of them are seasonally cultivated and exist as barren land that induce high run off rate. The higher susceptible is composed of sandy–loam soil, and the bareness of the lands insists it to be more prone to flood. Secondly, from 2000 to 2020, settlements have shifted toward the northern section due to flood in the lower Jaldhaka plains.

In the southeastern part of the study area, Khalaigram, East Dangapara, Salbari, and Malsagaon have been marked to be affected by frequent flood hazard. Construction of bridges and guide bunds also play an important role as during monsoon huge amount of water used to flow out through the narrow passage and in downstream water flashed out with high energy resulting flood and bank erosion. The comparison between the two land use maps enhances a significant outcome that the buildup area has been shifted and huge lands are transferred into an agricultural field, though it may be seasonally cultivated. Actually, these lands are most prone to be affected by floods in frequently.

Along with this, deaths of animals and people due to floods in the Himalayan foreland region also result in significant socioeconomic losses. Recurrent flooding affects a sizeable portion of the tea gardens and results in significant financial loss. After flood episodes, there is extensive sedimentation, which causes agricultural fields to lose fertility and production. Cropland flooding also destroys the agricultural output. A number of health problems are brought on by waterlogging in certain locations of Jalpaiguri, Alipurduar, and Cooch Behar. Building damage caused by bank failure is a frequent issue close to waterways.

Embankment breaches and spurs make the situation worse during a major flood. Occasionally, the percolation of dissolved minerals causes the quality of the groundwater to decrease. Taking an active, multidisciplinary approach is necessary for disaster management. Since the Himalayan foreland region experiences significant losses, flood management requires specific thought. Therefore, it is crucial to decrease flood threats' susceptibility. Building embankments along riverbanks can help shield the floodplain from repeated flooding episodes. Dykes and other structural control methods, such as spurs, may also be used. De-silting is a practical way to increase a river's carrying capacity in its lower sections, which can further aid to lessen flood susceptibility. To educate the general public about dangerous circumstances, community preparation is essential. Long-term watershed management should be implemented to reduce the negative consequences of flood episodes and to efficiently use the available natural resources.

**Fig. 4.12** (a) Land use/land cover map of 2000 depicting major land use pattern in the study area. (b) Land use/land cover map of 2020 depicting major land use pattern in the study area. (c) Percentage wise change from one land use pattern to another land use pattern between 2000 and 2020





## 11 Conclusion

The whole flood plains of West Bengal's Jalpaiguri and Alipurduar districts have experienced flooding. Environmental degradation, such as forest fires, forest cutting, deforestation, soil erosion, and slope divergence, makes rivers more sensitive to disruption, including the area of the Jaldhaka River basin investigated. The flood susceptibility map shows that the lowest reaches of all riverine portions are prone to flooding. The LU/LC pattern has shifted dramatically over the previous two decades. The majority of the flood-affected lands have been converted to agriculture, with large plots dedicated to seasonal cropping. The built-up area has grown. However, it is not concentrated or clustered in one location; rather, it is dispersed in a random pattern. However, natural vegetation coverage has reduced, potentially causing soil erosion, despite the fact that precipitation patterns have been consistent over the last 30 years, with the exception of a few exceptional years, such as floods in 1991, 1993, 1996, 2000, and 2013 (Govt. of West Bengal report 2013). However, the present study can be analyzed on block level to understand the vulnerability to floods in community level so that community preparedness programs can be adopted effectively. Along with the flood susceptibility mapping, flood hazard rating may be performed to analyze the flood risk zone. Flood hazard modeling may be executed to validate the susceptibility analysis.

## References

- Adnan, M., Dewan, A., Zannat, K., & Abdullah, A. (2019). The use of watershed geomorphic data in flash flood susceptibility zoning: A case study of the Karnaphuli and Sangu river basins of Bangladesh. *Natural Hazards*, 99(1), 425–448. <https://doi.org/10.1007/s11069-019-03749-3>
- Ahmad, M. (2018). Application of remote sensing and GIS for flood hazard management : A case study of Bihar (India). *Contemporary. Social Sciences*, 27(2), 69–77. <https://doi.org/10.29070/27/57466>
- Ahmed, A., Hewa, G., & Alrajhi, A. (2021). Flood susceptibility mapping using a geomorphometric approach in South Australian basins. *Natural Hazards*, 106(1), 629–653. <https://doi.org/10.1007/s11069-020-04481-z>
- Alam, A., Ahmed, B., & Sammonds, P. (2021). Flash flood susceptibility assessment using the parameters of drainage basin morphometry in SE Bangladesh. *Quaternary International*, 575–576, 295–307. <https://doi.org/10.1016/j.quaint.2020.04.047>
- Arabameri, A., Rezaei, K., Cerdà, A., Conoscenti, C., & Kalantari, Z. (2019). A comparison of statistical methods and multi-criteria decision making to map flood hazard susceptibility in Northern Iran. *Science of the Total Environment*, 660, 443–458. <https://doi.org/10.1016/j.scitotenv.2019.01.021>
- Astaras, T., Oikonomidis, D., & Mouratidis, A. (2011). *Psifiakí Chartografía kai Geografiká Systímata Pliroforión* [Digital Cartography and GIS]. Ekdóseis Dísigma [Disigma Publishing Group].
- Baez-Villanueva, O., Zambrano-Bigiarini, M., Ribbe, L., Nauditt, A., Giraldo-Osorio, J., & Thinh, N. (2018). Temporal and spatial evaluation of satellite rainfall estimates over different regions in Latin-America. *Atmospheric Research*, 213, 34–50. <https://doi.org/10.1016/j.atmosres.2018.05.011>

- Baky, M., Islam, M., & Paul, S. (2019). Flood hazard, vulnerability and risk assessment for different land use classes using a flow model. *Earth Systems and Environment*, 4(1), 225–244. <https://doi.org/10.1007/s41748-019-00141-w>
- Bhat, M., Alam, A., Ahmad, S., Farooq, H., & Ahmad, B. (2019). Flood hazard assessment of upper Jhelum basin using morphometric parameters. *Environmental Earth Sciences*, 78(2). <https://doi.org/10.1007/s12665-019-8046-1>
- Birkholz, S., Muro, M., Jeffrey, P., & Smith, H. (2014). Rethinking the relationship between flood risk perception and flood management. *Science of the Total Environment*, 478, 12–20. <https://doi.org/10.1016/j.scitotenv.2014.01.061>
- Biswas, M., & Banerjee, P. (2018). Bridge construction and river channel morphology—A comprehensive study of flow behavior and sediment size alteration of the river Chel, India. *Arabian Journal of Geosciences*, 1–23. <https://doi.org/10.1007/s12517-018-3789-7>
- Biswas, M., & Dhara, P. (2019). Evolutionary characteristics of meander cut-off—A hydro-morphological study of the Jalangi River, West Bengal, India. *Arabian Journal of Geosciences*, 12, 667. <https://doi.org/10.1007/s12517-019-4711-7>
- Bui, D. T., Ngo, P. T. T., Pham, T. D., Jaafari, A., Minh, N. Q., Hoa, P. V., & Samui, P. (2019, August). A novel hybrid approach based on a swarm intelligence optimized extreme learning machine for flash flood susceptibility mapping. *CATENA*, 179, 184–196. <https://doi.org/10.1016/j.catena.2019.04.009>
- Chakraborty, A., & Joshi, P. (2014). Mapping disaster vulnerability in India using analytical hierarchy process. *Geomatics, Natural Hazards and Risk*, 7(1), 308–325. <https://doi.org/10.1080/19475705.2014.897656>
- Chakraborty, S., & Mukhopadhyay, S. (2019). Assessing flood risk using analytical hierarchy process (AHP) and geographical information system (GIS): Application in Coochbehar district of West Bengal, India. *Natural Hazards*, 99(1), 247–274. <https://doi.org/10.1007/s11069-019-03737-7>
- Chang, H., & Franczyk, J. (2008). Climate change, land-use change, and floods: Toward an integrated assessment. *Geography Compass*, 2(5), 1549–1579. <https://doi.org/10.1111/j.1749-8198.2008.00136.x>
- Costache, R., Pham, Q., Sharifi, E., Linh, N., Abba, S., Vojtek, M., et al. (2019). Flash-flood susceptibility assessment using multi-criteria decision making and machine learning supported by remote sensing and GIS techniques. *Remote Sensing*, 12(1), 106. <https://doi.org/10.3390/rs12010106>
- CRED, U. (2015). *The human cost of natural disasters 2015: A global perspective*. Centre for Research on Epidemiology of Disasters, Université catholique de . . . , 2015.
- Dandapat, K., & Panda, G. (2017). Flood vulnerability analysis and risk assessment using analytical hierarchy process. *Modeling Earth Systems and Environment*, 3(4), 1627–1646. <https://doi.org/10.1007/s40808-017-0388-7>
- Darabi, H., Choubin, B., Rahmati, O., TorabiHaghighi, A., Pradhan, B., & Kløve, B. (2019). Urban flood risk mapping using the GARP and QUEST models: A comparative study of machine learning techniques. *Journal of Hydrology*, 569, 142–154. <https://doi.org/10.1016/j.jhydrol.2018.12.002>
- Das, S., & Sahu, A. (2017). Flood zonation mapping through RS and GIS techniques: A case study in Panskura of Purba Medinipur District, West Bengal. In S. Chatterjee (Ed.), *Indian journal of landscape systems and ecological studies* (pp. 126–135).
- Das, M., Chattopadhyay, A., & Basu, R. (2017). Spatial Flood Potential Mapping (SFPM) with flood probability and exposure indicators of flood vulnerability: Case study former Jalpaiguri District, West Bengal, India. *Journal of Geography & Natural Disasters*, 7(3). <https://doi.org/10.4172/2167-0587.1000210>
- Das, S. (2019). Geospatial mapping of flood susceptibility and hydro-geomorphic response to the floods in Ulhas basin, India. *Remote Sensing Applications: Society and Environment*, 14, 60–74. <https://doi.org/10.1016/j.rsase.2019.02.006>

- Dawod, G., Mirza, M., & Al-Ghamdi, K. (2012). GIS-based estimation of flood hazard impacts on road network in Makkah city, Saudi Arabia. *Environmental Earth Sciences*, 67(8), 2205–2215. <https://doi.org/10.1007/s12665-012-1660-9>
- Degiorgis, M., Gnecco, G., Gorni, S., Roth, G., Sanguineti, M., & Taramasso, A. (2012). Classifiers for the detection of flood-prone areas using remote sensed elevation data. *Journal of Hydrology*, 470–471, 302–315. <https://doi.org/10.1016/j.jhydrol.2012.09.006>
- Dewan, A. (2013). *Floods in a megacity: Geospatial techniques in assessing hazards, risk and vulnerability*. Springer.
- Dhar, O. N., & Nandargi, S. (2003). Hydrometeorological aspects of floods in India. *Natural Hazards*, 28(1), 1–33. <https://doi.org/10.1023/a:1021199714487>
- Domakinis, C., Mouratidis, A., Voudouris, K., Astaras, T., & Karypidou, M. (2020). Flood susceptibility mapping in Erythrotamos river basin with the aid of remote sensing and GIS. *AUC Geographica*, 55(2), 149–164. <https://doi.org/10.14712/23361980.2020.11>
- El Bastawesy, M., Attwa, M., Abdel Hafeez, T., & Gad, A. (2019). Flash floods and groundwater evaluation for the non-gauged dryland catchment using remote sensing, GIS and DC resistivity data: A case study from the Eastern Desert of Egypt. *Journal of African Earth Sciences*, 152, 245–255. <https://doi.org/10.1016/j.jafrearsci.2019.02.004>
- Ghosh, T. (2018). Floods and people, colonial North Bengal, 1871–1922. *Studies in People's History*, 5(1), 32–47. <https://doi.org/10.1177/2348448918759855>
- Ghosh, A., & Kar, S. (2018). Application of analytical hierarchy process (AHP) for flood risk assessment: A case study in Malda district of West Bengal, India. *Natural Hazards*, 94(1), 349–368. <https://doi.org/10.1007/s11069-018-3392-y>
- Hu, P., Zhang, Q., Shi, P., Chen, B., & Fang, J. (2018). Flood-induced mortality across the globe: Spatiotemporal pattern and influencing factors. *Science of the Total Environment*, 643, 171–182. <https://doi.org/10.1016/j.scitotenv.2018.06.197>
- Jarrett, R., & Tomlinson, E. (2000). Regional interdisciplinary paleoflood approach to assess extreme flood potential. *Water Resources Research*, 36(10), 2957–2984. <https://doi.org/10.1029/2000wr900098>
- Kabenge, M., Elaru, J., Wang, H., & Li, F. (2017). Characterizing flood hazard risk in data-scarce areas, using a remote sensing and GIS-based flood hazard index. *Natural Hazards*, 89(3), 1369–1387. <https://doi.org/10.1007/s11069-017-3024-y>
- Kale, V. S. (2004). *Floods in India: Their frequency and pattern. Coping with natural hazards: Indian context* (pp. 91–103). Orient Longman.
- Kaur, H., Gupta, S., Parkash, S., Thapa, R., & Mandal, R. (2017). Geospatial modelling of flood susceptibility pattern in a subtropical area of West Bengal, India. *Environmental Earth Sciences*, 76(9). <https://doi.org/10.1007/s12665-017-6667-9>
- Kazakis, N., Kougias, I., & Patsialis, T. (2015). Assessment of flood hazard areas at a regional scale using an index-based approach and analytical hierarchy process: Application in Rhodope–Evros region, Greece. *Science of the Total Environment*, 538, 555–563. <https://doi.org/10.1016/j.scitotenv.2015.08.055>
- Khosravi, K., Pourghasemi, H., Chapi, K., & Bahri, M. (2016). Flash flood susceptibility analysis and its mapping using different bivariate models in Iran: A comparison between Shannon's entropy, statistical index, and weighting factor models. *Environmental Monitoring and Assessment*, 188(12). <https://doi.org/10.1007/s10661-016-5665-9>
- Kowalzig. (2008). Climate, poverty, and justice: What the Poznań UN climate conference needs to deliver for a fair and effective global deal. *Oxfam Policy and Practice: Climate Change and Resilience*, 117–148.
- Li, C., Chai, Y., Yang, L., & Li, H. (2016). Spatio-temporal distribution of flood disasters and analysis of influencing factors in Africa. *Natural Hazards*, 82(1), 721–731. <https://doi.org/10.1007/s11069-016-2181-8>
- Mahmood, S., & Rahman, A. (2019). Flash flood susceptibility modeling using geo-morphometric and hydrological approaches in Panjkora Basin, Eastern Hindu Kush, Pakistan. *Environmental Earth Sciences*, 78(1). <https://doi.org/10.1007/s12665-018-8041-y>

- Malik, S., Chandra Pal, S., Chowdhuri, I., Chakraborty, R., Roy, P., & Das, B. (2020). Prediction of highly flood prone areas by GIS based heuristic and statistical model in a monsoon dominated region of Bengal Basin. *Remote Sensing Applications: Society and Environment*, 19, 100343. <https://doi.org/10.1016/j.rsase.2020.100343>
- Mandal, S., & Sarkar, S. (2016). Overprint of neotectonism along the course of River Chel, North Bengal, India. *Journal of Palaeogeography*, 5(3), 221–240. <https://doi.org/10.1016/j.jop.2016.05.004>
- Mojaddadi, H., Pradhan, B., Nampak, H., Ahmad, N., & Ghazali, A. H. B. (2017). Ensemble machine-learning-based geospatial approach for flood risk assessment using multi-sensor remote-sensing data and GIS. *Geomatics, Natural Hazards and Risk*, 8(2), 1080–1102. <https://doi.org/10.1080/19475705.2017.1294113>
- Mohamed, S., & El-Raey, M. (2019). Vulnerability assessment for flash floods using GIS spatial machine-learning-based sensed data in El-Arish City, North Sinai, Egypt. *Natural Hazards*, 102(2), 707–728. <https://doi.org/10.1007/s11069-019-03571-x>
- Mouratidis, A., & Sarti, F. (2012). Flash-flood monitoring and damage assessment with SAR data: Issues and future challenges for earth observation from space sustained by case studies from the Balkans and Eastern Europe. *Lecture Notes in Geoinformation and Cartography*, 125–136. [https://doi.org/10.1007/978-3-642-32714-8\\_8](https://doi.org/10.1007/978-3-642-32714-8_8)
- Mirzaei, S., Vafakhah, M., Pradhan, B., & Alavi, S. J. (2020, October 15). Flood susceptibility assessment using extreme gradient boosting (EGB), Iran. *Earth Science Informatics*, 14(1), 51–67. <https://doi.org/10.1007/s12145-020-00530-0>
- NBFCC. (1965). *Master plan of flood control and drainage improvement III the catchment of river Teesta, December, 1965*. Govt. of West Bengal.
- Patrikaki, O., Kazakis, N., Kougias, I., Patsialis, T., Theodossiou, N., & Voudouris, K. (2018). Assessing flood Hazard at river basin scale with an index-based approach: The case of Mouriki, Greece. *Geosciences*, 8(2), 50. <https://doi.org/10.3390/geosciences8020050>
- Paul, A., & Biswas, M. (2019). Changes in river bed terrain and its impact on flood propagation – A case study of River Jayanti, West Bengal, India. *Geomatics, Natural Hazards and Risk*, 10(1). <https://doi.org/10.1080/19475705.2019.1650124>
- Paul, G., Saha, S., & Hembram, T. (2019). Application of the GIS-based probabilistic models for mapping the flood susceptibility in Bansloi sub-basin of Ganga-Bhagirathi River and their comparison. *Remote Sensing in Earth Systems Sciences*, 2(2–3), 120–146. <https://doi.org/10.1007/s41976-019-00018-6>
- Quesada Román, A. (2021). Landslides and floods zonation using geomorphological analyses in a dynamic basin of Costa Rica. *Revista Cartográfica*, 102, 125–138. <https://doi.org/10.35424/rcarto.i102.901>
- Raha, A., & Biswas, M. (2022a). Himalayan foredeep neotectonics and deformed riverscape landforms: An integrated discussion, West Bengal, India. In H. N. Bhattacharya, S. Bhattacharya, B. C. Das, & A. Islam (Eds.), *Himalayan neotectonics and channel evolution* (Society of Earth Scientists Series). Springer. [https://doi.org/10.1007/978-3-030-95435-2\\_11](https://doi.org/10.1007/978-3-030-95435-2_11)
- Raha, A., & Biswas, M. (2022b). Quaternary alluvial fan dynamics of the Jaldhaka basin. *Journal of Mountain Science*, 19(8). <https://doi.org/10.1007/s11629-021-7005-y>
- Rahman, M., Ningsheng, C., Islam, M., Dewan, A., Iqbal, J., Washakh, R., & Shufeng, T. (2019). Flood susceptibility assessment in Bangladesh using machine learning and multi-criteria decision analysis. *Earth Systems and Environment*, 3(3), 585–601. <https://doi.org/10.1007/s41748-019-00123-y>
- Rai, P., & Mohan, K. (2014). Remote sensing data & GIS for flood risk zonation mapping in Varanasi District, India. *Forum Geografic*, XIII(1), 25–33. <https://doi.org/10.5775/fg.2067-4635.2014.041.i>
- Rastogi, A., Thakur, P., Rao, G., Aggarwal, S., Dadhwal, V., & Chauhan, P. (2018). Integrated flood study of bagmati river basin with hydro processing, flood inundation mapping & 1-D hydrodynamic modeling using remote sensing and GIS. *ISPRS Annals of the Photogrammetry*,

- Remote Sensing and Spatial Information Sciences, IV-5*, 165–172. <https://doi.org/10.5194/isprs-annals-iv-5-165-2018>
- Rimba, A., Setiawati, M., Sambah, A., & Miura, F. (2017). Physical flood vulnerability mapping applying geospatial techniques in Okazaki City, Aichi Prefecture, Japan. *Urban Science, 1*(1), 7. <https://doi.org/10.3390/urbansci1010007>
- Roy, S. (2011). *Flood hazards in Jalpaiguri District and its management* (Ph.D.). University of North Bengal.
- Roy, S., Bose, A., & Chowdhury, I. (2021). Flood risk assessment using geospatial data and multi-criteria decision approach: A study from historically active flood-prone region of Himalayan foothill, India. *Arabian Journal of Geosciences, 14*(11). <https://doi.org/10.1007/s12517-021-07324-8>
- Rozalis, S., Morin, E., Yair, Y., & Price, C. (2010). Flash flood prediction using an uncalibrated hydrological model and radar rainfall data in a Mediterranean watershed under changing hydrological conditions. *Journal of Hydrology, 394*(1–2), 245–255. <https://doi.org/10.1016/j.jhydrol.2010.03.021>
- Saaty, T. (1980). *The analytic hierarchy process: Planning, priority setting, resource allocation*. McGraw-Hill International Book Co. ISBN: 0070543712 9780070543713.
- Saaty, T. (1990). How to make a decision: The analytic hierarchy process. *European Journal of Operational Research, 48*(1), 9–26. [https://doi.org/10.1016/0377-2217\(90\)90057-1](https://doi.org/10.1016/0377-2217(90)90057-1)
- Sahu, A. (2014). A study on Moyna basin water-logged areas (India) using remote sensing and GIS methods and their contemporary economic significance. *Geography Journal, 2014*, 1–9. <https://doi.org/10.1155/2014/401324>
- Samanta, S., Koloa, C., Kumar Pal, D., & Palsamanta, B. (2016, August 2). Flood risk analysis in lower part of Markham river based on multi-criteria decision approach (MCDA). *Hydrology, 3* (3), 29. <https://doi.org/10.3390/hydrology3030029>
- Sankhua, R., Sharma, N., & Garg, P. (2015). Flood management through ANN-based spatio-temporal morphological model – A potential approach for the Brahmaputra.
- Sarkar, D., & Mondal, P. (2019). Flood vulnerability mapping using frequency ratio (FR) model: A case study on Kulik river basin, indo-Bangladesh Barind region. *Applied Water Science, 10*(1). <https://doi.org/10.1007/s13201-019-1102-x>
- Şener, Ş., Sener, E., & Karagüzel, R. (2010). Solid waste disposal site selection with GIS and AHP methodology: A case study in Senirkent–Uluborlu (Isparta) Basin, Turkey. *Environmental Monitoring and Assessment, 173*(1–4), 533–554. <https://doi.org/10.1007/s10661-010-1403-x>
- Shehata, M., & Mizunaga, H. (2018). Flash flood risk assessment for Kyushu Island. *Japan Environmental Earth Science*.
- Shrestha, U., Gautam, S., & Bawa, K. (2012). Widespread climate change in the Himalayas and associated changes in local ecosystems. *PLoS One, 7*(5), e36741. <https://doi.org/10.1371/journal.pone.0036741>
- Swain, K., Singha, C., & Nayak, L. (2020). Flood susceptibility mapping through the GIS-AHP technique using the cloud. *ISPRS International Journal of Geo-Information, 9*(12), 720. <https://doi.org/10.3390/ijgi9120720>
- Tehrany, M., Lee, M., Pradhan, B., Jebur, M., & Lee, S. (2014). Flood susceptibility mapping using integrated bivariate and multivariate statistical models. *Environmental Earth Sciences, 72*(10), 4001–4015. <https://doi.org/10.1007/s12665-014-3289-3>
- Tien Bui, D., Khosravi, K., Shahabi, H., Daggupati, P., Adamowski, J., Melesse, M. A., et al. (2019). Flood spatial Modeling in Northern Iran using remote sensing and GIS: A comparison between evidential belief functions and its ensemble with a multivariate logistic regression model. *Remote Sensing, 11*(13), 1589. <https://doi.org/10.3390/rs11131589>
- Woods, R., & Sivapalan, M. (1997). A connection between topographically driven runoff generation and channel network structure. *Water Resources Research, 33*(12), 2939–2950. <https://doi.org/10.1029/97wr01880>
- Yésou, H., Sarti, F., Tholey, N., Mouratidis, A., Clandillon, S., Huber, C., Stude R. M., & De Fraipont, P. (2013). *Addressing emergency flood mapping and monitoring of inland water*

- bodies with sentinel 1–2. Expectations and perspectives.* Living Planet Symposium, 9–13 September 2013, Edinburgh, UK, ESA SP-722.
- Youssef, A. M., Pradhan, B., & Hassan, A. M. (2010). Flash flood risk estimation along the St. Katherine road, southern Sinai, Egypt using GIS based morphometry and satellite imagery. *Environmental Earth Sciences*, 62(3), 611–623. <https://doi.org/10.1007/s12665-010-0551-1>
- Youssef, A., Pradhan, B., & Sefry, S. (2015). Flash flood susceptibility assessment in Jeddah city (Kingdom of Saudi Arabia) using bivariate and multivariate statistical models. *Environmental Earth Sciences*, 75(1). <https://doi.org/10.1007/s12665-015-4830-8>
- Zhong, S., Yang, L., Toloo, S., Wang, Z., Tong, S., Sun, X., et al. (2018). The long-term physical and psychological health impacts of flooding: A systematic mapping. *Science of the Total Environment*, 626, 165–194. <https://doi.org/10.1016/j.scitotenv.2018.01.041>
- Zhou, Z., Wang, X., Sun, R., Ao, X., Sun, X., & Song, M. (2014). Study of the comprehensive risk analysis of dam-break flooding based on the numerical simulation of flood routing. Part II: Model application and results. *Natural Hazards*, 72(2), 675–700. <https://doi.org/10.1007/s11069-013-1029-8>

# Chapter 5

## Flood Dynamics, River Erosion, and Vulnerability in the Catchment of Dharla and Dudhkumar Rivers in Bangladesh



Md Rejaur Rahman, Sabbir Ahmed Sweet, and A. H. M. Hedayatul Islam

**Abstract** Bangladesh is a land of rivers, and the major part of the country consists of deltaic landform by three large river systems, the Ganges, the Brahmaputra, and the Meghna. The livelihood of the people and environmental settings are mainly dependent on the hydrological characteristics of the rivers and associated resources in the catchment area. However, in the riverine areas of the country, flood is a common phenomenon that causes severe impact on people and properties. The effect of flood brings enormous sufferings to the inhabitants and causes riverbank erosion and loss and devastation to the resources and constructions. The alterations in river morphology as a result of flood have been related with bank line shifting, river widening, and extensive erosion of river bank. This chapter illustrates and analyzes the hydro-geomorphological conditions of the catchment of Dharla and Dudhkumar, which are the two perennial rivers in the north-western part of Bangladesh, and also provides a detailed understanding of inundation patterns and dynamics of floods in these catchments. This chapter further discusses and analyzes the causes and impact of floods, particularly on hydro-geomorphology, riverbank erosion, resource and live, and livelihood. Moreover, a flood vulnerability index was assessed considering the criteria for physical vulnerability, social vulnerability, and coping capacity indices. Finally, a management perspective approach and policy issues were drawn and discussed based on the findings. To fulfill the objectives, necessary data were collected and analyzed. Inundation data for the years 1954, 1974, 1988, 1998, 2004, and 2020 were used and analyzed for flood dynamics. Water level and discharge data of the two rivers were analyzed for hydrological conditions, and on the other hand, Landsat satellite data were analyzed to find out the geomorphological characteristics, river dynamics, and riverbank erosion. Flood vulnerability was assessed considering the IPCC vulnerability framework and GIS-aided multi-criteria analysis (GIS-MCA) modeling techniques. SRTM digital elevation model was used and analyzed for

---

M. R. Rahman (✉) · S. A. Sweet · A. H. M. H. Islam  
Department of Geography and Environmental Studies, University of Rajshahi, Rajshahi,  
Bangladesh  
e-mail: [rejaur@ru.ac.bd](mailto:rejaur@ru.ac.bd)

elevation and slope of the catchment area. Detail flood inundation and river dynamics, hydro-geomorphological characteristics, and erosion status of the Dharla and Dudhkumar Rivers were assessed and discussed in this chapter. Moreover, flood vulnerability assessment highlights the vulnerable areas with different magnitudes. Finally, this chapter concludes by discussing some management issues and policy implications for mitigating the adverse effects of such events, floods. The outcome of this work will be helpful to decisions and policymakers to minimize the exposure and vulnerability of floods. The overall approach discussed in this chapter can also help in achieving disaster risk reduction and ensure the safety of livelihood in the river floodplains.

**Keywords** Floods · River bank erosion · Flood vulnerability · Remote sensing · GIS-MCA · Flood management

## 1 Introduction

Flood is a main havoc to humans and the greatest hydrological hazard that causes huge destruction and losses. Bangladesh is a riverine country, and the riverine people mostly depend on the river and river-allied resources. Cyclones, storm surges, floods, riverbank erosions, and droughts are the major disaster in Bangladesh (Nasreen, 2004), and among them, flood became the most devastating disaster. In a river, flooding is a natural periodic event, and it occurs due to high flow of water that run over the river banks. Due to overflow and floods, water blow-outs over the river bank sides and usually causes indescribable misery for residents, crop damage, plants, infrastructure, hostile effects on economy, and so on. Since 80% of the total area of the country is under floodplain, these areas are subject to flooding regularly at different levels and cause pervasive damages (Sayed & Haruyama, 2016). Also, the majority of the population lives in floodplain with different exposure levels to river flooding and erosion (Tingsanchali & Karim, 2005). Flood is a key problem in Bangladesh and during the monsoon season, and at least 20–25% of areas are flooded. The occurrence and losses of flooding have amplified over the periods, and the flood of 1988 was the greatest one in terms of area inundation and damages in the last 100 years. In the year, the total inundated area was about 68% of the total area of the country, which was the highest in history (Islam et al., 2010), and 45 million people were directly affected (Brammer, 1990). The country faces huge losses due to the floods, and the total losses of 1988, 1998, and 2004 floods were about 2.0, 2.8, and 2.0 billion US dollars, respectively (Islam et al., 2010; Annual Flood Report, 2014). In the country, the rivers are unsteady, dynamics, and shifted over time mainly due to the bank erosion during the flood. Each year, bank erosion was observed about 2000 km along the river reaches mainly due to flood-induced flow dynamics (Pahlowan & Hossain, 2015). Changing patterns of the intensity and magnitude of floods in the last few decades is also one of the impacts of rainfall variability and climate change. It was reported that since 1950, the annual variability of floods and the area of major floods were increased (Bose & Navera, 2017). Similar



findings in rainfall and discharge were also observed. Therefore, rising water levels and flow patterns with high sediment load in the river during a flood are the main reasons for erosion (Bose & Navera, 2017). The Dharla and Dudhkumar are the two dominant perennial and trans-boundary rivers in the north-western part of Bangladesh, where river floods are a common phenomenon. In the monsoon season, about 25–30% of the area is inundated in these two river basin areas of the country. The causes of floods in the areas are monsoonal rainwater, melting of snow, upstream discharge, river siltation, etc. (FFWC, 2008). River morphology of Dharla and Dudhkumar and the Brahmaputra River, where these two rivers empty, has also great impact on floods. The floodplains of the rivers are mainly alluvial in nature and largely made by flood-borne deposits, whereas their bank materials be made of typically of fine-grained unified sediments (Azuma et al., 2007). All of these cause changes in the morphology of the river and over time affect the stability of the deposit, the river channel system, and its dynamics. The movement of rivers caused by floods is related to shifting, diverting, and extensive bank erosion.

Floods and floodplains are dynamic in nature. Adjacent areas along the river banks are floodplains that are regularly inundated. Due to erosion, accretion, and migration processes, river channels and floodplains are continuously changing. In addition, increased population pressures, various human activities, climate change, and variability are also accountable for floodplain change. The above conditions also affect the intensity, velocity, peak time, and risk of floods (Bradshaw et al., 2007; Vojinovic & Abbott, 2012). Owing to the constantly changing nature, it is necessary to examine how floodplains and other parts of river landform are influenced by floods. Among natural and anthropogenic hazards in the investigated area, i.e., Dharla and Dudhkumar River basin area, floods represent one of the main environmental hazards, causing major problems to humans, the environment, and development. Flood is a natural event and cannot be stopped completely. So, it would be better to take flood control and management measures and strategies to reduce the flood damage and risk. Nowadays, the involvement of advanced strategies, communities, and vulnerable people to implement a proper plan and policy and reduce the impact of floods is considered. Therefore, in addition to the engineering system, a nonengineering, i.e., nonstructural approach needs to be included. However, implementing structural solutions for flood control is more expensive, complex, and time-consuming. Thus, nonstructural measures can be an alternative solution to reduce flood damage and is more acceptable to avoid any adverse environmental conditions caused by floods. In order to formulate an effective nonstructural measure in a river basin, reliable and well-synthesized information on the historic inundation, nature, magnitude, causes and impact of flood along with the hydro-geomorphology, livelihood pattern, and flood vulnerability of the basin area are needed.

Understanding the dynamics and impacts and mitigating the floods are therefore very important since flood is controlled by deferent natural and human-induced processes. The frequency of floods has changed in recent times because of climate change, and it has become a major environmental concern, and it can affect the dynamics and vulnerability of floods. The potential relationship between existing human-induced outcomes on climate and flooding has been extensively discussed in

the Intergovernmental Panel on Climate Change (IPCC) assessment report (IPCC, 2007, 2014). Several reports indicate that the severity of future floods will be more intense with climate change and variability (Re, 2012; Rahman & Lateh, 2016, 2017). Therefore, researchers, policy makers, and concern authorities are more interested in understanding the underlying factors involved in flood vulnerability and risk (IPCC, 2012). Vulnerability assessment is considered an important tool for flood mitigation and management following nonstructural approaches (Nasiri et al., 2016). Floods increase economic losses through damage to infrastructure, resources, and farmland and cause indirect losses in flooded areas and even outside flooded areas. Thus, flood vulnerability assessment is crucial for formulating an appropriate management plan considering the various levels of vulnerability for flood adaptation and mitigation (Evans et al., 2004). The risks and risks of floods are both getting worse over time and have become a threat to society and the environment. Flood vulnerability in this century and beyond will be affected by the population growth, land use change, urbanization, economic growth in developing countries, climate change and its impact, etc. (He et al., 2013). Thus, physical, social, economic, and environmental parameters should be considered for flood vulnerability assessment in a river basin area. However, the level of vulnerability depends on the preparedness and ability to cope with the flood situation, which is called coping capacity, because vulnerability is associated with propensity, sensitivity, instability, weakness, and the absence of capability, which is in favor of destructive effects on exposed features (Cardona et al., 2012). Therefore, an extensive study of the process, components, and factors that affect temporal and spatial changes of flooding is important for flood risk reduction. Assessing the impact and vulnerability of floods on bank erosion, livelihoods, and assets is also imperative for flood hazard management to establish comprehensive planning and effective adaptation schemes.

Several studies indicate that the behavior of area inundation due to floods is an important issue to the researcher and policy makers (Bates et al., 2012). To understand the floodplain processes and flood inundation, laboratory experimentation (Knight & Shiono, 1996; Sellin & Willets, 1996), field investigation (Babaeyan-Koopaei et al., 2002; Nicholas & Mitchell, 2003), and remote sensing data interpretations and modeling (Alsdorf et al., 2007; Pavelsky & Smith, 2008; Schumann et al., 2008) are essential and playing a significant role. Nowadays, geoinformation technologies opened up scope of spatial data analysis and modeling the earth phenomena (Shekinah et al., 2004; Rahman, 2013; Rahman et al., 2018; Pandey et al., 2020), and particularly, these technologies are widely used in river and flood study and modeling (Xiong et al., 2019; Ge et al., 2020; He et al., 2021). On the other hand, several studies analyzed the impact of floods on riverbank erosion, bank line shift, and channel migration (Boyle et al., 1998; Kotoky et al., 2005; Pahlowan & Hossain, 2015); these all aspects of a river are vital and need to be addressed in the flood and river management related issues. Again, the underlying surface settings for assessing flood vulnerabilities (Ardıçlıoğlu & Kuriqi, 2019) require a broad consideration such as the effects of anthropogenic influences on floods, the effects of seasonality on flood events, the effects of floods on river geomorphology (Ali et al., 2019; Kuriqi et al., 2020), and the ambiguity of structural approaches to

flood management (Kuriqi et al., 2016). Owing to lack of information and flood hazard forecasting and many uncertainties in human activity, an inclusive evaluation of flood vulnerability is a major challenge at present.

The broad scope of this chapter is therefore to discuss the flood dynamics, erosion patterns, and vulnerability of floods in the two basin areas of Dharla and Dudhkumar Rivers, which are the two perennial rivers in the north-western part of Bangladesh. However, in particular, this chapter analyzes the nature and magnitude of inundation, hydro-geomorphological conditions, and erosion status of the catchment areas. This chapter also analyzes the causes and impact of floods, particularly riverbank erosion, which is the major natural disaster in the area. Further, this chapter analyzes and discusses the flood vulnerability considering the criteria for physical vulnerability, social vulnerability, and coping capacity, which highlights the vulnerable areas with different magnitudes. Finally, based on the results, a management perspective approach and policy issues were drawn and discussed.

## 2 Materials and Methods

### 2.1 Study Area

Dharla and Dudhkumar are the two trans-boundary rivers in the north-western part of Bangladesh. To analyze the flood dynamics, bank erosion, and flood vulnerability here in this chapter, the river catchment areas of these two rivers in Bangladesh are selected as study area (Fig. 5.1). The Dharla River runs among the countries India, Bhutan, and Bangladesh, and in Bangladesh, it enters at Lalmonirhat District. However, near Patgram upazila, it flows eastward and runs again into India. It then travels southwards direction and reenters Bangladesh at Fulbari upazila of Kurigram District and continue to flow up to falls into the river Jamuna near Kurigram District (Chowdhury, 2012). The Dharla River is a tributary of the Jamuna river and originates in Cooch Behar, India. The upper course of the Dharla River is known as the Jaldhaka or Singimari. In Bangladesh, the length of the river is about 54 km, and the total catchment area is about 1084 km<sup>2</sup>. During the monsoon, the river becomes wide and rough and suffers severe erosion. In 1947, it completely washed away the old place of Kurigram town.

Dudhkumar is a river in the northwestern part of Bangladesh (Fig. 5.1) and originates in the foothills of the Himalayas in Bhutan and flows southeast through India and then enters Bangladesh and empties as a tributary of the Jamuna River at Nunkhawa (BWDB, 2011). The name of this river in West Bengal, India, is Raidak or the Sankosh River, and when it enters Bangladesh near Pateshwari of Bhurungamari Upazila in Kurigram District, it is renamed as the Dudhkumar (Pal et al., 2017). The river is about 55 km long in Bangladesh, and the catchment area is about 490 km<sup>2</sup>. Satkuradara, Phulkumar River, Giraikhal, Dikdaridara, and Santashikhal are the notable tributaries of the Dudhkumar River in Bangladesh (Pal et al., 2017). Topography (elevation) within the catchment area varies from

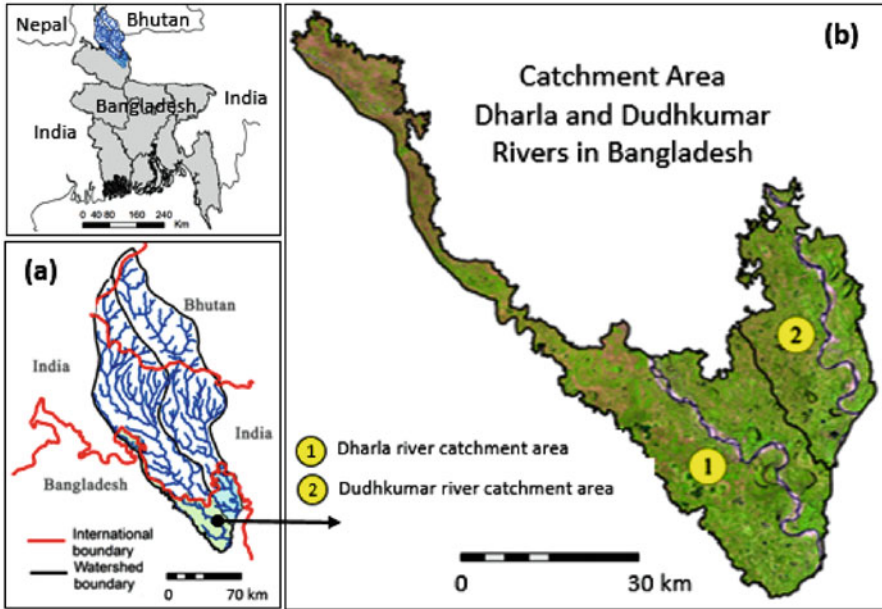


**Fig. 5.1** Catchment area: (a) total catchment area of Dharla and Dudhkumar Rivers and (b) study area: catchment area of Dharla and Dudhkumar River in Bangladesh

20 to 77 m, and the land slope (aspect) is from the northwest to the southeast. Although the area is generally flat, some localized low-lying areas are locally known as *beel*. In the catchment areas of Dharla and Dudhkumar, these two rivers lead the problems of flood, erosion, and drainage congestion significantly. During the monsoon, high water levels and discharges cause flooding along the river plains of Dharla and Dudhkumar, which in turn erodes river banks and destroys homes and human settlements along the river. Thus, availability of water, river, and flood dynamics and vulnerability of floods of these two important rivers are very vital for sustainable livelihood, flood planning and management, and optimum usage of natural resources.

## 2.2 Data Used and Methodology

To fulfill the objectives and required analysis here in this chapter, necessary data were collected, processed, and analyzed. The used data in this work are mainly secondary data and collected from various sources. A list of used data and their sources is given in Table 5.1.

Major flood maps of Bangladesh for the years 1954, 1974, 1988, 1998, 2004, and 2020 were collected from the Bangladesh Water Development Board (BWDB,

**Table 5.1** Data used and sources

Data	Source	Characteristics	Time
Flood maps	Bangladesh Water Development Board (BWDB), CEGIS	Affected area of major floods	1954, 1974, 1988, 1998, 2004, 2020
Elevation, slope	SRTM DEM ( <a href="https://earthexplorer.usgs.gov">https://earthexplorer.usgs.gov</a> )	Surface height from MSL, slope	
Rainfall	Bangladesh Meteorological Department, BMD (2000–2020)	Station wise data (Rangpur)	2000–2019
LULC	Esri Inc. USA <a href="https://www.arcgis.com/home/item.html?id=fc92d38533d440078f17678ebc20e8e2">https://www.arcgis.com/home/item.html?id=fc92d38533d440078f17678ebc20e8e2</a>	Land use/land cover using Sentinel-2, 10 m spatial resolution	2020
Water level	Bangladesh Water Development Board (BWDB)	Water level data of the two rivers, Dharla and Dudhkumar	1946–2008
Discharge	Bangladesh Water Development Board (BWDB)	Water level data of the two rivers, Dharla and Dudhkumar	1968–2005
Socioeconomic data	Population and housing census 2011 (Union wise), LGED	<i>Upazila</i> and <i>Union</i> wise data (Population, drinking water source, health center, educational institute)	2011
River bank line	Landsat TM and OLI images	Digital bank line	1992–2020

2021) and Centre for Environment and GIS (CEGIS, 2021), and digital flood maps were generated individually for the study area using GIS technique. All the flood maps were then superimposed, and the intensity of observed flooded areas was calculated spatially in the ArcGIS environment. To generate the elevation and slope maps, Shuttle Radar Terrain Mission Digital Elevation Model (SRTM DEM) (USGS, 2021) was used with the GIS technique. A land use/land cover map generated by Esri Inc. using Sentinel-2 was used (ESRI, 2020). Land use/land cover for the study area was extracted from this map. Riverbank lines were generated using geocoded Landsat TM and OLI images for the years 1992, 2000, 2011, and 2020. From the false color composite (FCC) of the three bands (near infrared, red, and green) of Landsat TM and OLI sensors, bank lines were digitized and extracted to define the river course extend in the stipulated time frame. After extraction of bank lines from the satellite images, to measure the temporal bank line shift, erosion, and accretion, bank lines were analyzed. Boolean logic and overlay with ArcGIS were used for these purposes. To identify the erosion and accretion areas of the rivers, two successive years of bank lines were superimposed and analyzed. Moreover, for analyzing the bank lines shift, accretion, and erosion, 20 fixed cross-sections covering each river (Dharla and Dudhkumar) reach were selected and analyzed (Fig. 5.5). Statistics of erosion and accretion for all the above years were calculated using ArcGIS software for polygon areas with the shifting bank lines. Moreover, the width of the river was calculated at each cross-section first, and then the average width was

measured. Besides, all the required socioeconomic data were processed, and spatial layers were generated in a GIS environment with ArcGIS. The river catchment area was delineated from the SRTM DEM through the GIS technique and ArcGIS.

For flood vulnerability mapping and vulnerable area identification, GIS-aided multi-criteria analysis (GIS-MCA) modeling technique was used. In the MCE process, the first step is the selection of the criteria. Thus, 15 criteria were selected and grouped into three vulnerability components, namely physical, social, and coping capacity (Table 5.2). Considering these three components, flood vulnerability was assessed. GIS and RS techniques were used to generate the spatial thematic layer for selected 15 criteria under three vulnerability components. Each spatial thematic level was then classified as very high, high, medium, low, and very low, which represented flood vulnerability levels (Table 5.2). Here, 1–5 scale levels of flood vulnerability were used where 1 refers to the lowest level and 5 refers to the highest level of vulnerability (Table 5.2). Afterwards, for more meaningful representation, all criteria were standardized into 0–10 scale using Eq. 5.1.

$$S_c = \frac{x - x_{\min}}{x_{\max} - x_{\min}} \times 10, \quad (5.1)$$

where  $s_c$  = standardized criteria,  $x$  = cell value of the criteria,  $x_{\min}$  = minimum value of each criteria, and  $x_{\max}$  = maximum value of each criteria.

After standardization, weights were assigned for each criterion considering the relative importance of the criterion with others for vulnerability. Here, we used the AHP decision-making algorithm to weight the criteria of physical, social, and coping capacity components, which is an important and meaningful method for evaluating multi-criteria (Rahman & Saha, 2007; Rahman et al., 2009, 2014, 2020; Shahabi & Hashim, 2015). For each vulnerability component, the pair-wise matrix was created with a 1–9 scale of relative importance proposed by Saaty (1977), and consistency ratio (CR) was considered within the acceptable level ( $\leq 0.1$ ) (Malczewski, 2010). The calculated weights are presented in Table 5.2. Once the weights for all the criteria were developed under the vulnerability components (i.e., physical, social, and coping capacity), the GIS-MCE approach was used to combine the criteria for generating each vulnerable component index map. Here, to complete the multi-criteria approach using Eq. 5.2, the weighted linear combination (WLC) method was followed (Voogd, 1983; Zopounidis & Doumpos, 2002). Afterwards, vulnerability maps were categorized into five classes namely very low, low, moderate, high, and very high zone.

$$S_i = \sum_{i=1}^n X_i \times W_i, \quad (5.2)$$

where  $S_i$  is the vulnerability index of the component  $i$  (i.e., physical, social, or coping capacity),  $X_i$  is the standardized score of criterion  $i$ ,  $W_i$  is the weight of criterion, and  $n$  is the total number of criteria.

**Table 5.2** Criteria and weights for flood vulnerability assessment

Component/ vulnerability	Criteria	Ranking (based on vulnerability concept)					Criteria weight	CR
		Very low (1)	Low (2)	Moderate (3)	High (4)	Very high (5)		
Physical vulnerability	Elevation (m)	>57	44-57	34-44	29-34	<29	0.113	0.01
	Slope (%)	>6.56	3.74-6.56	2.14-3.74	.93-2.14	<.93	0.050	
	Land use/land cover (LULC)	Water bodies	Bare land	Vegetation	Cropland	Built-up area	0.118	
	Rainfall (mm/year)	<2012	2012-2029	2029-2045	2045-2062	>2062	0.063	
	Distance to river (m)	>2400	1800-2400	1200-1800	600-1200	<600	0.260	
	Drainage density (per sq.km)	<.29	0.29-0.62	.62-.93	0.93-1.28	>1.28	0.118	
	Observed flood (flood frequency)	No flood	1	2-3	4-5	>5	0.332	
	Population density (per sq.km)	<700	700-900	900-1100	1100-1300	>1300	0.145	
	Female population (%)	<49.66	49.66-50.25	50.25-50.96	50.96-51.88	>51.88	0.353	
	Dependent population (%)	<22.95	22.95-23.91	23.91-24.93	24.93-26.44	>26.44	0.353	
Social vulnerability	Household with tube well water source (%)	>7.43	6.25-7.43	5.08-6.25	3.9-5.08	<3.9	0.058	
	Household with water-sealed sanitation (%)	>11.62	10.05-11.62	8.47-10.05	6.8-8.47	<6.8	0.091	
	Literacy rate (%)	>51.91	45.56-51.91	39.89-45.56	32.85-39.89	<32.85	0.122	
Coping capacity	Distance to school (m)	<600	1200	1800	2400	>2400	0.557	
	Distance to health center (km)	<2	2-4	4-6	6-8	>8	0.320	

Finally, by means of the physical and social vulnerability and coping capacity index maps, potential vulnerability to flooding (combining the two vulnerability components: physical and social) and flood vulnerability (considering the coping capacity with potential vulnerability) were assessed using Eqs. 5.3 and 5.4, respectively (Hoque et al., 2019, 2021; Biswas et al., 2015).

$$Pvi_f = Pv_f \times Sv_f, \quad (5.3)$$

$$Fvi = \frac{Pv_f \times Sv_f}{Cc_f}, \quad (5.4)$$

where  $Pvi_f$  is the potential vulnerability index to flood,  $Fvi$  is the flood vulnerability index,  $Pv_f$  is the physical vulnerability to flood,  $Sv_f$  is the Social vulnerability to flood, and  $Cc_f$  is the coping capacity to flood.

### 3 Flood Dynamics: Nature and Magnitude

Flood is a dynamic phenomenon and propagates through space and time. The catchment areas of the Dharla and Dudhkumar Rivers are very prone to flooding. The country has a record of historically devastating floods and has adversely affected people and resources, the study area is not an exception from this. In the country, historically, there were some major floods that occurred in 1954, 1974, 1988, and 1998. More recent major floods include 2004 and 2020. More than 65% of the country could be inundated during the catastrophic floods, as it was about 35%, 52%, and 67% in 1974, 1988, and 1998, respectively (Kabir & Hossen, 2019). Statistical analysis of the available records shows that there can be severe floods every 7 years and catastrophic floods every 33–50 years. In Dharla and Dudhkumar catchment areas, similar inundation pattern was observed (Fig. 5.2). In 1954, about 50% of the catchment area of the Dharla River was flooded, while about 48% of the catchment area of the Dudhkumar River was inundated (Fig. 5.2a). Except the year 1974, in all the major flooded years, i.e., 1988, 1998, 2004, and 2020, inundated areas were more than 50% of the catchment area of the Dharla and Dudhkumar Rivers. The highest recorded flooded area was noticed in 2020, which was about 66% and 71% of the total catchment area of Dharla and Dudhkumar, respectively. The Dharla River was at its peak in Taluk-Shimulbari and Kurigram, with 31.88 m and 27.57 m, respectively. On the other hand, the flood peak of the Dudhkumar River at Pateshwari and Nunkhawa were recorded 31.52 m and 28.07 m, respectively (BWDB, 2021). Figure 5.2a further indicates that the flooded area increased in the recent major floods in both the catchment areas. Moreover, Fig. 5.2a depicts the spatial pattern of the flooded area over space and time. Historically, in the lower river reach areas of Dharla and Dudhkumar catchments, more specifically southern, eastern and north



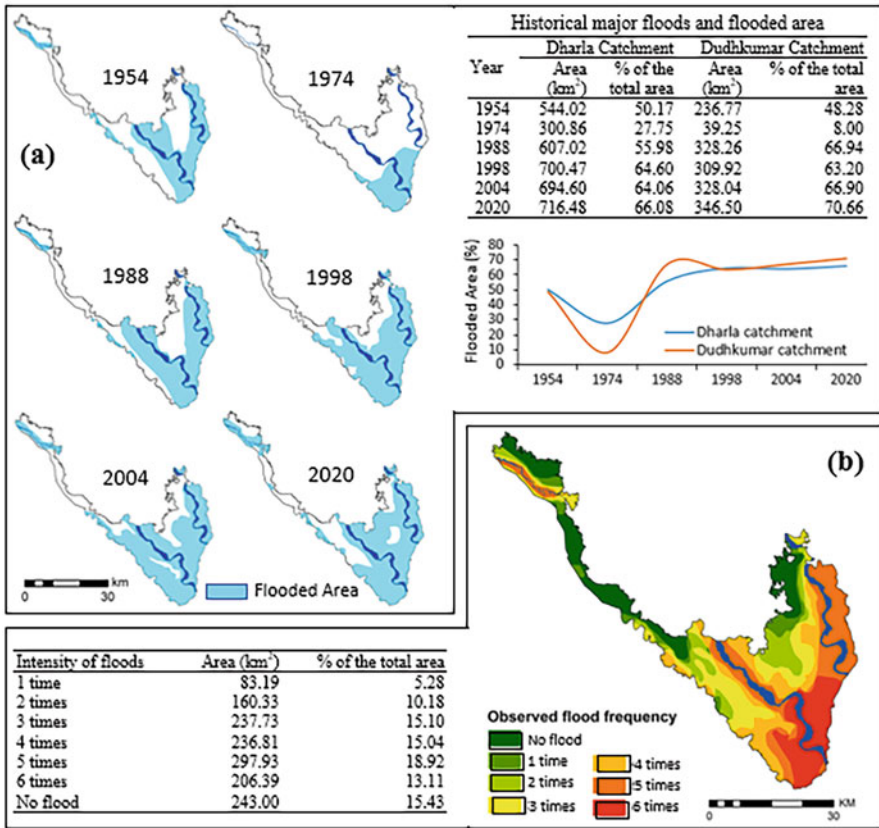


**Fig. 5.2** Flood dynamic and magnitude in Dharla and Dudhkumar catchment: (a) flooded area over space and time and (b) magnitude of flooded area

eastern parts of the area, floods are common and occurred frequently. Therefore, in these areas, the intensity of floods was observed very high (4–6 times) and located near the river course areas (Fig. 5.2b). Very high intensity flooded areas were observed in 47% of the total catchment areas. Thus, the dynamics of the flooded area and magnitudes indicate both the catchment areas of these two rivers are very prone to floods and flooding is a major problem in the areas.

### 4 Causing of Floods

Due to physico-environmental setting, flood occurs regularly in Bangladesh and in the study area as well. There are many factors that cause floods and allowed the floods to be worse. Flood happens naturally, but human activities intensified the flood risk in the area. In addition, severe floods due to extreme hydro- and weather-

related events at unexpected levels and frequencies can be detrimental to people, livelihoods, and resources. Broadly, the causes of river flooding can be grouped into two, natural and anthropogenic. These are discussed in the following sections.

#### **4.1 *Natural Causes***

The main natural causes of flooding in the catchment of Dharla and Dudhkumar Rivers are low topography, floodplain area, high rainfall in riverine areas and the upstream areas/country, high peak flow, and water level in the rivers, river siltation, lateral river contraction, etc. Almost all of the catchment areas consist of a meander floodplain (95% of the total catchment area), and the rest of the area is under active floodplain (BARC, 2016). About 41% area of the Dharla River catchment is found under the peak water level (31.88 m PWD), while about 59% of the Dudhkumar catchment area is found under the peak water level (31.52 m PWD), and these peak levels are much higher the danger level of the rivers. The catchment areas experience heavy monsoon rains, 1772 mm on average in the area, and the highest recorded rainfall was 2593 mm. The heavy rainfall in the monsoon season along with high flow from the upper stream increase the water level and peak flow that cause flood in the catchment areas. In the area, the peak water level was recorded 31.88 m PWD and 31.52 m PWD and peak flow (discharge)  $7600 \text{ m}^3 \text{ s}^{-1}$  and  $9250 \text{ m}^3 \text{ s}^{-1}$  in Dharla and Dudhkumar Rivers, respectively. These all can be linked with high flooded areas and areas to be flooded. Moreover, the Dharla and Dudhkumar Rivers were more navigable years ago and were presently a less navigable channel. The depth of the rivers reduces remarkably due to the flow variability and siltation. The rise of the river bed after sedimentation causes a reduction of the water-holding capacity of the river, resulting in floods. The reduced river bed height through sedimentation is an important cause for increased extreme flooding situations in Bangladesh (Choudhury, 2009). Filling the riverbed reduces the water holding capacity of the river causing the banks to overflow, and thus, reducing the depth of the riverbed increases the flooding in the catchment areas.

#### **4.2 *Anthropogenic Causes***

Human activities have a great influence on floods. Floods are gradually becoming more vulnerable due not only to natural causes but also to human influence in the floodplain areas. The rapid increase of population and urbanization has escalated the flood risk in the area; in the floodplains, the persistent poverty forces people to live in floodplains. In the catchment areas, during the last 40 years, total and urban populations have increased about 35% and 15%, respectively. Human-induced global warming is blamed to increase rainfall and variability in the area that causes increased magnitude and frequency of floods. In the catchments, during the last

40 years, rainfall increased about 5.5% and high rainfall variability (22.25–25.76% per year) were observed (Rahman & Lateh, 2017). Since Dharla and Dudhkumar are two trans-boundary rivers, the flooding in the catchments mostly depends on the upstream characteristics. Thus, deforestation or removal of vegetation, increased snowmelt, etc. increase runoff and add to deposition and flooding downstream. It was reported that deforestation within the Dharla and Dudhkumar catchments has resulted in increased siltation levels, flash surges, and soil erosion in crucial downstream areas. Also, the building of dams/embankments in the upstream in Indian part has increased the problem of sedimentation in the downstream in Bangladesh parts. Moreover, building embankments without consideration of long-term impact, poorly maintained embankments that cause outflow and collapse in times of high discharge and resultant flooding.

## 5 Impact of Floods

### 5.1 Impact on Hydro-Geomorphology

Flood is a recurring phenomenon in the study area and has a great impact on hydro-geomorphology. Due to the geographical and geological conditions including the drainage system, the floodplain of the study area is prone to flooding. This can be figured out by channel migration, bank line shifting, river width due to the high water level, and discharge in these two rivers, Dharla and Dudhkumar. The hydrology of the catchment area of the Dharla and Dudhkumar Rivers is mainly directed by rainfall, runoff, and cross-boundary flows through the rivers. The pattern and magnitude of floods in the catchment area largely depend on the discharge and water level of the two rivers. Mainly, when there is heavy rainfall and water level exceed the danger level in these two rivers, floods occurred in the catchment area. The severity and inundation depend on the peak of water level and discharge. Long-term water level and discharge hydrographs of the two rivers are shown in Fig. 5.3. The figure depicts that the water level and discharge in the river were found very low from November to May and very high from June to October (Fig. 5.3e, f). Based on the data available from Bangladesh Water Development Board (BWDB, 2011, 2021), the historical maximum and minimum water levels were found 27.57 and 20.91 m PWD and discharge 7600 and  $12 \text{ m}^3\text{s}^{-1}$  in Dharla River (Kurigram station), respectively (Fig. 5.3a, b), while recorded maximum and minimum water level and discharge were found 31.52 and 25.47 m PWD and 9250 and  $52.3 \text{ m}^3\text{s}^{-1}$  in Dudhkumar River, respectively (Fig. 5.3c, d). The historical peak water levels are remarkably higher than the danger levels of these two rivers (Fig. 5.3a, c). When water flows above the danger level, it overtops the river bank and submerges the catchment area. Due to the severe flood and physical processes of erosion and accretion, the river channel migrated.

Figure 5.4 shows the river channel migration pattern of the Dharla and Dudhkumar Rivers from 1992 to 2020. The figure depicts significant changes in

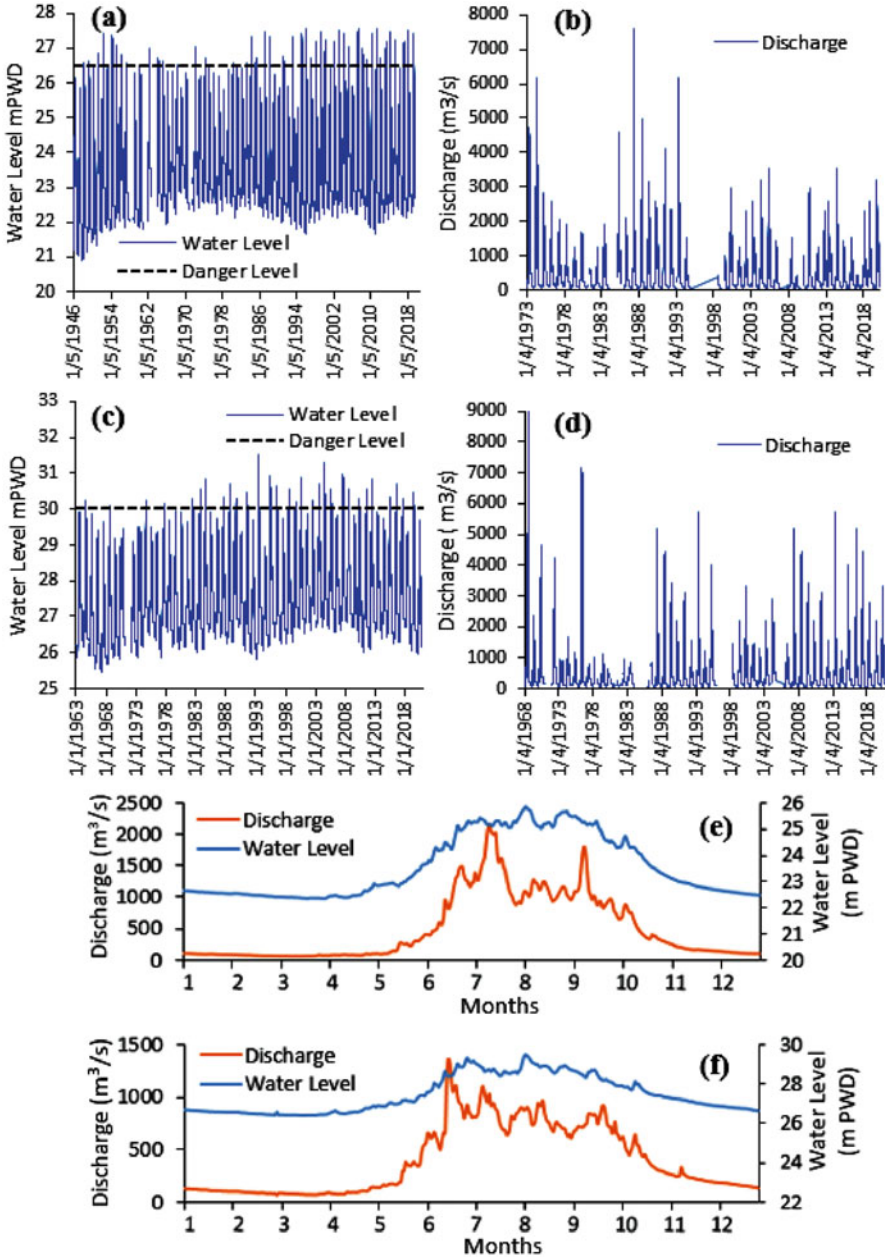


**Fig. 5.3** Long-term hydrographs of water level and discharge: (a and b) daily distribution at Kurigram station of Dharla River; (c and d) daily distribution at Pateshwari station of Dudhkumar River; (e) monthly average distribution at Kurigram station of Dharla River; and (f) monthly average distribution at Pateshwari station of Dudhkumar River. (Data source: BWDB (2011, 2021))

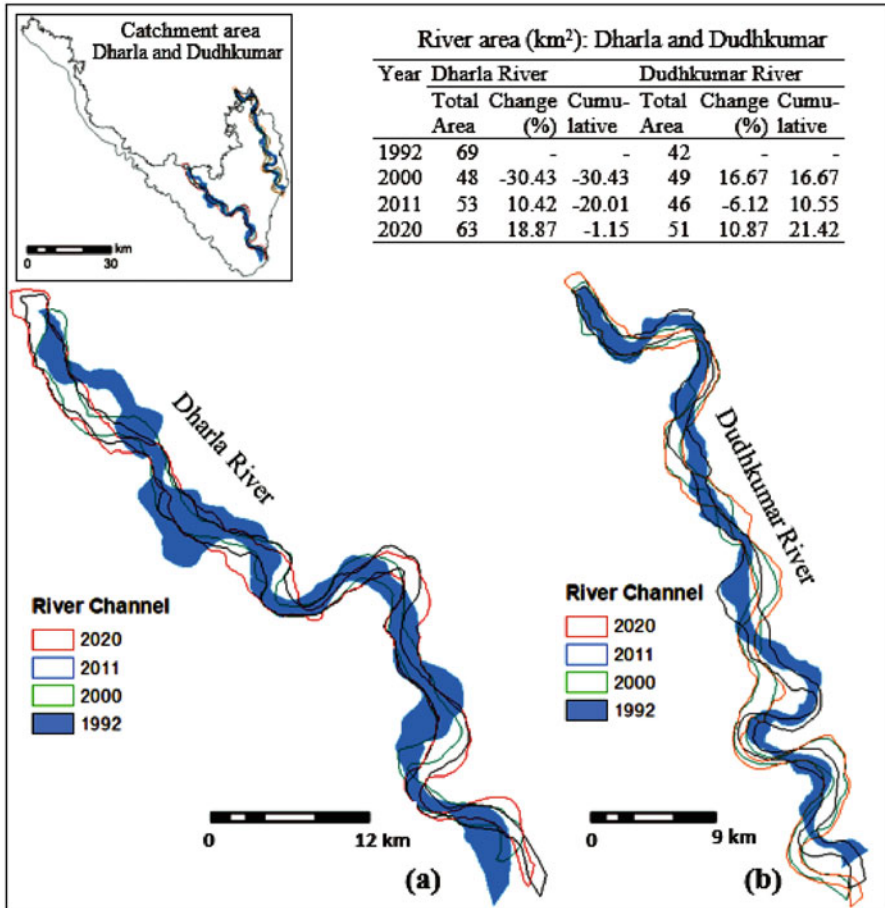


**Fig. 5.4** River channel migration: 1992–2020. (a) Dharla River and (b) Dudhkumar River

the spatial pattern of river migration, i.e., narrowing and widening both of the rivers and highly dynamic flow patterns over the last 28 years. The analysis shows changes in the surface area of the river and depicts that the extent of the Dharla River decreased from 69 to 60 km<sup>2</sup> during the period, while the area of the Dudhkumar River increased from 42 to 51 km<sup>2</sup> (Fig. 5.4). The river channel migration pattern also depicts that the changes in the river course with time were mainly due to erosion and deposition. Also, the river shifting is the resultant due to heavy rains and floods during the monsoon. Figure 5.4 also illustrated that there was a westward movement of the upper reach and eastward movement of the lower reach of the Dharla River between 1992 and 2020 (Fig. 5.4a). In contrast, both westward and eastward migrations were observed at the lower reach of the Dudhkumar River during the periods (Fig. 5.4b).

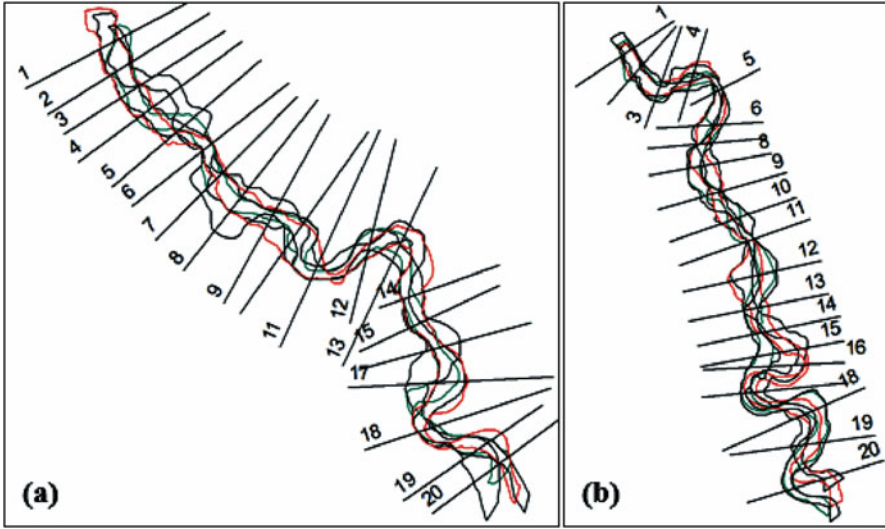


**Fig. 5.5** Selected cross-section (a) Dharla River and (b) Dudhkumar River

Due to the high water level, discharge, velocity, floods, and river morphometry, erosion and accretion processes increased along the bank lines of the river, and consequently, widening and narrowing the river channel have occurred that directly impact the width of the river. Thus, measuring the river width is important to identify the bank line shift, erosion, and accretion. The width of the Dharla and Dudhkumar Rivers was measured along the specific 20 cross-sections (Fig. 5.5). The river width analysis shows that a decrease, from 1.52 to 1.31 km, in the average width of the Dharla River between 1992 and 2020 was observed (Table 5.3), while a very negligible increase, from 1.03 to 1.09 km, of the average width of Dudhkumar River between 1992 and 2020 was witnessed (Table 5.3). However, the highest width of the Dharla River was observed at cross-section 8, which was 3.59 km in 1992, whereas the lowest width was at cross-section 18, which was 0.52 km in 2020. The rate of width change in the Dharla River from 1992 to 2020 at different cross-sections depicts that the highest widening of the river occurred at the upper (at cross-sections 1, 2, and 3) and middle (cross-sections 9, 10, and 11) parts of the river. The highest narrowing of the river was at the cross-sections 5, 7, and 8, followed by the cross-sections 15, 16, 18, and 20 at the lower part of the river (Table 5.3). In contrast, the highest width of the Dudhkumar River was observed at cross-section 12, 2.53 km in 2000, whereas the lowest width was at cross-section 16, 0.25 km in 2020. The rate of width change in the Dudhkumar River from 1992 to 2020 at different cross-sections depicts that the highest widening of the river occurred at the tiny part of the middle (at cross-section 9) and lower reach (cross-sections 15, 16 and 19) of the river. The highest narrowing of the river was at the cross-sections 5 and 6 and followed by the cross-sections 14, 17, and 20 at the lower part of the river

**Table 5.3** Temporal dynamics of river width of the Dudhkumar and Dharla Rivers along the cross-sections

Cross-section	Dharla River					Dudhkumar River				
	Width (km)				Rate (m year <sup>-1</sup> )	Width (km)				Rate (m year <sup>-1</sup> )
	1992	2000	2011	2020	1992–2020	1992	2000	2011	2020	1992–2020
1	0.80	1.10	1.34	1.32	19	0.80	0.95	1.05	0.82	1
2	0.98	1.60	1.45	1.63	23	0.88	1.18	1.54	1.12	9
3	1.19	0.95	1.44	1.65	16	1.20	1.15	1.4	1.20	0
4	0.92	0.96	0.72	1.06	5	0.63	1.66	0.91	0.81	6
5	2.28	1.23	0.92	0.99	-46	0.60	0.68	0.74	0.31	-10
6	0.73	0.82	0.89	0.88	5	1.40	1.61	0.88	0.60	-29
7	1.87	1.43	1.41	0.8	-38	1.13	0.78	0.75	0.98	-5
8	3.59	1.03	1.16	1.66	-69	1.08	1.54	0.84	1.01	-3
9	1.19	0.54	1.06	1.65	16	0.91	0.62	1.14	1.69	28
10	2.12	1.95	1.41	2.38	9	1.24	0.82	0.97	1.15	-3
11	0.93	0.56	1.1	1.63	25	0.45	0.41	0.75	0.58	5
12	1.34	1.59	1.01	1.10	-9	1.50	2.53	1.08	1.46	-1
13	1.17	1.26	1.23	1.06	-4	0.99	1.37	1.34	1.09	4
14	1.35	0.74	0.38	1.32	-1	1.45	0.98	0.4	0.74	-25
15	2.37	0.86	0.71	1.18	-43	0.80	1.39	1.25	1.82	36
16	1.44	0.57	0.76	0.87	-20	0.73	0.25	1.52	1.63	32
17	1.40	1.75	1.81	1.94	19	0.88	0.83	0.7	0.4	-17
18	0.95	1.29	1.08	0.52	-15	1.53	1.41	1.56	1.76	8
19	1.74	1.53	1.69	1.82	3	1.14	0.95	1.43	2.04	32
20	2.00	1.42	0.68	0.78	-44	1.23	1.24	0.6	0.68	-20
Average	1.52	1.16	1.11	1.31	-7	1.03	1.12	1.04	1.09	2
Minimum	0.73	0.54	0.38	0.52	-	0.45	0.25	0.4	0.31	-
Maximum	3.59	1.95	1.81	2.38	-	1.53	2.53	1.56	2.04	-

(Table 5.3). All these observations indicate a high rate of widening and narrowing both of the rivers during the study period, denoting more erosion and accretion in these parts of the river.

During floods and recession periods of floods, erosion, and accretion processes are going on along the bank lines of the river. Through these processes, floods impact the shifting of bank lines, and as a result, river channels migrated. The movement of bank lines of the Dharla and Dudhkumar Rivers from 1992 to 2020 was assessed and analyzed using 20 selected cross-sections on the banks of the rivers. Figure 5.6 represents the shifting of the bank lines from 1992 to 2020 of the Dharla and Dudhkumar Rivers from the initial observation bank line in 1992 at different fixed cross-sections. Figure 5.6a depicts that at cross-section 17, the highest shifting was observed on the left bank of the Dharla River, about 2.3 km toward the east due to erosion, whereas at cross-section 5, the highest shift was observed on the left bank, about 2.24 km toward the west due to accretion (Fig. 5.6a). In contrast, at

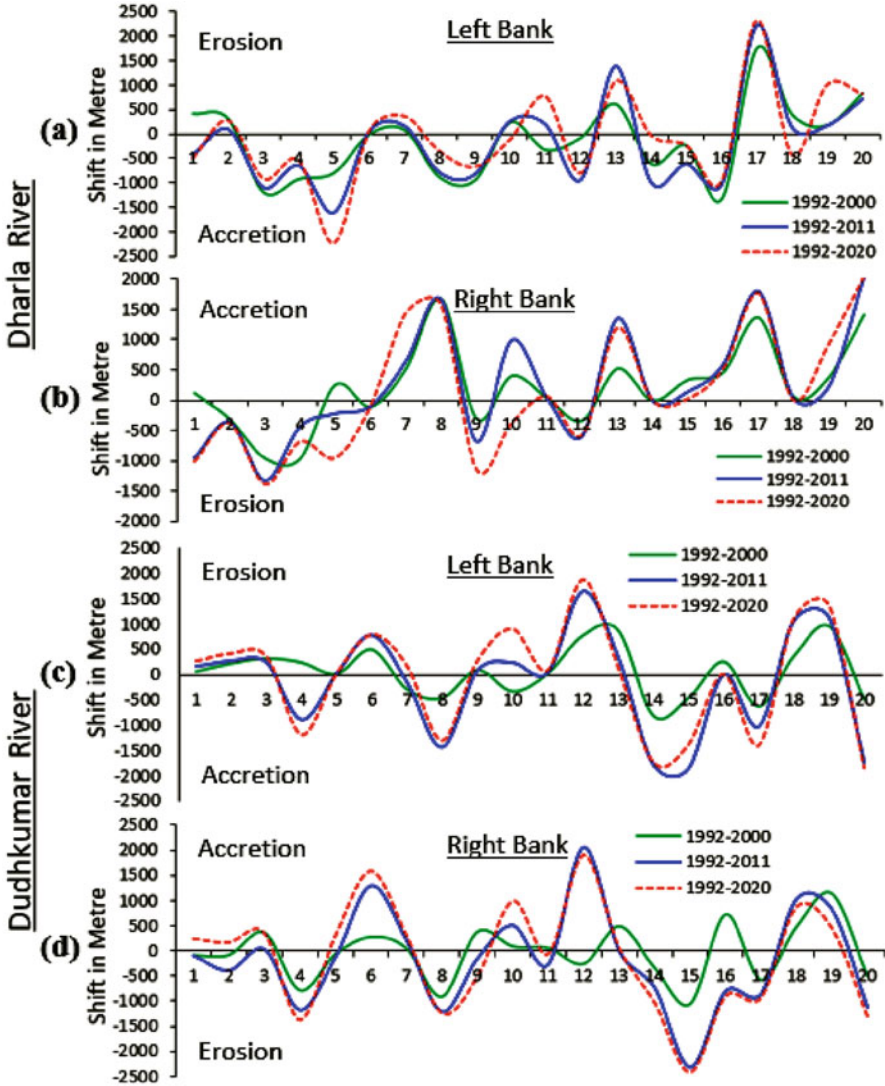


Fig. 5.6 Bank line shift: (a) left bank, (b) right bank of Dharla, and (c) left bank, (d) right bank of Dudhkumar

cross-sections 3 and 9, the highest shifting was observed on the right bank of the river, about 1.38 and 1.14 km toward the west due to erosion, while at cross-sections 8, 17, and 20, the maximum movement was observed on the right bank, about 1.57, 1.76 and 2.04 km, respectively, toward the east due to the accretion (Fig. 5.6b). Figure 5.6a further shows that eastward shifting of the left bank was noticed mainly at the lower reach of the Dharla River, whereas comparatively less shifting of the left bank was observed at the middle part of the river in both east and west directions.



However, the westward movement of the left bank was occurred at the upper part of the river, Dharla. Conversely, the right bank of the river shifted more toward the east, meaning more deposition on the right bank and noticed at the middle to lower reaches of the river. The westward movement of the right bank was observed at the upper part of the river (Fig. 5.6b).

On the other hand, Fig. 5.6c depicts that at cross-sections 12 and 19, the highest shifts are observed on the left bank of the Dudhkumar River, about 1.87 and 1.35 km, respectively, toward the east due to erosion, whereas at cross-sections 20, 14, 17, and 15, the maximum shifts are observed on the left bank, about 1.86, 1.75, 1.41, and 1.36 km, respectively, toward the west due to accretion (Fig. 5.6c). Conversely, at cross-sections 15, 4, and 20, the highest shifting was observed on the right bank of the Dudhkumar River, about 2.14, 1.38, and 1.30 km, respectively, toward the west due to erosion. While at cross-sections 12, 6 and 10, the maximum movement was observed on the right bank, about 1.91, 1.59, and 1.00 km, respectively, toward the east due to accretion (Fig. 5.6d). Figure 5.6c further shows that the east and westward shifts of the left bank of the Dudhkumar River are observed mainly at the middle and lower parts of the bank, respectively, whereas both east and westward shifting of the right bank was observed at the upper part of the bank, and westward movement of the right bank occurred more at the lower part of the bank (Fig. 5.6d). In the Dudhkumar River, both left and right banks shifted more, particularly, toward the west, meaning more erosion and deposition on the right bank and maximum noticed at the lower reach of the river (Fig. 5.6d).

## 5.2 *Impact on River Bank Erosion and Accretion*

Flood is a typical feature of the Dharla and Dudhkumar Rivers catchment area. The floods of this catchment are the leading reason for river channel shifting and hydrological changes. Flood and extreme discharge affect the channel behavior of the rivers. Thus, bank areas are prone to erosion and accretion because of the migration of bank lines over time. Bank line eroded to the landward and deposited to the riverward direction. Erosion and accretion analysis of Dharla and Dudhkumar Rivers discloses that about 50.10 km<sup>2</sup> and 56.27 km<sup>2</sup> land were eroded and accredited along the bank lines of the Dharla River during the period 1992–2020. Again, 57.05 km<sup>2</sup> and 48.12 km<sup>2</sup> land were eroded and accredited along the bank lines of the Dudhkumar River during the period 1992–2020, respectively (Table 5.4). Therefore, the erosion and accretion rates were 1.79 km<sup>2</sup> year<sup>-1</sup> and 2.01 km<sup>2</sup> year<sup>-1</sup>, respectively, during the period 1992–2020 in the Dharla River (Table 5.4). On the contrary, the erosion and accretion rates were 2.04 km<sup>2</sup> year<sup>-1</sup> and 1.72 km<sup>2</sup> year<sup>-1</sup>, respectively, during the same period in the Dudhkumar River. Thus, in Dharla, accretion was more than erosion, and in Dudhkumar, erosion was more than accretion. Table 5.4 also depicts that the Dharla River experienced more erosion on the left bank (28.05 km<sup>2</sup>) compared with the right bank (22.05 km<sup>2</sup>). And more erosion (30.35 km<sup>2</sup>) was observed on the right bank than the left bank

**Table 5.4** Erosion and accretion of Dharla and Dudhkumar Rivers

Year	Dharla River						Dudhkumar River					
	Erosion (km <sup>2</sup> )			Accretion (km <sup>2</sup> )			Erosion (km <sup>2</sup> )			Accretion (km <sup>2</sup> )		
	Left bank	Right bank	Total	Left bank	Right bank	Total	Left bank	Right bank	Total	Left bank	Right bank	Total
1992–2000	7.74	6.07	13.81	16.36	18.35	34.71	10.51	10.47	20.98	6.94	6.95	13.89
2000–2011	10.82	7.30	18.12	6.27	6.98	13.25	8.50	13.62	22.12	16.00	9.37	25.37
2011–2020	9.49	8.68	18.17	6.21	2.10	8.31	7.69	6.26	13.95	2.66	6.20	8.86
1992–2020	28.05	22.05	50.10	28.84	27.43	56.27	26.70	30.35	57.05	25.60	22.52	48.12

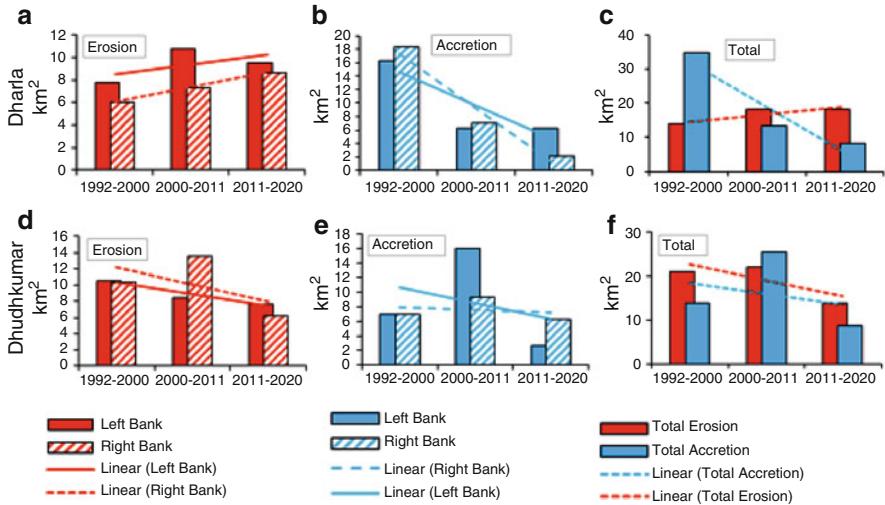


**Fig. 5.7** Erosion and accretion of Dharla and Dudhkumar Rivers: (a–c) Dharla River and (d–f) Dudhkumar River

(26.70 km<sup>2</sup>) of the Dudhkumar River (Fig. 5.7). So, *the left bank of Dharla and the right bank of Dudhkumar are more prone to erosion.* Moreover, if we see the statistics and trends of the erosion and accretion over time, except erosion in *the Dharla River* (also left and right banks), the accretion in Dharla River, and erosion and accretion in Dudhkumar River all were decreased and *showed* negative trends (Fig. 5.7). *Thus, it may be said that there is a big change in the erosion and accretion process in these two rivers of Bangladesh.* The spatial pattern of erosion and accretion depicts, overall, the middle and lower parts of the Dharla and Dudhkumar were more exposed to erosion and accretion (Fig. 5.8). In the Dharla River, erosion was increased both on the left and right banks in recent years and observed throughout the banks. However, erosion decreased gradually and was observed in almost every part of the banks of the Dudhkumar River (Fig. 5.8). *Further, Fig. 5.8 illustrates that in both the rivers, erosion and accretion are very dynamic in nature and frequently changes over time.*

### 5.3 Impact on Resources, Live, and Livelihood

Bangladesh is one of the most vulnerable countries to flooding disasters. The catchment of Dharla and Dudhkumar is also vulnerable to flood and causes damage to infrastructure, settlement, transport network, resources, agriculture, loss of lives, etc. The floods of 1954, 1974, 1988, 1998, 2004, and 2020 all caused enormous damages to properties and impacted the lives and livelihood of the inhabitants. Fatality by drowning, water-borne diseases, diarrhea, and snakebites are the major

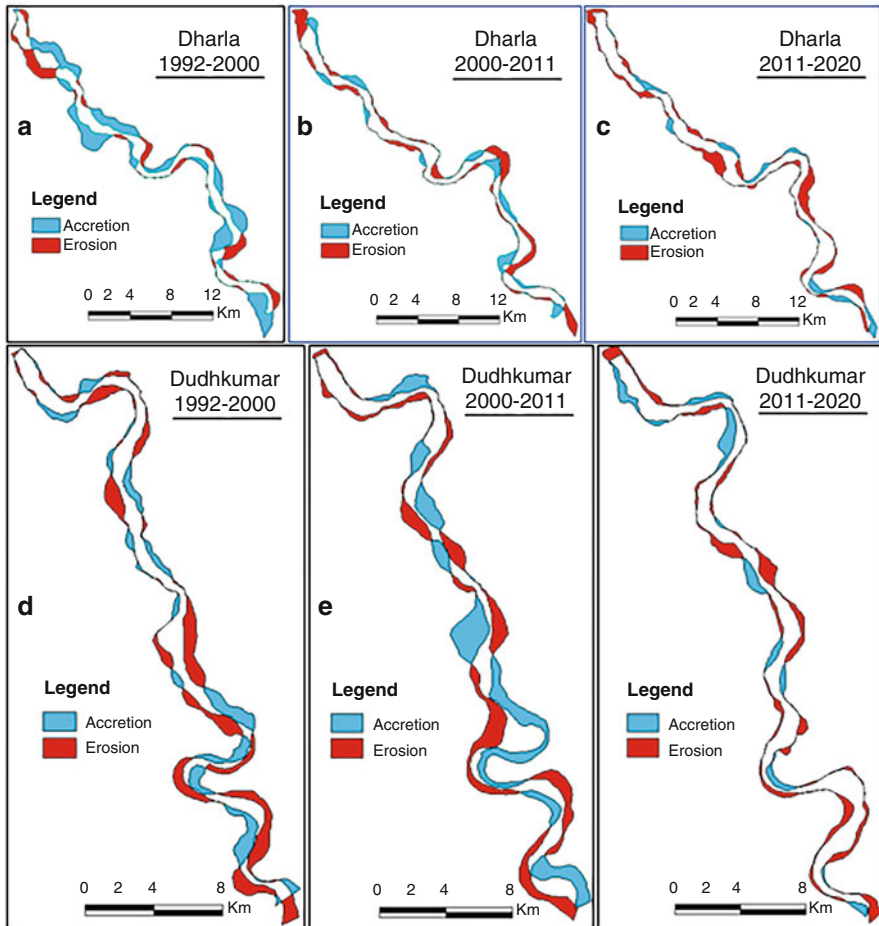


**Fig. 5.8** Erosion and accretion: Dharla River (a) 1992–2000, (b) 2000–2011, and (c) 2011–2020 and Dudhkumar River (d) 1992–2000, (e) 2000–2011, (f) 2011–2020

impacts of floods. There is a strong positive relationship between economic loss and flood-affected areas in Bangladesh, highlighting the overall economic risk of flooding. Two catastrophic floods, 1988 and 1998, each affects more than 60% of the total area of Bangladesh. The total damage from each flood was more than 8% of the country's gross domestic product (GDP) (Kabir & Hossen, 2019). The most affected sector of the country by floods is agriculture. Pre-monsoon rice called *Aus* and rain-fed rice called *Aman* cultivated/transplanted during monsoon season in Bangladesh are highly susceptible to floods and affected almost every year at different scales. In 1998 floods, about 69% of *Aus*, 82% of deep-water *Aman*, and 91% of transplanted *Aman* were damaged and causing the whole country to food insecure (Shaw, 2018). Floods also affect domestic animals like poultry and dairy,

which are the main sources of earnings in the rural and semi-urban areas. River erosion due to floods caused loss of land and resources and people became homeless. Consequently, a large number of riverine people migrated to the different parts of the country.

Table 5.5 shows some statistics of flood impact on resources, live, and livelihood in the Dharla and Dudhkumar catchment areas. The statistics of flood impacts show the severity of flooding issues in the catchment. Here, flood impacts were analyzed based on observed flood frequency of 1954, 1974, 1988, 1998, 2004, and 2020 floods (Fig. 5.2). Table 5.5 depicts that about 72% of the total people of the catchment area are affected by high-frequency floods (3–6 times). Floods also affect 70% and 72% of the total infant (<14 years) and elderly (>60 years) population, respectively. These dependent groups are highly vulnerable to floods in the area. The widespread impact of flooding on housing and households is common in the catchment area. About 67% of the settlement area of the catchment is subject to be affected by floods. During the flood, the source of drinking water is necessary, and safe drinking water can prevent many water-borne diseases. In the catchment area, about 71% of households with drinking water facilities and 69% of the household with toilet facilities are affected by floods that cause water-borne diseases, diarrhea, and other health-related problems. On the other hand, in the case of educational institutions in the area, out of 72 schools, 45 (62.5%) are affected by severe floods, which disrupt schooling during floods.

In the catchment, paddy, jute, maize, *Kaun*, and vegetables are cultivated extensively; however, crop fields are submerged in the floodwaters. Table 5.5 illustrates that about 64% agricultural land of the Dharla and Dudhkumar catchment are affected by floods and causing huge crop damage in the area. Road communication is the vital infrastructure of an area, and the road network can utilize to maintain communication with different locations. However, if road communication is affected due to the flood, communication with other areas is disrupted. Statistics show that about 67% of the total roads of the catchment area of Dharla and Dudhkumar is within the high magnitude flooded area (3–6 times) affected almost every year (Table 5.5). Individually, 77, 68, and 63% of the highways, *Upazila* road and *Union* road, are affected by floods. Thus, floods affect road communication and create tremendous problems in the area. Also, during floods, some roads are damaged. Besides, due to river erosion, more than 200 families have lost their land and became homeless during each and every severe flood.

## 6 Flood Vulnerability

Flood vulnerability (FV) is a geographic concept that identifies areas where people and resources are vulnerable to floods and flood-related problems. In previous sections, flood dynamics, causes of flood, and impact of flood in the Dharla and Dudhkumar catchment areas have been discussed. From the discussions, it is clear that flood is a serious natural hazard and causes hydro-geomorphological changes of

**Table 5.5** Flood impact on resources, live, and livelihood (Dhatla and Dudhkumar catchment area)

Impact/affect	Flooded area				No flood				Total	
	5-6 times	%	3-4 times	%	1-2 times	%	No flood	%	Total	%
Population (number)	642,013	37.83	585,137	34.48	258,426	15.23	211,398	12.46	1,696,974	100
Infant population (<14 years in number)	218,097	38.23	180,646	31.67	90,241	15.82	81,446	14.28	570,430	100
Elderly population (>60 years in number)	49,371	39.37	41,139	32.80	19,220	15.33	15,681	12.50	125,411	100
Settlement (km <sup>2</sup> )	167.81	31.96	184.39	35.11	90.11	17.16	82.81	15.77	525.12	100
Households with drinking water facilities	147,589	38.62	123,537	32.33	59,581	15.59	51,401	13.45	382,108	100
Households with toilet facilities	79,888	35.86	73,324	32.92	38,176	17.14	31,361	14.08	222,749	100
School (number)	17	23.61	28	38.89	15	20.83	12	16.67	72	100
Agricultural land (km <sup>2</sup> )	254.12	33.94	221.84	29.63	133.12	17.78	139.72	18.66	748.8	100
Total roads (km)	289.01	29.70	361.61	37.16	168.17	17.28	154.41	15.87	973.2	100
Highways (km)	47.71	27.92	83.98	49.14	32.32	18.91	6.88	4.03	170.89	100
Upazila road (km)	120.31	39.14	88.8	28.89	64.42	20.96	33.89	11.02	307.42	100
Union road (km)	120.99	24.45	188.83	38.16	71.43	14.43	113.64	22.96	494.89	100

the river such as bank line shift, channel migration, erosion, and accretion and impacts on the resources, life, and livelihood of the area as well. Low topography, floodplain area, and high seasonal rainfall in the upstream country or the mainland areas are the main natural causes, and on the other hand, high population density, marginalized communities who are unprepared for and unable to deal with this disaster, lack of proper knowledge, limitation of the resources, and proper response to government initiatives are the main anthropogenic causes of flood vulnerability in this catchment area. Thus, for the management approaches to mitigate the effect of flood on people, property, and environment and continue the sustainable development of the area, flood vulnerability (FV) assessment is required. Here, flood vulnerability was assessed combining physical vulnerability, social vulnerability, and coping capacity to floods following GIS-aided multi-criteria analysis (GIS-MCA) modeling technique, and the processes that were followed are discussed in the methodology section. For effective management, flood vulnerability zoning (FVZ) based on physical, social, and coping capacity can be used as an important tool in flood-prone area, as vulnerability zoning describes the spreading of flood-affected areas to varying degrees.

Physical vulnerability to floods was assessed based on seven criteria that expose the magnitude of flood vulnerability, viz., elevation, slope, land use/land cover, rainfall, distance to the river, drainage density, and observed flood frequency (Table 5.2 and Fig. 5.9a). Social vulnerability refers to the inability of people, organizations, and societies to deal with the negative impacts of hazards like floods. Thus, the social vulnerability was evaluated based on five criteria (population density, female population, dependent population, household with tube well as the water source, and household with water-sealed sanitation) (Table 5.2 and Fig. 5.9b). Coping capacity refers to the capability of people, organizations and systems to manage the impact of disaster using available skills and resources, and it represents the scale of vulnerability reduction capability of a hazard-prone area. A very high coping capacity index specifies a region having vulnerability-reduction strategies in place. Conversely, a very low coping capacity index represents an area having less vulnerable reduction capability in place. For the effective evaluation of flood vulnerability, coping capacity, therefore, should be considered in the evaluation process. So, considering three criteria, i.e., literacy rate, distance to school, and distance to the health center, coping capacity to floods was measured (Table 5.2 and Fig. 5.9c).

Physical vulnerability depicts that in the catchment area of Dharla and Dudhkumar about 32% of the area is found under very high and high vulnerability zones (Table 5.6). Social vulnerability to floods indicates that about 43% of the catchment area was vulnerable to floods with a scale very high to high. However, about 46% of the catchment (almost half) exhibits very low to low coping capacity zones; another 24% area was with a moderate coping capacity to floods. Only 23% of the catchment area was categorized as high to very high coping capacity (Table 5.6), indicating that only one-fourth area of the catchment was under the capability to manage the impact of disaster using available skills and resources and having under vulnerability-reduction strategies. Following the IPCC vulnerability

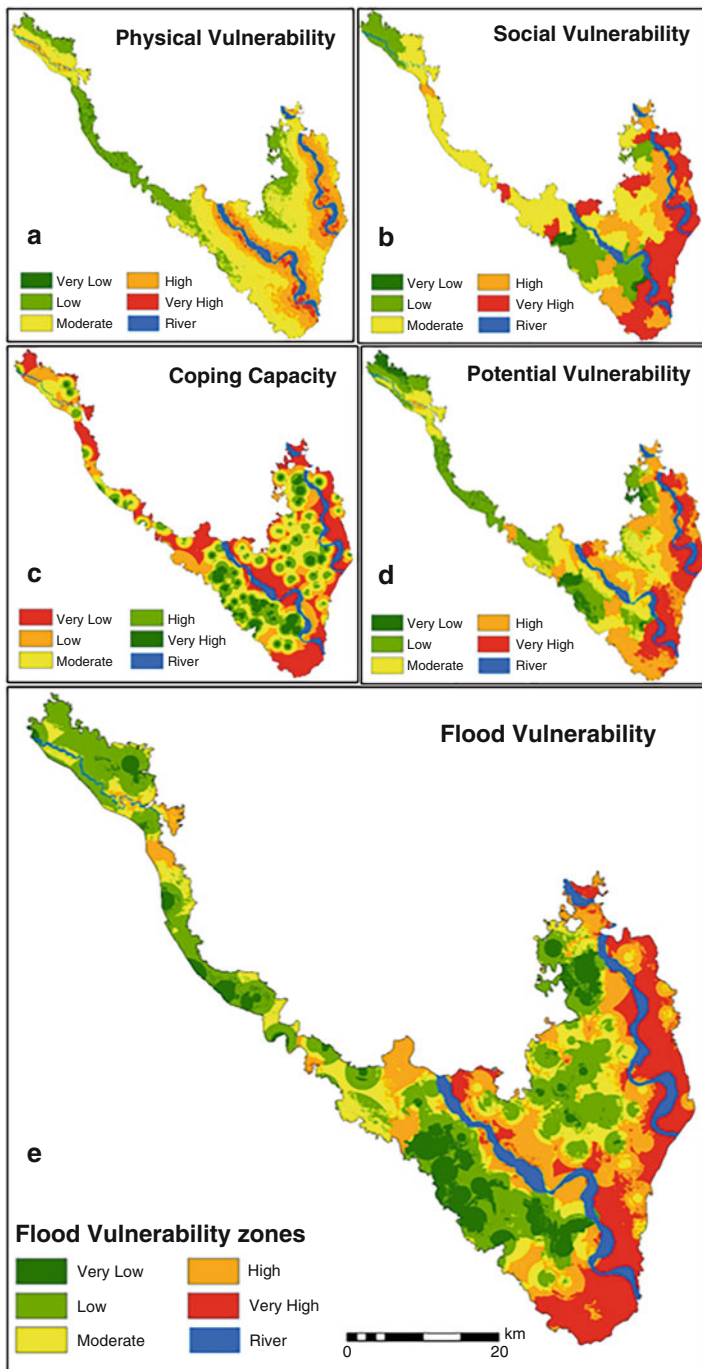


**Fig. 5.9** Spatial pattern of vulnerability. (a) Physical vulnerability to flood, (b) social vulnerability to flood, (c) coping capacity to flood, (d) potential vulnerability to flood, and (e) flood vulnerability



**Table 5.6** Flood vulnerability in Dharla and Dudhkumar Rivers catchment area (km<sup>2</sup>)

Vulnerable zone	Physical vulnerability		Social vulnerability		Coping capacity		Potential vulnerability		Flood vulnerability	
	Area	%	Area	%	Area	%	Area	%	Area	%
Very low	13.28	0.85	25.32	1.62	380.48	24.28	85.60	5.46	176.94	11.29
Low	327.98	20.93	261.96	16.71	346.12	22.08	338.11	21.57	445.20	28.41
Medium	618.98	39.49	497.78	31.76	370.11	23.61	318.94	20.35	225.46	14.39
High	456.98	29.16	293.93	18.75	264.22	16.86	481.17	30.70	344.79	22.00
Very high	40.79	2.60	379.01	24.18	97.08	6.19	234.23	14.94	265.62	16.95
River	109.28	6.97	109.28	6.97	109.28	6.97	109.28	6.97	109.28	6.97
Total	1567.29	100.00	1567.29	100.00	1567.29	100.00	1567.33	100.00	1567.29	100.00

concept (IPCC, 2007, 2014) and Eq. 5.3, a potential vulnerability index was calculated and scaled as very high, high, medium, low, and very low (Table 5.6 and Fig. 5.9d). The degree of potential vulnerability on a system is defined as the combination of physical and social vulnerabilities (Schauser et al., 2010). Potential vulnerability to floods of the Dharla and Dudhkumar Rivers depicts that about 45% of the total area comes under the very high to highly vulnerable zones (Table 5.6) and indicates nearly half of the area comes under very high to high potential vulnerability zone, and this area of potential vulnerability is the combined impact of physical and social vulnerabilities.

Finally, assessment of flood vulnerability is initiated with the IPCC's vulnerability definition (IPCC, 2007) and the extended definition of IPCC's by Schauser et al. (2010), which is based on three key components: physical vulnerability (exposure), social vulnerability (sensitivity), and coping capacity (adaptive capacity) (Eq. 5.4). The statistics of the flood vulnerability are given in Table 5.6. The table illustrates that a very high flood vulnerability zone covered about 17%, and in contrast, the high vulnerability zone covered about 22% of the catchment area. Altogether very high and high vulnerable areas were about 39% of the catchment and mainly located in the north-eastern, eastern, and southern parts of the catchment. Most of these areas are nearby the riverside, have more physical and social sensitivity to flooding hazards, and have inadequate coping capacity. Coping capacity plays a significant role in reducing the vulnerability of the area; hence, some very high to high potential vulnerability areas change to moderate to low flood vulnerability due to very high and high coping capacity (Fig. 5.9c, d). In contrast, about 40% of the area was at the low and very low vulnerable zones, where about 29% and 11% were found in the low and very low vulnerable zones, respectively. These areas were located in the north-western, western, and northern parts of the catchment, generally far from the river, comparatively high elevation areas, and very high to high coping capacity areas. Thus, the inclusion of coping capacity is essential to illustrate actual vulnerability and to make available information where robust flood control and action plan need to be implemented.

## 7 Management of Floods

Flood is a natural and dynamic phenomenon and cannot be stopped. Since it has a huge impact on resources, live, and livelihood, therefore, management practices need to be followed to reduce the impacts of floods. Management of flood hazards reveals the vital strategy, including structural and nonstructural measures, to mitigate the probable impacts of flood. Bangladesh practices both structural and nonstructural approaches to alleviate the flood problems of the country. The country initially followed a structural approach for post-disaster recoveries dating back to the 1950s. From 1947 to 1987, the government has focused on large and small-scale engineering works for flood prevention and irrigation, while the periods of 1987 to 1995 and 1995 to present considered as structural and nonstructural, respectively, and implemented under flood action plan (FAP) (Haque et al., 2019). The structural

and nonstructural initiatives, which have been taken in the catchment area, particularly in the Dharla and Dudhkumar Rivers are discussed in the following sections.

### ***7.1 Structural Approach***

In structural approach, construction of engineering structures such as embankments, dams, reservoirs, etc. is planned to control the flow of flood water and rivers. The structural system has given priority to the safety management of the residents of flood-prone areas. Engineering work is done to reduce the risk of floods and flood damage. Bangladesh is practicing a limited range of structural solutions to control the flood situation. In the Dharla and Dudhkumar catchment areas, two projects, the North and South Kurigram Irrigation project and the Flood Control project, were implemented between 1975 and 2010. Under these projects, a 210 km long flood protection embankment was constructed to protect Kurigram and a part of Lalmonirhat from the flood of Teesta, Dharla, Dudhkumar, and Brahmaputra Rivers. Moreover, 39 regulators and sluice gates, 11 groynes, and spars were built. Additionally, more than 13 km of the riverbank were protected under these two projects (The Daily Sun, 2020). The flood protection embankment, protected riverbank, and associated structures were either destroyed or washed away due to excessive flooding every year. Considering the flood situation worsening in Kurigram, the Water Resources Ministry (WRM) has initiated a new project, “Left and Right Embankment Protection of the Dharla River,” which will be constructed by the end of June 2023. Under the new scheme, 16.84 km of riverbank and 16.65 km of alternative flood protection embankment will be constructed, and 17.9 km of flood protection embankment will be reconstructed (The Daily Sun, 2020). However, structural work has some negative effects, such as preventing sedimentation in the floodplain, which in turn raises the riverbed again and flooded the area behind the dam as the water holding capacity decreases and the water level rises. In addition, structural work can result in changes in river course, extensive erosion, and potential human displacement.

### ***7.2 Nonstructural Approach***

Nonstructural methods are initially applied for flood mitigation and recovery. Various activities such as proper land use planning, floodplain area mapping, early warning system, floodplain management, flood preparedness and awareness, susceptibility and hazard zoning, etc. can be done for flood vulnerability and risk reduction, anticipation, fortification, and mitigation. The catastrophic floods of 1987 and 1988 in the country, which caused more than two billion dollars in damages, discovered that structural measures alone cannot protect and prevent the severity of floods. The nonstructural approach adopted by the Government of

Bangladesh focuses on preparation and action to reduce risk among different stakeholders and for better coordination. In the country, nonstructural measures include flood forecasting and early warning, flood zoning, flood proofing, building awareness, disaster preparedness, and response that were carried out and implemented time to time. The flood vulnerability zoning of the Dharla and Dudhkumar catchment, which has been discussed earlier in this chapter, is an example of the nonstructural approach to flood management. This kind of vulnerability map is useful to develop effective flood management strategies.

### ***7.3 Coping Strategies, Policy Issues, and Local Level Implementation***

During floods in Kurigram, many people take shelter on the banks of Dharla, Dudhkumar, and Brahmaputra Rivers, different flood centers, and nearby high-raised roads or marketplace. The IPCC notified that South Asia's mega delta would be at risk because of increased flooding and poverty in these regions that can reduce the adaptation capacities of inhabitants (IPCC, 2007). Besides poverty, frequent floods and riverbank erosion make their life unbearable. However, people used their indigenous knowledge to predict floods and coping strategies to deal with these situations. During floods, locals usually commute using boats made of banana trees for moving from one place to another, pack dry food as cooking is not possible, use tablets for water purification or boiled water for drinking, keep livestock as resources, and build homes at high elevation or raised places. The Government of Bangladesh has initiated structural and nonstructural measures to build a flood resilient community, as well as different NGOs, who work to improve the adaptation capacities of local people, especially in vulnerable communities.

## **8 Conclusions and Recommendations**

Floods cause about 43% of the total damage from all-natural disasters and are considered one of the most devastating disasters in the world today. This chapter deals with the flood dynamics, hydro-geomorphological conditions, and erosion status, the causes and impact of floods, and flood vulnerability considering the criteria for physical vulnerability, social vulnerability and coping capacity in the Dharla and Dudhkumar catchment area. The study reveals that about half of the catchment area is very prone to floods, and thus, flooding is a major problem in the area. Over the last 28 years, the remarkable area of the Dharla River decreased, and the area of the Dudhkumar River increased due to erosion and accretion processes. Accretion was observed more than erosion in Dharla, and on the contrary, erosion was noticed more than accretion in Dudhkumar River. Besides, the left bank of

Dharla and the right bank of Dudhkumar were more prone to erosion. Due to erosion and accretion, the westward movement of upper reach and eastward movement of lower reach of the Dharla River have been observed from 1992 to 2020. Conversely, westward and eastward migration has been observed in the lower reaches of the Dudhkumar. In the catchment area of Dharla and Dudhkumar, more than 70% of people, 67% of the settlement area, 62.5% of schools, 64% of agricultural land, and 67% of the total roads were within the high-intensity flooded area and were affected consequently by the flood. Also, more than 200 families have lost their land and become homeless during each severe flood due to erosion.

Again, vulnerability analysis indicates the north-eastern, eastern, and southern parts of the catchment are very high and high vulnerable to floods, and coping capacity plays a significant role in reducing the vulnerability of the area. Thus, by vulnerability zoning, different levels of vulnerable area can be identified, and needful action can be taken accordingly under appropriate management and action plan. In the catchment area, mainly structural and some nonstructural methods were followed to deal with the impact of floods. However, they were not enough and received little attention. Structural means of action alone is not a perfect solution and safeguard from flooding; therefore, modified and inventive flood protection system and mitigation solutions are needed. Therefore, the integrated flood management (IFM) approach needs to be followed. Under a holistic approach, structural and nonstructural solutions are considerate together in IFM and thus cover all aspects of floods. Thus, decision and policymakers should consider the IFM approach and flood vulnerability with exposure, sensitivity, and adaptive capacity in flood management initiatives. Since human activities play a major role in flood disaster management, human behavior (preparedness, flood risk perception, etc.) also need to be incorporated into flood disaster management plan, because the Sendai Framework for Disaster Risk Reduction considers and accepts the spatial pattern of flood risk and flood-affected people in the flood management planning process (Aitsi-Selmi et al., 2016). On the other hand, as a part of the nonstructural measure, each zoning of vulnerability can be considered as a basic unit of measurement and planning and helps to develop a sustainable management plan under IFM with care of specific activities. The very high and high vulnerable areas are the most exposed areas and need to be given more attention in the management plan due to their vulnerability. Most of these areas are nearby the riverside, have more physical and social sensitivity to flooding hazards, and have inadequate coping capacity. Therefore, in these areas, priority should be given to protect the area from floods through emergency response and action plans. To protect such an area, river management initiatives also need to be taken by means of structural measures. The area under moderate vulnerability considers as the focal regions of development, and therefore, preparedness, prevention, mitigation, and recovery measures need to be taken for long-term solutions. Additionally, planning needs to be formulated to prevent the area from further inundation, reducing the intensity of floods and articulating an appropriate land use plan. Finally, it could be concluded that since

flood vulnerability is varied spatially, dynamic in nature, and dependent on several factors, execution of a comprehensive flood management plan and a synchronized approach with spatial characteristics among the different flood management factors will foster flood risk reduction in the area.

## References

- Aitsi-Selmi, A., Murray, V., Wannous, C., Dickinson, C., Johnston, D., Kawasaki, A., Stevance, A. S., & Yeung, T. (2016). Reflections on a science and technology agenda for 21st century disaster risk reduction. *International Journal of Disaster Risk Science*, 7, 1–29. <https://doi.org/10.1007/s13753-016-0081-x>
- Ali, R., Kuriqi, A., Abubaker, S., & Kisi, O. (2019). Hydrologic alteration at the upper and middle part of the yangtze river, China: Towards sustainable water resource management under increasing water exploitation. *Sustainability*, 11(19), 5176.
- Alsdorf, D., Bates, P., Melack, J., Wilson, M., & Dunne, T. (2007). The spatial and temporal complexity of the Amazon flood measured from space. *Geophysical Research Letter*, 34(8). <https://doi.org/10.1029/2007GL029447>
- Annual Flood Report. (2014). Flood Forecasting and Warning Centre, Bangladesh Water Development Board. Ministry of Water Resources.
- Ardıçlıoğlu, M., & Kuriqi, A. (2019). Calibration of channel roughness in intermittent rivers using HEC-RAS model: Case of Sarımsaklı creek, Turkey. *SN Applied Sciences*, 1(9), 1080.
- Azuma, R., Sekiguchi, H., & Ono, T. (2007). *Studies of high resolution morpho-dynamics with special reference to river bank erosion* (Vol. 50 (C), pp. 199–209). Annuals of Disaster Prevention Research Institute, Kyoto University.
- Babaeyan-Koopaei, K., Ervine, D. A., Carling, P. A., & Cao, Z. (2002). Velocity and turbulence measurements for two overbank flow events in River Severn. *Journal of Hydraulic Engineering*, 128(10), 891–900. [https://doi.org/10.1061/\(ASCE\)0733-9429\(2002\)128:10\(891\)](https://doi.org/10.1061/(ASCE)0733-9429(2002)128:10(891))
- BARC. (2016). *Physiography and soil maps of Bangladesh*. Bangladesh Agricultural Research Council. Retrieved from <http://barc.gov.bd/>
- Bates, P. D., Pappenberger, F., & Romanowicz, R. (2012). Uncertainty and risk in flood inundation modelling. In K. J. Beven & J. Hall (Eds.), *Flood forecasting*. Wiley.
- Biswas, A., Zaman, A. M., Sattar, M. A., Islam, M. S., Hossain, M. A., & Faisal, M. (2015). Assessment of disaster impact on the health of women and children. *Journal of Health and Environmental Research*, 1(3), 19–28.
- Bose, I., & Navera, U. K. (2017). Flood maps and bank shifting of Dharla River in Bangladesh. *Journal of Geoscience and Environment Protection*, 5, 109–122. <https://doi.org/10.4236/gep.2017.59008>
- Boyle, S. J., Tsanis, I. K., & Kanaroglou, P. S. (1998). Developing geographic information systems for land use impact assessment in flooding condition. *Journal of Water Resources Planning and Management*, 124(2), 89–98. [https://doi.org/10.1061/\(ASCE\)0733-9496\(1998\)124:2\(89\)](https://doi.org/10.1061/(ASCE)0733-9496(1998)124:2(89))
- Bradshaw, C. J. A., Sodhi, N. S., Peh, K. S. H., & Brook, B. W. (2007). Global evidence that deforestation amplifies flood risk and severity in the developing world. *Global Change Biology*, 13, 2379–2395. <https://doi.org/10.1111/j.1365-2486.2007.01446.x>
- Brammer, H. (1990). Floods in Bangladesh II: Flood mitigation and environmental aspects. *The Geographical Journal*, 156(2), 158–165.
- BWDB. (2011). *Rivers of Bangladesh*. Bangladesh Water Development Board.
- BWDB. (2021). Bangladesh Water Development Board.
- Cardona, O. D., van Aalst, M. K., Birkmann, J., Fordham, M., McGregor, G., Perez, R., Pulwarty, R. S., Schipper, E. L. F., & Singh, B. T. (2012). Determinants of risk: Exposure and vulnerability. In: *Managing the risks of extreme events and disasters to advance climate change*

- adaptation. In C. B. Field, V. Barros, T. F. Stocker, D. Qin, D. J. Dokken, K. L. Ebi, M. D. Mastrandrea, K. J. Mach, G.-K. Plattner, S. K. Allen, M. Tignor, & P. M. Midgley (Eds.), *A special report of working groups I and II of the Intergovernmental Panel on Climate Change (IPCC)* (pp. 65–108). Cambridge University Press.
- CEGIS. (2021). Centre for Environment and Geographic Information System.
- Choudhury, A. M. (2009). *Protecting Bangladesh from natural disasters* (p. 1209). Academic Press/Publishers Library.
- Chowdhury, M. H. (2012). Dharla River. In S. Islam & A. A. Jamal (Eds.), *Banglapedia: National encyclopedia of Bangladesh* (2nd ed.). Asiatic Society of Bangladesh.
- ESRI. (2020). Esri Inc. <https://www.arcgis.com/home/item.html?id=fc92d38533d440078f17678ebc20e8e2>
- Evans, E., Ashley, R., Hall, J., Penning-Rowsell, E., Sayers, P., Thorne, C., & Watkinson, A. (2004). *Future flooding. Scientific summary: Volume I-future risks and their drivers*. Office of Science and Technology.
- FFWC. (2008). *Annual flood report 2008. Technical report*. Flood Forecasting and Warning Centre. Bangladesh Water Development Board, Ministry of Water Resources, Government of the People's Republic of Bangladesh.
- Ge, Y., Cui, P., & Chen, X. (2020). Strategy of the international cooperation with respect to disaster prevention and reduction in the Belt and Road areas. *Science & Technology Review*, 38, 29–34. <https://doi.org/10.3981/j.issn.1000-7857.2020.16.003>
- Haque, C. E., Azad, M. A. K., & Choudhury, M. U. I. (2019). Discourse of flood management approaches and policies in Bangladesh: Mapping the changes, drivers, and actors. *Water*, 11, 2654. <https://doi.org/10.3390/w11122654>
- He, Y., Pappenberger, F., Manful, D., Cloke, H., Bates, P., Wetterhall, F., & Parkes, B. (2013). Flood inundation dynamics and socioeconomic vulnerability under environmental change. In R. Pielke Sr. (Ed.), *Climate vulnerability: Understanding and addressing threats to essential resources*. Elsevier/Academic Press. 241–255 pp. ISBN: 9780123847034.
- He, Y., Maa, D., Xionga, J., Chengb, W., Jia, H., Wangb, N., Guod, L., Duan, Y., Liu, J., & Yang, G. (2021). Flash flood vulnerability assessment of roads in China based on support vector machine. *Geocarto International*, 37, 6141. <https://doi.org/10.1080/10106049.2021.1926560>
- Hoque, M. A. A., Tasfia, S., Ahmed, N., & Pradhan, B. (2019). Assessing spatial flood vulnerability at Kalapara Upazila in Bangladesh using an analytic hierarchy process. *Sensors*, 19(6), 1302.
- Hoque, M. A. A., Pradhan, B., Ahmed, N., Ahmed, B., & Alamri, A. M. (2021). Cyclone vulnerability assessment of the western coast of Bangladesh. *Geomatics, Natural Hazards and Risk*, 12(1), 198–221.
- IPCC. (2007). *Climate change 2007: Impacts, adaptation and vulnerability: Working group II contribution to the Intergovernmental Panel on Climate Change, fourth assessment report*. Cambridge University Press.
- IPCC. (2012). Managing the risks of extreme events and disasters to advance climate change adaptation. In C. B. Field et al. (Eds.). *Special Report of the Intergovernmental Panel on Climate Change*, Cambridge University Press, 582 pp.
- IPCC. (2014). Summary for policymakers. In: *Climate change 2014: Impacts, adaptation, and vulnerability. Part A: Global and sectoral aspects*. In C. B. Field et al. (Eds.), *Contribution of working group II to the Fifth Assessment Report of the Intergovernmental Panel on Climate Change* (pp. 1–32). Cambridge University Press.
- Islam, A. S., Bala, S. K., & Haque, M. A. (2010). Flood inundation map of Bangladesh using MODIS time-series images. *Journal of Flood Risk Management*, 3(3), 210–222.
- Kabir, M. H., & Hossen, M. N. (2019). Impacts of flood and its possible solution in Bangladesh. *Disaster Advances*, 12(10), 48–57.
- Knight, D. W., & Shiono, K. (1996). River channel and floodplain hydraulics. In M. G. Anderson, D. E. Walling, & P. D. Bates (Eds.), *Floodplain processes* (pp. 139–182). Wiley.
- Kotoky, P., Bezbaruah, D., Baruah, J., & Sarma, J. N. (2005). Nature of bank erosion along the Brahmaputra River channel, Assam, India. *Current Science*, 88(4), 634–640.

- Kuriqi, A., Ardiçlioglu, M., & Muceku, Y. (2016). Investigation of seepage effect on river dike's stability under steady state and transient conditions. *Pollack Periodica*, *11*(2), 87–104.
- Kuriqi, A., Koçileri, G., & Ardiçlioglu, M. (2020). Potential of Meyer-Peter and Müller approach for estimation of bed-load sediment transport under different hydraulic regimes. *Modeling Earth Systems and Environment*, *6*(1), 129–137.
- Malczewski, J. (2010). Multiple criteria decision analysis and geographic information systems. In *Trends in multiple criteria decision analysis* (pp. 369–395). Springer Science and Business Media.
- Nasiri, H., Yusof, M. J., & Ali, T. A. (2016). An overview to flood vulnerability assessment methods. *Sustainable Water Resources Management*, *2*(3), 331–336. <https://doi.org/10.1007/s40899-016-0051-x>
- Nasreen, M. (2004). Disaster research: Exploring sociological approach to disaster in Bangladesh. *Bangladesh e-Journal of Sociology*, *1*(2), 21–28.
- Nicholas, A. P., & Mitchell, C. A. (2003). Numerical simulation of overbank processes in topographically complex floodplain environments. *Hydrological Processes*, *17*(4), 727–746.
- Pahlowan, E. U., & Hossain, A. T. M. S. (2015, May 11–15). Jamuna river erosional hazards, accretion and annual water discharge—a remote sensing and GIS approach. *The International Archives of the Photogrammetry, Remote Sensing and Spatial Information Sciences*, *XL-7/W3*. In *36th international symposium on remote sensing of environment*. <https://doi.org/10.5194/isprsarchives-XL-7-W3-831-2015>
- Pal, P. K., Rahman, A., & Yunus, A. (2017). Analysis on riverbank erosion-accretion and bar dynamics using multi-temporal satellite images. *American Journal of Water Resources*, *5*(4), 132–141. <https://doi.org/10.12691/ajwr-5-4-6>
- Pandey, V. K., Pourghasemi, H. R., & Sharma, M. C. (2020). Landslide susceptibility mapping using maximum entropy and support vector machine models along the Highway Corridor, Garhwal Himalaya. *Geocarto International*, *35*, 168–187.
- Pavelsky, T. M., & Smith, L. C. (2008). Remote sensing of hydrologic recharge in the Peace-Athabasca Delta, Canada. *Geophysical Research Letters*, *35*(8), paper no. L08403. <https://doi.org/10.1029/2008GL033268>
- Rahman, M. R. (2013). Agro-spatial diversity in Bangladesh—a special reference to climate change and crop diversification in Rajshahi Division. *Journal of Geo-Environment*, *10*, 1–15.
- Rahman, M. R., & Lateh, H. (2016). Spatio-temporal analysis of warming in Bangladesh using recent observed temperature data and GIS. *Climate Dynamics*, *46*, 2943–2960. <https://doi.org/10.1007/s00382-015-2742-7>
- Rahman, M. R., & Lateh, H. (2017). Climate change in Bangladesh: A spatio-temporal analysis and simulation of recent temperature and rainfall data using GIS and time series analysis model. *Theoretical and Applied Climatology*, *128*(1–2), 27–41. <https://doi.org/10.1007/s00704-015-1688-3>
- Rahman, M. R., & Saha, S. K. (2007). Flood hazard zonation—A GIS aided multi criteria evaluation (MCE) approach with remotely sensed data. *International Journal of Geoinformatics*, *3*(3), 25–35.
- Rahman, M. R., Shi, Z. H., & Chongfa, C. (2009). Soil erosion hazard evaluation—An integrated use of remote sensing, GIS and statistical approaches with biophysical parameters towards management strategies. *Ecological Modelling*, *220*(13–14), 1724–1734.
- Rahman, M. R., Shi, Z. H., & Chongfa, C. (2014). Assessing regional environmental quality by integrated use of remote sensing, GIS, and spatial multi-criteria evaluation for prioritization of environmental restoration. *Environmental Monitoring and Assessment*, *186*(11), 6993–7009.
- Rahman, M. R., Lateh, H., & Islam, M. N. (2018). Climate of Bangladesh: Temperature and rainfall changes, and impact on agriculture and groundwater—A GIS-based analysis. In M. Islam & A. van Amstel (Eds.), *Bangladesh I: Climate change impacts, mitigation and adaptation in developing countries*. Springer Climate/Springer. [https://doi.org/10.1007/978-3-319-26357-1\\_2](https://doi.org/10.1007/978-3-319-26357-1_2)
- Rahman, M. R., Islam, A. H. M., & Islam, M. N. (2020). Geospatial modelling on the spread and dynamics of 154 day outbreak of the novel coronavirus (COVID-19) pandemic in Bangladesh



- towards vulnerability zoning and management approaches. *Modeling Earth Systems and Environment*, 7, 1–29.
- Re, S. (2012). Flood-An underestimated risk: Inspect, inform, insure. *Swiss Re*, 28 pp. Available online at <http://media.swissre.com/documents/Flood.pdf>
- Saaty, T. L. (1977). A scaling method for priorities in hierarchical structures. *Journal of Mathematical Psychology*, 15(3), 234–281.
- Sayed, M. B., & Haruyama, S. (2016). Evaluation of flooding risk in Greater Dhaka District using satellite data and geomorphological land classification map. *Journal of Geoscience and Environment Protection*, 4, 110–127. <https://doi.org/10.4236/gep.2016.49009>
- Schauser, I., Otto, S., Schneiderbauer, S., Harvey, A., Hodgson, N., Robrecht, H., Morchain, D., Schrandner, J. J., Khovanskaia, M., Celikyilmaz-Aydemir, G., Prutsch, A., & McCallum, S. (2010). *Urban regions: Vulnerabilities, vulnerability assessments by indicators and adaptation options for climate change impacts- scoping study* (ETC/ACC Technical Paper 2010/12). The European Topic Centre on Air and Climate Change (ETC/ACC) is a consortium of European institutes under contract of the European Environment Agency. Retrieved from <http://air-climate.eionet.europa.eu/>
- Schumann, G., Matgen, P., & Pappenberger, F. (2008). Conditioning water stages from satellite imagery on uncertain data points. *IEEE Geoscience and Remote Sensing Letters*, 5(4), 810–813. <https://doi.org/10.1109/LGRS.2008.2005646>
- Sellin, R. H. J., & Willets, B. B. (1996). Three-dimensional structures, memory, and energy dissipation in meandering compound channel flow. In M. G. Anderson, D. E. Walling, & P. D. Bates (Eds.), *Floodplain processes* (pp. 255–298). Wiley.
- Shahabi, H., & Hashim, M. (2015). Landslide susceptibility mapping using GIS-based statistical models and remote sensing data in tropical environment. *Scientific Reports*, 5(1), 1–15.
- Shaw, R. (2018). Flood and sustainable agriculture in the Haor Basin of Bangladesh: A review paper. *Universal Journal of Agricultural Research*, 6(1), 40–49.
- Shekinah, D. E., Saha, S. K., & Rahman, M. R. (2004). Land capability evaluation for land use planning using GIS. *Journal of the Indian Society of Soil Science*, 52(3), 232–237.
- The Daily Sun. (2020, March 2). Move to protect Kurigram. *The Daily Sun*.
- Tingsanchali, T., & Karim, M. F. (2005). Flood hazard and risk analysis in the southeast region of Bangladesh. *Hydrological Processes*, 19, 2055–2069.
- USGS. (2021). *USGS Global Visualization Viewer (GloVis)*. United State Geological Survey.
- Vojinovic, Z., & Abbott, M. B. (2012). *Flood risk and social justice: From quantitative to qualitative flood risk assessment and mitigation*. IWA. 550 pp.
- Voogd, H. (1983). *Multi-criteria evaluation for urban and regional planning*. Pion Ltd.
- Xiong, J. N., Ye, C. C., Cheng, W. M., Guo, L., Zhou, C. H., & Zhang, X. L. (2019). The spatiotemporal distribution of flash floods and analysis of partition driving forces in Yunnan Province. *Sustainability*, 11(10), 2926.
- Zopounidis, C., & Doumpos, M. (2002). Multicriteria classification and sorting methods: A literature review. *European Journal of Operational Research*, 138, 229–246.

## Chapter 6

# Assessing Human Control on Planform Modification over Floods: A Study of Lower Mahananda–Balason River System, India



Suman Mitra , Mehebab Mondal, Khusbu Khatoon, Susmita Oraon, and Lakpa Tamang 

**Abstract** An indicator-based assessment, using five indicators each on anthropogenic interventions and channel planform, for three major flood events in 1968, 1993, and 2017, was carried out to identify the predominance between floods and human activities in modifying the planform of the Mahananda-Balason system (MBS). Initially, the unconfined stretches of the studied system were segmented into 20 equidistant reaches and used as the assessment units. The land use/land cover practices of the study region were classified using the support vector machine algorithm. The impact of human activities on channel planform was quantified through panel data regression. Planform attributes, measured for pre- and post-flood for the selected years, were tested using the two-tailed “t-test.” A total of four cross-sections were measured, and the flood level of 1968 was superimposed to assess if that level of discharge can cause flooding or not. Results showed that built-up areas had expanded by 197.85% during these 49 years, for the entire area, at the expense of agricultural land or grassland and river. Accordingly, embankments were increased from 2.63% in 1968 to 51.85% in 2017, and almost the entire channel bed (82%) was experiencing large-scale sediment extraction, and significant portions of the adjoining floodplain were concretized (24.10%). Following that, CA, CW, CL, and BI were reduced significantly by  $\geq 40\%$ . The reduction of CCB was also significant but relatively lower in percentage (10.69%). All these fluctuations in channel planform properties were well explained by anthropogenic interventions since the  $R^2$  values were measured  $>0.70$  indicating a strong correlation between the anthropogenic interventions and channel planform alterations. Increased human activities had impacted the channel planform in such a way that except in 1968, no significant inter-seasonal fluctuations regarding channel planform were measured. In few reaches, planform properties responded to the occurrence of floods in 1993 and 2017. Conversely, several reaches even experienced channel narrowing after the flood discharge. Embanking was done on such a large scale that in most areas, even

---

S. Mitra · M. Mondal · K. Khatoon · S. Oraon · L. Tamang (✉)  
Department of Geography, University of Calcutta, Kolkata, India  
e-mail: [ltgeog@caluniv.ac.in](mailto:ltgeog@caluniv.ac.in)

the flood levels of 1968 could not overtop it. Coupled effect of these anthropogenic interventions is transforming this river system into a controlled one where natural channel forming factors have limited roles in reshaping channel planform, which in return is causing socio-hydrological hazards in the form of undersupply of sediments, lack of groundwater, and destabilization of bridges. This cost and time effective methodology can be adopted in other rivers also to assess the extent of anthropogenic interventions and planform alteration along with identifying the responsible factors behind the planform adjustment; however, more in-depth and long-term study is required to fully understand the interrelationship among the anthropogenic interventions and change in channel planform.

**Keywords** Anthropogenic interventions · High flood level · Planform alterations · Sub-Himalayan foothills

## 1 Introduction

Channel planform, the function of a complex interplay between water and sediment discharge, is eventually modified by natural phenomena such as floods, tectonic movement, glacial outbursts, and landslides (Benda et al., 2003; Kiss & Blanka, 2012; Scorpio & Roszkopf, 2016; Righini et al., 2017). Among these, flood is the most predominant since it is the most frequent event which actively influences the fluctuation of sediment and water discharge, but in this era of Anthropocene, anthropogenic activities are becoming predominant in short-term channel planform adjustment (Bandyopadhyay & De, 2017; Bhattacharya et al., 2019). These anthropogenic activities or human modifiers of channel planform can be grouped into some active and passive modifiers. Longitudinal alterations in the form of dams, barrages, retention dams, and sediment mining from channel beds are among the modifiers that directly alter the fluctuation of water and sediment flow (Kondolf, 1994; Kondolf, 1997). On the other hand, lateral disconnection, increase in imperviousness, and removal of vegetation cover can be termed as passive modifiers since these trigger the fluctuation of sediment and water flow by altering the overland flow (Chin & Gregory, 2005; Gregory, 2006; Comiti et al., 2011). At present, the large rivers, especially in Southeast Asia, are undergoing tremendous degradation regarding their hydromorphological properties, hydro-chemical characteristics, and biota assemblage as well (Pamayotou, 1993; Douglas, 1999; Best, 2019; Macklin & Lewin, 2019; Liu et al., 2020). Large-scale flow regulation by damming, embanking, and channelizing along with extensive sediment mining from channel bed is reconfiguring the channel planform at an alarming pace. Rapid urbanization, in this twenty-first century, along the river banks by eliminating the natural floodplain features and vegetation cover, has intensified this process (Paul & Meyer, 2001; Chin, 2006). In response to that channel, the planform is reshaping in such a way that it could bring enormous socio-hydrological hazards such as lowering of groundwater, undersupply of water, sediments and biota, lowering of the channel bed, destabilization of bridge pillars, embankment, etc. (Gregory, 2006; Biswas, 2018).

Channel planform, altered by natural factors, can quickly regain its previous equilibrium condition, but if the anthropogenic activities take part in the reshaping process, then it would create noticeable obstacles in regaining its intrinsic physiography (Kiss & Blanka, 2012; Khaleghi & Surian, 2019). The natural channel-forming factors such as floods are not a day-to-day phenomenon; it occurs once or a few times annually, whereas human activities can be experienced relentlessly with a continuous increase in intensity. Presently developed engineering techniques and river management activities have significantly mitigated the flood hazards by halting and regulating the suddenly increased discharge (Chandra, 2003; Sen, 2010; Abbas et al., 2016; Mohanty et al., 2020). Dams and barrages are used as the major tools of such flood control. Channel planform modification induced by flood discharge can also be overwhelmed by other human activities, such as deforestation, urbanization, and lateral disconnection; sediment extraction can also become the major channel-forming factor.

India being a developing country in Southeast Asia is also not exempted from these intensified anthropogenic interventions on rivers and their effects on channel planform. The massive infrastructural developments started in the 1990s have noticeably modified the country's river-dominated landscapes (Siddiqui, 2010; Mukherji, 2013; Das, 2015). Similarly, such urbanization, channelization, embanking of the river banks, and sediment extraction from channel beds have become a serious issue for the rivers of sub-Himalayan foothills also. Sub-Himalayan foothill, popularly known as "Terai," is presently undergoing a large-scale land use transformation (Prokop & Sarkar, 2012; Prokop, 2018). For ages, rivers were getting modified by human activities, but the rate of such has increased manifold during the last decade. After the adoption of new economic reforms in 1991, this region, sharing boundaries with Nepal, Bhutan and China, serving as a gateway to north-east India has gained immense economic potential, which ultimately results in massive infrastructural development. With this, large-scale immigration, not only from the neighboring states but also from the countries as well, followed by unplanned urbanization became inevitable (Ghosh, 2018). In response to this, the rivers of the "Terai," characterized by heavy monsoon discharge, wide gravelly beds, and braided channel patterns are experiencing notable adjustments toward narrowing, lowering, and becoming single-threaded sinuous rivers (Mitra et al., 2020). Siliguri, the largest urban center of the "Terai" of West Bengal, is situated at the banks of Mahananda and Balason (M and B), immensely pressurizes the adjoining river system. Mostly, the unconfined stretches of these rivers are affected as the topographical hindrances of the hills have restricted the intense human activities only to the floodplain. Since the area receives ample rainfall (2500 mm) from May end to early November, and no major longitudinal obstructions are there, hence heavy flood discharge is inevitable. The largest flood in the recent times of this region occurred in October 1968, and from then onwards numerous major flood events were witnessed in this region (Roy, 2011). But despite having such dominance of floods, the channel planform exhibits no intent of regaining its intrinsic channel planform. Ecologically sensitive and geomorphologically unique sub-Himalayan river systems are an integral part of that landscape, which provides

numerous ecosystem services; now excessive human control would reduce the resources' potentiality, which will ultimately affect all kinds of stakeholders of this river system. In this regard, recently several studies on the rivers such as Teesta, Torsa, Kaljani, Jaldhaka, and Chel Rivers have assessed the planform adjustment scenario (Ayaz et al., 2018; Biswas & Banerjee, 2018; Saha & Bhattacharya, 2019; Dhali et al., 2020; Hasanuzzaman et al., 2021; Saha & Bhattacharya, 2021). But surprisingly, such studies on the channel planform of the Mahananda-Balason system (MBS), which experiences one of the most intensive human activities in this region, are still due. Now to fulfill that research gap, this study was formulated with the prime objectives:

- To quantify the nature and intensity of anthropogenic alterations and channel adjustment and to assess the relationship between them.
- To analyze if the flood discharge is significantly modifying the channel planform or not.

Responsibility of floods, in channel planform modification, is predominant; however, considering the ongoing intensive human alterations, this study has further tested this notion in the unconfined stretch of the MBS.

## **2 Database and Methodology**

### ***2.1 The Spatiotemporal Framework Selected for This Study***

The MBS can be divided into two segments from the geomorphological perspective, i.e., the confined rugged hilly region and the unconfined gently sloped floodplains. The debouching points of M and B at Gulma and Dudhia, respectively, mark the boundary between these two segments. The topographic characteristics eventually determine the intensity of human activities, since hilly rugged topography offers relatively lower accessibility and, therefore, experiences lesser human interventions. Hence, the anthropogenic activities, mostly restricted to the floodplains, extending between the debouching points to Naukaghat (26°40' N to 26°50' N and 88°12' E to 88°28' E), are selected for the study. Delineation of the study area began with the demarcation of the mountain front, a clear dividing line between the confined and unconfined areas. Following that, the unconfined floodplain having the highest and lowest elevation of 300 m and 114 m and a 244.2 km<sup>2</sup> of areal coverage was delineated by processing the digital elevation map (DEM) in ArcGIS (Fig. 6.1). The selected study region, characterized by gentle slopping, covered with thick quaternary deposits, is dissected by wide, multi-threaded rivers namely Mahananda, Balason, Rakti, Rohini, and several other small tributaries (Sarkar, 1989; De, 1998). Annually, the region receives heavy rainfall of over 250 cm, resulting in high monsoonal discharge and sediment yields (Gansser, 1964; Sarkar, 1989; De, 1998; Tamang, 2013; Roy, 2011). Apart from the rivers, this floodplain region is mostly covered by the urban agglomeration of the Siliguri urban region, along with ten

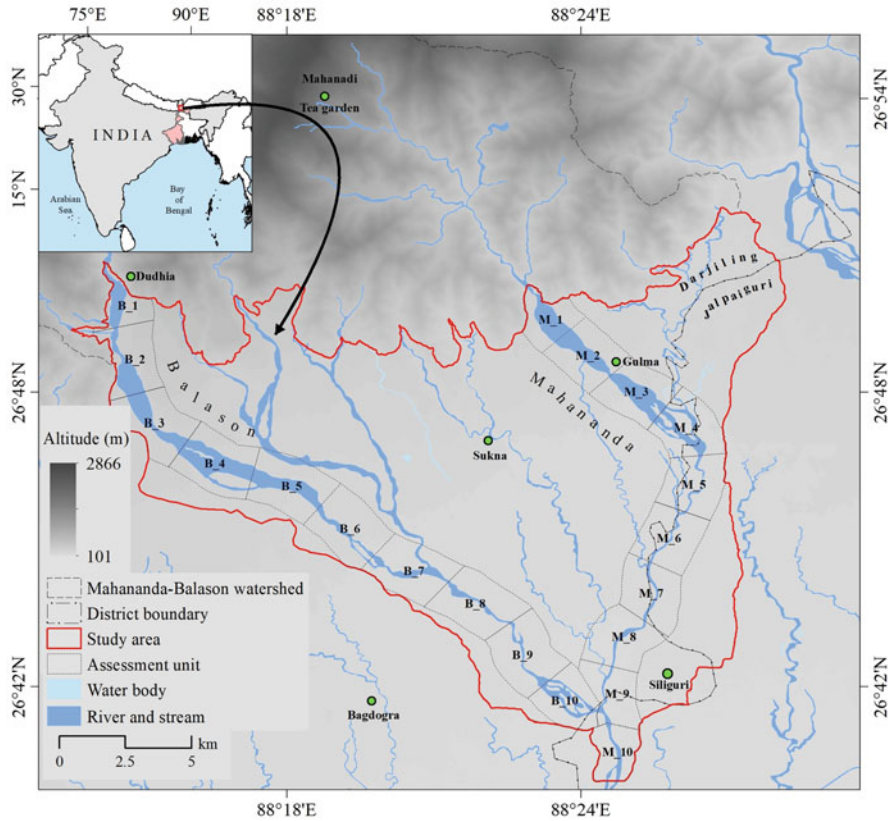


**Fig. 6.1** The location of the study area, its altitude, drainage network, and segmented reaches. (Figure prepared by the author)

census towns (CTs) and several larger villages, tea gardens, dense vegetation patches, and fallow land (Census, 2006, 2014a, b).

Usually, the rivers of the “Terai” of West Bengal experience massive flood discharges annually. High, concentrated rainfall from June to October along with runoff coming from the hills is primarily responsible for this. The first documented flood event in this region occurred in 1787, resulting in the massive avulsion of Teesta (Roy, 2011). Afterwards, during 235 years (1787–2021), this region had witnessed several devastating floods. Now to comply with the data availability, this study was constrained to only the last 49 years (1968–2017). The 1968 flood was the most devastating and well-documented flood event, witnessed by the “Terai” in the last century (Sen, 2011). The flood level of 1968 is marked as the high flood level (HFL) for the rivers of this study area (Table 6.1). Afterwards, in 1993, 25 years later, another high flood discharge was experienced due to heavy rainfall in Bhutan-Darjeeling Himalaya induced by a cloud burst. Very recently in 2017, 24 years later, another heavy flood was observed, affecting almost 4 million people in northern

**Table 6.1** Selected flood events for this study, their levels and cause of flooding

Years	Flood levels (m)		Cause	Date of peak flood discharge	References
	M (Airview)	B (Matigara)			
1968	117.05	124.31	Cloud burst over the sub-Himalayan West Bengal and 1200 mm rainfall triggered a massive landslide and channel blocking. Continued rainfall ultimately breached those blocks and water with a high sediment load caused enormous flooding	02/10/1968	Roy (2011)
1993	114.70	NA	Cloud burst over the lower Bhutan and Darjeeling Himalaya	20/07/1993	Roy (2011) and Government of West Bengal (1993)
2017	115.60	NA	A high amount of rainfall over the sub-Himalayan West Bengal	12/08/2017	Government of West Bengal (2017)

West Bengal and Bihar (Kundu, 2017; The Times of India, 2017; State IAG-West Bengal, 2017). During this time, several other floods had occurred in 1980, 1998, 2000, 2003, 2007, and 2013, but they were either of relatively lower magnitude or distant events from the study area (Roy, 2011). Therefore, three major flood events of the study region, i.e., 1968, 1993, and 2017, having an interval of nearly 25 years were selected for this study.

This indicator-based assessment was initiated after the segmentation of both the major rivers, i.e., M and B into 20 equidistant reaches having a length of 2.25 km and 2.60 km, respectively (Goswami et al., 1999). Their adjoining floodplains, demarcated with a 1 km buffer on each bank, were characterized by dense forest, tea gardens in the upstream, and conversely extensive urban areas, fallow lands, the downstream. The reaches of M and B were denoted as M1, M2, . . . . .M10 and B1, B2, . . . . .B10, respectively.

## 2.2 Dataset Procurement and Preprocessing

This multi-temporal study incorporated four multispectral and two panchromatic satellite images with varying spatial and temporal resolutions (Table 6.1). At first to delineate the floodplain ALOS PALSAR DEM of 12.5 m spatial resolution, dated

**Table 6.2** Geospatial dataset used in this study

Season	Satellite ID	Sensor	Date of acquisition	Path/row	Resolution (m)
Preflood	CORONA	–	06-02-1968	–	1.83
	Landsat 5	TM	02-03-1993	139/041	30
	Sentinel 2A	–	02-04-2017	T45RXX	10
	Landsat/Copernicus <sup>a</sup>	–	05-03-2017	–	–
Post-flood	CORONA	–	22-12-1968	–	1.83
	Landsat 5	TM	15-12-1993	139/041	30
	Sentinel 2A	–	26-12-2017	T45RXX	10
	Landsat/Copernicus <sup>a</sup>	–	13-12-2017	–	–

<sup>a</sup>Acquired from the Google Earth platform

11/02/2009 was downloaded from <https://asf.alaska.edu>. Thereafter, three pre-monsoon images and three post-monsoon images from 1968, 1993, and 2017 were freely downloaded from <https://earthexplorer.usgs.gov/> (Table 6.2). All the geo-rectifications and radiometric corrections were performed afterwards. Rigorous field surveys were carried out from February 2017 to April 2018 for understanding the nature and extent of anthropogenic activities and ground verifying the results derived from image analysis. At that time, four cross profiles across M and B were measured using Leica TC-805 total station. During the field survey, 66 persons, residing adjacent to the rivers for more than 10 years and who had a close association with these rivers, were communicated regarding the past conditions of the rivers along with the ongoing anthropogenic activities and associated adjustments in channel planform. The interviewed persons were mostly the sediment mining labors, fishermen, and the local populace. Besides this, data related to sediment extraction, and embankments were procured from the District Land Reforms Office (DLRO) of Darjeeling District and the office of the Irrigation and Waterways Department, Siliguri Division, Government of West Bengal. The previous research works, governmental reports, news reports, and blog posts were also taken into consultation to develop an understanding of the past floods that occurred in the study area. All the geo-rectification and image classification were done in QGIS 3.16 and ENVI 5.3; the entire geospatial analysis was done in ArcGIS 10.3.1, and the statistical analyses were carried out using R studio.

### 2.3 LULC Classification

Preprocessed satellite images of 1993 and 2017 were classified to obtain the land use/land cover (LULC) using the support vector machine (SVM) algorithm (Mondal et al., 2021). The image of 1968 could not be classified due to its panchromatic nature; therefore, manual digitization was performed. To perform this, intensive fieldwork was carried out in February 2017 to identify the land use practices of the studied region. Based on that, five classes, namely vegetation, river, tea garden, open



land, and built-up, were selected as LULC classes of 1968. For the images of 1993 and 2017, the open land was further classified into agricultural land and fallow land. Since an ambiguity was arisen in separating the agricultural areas with crops and without crops, therefore, to avoid an erroneous result, these two classes were merged in 1968. For accuracy assessment, 156 ground control points (GCP) were collected for seven classes (higher numbers of GCPs were collected for built-up and vegetation) using handheld Garmin e-Trex 20 GPS and Google Earth. Finally, using these GCPs, user's accuracy, producer's accuracy, and Kappa coefficient were calculated (Sarkar & Islam, 2020). Afterwards, the class-wise areal coverage and the temporal changes among them were measured.

## 2.4 Formulation and Measurement of the Indicators

A total of ten indicators (Table 6.3), grouped into two sets of five indicators each, were formulated to estimate the extent of human interventions and the dynamicity of the planform attributes. Thorough ground verification was carried out afterwards and along with it; personal interviews, literature, governmental reports, and high-resolution satellite images of CORONA and Google Earth were consulted. The indicators were formulated to measure anthropogenic interventions mostly focused on measuring the extent of lateral disconnection, in-channel sediment extraction, land use transformation, and longitudinal alterations. On the other side, the indicators measuring the planform attributes were concentrated on changing channel morphology and channel pattern. The measurements of the anthropogenic interventions were solely done from the images of the post-monsoon season, but the planform attributes were measured from both pre- and post-monsoon images to

**Table 6.3** The indicators selected for this study

Indicators		Equation
Anthropogenic interventions	EM (%)	$\frac{\text{Length of the embanked river banks}}{\text{Total length of the banklines}} * 100$
	SM (%)	$\frac{\sum \text{Numbers of mined sub reaches}}{\text{Total number of sub reaches}} * 100$
	BA (%)	$\frac{\text{The area under built up of a reach}}{\text{Total area of the adjoining floodplain of that reach}} * 100$
	VA (%)	$\frac{\text{The area under vegetation cover of a reach}}{\text{Total area of the adjoining floodplain of that reach}} * 100$
	CS (structures/km)	$\frac{\text{Number of crossing structures in a reach}}{\text{Total length of that reach}}$
Channel planform	CA (km <sup>2</sup> )	Total area of the channel corridor of a reach
	CW (m)	$\frac{\sum \text{Width measured}}{\text{Total number of observation}}$
	CL (km)	Total length of the channels in a reach
	CCB (%)	$\frac{\sum \text{Area covered by the bar in the channel of a reach}}{\text{Total area of the channel of that reach}} * 100$
	BI	$\frac{2(\sum \text{Length of all the islands and bars in a reach})}{\text{Total length of the reach}}$

obtain the impact of flood discharge on channel planform. Due to the lack of previous data, channel hydrology was not included in this study.

The quantification of the anthropogenic indicators started with measuring the lateral obstructions in the form of the percentage of the embanked river bank in a reach (EM). All the embankments were initially measured from the geospatial dataset, and thereafter, percentage was calculated (Huang et al., 2019). However, to quantify the embankments of 1993, secondary data, collected from Irrigation and waterways department, were used. The measurement of the reach under active sediment extraction (SM) was initiated by further subdividing the reaches into five equidistant sub-reaches. Now, the mining/extraction activities were traced sub-reach-wise from the geospatial database, literature, and personal interviews, and ultimately, the percentage of sub-reaches identified with active in-channel sediment extraction was calculated (Rinaldi et al., 2005). After covering the aspects of lateral obstruction and sediment extraction, two separate indicators measuring the percentage of built-ups in the adjoining floodplain (BA) and the percentage of vegetation cover in the adjoining floodplain (VA) were quantified to assess the intensity of land use transformation (Chin & Gregory, 2005; Kang & Marston, 2006; Keen-Zebert, 2007; Comiti et al., 2011; Del Tánago et al., 2015). These land use practices control the channel planform adjustments by fluctuating the runoff and sediment load. Now, the reach-wise areal coverages were obtained from the previously classified images, and following that, the percentages of those areal coverages were calculated. It was observed that significant longitudinal obstructions were absent in this study area, but structures altering longitudinal connectivity in the form of bridge pillars were often identified. Therefore, the intensity of these alterations was measured as the occurrence of urban crossing structures on the river channel per km (CS) (Rinaldi et al., 2013). These crossing structures alter the channel in two ways: firstly, its pillars and piers obstruct and deflect the flow, and secondly, it increases accessibility, which ultimately resulted in increasing settlements or impervious surfaces. The crossing structures were primarily identified from the satellite images, and then, the density of them was measured per kilometer of channel length.

Before starting the quantification of the planform attributes, the bank lines were digitized from all six images, and depending on the digitized bank lines, the reach-wise channel area (CA) and reach-wise mean channel width (CW) were calculated. For CW, bank-to-bank channel width was measured at every 50 m interval and thereafter averaged reach wise (Surian, 1999; Galster et al., 2008; Rinaldi et al., 2013; Scorpio & Rosskopf, 2016; Yousefi et al., 2019). Now within the digitized bank lines, all the channels and bars were measured as the total length of the channels in kilometer (CL) and areal coverage of bars in percentage (CCB) (Hajdukiewicz & Wyzga, 2018). Afterwards, to analyze the channel pattern, the braiding index (BI) after Brice (1964) was calculated reach wise. For this, the lengths of the reaches were measured midway between the banks in the channel belt, and similarly, the length of the islands and bars were also measured following its longest axis (Leopold & Wolman, 1957; Ferguson & Werritty, 1983; Ashmore, 1991; Friend & Sinha, 1993; Goswami et al., 1999; Bertoldi et al., 2009).

During all of these measurements, no data gap was observed. The changes measured through these indicators were further statistically tested using a two-tailed T-test with at least a 95% confidence interval. At the time of testing, the channel planform data from post-monsoon was taken into consideration.

## ***2.5 Assessment of the Impact of Flood Discharge on Channel Planform***

The impact of flood discharge on channel planform was assessed by analyzing the seasonal measurements of channel attributes. Those seasonal measurements were further statistically tested using a one-tailed T-test with at least a 95% confidence interval (Nandi et al., 2020). The null hypothesis of this testing was fixed as there was no difference between pre- and post-flood conditions of channel planform attributes. Now, this test was performed three times (1968, 1993, and 2017) for the entire system and for the M and B Rivers separately to identify any inter-river variations. Furthermore, the high flood levels (HFL) of both these rivers (1968 flood levels are the HFL in this region) were superimposed in the present cross-sections to understand if such floods possess any chance of flooding the adjoining areas or not. The HFLs were measured from the bridge pillars and used in superimposition.

## ***2.6 Estimating the Relationship Between the Anthropogenic Intervention and Planform Properties***

Since the structure of the data had spatial and temporal resolution, therefore, panel data regression was opted to measure the impact of the anthropogenic intervention on channel planform. It is found suitable as it deals with heterogeneous datasets and gives a standard effect in longitudinal data. For this study, a fixed effects model (FE) was used for regression analysis (Galvao Jr., 2011; Makuta & O'Hare, 2015) using the following equation:

$$y_{it} = \beta_1 X_{it} + \alpha_i + u_{it} \quad (6.i)$$

where  $\alpha_i$  ( $i = 1 \dots n$ ) is the unknown intercept for each entity ( $n$  entity-specific intercepts) and  $Y_{it}$  is the channel planform properties, where  $i = \text{entity}$  and  $t = \text{time}$ .  $X_{it}$  represents one indicator of anthropogenic intervention,  $\beta_1$  is the coefficient for that indicator measuring anthropogenic interventions, and  $u_{it}$  is the error term.

The selection of the fixed effects model was backed by the Hausman specification test, which confirmed the suitability of the FE model over RE (Random Effects). This model helps to understand the relationship between the multiple dependent and independent variables within an entity on a longitudinal scale. The analysis was

primarily performed for the whole system, but to obtain an inter-system comparative assessment, the analysis was repeated for M and B separately as well. This assessment incorporated the measurements of the post-monsoon for both groups of indicators.

### 3 Results

#### 3.1 Spatiotemporal Dynamics of LULC

The LULC classification (Fig. 6.2) has identified an intense urbanization process in the studied region over the past 49 years. While, in 1968, the urban region was confined to a small pocket in the southern part of the study area (M8 and M9 reach),

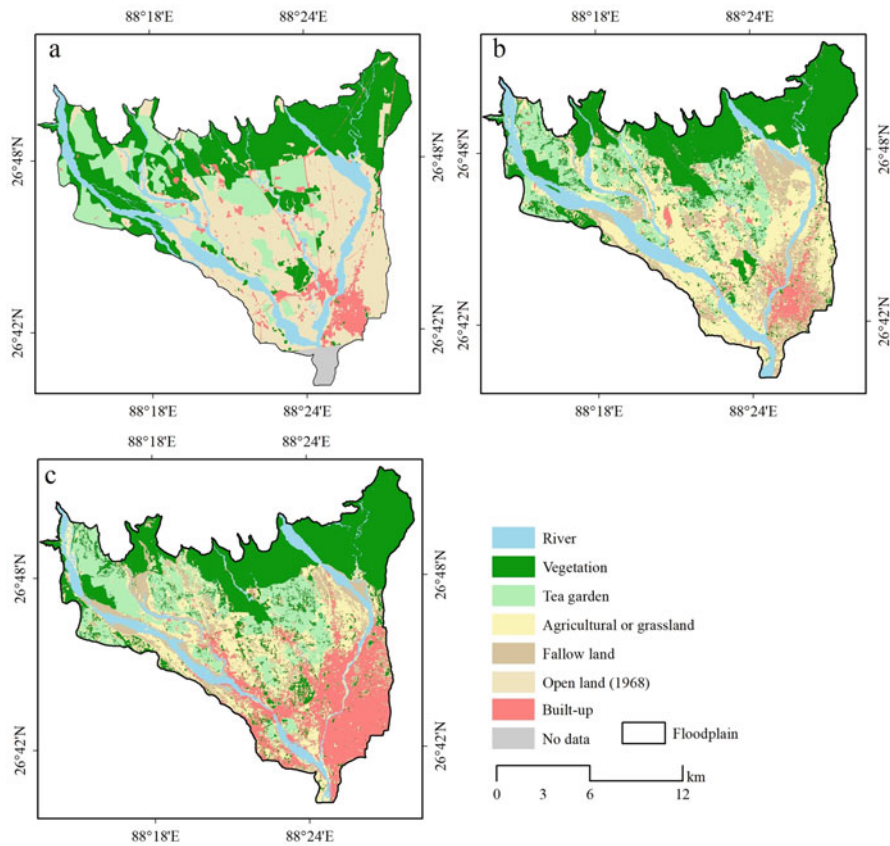


**Fig. 6.2** LULC of the studied system; (a) 1968, (b) 1993, and (c) 2017. (Figure prepared by the author)

**Table 6.4** Areal coverage and change detection data of LULC types

LULC	Areal coverage (%)			Change (%)	
	1968	1993	2017	1968–93	1993–17
River	12.34	11.87	7.79	–3.80	–34.34
Vegetation	30.89	29.76	29.63	–3.67	–0.43
Tea garden	14.64	12.88	15.47	–11.99	20.03
AG/GL (OL <sup>1968</sup> )	34.47	25.65	17.03	7.74	–33.59
Fallow land		11.49	12.06		4.95
Built-up area	6.05	7.35	18.02	21.49	145.17

AG/GL, agricultural land or grassland and OL<sup>1968</sup>, open land for 1968

it was gradually expanded upward and acquired almost one-fifth (18.02%) (Table 6.4) of the study area by 2017 (the areas of M5 to M10 and B7 to B10). The overall increase (1968–2017) of built-ups during the entire study period was estimated at 197.85%, which was mostly accelerated in the second half (1993–2017) with an increase of 145.17%. The reduction of riverine landscape and agricultural land had fueled this growth as they lost their areal coverage by 36.87% (1968–2017) and 33.48% (1993–2017), respectively. A notable 34.34% reduction of the river was estimated during the second half, which was almost ten times higher than that of the first half. The reduction of channels was mostly observed in B4–B7 and B10 along with M3–M6. Conversely, the river flowing through the vegetated areas had not reduced but rather widened in some reaches (M1 and M2). The decrease in agricultural land was mostly observed adjoining the rivers. Interestingly, the fallow land was not reduced rather slightly increased by 4.96% from 1993 to 2017, and overall, the open land decreased by 15.6% (1968–2017). The adjoining Siliguri showed the negligible presence of vegetation from the beginning, and during this period, the reduction of vegetation was also not very alarming (4.07%). The reduction measured in the first half (3.67%), adjacent to B River in B1–B4, was largely compensated in the second half (0.43%). A relatively large vegetation patch, adjacent to M8, was gradually converted into housing. Surprisingly, tea gardens were increased (20.03%) in the second half, after being reduced (11.99%) in the previous one, which might be the reflection of seasonal cutting and replanting of tea or the ambiguity created by similar spectral characteristics of the canopy cover of the trees planted in the tea gardens to provide shade for tea plants. The estimated accuracy for these 1968, 1993, and 2017 were 85.3%, 90.8%, and 91.2% with the kappa coefficient of 82.3, 88.5, and 89.4. The highest accuracy was achieved for built-up with 93.5%, 94.2%, and 94.6% for 1968, 1993, and 2017, respectively.

### 3.2 Measurement of the Indicators

The indicators measuring anthropogenic intervention showed (Fig. 6.3, Table 6.5, Supplementary Table 6.1) a sharp change through time in most cases. At the

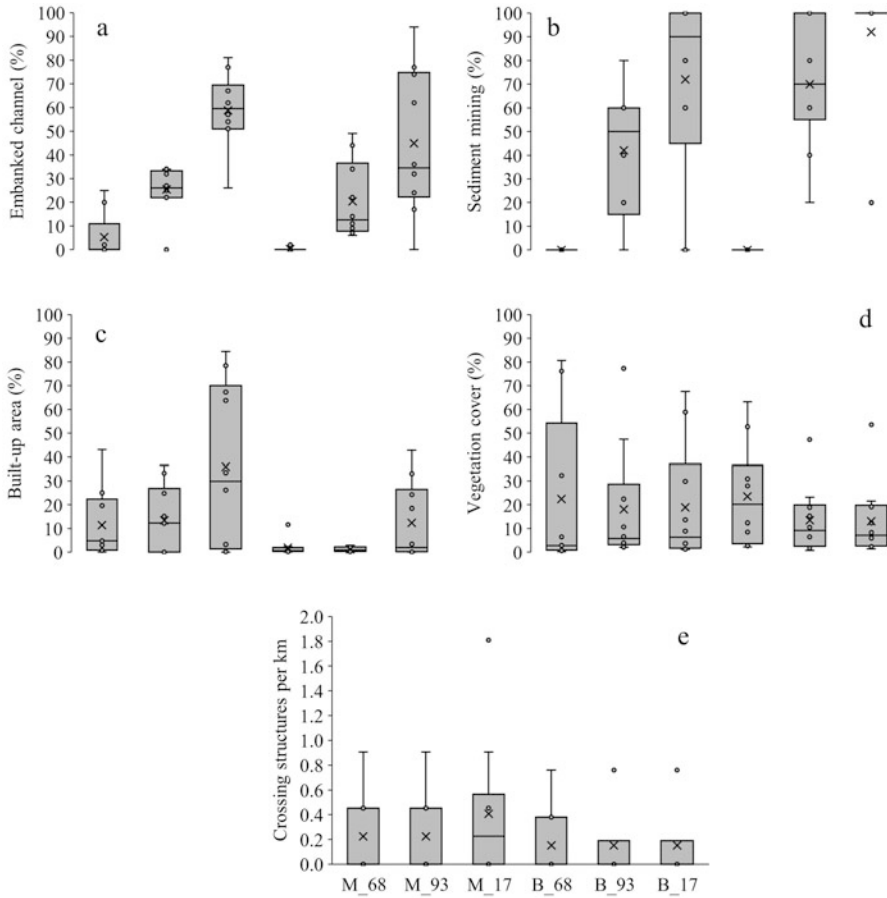


**Fig. 6.3** The dynamicity of the indicators measuring anthropogenic interventions: (a) EM (%), (b) SM (%), (c) BA (%), (d) VA (%), and (e) CS (structures/km). (Figure prepared by the author)

beginning of 1968, the presence of concrete embankments (EM) and practice of in-channel sediment extraction (SM) was negligible, which in 49 years, increased to such an extent that more than half of the channel banks are now embanked (58.80% of M and 44.90% of B) and almost entire channel bed is under active sediment mining (72% of M and 92% of B). Since Siliguri is situated at the banks of M, therefore, it was heavily embanked to protect the urban setup. On the other side, B having a larger catchment area (287 km<sup>2</sup> compared with 116 km<sup>2</sup> of M) produces more sediment and hence more extracted. In 1968, negligible bank protection measures were identified in the reaches such as M8 and M9, but with time, embankments were built in the upstreams (M2–M6 and B5 and B6). Similarly, extraction from channel beds was initiated in the late 1980s in the reaches adjoining the Siliguri (M8–M10 and B8–B10) and expanded upstreams. Following this, the

**Table 6.5** Measurements of the indicators, change detection, and test of significance for the overall system (S) and separately for Mahananda and Balason

Indicators	Overall System						Mahananda						Balason					
	1968	1993	2017	Change (%) (1968-2017)	<i>t</i> -test	<i>df</i>	1968	1993	2017	Change (%) (1968-2017)	<i>t</i> -test	<i>df</i>	1968	1993	2017	Change (%) (1968-2017)	<i>t</i> -test	<i>df</i>
EM (%)	2.63	22.90	51.85	1871.48	-8.649**	37	5.33	25.40	58.80	131.50	-9.105***	17	0.20	20.40	44.90	120.10	-4.682**	18
SM (%)	0.00	56.00	82.00	8200.00	-10.699**		0.00	42.00	72.00	7200.00	-5.660***		0.00	70.00	92.00	9200.00	-11.5**	
BA (%)	6.42	7.38	24.10	275.39	-2.532*		11.46	13.52	35.88	165.38	-2.030*		1.89	1.24	12.31	892.74	-1.993*	
VA (%)	23.04	15.77	15.94	-30.82	0.920		22.49	18.09	18.89	4.42	0.264		23.53	13.45	12.98	-3.49	1.243	
CS (structures/km)	0.19	0.19	0.28	47.37	-0.727	38	0.23	0.23	0.41	78.26	-0.861	18	0.15	0.15	0.15	0.00	0.000	
CA (km <sup>3</sup> )	25.08	23.03	14.94	-40.43	4.504**	37	8.31	8.57	6.32	-23.95	1.988*	17	16.77	14.46	8.62	-48.60	7.541**	
CW (m)	482.24	450.54	291.55	-39.54	4.490**		408.92	343.31	271.89	-33.51	2.228*		548.24	557.77	311.21	-43.23	4.561**	
CL (km)	239.34	169.93	122.37	-48.87	4.213**		81.05	54.51	42.11	-48.04	-9.861**		158.29	115.42	80.26	-49.30	5.460**	
CCB (%)	80.55	74.66	71.94	-10.69	2.104*		75.82	68.78	68.71	-9.38	1.002		84.80	80.53	75.16	-11.37	2.436*	
BI	9.13	6.63	4.99	-45.35	4.148**		7.24	5.17	3.91	-45.99	2.025*		10.84	8.09	6.07	-44.00	5.698**	

\* Significant at 95%; \*\*Significant at 99%

BA was also expanded from 11.46% in 1968 to 35.88% in 2017 in the adjacent floodplain of M. For B, the initial BA was much lower than that of M, amounting to only 1.89%, which rose to 12.31% during this period. Since Siliguri was already urbanized in 1968, therefore reaches such as M8, M9, and M10 showed lower rates of increase than M3, M5, and M6 in the upstreams. Conversely, the upstreams of B were not at all urbanized, and the main agglomeration was seen in the lower reaches, adjacent to Siliguri urban region, namely B8, B9, and B10. Drastic decrease in vegetation cover (VA) was evident in the floodplains of both rivers, but the floodplains of M experienced a sharp decrease until 1993, which was further arrested and showed a slight increase from 1993 to 2017. But in the case of B, the trend was gradually declining. Overall, VA was decreased by 30.81%, which was even greater in the floodplains of B, measuring 44.83%. But the loss was concentrated in most of the upstream reaches such as M1, M2, M3, B1, B2, B3, B4, B5, and B6, since the lower reaches were already devoid of subsequent vegetation cover in 1968. In the beginning, there were only 8 bridges in the entire study region (4 on M and 4 on B), but those on M alone were gradually increased to 8 in later years. However, the CS on B remained constant during these 49 years. Most of the bridges were identified in the close vicinity of Siliguri (M7–M10 and B9) with a few adjacent to hills in M2 and B2.

A reversal of the sharp increase of anthropogenic interventions was observed in the measurement of planform properties (Fig. 6.4, Table 6.5, and Supplementary Table 6.2). The overall CA was reduced by 40.43%, and the rate was even higher in the case of B, amounting to 48.60% compared with a reduction of 23.95% in the case of M. Similarly, the overall CW was also heavily decreased by 39.54%, and the rate of this for B was higher (43.23%) than that of M. The rate of narrowing was mostly accelerated in the second half for both rivers. Most of the loss of CA and CW was observed in the reaches from M3 to M8 and for the entire B. Interestingly, M1 and M2, devoid of interventions, exhibited channel widening. Following the general trend, nearly half of the CL (48.87%) for the entire system was reduced during this period. While B had lost 49.30% of its CL, M being slightly on the lower side got reduced by 48.04%. Reaches such as M3–M8 along with B1–B4, and B6–B10 had experienced a relatively higher reduction of CL. As a result, this multi-threaded channel pattern had become single-threaded in many reaches. The reduction rate was much lower in the case of CCB. Overall, 10.69% of CCB was reduced. Contrary to this, CCB was increased in some of the reaches such as M1, M9, and M10. Following the reduced CL, BI was also reduced noticeably. The reduction rate was 45.35% for the whole system. Interestingly, in this case, the BI of M was largely reduced (45.99%) than that of B (44.00%). Relatively upstream reaches such as M2–M7 and B1–B4 and B6–B8 had experienced higher alterations regarding BI. In some reaches, the BI was reduced to such an extent that it resembled a pseudo-meandering channel.

Test of significance also proved the sharp increase of anthropogenic alterations and drastic decrease in the channel planform properties. Except for VA and CS, the



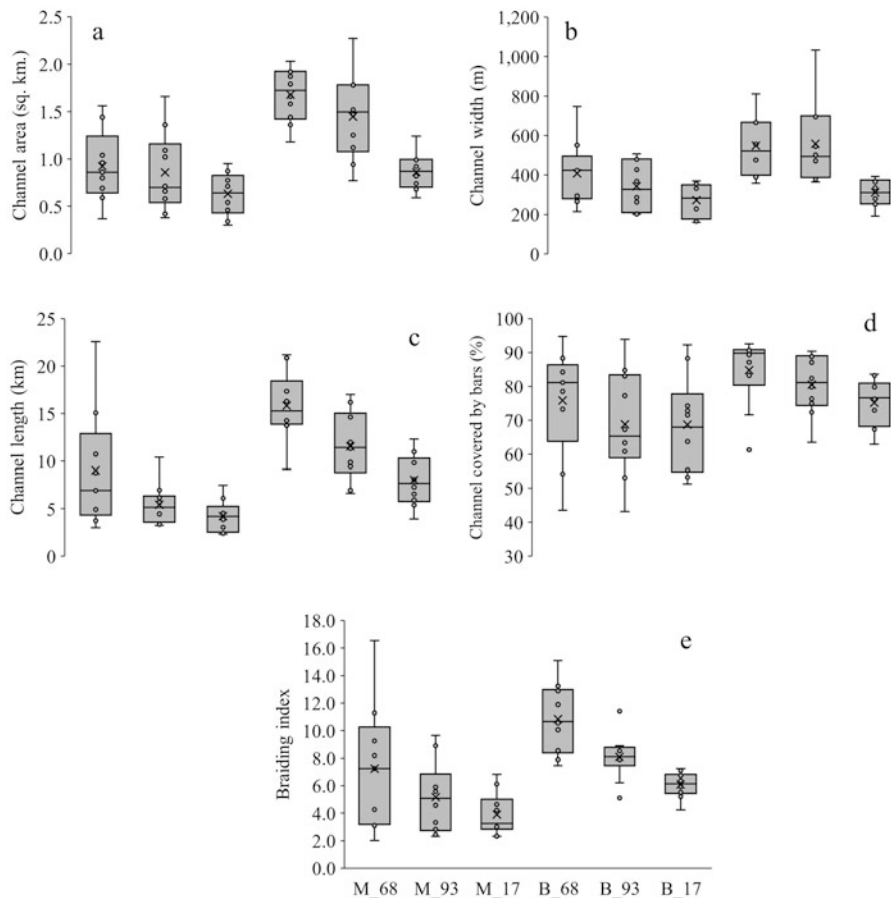


**Fig. 6.4** The dynamicity of the indicators measuring channel planform properties: (a) CA (km<sup>2</sup>), (b) CW (m), (c) CL (km), (d) CCB (%), and (e) BI. (Figure prepared by the author)

other three indicators, i.e., EM, SM, and BA, showed a significant increase from 1968 to 2017. Besides this, all the channel planform indicators, except CCB in M, showed a significant decrease during this period. B exhibited a higher level of significance than those of M for all these indicators.

### 3.3 Impact of Flood on Channel Modification

Inter-season comparison (Fig. 6.5, Table 6.6, and Supplementary Table 6.3) of channel planform properties revealed that in most cases, after the flood discharge, the measurements were increased. In between the pre- and post-flood season of

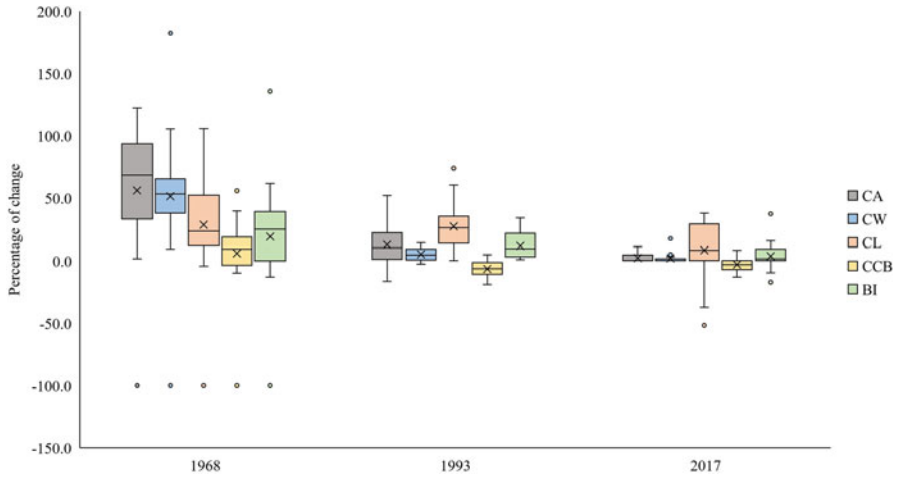


**Fig. 6.5** Sharp decrease in inter-seasonal changes of the planform properties in 1968, 1993, and 2017. (Figure prepared by the author)

1968, overall CA, CW, CL, and CCB were significantly increased by 74.29%, 54.55%, 63.46%, and 14.71%. BI was also increased by 26.98% but not significantly since those increases were confined to a few reaches only. Marked changes on such a scale were completely absent in the later years, i.e., 1993 and 2017. The percentage of change mostly had become  $<10\%$ , and even negative change of 4.5% and 3.15% was measured for CCB after the floods of 1993 and 2017, respectively. However, CL had increased by 33.67% between the pre- and post-monsoon of 1993, but most of this increase was insignificant, since they were restricted to a few reaches such as M4 and M6 and B4, B6, B7, and B8. The seasonal changes of B in 1968 were relatively more significant than those of M. During the initial year (1968), while CA, CW, CL, and CCB were significantly changed by the flood discharge in B, only the CA and CW were increased significantly in M. The percentage of change was also higher in B than in M. Despite being increased by 41.13%, the change of BI in M was not significant since it was confined in M4, M6, and M8. During the later years, no significant inter-seasonal changes in planform properties were observed. But among those, an increase of CL by 62.77% and BI by 24.88% in 1993 along with a reduction of CL and BI by 12.73 and  $-6.68\%$  in 2017 was noticeable.

### 3.4 Relationship Between Human Interventions and Channel Planform

It was observed from the calculated  $R^2$  values (Table 6.7) that in the case of the whole system, all the planform properties showed high correlations with anthropogenic interventions. But when B and M were evaluated separately, some intersystem

**Table 6.6** The indicator-wise measurements of channel planform for pre- and post-flood period along with their change detection and test of significance

Extents	Indicators	1968			1993			2017			<i>t-test</i> ( <i>df</i> )
		Pre-flood	Post-flood	<i>t-test</i> ( <i>df</i> )	Pre-flood	Post-flood	<i>t-test</i> ( <i>df</i> )	Pre-flood	Post-flood		
S	CA	14.39	25.08	-2.955** (34)	21.26	23.03	-0.533 (38)	14.59	14.94	-0.240 (38)	
	CW	312.02	482.24	-3.739** (34)	431.64	450.54	-0.306 (38)	286.15	291.55	-0.221 (38)	
	CL	146.42	239.34	-2.283* (34)	127.13	169.93	-1.173 (36)	113.38	122.37	-0.532 (38)	
	CCB	70.22	80.55	-2.094* (34)	78.18	74.66	0.783 (36)	74.28	71.94	0.650 (38)	
	BI	7.19	9.13	-1.445 (34)	5.87	6.63	-0.950 (36)	4.83	4.99	-0.299 (38)	
M	CA	5.52	8.31	-2.470* (17)	7.02	8.57	-0.931 (18)	6.14	6.32	-0.187 (18)	
	CW	296.87	408.92	-1.688* (17)	318.31	343.31	-0.454 (18)	270.38	271.89	-0.039 (18)	
	CL	64.81	81.05	-1.047 (17)	33.49	54.51	-1.527 (16)	48.25	42.11	0.691 (18)	
	CCB	72.59	75.82	-0.400 (17)	68.46	68.78	-0.044 (16)	67.87	68.71	-0.442 (18)	
	BI	5.13	7.24	-1.107 (17)	4.14	5.17	-0.914 (16)	4.19	3.91	0.350 (18)	
B	CA	8.87	16.77	-2.652** (15)	14.24	14.46	-0.109 (18)	8.45	8.62	-0.198 (18)	
	CW	333.66	548.24	-3.979** (15)	544.97	557.77	-0.146 (18)	301.92	311.21	-0.307 (18)	
	CL	81.61	158.29	-2.402* (15)	93.64	115.42	-1.612 (18)	65.13	80.26	-1.351 (18)	
	CCB	66.84	84.80	-3.667** (15)	85.96	80.53	1.639 (18)	80.69	75.16	1.679 (18)	
	BI	10.14	10.84	-0.526 (15)	7.25	8.09	-1.227 (18)	5.48	6.07	-1.341 (18)	

\* Significant at 95%; \*\*Significant at 99%

S system, M Mahananda, B Balason

**Table 6.7** Estimated  $R^2$  values for each planform parameter indicating the correlation between anthropogenic alterations and channel planform adjustment

Indicator	$R^2(S)$	$R^2(M)$	$R^2(B)$
Channel area in sq. km	0.811	0.939	0.729
Channel width in m	0.713	0.945	0.606
Channel length in km	0.849	0.778	0.889
Reach covered by bar (%)	0.738	0.896	0.458
Braiding index	0.807	0.820	0.790

differences were identified. For the whole system, all the channel planform indicators showed a high correlation with an  $R^2$  value of over 0.700. The correlations of CL, CA, and BI were even higher with an  $R^2$  value of  $>0.800$ . Intra-system comparisons between M and B revealed that the channel planform of M was more impacted by anthropogenic interventions than that of B. While all the channel planform indicators were measured with  $R^2$  values of  $>0.750$  at M, only BI was correlated with an  $R^2$  value of  $>0.750$  at B. The CCB has not even showed significant correlations with the ongoing anthropogenic interventions. Therefore, it was affirmed that the dynamicity of channel planform was profoundly explained by the selected variables of anthropogenic intervention. However, the reduction of bars remained less explained. This statistical analysis clearly explains that the anthropogenic interventions in the form of embanking, sediment extraction, and landscape alteration have significantly affected the planform attributes. The rivers were noticeably narrowed; their channel length was lost, which ultimately altered them from wide multi-threaded, braided channels to single-threaded sinuous ones. Since anthropogenic interventions were recently intensified in the floodplains of Balason, therefore, it had still managed to retain its intrinsic equilibrium, which was already lost for Mahananda due to remarkable alterations at its floodplain for a long time.

## 4 Discussions

### 4.1 *Spatiotemporal Pattern of Anthropogenic Interventions and Planform Modification of MBS*

It was revealed from the LULC analysis that the areal coverage of impervious surfaces had increased significantly in the past 49 years by engulfing the adjoining rural areas. The rate of urbanization was relatively less in the first half (1968–1993), but the adoption of new economic policies in 1991 by the Government of India had accelerated the growth of Siliguri in the second half (1993–2017) (Datta, 1998, 2003; Debnath et al., 2017; Ghosh, 2018, Ahluwalia, 2019). New development policies had increased the economic potency of the Siliguri, and to take advantage of that, people in large numbers from the adjoining areas immigrated to this region. With increasing population, an increase in impervious areas became inevitable, and thus, Siliguri urban region had expanded in such an ill-planned manner by creating enormous pressure on natural resources, especially riverine resources.



**Fig. 6.6** Glimpses of ongoing anthropogenic interventions in the study area: (a) large embankments with groynes and bed stabilization structures along the banks of M, (b) intensive sediment extraction from the B river bed, (c) encroached banks of M, and (d) bridge pillars altering the flow of M. Pictures were taken by the author in December 2016 and April 2017. (Figure prepared by the author)

Measurements of the anthropogenic indicators exhibited exact accordance with this expanding urbanization. Urbanization or concretization needs loads of construction aggregates, which are mostly fulfilled by extracting riverine sediments (Fig. 6.6). The MBS had experienced a similar phenomenon since the late 1980s (Mitra et al., 2020). Initially, a notable portion of the immigrated populace had chosen sediment extraction from rivers as their livelihood and started living adjacent to the extraction sites, mostly at the river banks. Thus, areas alongside both rivers were mostly encroached and converted into built-ups. Now to provide a safe allocation of their newly built dwellings, embankments were introduced (Fig. 6.7). Earlier, the riverbanks adjoining the main city region and the bridges were embanked, but now with increasing settlements, the adjacent river banks were also embanked. Now with the accelerated urbanization, the need for the riverine sediments started increasing, and to meet that demand, extraction activities had occupied nearly the entire unconfined stretch of MBS. Following the emergence of the Siliguri urban region, further immigration had taken place, which in return again escalated the intensity of urbanization, embanking, and sediment extraction. Expanded urban areas need ease of access, and to provide that, several bridges were introduced, and the pillars of those being situated at the river beds eventually altered the discharge. Coupled

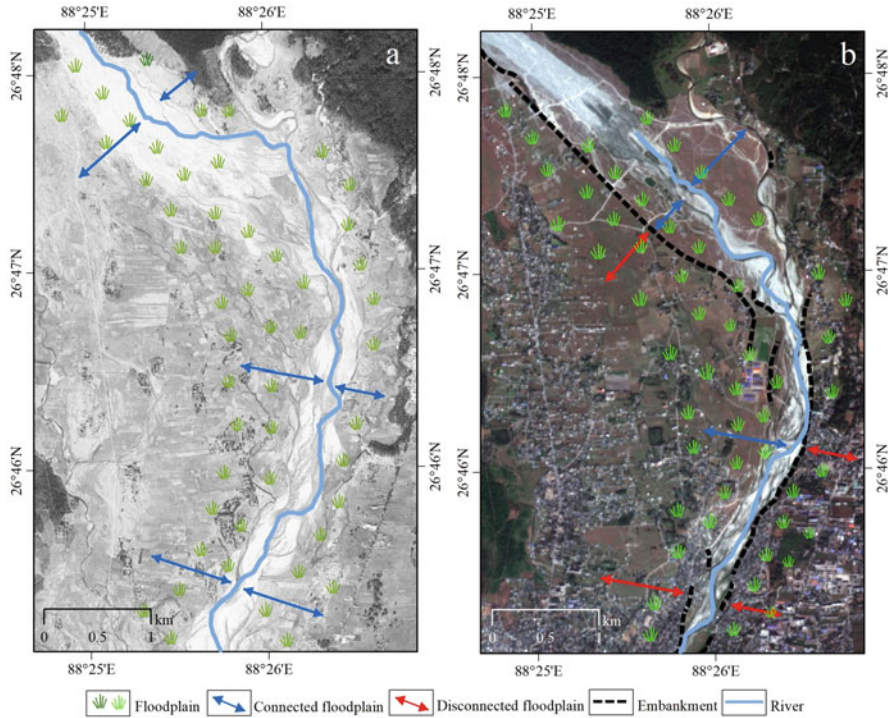


**Fig. 6.7** Concretized embankments are laterally disconnecting the river from its floodplain and narrowing the channel corridor: (a) planform in 1968 with no embankments and laterally connected floodplains of M and (b) planform in 2017 with mostly embanked, laterally disconnected and narrowed. (Figure prepared by the author)

effects of these ultimately resulted in the loss of naturalness of this river system and the region.

In response to this, channel planform started modifying and ultimately pushed to such an extent that regaining its intrinsic equilibrium become mostly unachievable (Fig. 6.8). The predominance of the impervious areas in the adjoining floodplains made the runoff free from sediment load, and protected embankments prevented the lateral migration of the river. Along with these, extraction of sediment from the channel bed helped in initiating channel incision. Now, coupled effect of these would eventually increase the erosion potentiality of the river, which in return made the river system narrower, incised, and ultimately the whole drainage pattern became altered. It was evident that during this period, significant alterations had happened, which were relatively higher in the case of B than M. The adjoining of M was urbanized, and the banks were embanked from several decades earlier; however, B had experienced such interventions at a later stage. So it can be understood that to some extent, the channel pattern and hydraulics of M had adjusted with these interventions. Interestingly, the upper reaches of M, covered by dense natural vegetation, portrayed noticeable channel widening. Other than that, most of the

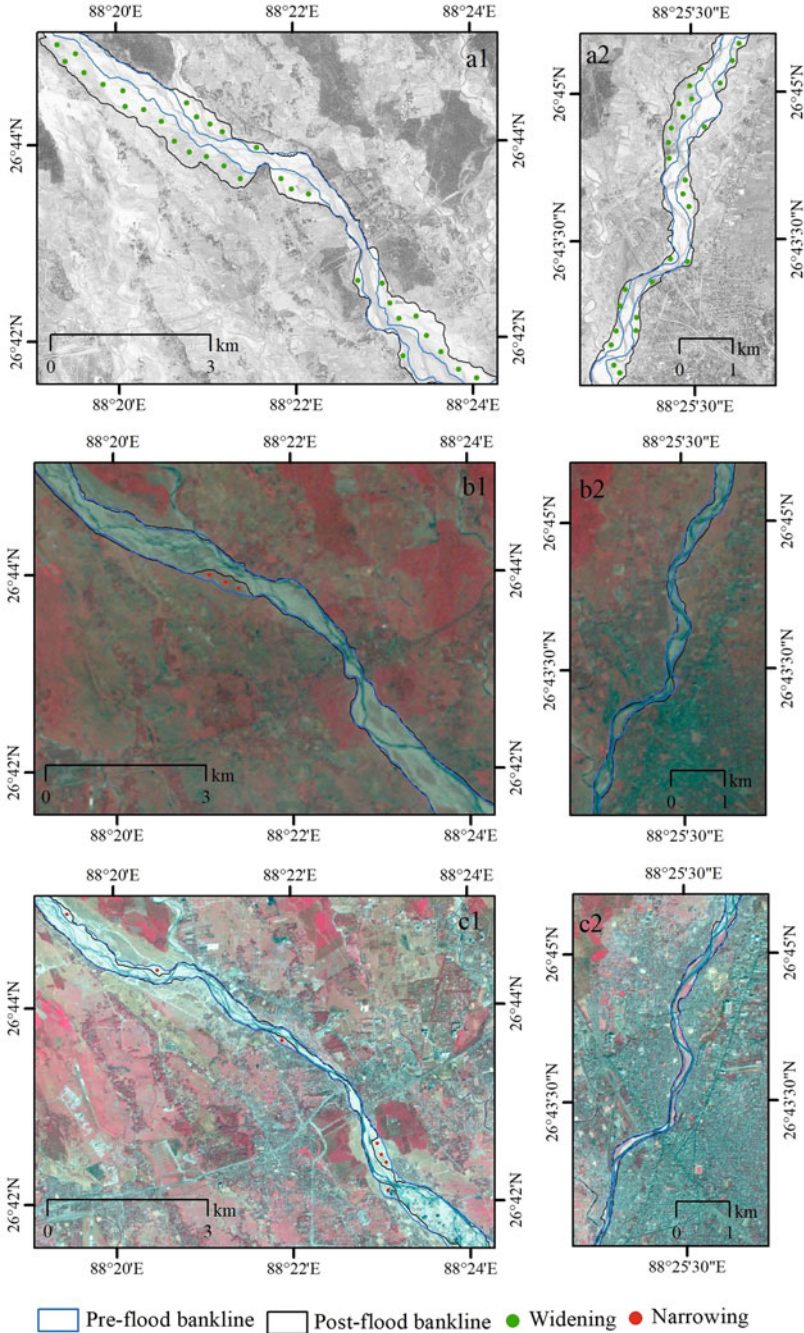


**Fig. 6.8** Channel narrowing through time along with pre and post-flood changes in bank lines: (**a1** and **a2**) conditions of B and M in 1968 is showing extensive widening after the flood, (**b1** and **b2**) conditions of the same in 1993 is showing nearly no widening but slight narrowing after the floods, and (**c1** and **c2**) intensively narrowed river reaches of B and M in 2017 along with notable narrowing after the floods. (All of the used images were post-flood images and the figure was prepared by the author)

reduction of the channel planform properties was observed in relatively upstream reaches of the main urban region, and the spatial extent of those was found in exact accordance with increasing interventions. During the study period, there was hardly any sudden and intensive tectonic event; changes in rainfall patterns or other events that can control the channel pattern were observed in the studied region (Mitra et al., 2020). Therefore, it can be affirmed that the ongoing rapid changes regarding channel planform are being significantly controlled by ongoing anthropogenic interventions.

## ***4.2 Comparing the Role of Flood and Human Activities on Planform Modification***

It is evident from the analysis that in the studied system, anthropogenic interventions are predominantly controlling the channel planform adjustments. Anthropogenic activities had increased through time and in response to that channel planform had adjusted to such an extent that even high flood discharges could not significantly alter the planform (Fig. 6.8). Inter-seasonal measurements of the planform indicators exhibited that except for 1968, other years did not show significant changes; however, some of the changes were notable in those years but confined to a few reaches. As mentioned earlier, the selected years were characterized by large-scale floods across northern West Bengal, but despite that, only the changes in 1968 were found significant. It was also evident that the post-flood changes were gradually becoming more diminishing in the later years (1993 and 2017). At present, a significant portion of the study reach is embanked by huge concrete embankments; the height of those is even exceeding 13 m. So when the storm flux sets in, the excess water cannot be spilt in the floodplains, which triggers the down-cutting process. Sediment-free runoff from the impervious landscape and intense sediment extraction from the channel bed fuel this process. So eventually, storm flux or monsoonal discharge, instead of helping to regain the river's intrinsic channel pattern, ended up enkindling the incision and narrowing process. Among the indicators, the seasonal change of BI was not significant for these years. Several reaches had even experienced a decrease in seasonal change of BI, indicating the reduction of bars and channel length.

The superimposition of the HFLs on the present cross-sections (Fig. 6.9) depicts that most of the sites are protected with such huge embankments that even a flood-like 1968 cannot overtop it. Areas such as Airview more, where the river can spill its water, are now being embanked also, and the remaining chances of lateral migration and spilling of flood discharge are being reduced at an alarming pace. So with such rapid anthropogenic interventions, channel modification due to floods is becoming negligible.



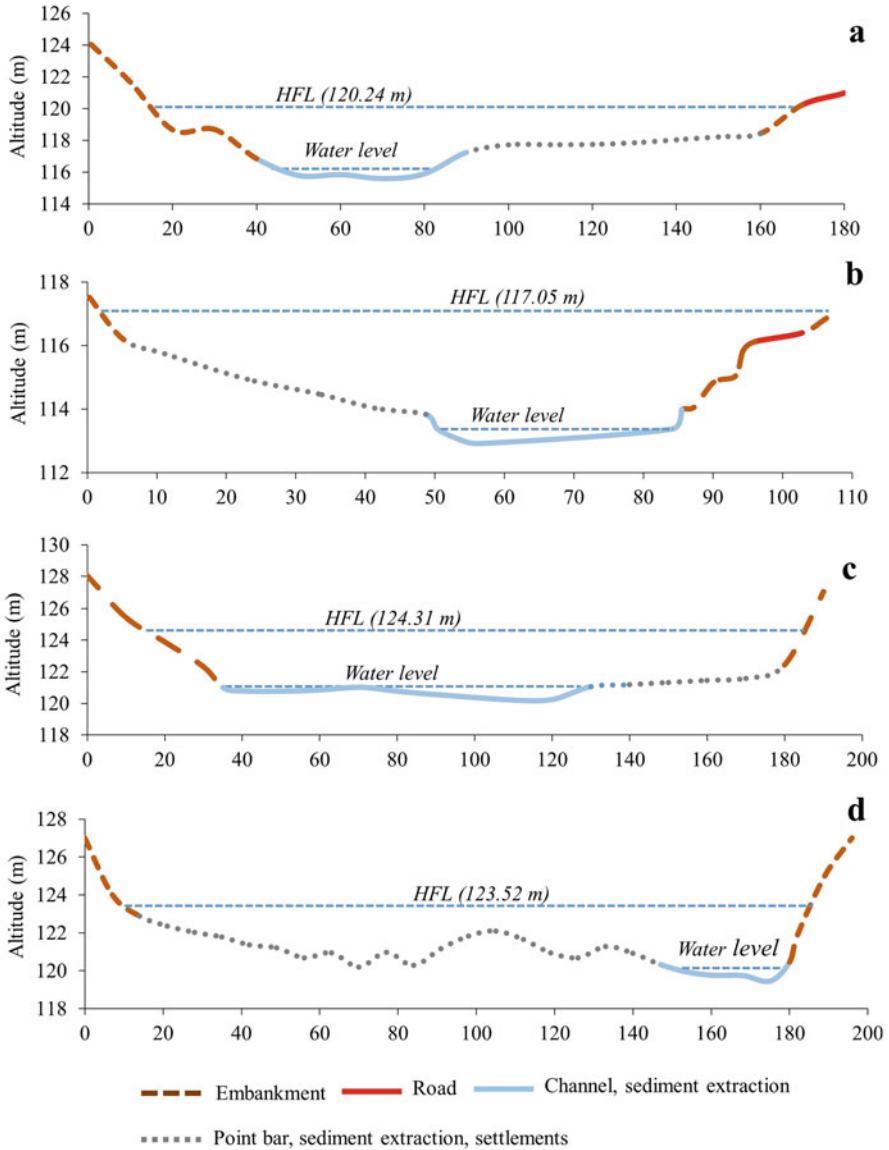


**Fig. 6.9** Superimposition of the HFL (1968 flood level) on the present cross-section shows in most of the reaches embankments are so high that they can be hardly overtopped even with the largest scale of flood discharge in the recorded history. The cross-sections are situated at (a) Champasari (M7), (b) Airview more (M8), (c) Matigara-Balason bridge (B9), and (d) Matigara-Balason Railway bridge (B9). (Figure prepared by the author)

### 4.3 *Possible Future Pattern of Channel Planform and Its Effects*

If anthropogenic interventions and planform alteration would continue at this pace, then there will be an irreparable alteration regarding channel pattern. Along with this, the entire system would experience severe undersupply of riverine resources and related hazards in the socio-hydrological domain. Initial tendencies are indicating this. Already the channel flowing through the main urban region has become single threaded, and this tendency is spreading upstream. Interviews with the local mining workers have highlighted that the lowermost reaches of these systems are experiencing insufficiency regarding sediments of the required grade. Excessive extraction in the past had deteriorated the condition. The upper reaches will experience this in near future as at present those are being extracted extensively to compensate for the nonavailability in their lower counterparts. Increased sediment extraction from the upstreams has further fueled the embanking and urbanization. Coupled effect of these has started reconfiguring this broad, multi-threaded, braided river system into a narrower, single-threaded, and sinuous one. It was observed during the field visit at Matigara and Champasari that secondary bank protection measures are being introduced. This will further restrict the rivers from lateral migration during the heavy seasonal discharge. With such intense human activities, incisions become inevitable. According to Mitra et al. (2020), the unconfined M and B had experienced >2 m of an incision during 1987–89 to 2019, which was similar to Tamang and Mandal (2015).

Reshaping of the rivers in the unconfined floodplains would have an impact on the entire system such as incision tendencies can migrate upstream and accumulation of sediments in the debouching areas can increase. The recharge–discharge cycle of groundwater also is being disturbed as incised river channels have a lower level than the vadose zone; therefore, recharge of that zone from river water has become impossible (Fig. 6.10). On the other side, the groundwater table maintains an equilibrium with the water level of the nearby river; now if the water level of that river goes down, the groundwater level should go down to maintain that equilibrium. The floodplain region of M7–M8 and B5–B9 is experiencing similar problems where the continuous discharge of vadose water can be seen along the river banks, and as a result of that, the non-monsoon lack of groundwater is becoming prominent (Biswas, 2016). Furthermore, the finer particles released during the sediment extraction can also clog the pores, which will obstruct the hyporheic exchange. Finally, the living biota, especially fishes, will suffer enormous habitat destruction. Fishes of these rivers are mostly benthopelagic, bottom feeders, and live in shallow rivers with a rocky or sandy bottom and higher currents. Now with such alteration in channel planform, all these preferable living conditions shall be altered, which will ultimately reshape the biotic assemblage of these river systems. Personal interviews with fishermen supported this notion as they confirmed the large-scale lowering of consumable fishes, observed by Paul et al., 2009.



**Fig. 6.10** Problems associated with channel adjustments: (a) recent incision noticed on B in December 2017, (b) signs of bed lowering on B at Matigara Railway bridge, (c) destabilized bridge pillar on M at Champasari, and (d) discharge of vadose water noticed from the black clay layer along the banks of B. Pictures were taken in December 2017 by the author. (Figure prepared by the author)

## 5 Conclusion

After analyzing the results, it can be affirmed that the unconfined stretch of the MBS is undergoing planform alterations at an alarming pace. Analysis of the anthropogenic interventions and inter-seasonal fluctuations in channel planform properties also exhibit that as the intensity of human activities is increasing, the effect of flood on channel planform is diminishing. As a result of that, the river is steadily losing its inherent equilibrium condition or the river is becoming narrower and sinuous, and showing no tendencies of reshaping with even large-scale flood discharge. The channel is embanked to such an extent that even the discharge of the HFL will not overtop them. Intensive sediment extraction has disturbed the sediment budget, which leads to undersupply of the required sediment grade. Now with less bed load, the river has started down cutting and flood discharge with high energy is fueling that process. Therefore, the incised river shall further become narrower, and ultimately irreparable adjustments regarding channel planform would become inevitable. This may bring imbalance in the socio-hydrological domain regarding lack of groundwater, loss of jobs due to insufficiency of riverine resources, and risking the

road network connectivity. To overcome this, immediate restoration activities should be started in the form of halting any new embankment building, freeing the modern floodplains from settlements, imposing strict regulations on sediment extraction, and afforesting the adjoining areas, especially bank lines.

Floods being the most important natural channel-forming factor eventually act as a feedback mechanism for the channel planform, since it helps the river planform to regain its intrinsic equilibrium condition. Along with this, it also cleans the river, provides sediments to the channel bed, nurtures the riparian zone, adds minerals to the soil of the floodplain and nutrition to the river water essential for the biota, and enormously recharges the groundwater. Now with such intensive anthropogenic activities, flood discharge cannot perform most of these ecosystem services. Along with this, if the flood discharge starts altering the planform in the way how human intervention alters, then it shall permanently modify the channel planform, which will be hazardous for its stakeholders and the present tendencies are indicating this.

**Acknowledgments** Authors are grateful to Dr. Debajit Datta, Assistant Professor, Department of Geography, Jadavpur University; for his valuable support during the preparation of the manuscript. We also express our gratitude toward those who provided their logistic support during fieldwork.

**Conflict of Interest** The authors declare no conflict of interest.

**Funding** This study received financial support (Fellowship Reference No. 3128/NET-JUNE 2014) extended by the University Grants Commission, India to the first author

## Appendix

**Supplementary Table 6.1** Indicators of anthropogenic interventions measured reach-wise and change detection (1968–2017) in %

R_ID	EM_68	EM_93	EM_17	Change (%) (68–17)	SM_68	SM_93	SM_17	Change (%) (68–17)	BA_68	BA_93	BA_17	Change (%) (68–17)	VA_68	VA_93	VA_17	Change (%) (68–17)	CS_68	CS_93	CS_17	Change (%) (68–17)
M_1	0.0	0.0	26.0	2600.0	0.0	0.0	0.0	0.0	0.0	0.0	0.0	0.0	80.7	77.3	58.9	-27.0	0.0	0.0	0.0	0.0
M_2	1.0	22.0	54.0	5300.0	0.0	0.0	0.0	0.0	3.0	0.0	0.2	-93.2	76.1	47.4	67.6	-11.2	0.5	0.5	0.5	0.0
M_3	0.0	25.0	51.0	5100.0	0.0	40.0	100.0	10000.0	0.9	0.0	3.2	255.5	32.3	22.4	29.9	-7.5	0.0	0.0	0.0	0.0
M_4	0.0	22.0	57.0	5700.0	0.0	40.0	100.0	10000.0	0.7	0.8	1.8	166.0	6.4	10.7	13.6	112.4	0.0	0.0	0.0	0.0
M_5	0.0	27.0	62.0	6200.0	0.0	60.0	100.0	10000.0	6.1	12.5	26.2	328.5	2.8	4.8	8.9	214.5	0.0	0.0	0.0	0.0
M_6	0.0	34.0	77.0	7700.0	0.0	80.0	100.0	10000.0	4.8	15.1	67.3	1316.3	0.7	2.2	1.2	82.7	0.0	0.0	0.0	0.0
M_7	2.0	25.0	81.0	3950.0	0.0	60.0	80.0	8000.0	25.0	33.3	84.5	237.9	0.2	3.5	2.1	1055.0	0.5	0.5	0.5	0.0
M_8	25.0	32.0	67.0	168.0	0.0	60.0	60.0	6000.0	43.1	36.5	78.5	82.1	0.9	3.9	1.9	109.5	0.9	0.9	1.8	100.0
M_9	20.0	33.0	51.0	155.0	0.0	60.0	80.0	8000.0	19.7	24.8	63.7	224.2	2.3	6.6	1.2	-49.5	0.0	0.0	0.5	450.0
M_10	NA	34.0	62.0	NA	NA	20.0	100.0	10000.0	NA	12.2	33.5	NA	NA	2.1	3.7	NA	0.5	0.5	0.9	100.0
B_1	0.0	8.0	24.0	2400.0	0.0	20.0	20.0	2000.0	0.0	2.1	0.0	0.0	27.9	15.2	19.2	-31.4	0.4	0.0	0.0	-100.0
B_2	0.0	9.0	17.0	1700.0	0.0	40.0	100.0	10000.0	0.5	1.6	0.3	-32.2	31.1	18.9	21.5	-30.9	0.4	0.8	0.8	100.0
B_3	0.0	6.0	6.0	0.0	0.0	60.0	100.0	10000.0	0.4	0.8	0.0	-90.4	52.7	47.3	53.5	1.6	0.0	0.0	0.0	0.0
B_4	0.0	7.0	36.0	3600.0	0.0	60.0	100.0	10000.0	0.2	0.3	0.3	70.7	63.2	23.1	12.3	-80.5	0.0	0.0	0.0	0.0
B_5	0.0	22.0	74.0	7400.0	0.0	60.0	100.0	10000.0	0.9	0.1	0.4	-53.5	30.9	7.8	2.6	-91.4	0.0	0.0	0.0	0.0
B_6	0.0	34.0	77.0	7700.0	0.0	80.0	100.0	10000.0	0.4	0.4	3.4	777.1	12.3	1.7	2.3	-81.0	0.0	0.0	0.0	0.0
B_7	0.0	11.0	32.0	3200.0	0.0	80.0	100.0	10000.0	1.8	0.8	18.5	939.2	8.5	2.8	1.4	-83.9	0.0	0.0	0.0	0.0
B_8	0.0	14.0	33.0	3300.0	0.0	100.0	100.0	10000.0	2.3	0.9	42.7	1766.3	3.8	6.5	8.3	117.2	0.0	0.0	0.0	0.0
B_9	2.0	49.0	62.0	3000.0	0.0	100.0	100.0	10000.0	11.6	2.6	33.1	184.6	2.7	10.5	6.0	124.6	0.8	0.8	0.8	0.0
B_10	0.0	44.0	94.0	9400.0	0.0	100.0	100.0	10000.0	0.8	2.9	24.3	2894.5	2.2	0.7	2.7	24.9	0.0	0.0	0.0	0.0

**Supplementary Table 6.2** Indicators of channel platform measured reach-wise and change detection (1968–2017) in %

R_ID	CA_68	CA_93	CA_17	Change (%) (68-17)	CW_68	CW_93	CW_17	Change (%) (68-17)	CL_68	CL_93	CL_17	Change (%) (68-17)	CCB_68	CCB_93	CCB_17	Change (%) (68-17)	BL_68	BL_93	BL_17	Change (%) (68-17)
M_1	0.4	0.7	0.9	135.1	214.3	286.4	347.1	62.0	3.0	7.0	7.5	147.5	81.1	83.0	88.3	8.8	3.2	6.2	6.8	110.8
M_2	0.7	1.0	0.7	2.9	266.1	426.9	342.3	28.6	6.9	4.6	5.0	-28.3	94.8	93.9	92.3	-2.6	9.3	5.9	6.1	-33.9
M_3	1.6	1.7	1.0	-39.1	550.8	486.7	370.2	-32.8	15.1	4.5	2.6	-82.8	88.3	84.7	72.8	-17.6	11.3	8.9	4.6	-58.9
M_4	1.4	1.4	0.8	-46.3	747.5	479.2	356.2	-52.3	22.6	10.4	6.1	-73.0	84.2	77.2	71.5	-15.0	16.5	9.7	3.2	-80.4
M_5	1.0	0.7	0.6	-45.2	439.0	368.3	235.3	-46.4	10.7	6.2	4.5	-57.6	78.5	63.3	63.7	-18.8	8.2	5.6	4.2	-48.6
M_6	1.0	0.7	0.5	-52.1	423.3	262.9	228.4	-46.0	8.8	5.7	3.0	-65.4	73.3	67.3	53.3	-27.2	7.2	4.6	3.2	-56.5
M_7	0.9	0.4	0.3	-60.5	440.9	211.6	165.3	-62.5	5.3	3.6	2.3	-56.6	84.3	60.8	55.4	-34.4	4.3	2.8	2.3	-45.6
M_8	0.8	0.4	0.3	-62.5	304.6	202.3	159.9	-47.5	4.9	3.4	2.4	-51.1	54.3	53.1	51.2	-5.5	3.1	2.5	2.3	-25.1
M_9	0.6	0.6	0.5	-8.5	293.9	202.2	181.8	-38.1	3.7	3.2	3.9	4.0	43.6	43.2	64.4	47.8	2.0	3.3	3.0	49.8
M_10	NA	1.1	0.8	NA	NA	506.8	332.5	NA	NA	6.0	4.8	NA	NA	61.3	74.2	NA	NA	2.3	3.3	NA
B_1	1.2	0.8	0.7	-37.3	358.9	390.1	287.6	-19.9	13.7	9.9	7.3	-46.9	89.4	87.1	72.9	-18.4	10.1	8.8	5.5	-45.1
B_2	1.4	0.9	0.7	-52.8	555.7	365.4	279.7	-49.7	9.1	6.6	3.9	-57.1	91.5	72.4	62.9	-31.2	7.9	5.1	4.3	-46.1
B_3	1.9	1.5	1.0	-49.0	403.3	501.4	365.5	-9.4	16.3	6.9	6.5	-59.8	90.6	82.3	79.9	-11.9	10.6	8.5	5.9	-43.8
B_4	1.8	2.3	0.9	-48.6	389.9	1033.2	334.8	-14.1	17.6	16.2	9.8	-44.4	90.6	88.8	83.6	-7.7	11.9	11.4	6.7	-43.3
B_5	1.9	1.5	1.0	-46.0	666.2	486.4	380.4	-42.9	13.9	11.3	12.3	-11.4	90.3	76.3	76.2	-15.6	10.8	7.9	7.2	-32.7
B_6	2.0	1.8	0.9	-54.7	668.5	694.6	371.8	-44.4	20.8	17.0	10.1	-51.7	92.6	79.8	77.1	-16.7	12.9	8.1	6.6	-49.1
B_7	1.9	1.1	0.7	-63.0	811.2	544.3	252.5	-68.9	21.2	14.6	11.0	-48.2	87.1	63.5	68.5	-21.5	15.1	8.9	7.1	-53.0
B_8	1.6	1.8	0.6	-62.7	475.9	378.2	192.4	-59.6	17.3	12.0	5.9	-65.9	83.2	75.0	67.3	-19.1	13.2	6.2	5.2	-60.6
B_9	1.4	1.3	0.8	-39.7	487.5	471.6	255.2	-47.7	14.0	11.5	5.4	-61.6	61.3	89.8	80.1	30.7	7.5	7.9	5.8	-22.3
B_10	1.7	1.6	1.2	-25.3	665.2	712.6	392.5	-41.0	14.2	9.4	8.1	-43.3	71.5	90.4	83.2	16.3	8.5	8.1	6.4	-25.6

**Supplementary Table 6.3** Reach-wise inter-seasonal change of planform properties

R_ID	Seasonal change (%)														
	CA_68	CA_93	CA_17	CW_68	CW_93	CW_17	CL_68	CL_93	CL_17	CCB_68	CCB_93	CCB_17	BI_68	BI_93	BI_17
M_1	42.31	1.47	7.41	58.00	5.45	1.73	-4.44	51.75	-14.47	2.43	-7.70	7.19	-9.24	1.89	-9.43
M_2	68.29	30.77	2.90	9.33	7.10	0.73	14.00	NA	-37.14	-2.54	NA	5.71	3.35	NA	-16.73
M_3	83.53	44.35	1.06	47.96	8.47	0.34	36.32	NA	-51.68	-6.28	NA	0.28	31.78	NA	0.60
M_4	56.52	19.30	9.01	42.11	8.34	1.45	58.05	73.91	0.99	18.19	-9.35	1.85	46.50	18.26	-1.52
M_5	103.92	14.52	1.79	25.68	10.41	0.15	46.65	26.80	31.59	-4.68	-12.45	-8.28	29.06	3.04	-17.07
M_6	113.33	29.41	4.55	50.69	14.51	0.02	22.73	60.45	3.40	-9.85	-3.03	-6.87	135.83	22.46	1.29
M_7	120.51	23.53	0.00	65.30	6.97	0.00	10.10	26.83	0.00	16.47	1.98	0.00	31.48	34.31	0.00
M_8	122.22	52.00	0.00	39.92	9.65	0.00	31.47	15.46	0.00	5.26	-14.72	0.00	48.80	5.60	0.00
M_9	34.09	13.73	0.00	65.68	11.54	0.00	3.32	14.08	0.00	11.29	4.75	0.00	1.52	9.04	0.00
M_10	NA	4.81	0.00	NA	2.31	0.00	NA	1.35	-8.19	NA	-9.46	8.22	NA	2.67	1.87
B_1	NA	4.05	0.00	NA	0.42	0.00	NA	0.10	6.28	NA	-1.30	-2.60	NA	0.88	11.74
B_2	NA	1.08	0.00	NA	0.52	0.00	NA	28.16	26.05	NA	-3.20	-3.65	NA	10.37	9.25
B_3	NA	-4.40	11.24	NA	1.02	1.17	NA	11.22	27.24	NA	-2.71	-5.18	NA	4.73	16.02
B_4	36.64	-2.16	4.55	36.09	11.36	6.79	105.83	25.91	20.37	22.11	-5.12	-5.18	61.77	23.89	13.28
B_5	3.31	-0.68	0.00	55.40	0.26	4.92	23.56	15.75	30.54	15.28	-7.28	-6.16	-1.19	12.07	8.87
B_6	32.68	1.13	0.00	55.18	-2.65	3.18	20.81	49.47	10.54	19.83	-10.24	-12.90	0.78	26.96	6.67
B_7	82.86	-16.42	4.41	182.44	0.77	17.75	42.50	29.96	25.09	55.92	-18.96	-11.51	5.94	21.74	0.85
B_8	79.55	14.10	0.00	53.36	3.56	0.00	59.76	30.85	38.08	39.73	-13.56	-10.63	25.14	10.11	5.25
B_9	1.49	17.92	0.00	81.67	0.69	0.00	21.09	13.60	29.95	7.04	-0.88	-2.67	-12.97	4.17	37.53
B_10	74.74	6.90	0.00	105.46	1.60	0.00	96.41	19.82	31.22	9.27	-1.30	-7.26	29.98	2.79	6.90

## References

- Abbas, A., Amjath-Babu, T. S., Kächele, H., Usman, M., & Müller, K. (2016). An overview of flood mitigation strategy and research support in South Asia: Implications for sustainable flood risk management. *International Journal of Sustainable Development & World Ecology*, 23(1), 98–111.
- Ahluwalia, M. S. (2019). India's economic reforms: Achievements and next steps. *Asian Economic Policy Review*, 14(1), 46–62.
- Ashmore, P. (1991). Channel morphology and bedload pulses in braided, gravel-bed streams. *Geografiska Annaler: Series A, Physical Geography*, 73(1), 37–52.
- Ayaz, S., Biswas, M., & Dhali, M. K. (2018). Morphotectonic analysis of alluvial fan dynamics: Comparative study in spatio-temporal scale of Himalayan foothill, India. *Arabian Journal of Geosciences*, 11(2), 1–16.
- Bandyopadhyay, S., & De, S. K. (2017). Spatio-temporal changes in pollution status of the Haora River. In *Human interference on river health* (pp. 169–181). Springer.
- Benda, L., Miller, D., Bigelow, P., & Andras, K. (2003). Effects of post-wildfire erosion on channel environments, Boise River, Idaho. *Forest Ecology and Management*, 178(1–2), 105–119.
- Bertoldi, W., Zanoni, L., & Tubino, M. (2009). Planform dynamics of braided streams. *Earth Surface Processes and Landforms*, 34(4), 547–557.
- Best, J. (2019). Anthropogenic stresses on the world's big rivers. *Nature Geoscience*, 12(1), 7–21.
- Bhattacharya, R., Dolui, G., & Chatterjee, N. D. (2019). Effect of instream sand mining on hydraulic variables of bedload transport and channel planform: An alluvial stream in South Bengal basin, India. *Environmental Earth Sciences*, 78(10), 303.
- Biswas, M., & Banerjee, P. (2018). Bridge construction and river channel morphology - A comprehensive study of flow behavior and sediment size alteration of the River Chel, India. *Arabian Journal of Geosciences*, 11(16), 1–23.
- Biswas, P. (2016). West Bengal: In this village of 70 wells, 65 dry up in four months. *The Indian Express*. <https://indianexpress.com/article/elections-2016/cities/kolkata/west-bengal-in-this-village-of-70-wells-65-dry-up-in-four-months-2754117>. Accessed 20 Nov 2018.
- Census of India. (2006) *District census handbook 2001: Darjiling District, West Bengal*.
- Census of India. (2014a). *District census handbook 2011: Darjiling District, West Bengal*.
- Census of India. (2014b). *District census handbook 2011: Jalpaiguri District, West Bengal*.
- Chandra, S. (2003). *India: Flood management-Damodar river basin*. World Meteorological Organization and the Associated Programme on Flood Management. *Integrated Flood Management. Case Study*. [https://www.floodmanagement.info/publications/casestudies/cs\\_india\\_sum.pdf](https://www.floodmanagement.info/publications/casestudies/cs_india_sum.pdf). Accessed on 21 July 2020.
- Chin, A. (2006). Urban transformation of river landscapes in a global context. *Geomorphology*, 79(3–4), 460–487.
- Chin, A., & Gregory, K. J. (2005). Managing urban river channel adjustments. *Geomorphology*, 69(1–4), 28–45.
- Comiti, F., Da Canal, M., Surian, N., Mao, L., Picco, L., & Lenzi, M. A. (2011). Channel adjustments and vegetation cover dynamics in a large gravel bed river over the last 200 years. *Geomorphology*, 125(1), 147–159.
- Das, R. J. (2015). Critical observations on neo-liberalism and India's new economic policy. *Journal of Contemporary Asia*, 45, 715–726. <https://doi.org/10.1080/00472336.2014.1003143>
- Datta, A. (2003). *Human migration: A social phenomenon*. Mittal Publications.
- Datta, P. (1998). *Migration in India with special reference to Nepali Migration*. Unpublished PhD thesis. Department of Economics. University of Calcutta, Kolkata, West Bengal. <http://hdl.handle.net/10603/158869>
- De, S. K. (1998). *A study of the fluvial dynamics of the river Balasan*. Unpublished PhD thesis. Department of Geography. University of Calcutta, Kolkata, West Bengal. <http://hdl.handle.net/10603/159910>



- Debnath, M., Ray, S., Islam, N., & Sar, N. (2017). Migration patterns and urban growth in north-east India: A study in Siliguri city. *Quest-The Journal of UGC-HRDC Nainital*, 11(2), 118–123. <https://doi.org/10.5958/2249-0035.2017.00016.X>
- Del Tánago, M. G., Bejarano, M. D., de Jalón, D. G., & Schmidt, J. C. (2015). Biogeomorphic responses to flow regulation and fine sediment supply in Mediterranean streams (the Guadalete River, southern Spain). *Journal of Hydrology*, 528, 751–762.
- Dhali, M. K., Ayaz, S., Sahana, M., & Guha, S. (2020). Response of sediment flux, bridge scouring on river bed morphology and geomorphic resilience in middle-lower part of river Chel, Eastern Himalayan foothills zone, India. *Ecological Engineering*, 142, 105632.
- Douglas, I. (1999). Hydrological investigations of forest disturbance and land cover impacts in South–East Asia: A review. *Philosophical Transactions of the Royal Society of London. Series B: Biological Sciences*, 354(1391), 1725–1738.
- Ferguson, R. L., & Werritty, A. (1983). Bar development and channel changes in the gravelly river Feshie, Scotland. *Modern and Ancient Fluvial Systems*, 181–193.
- Friend, P. F., & Sinha, R. (1993). Braiding and meandering parameters. *Geological Society, London, Special Publications*, 75(1), 105–111.
- Galster, J. C., Pazzaglia, F. J., & Germanoski, D. (2008). Measuring the impact of urbanization on channel widths using historic aerial photographs and modern surveys 1. *JAWRA Journal of the American Water Resources Association*, 44(4), 948–960.
- Galvao, A. F., Jr. (2011). Quantile regression for dynamic panel data with fixed effects. *Journal of Econometrics*, 164(1), 142–157.
- Gansser, A. (1964). *Geology of the Himalayas*. Inter-science Publishers.
- Ghosh, A. (2018). The importance of being Siliguri: Border effect and the ‘untimely’ city in North Bengal. In *Logistical Asia* (pp. 135–154). Palgrave Macmillan.
- Goswami, U., Sarma, J. N., & Patgiri, A. D. (1999). River channel changes of the Subansiri in Assam, India. *Geomorphology*, 30(3), 227–244.
- Government of West Bengal. (1993). *Annual flood report for the year 1993*. Irrigation and Waterways Directorate. [https://wbiwd.gov.in/uploads/annual\\_flood\\_report/ANNUAL\\_FLOOD\\_REPORT\\_1993.pdf](https://wbiwd.gov.in/uploads/annual_flood_report/ANNUAL_FLOOD_REPORT_1993.pdf). Accessed on 29 Jan 2018.
- Government of West Bengal. (2017). *Annual flood report for the year 2017*. Irrigation and Waterways Directorate. [https://wbiwd.gov.in/uploads/annual\\_flood\\_report/ANNUAL\\_FLOOD\\_REPORT\\_2017.pdf](https://wbiwd.gov.in/uploads/annual_flood_report/ANNUAL_FLOOD_REPORT_2017.pdf). Accessed on 29 Jan 2018.
- Gregory, K. J. (2006). The human role in changing river channels. *Geomorphology*, 79(3–4), 172–191.
- Hajdukiewicz, H., & Wyzga, B. (2018). Hydromorphological changes of a mountain river over the last six decades: Case study of the Czarny Dunajec, Polish Carpathians. In *5th Forum Carpaticum*.
- Hasanuzzaman, M., Gayen, A., & Shit, P. K. (2021). Channel dynamics and geomorphological adjustments of Kaljani River in Himalayan foothills. *Geocarto International*. <https://doi.org/10.1080/10106049.2021.1882008>
- Huang, X., Liu, J., Zhang, Z., Fang, G., & Chen, Y. (2019). Assess river embankment impact on hydrologic alterations and floodplain vegetation. *Ecological Indicators*, 97, 372–379.
- Kang, R. S., & Marston, R. A. (2006). Geomorphic effects of rural-to-urban land use conversion on three streams in the Central Red bed Plains of Oklahoma. *Geomorphology*, 79(3–4), 488–506.
- Keen-Zebert, A. (2007). Channel responses to urbanization: Scull and Mud creeks in Fayetteville, Arkansas. *Physical Geography*, 28(3), 249–260.
- Khaleghi, S., & Surian, N. (2019). Channel adjustments in Iranian Rivers: A review. *Water*, 11(4), 672. <https://doi.org/10.3390/w11040672>
- Kiss, T., & Blanka, V. (2012). River channel response to climate-and human-induced hydrological changes: Case study on the meandering Hernád River, Hungary. *Geomorphology*, 175, 115–125.
- Kondolf, G. M. (1994). Geomorphic and environmental effects of instream gravel mining. *Landscape and Urban Planning*, 28(2–3), 225–243.

- Kondolf, G. M. (1997). PROFILE: Hungry water: Effects of dams and gravel mining on river channels. *Environmental Management*, 21(4), 533–551. <https://doi.org/10.1007/s002679900048>
- Kundu, I. (2017). Heavy rains trigger flash floods and landslide in North Bengal, 3 dead. *India Today*. <https://www.indiatoday.in/india/story/bengal-floods-rain-cooch-behar-landslide-1029356-2017-08-12>. Accessed on 14 Aug 2017.
- Leopold, L. B., & Wolman, M. G. (1957). *River channel patterns: Braided, meandering, and straight*. US Government Printing Office.
- Liu, C., Yang, K., Bennett, M. M., Lu, X., Guo, Z., & Li, M. (2020). Changes to anthropogenic pressures on reach-scale rivers in South and Southeast Asia from 1990 to 2014. *Environmental Research Letters*, 16(1), 014025.
- Macklin, M. G., & Lewin, J. (2019). River stresses in anthropogenic times: Large-scale global patterns and extended environmental timelines. *Progress in Physical Geography: Earth and Environment*, 43(1), 3–23.
- Makuta, I., & O'Hare, B. (2015). Quality of governance, public spending on health and health status in Sub Saharan Africa: A panel data regression analysis. *BMC Public Health*, 15(1), 932.
- Mitra, S., Roy, A. K., & Tamang, L. (2020). Assessing the status of changing channel regimes of Balason and Mahananda River in the Sub-Himalayan West Bengal, India. *Earth Systems and Environment*, 4(2), 409–425.
- Mohanty, M. P., Mudgil, S., & Karmakar, S. (2020). Flood management in India: A focussed review on the current status and future challenges. *International Journal of Disaster Risk Reduction*, 49, 101660.
- Mondal, S., Mitra, S., Dey, J., & Tamang, L. (2021). Assessment of the anthropogenic interventions and related responses of Karala River, Jalpaiguri, India: A multiple indicator-based analysis. *Environmental Monitoring and Assessment*, 193(10), 1–23.
- Mukherji, R. (2013). Ideas, interests, and the tipping point: Economic change in India. *Review of International Political Economy*, 20, 363–389. <https://doi.org/10.1080/09692290.2012.716371>
- Nandi, G., Neogy, S., Roy, A. K., & Datta, D. (2020). Immediate disturbances induced by tropical cyclone Fani on the coastal forest landscape of eastern India: A geospatial analysis. *Remote Sensing Applications: Society and Environment*, 20, 100407.
- Pamayotou, T. (1993). The environment in Southeast Asia-problems and policies. *Environmental Science & Technology*, 27(12), 2270–2274.
- Paul, M., Gupta, S., & Banerjee, S. (2009). Fish fauna of major rivers of Darjeeling district, with special reference to their conservation status. *Rec Zoological Survey of India*, 109(4), 15–23.
- Paul, M. J., & Meyer, J. L. (2001). Streams in the urban landscape. *Annual Review of Ecology and Systematics*, 32(1), 333–365.
- Prokop, P., & Sarkar, S. (2012). Natural and human impact on land use change of the Sikkimese-Bhutanese Himalayan piedmont, India. *Quaestiones Geographicae*, 31, 63–75. <https://doi.org/10.2478/v10117-012-0010-z>
- Prokop, P. (2018). Tea plantations as a driving force of long-term land use and population changes in the Eastern Himalayan piedmont. *Land Use Policy*, 77, 51–62.
- Righini, M., Surian, N., Wohl, E., Marchi, L., Comiti, F., Amponsah, W., & Borga, M. (2017). Geomorphic response to an extreme flood in two Mediterranean rivers (northeastern Sardinia, Italy): Analysis of controlling factors. *Geomorphology*, 290, 184–199.
- Rinaldi, M., Surian, N., Comiti, F., & Bussetini, M. (2013). A method for the assessment and analysis of the hydromorphological condition of Italian streams: The Morphological Quality Index (MQI). *Geomorphology*, 180, 96–108.
- Rinaldi, M., Wyzga, B., & Surian, N. (2005). Sediment mining in alluvial channels: Physical effects and management perspectives. *River Research and Applications*, 21(7), 805–828. <https://doi.org/10.1002/rra.884>
- Roy, S. (2011). *Flood hazards in Jalpaiguri district and its management* (Doctoral dissertation, University of North Bengal). Unpublished PhD thesis. Department of Geography & Applied

- Geography. University of North Bengal, Darjeeling, West Bengal. <http://hdl.handle.net/10603/149931>
- Saha, U. D., & Bhattacharya, S. (2019). Reconstructing the channel shifting pattern of the Torsa River on the Himalayan Foreland Basin over the last 250 years. *Bulletin of Geography. Physical Geography Series*, 16(1), 99–114.
- Saha, U. D., & Bhattacharya, S. (2021). Channel avulsion in the Torsa River course and its response to topographic and hydrological controls on the Himalayan Foreland Basin. *Journal of Earth System Science*, 130(4), 1–29.
- Sarkar, S. (1989). *A Geo- environmental appraisal of the upper Mahananda basin of the Darjeeling Himalaya West Bengal*. Unpublished PhD thesis. Department of Geography and Applied Geography. University of North Bengal, Darjeeling, West Bengal. <http://hdl.handle.net/10603/182332>
- Sarkar, B., & Islam, A. (2020). Drivers of water pollution and evaluating its ecological stress with special reference to macrovertebrates (fish community structure): A case of Churni River, India. *Environmental Monitoring and Assessment*, 192(1), 1–31.
- Scorpio, V., & Roskopf, C. M. (2016). Channel adjustments in a Mediterranean river over the last 150 years in the context of anthropic and natural controls. *Geomorphology*, 275, 90–104.
- Sen, D. (2010). Flood hazards in India and management strategies. In Jha M. Kumar (Ed.), *Natural and anthropogenic disasters* (pp. 126–146). Springer.
- Sen, S. (2011, August 29). Bridge on the Untamed Teesta. *Reflections*. <http://akdcts.blogspot.com/2011/08/bridge-on-untamed-teesta.html>. Accessed on 12 June 2019.
- Siddiqui, K. (2010). Globalisation and neo-liberal economic reforms in India: A critical review. In S. K. Pramanick & R. Ganguly (Eds.), *Globalization in India: New Frontiers emerging challenges* (pp. 219–243). Prentice Hall India. <http://eprints.hud.ac.uk/id/eprint/3599/> (Accessed on 25 Jan 2020)
- State Inter Agency Group-West Bengal. (2017). *Sit Rep-II: North Bengal flood report*. Department of Disaster Management, Government of West Bengal. <https://reliefweb.int/report/india/sit-rep-iii-north-bengal-flood-report-17-august-2017>. Accessed on 20 July 2018.
- Surian, N. (1999). Channel changes due to river regulation: The case of the Piave River, Italy. *Earth Surface Processes and Landforms: The Journal of the British Geomorphological Research Group*, 24(12), 1135–1151.
- Tamang, L. (2013). *Effects of boulder lifting on the fluvial characteristics of lower Balason basin in Darjeeling district, West Bengal*. Unpublished PhD thesis. Department of Geography and Applied Geography. University of North Bengal, Darjeeling, West Bengal. <http://hdl.handle.net/10603/33129>
- Tamang, L., & Mandal, D. K. (2015). Bed material extraction and its effects on the forms and processes of the lower Balason River in the Darjeeling Himalayas, India. *Geographia Polonica*, 88(3), 393–405.
- The Times of India. (2017). *Flood cuts off north Bengal, more misery in store*. <https://timesofindia.indiatimes.com/city/kolkata/flood-cuts-off-n-bengal-more-misery-instore/articleshow/60050712.cms>. Accessed on 16 Aug 2017.
- Yousefi, S., Moradi, H. R., Keesstra, S., Pourghasemi, H. R., Navratil, O., & Hooke, J. (2019). Effects of urbanization on river morphology of the Talar River, Mazandaran Province, Iran. *Geocarto International*, 34(3), 276–292. <https://doi.org/10.1080/10106049.2017.1386722>

# Chapter 7

## Exploring the Flooding Under Damming Condition in Punarbhaba River of India and Bangladesh



Swapan Talukdar, Swades Pal, Mohd Waseem Naikoo, and Atiqur Rahman

**Abstract** The flooding in India and Bangladesh causes enormous damage to life, property, and infrastructure loss. The present study, Punarbhaba River, a flood-prone transboundary river of India and Bangladesh, has witnessed many floods since historical times. It needs to be monitored closely. Therefore, we explored the flooding conditions and their effect on river ecology with management in the present study. The present study analyzed the flood condition using flood frequency, basic regional hydrology analysis, and probability analysis. We also reconstructed flooding scenarios using a 2-D hydraulic model at different flood return periods. The wetland transformation has been explored under the reconstructed flooding scenarios. The wetland habitat health was also modeled under different flood scenarios using logistic regression. We proposed flood management plans with the help of a random forest-based flood susceptibility model. Also, we proposed a wetland management plan in floodplain areas with a nature-based solution technique. The average water level (W.L.) during pre- and post-monsoon was 52% and 32%, respectively, but the flow level increased to 3% in postdam periods. The study area witnessed 18% more sudden flooding. Results showed that 4% and 5.1% wetland areas were predicted to be very high and high vulnerable zones during pre-dam conditions, while these have been increased to 34% (very high) and 20% (high) during postdam phase. Findings showed that the flood susceptibility model predicted 11.65% of the area as very high flood susceptible zones, which must be monitored closely. This study will provide a comprehensive foundation for flood management.

**Keywords** Hydrological alteration · Damming condition · Wetland habitat health · Nature based solution · Remote sensing · Machine learning

---

S. Talukdar · M. W. Naikoo · A. Rahman (✉)

Department of Geography, Faculty of Natural science, Jamia Millia Islamia, New Delhi, India  
e-mail: [arahman2@jmi.ac.in](mailto:arahman2@jmi.ac.in)

S. Pal

Department of Geography, University of Gour Banga, Englishbazar, India

## 1 Introduction

Natural disasters and their consequences have increased in recent years due to poor environmental quality, climate change, rapid population growth, and artificial land use intensification (Tehrany et al., 2014). Natural disasters such as landslides, floods, earthquakes, and tsunamis cause significant damage, fatalities, property and infrastructure damage, economic losses, and social disturbance (Lee & Kim, 2018). Floods are one of the most devastating natural disasters in the world, causing damage to property, infrastructure, and human lives (Paul et al., 2019; Yalcin & Akyurek, 2004). Globally, floods have increased by 40% over the past two decades (Hirabayashi et al., 2013). Between 1995 and 2015, floods affected 109 million people and caused damage of up to \$75 billion in damage (Khosravi et al., 2019).

Floods occur when huge amounts of water exceed their carrying capacity and inundate river banks (Sarkar & Mondal, 2020). Climate change is often blamed for the increase in severe flooding (Gersonius et al., 2013). Floods are caused by both natural and human factors (Samanta et al., 2018). Climate change leads to changes in flood patterns, severity, and amplitude (Hens et al., 2018). Floods are common in the monsoon climate zone because of a highly irregular rainfall pattern (Wu et al., 2020). Floods are induced by rapid changes in channel shape due to agricultural expansion, drainage, settlement development, and piracy of distributaries, deforestation, and filling of wetlands (Dash & Punia, 2019). Artificial control, such as dam construction, reduces the magnitude of the flood, while the breach of levees increases the effect of the flood (Talukdar & Pal, 2017). Asian countries, such as India, have very weak flood prevention systems because of the high population density along the river bank and lack of infrastructural development (Du et al., 2019). Excessive rainfall, tidal surges, cyclone storms, strong current from dams and barrages, and inappropriate human intervention contributed to the floods in India (Samanta et al., 2018).

Leopold (1956) correctly predicted that the dam would be the primary contributor to a paradigm shift in the flow regime of rivers. For example, there were 427 large dams exceeding 15 m in 1900, 5268 in 1950, and 39,000 in 1986 (ICOLD, 1998). Currently, India has 5193 large dams, or 15% of the world's total (Graf, 1999). In the twentieth century, approximately 47,000 large dams (>15 m) and 800,000 small dams (World Commission on Dam, 2000) affected nearly half of the 292 significant river systems (Nilsson et al., 2005). Dams are increasingly common along rivers, in both developed and developing countries. Hence, the increasing artificial control over river flow dams has transformed natural flow into artificial (Garf, 2006).

The existence of floodplain ecosystem is inextricably linked to the overflow of periodic rivers of optimal size (Pal & Talukdar, 2019). Previous literature reported that the loss of repeated flood and new sediment deposition on a floodplain due to damming over the river causes changes in river processes and floodplain hydroecology (Paul & Pal, 2020; Talukdar et al., 2020). Regulated streamflow can limit the lateral expansion of river water (Pal & Talukdar, 2018), causing pressure in the habitat and ecosystem beyond the flood threshold.

The Punarbhaba River, a transboundary river between India and Bangladesh, is a highly important river in North Bengal, especially Dakshin Dinajpur, and some parts of Malda District (West Bengal, India) and the Dinajpur District of Bangladesh (Talukdar et al., 2023). Farmers in the basin area are dependent on it for irrigation, which is the only source of water. In addition, huge numbers of fishermen live in Dakshin Dinajpur District, who are totally dependent on it for livelihood. Most importantly, the Gangarampur town is situated along the bank of the river; therefore, this river meets the water requirement of the town. However, in 1992, a dam was constructed at Birganj (Bangladesh) over the river for fishing and irrigation. Since then, the river has witnessed a hydrological paradigm shift, which produces regulated and erratic flow. As a result, sporadic flooding occurred downstream. Therefore, effective flood management is crucial to prevent irregularities and frequent flooding downstream. Based on the obtained information, we determined to analyze and reconstruct the flooding scenarios of the Punarbhaba River. Therefore, to propose effective flood and wetland management in the study area, this research provided a comprehensive study of basic flood frequency analysis, statistical technique-based wetland habitat vulnerability under damming condition, and machine learning-based flood susceptibility to nature-based solution. To the best of authors' knowledge, this is the first attempt to provide a comprehensive study on wetland research under flood scenarios considering the damming condition.

## 2 Study Area

The Punarbhaba River Basin covers 5265.93 km<sup>2</sup> in India and Bangladesh. Punarbhaba is a 160 km river with a 3–8 km width (Fig. 7.1). It begins in Bangladesh's lowlands and goes through Dakshin Dinajpur's Gangarampur block (India). In India, it passes through four blocks of West Bengal (Gangarampur, Banshihari, Kushmandi, and Nalagola), while in Bangladesh, it passes through five districts (Panchagarh, Thakurgaon, Dinajpur, Bochaganj, and Biral). When the

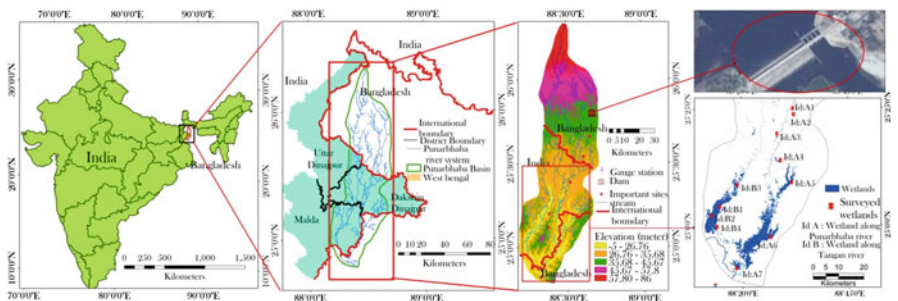


**Fig. 7.1** Location of the study area with altitude and dam location. (Kamardanga dam, Birganj, Bangladesh)

Teesta River ran through it, it was hydrologically active. Neo-tectonic action diverted the Teesta flow toward Bangladesh, cutting off the Punarbhaba River (Rashid et al., 2015). This geological event caused a significant alteration in the river's and riparian environment's hydrological structure. Both ice and rain-fed perennial river flow became rain-fed seasonal river flow. Another source of flow changes in this river was the damming of the river in 1992 (Fig. 7.1). The riparian ecosystem has been severely affected in the post-hydrological modification period because of dam building in this river and considerable water lifting in such a densely populated region. This significantly influences the periodically inundated riparian wetlands, particularly those near the principal river. The dam installation causes dramatic changes. The river's cross-border difficulties between Bangladesh and India are additional causes to investigate its basin.

### 3 Historical Perspective of Floods in the Punarbhaba River

The Punarbhaba River is a small river compared with other rivers in West Bengal and India; therefore, the information is limited. However, the present research has prepared a historical flooding inventory based on the previous literature, local history, and government records. We found historical information about flooding about this river from the work of Agarwal and Narain (1991). They said that prior to 1787 the Teesta River flowed south (from Jalpaiguri to Dinajpur) through the Karatoya to the east, the Atreyee to the center, and the Punarbhaba to the west, where it joined the Ganga. Trisrota (three streams) was the name given to the three channels combined, which is today known as Teesta. In 1787, a disastrous flood occurred in Trisrota, which caused the Teesta River to change course and flow to the southeast, eventually flowing into the Brahmaputra River and separating from the Trisrota.

Subsequently, no data on flooding were available. However, the West Bengal Government's Disaster Management Department (<https://ddinajpur.nic.in/>) has retained flood data for the past 32 years. According to the archives, three types of floods have been recorded since 1987.

Floods of lesser intensity occurred in the following years: 1997, 1999, 2000, 2004, and 2005 (confined to water logging only).

Floods of moderate intensity occurred in 1987, 1992, 1995, and 1998.

In 2017, a severe flood occurred, killing 29 people and destroying Kutcha houses (fully, 40,996; severely, 12,477; and partially, 41,079; Hut-1309, animals, agricultural output, and other things).

## 4 Materials and Methods

### 4.1 Materials

In this present chapter, we used a variety of data collected from different sources. The river and road network was created from a Google Earth image. In ArcGIS, a drainage density map was created using the river network. Details of the materials can be found in Table 7.1.

### 4.2 Method for Flood Frequency and Magnitude Analysis

After dam construction (1992), the flood frequency and duration of high flow were determined. Fluctuations in water flow are studied closely to determine how they affect channel processes. It is possible to fit the lines through the data series with the Gumbel extreme value distribution (type 1). However, in artificially controlled

**Table 7.1** Data types used for different purposes and their respective sources

Data type	Specification	Purpose	Sources of data
Water level data (1982–2016)	Three to six hour intervals in each day	Identifying missing flow, flood simulation	North Bengal Planning Division, Malda, Govt. of West Bengal
Landsat images (4–5 TM and 8 OLI)	Path/row: 139, 42, and 43; spatial resolution: 30 m. Pre-monsoon: 1980, 1982, 1983, 1985, 1986, 1987, 1988, 1989, 1990, 1991, 1993, 1995, 1996, 1997, 1998, 1999, 2000, 2001, 2004, 2005, 2006, 2008, 2009, 2010, 2014, 2015, 2017 Post monsoon: 1980, 1983, 1984, 1985, 1986, 1987, 1988, 1989, 1990, 1991, 1993, 1994, 1996, 1999, 2000, 2003, 2004, 2006, 2008, 2009, 2010, 2012, 2014, 2015, 2016, 2017	For wetland image preparation	USGS Earth explorer
SRTM DEM	Spatial resolution: 30 m	For generating surface	USGS Earth explorer
Wetland-related information	Depth of wetland, areas of wetlands, different land uses over the wetlands and its adjacent areas, channel linkage with wetlands, flood conditions on wetlands	For validating the result	Primary survey in Daiduba, Jatradanga, Jalakar Bithan and Bhatra wetlands along Tangon River; Gojamari and Bakla wetlands along Punarbhaba River

Collected from Talukdar and Pal (2021)



rivers, total probability techniques or other similar approaches should be used to explain flood probabilities better, as noted by Durrans (1988) and USACE (1993). In lieu of Gumbel's technique, a line graph of primary extreme flow distribution for each year was created, with primary, danger, and extreme danger levels (PDL, DL, and EDL) drawn on it. Flood frequency and magnitude have been approximated using this graphical method. On the normal graph, rating curves were created for both pre- and post-reservoir eras to identify changes in normal and critical flood-spilling discharge limitations and the pattern of inflection.

### ***4.3 Instability of Flow***

The instability index is used to comprehend continuous events or time-series data, such as river flow change. Significant changes in flow regime can be identified using instability analysis when water is diverted via a reservoir or canals. The instability index can well capture the internal variability and trend of flow data. Therefore, this method can detect dynamism in discharge data series. For detailed method, please see the work of Talukdar and Pal (2017).

### ***4.4 Methods for Regional Hydrologic Analysis***

Regional analysis of baseline hydrological conditions helps identify regional variance in the data series due to damming over the river. It is computed by comparing maximum/minimum annual flow ratios and maximum/mean flow ratios. The maximum/minimum flow ratio shows the flow range. This shows a significant degree of flow variability. It captures the basic hydrological essence of flows by comparing maximum and average daily flows over time. High max/mean ratios indicate rivers with high floods compared with typical flows, which result in complex geomorphology. Rivers with low max/mean ratios have less fluctuation in flow, simpler designs, and less change. Benn and Erskine (1994) recommended that water discharge be defined by a standardized percentage change (Pc).

In addition to this, Garf (2006) identified a few distinctive hydrological metrics for computing the regional hydrological situation under damming condition, such as maximum/mean daily flow, instantaneous minimum flow, one-day minimum flow, date of minimum flow, range of daily flows, mean up-ramp rate, mean down-ramp rate, etc.

#### 4.5 Method for Simulating Flooding

A flood model can be created in one-dimension (1-D), two-dimensions (2-D), or three-dimensions (3-D). In the case of prismatic channels, the one-dimensional model is often used (channel with uniform cross-section). A two-dimensional model might be used to represent flood inundation as it travels through a non-prismatic channel (one with changing cross-section and alignment) such as a river, river overflowing, or floodplain (Al Amin et al., 2017). In this present chapter, we used HEC-RAS software, provided by the US Army Corps of Engineers, to model flood simulation based on 2-D hydraulic model. Three-dimensional hydraulic models describe flow parameters in three directions: longitudinal (along  $x$ ), transversal (along  $y$ ), and vertical (along  $z$ ). Because of the high computing requirements, 3-D modeling is seldom used in hydraulic investigations. The 2-D hydraulic model, on the other hand, is reasonably time-efficient and straightforward, and it can display spatial flooding. Therefore, it has been frequently used worldwide. As a result, Tonina and Jorde (2013) suggested that 2-D modeling could be enough for most hydraulics and ecological applications.

The new HEC-RAS-v5 solves the complete 2-D Saint Venant equations and the 2-D diffusive wave equations:

$$\frac{\partial s}{\partial t} + \frac{\partial x}{\partial p} + \frac{\partial y}{\partial q} = 0 \quad (7.1)$$

$$\begin{aligned} \frac{\partial x}{\partial t} + \frac{\partial}{\partial p} \left( \frac{x^2}{h} \right) + \frac{\partial}{\partial q} \left( \frac{xy}{h} \right) = & - \frac{n^2 x g \sqrt{x^2 + y^2}}{h^2} - gh \frac{\partial s}{\partial p} + xf + \frac{\partial}{\omega \partial p} (h\tau_{pp}) \\ & + \frac{\partial}{\omega \partial q} (h\tau_{pq}) \end{aligned} \quad (7.2)$$

$$\begin{aligned} \frac{\partial y}{\partial t} + \frac{\partial}{\partial q} \left( \frac{y^2}{h} \right) + \frac{\partial}{\partial p} \left( \frac{xy}{h} \right) = & - \frac{n^2 y g \sqrt{x^2 + y^2}}{h^2} - gh \frac{\partial s}{\partial q} + yf + \frac{\partial}{\omega \partial q} (h\tau_{qq}) \\ & + \frac{\partial}{\omega \partial p} (h\tau_{pq}) \end{aligned} \quad (7.3)$$

where  $h$  is the water depth (m),  $x$  and  $y$  are the specific flow in the  $p$  and  $q$  directions ( $m^2/s$ ),  $s$  is the surface elevation (m),  $g$  is the acceleration due to gravity ( $m/s^2$ ),  $n$  is the Manning resistance,  $\omega$  is the water density ( $kg/m^3$ ), and  $f$  is the Coriolis ( $s$ ). The inertial components of the momentum equations (Eqs. 7.2 and 7.3) should be neglected while choosing the diffusive wave (Quirogaa et al., 2016).

For computing flood simulation modeling (FSM) or flood reconstruction model at different return periods, the cumulative discharge of maximum flow level at Haripur and Bamangola Gauge stations has been used.

#### **4.6 Method for Wetland Mapping**

Extraction of objects from satellite based on spectral value is not new methods. There are several spectral indices that are available for extracting water-bodies, such as Normalized Difference Vegetation Index (NDVI) (Townshend & Justice, 1986), the Normalized Difference Water Index (NDWI) (McFeeters, 1996), the Modified Normalized Difference Water Index (MNDWI) (Xu, 2006), the Water Index (WI), and so on. All these techniques have some advantages and disadvantages. Therefore, before using the spectral indices, researchers have to conduct pilot study and confirmed about the indices. In the present study, Das and Pal (2016) have conducted a study for extracting water bodies from spectral indices. They reported that NDWI is the best method for detecting water bodies and established the optimal threshold for distinguishing water bodies from nonwater bodies in the present study area. As a result, in the present study, we used NDWI with a thresholding approach to map the time series wetland areas.

#### **4.7 Method for Wetland Habitat Vulnerability Under Flooding Conditions Considering Damming Effect**

Wetland habitat vulnerability is crucial for wetland management and conservation. The ecological vulnerability assessment approach is often used to analyze wetland degradation risk and vulnerability (Walker et al., 2001). Researchers have frequently used several framework to calculate the habitat vulnerability, such as USEPA's "Three-Step Framework" (USEPA, 1998), PETAR (Moraes & Molander, 2004), RRM (O'Brien & Wepener, 2012), and PSR (Islam et al., 2021).

The pressure, state, and response (PSR) model were devised by Rapport and Friend (1979), and it was extensively expanded by the Organization for Economic Cooperation and Development (1993). This model has effectively monitored the conditions of marsh, forest, river, and other natural resources. Since the model established a cause-and-effect link between physical and anthropogenic indicators, it can accurately model the wetland habitat vulnerability.

We selected seven parameters to assess wetland habitat vulnerability, such as water presence frequency, agricultural presence frequency, fragmentation of wetland bodies, built-up indices, wetland change rate, flood inundation model or flood reconstructed model, and nonpermanent pixel frequency. To build wetland vulnerability models, selected factors are collected for both before and after dam phases. Then, all the parameters have been integrated together using logistic regression model to generate the habitat vulnerability assessment. It is a multivariate analytic model that predicts several predictor variables to estimate the probability of a dichotomous or binary event (presence or absence). It is used to discover the model that best fits a dependent indicator (vulnerability) and a collection of independent indicators (continuous, discrete, or both) (Basu & Pal, 2017). However, it

does not need linearity or equal variances in the independent indicators' relationships (Solaimani et al., 2013). It is recommended to employ an equal number of vulnerability and non-vulnerable sample sites to establish a better sampling pattern (Suzen & Doyuran, 2004). Therefore, in the present chapter, we selected 1500 wetland vulnerable points and similar number of non-vulnerable points (details can be found in Talukdar & Pal, 2018). We split the dataset into 83:17 ratio as training and testing datasets for model building and validation.

Further, we validate the wetland habitat vulnerability model using ROC curve. It plots the true positive rate against the false positive rate of various diagnostic tests cut points. The area under the ROC curve measures the goodness of fit. The accuracy has been judged based on the area values under the curve (AUC). It ranges from 0 to 1. Close to 1 shows very high accuracy and vice versa (Rasyid et al., 2016).

#### ***4.8 Method for Flood Susceptibility Model***

Flood susceptibility mapping is crucial in the present study for flood prevention and control. Therefore, we chose 12 flood conditioning factors for flood susceptibility modeling, such as elevation, slope, aspect, curvature, flow direction, flow accumulation, Stream Power Index (SPI), Normalized Difference Water Index (NDWI), Normalized Difference Vegetation Index (NDVI), Normalized Difference Moisture Index (NDMI), and Normalized Difference Built-up Index (NDBI).

Alike wetland habitat vulnerability modeling, flood inventory is also required to predict flood susceptibility. We collected the flood and non-flood locations from the field survey and historical Google Earth Image. All flood conditioning variables and flood inventories were integrated with machine learning algorithm (random forest) to generate a flood susceptibility map. Breiman (2001) invented random forest, a widely used robust ensemble machine learning approach used for regression, classification, and unsupervised learning. It is widely used in natural hazard modeling, hydrology, LULC categorization, and finance (Sevgen et al., 2019).

The random forest model combines the random subspace and bagging ensemble models (Naikoo et al., 2023; Chen et al., 2020). This model is less sensitive to multicollinearity and can manage imbalanced and missing data. The RF model works by:

1. Generating subsets from the original datasets using bootstrap-based re-sampling.
2. Producing decision trees using the subsets.
3. Combining the classification or prediction results from all decision trees.

The number of decision trees (Ntree) and the characteristics of the candidate included in the subsets (mtry) are claimed to affect the performance of the RF method (Chen et al., 2020). A considerable Ntree value may increase modeling durations, whereas a little amount might cause problems.

The generated flood model has been validated using ROC curve as like wetland vulnerability model.

#### 4.9 Method for Wetland Creation and Restoration Using Nature-Based Solution

In this work, we used a nature-based solution method to restore and protect a wetland. To do so, we first selected wetland restoration and conservation areas based on a variety of surface water, topographical, water quality, and land cover factors. Then, we created wetlands in the GIS platform on the appropriate places in vector form. Then, we rasterized the new wetland map with base resolution from the polygon format. Finally, we used new wetland model with other parameters to evaluate the wetland habitat vulnerability condition using logistic regression model.

### 5 Results and Discussion

#### 5.1 Monitoring Flooding Conditions in the Punarbhaba River

Storage of reservoirs delays and reduces downstream flooding (Williams & Wolman, 1984), although the delay varies with reservoir size and operational restrictions (Kondolf, 1994). The maximum flood peaks (66%) in pre-dam condition occurred during the pre-monsoon months; however, peak water levels are reduced in postdam condition. Over the past 37 years, the pre-monsoon months have witnessed 55% reduction in the peak discharge. Despite the fact that the dam's storage capacity is only 6,540,000 cubic meters, large volumes of water are channeled through canals for farming, lowering peak discharge levels. Figure 7.2 also shows the frequency of peak flows during the monsoon months. The modal discharge class is also shown on

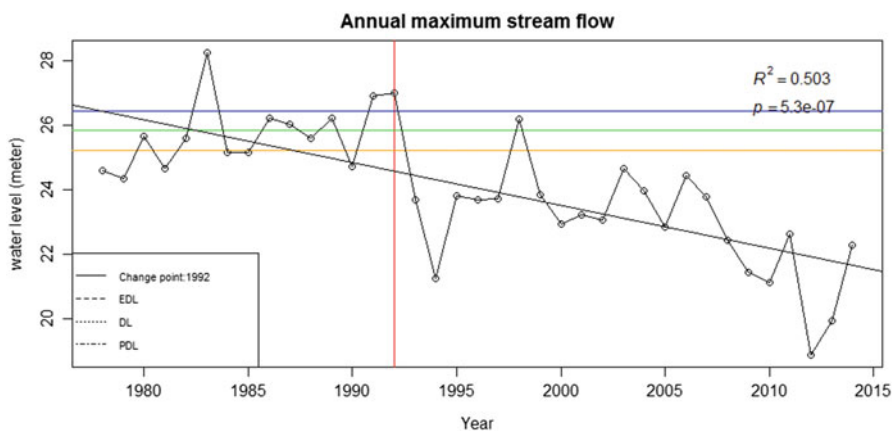


**Fig. 7.2** Annual streamflow level in different years in reference to primary danger level (PDL), danger level (DL), and extreme danger level (EDL)

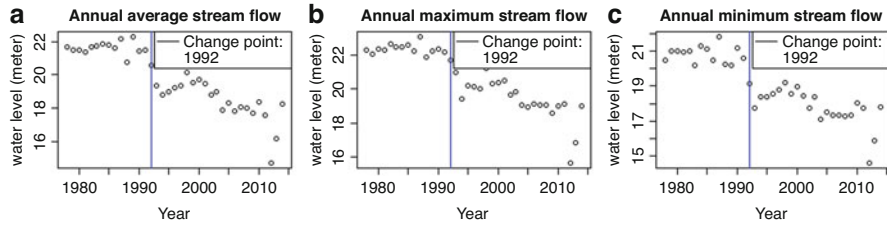


**Fig. 7.3** Location of change point in annual (a) average water level, (b) maximum, and (c) minimum streamflow data (1978–2016)

this graph. It also displays the months with the highest concentration of discharge. We found that the maximum water level (24–26 m) frequency in pre-dam condition was 10 times, but in postdam condition, the height of maximum water flow has reduced to 22–24 m. The frequency was 13 times in 26 years of postdam period. It is surprising to know that the discharge has reached to 28 m just once in pre-dam condition. Since then, the river has never got that level. According to a flood frequency analysis, only three times (20% of the 15 years) had water levels over the extreme danger level (EDL = 26.42 m). However, after the dam construction, water levels are constantly lower than the EDL. Only one year (1998) exceeded the DL (Fig. 7.2). These evidences indicate that the number of flood peaks has decreased since the reservoir was built.

Furthermore, the average annual streamflow levels at pre- and postdam conditions were 21.55 and 18.43 m, respectively (Fig. 7.3). The average water level has declined by 3.12 m since the dam was built. Following the damming in 1992, trend analysis was carried out in order to compare the pattern from before to after the change point.

On average, during the monsoon, maximum high flow duration has decreased by up to 73%, while the diurnal fluctuation coefficient of discharge has increased by 37%. Maximum and mean flow ratios have dwindled in reservoirs condition. After damming, the Punarbhaba River has a large (63.89%) shift in flow (Table 7.2).

The Punarbhaba River's flood probability and return period with specific magnitudes were estimated using Gumbel's extreme value distribution method (Table 7.3). Figure 7.4a, b show the recurrence interval curves for the Punarbhaba River concerning flow magnitudes and the best-fit approach for selection. According to this result, the probable water level in the Punarbhaba River in 2 years return period would be 21 m. The water level of the river would be 30 m at 50-year return periods (Table 7.3).

## 5.2 Reconstruction of Flooding Under Damming Scenario

The flood levels for varied return durations were utilized to simulate spatial floods. Figure 7.4a–e shows flooded areas at 2, 5, 10, 25, and 50 years of return period. The

**Table 7.2** Hydrological parameters for regional analysis in pre- and postdam conditions

Hydrologic parameters	Before reservoir(1978–1992)	After reservoir(1993–2014)
Instantaneous maximum flow (number)	08	16
Year of instantaneous maximum flow	1981, 82, 83, 84, 86, 89, 91	1995, 96, 97, 99, 2001, 03, 04, 06, 08 (January), 08 (June), 10 (January), 10 (June), 11, 13, 14
Thirty-day maximum flow	28.47 m	23.8 m
Month of maximum flow	August 1983	September 1998
Mean monthly flow	21.55 m	18.35 m
Instantaneous minimum flow (number)	7	14
Year of instantaneous minimum flow	1981, 82, 83 (March), 83 (September), 86 (June), 86 (December), 89, 91 (May), 91 (November)	1993 (April), 93 (November), 98, 2001, 02 (March), 02 (December), 03 (February), 03 (September), 06 (March), 06 (August), 06 (December), 09, 2012
Thirty-day minimum flow	14.83 m	11.87 m
Month of minimum flow	May 1991	March 2013
Range of flows (max.-min.)	17.78–28.47 m (during 1983)	18.07–23.8 m (during 1998)
Mean up-ramp rate of water level	1.45 m/month	1.40 m/month
Mean down-ramp rate of water level	1.35 m/month	1.25 m/month
Number of high flow pulses above PDL (P.D.L. = 25.22 m)	12	0
Year of high flow pulses	1983 (July), 83 (August), 86, 87 (July), 87 (August), 87 (September), 89 (July), 89 (September), 89 (October), 91, 92 (July), 92 (August)	–
Number of low flow pulses	9	17
Year of low flow pulses	1882, 83, 86, 87, 88, 89, 90, 91, 92	1995, 96, 99, 2001, 02, 03, 04, 05, 06, 07, 08, 09, 10, 11, 12, 13, 14

Collected from Talukdar and Pal (2017)

**Table 7.3** Estimation of the return periods and flood magnitudes with Gumbel extreme value and log-Pearson type III

Return periods (years)	Percent of chance	Punarbhaba (water level in meters)	
		Gumbel	Log-Pearson type III
2	50	23.68	24.13
5	20	25.73	25.8
10	10	27.06	26.63
25	4	28.78	27.48
50	2	29.98	28.01
100	1	31.24	28.47
200		32.40	28.88

Collected from Pal and Talukdar (2019)

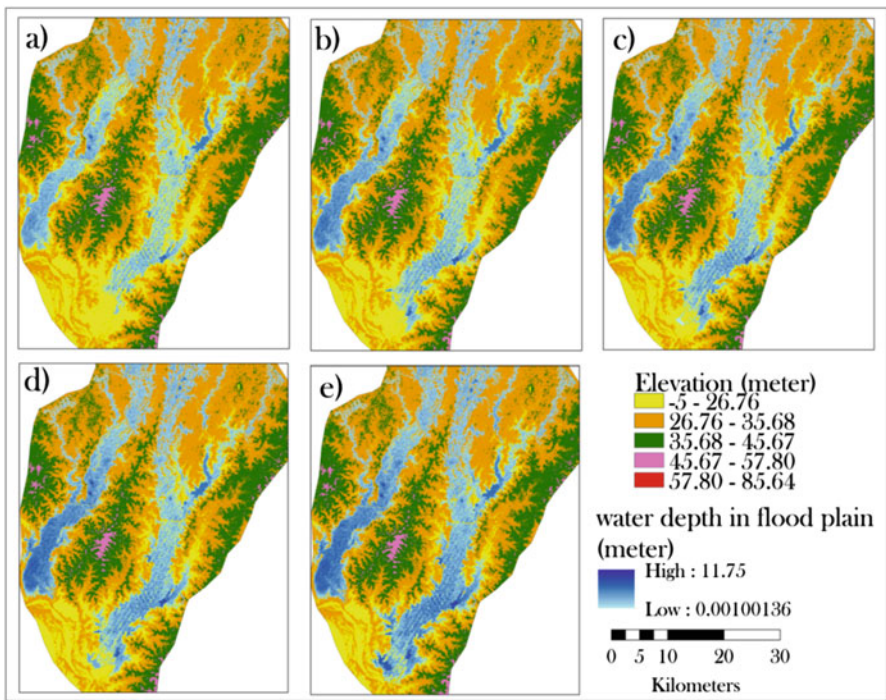


**Fig. 7.4** Reconstruction of flooding scenarios using 2-D hydraulic model at (a) 2 years, (b) 5 years, (c) 10 years, (d) 20 years, and (e) 50 years return periods

areal extent and depth of floodwater in flooded areas for Punarbhaba Rivers were also calculated, such as 737.63 km<sup>2</sup> flooded areas with water level of 29.98 m (recurrence interval 50 years), 671.14 km<sup>2</sup> with water level of 28.78 m (recurrence interval 20 years), 634.83 km<sup>2</sup> with water level of 27.07 m (10 years interval), and 597.66 km<sup>2</sup> with water level of 25.73 m (5 years interval). We found that high discharge caused higher extent of lateral flooding. Based on this, we classified the



lateral flooded areas as active flooded areas (5 years of return period) because these regions would get flood water in every 5 years interval, dormant flooded areas (20 years), and moribund flooded areas (50 years). We also computed the lateral expansion of flooded areas in pre- and post-conditions. It is found that huge parts of active floodplain (found in pre-dam period) have transformed into dormant and moribund flooded areas.

Punarbhaha River has a maximum lateral flood reach of 10 km, and the right bank extends even farther. For 50 years, the lateral flood extent (width) of this basin at the confluence section is 7.7 km; for 10 years, the lateral flood extent (width) is 5 km; and for 5 years, it is 3.9 km. A flood breadth of 7.7 km in pre-dam conditions was reduced to 3.36 km after a dam was built.

### 5.3 Impact of Flooding Under Dam Condition on Wetland Habitat Vulnerability

Figure 7.5a depicts the current wetland cover across floodplain at pre- and postdam conditions. Figure 7.5b, c show the wetland status before and after the dam. As noted in the methodology section, they are categorized as safe, stress, and critical wetland based on the frequency of receiving floodwater from the river. The wetland area decreases in postdam condition from 215.70 km<sup>2</sup> to 90.40 km<sup>2</sup>. The majority of the lost water body is turned into farmland. From pre-dam to postdam, the percentage of safe, stress, and critical wetland decreased from 69.09% to 53.80%, 19.95% to 25.50%, and 10.96% to 20.71%. It means that 53.80% of wetland now gets regular water from the concerned rivers. The percentage of the wetland now in a stress zone is 5.55%. These regions are beyond the current flood limit but not above the pre-dam flood limit. Approximately 9% of wetland area is in critical condition due to

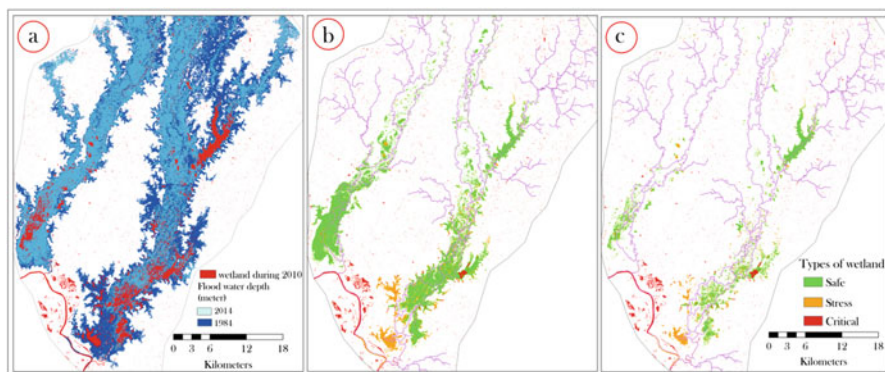


**Fig. 7.5** Effect of flooding under damming scenario on the floodplain wetlands: (a) active floodplain for pre- and postdam condition, (b) wetland states during pre-dam, and (c) postdam periods

exceeding flooding threshold of pre-dam periods. Wetlands without inundation water in a controlled environment are changing. Most species will likely relocate to other wetlands with reliable water supplies. The research area's wetland is becoming more hydro-ecologically vulnerable. Reduced flooded areas and increased flood irregularity are the main reasons for increasing habitat vulnerability. Rainfall has not decreased much in this region during the previous 50 years. Thus, the dam's flow control is critical for such rapid wetland degradation.

We also assessed the health condition of the wetlands under flooding and other factors for pre- and postdam conditions. Before integrating all seven data layers, each indicator's geographical variation status may be quantified to better understand the control of each indicator on the final integrated vulnerability layer. The LWPF area increased by 3.32% following dam construction, showing that these areas experienced water scarcity and isolation from the channel. This indicates that, after dam building, about half of the wetland area had low depth water availability and quickly dried up, exposing it to damage, i.e., vulnerable wetland existence. Patch and edge areas rose from 11.61 to 13.65% and 23.37 to 24.46%, respectively, after dam building. Increased patch and edge wetland area imply decreasing core wetland area due to increasing disturbance, resulting in wetland susceptibility. The area of >80% wetland conversion increased by 23–25% from pre- to postdam; the area of high agriculture presence frequency increased by 23–25% from pre- to postdam, indicating that permanent agricultural land was extended by converting low water presence and low water depth flood plain region. In the NDBI dataset, there was evidence of built-up areas encroaching into the marsh. Because the susceptible zone in each dataset is not concentrated in the same geographical unit or because these datasets exhibit spatial variability, it is necessary to aggregate these datasets using the weights established by the FR and LR models.

Before aggregating the selected seven indicators, the geographical discrepancy condition of each indicator may be stated to assess the impact of each sign on the vulnerability state.

This study uses logistic regression to analyze the spatial relationship between the wetland's irregular and low water presence frequency zones and the conditioning factors (WPF, FIM, NPW, APF, FoW, NDBI, and WC). Figure 7.6 shows the composite LR models of physical wetland vulnerability before and after dams. When the components are combined, WVI maps for pre- and post-dam eras are constructed. A value of extremely low, low, moderate, high, or very high is computed (Fig. 7.6). A higher WVI indicates more susceptibility. The model predicts that pre-dam wetland areas of 7.44 km<sup>2</sup> (3.82%) and 9.78 km<sup>2</sup> (5.02%) are very high and highly vulnerable, whereas postdam regions of 42.97 km<sup>2</sup> (34.07%) and 25.46 km<sup>2</sup> (20.19%) are very high and extremely vulnerable. LR models also reveal that a large quantity of wetland is now vulnerable. Migratory birds prey on marginal and little wetlands.

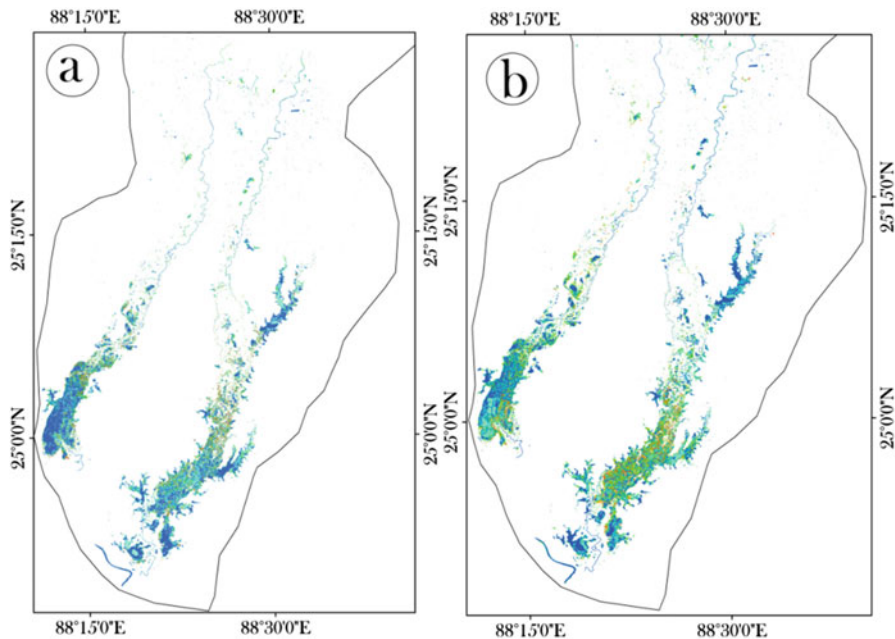


**Fig. 7.6** Wetland habitat modeling under flooding condition using LR model for (a) pre- and (b) postdam condition

#### 5.4 Drivers for Flooding

Floods are often classified as natural disasters whether catastrophes are classified as natural or man-made. Floods, for example, are listed under the subhead “natural catastrophes” by the National Institute of Disaster Management. Floods are sometimes referred to as “the most common sort of natural catastrophe” by the World Health Organization. As like earthquakes, landslides, avalanches, storms, and tsunamis, floods have been a component of the earth’s natural system since the dawn of time. Human activity, on the other hand, has been directly contributing to floods since the advent of agriculture and urbanization. We did, however, provide a list of causes for flooding.

Floods caused by a dam failure and breaching are abrupt, and their effects are more damaging to lives and property due to the intensity of the flood and the unpreparedness of the inhabitants of the surrounding regions. Communities are vulnerable due to the unexpected nature of flooding caused by dam failure and the reluctance of the authorities to share information with the public. Flood water rises in an undammed river not suddenly, but with time, giving people time to react. Furthermore, the dam alters the riverbed’s contours, the river’s down streamflow, and even the floodplains.

The gradual shrinking of wetlands and lower water level are making it easier for farmers to reclaim wetlands for agricultural purposes. According to Pal and Talukdar (2018), the agriculture area of the Punarbhaba River increased from 59.19% to 84.2% (out of total basin area) in postdam condition, while the built-up area is increased from 2.54% to 5.72%. Many researchers, such as Pal and Saha (2018), have reported on the conflict between farmland and wetland. As a result of decreasing wetland areas (act as natural water container), the study area has experienced flooding with less amount of rainfall (e.g., flooding at Gangarampur along the Punarbhaba river on 14 August, 2017). As per the government report, damages were more in 2017 flood with 26 m water level recorded at gauge station, while 1987 flood caused less damage with 28 m recorded water level. The major factor is the decrease of wetland water storage capacity.

### 5.5 Recommendation for Flood and Floodplain Wetland Management

#### 5.5.1 Flood Susceptibility Model

The flood susceptibility model has been prepared for future flood management to reduce the damage. Landsat image and SRTM DEM datasets were used to create flood conditioning parameters, which were used to prepare susceptibility model using RF. Following natural break principles, the generated flood susceptibility model was divided into five susceptibility zones: very high, high, moderate, low, and very low (Fig. 7.7). The model identified riparian corridors along major rivers as very high flood-prone zones, accounting for 7–15% of the overall area. The high flood susceptible zone, on the other hand, changes only 15–16% (smaller

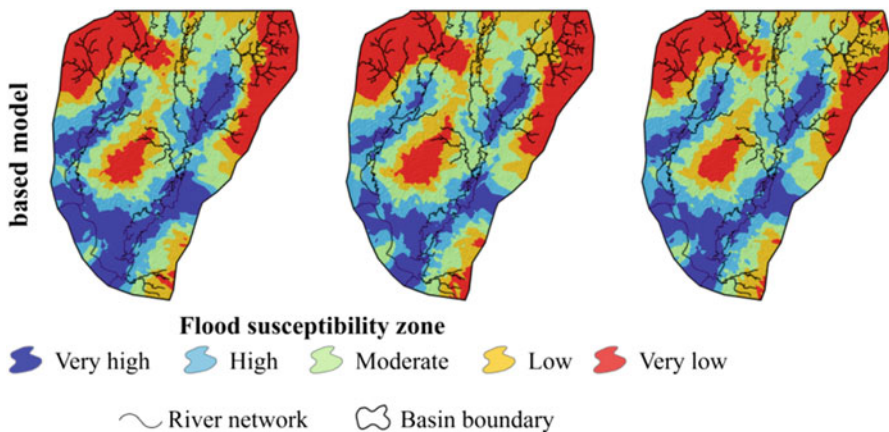
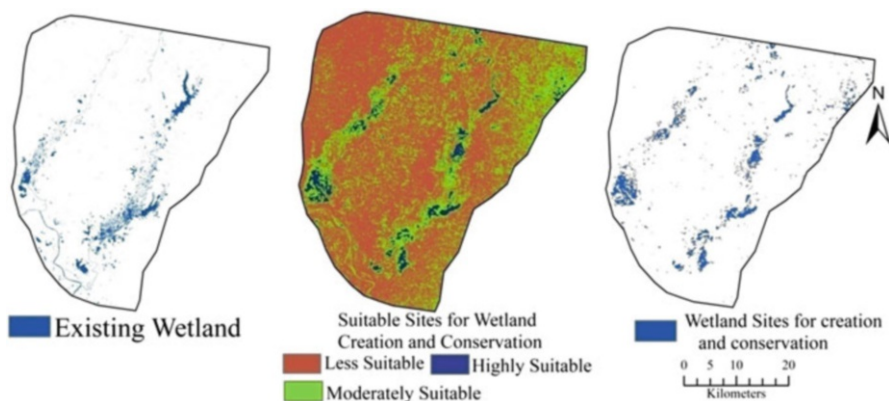


Fig. 7.7 Flood susceptibility model using RF at different tree number

fluctuation), yet the variance is large (area: 19–26%). The distant from major rivers and interfluvial zones of the major rivers have very low and low flood sensitive zones. Low and extremely flow flood-sensitive zones have been discovered in around 16–25% and 32–44% of the areas, respectively.

### 5.5.2 Wetland Conservation and Restoration Using Nature-Based Solution

The first task was to predict the appropriate location of the wetland to be restored and conserved. For this, wetland restoration and conservation suitability model was constructed using several factors and analytical hierarchy process (AHP) model. The AHP model has calculated weights for different parameters based on expert opinion and pair-wise matrix comparisons. Then, the weights were assigned to the factors and generated wetland restoration and conservation suitability map. The map was classified into three classes, such as less suitable, somewhat appropriate, and very suitable. We selected the very suitable class for the best choice of the wetland conservation and restoration. The less suitable and somewhat appropriate groupings are dominated by agricultural land and other land use/land coverings (Fig. 7.8). Agricultural landscapes and towns inhibit the creation of new wetlands by fragmenting existing wetlands, putting habitat quality and wetland health at risk. As a consequence, human intrusion should be avoided in newly developed wetlands. The areas with the worst quality require extra conservation efforts. Then, we converted this class into polygon format and combined it with the existing wetland map. Thus, we created a new wetland map, which then rasterized in ArcGIS software.



**Fig. 7.8** Modeling of suitable sites for wetland conservation and restoration: (a) existing wetland (2020), (b) suitable site model, and (c) selected sites for wetland conservation and restoration (N.B. highly suitable site for wetland conservation and restoration has been selected as wetland conservation and restoration sites)

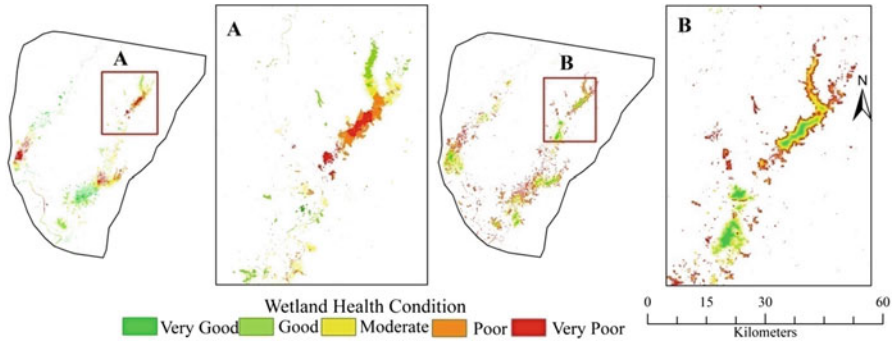


**Fig. 7.9** Comparisons of wetland health condition models between (a) health condition model using existing data and (b) health condition model using existing data and new wetland data (N.B. new wetland map has been prepared by integrating existing wetland area (2020) and selected sites for wetland conservation and restoration)

Then we used new wetland map as parameters for wetland habitat health condition modeling with other parameters. Thus, we created two wetland habitat health condition models, such as the current condition and the new condition (Fig. 7.9). Figure 7.9 shows the health of wetland habitats using existing data (Fig. 7.9a) and the health of freshly developed wetland data using existing data (Fig. 7.9b). The facts that Fig. 7.9a depicts regions dominated by poor and very poor wetland health, while the percentage of poor and very poor areas decreased dramatically when new wetland data was included, is a remarkable finding. The area of superior quality wetland, on the other hand, has increased from 28% in current wetland data to 62.28% using new wetland data. The state of wetlands would undoubtedly improve if additional wetlands could be developed in a sustainable way.

## 6 Conclusion

It is obvious from this study that the Punarbhaba River has seen hydrological changes as a result of the dam's construction. As a result, the average water level has decreased from 42% to 62%. As a result, the river's floodplain wetlands, which are mostly nourished by river water, have faced water shortage. It results in a large reduction in the marsh area. Factors such as agricultural growth, continual urbanization, groundwater depletion, river separation, and other developmental projects hasten the process. Existing wetland vulnerability is considerable, according to the data. Sudden and erratic floods have been reported in the research region as a result of damming. As a result, flood vulnerable mapping has been completed in order to monitor the floods. The lower reaches of the river basin, particularly the very close riparian corridor of the main river, which accounts for 19% of the overall study area, has been determined to be very vulnerable to flooding. These locations must be closely monitored. We also recommended adopting the natural-based solution approach for flood and wetland managements.

## References

- Agarwal, A., & Narain, S. (1991). *Floods, flood plain and environmental myths* (State of India's environment: A citizens' report, 3) (pp. 32–39). Centre for Science and Environment. <http://csestore.cse.org.in/usd/soe3.html>
- Al Amin, M. B., & Haki, H. (2017). Floodplain simulation for Musi River using integrated 1D/2D hydrodynamic model. In *MATEC web of conferences* (Vol. 101, p. 05023). EDP Sciences.
- Basu, T., & Pal, S. (2017). Exploring landslide susceptible zones by analytic hierarchy process (AHP) for the Gish River Basin, West Bengal, India. *Spatial Information Research*, 25(5), 665–675.
- Benn, P. C., & Erskine, W. D. (1994). Complex channel response to flow regulation: Cudgegong River below Windamere Dam, Australia. *Applied Geography*, 14(2), 153–168.
- Breiman, L. (2001). Random forests. *Machine Learning*, 45(1), 5–32.
- Chen, T., Zhu, L., Niu, R. Q., Trinder, C. J., Peng, L., & Lei, T. (2020). Mapping landslide susceptibility at the Three Gorges Reservoir, China, using gradient boosting decision tree, random forest and information value models. *Journal of Mountain Science*, 17(3), 670–685.
- Das, R. T., & Pal, S. (2016). Spatial association of wetlands over physical variants in barind tract of West Bengal, India. *Journal of Wetlands Environmental Management*, 4(2).
- Dash, P., & Punia, M. (2019). Governance and disaster: Analysis of land use policy with reference to Uttarakhand flood 2013, India. *International Journal of Disaster Risk Reduction*, 36, 101090.
- Du, S., Cheng, X., Huang, Q., Chen, R., Ward, P. J., & Aerts, J. C. (2019). Brief communication: Rethinking the 1998 China floods to prepare for a nonstationary future. *Natural Hazards and Earth System Sciences*, 19(3), 715–719.
- Durrans, S. R. (1988). 18. Total probability methods for problems in flood frequency estimation. In *International conference on statistical and Bayesian methods in hydrological sciences in honor of professor Jacques Bernier, Paris, Paris, France* (pp. 299–326).
- Gersonius, B., Ashley, R., Pathirana, A., & Zevenbergen, C. (2013). Climate change uncertainty: Building flexibility into water and flood risk infrastructure. *Climatic Change*, 116(2), 411–423.
- Graf, W. L. (1999). Dam nation: A geographic census of American dams and their large-scale hydrologic impacts. *Water Resources Research*, 35(4), 1305–1311.
- Graf, W. L. (2006). Downstream hydrologic and geomorphic effects of large dams on American rivers. *Geomorphology*, 79(3–4), 336–360.
- Hens, L., Thinh, N. A., Hanh, T. H., Cuong, N. S., Lan, T. D., Van Thanh, N., & Le, D. T. (2018). Sea-level rise and resilience in Vietnam and the Asia-Pacific: A synthesis. *Vietnam Journal of Earth Sciences*, 40(2), 126–152.
- Hirabayashi, Y., Mahendran, R., Koirala, S., Konoshima, L., Yamazaki, D., Watanabe, S., Kim, H., & Kanae, S. (2013). Global flood risk under climate change. *Nature Climate Change*, 3(9), 816–821.
- ICOLD. (1998). *World register of dams*.
- Islam, A. R. M., Talukdar, S., Mahato, S., Ziaul, S., Eibek, K. U., Akhter, S., Pham, Q. B., Mohammadi, B., Karimi, F., & Linh, N. T. T. (2021). Machine learning algorithm-based risk assessment of riparian wetlands in Padma River Basin of Northwest Bangladesh. *Environmental Science and Pollution Research*, 28(26), 34450–34471.
- Khosravi, K., Shahabi, H., Pham, B. T., Adamowski, J., Shirzadi, A., Pradhan, B., Dou, J., Ly, H. B., Gróf, G., Ho, H. L., & Hong, H. (2019). A comparative assessment of flood susceptibility modeling using multi-criteria decision-making analysis and machine learning methods. *Journal of Hydrology*, 573, 311–323.
- Kondolf, G. M. (1994). Geomorphic and environmental effects of instream gravel mining. *Land-scape and Urban Planning*, 28(2–3), 225–243.
- Lee, E. H., & Kim, J. H. (2018). Development of a flood-damage-based flood forecasting technique. *Journal of Hydrology*, 563, 181–194.
- Leopold, L. B. (1956). Land use and sediment. *Man's Role in Changing the Face of the Earth*, 2, 639–647.

- McFeeters, S. K. (1996). The use of the Normalized Difference Water Index (NDWI) in the delineation of open water features. *International Journal of Remote Sensing*, 17(7), 1425–1432.
- Moraes, R., & Molander, S. (2004). A procedure for ecological tiered assessment of risks (PETAR). *Human and Ecological Risk Assessment*, 10(2), 349–371.
- Naikoo, M. W., Talukdar, S., Ishtiaq, M., & Rahman, A. (2023). Modelling built-up land expansion probability using the integrated fuzzy logic and coupling coordination degree model. *Journal of Environmental Management*, 325, 116441.
- Nilsson, C., Reidy, C. A., Dynesius, M., & Revenga, C. (2005). Fragmentation and flow regulation of the world's large river systems. *Science*, 308(5720), 405–408.
- O'Brien, G. C., & Wepener, V. (2012). Regional-scale risk assessment methodology using the Relative Risk Model (RRM) for surface freshwater aquatic ecosystems in South Africa. *Water SA*, 38(2), 153–166.
- Organization for Economic Cooperation & Development, and OECD Group of the Council on Rural Development. (1993). *What future for our countryside?: A rural development policy*. Organisation for Economic Co-operation and Development.
- Pal, S., & Talukdar, S. (2018). Drivers of vulnerability to wetlands in Punarbhaba river basin of India-Bangladesh. *Ecological Indicators*, 93, 612–626.
- Pal, S., & Talukdar, S. (2019). Impact of missing flow on active inundation areas and transformation of paraffluvial wetlands in Punarbhaba–Tangon river basin of Indo-Bangladesh. *Geocarto International*, 34(10), 1055–1074.
- Paul, G. C., Saha, S., & Hembram, T. K. (2019). Application of the GIS-based probabilistic models for mapping the flood susceptibility in Bansloi sub-basin of Ganga-Bhagirathi river and their comparison. *Remote Sensing in Earth Systems Sciences*, 2(2), 120–146.
- Paul, S., & Pal, S. (2020). Exploring wetland transformations in moribund deltaic parts of India. *Geocarto International*, 35(16), 1873–1894.
- Pal, S., & Saha, T. K. (2018). Identifying dam-induced wetland changes using an inundation frequency approach: The case of the Atreyee River basin of Indo-Bangladesh. *Ecology and Hydrobiology*, 18(1), 66–81.
- Quiroga, V. M., Kurea, S., Udoa, K., & Manoa, A. (2016). Application of 2D numerical simulation for the analysis of the February 2014 Bolivian Amazonia flood: Application of the new HEC-RAS version 5. *Ribagua*, 3(1), 25–33.
- Rashid, B., Islam, S. U., & Islam, B. (2015). Evidences of Neotectonic activities as reflected by drainage characteristics of the Mahananda River floodplain and its adjoining areas, Bangladesh. *American Journal of Earth Sciences*, 2(4), 61–70.
- Rasyid, A. R., Bhandary, N. P., & Yatabe, R. (2016). Performance of frequency ratio and logistic regression model in creating GIS based landslides susceptibility map at Lompobattang Mountain, Indonesia. *Geoenvironmental Disasters*, 3(1), 19.
- Samanta, S., Pal, D. K., & Palsamanta, B. (2018). Flood susceptibility analysis through remote sensing, GIS and frequency ratio model. *Applied Water Science*, 8(2), 1–14.
- Sarkar, D., & Mondal, P. (2020). Flood vulnerability mapping using frequency ratio (FR) model: A case study on Kulik river basin, Indo-Bangladesh Barind region. *Applied Water Science*, 10(1), 1–13.
- Sevgen, E., Kocaman, S., Nefeslioglu, H. A., & Gokceoglu, C. (2019). A novel performance assessment approach using photogrammetric techniques for landslide susceptibility mapping with logistic regression, ANN and random forest. *Sensors*, 19(18), 3940.
- Solaimani, K., Mousavi, S. Z., & Kavian, A. (2013). Landslide susceptibility mapping based on frequency ratio and logistic regression models. *Arabian Journal of Geosciences*, 6(7), 2557–2569.
- Süzen, M. L., & Doyuran, V. (2004). A comparison of the GIS based landslide susceptibility assessment methods: Multivariate versus bivariate. *Environmental Geology*, 45(5), 665–679.
- Talukdar, S., & Pal, S. (2017). Impact of dam on inundation regime of flood plain wetland of punarbhaba river basin of barind tract of Indo-Bangladesh. *International Soil and Water Conservation Research*, 5(2), 109–121.



- Talukdar, S., & Pal, S. (2018). Impact of dam on flow regime and flood plain modification in Punarbhaba River Basin of Indo-Bangladesh Barind tract. *Water Conservation Science and Engineering*, 3(2), 59–77.
- Talukdar, S., Pal, S., Chakraborty, A., & Mahato, S. (2020). Damming effects on trophic and habitat state of riparian wetlands and their spatial relationship. *Ecological Indicators*, 118, 106757.
- Talukdar, S., & Pal, S. (2021). *Impact of hydrological alteration of riparian wetlands in Punarbhaba river basin of Indo-Bangladesh (unpublished thesis)*. University of Gour Banga.
- Talukdar, S., Pal, S., Shahfahad., Naikoo, M.W., Parvez, A., Rahman, A. (2023). Trend analysis and forecasting of streamflow using random forest in the Punarbhaba River basin. *Environmental Monitoring and Assessment*, 195(1), 153.
- Tehrany, M. S., Pradhan, B., & Jebuv, M. N. (2014). A comparative assessment between object and pixel-based classification approaches for land use/land cover mapping using SPOT 5 imagery. *Geocarto International*, 29(4), 351–369.
- Tonina, D., & Jorde, K. (2013). *Hydraulic modeling approaches for ecohydraulic studies: 3D, 2D, 1D and non-numerical models* (pp. 31–66). An integrated approach.
- Townshend, J. R., & Justice, C. O. (1986). Analysis of the dynamics of African vegetation using the normalized difference vegetation index. *International Journal of Remote Sensing*, 7(11), 1435–1445.
- USACE. (1993). *Engineering Manual EM 1110–2-1415, Chapter 3. Flood Frequency Analysis*, US Army Corps of Engineers.
- USEPA (US Environmental Protection Agency). (1998). *Method 3051a—Microwave assisted acid digestion of sediments, sludges, soils, and oils*.
- Walker, R., Landis, W., & Brown, P. (2001). Developing a regional ecological risk assessment: A case study of a Tasmanian agricultural catchment. *Human and Ecological Risk Assessment*, 7(2), 417–439.
- Williams, G. P., & Wolman, M. G. (1984). *Downstream effects of dams on alluvial rivers* (Vol. 1286). US Government Printing Office.
- World Commission on Dams. (2000). *Dams and development: A new framework for decision-making*. In *A report of the World Commission on Dams*. Earthscan. <http://www.dams.org/report>. Accessed 5 Sept 2004.
- Wu, Z., Zhou, Y., Wang, H., & Jiang, Z. (2020). Depth prediction of urban flood under different rainfall return periods based on deep learning and data warehouse. *Science of the Total Environment*, 716, 137077.
- Xu, H. (2006). Modification of normalised difference water index (NDWI) to enhance open water features in remotely sensed imagery. *International Journal of Remote Sensing*, 27(14), 3025–3033.
- Yalcin, G., & Akyurek, Z. (2004, July). Analysing flood vulnerable areas with multicriteria evaluation. In *20th ISPRS Congress* (pp. 359–364).

# Chapter 8

## Morphometric Analysis and Prioritization of Watersheds for Flood Susceptibility Mapping in the Eastern Himalayan Foothills, India



Md Hasanuzzaman, Biswajit Bera, Aznarul Islam, and Pravat Kumar Shit

**Abstract** Flood vulnerability mapping is a significant footstep for policymakers for disaster management and water resource management and restoration. In this chapter, we analyzed the morphometric parameters sub-watersheds prioritization (MPSWP) of the Kaljani River Basin for flood susceptibility zone identification. Characteristics of this Himalayan foothills river are a sixth-order drainage system, a dendritic drainage pattern, and a funnel-shaped basin. This present chapter has integrated with morphometric analysis using ALOS PALSAR DEM (12.5 m) for assessing the flood susceptibility area spatially. We have used the total ranking approach for the final flood susceptibility sub-watershed prioritization. Research findings show that about 40.62% area of the basin and 11 sub-watersheds were identified as high to very high flood susceptibility zone. Out of the 12 morphometric factors, five factors ( $R_r$ ,  $R_v$ ,  $S_f$ ,  $L_o$ , and  $R_n$ ) were the most significant factors for the flooding. The receiver operating characteristic (ROC) curve was employed for the validation of the model. The result of the ROC accuracy rate is 87%. Therefore, MPSWP has been successfully and efficiently employed to determine sub-watershed sensitivity to flooding. This result can be helpful as a primary guideline for flood mitigation and sub-watersheds management.

**Keywords** Kaljani River Basin · Flood · Morphometric analysis · Sub-watersheds · Prioritization · Himalayan foothills

---

M. Hasanuzzaman · P. K. Shit (✉)

PG Department of Geography, Raja N. L. Khan Women's College (Autonomous), Midnapore, West Bengal, India

B. Bera

Department of Geography, Sidho Kanho Birsha University, Purulia, West Bengal, India

A. Islam

Department of Geography, Aliah University, Kolkata, West Bengal, India

e-mail: [aznarul.geog@aliah.ac.in](mailto:aznarul.geog@aliah.ac.in)

## 1 Introduction

Flood is a common hydrological, catastrophic, and destructive quasi-natural hazard (Ali et al., 2020). Flood mapping is very significant for the management of flood threats and their damage (Hasanuzzaman et al., 2022a). According to Smith (1996), 75 million people and 20,000 lives per year lost their life by flood worldwide. UNISDR reported that 150 thousand people died in the flood event from 1996 to 2015 in the world. It was 11% of the total mortality rate in the world. It's very high in underdeveloped and developing countries, such as Sri Lanka, Bangladesh, and India. A strong controlling factor of flooding is precipitation in the tropical monsoon climatic region (Wu et al., 2019; Islam & Ghosh, 2022). In the high land area of the small watershed (1000 km<sup>2</sup>), floods originate due to the complex orography and short response time (Toduse et al., 2020). Watershed shape, watershed size, watershed drainage characteristics, and watershed relief features, directly and indirectly, impact flood intensity and frequency (Jodar-Abellan et al., 2019; Azmeri & Vadiya, 2016; Islam & Deb Barman, 2020). Thus, flood susceptibility area identification is a very significant research for the protection of human life and resources (Destro et al., 2018). In the wake of the development of RS and GIS, various approaches and models are used for flood susceptibility mapping such as machine learning, bivariate mathematical method, multi-criteria decision analysis, etc.

All these models are requiring historical flood data and appropriate influencing factor data. But this type of data is not present worldwide, especially in underdeveloped and developing countries. The digital elevation model (DEM)-based morphometric parameters sub-watershed prioritization (MPSWP) method is a very accurate and acceptable method for flood susceptibility mapping (Obeidat et al., 2021). In current times, USGS DEM and NASA ALOS PALSAR DEM are freely available worldwide.

Many research scholars have successfully used MPSWP methods of flood susceptibility mapping (Rajasekhar et al., 2020; Aher et al., 2014; Borga et al., 2008; Alam et al., 2020; Kannan et al., 2018; Hasanuzzaman et al., 2022b; Charizopoulos et al., 2019). Smith (1950), Horton (1932, 1945), Miller (1953), Schumm (1956), and Strahler's (1952) research work have been used as base work for MPSWP methods. Therefore, the watershed-wise morphometric parameters play a significant role in their hydrological response to precipitation (Shivhare et al., 2018). Current research is an attempt to identify the flooding area of the Himalayan foothill Kaljani River Basin. Here, historical flood data and proper flood influencing factor data are completely not present at the local scale and national scale. But ALOS PALSAR DEM is freely available here. Therefore, the MPSWP method is an important and appropriate model in the study region condition. The major objective of the research is sub-watershed prioritization of the Kaljani River Basin regarding flood probability. The result of the research can help decision-makers or planners to select the flood susceptibility sub-watershed for the preparation of flood watershed management strategies.

## 2 Study Area

### 2.1 Location of the Study Area

An important tributary of the Torsha River is the Kaljani River. Its origin in Bhutan flows from north to south at the foothills of the Himalayas to meet the Brahmaputra River (Fig. 8.1). The Kaljani River covers the flow path of various geomorphological features. Dima, Bala, Pana, Garam, Bania, Ghargharia, and Nonai are the major tributaries of this river. Most parts of the Alipurduar District and some parts of the Cooch Behar Districts of West Bengal cover this basin. The longitude and latitude extension of the Kaljani River is  $89^{\circ}30' 17''$  E to  $89^{\circ}34' 56''$  E and  $26^{\circ}16' 0''$  N to  $26^{\circ}55' 37''$  N. The basin area is  $1137.23 \text{ km}^2$ , and the length is 238.87 km.

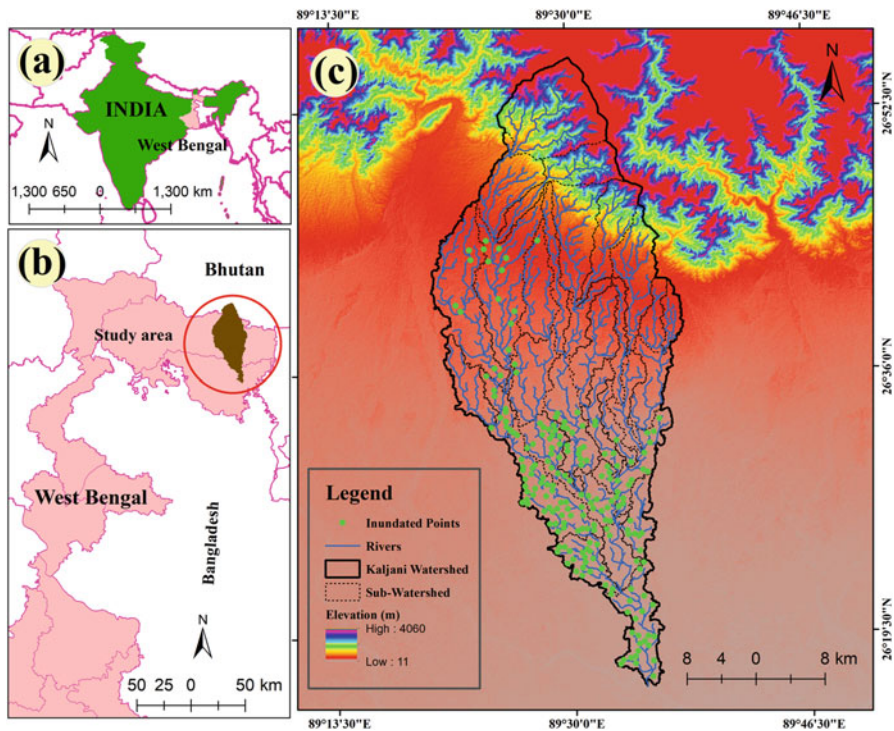
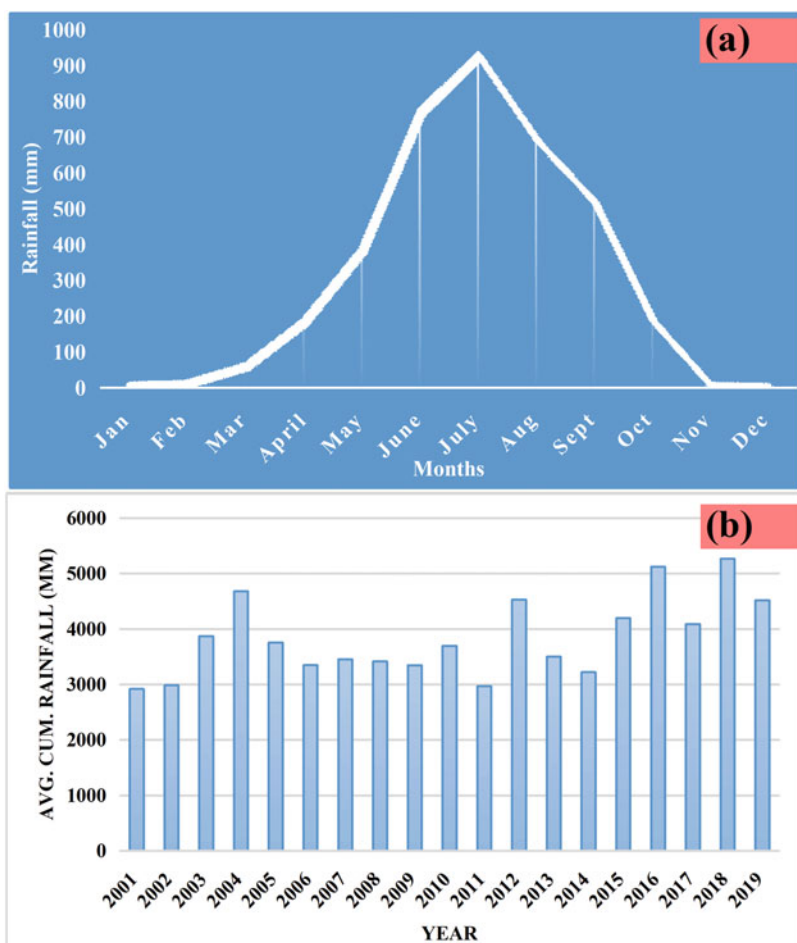


Fig. 8.1 Location map of the Kaljani basin

## 2.2 Flood Perspective of the Study Area

The Kaljani River Basin is situated in the heavy rainfall area according to the West Bengal rainfall zonation map. Due to the geographical location of the basin, this area generally receives more than 4000 mm of cumulative rainfall per year (Fig. 8.2). The heavy rainfall occurs mainly from June to September month (monsoon season), i.e., about 75% of the total rainfall a year recorded during the time of monsoon season (Fig. 8.2).

The Himalayan Mountain range is present in the northern part of the study basin. This mountain range has blocked the Bay of Bengal branch of the monsoon that is occurred in the orographic rainfall of this basin. After the 19-year rainfall data



**Fig. 8.2** Rainfall trend of the river Kaljani basin: (a) monthly rainfall and (b) rainfall of the study area during 2001–2019. (Source: District Disaster Management Plan, 2020)

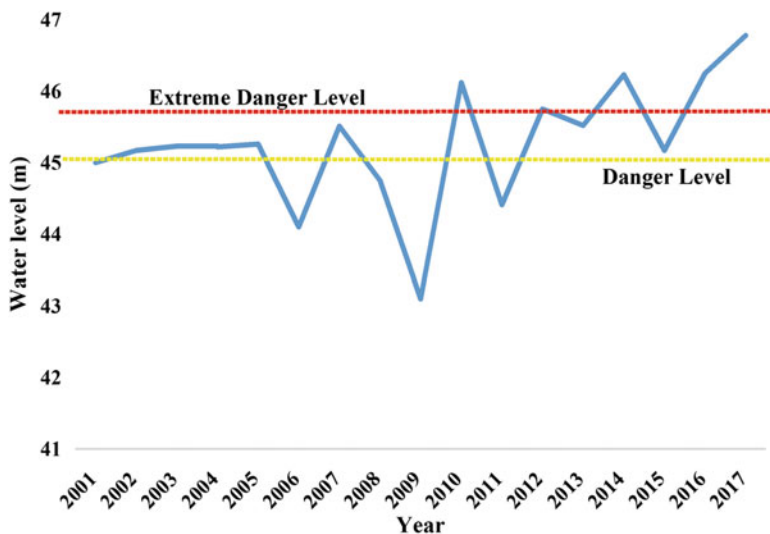


**Fig. 8.3** Water level of the study river from 2001 to 2017. (Source: District Disaster Management Plan, 2020)

analysis, we observed that the monsoon rainfall pattern has changed. Rainfall has become sporadic and incisive by the monsoon trough. The lower part of this basin deposits sediments of the Kaljani River and its tributary rivers each year during the flooding period (Hasanuzzaman et al., 2021). Every year flood is a common factor in the Kaljani River Basin during the monsoon season (District Disaster Management Plan, 2020; Hasanuzzaman et al., 2022c). Figure 8.3 shows the number of times the river is crossing the danger level and the extreme danger level.

According to the report of the District Disaster Management Plan (2020), the floods in this basin significantly impact the life of the people, the livelihoods of a million people, damage standing crops of hectares, the life of cattle, and embankments, bridge, etc. (Table 8.1).

### 3 Data and Methods

We selected and demarcated 22 morphometric parameters for the flood susceptibility of sub-watershed prioritization of the Kaljani River Basin (Table 8.2). The ranking of sub-watersheds (watershed prioritization) of this basin area was demarcated according to their order (Patel et al., 2012). Relief, basic, shape, and linear parameters of the basin were included as morphometric parameters (Melton, 1957; Strahler, 1964). We demarcated sub-watersheds of the study basin using DEM (12.5 m). The ALOS PALSAR DEM of 2007 (12.5 m) was downloaded from Alaska satellite facility (<https://search.asf.alaska.edu>). After that, we calculated

**Table 8.1** Flood events from 1991 to 2019 and their impact on the study area

Year	Flood	Remarks
1991	Yes	Cattle died. Crops were damaged. Villages were affected.
1992	No	
1993	Yes	Heavy and continuous rainfall occurred in the remarkable flood. It damaged roads, crops, cattle, houses, etc. This flood was occurrence left a deep mark on the local people.
1994	No	
1995	Yes	Crops were damaged. Villages were affected. Houses beside the river bank were destroyed.
1996	Yes	Seven consecutive days of heavy rainfall occurred inundated the riverside region. Houses were destroyed, people died, and crops and land were affected.
1997	No	
1998	Yes	Cattle died. Crops were damaged. Villages were affected.
1999	Yes	Due to heavy precipitation in the last week of August month, the river Kaljani was flooded. The agricultural area was affected, and people died.
2000	No	
2001	Yes	The flash flood occurred because of the heavy precipitation. Farmland was damaged, cattle died, and the embankment collapsed.
2002	Yes	The agricultural area was destroyed due to heavy rainfall and resultant flooding.
2003	No	
2004	Yes	Cattle died and farmland and people were affected because of pre-monsoonal precipitation and flood.
2005	Yes	Cattle died. Crops were damaged. Villages were affected. Houses were collapsed.
2006	Yes	Houses were collapsed. Cattle died. Crops were damaged. Villages were affected.
2007	Yes	The upper part of the basin was flooded, and houses were damaged by mudslides or landslides.
2008	No	
2009	No	
2010	Yes	Cattle died. Crops were damaged. Villages were affected. Houses were collapsed.
2011	Yes	Agricultural products, houses, and people were affected by the earthquake and flood.
2012	Yes	The agricultural area was destroyed due to heavy rainfall and resultant flooding.
2013	Yes	Crops were damaged. Villages were affected. House beside the river bank were destroyed.
2014	Yes	The agricultural area was destroyed due to heavy rainfall and resultant flooding.
2015	Yes	Agricultural products, houses, and people were affected by the earthquake and flood.
2016	Yes	Crops, houses, and people were affected by the flood.
2017	Yes	Heavy and continuous rainfall occurred during the extreme flood. It damaged roads, crops, cattle, houses, culverts, bridges, etc. This flood was occurrence left a deep mark on the local people.
2018	Yes	Some people lost their houses, crops, and cattle to the flood and thunderstruck.
2019	Yes	The agricultural products were destroyed due to heavy rainfall and resultant flooding.

Source: District Disaster Management Plan (2020)

**Table 8.2** Analysis of the morphometric parameters using the algorithm and formula

Sl. no.	Dimensions	Morphometric parameters	Short form	Algorithm	References	
1.	Basic	Basin area	$A$	Area of the basin (km <sup>2</sup> )	Horton (1945)	
2.		Basin perimeter	$P$	Outline of the basin (km)		
3.		Basin length	$L_b$	Length of the watershed (km)		
4.		Stream order	$U$	Hierarchical rank		
5.		Total number of streams	$N_u$	Total number of streams of all orders		
6.		Stream length	$L_u$	Length of the stream (km)		
7.		Mean stream length	$L_{sm}$	$L_{sm} = L_u/N_u$		
8.		Stream length ratio	$R_L$	$R_L = L_u/N_u - 1$		
9.	Linear	Bifurcation ratio	$R_b$	$R_b = L_u/N_u + 1$	Strahler (1952)	
10.		Bifurcation ratio	$R_{bm}$	$R_{bm}$ = average of the bifurcation ratio of all orders		
11.		Drainage density	$D_d$	$D_d = L_u/A$		Horton (1945)
12.		Length of overland flow	$L_o$	$L_o = 1/(2*D_d)$		
13.		Stream frequency	$F_s$	$F_s = N_u/A$ ,		
14.	Shape	Elongation ratio	$R_e$	$R_e = 1.128*(A \wedge 0.5)/L_b$	Strahler (1957)	
15.		Circularity ratio	$R_c$	$R_c = 4 \times \pi \times A/P^2$ ,	Schumm (1956)	
16.		Shape factor	$S_f$	$S_f = L_b^2/A$ ,	Miller (1953)	
17.	Relief	Basin relief	$H$	$H = h - h_1$ , where	Horton (1945)	
				$h$ = highest height (m)		
				$h_1$ = lowest height (m)		
18.		Relief ratio	$R_r$	$R_r = H/L_b$ ,	Malik et al. (2011)	
19.		Relative relief ratio	$R_v$	$R_v = R_r = H/P$ , where	Schumm (1956)	
				$H$ = total relief (km)		
			$P$ = perimeter of the basin (km)			
20.	Basin slope	$B_s$	$B_s = H/L_b * 60$ , where	Melton (1957)		
			$H$ = total relief (km)			
			$L_b$ = basin length (km)			
21.	Ruggedness number	$R_n$	$R_n = D_d * H$ , where	Farhan and Anaba (2016)		
			$H$ = basin relief (km)			
			$D_d$ = drainage density			

(continued)



**Table 8.2** (continued)

Sl. no.	Dimensions	Morphometric parameters	Short form	Algorithm	References
22.		Hypsometric integral	HI	$HI = (E_{\text{mean}} - E_{\text{min}})/(E_{\text{max}} - E_{\text{min}})$ , where $E_{\text{mean}}$ = the weighted mean elevation $E_{\text{max}}$ = highest elevation $E_{\text{min}}$ = lowest elevation	Schumm (1956)

directly basic parameters ( $A, P, L_b, N_u, L_u$ , etc.) of the watershed from DEM by hydrology tool of ArcGIS 10.4 software. Relief parameters, shape parameters, and linear parameters were calculated using the mathematical equations. All mathematical equations were depicted in Table 8.2.

Out of 22 morphometric parameters, 12 parameters were directly used for preparing the final flood susceptibility map (Table 8.1).  $A, D_d, F_s, R_r, R_c, R_n, B_s$ , and  $R_v$  have a direct relationship with flood susceptibility. Therefore, in all of these morphometric parameters, higher values depicted a higher degree of susceptibility to flooding risk. The morphometric ranking method (total rank) was employed for the sub-watershed (SW) prioritization (Puno & Puno, 2019). We divided five categories of the morphometric parameter, and each category defines a certain degree of vulnerability. Therefore, weight value 1 denotes a very low, and value 5 denotes a very high degree of flood risk possibility (Obeidat et al., 2021). Moreover, the total rank values were summed to divide the SWs to prepare for their susceptibility to flooding (Farhan & Anaba, 2016). We normalized the summed parameters' rank values between 0 and 1 to the determine floods susceptibility index of each SW. The same values denoted similar rankings and finally prepared the flood's priority map. The final flood susceptibility map was classifying five classes: very low (VL), low (L), moderate (M), high (H), and very high (VH) flood priority.

## 4 Validation

Validation is a very necessary and crucial step for scientific research. We used the ROC curve for the validation of the final output susceptibility map. For the validation of the research, we have extracted the 200 flood or inundation points of the 2016 major flood inundation area map using a simple random sampling method. We used the Landsat-8 OLI syn-flood image of August 2016 by the "Iso Cluster Unsupervised Classification" technique to develop the 2016 flood inundation area map (Roy & Das, 2021). We considered moderate, low, and very low flood priority classes of sub-watersheds to be non-flood areas. On the other hand, VH and H categories were considered flood areas for the calculation of the ROC. Therefore, the

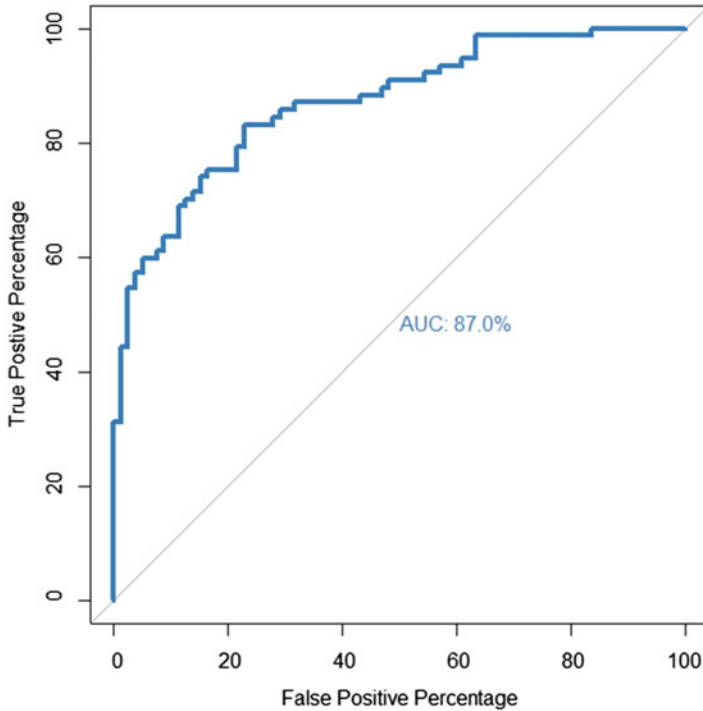


**Fig. 8.4** ROC for validation

result of the ROC measures the location of non-flood and flood areas out of the 200 sample points. The result of the ROC curve was 87% (Fig. 8.4). This result represents that the MPSWP method is very accurate and acceptable for flood estimation.

## 5 Results and Discussion

### 5.1 Morphometric Parameters

We extract 31 sub-watersheds from the Kaljani River Basin by the SWAT hydrological modeling extension tool of ArcGIS software (Fig. 8.5). Table 8.3 presented the outcome of the research using the morphometric analysis of all SWs. We prepare the final flood prioritization map of all SWs based on the result of this research.

#### 5.1.1 Basic Parameters

The basin area is an important basic morphometric parameter, which is demarcated by the water quantity that could be originated from precipitation. It ranged from

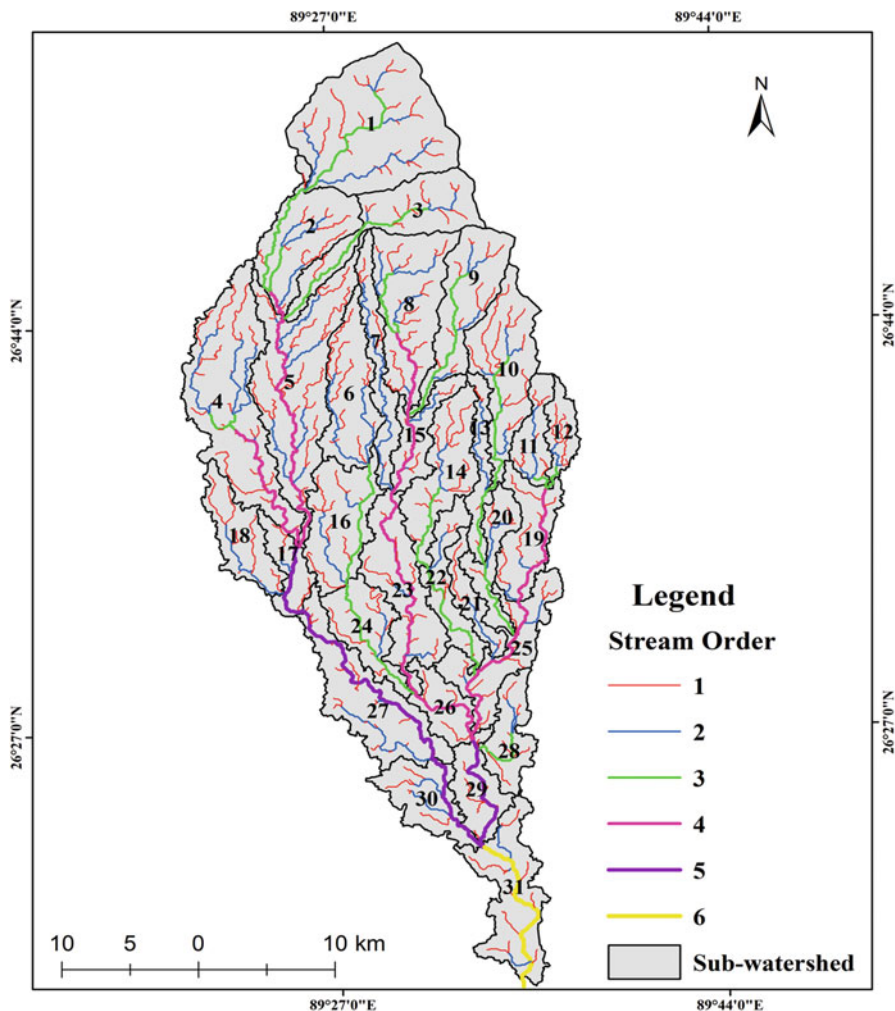


**Fig. 8.5** Sub-watersheds, stream order, and drainage pattern of the Kaljani River Basin

13.82 km<sup>2</sup> (SW 21) to 97.68 km<sup>2</sup> (SW 1). The perimeter of the basin is a significant feature of the watershed, which is depicted as the length of the line of the watershed. We find that the result of the maximum basin perimeter value was 81.09 km (SW 5) whereas the minimum basin perimeter value was 17.23 km (11 SW). A positive high correlation relationship is present between the watershed area and the perimeter (Obeidat et al., 2021). Basin length is an important hydrological computation. It defines as the length calculated along the major channel from the outlet of the basin to the watershed divide (Bhat et al., 2019). In the current study, watershed length ranges between 7.44 km (26 SW) and 24.87 km (5 SW). Therefore, a positive

**Table 8.3** Summary of final calculation of 31 sub-watersheds

SW	A	D <sub>d</sub>	L <sub>o</sub>	F <sub>s</sub>	R <sub>e</sub>	R <sub>c</sub>	S <sub>f</sub>	R <sub>r</sub>	R <sub>v</sub>	B <sub>s</sub>	R <sub>n</sub>	HI	Total rank	Normalization	Prioritized rank	Priority
1	2	1	1	2	5	2	2	2	3	2	2	2	26	0	1	Very low
2	1	3	4	1	5	1	1	4	4	3	4	2	33	0.35	7	Moderate
3	1	4	1	1	2	2	5	2	2	2	1	4	27	0.05	2	Very low
4	1	2	3	3	1	5	5	4	2	2	2	5	35	0.45	8	High
5	1	5	2	5	4	4	3	2	4	2	3	2	37	0.55	9	High
6	1	5	2	5	3	1	4	1	1	1	1	5	30	0.20	4	Low
7	1	4	1	5	5	4	2	2	1	2	1	1	29	0.15	3	Low
8	1	4	4	2	5	1	1	3	4	3	2	3	33	0.35	7	Moderate
9	2	4	1	2	1	5	5	1	1	1	1	2	26	0	1	Very low
10	1	4	1	2	1	3	5	4	3	4	1	2	31	0.25	5	Low
11	4	5	1	2	3	1	4	1	1	2	1	5	30	0.20	4	Low
12	1	3	2	3	3	3	2	1	2	2	3	4	29	0.15	3	Low
13	3	2	3	1	1	4	2	4	2	2	3	3	30	0.20	4	Low
14	1	4	2	4	4	1	2	1	2	1	3	4	29	0.15	3	Low
15	5	2	3	4	2	5	5	1	1	1	1	3	33	0.35	7	Moderate
16	1	5	2	4	3	2	2	2	3	2	2	4	32	0.30	6	Moderate
17	3	5	2	4	3	3	2	1	1	1	2	5	32	0.30	6	Very high
18	3	1	1	3	3	3	4	2	1	2	1	5	29	0.15	3	Low
19	1	1	5	2	2	5	4	3	5	3	1	1	33	0.35	7	Moderate
20	1	5	2	5	3	4	3	2	3	2	2	1	33	0.35	7	Moderate
21	4	2	2	3	4	1	3	2	2	2	3	1	29	0.15	3	Low
22	4	5	2	5	4	2	1	1	1	1	3	3	32	0.30	6	Moderate
23	3	4	4	2	1	5	5	3	3	4	2	2	38	0.60	10	High
24	2	5	5	3	2	3	4	3	3	3	4	4	41	0.75	12	High
25	1	5	5	4	4	2	2	4	4	4	4	5	44	0.90	14	Very high

(continued)

Table 8.3 (continued)

SW	A	$D_d$	$L_o$	$F_s$	$R_e$	$R_c$	$S_f$	$R_r$	$R_v$	$B_s$	$R_n$	HI	Total rank	Normalization	Prioritized rank	Priority
26	3	5	2	4	3	3	2	1	1	1	2	5	32	0.30	6	Moderate
27	3	5	5	2	1	5	5	4	4	4	5	3	46	1	15	Very high
28	1	2	2	2	3	2	5	5	4	5	2	5	38	0.60	10	High
29	2	4	5	1	4	2	2	4	5	4	5	4	42	0.80	13	Very high
30	2	5	5	3	2	3	4	3	3	3	4	4	41	0.75	12	High
31	2	4	4	3	4	1	3	4	4	4	4	3	40	0.70	11	High

SW sub-watershed

relationship is present between basin length and stream length (Christopher et al., 2010).

Stream order of the Kaljani River 31 watershed was ranging from the first order to six orders. High stream numbers of the watershed are indicated as rapid peak flow and high surface flow water (Christopher et al., 2010). Stream length is the length of various orders of the stream (Horton, 1945). According to Magesh et al. (2011), it is a significant indicator of the contributing area of water for a particular stream order. Less stream length is representing low surface flow water of the watershed (Strahler, 1952). The Kaljani River Basin's total stream length is 1087.70 km whereas 31 sub-watersheds is varying in all orders.

### 5.1.2 Linear Parameters

Surface topography is the main influencing factor of drainage density. A high drainage density value is indicating low relief, low slope, low runoff, and high flood possibility (Magesh et al., 2011). Therefore, a direct relationship is present between the drainage density and flood. The highest drainage density was given as SW 5, 6, 11, 16, 17, 20, 22, 24, 25, 26, and 30. The length of overland flow is the length of surface runoff area before it becomes accumulated into a particular river (Horton, 1945). Sub-watersheds 19, 24, 25, 27, 29, and 30 were found the maximum rank (5). It means these SWs have indicated the maximum possibility of a flood. Stream frequency is the ratio between per unit basin area and all order total stream number (Horton, 1932). This is a high value, which means higher surface runoff and high flood possibility (Melton, 1957). We observed that SW 5, 6, 7, and 20 were found higher stream frequency values.

### 5.1.3 Shape Parameters

The elongation ratio denoted the diameters of the same area circle as that of the drainage basin and the highest length of the basin (Horton, 1932). In this work, SW4, 9, 10, 13, 23, and 27 were the lowest sensitivity to flooding, whereas SW 1, 2, 7, and 8 were the lowest indicating a high possibility of flooding. According to Miller (1953), a direct relationship is present between flood and the circulatory ratio. The minimum value is indicated as the high availability of time for the water flow of the surface to infiltrate and therefore the low possibility of flooding. In this work, sub-watershed 4, 9, 15, 19, 23, and 27 were found the maximum rank (5) due to maximum circulatory ratio value, whereas SWs 2, 6, 8, 11, 14, and 31 were found to the minimum rank (1). The shape factor minimum value revealed high elevation and very steep slopes. It indicates the high possibility of a flood (Farhan et al., 2017). Sub-watersheds 3, 4, 10, 23, 27, and 28 with low shape factor values were found to be the maximum rank (5).

### 5.1.4 Relief Parameters

Basin relief is a significant controlling impact on drainage development and landform development (Macka, 2001). A high relief ratio value was indicating less lag time and sudden peak discharge, which depicted the probability of flood occurrence (Magesh et al., 2011). The high relief ratio value was found in SW 28. A strong and direct relationship is present between the relative relief ratio and flood (Ameri et al., 2018). In the current research, sub-watershed 29 with a high relative relief ratio value is given the highest rank (5). Basin slope is a determining impact on the hydrological processes (Patton & Baker 1976). SW 6, 9, 14, 15, 17, 22, and 26 were found to be in the lowest rank (1) due to the low basin slope value. Moreover, only SW 5 was found to be in the maximum rank (5). The high ruggedness number of the watershed refers to steep slopes, which indicate flash floods and erosion (Meraj et al., 2013). It has a direct relationship with flooding (Pavano et al., 2018). The ruggedness number value was found highest of SW27 and SW29, so they were given the highest rank (5). On the other hand, SW 7, 8, 9, 11, 15, and 19 were found to have lowest values, so they were given the lowest rank (1). Hypsometric integral denotes an activity of ruggedness of the earth’s surface (Obeidat et al., 2021). It is a very important factor to determine interactions existing among the tectonic uplift, geology, erosion, and climate. Highest hypsometric integral values were found in SW 7, 19, 20, and 21. Therefore, they were given the lowest rank (1). Another side, SW 4, 6, 11, 17, 18, 25, 26, and 28 were found to be in the highest rank (5).

We have calculated the Pearson correlation coefficient matrix between the eight direct morphometric parameters ( $A$ ,  $F_s$ ,  $D_d$ ,  $R_c$ ,  $R_r$ ,  $R_v$ ,  $B_s$ , and  $R_n$ ) and four indirect parameters ( $S_f$ ,  $L_o$ ,  $R_e$ , and  $HI$ ) weight values for the observed relationship (Fig. 8.6). This correlation coefficient represented among the 12 factor weight value. Based on

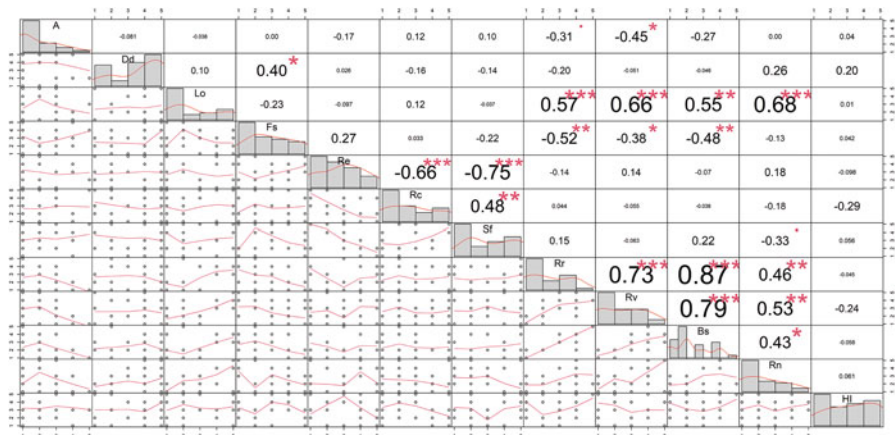


Fig. 8.6 Pearson correlation coefficient matrix of all selected parameters weight value

the outcome of the Pearson correlation coefficient matrix, a high positive correlation was found between the basin slope and the relief ratio ( $r = 0.87$ ). Moreover, the elongation ratio and shape factor observed a high negative correlation ( $r = -0.75$ ).

## 5.2 Flood Prioritization of the Kaljani River Basin

Flood prioritization mapping of the watershed is a very crucial step for flood and watershed management. We have prepared the flood prioritization map of the Kaljani River Basin using the morphometric parameters sub-watershed prioritization (MPSWP) approach (Fig. 8.7). Detailed outcomes of the study were represented in Table 8.2 and Fig. 8.5. In this study, all 12 morphometric parameters ranking scores of each sub-watershed were employed for the flood prioritization of SWs. According to the total score values of all selected factors, the 31 SWs were grouped into five classes (VL, L, M, H, and VH) for flooding prioritization of SWs (Fig. 8.7). SW 17, 25, 27, and 29 found a very high possibility of flood, which covered about 11.32% of the total Kaljani River Basin area. These SWs were located in the middle-east part of the basin. Seven sub-watersheds (SW 4, 5, 23, 24, 28, 30, and 31) forming 29.30% of the total basin area were found in the high flood possibility, which was located in the middle and lower part of the basin. A total of eight sub-watersheds (SW 2, 8, 15, 16, 19, 20, 22, and 26) were found to be the moderate class of flood susceptibility, which covers 22.01% of the total area of the basin. Nine sub-watershed (SW 6, 7, 10, 11, 12, 13, 14, 18, and 21) covering about 20.99% and three sub-watersheds (SW 1, 3, and 9) covering about 16.22% of the basin were found the low to very low flood possibility. These SWs were located in the upper and middle-east parts of the river Kaljani River.

The present study depicted that the middle west part of the basin was very active for floods and the northern comparatively low active. We observed that the flood-plain side of the main river channel at the middle and lower of the basin faced frequent flooding. One of the valid reasons has sediment deposition in the river bed of this area. River bank failure, landslide, and river deposition are common phenomena of the basin during heavy and intensive rainfall (Chakraborty and Mukhopadhyay, 2019). It increased the flood possibility year by year in this area. This MPSWP model was validated with the ROC curve and field survey photo (Fig. 8.8). ROC curve value was 87%. This work will help policymakers to develop an appropriate policy for flood risk mitigation and watershed restoration management. Moreover, this work can be replicated in another region, when the appropriate flood influencing factors and historical flood data are absent.



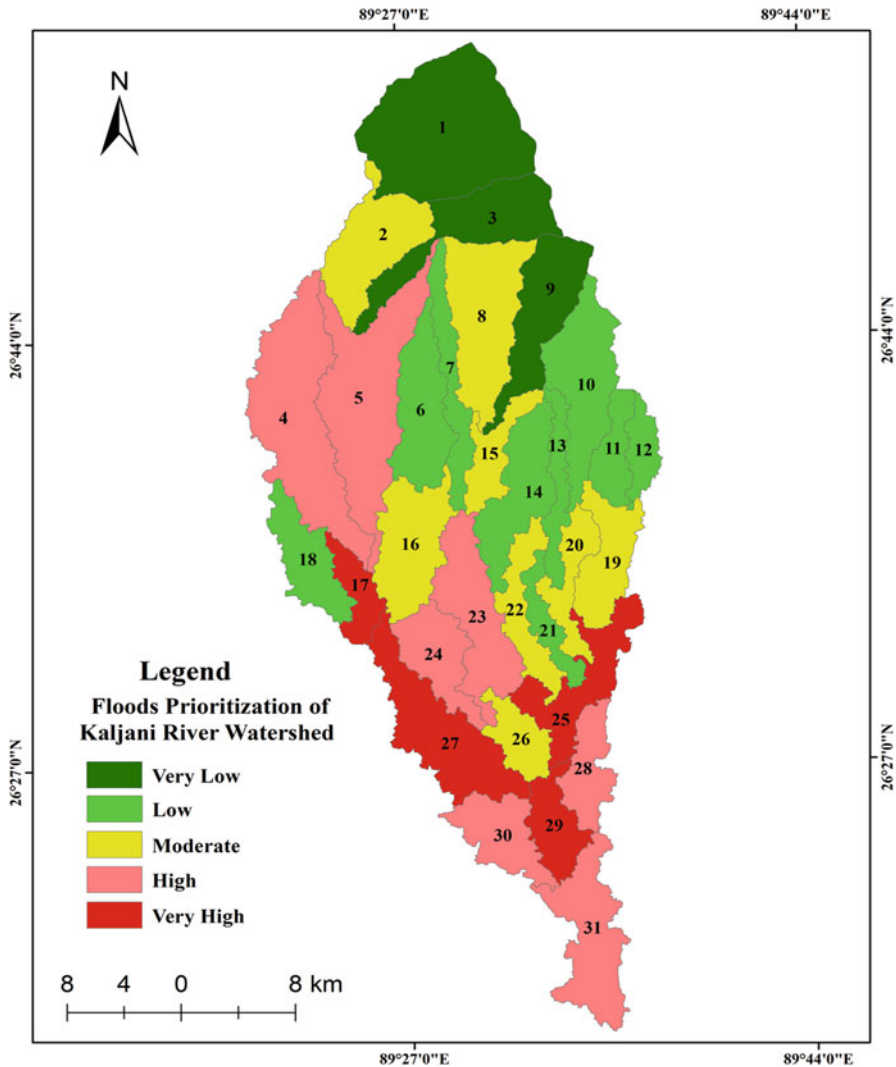


Fig. 8.7 Flood prioritization of river Kaljani sub-watersheds

## 6 Conclusions

In recent research, we have identified flood susceptibility at the sub-watershed level of the Kaljani River Basin using hydro-morphometric analysis and modern high-resolution satellite data. Since there was inadequate government and private historical flood data at the national or local level, which could help flood susceptibility modeling, the MPSWP method has been employed for flood prioritization of sub-watersheds using NASA ALOS PALSAR DEM (12.5 m). The research revealed



**Fig. 8.8** Field photos (a), (b), and (c) at Alipurduar town surrounding area and (d), (e), and (f) at beside of the Kaljani River during the flooding. (Source: (f) photo published Anandabazar 27/06/2019)

that about 40.62% of the total basin area is under H to VH flood probability. Out of the 12 morphometric factors, five factors ( $R_r$ ,  $R_v$ ,  $S_f$ ,  $L_o$ , and  $R_n$ ) were the most significant factors for the flooding. In the research, we have successfully used the ROC for the validation with an accuracy rate of 87%. Four sub-watersheds (SW 17, 25, 27, and 29) were under the very high flood zone, which covered about 11.32% area. Therefore, seven SWs (SW 4, 5, 23, 24, 28, 30, and 31) formed 29.30% area under the high flood category. Construction of the dam is highly recommended in high flood-prone areas for multipurpose water resources development, such as reducing the flood possibility, utilization of runoff water for irrigation, and increasing the sub-watershed management and restoration. Moreover, the outcome of the study will help decision-makers and policymakers with sustainable watershed management through the combination of MPSWP with GIS. It can contribute to further research on the other basins of the Himalayan foothills river basin.

## References

- Aher, P. D., Adinarayana, J., & Gorantiwar, S. D. (2014). Quantification of morphometric characterization and prioritization for management planning in semi-arid tropics of India: A remote sensing and GIS approach. *Journal of Hydrology*, *511*, 850–860.
- Alam, A., Ahmed, B., & Sammonds, P. (2020). Flash flood susceptibility assessment using the parameters of drainage basin morphometry in SE Bangladesh. *Quaternary International*. <https://doi.org/10.1016/j.quaint.2020.04.047>
- Ali, S. A., Parvin, F., Pham, Q. B., Vojtek, M., Vojtekova, J., Costache, R., et al. (2020). GIS-based comparative assessment of flood susceptibility mapping using hybrid multi-criteria decisionmaking approach, nave Bayes tree, bivariate statistics and logistic regression: A case study of Topl'a basin, Slovakia. *Ecological Indicators*, *117*, 106620. <https://doi.org/10.1016/j.ecolind.2020.106620>
- Ameri, A. A., Pourghasemi, H. R., & Cerda, A. (2018). Erodibility prioritization of sub-watersheds using morphometric parameters analysis and its mapping: A comparison among TOPSIS, VIKOR, SAW, and CF multi-criteria decision-making models. *Science of the Total Environment*, *613–614*, 1385–1400.
- Azmeri, H. I. K., & Vadiya, R. (2016). Identification of flash flood hazard zones in mountainous small watershed of Aceh Besar Regency, Aceh Province, Indonesia. *The Egyptian Journal of Remote Sensing and Space Sciences*, *19*, 143–160.
- Bhat, M. S., Alam, A., Ahmad, S., Farooq, H., & Ahmad, B. (2019). Flood hazard assessment of upper Jhelum basin using morphometric parameters. *Environmental Earth Sciences*, *78*, 54. <https://doi.org/10.1007/s12665-019-8046-1>
- Borga, M., Gaume, E., Creutin, J. D., & Marchi, L. (2008). Surveying flash floods: Gauging the ungauged extremes. *Hydrological Processes*, *22*, 3883–3885.
- Chakraborty, S., & Mukhopadhyay, S. (2019). *Assessing flood risk using analytical hierarchy process (AHP) and geographical information system (GIS): application in Coochbehar district of West Bengal*. Natural Hazards. <https://doi.org/10.1007/s11069-019-03737-7>
- Charizopoulos, N., Mourtziou, P., Psilovikos, T., Psilovikos, A., & Karamotsou, L. (2019). Morphometric analysis of the drainage network of Samos Island (northern Aegean Sea): Insights into tectonic control and flood hazards. *Comptes Rendus-Geoscience*, *351*, 375–383.
- Christopher, O., Idowu, A., & Olugbenga, A. (2010). Hydrological analysis of Onitsha North East drainage Basin using Geoinformatic techniques. *World Applied Sciences Journal*, *11*(10), 1297–1302.
- Destro, E., Amponsah, W., Nikolopoulos, E. I., Marchi, L., Marra, F., Zoccatelli, D., & Borga, M. (2018). Coupled prediction of flash flood response and debris flow occurrence: Application on an alpine extreme flood event. *Journal of Hydrology*, *558*, 225–237.
- District Disaster Management Plan. (2020). A publication of the District Disaster Management Authority, Alipurduar, March 2020.
- Farhan, Y., & Anaba, O. (2016). Flash flood risk estimation of Wadi Yutum (southern Jordan) watershed using GIS based: Morphometric analysis and remote sensing techniques. *Open Journal of Modern Hydrology*, *6*, 79–100.
- Farhan, Y., Anbar, A., Al-Shaikh, N., & Mousa, R. (2017). Prioritization of semi-arid agricultural watershed using morphometric and principal component analysis, remote sensing, and GIS techniques, the Zerqa River Watershed, Northern Jordan. *Agricultural Sciences*, *8*, 113–148.
- Hasanuzzaman, M., Gayen, A., & Shit, P. (2021). Channel dynamics and geomorphological adjustments of Kaljani River in Himalayan foothills. *Geocarto International*, 1–28. <https://doi.org/10.1080/10106049.2021.1882008>
- Hasanuzzaman, M., Adhikary, P., Bera, B., & Shit, P. (2022a). Flood vulnerability assessment using AHP and frequency ratio techniques. *Spatial Modelling of Flood Risk and Flood Hazards*, 91–104. [https://doi.org/10.1007/978-3-030-94544-2\\_6](https://doi.org/10.1007/978-3-030-94544-2_6)

- Hasanuzzaman, M., Islam, A., Bera, B., & Shit, P. (2022b). Flood susceptibility mapping using morphometric parameters and GIS. *Spatial Modelling of Flood Risk and Flood Hazards*, 15–31. [https://doi.org/10.1007/978-3-030-94544-2\\_2](https://doi.org/10.1007/978-3-030-94544-2_2)
- Hasanuzzaman, M., Gayen, A., Mafizul Haque, S., & Shit, P. (2022c). Spatial modeling of river bank shifting and associated LULC changes of the Kaljani River in Himalayan foothills. *Stochastic Environmental Research and Risk Assessment*, 36(2), 563–582. <https://doi.org/10.1007/s00477-021-02147-1>
- Horton, R. (1932). Drainage basin characteristics. *Transactions, American Geophysical Union*, 13, 350–361.
- Horton, R. E. (1945). Erosional development of streams and their drainage basins; hydrophysical approach to quantitative morphology. *Bulletin of the Geological Society of America*, 56, 275–370.
- Islam, A., & Deb Barman, S. (2020). Drainage basin morphometry and evaluating its role on flood-inducing capacity of tributary basins of Mayurakshi River, India. *SN Applied Sciences*, 2(6), 1–23.
- Islam, A., & Ghosh, S. (2022). Community-based riverine flood risk assessment and evaluating its drivers: evidence from Rarh Plains of India. *Applied Spatial Analysis and Policy*, 15(1), 1–47.
- Jodar-Abellan, A., Valdes-Abellan, J., Pla, C., & Gomariz- Castillo, F. (2019). Impact of land use changes on flash flood prediction using a sub-daily SWAT model in five Mediterranean ungauged watersheds (SE Spain). *Science of the Total Environment*, 657, 1578–1591.
- Kannan, R., Venkateswaran, S., Vijay Prabhun, M., & Sankar, K. (2018). Drainage morphometric analysis of the Nagavathi watershed, Cauvery river basin in Dharmapuri district, Tamil Nadu, India using SRTM data and GIS. *Data in Brief*, 19, 2420–2426.
- Macka, Z. (2001). Determination of texture of topography from large scale contour maps. *Geografski Vestnik*, 73(2), 53–62.
- Magesh, N. S., Chadrasekar, N., & Soundranagyagam, J. P. (2011). Morphometric evaluation of Papanasam and Manimuthar watersheds, part of Western Ghats. Tirunelveli District, Tamil Nadu, India: A GIS approach. *Environmental Earth Sciences*, 64, 374–381.
- Malik, M. I., Bhat, M. S., & Kuchay, N. A. (2011). Watershed based drainage morphometric analysis of Lidder catchment in Kashmir valley using Geographical Information System. *Recent Research in Science and Technology*, 3(4), 118–126.
- Melton, M. A. (1957). Correlations structure of morphometric properties of drainage systems and their controlling agents. *Journal Geology*, 66, 442–460.
- Meraj, G., Yousuf, A. R., & Romshoo, S. A. (2013). *Impacts of the geo-environmental setting on the flood vulnerability at watershed scale in the Jhelum basin*. M.Phil dissertation, University of Kashmir, India. <http://dspace.uok.edu.in/jspui/handle/1/1362>
- Miller, V. C. (1953). *A quantitative geomorphic study of drainage basin characteristics on the Clinch Mountain area, Virginia and Tennessee* (Proj. NR 389–402, Tech Rep 3). Columbia University, Department of Geology, ONR.
- Obeidat, M., Awawdeh, M., & Al-Hantouli, F. (2021). Morphometric analysis and prioritisation of watersheds for flood risk management in Wadi Easal Basin (WEB), Jordan, using geospatial technologies. *Journal of Flood Risk Management*, 14(2). <https://doi.org/10.1111/jfr3.12711>
- Patel, D., Dholakia, M., Naresh, N., & Srivastava, P. (2012). Water harvesting structure positioning by using geo-visualization concept and prioritization of mini-watersheds through morphometric analysis in the Lower Tapi Basin. *Journal of the Indian Society of Remote Sensing*, 40, 299–312.
- Patton, P. C., & Baker, V. R. (1976). Morphometry and floods in small drainage basins subject to diverse hydrogeomorphic controls. *Water Resources Research*, 12, 941–952.
- Pavano, F., Catalano, S., Romagnoli, G., & Tortorici, G. (2018). Hypsometry and relief analysis of the southern termination of the Calabrian arc, NE Sicily (southern Italy). *Geomorphology*, 304, 74–88.
- Puno, G. R., & Puno, R. C. C. (2019). Watershed conservation prioritization using geomorphometric and land use-land cover parameters. *Global Journal of Environmental Science and Management*, 5(30), 279–294.

- Rajasekhar, M., Sudarasana Raju, G., & Siddi Raju, R. (2020). Morphometric analysis of the Jilledubanderu River Basin, Anantapur District, Andhra Pradesh, India, using geospatial technologies. *Groundwater for Sustainable Development*, 11, 100434. <https://doi.org/10.1016/j.gsd.2020.100434>
- Roy, L., & Das, S. (2021). GIS-based landform and LULC classifications in the Sub-Himalayan Kaljani Basin: Special reference to 2016 Flood. *The Egyptian Journal of Remote Sensing and Space Science*, 24(3), 755–767. <https://doi.org/10.1016/j.ejrs.2021.06.005>
- Schumm, S. (1956). Evolution of drainage systems and slopes in badlands at Perth Amboy, New Jersey. *Geological Society of America Bulletin*, 67, 597–646.
- Shivhare, N., Rahul, A. K., Omar, P. J., Chauhan, M. S., Gaur, S., Dikshit, P. K. S., & Dwivedi, S. B. (2018). Identification of critical soil erosion prone areas and prioritization of microwatersheds using geoinformatics techniques. *Ecological Engineering*, 121, 26–34.
- Smith, K. (1950). Standards for grading texture of erosional topography. *American Journal of Science*, 248(9), 655–668.
- Smith, K. (1996). *Environmental hazards: Assessing risk and reducing disaster* (2nd ed.). Routledge.
- Strahler, A. (1952). Hypsometric (area-altitude) analysis of erosional topography. *Geological Society of America Bulletin*, 63, 1117–1142.
- Strahler, A. (1957). Quantitative analysis of watershed geomorphology. *Transactions, American Geophysical Union*, 38, 913–920.
- Strahler, A. (1964). Quantitative geomorphology of drainage basins and channel networks. In V. Chow (Ed.), *Handbook of applied hydrology* (pp. 439–476). McGraw Hill.
- Toduse, N. C., Ungurean, C., Davidescu, S., Clinciu, I., Marin, M., Nita, M. D., et al. (2020). Torrential flood risk assessment and environmentally friendly solutions for small catchments located in the Romania Natura 2000 sites Ciucas, Postavaru and Mare. *Science of the Total Environment*, 698, 134271. <https://doi.org/10.1016/j.scitotenv.2019.134271>
- UNISDR. (2015). Making development sustainable: The future of disaster risk management. In *Global assessment report on disaster risk reduction*. United Nations Office for Disaster Risk Reduction (UNISDR).
- Wu, Y., Ji, H., Wen, J., Wu, S. Y., Xu, M., Tagle, F., He, B., Duan, W., & Li, J. (2019). The characteristics of regional heavy precipitation events over eastern monsoon China during 1960–2013. *Global Planet Change*, 172, 414–427.

# Chapter 9

## Application of Multi-Criteria Decision-Making Approach for Assessing Flood Susceptibility of the Tal-Diara and Barind Region in Malda District, India



Kunal Chakraborty, Mantu Das, and Snehasish Saha

**Abstract** The most frequent natural occurrence in low-lying flat land or floodplain regions is flooding, which not only results in a boost to the soil fertility but is also almost invariably accompanied by a major loss of lives, property, and the economy. The major objective of the present study is to identify areas, which are vulnerable to flood in the Malda District of West Bengal, lying under the lower Gangetic floodplain using the remote sensing, GIS with the integration of multi-criteria decision-making (MCDM) approach by applying the analytical hierarchy process (AHP) model. Spatial distribution under GIS platform has been employed, and eight relevant parameters have been selected, and weights were given from the calculation of pair matrix of AHP model namely elevation (27.7%), slope (21.5%), distance from river (15.4%), confluence (10.4%), geomorphology (7.6%), soil (5.7%), and LULC (4.1%) for the identification of flood susceptible areas. From the assessment, five flood-susceptible zones have been identified as very least susceptible, least susceptible, moderately susceptible, high susceptible, and very high susceptible. For the validation of MCDM-based model area within and under the curve (AUC) has prepared using the 50 number of flood inventory points. The high AUC value (0.847) indicates that flood susceptibility zonation of Malda District is quite precise and can be useful for planning, mitigating, and reducing future flood inundation problems.

**Keywords** Flood susceptibility zonation (FSZ) · MCDM · AHP · Lower Gangetic floodplain · Malda

---

K. Chakraborty · M. Das · S. Saha (✉)

Department of Geography & Applied Geography, University of North Bengal, Siliguri, India  
e-mail: [kunalgeo92@nbu.ac.in](mailto:kunalgeo92@nbu.ac.in); [rs\\_mantudas@nbu.ac.in](mailto:rs_mantudas@nbu.ac.in)

## 1 Introduction

Humans have experienced major natural catastrophes, including floods, cyclones, earthquakes, and landslides, from the beginning of civilization (Sarkar & Mondal, 2020). Flood is a natural catastrophe that often results from heavy rainfall (Tripathi, 2015; Beniston, 2009; Archer & Fowler, 2018) and chaotic river discharge (Singh & Kumar, 2017). It turns disastrous when it causes significant loss of life (including that of plants and animals), human settlements, and damage to infrastructure and property (Sanyal & Lu, 2005; Islam & Dharanirajan, 2017). Flood being a natural hazard sometimes accentuates its devastating power due to anthropogenic activities, i.e., bridge construction across the channel, channel encroachment, weak embankment, etc.; therefore, now, it's called quasi-natural hazard (Beniston, 2009; Hammami et al., 2019). Flood is a common hydrologic natural event (Mehebut et al., 2015) in plain land, specifically at the junction point of various active channels, low-lying areas where low discharge capacity means low bank-full height is the main scenario to create lateral spreading of water as a flood. According to Carter (2008), floods have the following characteristics, i.e., depending on the nature of flood (e.g., while flash floods may not give any real advance warning, flooding within some areas of a major river system may build over the course of days or even weeks); there may be a long, short, or no warning; there might be seasonal patterns of floods and gradual or abrupt changes in pace or start. Floods can happen seasonally in the same part of the world, or they can happen unexpectedly anywhere in the world owing to physical phenomena or human activities (Kireeva et al., 2015).

India, fittingly known as the “Land of Rivers,” is crisscrossed by several rivers and is subject to annual floods. Floods may be seen as both a blessing and a curse for the economy since; while high-intensity floods are dangerous, they also help to restore river ecology and soil fertility (Sinha et al., 2012; Gourav et al., 2020). The climatic and geographic aspects of India's varied regions leave them vulnerable to a variety of natural disasters (Pandey & Jha, 2012). It is reported that 40 million hectares of land are very sensitive to flooding, while 54% of land regions are extremely vulnerable to earthquakes. It is noteworthy, with a risk management score of 5.7 and an index for flood hazard of 8.5, that India is categorized under highly susceptible (risk) zone nation for humanitarian exigency and catastrophes (Andrew et al. 2018). However, the country's total flood-affected land area is just about 5.74 million hectares, affecting an estimated 18.64 million people (Vignesh et al., 2021).

Flood hazards are normally announced as extreme events grasping habitants residing side by side. It suddenly disrupts social structure cum operative social processes and impairs life-supporting functions that are inevitable to continue human sustenance (Ismail & Mustaqim, 2013; Dandapat & Panda, 2017). In the case of managing the surrounding fluvial systems to refigure the lifestyle of local people, there should be fruitful planning objectives. Malda District is one of the important areas that are normally vulnerable to floods. Malda is one of West Bengal's districts that experience the greatest flooding, which is caused by the

overflow of the rivers Ganga, Mahananda, and their tributaries (Ghosh & Kar, 2018). The shifting course of river Ganga is a serious cause of flood and bank failures in Malda District of West Bengal. This has become chronic since the early 1960s and the occurrence manifested significantly to a formidable degree during 1906, 1971, 1987, 1988, 1991, 1996, 1998, 2000, 2006, 2007, 2008, 2014, 2016, and 2017 (Ghosh & Kar, 2018). Though all these are natural processes in a riverine environment. Havoc inundations and destruction of houses by the rising water table of the rivers like the Ganga, Mahananda, Tangan, and Fulahar in Malda is the main reason for flooding here. During the severe flood of 1998, the entire district was seriously affected irrespective of the flood-prone blocks.

The majority of flood occurrences and riverbank erosion occur in flood plain areas (Ghosh & Kar, 2018). Therefore, it is crucial for the welfare of society to understand environmental concerns and risk management. There is no comprehensive database for flood monitoring and risk reduction, even though most wealthy nations have accurate flood hazard maps, current flood data, and post-disaster mitigation help. It is noticed that rural riverine residents are far away from knowing the management scenario of flood hazard at pre-, during and post-phases of occurrence.

From the available literary sources, a few researches (i.e., Mukherjee et al., 2018; Ghosh & Kar, 2018; Meheub et al., 2015; Ismail & Mustaqim, 2013; Mazumder, 2004) have been found regarding the identification of flood susceptible areas of Malda District. As flood is occurring frequently in the district almost in every monsoonal month of the year, it is very necessary to take up such kind of research for implementing the regional-level planning and risk management purpose.

Several attempts have been made in the last few decades to preserve flood data and mapping flood susceptibility, sensitivity, and risk zones to raise societal awareness at both the local and regional levels with the use of statistical methods, quantitative techniques, remote sensing data analysis, and GIS technology. Relevant geomorphological, hydro-geological, socioeconomic, climatic, and other data must be included in the field of this type of research, which leads toward micro-level assessment and planning (Barman et al., 2016; Sanyal & Lu, 2005; Aydin & Uysal, 2014; Masood & Takeuchi, 2012). Multi-criteria decision-making (MCDM) methods can be used to improve flood risk management. An acronym known as MCDM is used to designate a group of techniques for organizing and assessing options based on a variety of criteria and goals. Due to its ability to overcome the underlying ambiguity and difficulty of such situations and the knowledge gained through the involvement of several individuals, these approaches offer targeted judgments (Lee et al., 2013; Hammami et al., 2019; Mishra & Satapathy, 2020). The present study has been focused on two aspects, i.e., first, historical scenario of flood hazard in Malda District and second, to mapping spatial distribution of flood susceptibility based on the AHP model using GIS analytics (Mondal & Maiti, 2013).



## 2 A Succinct Outline of the Research Area

Geographically Malda District comprises about 3566.17 km<sup>2</sup> area and is located within 24°40'20"N to 25°32'08"N and from 87°45'50"E to 88°30'0"E, respectively (Fig. 9.1). The Ganga River defines the district's western border, while the northern portion of the district is bordered by the North Dinajpur District. Dakshin Dinajpur District is situated at the north-eastern part of the district, Bangladesh is situated along the south-eastern boundary, and Murshidabad District delimits the western boundary of the district. The district is generally divided into two equal halves by the river Mahananda's north and south flows, which corresponds to the former Rarh and Barendra border. The district is divided into ten police stations and two subdivisions: Sadar, with its headquarters in English Bazar, and Chanchal, with its headquarters in Chanchal. As per the Census of India 2011, the district comprises 15 community development (CD) blocks and that are namely Gazole, Habibpur, and Bamangola (in the east); English Bazar and Old Malda (in the central part); Manikchak, Kaliachak-I, Kaliachak-II, and Kaliachak-III (in the west); and Harishchandrapur-I and Harishchandrapur-II, Ratua-I, Ratua-II, Chanchal-I, and Chanchal-II (at the North). All the blocks in the northern part of the district are under the jurisdiction of the Chanchal subdivision, and the rest nine blocks are under the jurisdiction of Malda Sadar subdivision.

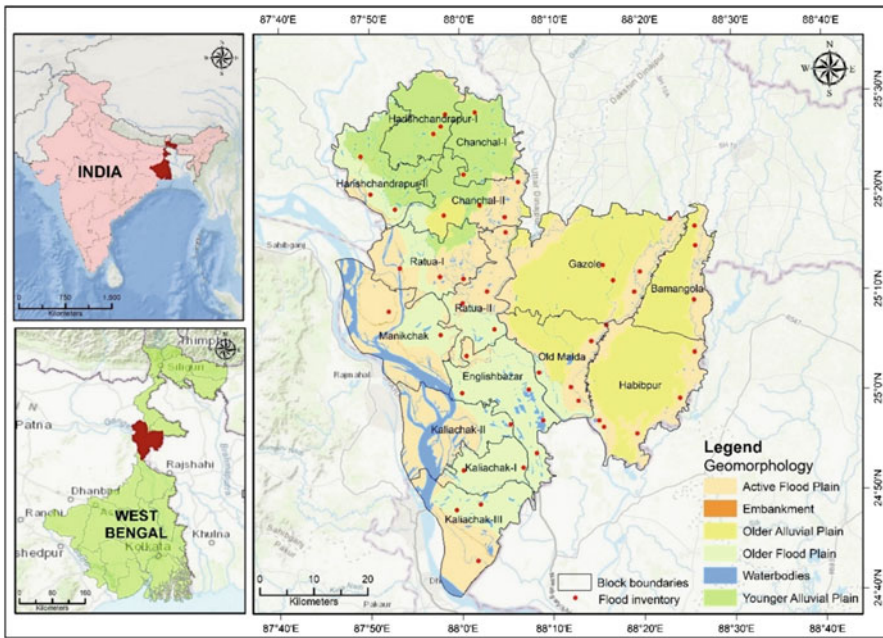


**Fig. 9.1** Locational settings of the Malda District with block boundaries and major geomorphological units in the lower Gangetic floodplain region with reference to India and West Bengal

Malda District, basically, the Diara region, which is in the Ganga-Mahananda interfluvial basin, has frequent flood risk due to the region's high annual rainfall average. The studied region is subject to flooding during flood withdrawal periods and has diluvial and alluvial tracts, respectively. In terms of historical comparison, the Malda area had three significant inundations between 1850 and 1870, particularly in the lowlands near the rivers. Following the notable flood of 1870, the high flood years were 1875, 1885, and 1906, indicating a possible scenario of flooding occurring every approximately 10 years (Carter, 1935). Floods also happened in the years 1918, 1922, 1935, 1948, and 1970, according to records. The recent history has seen significant flooding in the years 1987, 1988, 1991, 1995, and 1996. Surveys conducted by government personnel during the flood of 1938 revealed a 153,329 cusecs of water level, which demonstrated a superior ability flooding in the past (Samad, 2005). Disastrous flooding happened in 1998 because of continuous rain that was measured at 418 mm in 48 h (August 24–25). The Ganga and Mahananda Rivers' water levels increased as a result, and the fifth retired embankment at Gopalpur near Manikchak was breached. Total 2.1 million of the district's residents were vulnerable to flooding. 150,000 ha of agriculture were damaged, 2000 homes were destroyed, and 150,000 homes were damaged by the flood, which claimed the lives of 450 people (Mazumder, 2000). The district witnessed several floods in 2017, 2019, and 2021, all of which registered as relatively recent occurrences.

### 3 Materials and Methods

#### 3.1 Data Sources and Preparation of Thematic Layers

For recognition and identification of the flood susceptible zone of the Malda District in the Gangetic floodplain landscape, eight parameters have been selected, viz., geomorphology, distance from the major river, distance from the river confluence point, LULC, type of soil, rainfall pattern, slope, and elevation. Based on the research from both the existing literature and the field to determine the final output of flood susceptibility, GIS analytics have been used to examine and perform on each of these eight thematic layers (ArcMap 10.5). All the chosen theme layers have been converted into rasterized formats, which have then been projected onto the Northern Hemisphere's Zone 45 of the UTM Projection.

SRTM-DEM extracted from the website of USGS Earth Explorer featured by 30 m spatial resolution was processed to extract and create the elevation, slope, and drainage network maps as well as the distance from major rivers and the distance from river confluence point maps. A stream order tool was then employed after the DEM had initially been preprocessed in the GIS platform (ArcMap 10.5) utilizing the consecutive techniques of sink-filling, flow accumulation, and flow direction. Landsat 8 OLI data (30 m resolution) scenes were gathered from the USGS for the creation of LULC. Two Landsat images (Row 42 and 43 and Path 139) were combined at the first step, and thereafter, mosaic was done; after then atmospheric

correction was done, DN's value conversion for each band using the method called spectral radiance scaling and ultimately conversion to ToA reflectance was achieved associated with edge enhancement and band composition techniques. The ultimate outcome of the LULC map bearing seven-fold classes was produced following supervised classification using a maximum likelihood technique (i.e., water body, barren land, vegetation cover, agricultural land, marshy land, settlement, and sand deposit). The Bhukosh GSI website provided the data for geomorphology. The layer was originally processed in the GIS environment and further transformed purposefully into a raster layer. It is available in vector format (30 m spatial resolution). The NBSS and LUP were used to collect the soil map for the study region, which was then georeferenced, digitalized, and extracted using the GIS platform. Then, block-wise rainfall data with a CSV extension were collected from NASA's high-resolution satellite-based point data with a 30-year average. Point data were added to the vector layer, and afterwards, the interpolation (Kriging method) was done to generate the rainfall zoning map. Several research works suggested that the Kriging interpolation approach is the most accurate and trustworthy method for defining rainfall maps (Ly et al., 2013; Kim et al., 2011). Additionally, all data sources are included in Table 9.1 along with a summary of each one.

Reclassification was carried out once all the chosen theme layers were converted to a raster format having equal cell size (30 m). Furthermore, weighted overlay analysis (WOA) as a method was carried out through the raster thematic layer (RTL) integration approach using all RTLs under the GIS environment by using weighted overlay tool (WOT) to delineate the final flood susceptibility map of Malda District after assigning the weights applying the Saaty's scale using the AHP-Excel sheet featured by K. D. Geopel version 15.08.2018.

### ***3.2 Factors that Affect Flood Conditions***

Selecting the most important criteria for creating an accurate flood susceptibility map is a complex undertaking that depends on both subjective knowledge and practical experience. And a crucial task is understanding and determining of fundamentally critical flood conditioning elements (Kia et al., 2012; Das, 2020). Because of their varying importance in a constantly shifting quasi-natural environment, flood causation elements vary from location to location. Therefore, eight causative factors were primarily selected as elevation, distance from major river, slope, distance from confluence point, rainfall, geomorphology, soil, and LULC (Figs. 9.2, 9.3, 9.4 and 9.5).

#### **3.2.1 Elevation (EL)**

The most important element influencing the likelihood of flooding is elevation (Mojaddadi et al., 2017). Water rushes quickly from highland to lowland places

**Table 9.1** Information about the several data sets utilized in this study

Type of data	Data specifics	Data format available	Type of extracted layer	Type of generated layer	GIS data type
Satellite data <sup>a</sup>	Landsat 8 OLI Path – 139 Row – 42 & 43 Dated: 10.03.2021	TIFF (.tif)	LULC	LULC	Raster
Geomorphology <sup>b</sup>	Bhukosh-GSI	ESRI shapefile (.shp)	Geomorphology	Geomorphology	Raster
Soil map <sup>c</sup>	NBSS and LUP Soil-sheet 1 West Bengal Scale: 1:5,00,000	JPG	Types of soil	Types of soil	Raster
SRTM-DEM <sup>a</sup>	Entity ID: SRTM1N25E087V3 SRTM1N25E088V3 SRTM1N24E087V3 SRTM1N24E088V3 Spatial resolution-30 meters Dated: 23 September 2014	TIFF (.tif)	1. Contour. 2. Elevation. 3. Drainage network.	1. Average slope. 2. Elevation. 3. Distance from major river. 4. Distance from confluence point.	Raster
Rainfall map <sup>d</sup>	Monthly point data, Measuring unit – Millimeter 30 years average data	CSV	Station wise rainfall distribution	Rainfall zonation map	Raster

Source: <sup>a</sup>USGS Earth Explorer (<https://earthexplorer.usgs.gov/>)

<sup>b</sup>Bhukosh – Geological Survey of India (<https://bhukosh.gsi.gov.in/>)

<sup>c</sup>NBSS and LUP (<https://esdac.jrc.ec.europa.eu/>)

<sup>d</sup>NASA, USA (<https://power.larc.nasa.gov/>)

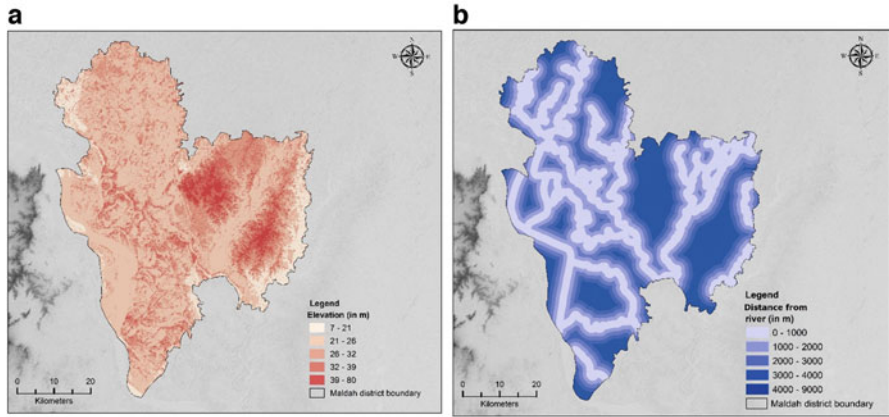


Fig. 9.2 (a) Elevation map and (b) distance from major river map

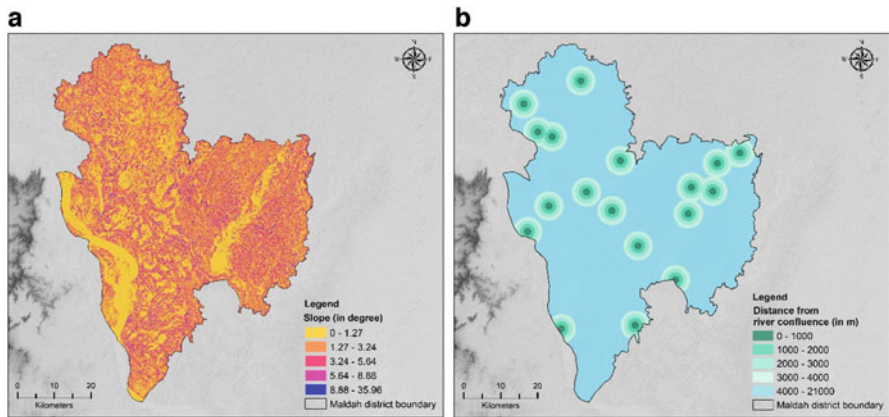


Fig. 9.3 (a) Slope map and (b) distance from river confluence point map

due to gravity, and the water spreads out across the lower raised plains, causing inundation. Elevation of the district ranges from 7 to 80 m from MSL. A total district area was categorized into five elevation zones, viz., very low elevated surface (7–21 m), low elevated (21–26 m), moderate (26–32 m), high elevated (32–39 m), and very high elevated surface (39–80 m) comprising of 270.06 km<sup>2</sup>, 1894.35 km<sup>2</sup>, 945.70 km<sup>2</sup>, 440.62 km<sup>2</sup>, and 137.15 km<sup>2</sup> areas, respectively. Most of the area (58.59%) comes under the zones of very low to low category (Fig. 9.2a). Basically, elevated surfaces are seen along the north-eastern parts of Malda District (i.e., Gazole, Habibpur, and Bamangola blocks). Low-elevated blocks are highly susceptible to flood catastrophes (Ghosh & Kar, 2018).

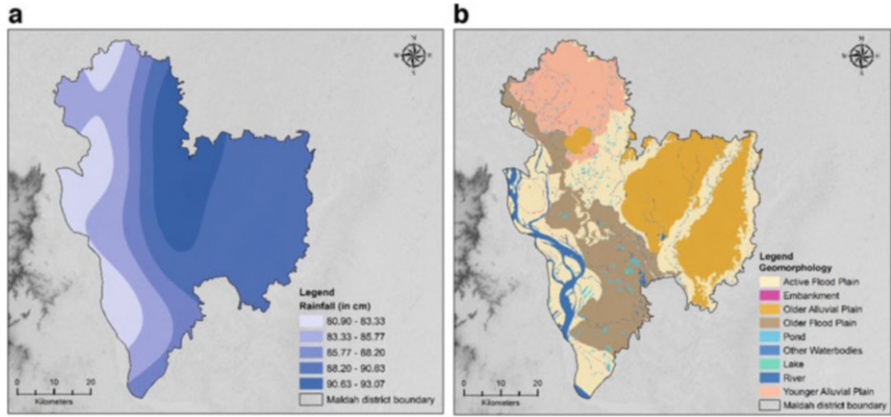


Fig. 9.4 (a) Rainfall map and (b) geomorphology map

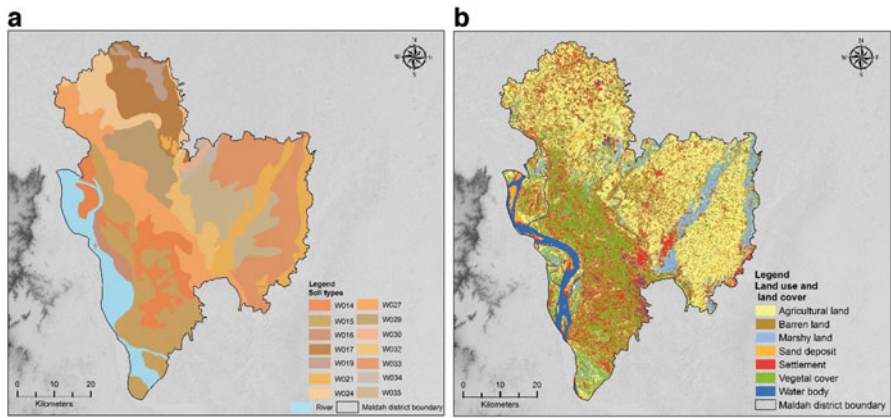


Fig. 9.5 (a) Soil map and (b) LULC map

### 3.2.2 Distance from Major Rivers (DR)

According to Das (2020), the distance between a riverine flood event and the drainage network is crucial in determining how far it spreads. Flooding is less likely in regions far away from streams. At the same time, regions close to rivers frequently flood (Pham et al., 2020). The threshold distance does not exist that can be considered as highly susceptible. Several factors simultaneously have played almost equal roles, i.e., channel width, water supply, channel geometry, and so on. Several researchers stated that 90–100 m buffer areas are highly sensitive to flood events every year (Samanta et al., 2016; Pradhan, 2010). The overall district area has been split into five areas that are separated from the district’s major rivers. Spatial coverage of each zone is 1208.78 km<sup>2</sup> (0–1 km), 848.10 km<sup>2</sup> (1–2 km),

591.67 km<sup>2</sup> (2–3 km), 414.65 km<sup>2</sup> (3–4 km), and 624.25 km<sup>2</sup> (4–9 km). It is noteworthy that based on literature, 1 km buffer area is highly sensitive to flood (Fig. 9.2b).

### 3.2.3 Slope (SP)

The process of surface runoff and flow accumulation depends on the surface slope in all lithologic and geomorphic environments (Fernandez & Lutz, 2010). The slope factor completely controls flow rate, river discharge, and flood inundation, among other things. Higher slope indicates frequent flood events and vice-versa in the downstream section. Therefore, low-lying places with high drainage networks and low relative relief surfaces are quite vulnerable to flooding occurrences. Five zones were created from the slope map as 0.00–1.27, 1.27–3.24, 3.24–5.64, 5.64–8.88, and 8.88–35.96 degree, comprising of 1603.94 km<sup>2</sup>, 1046.55 km<sup>2</sup>, 673.48 km<sup>2</sup>, 294.23 km<sup>2</sup>, and 69.74 km<sup>2</sup> areas, respectively (Fig. 9.3a). In Malda District, 43.49% area indicates high proficiency in flood hazard.

### 3.2.4 Distance from River Confluence Point (DC)

River confluence has played a very crucial role to create flood by spreading channel water and backwater of the next order channel. Junction point of several channels is high proficiency to flood hazard due to huge flow accumulation (Roca et al., 2009). Large number of river confluence points simultaneously has closer proximity in any geomorphic setting indicating high flood susceptibility. Here, the distance from the river confluence point map was categorized into four zones to 1 km buffer and last zone as 4–21 km (Fig. 9.3b). The Malda District is geographically made up of several river confluences.

### 3.2.5 Rainfall (RF)

According to a vast number of available research (e.g., Bouilloud et al., 2010; Zhang & Smith, 2003), rainfall is a direct cause of severe flooding. As a result, it is regarded as among the most crucial elements in mapping flood susceptibility. The study region is experiencing a monsoon climate; hence, flood in Malda District basically happened because of monsoon rainfall (June–September). The district has been divided into five rainy zones based on the distribution of rainfall (Fig. 9.4a). Results show a comparatively high rainfall zone exists in the district's northern and northern-eastern region and gradually decreases toward west, south-west, and north-west direction. Here, some part of the following blocks, i.e., Chanchal-II, Ratua-II, English Bazar, Old Malda, and Gazole, are experiencing high rainfall. From the analysis, it can be estimated that the 30 years of average annual rainfall of the district is about 87 cm per year and 90% of the rainfall occur during the monsoonal months.

### 3.2.6 Geomorphology (GM)

Flooding is significantly influenced by geomorphological variance in a region. The entire district has been categorized into nine morphological units, viz., active flood plain, older or *Bhabar* alluvial plain, older flood plain, younger or Khadar alluvial plain, embankment, river, lakes, pond bogs, and other water bodies. Basically, first four morphological units are dominated here comprising an area about 1175.43 km<sup>2</sup>, 935.17 km<sup>2</sup>, 765.25 km<sup>2</sup>, and 536.18 km<sup>2</sup>, respectively. According to several literatures (Syvitski et al., 2012; Predick et al., 2009), alluvium of two distinct eras covers the area, which has various physical and physiographic properties. The Tal and Diara regions are dominated by younger alluvial whereas the Barind region is dominated by older alluvium (Lambourn, 1918). River terraces found in the lower Gangetic region are frequently reflected as geologically older floodplains, which are one of the most dominant landforms constructed by the ancient streams. These are historic floodplains, which are still significantly elevated above the current floodplain and show where a stream formerly flowed and left several meander cutoffs. It is obvious that active flood plain is highly sensitive to flood hazard during long torrential rainfall, over bank-full discharge at every monsoon period, etc. that's why riverine settlements have direct, devastating experience of natural calamities like flood, bank failure, waterlogged, and so on.

### 3.2.7 Soil (SL)

Both infiltration and surface runoff depend upon the soil characteristics defining the soil texture, soil structure, composition, and porosity. Generally, loose composition, high porosity, and weak structural form are equally important to generating a high rate of infiltration. Therefore, torrential rainfall is sometimes going in favor of groundwater recharge. By contrast, structurally strong, low pore space, and concentration of clay composition are the dominating parameters to create surface runoff, and as a result, flood occurred in the monsoon period (Das, 2020). Soil category map has been executed based on the NBSS and LUP. In Malda District, a total of 14 soil types have been identified, viz., W014, W015, W016, W017, W019, W021, W024, W027, W029, W030, W032, W033, W034, and W035 (Fig. 9.5a). Out of which most dominating soil types are W033 (543.19 km<sup>2</sup>), W015 (532.89 km<sup>2</sup>), and W027 (408.88 km<sup>2</sup>). Different type of soil characteristics have been discussed on the basis of NBSS & LUP soil classes of West Bengal. Few soil samples were tested of Diara of Manikchak and Panchanandapur in the Pedological Laboratory of the Department of Geography and Applied Geography, NBU, alongside the eastern bank of Ganga and found that W015 and 17 were of the type of 70–80% of sands, 15–25% of silts, and 5–6% of clay and subject to ready collapse (based on field investigation, 2019) and flood inundation are very devastating.



### 3.2.8 LULC

LULC is the major force behind a certain area's transformation. A region's pattern of land utilization affects several hydrological processes, including surface runoff, infiltration rate, and evapotranspiration (Yalchin et al., 2011). In relation to identifying flood vulnerability, LULC is consequently viewed as a significant conditioning factor (Komolafe et al., 2018). There are seven main LULC classes: (i) agricultural land 1410 km<sup>2</sup>, (ii) Barren land 440 km<sup>2</sup>, (iii) Marshy land 214 km<sup>2</sup>, (iv) sand deposit 93 km<sup>2</sup>, (v) settlement 589 km<sup>2</sup>, (vi) vegetal cover 778 km<sup>2</sup>, and (vii) water body 164 km<sup>2</sup> (Fig. 9.5b).

### 3.3 AHP Model for Flood Susceptibility Zones

The AHP model is considered as one of the finest models for identifying the flood susceptibility zone map, which is an MCDM approach first developed by Saaty (Saaty, 1980). In order to simplify decision-making, the approach was used to a set of parameters for creating a hierarchical structure by assigning the weights (Kiker et al., 2005; Pramanik, 2016) to each of the criterion. AHP is a methodical and potent strategy that uses the GIS platform to examine many factors based on expert opinions and experiences, integrating practical information with subjective notions to perform decision-making (Sener et al., 2011; Hammami et al., 2019). The assignment of weights to each of the parameters and their normalization is an important step in producing correct findings since the outcome depends only on the selection of the suitable weight assignments (Muralitharan & Palanivel, 2015). Although several other weight estimating methods are also used, AHP is thought to be one of the popular and successful method for flood susceptibility modeling since it offers the most accurate and economical results (Murmu et al., 2019).

The four phases of functions used to construct the AHP model are weight assignment, pairwise comparison matrix, weight normalization, and consistency ratio (CR) check (Ghosh et al., 2020; Hammami et al., 2019; Benjmel et al., 2020). Eight criteria in total were selected for the present pursuing study with the goal of controlling flood susceptibility in the flood-prone Malda region. Here, each parameter is given a weight based on professional judgment, domain knowledge, and extensive literature studies (Magesh et al., 2012). A high weight parameter suggests a significant influence or impact, whereas a weight of low indicates negligible influence or impact on flood vulnerability.

At first, researchers have selected comparatively high important controlling factors and described the factors based on their importance and determining influence on flood vulnerability. Then, for comparing all the characteristics combining all the thematic layers synced in a matrix format and which is required in determining the measurement, the assigned weights for each criterion were loaded based on Saaty's scale (varies between 1 and 9) of relative importance. On Saaty's scale,

**Table 9.2** Saaty’s significance scale for determining parameter weights

Intensity	Definition	Explanation
1	Equivalent significance	The goal is influenced equally by two factors.
3	Medium significance	One ingredient is slightly more preferred than the other by experience and judgment.
5	High significance	One ingredient is greatly preferred over another by experience and judgment.
7	Very high significance	One element is greatly preferred over another, and its dominance is seen in action.
9	Utmost significance	The strongest form of affirmation is used to support the evidence accepting favorably one element over the another.

To indicate an intermediate value, use 2, 4, 6, or 8.

**Table 9.3** Matrix for pairwise comparisons in the AHP process

Matrix											normalized principal Eigenvector
	Elevation	Slope	Distance from River	Confluence	Rainfall	Geomorphology	Soil	LULC	0	0	
Elevation	1	1	2	3	4	4	5	6	-	-	$\begin{pmatrix} 27.73\% \\ 21.47\% \\ 15.41\% \\ 10.44\% \\ 7.55\% \\ 7.55\% \\ 5.69\% \\ 4.14\% \\ 0.00\% \\ 0.00\% \end{pmatrix}$
Slope	2	1	1	2	3	3	4	5	-	-	
Distance from River	3	1/2	1	1	2	2	3	4	-	-	
Confluence	4	1/3	1/2	1	1	1	2	3	-	-	
Rainfall	5	1/4	1/3	1/2	1	1	1	2	-	-	
Geomorphology	6	1/4	1/3	1/2	1	1	1	2	-	-	
Soil	7	1/5	1/4	1/3	1/2	1	1	1	-	-	
LULC	8	1/6	1/5	1/4	1/3	1/2	1/2	1	-	-	
0	9	-	-	-	-	-	-	-	1	-	
0	10	-	-	-	-	-	-	-	-	1	

Consistency ratio = 1.20%, for more than four components, the maximum acceptance level is 10% Using AHP-Excel framework by K. D. Geopel version 15.09.2018

1 denotes equal relevance in relation to the dominating component and 9 denotes extraordinary importance (Table 9.2).

The pairwise comparison matrix for flood susceptibility factors is shown in Table 9.3, where parameters are grouped in a hierarchy and given values based on their relative weights (Table 9.4). To create the standardized comparison matrix for

**Table 9.4** Distinct aspects of the eight conditioning factors have been given assigned and normalized rankings for flood susceptibility mapping

Table	Criterion	Comment	Weights	+/-
1	Elevation		27.7%	3.4%
2	Slope		21.5%	3.3%
3	Distance from River		15.4%	3.1%
4	Confluence		10.4%	2.6%
5	Rainfall		7.6%	1.3%
6	Geomorphology		7.6%	1.3%
7	Soil		5.7%	1.2%
8	LULC		4.1%	0.7%
9		for 9&10 unprotect the input sheets and expand the	0.0%	0.0%
10		question section ("+" in row 66)	0.0%	0.0%

Result	Eigenvalue	Lambda:	8.118	MRE:	18.4%
	Consistency Ratio	0.37	GCI: 0.04	Psi: 0.0%	CR: 1.2%

Source: Weightage assigned by authors based on Saaty’s scale (1980, 1994, and 1996)

mapping flood susceptibility, pairwise comparison scores are normalized. The following equations then assess the consistency of the AHP technique (Das, 2020):

$$CR = \frac{CI}{RI} \tag{9.1}$$

where

$$CI = \frac{\lambda_{max} - n}{n - 1} \tag{9.2}$$

where CR stands for consistency ratio, consistency index is denoted by CI, RI stands for random index,  $\lambda_{max}$  is the matrix’s primary eigenvalue, and the argument count is  $n$ . The consistency ratio (CR) value in the current study is 1.20%, or 0.012, which is less than Saaty’s 1980 upper acceptability value (0.10 for more than 4 components) (Table 9.5).

### 3.4 Weighed Overlay Model (WOM)

The weighted overlay as a model is a quick, accurate, plus straightforward tool to assessing vulnerability in flood-prone belts. For the assessment of flood vulnerability mapping in this study, eight maps depicting flood generating factor were used. It is necessary to reclassify each cell from each map layer into one shared preference

**Table 9.5** Calculated weights for key governing parameters in establishing the flood susceptible zones (FSZ)

i	j	Criteria	Which is more significant?		Scale (1 - 9)	
			A	B		
1	2	Elevation		Slope	A	1
1	3			Distance from River	A	2
1	4			Confluence	A	3
1	5			Rainfall	A	4
1	6			Geomorphology	A	4
1	7			Soil	A	5
1	8			LULC	A	6
2	3	Slope		Distance from River	A	1
2	4			Confluence	A	2
2	5			Rainfall	A	3
2	6			Geomorphology	A	3
2	7			Soil	A	4
2	8			LULC	A	5
3	4	Distance from River		Confluence	A	1
3	5			Rainfall	A	2
3	6			Geomorphology	A	2
3	7			Soil	A	3
3	8			LULC	A	4
4	5	Confluence		Rainfall	A	1
4	6			Geomorphology	A	1
4	7			Soil	A	2
4	8			LULC	A	3
5	6	Rainfall		Geomorphology	A	1
5	7			Soil	A	1
5	8			LULC	A	2
6	7	Geomorphology		Soil	A	1
6	8			LULC	A	1
7	8	Soil		LULC	A	1

Source: Prepared by authors using AHP-Excel framework by K. D. Geopel version 15.09.2018 Using AHP-Excel by K. D. Geopel version 15.09.2018

scale (Saaty’s scale) to combine these for the study. Utilizing WOM, all thematic maps were combined (Das et al., 2021; Hammami et al., 2019; Shit et al., 2016):

$$S = \frac{\sum WiSij}{\sum Wi} \tag{9.3}$$

Wi is the weight of the ith factor map, Sij is the weight of the ith spatial class of the jth factor map, and S is the value in the output map of the spatial unit.

A flood susceptibility zonation (FSZ) map was prepared by integrating these weighted factor maps in the GIS environment using weighted overlay analysis (Fig. 9.7).

### 3.5 Modeling Flood Susceptibility Zone

The Malda District's vulnerable flood zones were created by superimposing several chosen thematic layers that contribute to flood susceptibility using GIS and AHP technology (Table 9.6). Using Eq. 9.2, the weighted integration approach is utilized to identify locations that are susceptible to flooding (Bhattacharya et al., 2020; Malczewski, 1999; Muralitharan & Palanivel, 2015):

$$FSI = \sum_{w=1}^n W_j \times X_i \quad (9.4)$$

where  $m$  is the total number of theme layers employed and  $n$  signifies the total classes of thematic layers,  $W_j$  is taken into consideration like one normalized weight of the  $j$ th thematic layer, and  $X_i$  is the rank linked to the classes of the  $i$ th thematic layer. Additionally, FSI modeling was carried out using the following equation (Berhanu & Hatiye, 2020; Kumar et al., 2020; Thabile et al., 2020; Rao & Kishore, 1991):

$$\begin{aligned} FSI = & (EL_w \times EL_r) + (DR_w \times DR_r) + (SP_w \times SP_r) \\ & + (DC_w \times DC_r) + (RF_w \times RF_r) + (GM_w \times WM_r) \\ & + (SL_w \times SL_r) + (LULC_w \times LULC_r) \end{aligned} \quad (9.5)$$

where EL is elevation, DR is distance from major river, SP is slope, DC is designated as distance from the point of the confluence of the river, RF is rainfall, GM is geomorphology, SL is soil, and LULC is land use and land cover. The AHP normalized weight, and the subclass ranks are also shown by the subscripts "w" and "r" for each layer.

Using the aforementioned calculations, there are five zones of vulnerability to flooding over the whole Malda District, viz., very least susceptible zone (VLSZ), least susceptible zone (LSZ), moderate susceptible zone (MSZ), high susceptible zone (HSZ), and very high susceptible zone (VHSZ) to flood.

### 3.6 Validation of the Map of Flood Susceptibility

Model-based output should be validated with standard precession; it's a part of complete task in the field of GIS-dominated research work. Evaluating the accuracy

**Table 9.6** Assigned ranks of subclasses of each conditioning factor

Sl. no.	Conditioning factor	Subclasses	Rank
1	Elevation (in meter)	7–21	5
		21–26	4
		26–32	3
		32–39	2
		39–80	1
2	Slope (in degree)	1–1.27	5
		1.27–3.24	4
		3.24–5.64	3
		5.64–8.88	2
		8.88–35.96	1
3	Distance from major river (in meter)	0–1000	5
		1000–2000	4
		2000–3000	3
		3000–4000	2
		4000–9000	1
4	Distance from river confluence (in meter)	0–1000	5
		1000–2000	4
		2000–3000	3
		3000–4000	2
		4000–21,000	1
5	Rainfall (in millimeter)	80.90–83.33	1
		83.33–85.77	2
		85.77–88.20	3
		88.20–90.63	4
		90.63–93.07	5
6	Geomorphology	Active flood plain	5
		Embankment	1
		Older alluvial plain	5
		Older flood plain	5
		Pond	3
		River	3
		Lakes	3
		Other water bodies	3
		Younger alluvial plain	4
		River	5
7	Soil types	W014	4
		W015	4
		W016	4
		W017	3
		W019	3
		W021	3
		W024	3

(continued)

**Table 9.6** (continued)

Sl. no.	Conditioning factor	Subclasses	Rank
		W027	2
		W029	2
		W030	2
		W032	1
		W033	1
		W034	1
		W035	2
8	LULC	Water body	5
		Settlement	5
		Vegetal cover	1
		Barren land	2
		Agricultural land	3
		Marshy land	4
		Sand deposit	5

*Source:* Prepared by authors

of the output models is one of the important steps in any of the multi-criteria decision-making (MCDM) processes. The area under the curve (AUC) based on incidence data (previous floods in this study) is a well-established method for validating such MCDM models because of its straightforwardness, comprehensiveness, and fair agreement with the forecast (Pourghasemi et al., 2012; Tehrany et al., 2013;). The maximum accuracy level, baselessly, is indicated by a value of 1, under the area. An appropriate model is one that has an AUC value greater than 0.8 and is usually thought to be exceptionally accurate.

The AHP-based flood susceptibility map was separated into four groups for this investigation. Total 50 past flood-affected places were taken over the district as test locations to verify the FSM or the flood susceptibility map. The prepared flood susceptibility map and the flood inventory points were compared to compute the total flood episodes in number for each class. Under the GIS environment, the ArcSDM tool has been used to run all of the operations. Initially, a raster flood susceptibility map was used as a classification model for generating the ROC curve and AUC value, and inventory points were used as true positives in GIS contexts. The result came out as a PNG format (Fig. 9.6).

The accurate flood susceptibility mapping in the flood-prone Malda District is indicated by the high AUC value (0.847) (Das, 2020), which, if used effectively, might be used to manage, regulate, plan, and lessen the likelihood of future floods.

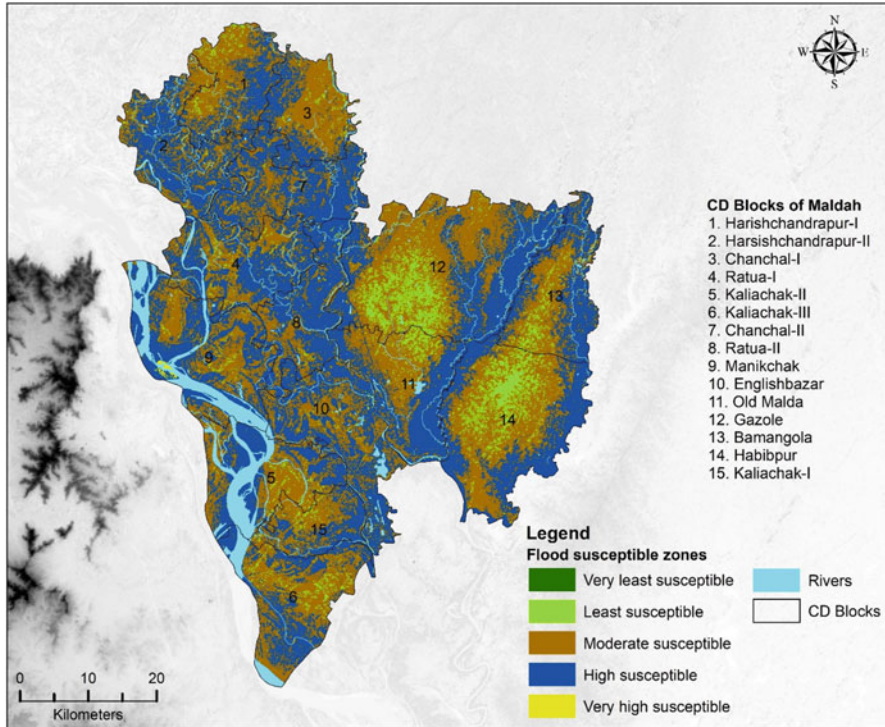


**Fig. 9.6** Analytical hierarchy process (AHP)-based flood susceptibility map of the Malda District showing flood-prone areas and administrative blocks

## 4 Results and Discussion

Assessing flood susceptibility zone (FSZ) in Malda District is represented in Fig. 9.7. There are five different flood-prone zones that make up the district’s whole geographic territory, viz., very least susceptible zone, least susceptible zone, moderate susceptible zone, high susceptible zone, and most susceptible zone in flood hazard that has derived using the MSDM-AHP semi-controlled GIS-based application. Area coverage and percentage of each class under the FSZ have been calculated and described in Table 9.7. Considering the district’s whole geographic coverage, about 0.99 ha (0.0003%) falls under the very least susceptible zone while 636.56 ha (0.17%) are recognized as very high susceptible to flood. Simultaneously, 22686.30 ha (6.19%), 172896.35 ha (47.20%), and 170105.96 ha (46.44%) surface area fall under least susceptible, moderate susceptible, and high susceptible zone in flood hazard, respectively. Based on acceptable output (with AUC = 0.847), most of the district is experiencing moderate susceptible to high susceptible circumstances.



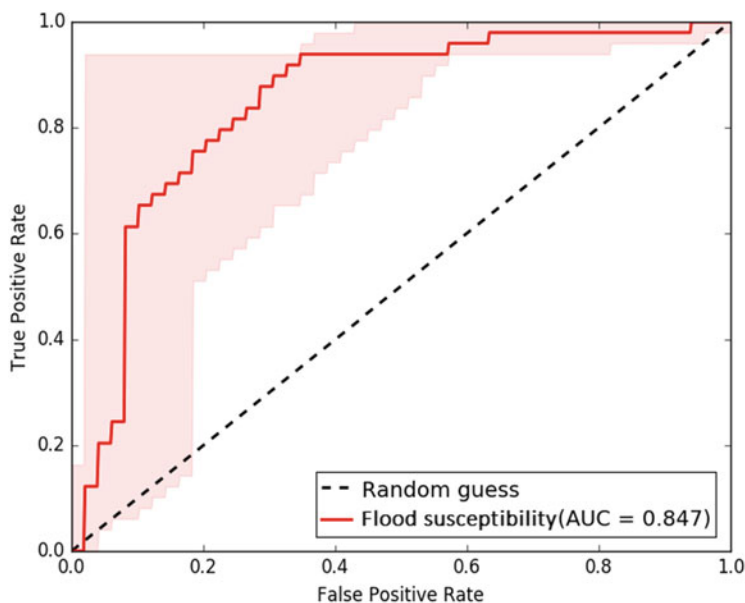


**Fig. 9.7** ROC curve and AUC value based on flood-susceptible zones. Results show a good level of satisfaction (AUC = 0.847, 84.70%), where  $n = 50$  sample points

**Table 9.7** Flood susceptibility status of Malda District

Sl. no.	Zone	Area (hectare)	Percentage
1	Very least susceptible	0.99	0.0003
2	Least susceptible	22686.30	6.19
3	Moderate susceptible	172896.35	47.20
4	High susceptible	170105.96	46.44
5	Very high susceptible	636.56	0.17

*Source:* Calculated by authors

Additionally, Table 9.8 also includes a presentation of the block-wise FSZ. The Malda District consists of 15 administrative blocks. Here, block-wise flood susceptibility status has also been analyzed. As a result, we have seen 11 blocks that are most susceptible among those blocks, where only Old Malda block is experiencing high susceptible to flood hazard with spatial coverage of 348.50 ha (1% land of the block area) in every monsoon due to closer proximity of the Mahananda and Tangon Rivers (major driving force in Malda flood catastrophe), active flood plain area, low surface elevation, and interfluvial position of the Malda (old) block. That's why the total block area (Old Malda) is categorized as least susceptible to very high susceptible. It is noteworthy that 58.97% (19053.42 ha) area of the Old-Malda block is identified as high susceptible flood zone and 38.15% (12327.53 ha) area as moderate susceptible zone. Meanwhile, all the blocks are recognized as moderate susceptible to high susceptible zones with greater spatial coverage. Based on spatial scale, the

**Table 9.8** Block wise aerial (in hectare) distribution of flood susceptibility status in Malda

Sl. no.	Block name	VLSZ	LSZ	MSZ	NMSZ	MSZ
1	Bamangola	–	1480.18	9896.88	9200.73	5.16
2	Chanchal-I	–	557.70	10612.62	5076.11	–
3	Chanchal-II	–	129.16	7698.83	12854.22	0.51
4	English bazar	–	331.08	10808.60	14166.91	91.08
5	Gazole	0.44	7086.76	27109.17	17761.75	38.95
6	Habibpur	–	6436.17	19758.66	11890.97	14.71
7	Kaliachak-I	0.12	934.73	10441.82	5814.83	–
8	Kaliachak-II	–	514.11	6373.94	4339.17	4.28
9	Kaliachak-III	0.25	723.85	10565.76	12122.97	–
10	Manikchak	0.06	1209.92	12811.05	10343.14	5.66
11	Malda (old)	–	581.15	12327.53	19053.42	348.30
12	Ratua-I	0.06	1505.30	10262.52	10856.08	41.45
13	Ratua-II	–	635.59	9765.66	12236.40	–
14	Harishchandrapur-I	–	152.68	5374.55	5374.55	70.08
15	Harishchandrapur-II	0.06	407.91	9088.76	19014.70	16.38

Source: Calculated by authors

VLSZ Very least susceptible zone, LSZ Least susceptible zone, MSZ Moderate susceptible zone, HSZ High susceptible zone, VHSZ Very high susceptible zone

following blocks, viz., Chanchal-I, Gazole, Habibpur, Kaliachak-I, Kaliachak-II, and Manikchak, are recognized as MSZ with >50% spatial coverage to individual block area. Least susceptible but not very least susceptible, all the blocks came under this category with spatial coverage <8% (except Gazole and Habibpur) geographical area. Here, have also been distinguished six blocks namely Chanchal-II (12854.22 ha), English bazar (14166.91 ha), Kaliachak-III (12122.97 ha), Old Malda (19053.42 ha), Ratua-II (12236.40 ha), and Harishchandrapur-II (19014.70 ha) with spatial coverage >50% area fall in the NMSZ group. Based on spatial coverage, only six blocks, i.e., Gazole, Kaliachak-I, Kaliachak-III, Manikchak, Ratua-I, and Harishchandrapur-II, have small unit of very least susceptible area due to high topographic elevation, distant position from river, higher slope angle, and being a part of old alluvial plain. Results of this study clearly shown Malda is a flood prone district in West Bengal. There are some favorable environments, which help to create Malda flood in every year.

#### 4.1 Location Factor

Malda being located along the outlets of the Ganga–Brahmaputra drainage system is geographically handicapped to the fact of immense discharge volume through the Ganga system. These two river systems enter the sub-Himalayan North Bengal plains through a 200 km Rajmahal-Meghalaya gap (Rudra, 1987). It is thought that through this gap, two mighty rivers discharge no less than  $1062.26 \times 10^9$  cubic

m of water annually. The annual sediment load is estimated to be  $167\text{--}175 \times 10^6$  tons (Rudra, 2000). Not only this trunk flow of discharge of about 80% passes through the channel during the months of July to September. The situation becomes alarming when an uninterrupted rainfall ( $>300$  mm) in the upstream areas of Bihar and Uttar Pradesh can produce huge discharge overburden in the lower reaches during further debouchments. Thus, the consequence is an inevitable flood event in the lower reach. On the other hand, Malda is such a place, which is comparatively nearer to the junctions of all North Bengal Rivers, Rivers of Nepal. Malda is also facing the molding of direction of the Ganga channel system from an east-west to more southwest direction, which results in tremendous shearing stress on banks and consequent flood.

## ***4.2 Breaching of Embankment***

Over the years 1971–2001, the river has been gradually shifting toward the left bank (Malda side), i.e., upstream of the barrage. Both the districts of Malda and Murshidabad are subjected to devastating erosion (Banerjee, 1999). Particularly excessive erosional phases and bank-side land failures of Ganga River compelled the newly constructed fifth retired embankment to be breached concurrently, which became the triggering factor of 1998 flood occurrence of Malda.

## ***4.3 Inability of River Systems Vis-À-Vis Human Impact***

From the geographical point of view, the abrupt fall of the river from the precipitous hill to plains and resultant decline of slope compel the rivers to deposit the sediment load on the bed.

Ganga, Mahananda, Fulahar, etc. are having siltation problems, which causes reduction of the cross-sectional area and thereby water holding capacity of the rivers. For example, near Panchanandapur, the Ganga is about 8.5–10 km of width and hydraulic average depth of 12.0–13.5 m, which is 2.6 km only near Barrage. Due to siltation about 54 bays of Farakka Barrage, out of 109 numbers of bays had become totally inactive. So, among the right side, 54 bays facilitate to accumulate about 65 cumecs of water through vertical passage of each of the bays. The feeder canal only allows 1120 cumecs of water to pass in the rainy season.

Most of the rivers like Kalindi, Chota Bhagirathi, and Pagla are decaying and over-silted, due course of time and are mostly unable to hold water during floods for which out flash is a general character of the rivers.

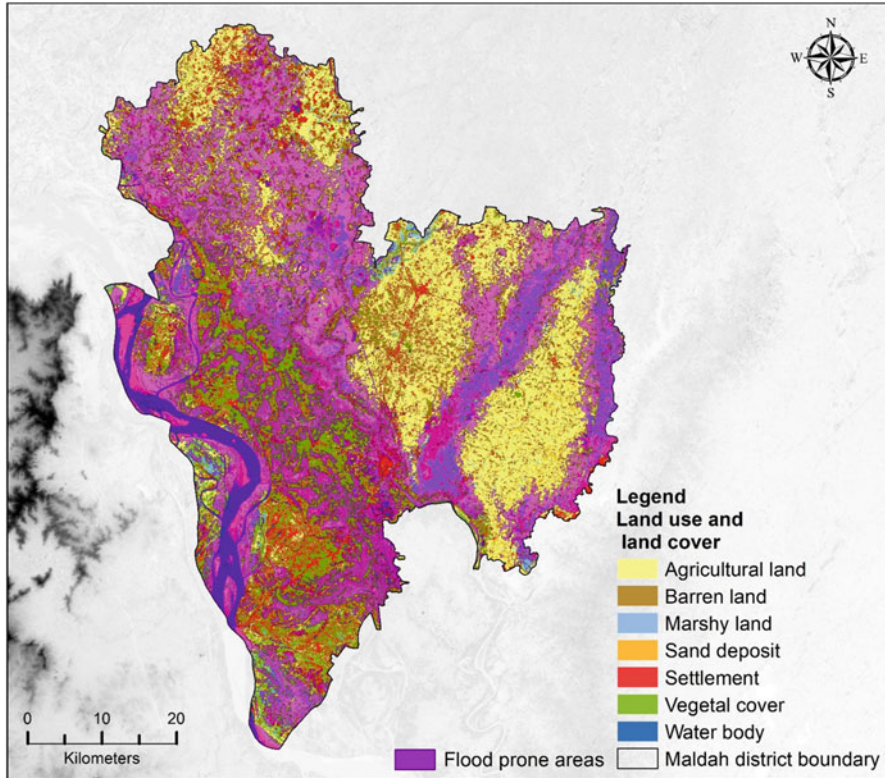


**Fig. 9.8** Flood prone areas of Malda District: land use and land cover classes under the risk of flood vulnerability

Irregular embankment and spur building is a continuously long-run process in the western part of the district creating artificial depressions over the land, and pocket inundations along the marginal and transverse spurs is also noticeable in the district.

In this present research, seven categories of LULC classes have been identified, and about 47.11% of the total area is under the threat of flood risk every year. For identifying the flood-prone areas, two categories under the flood susceptible zones, viz., high susceptible and very high susceptible zones, have been merged (Fig. 9.8). Using the GIS tool, it is estimated that 595.95 km<sup>2</sup> area of agricultural land possess under the flood risk, where 161.51 km<sup>2</sup> of barren land, 171.28 km<sup>2</sup> of marshy land, 48.59 km<sup>2</sup> of newer alluvial tracts (sand depositions), 347.79 km<sup>2</sup> of vegetal cover especially the mango orchards, and 275.12 km<sup>2</sup> areas of settled areas are lying under the vulnerable situation due to flood. Most of the areas affected by flood, flood water logging, and inundation in the low-lying areas are very often a problem of the district faced by the local inhabitants. From the field survey, it is observed that 15–30 days were taken to get out of this water logging problem in the flood regions, and almost 1744.95 km<sup>2</sup> of the total area of the district is estimated as flood prone.

## 5 Conclusion

Flood-sensitive zonation is a highly helpful tool that aids planners and decision-makers in creating an effective management strategy to lessen the potentially dangerous effects of flooding. Malda District consists of active alluvial floodplain in Diara, boggy, and marshy lands in the Tal and the older floodplain in the Barind region, and the district is basically sloping toward north to south direction favorable for inundation in every monsoonal month almost in every year. Most of the rivers are perennial in nature and very much susceptible to flood as the elevation is lower than the surroundings, i.e., Rajmahal Hill in the western side and the elevated Barind Tract in the eastern side. Multi-criteria AHP model is based on mathematical algorithms under remote sensing and GIS environs, and it is a sound alternative to identify the flood susceptibility zones in Malda District of West Bengal, India. For the evaluation, eight primary criteria have been selected based on their relative level of influence and the proximity causing flood situation. Every criterion was assigned by an authentic weight after the results from the decision matrix of AHP calculation. So, Saaty's AHP model with GIS techniques has helped to identify and ranked five flood-susceptible zones in the study area from very high susceptibility to very least susceptibility. The study insights a useful flood zone mapping of the study area using the most appropriate parameters under GIS platform and most of the susceptible areas were undergone flooding during the years 2017 and 2019. So, this study may be helpful to the stakeholders and planners to make some alternatives at the alarming situation to resist the harsh effect of the catastrophic event of flood. Integration of MCDM based on other approaches with this study may be useful for future research in this study area.

**Acknowledgments** The authors sincerely offer their appreciation to DSTBT, Government of West Bengal, for funding the Research Project and to carry the fieldwork as the present academic paper is partially related with the expected outcome of the ongoing research project. They are also in debt to the Department of Geography and Applied Geography, University of North Bengal, for continuous support. Further, they want to thank Mr. Sujoy Kumar Malo and Mr. Saidur Rahaman for their unconditional help during the field.

**Conflict of Interest** The authors are not associated in any way with any conflict of interest (s).

## References

- Andrew, T., Luca, V., Montserrat, M. F., Brian, D. (2018). *Inform global risk index*. <https://doi.org/10.2760/754353>
- Archer, D. R., & Fowler, H. J. (2018). Characterising flash flood response to intense rainfall and impacts using historical information and gauged data in Britain. *Journal of Flood Risk Management*, 11, S121–S133. <https://doi.org/10.1111/jfr3.12187>
- Aydin, S., & Uysal, S. (2014). Risk assessment of coastal erosion of Karasu coast in Black Sea. *Journal of Coastal Conservation*, 18, 673–682. <https://doi.org/10.1007/s11852-014-0343-y>

- Banerjee, M. (1999). A report on the impact of Farakka Barrage on the human fabric: a study of the upstream and downstream areas of Farakka Barrage. South Asia Network On Dams, Rivers and People, New Delhi, 1–29.
- Barman, N. K., Chatterjee, S., & Paul, A. K. (2016). Estimate the coastal vulnerability in the Balasore Coast of India: A statistical approach. *Earth Systems and Environment Model*, 2(1), 1–10. <https://doi.org/10.1007/s40808-015-0074-6>
- Beniston, M. (2009). Trends in joint quantiles of temperature and precipitation in Europe since 1901 and projected for 2100. *Geophysical Research Letter*, 36(7). <https://doi.org/10.1029/2008GL037119>.
- Benjmel, K., Amraoui, F., Boutaleb, S., Ouchchen, M., Tahiri, A., & Touab, A. (2020). Mapping of groundwater potential zones in crystalline terrain using remote sensing, GIS techniques, and multicriteria data analysis (case of the Ighrem region, Western Anti-Atlas, Morocco). *Water*. <https://doi.org/10.3390/w12020471>
- Berhanu, K. G., & Hatiye, S. D. (2020). Identification of groundwater potential zones using proxy data: Case study of Megech watershed, Ethiopia. *Journal of Hydrology: Regional Studies*, 28, 100676. <https://doi.org/10.1016/j.ejrh.2020.100676>
- Bhattacharya, R., Chatterjee, N. D., & Das, K. (2020). An integrated GIS approach to analyze the impact of land use change and land cover alteration on ground water potential level: A study in Kangsabati Basin, India. *Groundwater for Sustainable Development*. <https://doi.org/10.1016/j.gsd.2020.100399>
- Bouilloud, L., Delrieu, G., Boudevillain, B., & Kirstetter, P. E. (2010). Radar rainfall estimation in the context of post-event analysis of flash-flood events. *Journal of Hydrology*, 394(1–2), 17–27.
- Carter, M. O. (1935). *Final Report on the Survey and Settlement Operations in the District of Malda*. (pp. 2–32). Bengal Government Press.
- Carter, W. N. (2008). *Disaster management: A disaster manager's handbook*.
- Dandapat, K., & Panda, G. K. (2017). Flood hazard assessment at block level and its management strategy in Paschim Medinipur District, West Bengal, India. *IOSR Journal of Humanities and Social Science*, 22(6), 7–14.
- Das, S. (2020). Flood susceptibility mapping of the Western Ghat coastal belt using multi-source geospatial data and analytical hierarchy process (AHP). *Remote Sensing Applications: Society and Environment*, 20, 100379. <https://doi.org/10.1016/j.rsase.2020.100379>
- Das, M., Parveen, T., Ghosh, D., & Alam, J. (2021). Assessing groundwater status and human perception in drought-prone areas: A case of Bankura-I and Bankura-II blocks, West Bengal (India). *Environmental Earth Sciences*, 80(18), 1–23. <https://doi.org/10.1007/s12665-021-09909-8>
- Fernandez, D. S., & Lutz, M. A. (2010). Urban flood hazard zoning in Tucumán Province, Argentina, using GIS and multicriteria decision analysis. *Engineering Geology*, 111(1–4), 90–98. <https://doi.org/10.1016/j.enggeo.2009.12.006>
- Field Investigation (2019). This is not actually a citation and has been modified into a new form.
- Ghosh, A., & Kar, S. K. (2018). Application of analytical hierarchy process (AHP) for flood risk assessment: A case study in Malda district of West Bengal, India. *Natural Hazards*, 94(1), 349–368. <https://doi.org/10.1007/s11069-018-3392-y>
- Ghosh, A., Mandal, M., Banerjee, M., & Karmakar, M. (2020). Impact of hydro-geological environment on availability of groundwater using Analytical Hierarchy Process (AHP) and geospatial techniques: A study from the upper Kangsabati river basin. *Groundwater for Sustainable Development*. <https://doi.org/10.1016/j.gsd.2020.100419>
- Gourav, P., Kumar, R., Gupta, A., & Arif, M. (2020). Flood hazard zonation of Bhagirathi river basin using multi-criteria decision-analysis in Uttarakhand, India. *International Journal of Emerging Technologies*, 11(1), 62–71.
- Hammami, S., Zouhri, L., Souissi, D., Souei, A., Zghibi, A., Marzougui, A., & Dlala, M. (2019). Application of the GIS based multi-criteria decision analysis and analytical hierarchy process (AHP) in the flood susceptibility mapping (Tunisia). *Arabian Journal of Geosciences*, 12(21), 1–16. <https://doi.org/10.1007/s12517-019-4754-9>

- Islam, N., & Dharanirajan, K. (2017). Flood impact assessment in Murshidabad District of West Bengal using remote sensing and GIS. *International Journal of Remote Sensing GIS*, 5(1), 48–57.
- Ismail, M. D., & Mustaqim, M. D. (2013). Socio-economic status of population in flood prone areas of Chanchal sub-division in Malda district, West Bengal. *International Journal of Research in Applied, Natural and Social Sciences*, 1(3), 141–152.
- Kia, M. B., Pirasteh, S., Pradhan, B., Mahmud, A. R., Sulaiman, W. N. A., & Moradi, A. (2012). An artificial neural network model for flood simulation using GIS: Johor River Basin, Malaysia. *Environmental Earth Sciences*, 67(1), 251–264. <https://doi.org/10.1007/s12665-011-1504-z>
- Kiker, G. A., Bridges, T. S., Varghese, A., Seager, T. P., & Linkov, I. (2005). Application of multicriteria decision analysis in environmental decision making. *Integrated Environmental Assessment and Management*, 2, 95–108. [https://doi.org/10.1897/IEAM\\_2004a-015.1](https://doi.org/10.1897/IEAM_2004a-015.1)
- Kim, S., Lee, W., Shin, K., Kafatos, M., Seo, D. & Kwak, H. (2011). Comparison of spatial interpolation techniques for predicting climate factors in Korea. *Forest Science and Technology*. <https://doi.org/10.1080/21580103.2010.9671977>
- Kireeva, M. B., Frolova, N. L., Rets, E. P., Telegina, E. A., Telegina, A. A., & Ezerova, N. N. (2015). The role of seasonal and occasional floods in the origin of extreme hydrological events. *Proceedings of the International Association of Hydrological Sciences*, 369, 109–113. <https://doi.org/10.5194/piahs-369-109-2015>
- Komolafe, A. A., Herath, S., & Avtar, R. (2018). Methodology to assess potential flood damages in urban areas under the influence of climate change. *Natural Hazards Reviews*, 19, 05018001.
- Kumar, V. A., Mondal, N. C., & Ahmed, S. (2020). Identification of groundwater potential zones using RS, GIS and AHP techniques: A case study in a part of Deccan Volcanic Province (DVP), Maharashtra, India. *Journal of the Indian Society of Remote Sensing*, 48(3), 497–511. <https://doi.org/10.1007/s12524-019-01086-3>
- Lambourn, G. E. (1918). *Bengal District Gazetteers: Malda District*. N.L Publishers (The Bengal Secretariat Book Depot.), 1st Reprint (2003). (pp. 1–7, 58–59, 61, and 68). ISBN-81-86860-21-5.
- Lee, G., Chung, E. S., & Jun, K. S. (2013). MCDM approach for flood vulnerability assessment using TOPSIS method with  $\alpha$  cut level sets. *Journal of Korea Water Resources Association*, 46(10), 977–987. <https://doi.org/10.3741/JKWRA.2013.46.10.977>
- Ly, S., Charles, C., & Degré, A. (2013). Different methods for spatial interpolation of rainfall data for operational hydrology and hydrological modeling at watershed scale. A review. *Biotechnology, Agronomy and Society and Environment*, 17(2), 392–406.
- Magesh, N. S., Chandrasekar, N., & Soundranayagam, J. P. (2012). Delineation of groundwater potential zones in Theni district, Tamil Nadu, using remote sensing, GIS and MIF techniques. *Geoscience Frontiers*, 3(2), 189–196. <https://doi.org/10.1016/j.gsf.2011.10.007>
- Malczewski, J. (1999). *GIS and multicriteria decision analysis*. Wiley.
- Masood, M., & Takeuchi, K. (2012). Assessment of flood hazard, vulnerability and risk of mid-eastern Dhaka using DEM and 1D hydrodynamic model. *Natural Hazards*, 61, 757–770. <https://doi.org/10.1007/s11069-011-0060-x>
- Mazumdar, S. K. (2000). Role of Farakka Barrage on the disastrous flood at Malda (West Bengal) in 1998. In Role of drainage and challenges in 21st century. Vol. II. Proceedings of the Eighth ICID International Drainage Workshop, New Delhi, India, 31 January–4 February 2000. (pp. 103–112). International Commission on Irrigation and Drainage.
- Mazumder, S. K. (2004). Role of Farakka barrage on the disastrous 1998 flood in Malda (West Bengal). In *The Ganges water diversion: Environmental effects and implications* (pp. 39–48). Springer. [https://doi.org/10.1007/1-4020-2480-0\\_3](https://doi.org/10.1007/1-4020-2480-0_3)
- Mehabub, S., Raihan, A., Nuhul, H., & Haroon, S. (2015). Assessing flood inundation extent and landscape vulnerability to flood using geospatial technology: A study of Malda district of West Bengal, India. In *Forum geografic* (Vol. 14, No. 2, p. 156). University of Craiova, Department of Geography. <https://doi.org/10.5775/fg.2067-4635.2015.144.d>

- Mishra, D., & Satapathy, S. (2020). MCDM approach for mitigation of flooding risks in Odisha (India) based on information retrieval. *International Journal of Cognitive Informatics and Natural Intelligence (IJCINI)*, 14(2), 77–91. <https://doi.org/10.4018/IJCINI.2020040105>
- Mojaddadi, H., Pradhan, B., Nampak, H., Ahmad, N., & Ghazali, A. H. B. (2017). Ensemble machine-learning-based geospatial approach for flood risk assessment using multi-sensor remote-sensing data and GIS. *Geomatics, Natural Hazards and Risk*, 8(2), 1080–1102. <https://doi.org/10.1080/19475705.2017.1294113>
- Mondal, S., & Maiti, R. (2013). Integrating the analytical hierarchy process (AHP) and the frequency ratio (FR) model in landslide susceptibility mapping of Shiv-khola watershed, Darjeeling Himalaya. *International Journal of Disaster Risk Science*, 4(4), 200–212. <https://doi.org/10.1007/s13753-013-0021-y>
- Mukherjee, K., Pal, S., & Mukhopadhyay, M. (2018). Impact of flood and seasonality on wetland changing trends in the Diara region of West Bengal, India. *Spatial Information Research*, 26(4), 357–367. <https://doi.org/10.1007/s41324-018-0177-z>
- Muralitharan, J., & Palanivel, K. (2015). Groundwater targeting using remote sensing, geographical information system and analytical hierarchy process method in hard rock aquifer system, Karur district, Tamil Nadu, India. *Earth Science Informatics*, 8(4), 827–842. <https://doi.org/10.1007/s12145-015-0213-7>
- Murmu, P., Kumar, M., Lal, D., Sonkerb, I., & Singh, S. K. (2019). Delineation of groundwater potential zones using geospatial techniques and analytical hierarchy process in Dumka district, Jharkhand, India. *Groundwater for Sustainable Development*. <https://doi.org/10.1016/j.gsd.2019.100239>
- Pandey, R., & Jha, S. (2012). Climate vulnerability index-measure of climate change vulnerability to communities: a case of rural Lower Himalaya, India. *Mitigation and Adaptation Strategies for Global Change*, 17(5), 487–506.
- Pham, B. T., Avand, M., Janizadeh, S., Phong, T. V., Al-Ansari, N., Ho, L. S., Das, S., Le, H. V., Amini, A., Bozchaloei, S. K., Jafari, F., & Prakash, I. (2020). GIS based hybrid computational approaches for flash flood susceptibility assessment. *Water*, 12, 683. <https://doi.org/10.3390/w12030683>
- Pourghasemi, H. R., Mohammady, M., & Pradhan, B. (2012). Landslide susceptibility mapping using index of entropy and conditional probability models in GIS: Safarood Basin, Iran. *Catena*, 97, 71–84. <https://doi.org/10.1016/j.catena.2012.05.005>
- Pradhan, B. (2010). Flood susceptible mapping and risk area delineation using logistic regression, GIS and remote sensing. *Journal of Spatial Hydrology*, 9(2), 1–18.
- Pramanik, M. K. (2016). Site suitability analysis for agricultural land use of Darjeeling district using AHP and GIS techniques. *Earth Systems and Environment*. <https://doi.org/10.1007/s40808-016-0116-8>
- Predick, K. I., Gergel, S. E., & Turner, M. G. (2009). Effect of flood regime on tree growth in the floodplain and surrounding uplands of the Wisconsin River. *River Research and Applications*, 25(3), 283–296. <https://doi.org/10.1002/rra.1156>
- Rao, B. V., & Briz-Kishore, B. H. (1991). A methodology for locating potential aquifers in a typical semi-arid region in India using resistivity and hydrogeologic parameters. *Geoexploration*, 27(1–2), 55–64. [https://doi.org/10.1016/0016-7142\(91\)90014-4](https://doi.org/10.1016/0016-7142(91)90014-4)
- Roca, M., Martín-Vide, J. P., & Moreta, P. J. M. (2009). Modelling a torrential event in a river confluence. *Journal of Hydrology*, 364(3–4), 207–215. <https://doi.org/10.1016/j.jhydrol.2008.10.020>
- Rudra, K. (1987). Quaternary history of the lower Ganga distributaries. *Geographical Review of India*, 49(3), 38–48.
- Rudra, K. (2000). Living on the edge: the experience along the bank of the Ganga in Malda district, West Bengal. *Indian Journal of Geography & Environment*, 5, 57–67.
- Saaty, T. L. (1980). *The analytic hierarchy process: Planning, priority setting, resource allocation*. McGraw-Hill International Book.



- Samad, A. (2005). *Jella Maldaher Itihas O Malda Samagra, 1st part I* (pp. 3, 4–5, 7, 24–31). T.A Printers.
- Samanta, S., Koloa, C., Kumar Pal, D., & Palsamanta, B. (2016). Flood risk analysis in lower part of Markham River based on multi-criteria decision approach (MCDA). *Hydrology*, 3, 29. <https://doi.org/10.3390/hydrology3030029>
- Sanyal, J., & Lu, X. X. (2005). Remote sensing and GIS-based flood vulnerability assessment of human settlements: A case study of Gangetic West Bengal, India. *Hydrological Processes*, 19, 3699–3716. <https://doi.org/10.1002/hyp.5852>
- Sarkar, D., & Mondal, P. (2020). Flood vulnerability mapping using frequency ratio (FR) model: A case study on Kulik river basin, Indo-Bangladesh Barind region. *Applied Water Science*, 10(1), 1–13. <https://doi.org/10.1007/s13201-019-1102-x>
- Sener, S., Sener, E., & Karagüzel, R. (2011). Solid waste disposal site selection with GIS and AHP methodology: A case study in SenirkentUluborlu (Isparta) Basin, Turkey. *Environ Monit Assess*, 173(1–4), 533–554. <https://doi.org/10.1007/s10661-010-1403-x>
- Shit, P. K., Bhunia, G. S., & Maiti, R. (2016). Potential landslide susceptibility mapping using weighted overlay model (WOM). *Modeling Earth Systems and Environment*, 2(1), 21. <https://doi.org/10.1007/s40808-016-0078-x>
- Singh, O., & Kumar, M. (2017). Flood occurrences, damages, and management challenges in India: A geographical perspective. *Arabian Journal of Geosciences*, 10(5), 102. <https://doi.org/10.1007/s12517-017-2895-2>
- Sinha, R., Jain, V., Tandon, S. K., & Chakraborty, T. (2012). Large river systems of India. *Proceedings of the Indian National Science Academy*, 78, 277–294.
- Syvitski, J. P., Overeem, I., Brakenridge, G. R., & Hannon, M. (2012). Floods, floodplains, delta plains—A satellite imaging approach. *Sedimentary Geology*, 267, 1–14. <https://doi.org/10.1016/j.sedgeo.2012.05.014>
- Tehrany, M. S., Pradhan, B., & Jebur, M. N. (2013). Spatial prediction of flood susceptible areas using rule based decision tree (DT) and a novel ensemble bivariate and multivariate statistical models in GIS. *Journal of Hydrology*, 504, 69–79. <https://doi.org/10.1016/j.jhydrol.2013.09.034>
- Thabile, G., Das, D. M., & Raul, S. K. (2020). Assessment of groundwater potential in the Kalahandi district of Odisha (India) using remote sensing, geographic information system and analytical hierarchy process. *Journal of the Indian Society of Remote Sensing*, 48, 1755. <https://doi.org/10.1007/s12524-020-01247-9>
- Tripathi, P. (2015). Flood disaster in India: An analysis of trend and preparedness. *Interdisciplinary Journal of Contemporary Research*, 2(4), 91–98.
- Vignesh, K. S., Anandakumar, I., Ranjan, R., & Borah, D. (2021). Flood vulnerability assessment using an integrated approach of multi-criteria decision-making model and geospatial techniques. *Modeling Earth Systems and Environment*, 7(2), 767–781. <https://doi.org/10.1007/s40808-020-00997-2>
- Yalcin, A., Reis, S., Cagdasoglu, A., & Yomralioglu, T. (2011). A GIS-based comparative study of frequency ratio, analytical hierarchical process, bivariate statistics and logistic regression methods for landslide susceptibility mapping in Trabzon, NE Turkey. *Catena*, 85, 274–228. <https://doi.org/10.1016/j.catena.2011.01.014>
- Zhang, Y., & Smith, J. A. (2003). Space–time variability of rainfall and extreme flood response in the Menomonee River basin, Wisconsin. *Journal of Hydrometeorology*, 4(3), 506–517.

# Chapter 10

## Agrarian and Socio-Infrastructural Vulnerability in the Wake of Flood: An Example from the Mayurakshi River Basin, India



Aznarul Islam , Susmita Ghosh, Mohan Sarkar, Suman Deb Barman, Pravat Kumar Shit, and Abdur Rahman

**Abstract** The present work intends to portray the impact of the flood on the agrarian decline and socio-infrastructural vulnerability in a tropical river basin like the Mayurakshi River Basin (MRB), India. The study has been carried out based on the questionnaire survey of over 2366 households spreading over 43 villages and two municipality wards across the five community development (C.D.) blocks coupled with some secondary data (annual flood reports, district census reports, topographical maps, and satellite images). The flood magnitude has been portrayed in terms of flood frequency, depth, duration, and inundation over MRB while the agricultural and socio-infrastructural vulnerability is measured using cropping intensity, crop diversification index, and relative importance index. The results portray that during the last 20 years (1998–2017), the average flood frequency ranged from 9 to 12 times and flood depth on agricultural land varied from 1.89 to 3.72 m and average flood duration ranged from 15 to 40 days. The severity of floods wrecks havoc on the agrarian economy reducing the cropping intensity and crop diversity of the study regions especially those located in low-lying areas like Kandi. Thus, flood triggers seasonal unemployment in these areas acting as the catalyst for labor migration mainly in the Middle East countries. Besides, infrastructural vulnerabilities like the collapse of the kutchha houses, and rural muddy roads are notable. More than 90% of

---

A. Islam (✉) · S. Ghosh

Department of Geography, Aliah University, Kolkata, West Bengal, India

M. Sarkar

Department of Geography, Visva-Bharati, Santiniketan, West Bengal, India

S. D. Barman

Independent Researcher, Barasat, Kolkata, India

P. K. Shit

PG Department of Geography, Raja N. L. Khan Women's College (Autonomous), Midnapore, West Bengal, India

A. Rahman

Department of Geography, Dr. Kanailal Bhattacharyya College, Howrah, West Bengal, India

people were affected with diarrhea during floods due to the intake of contaminated flood water. Furthermore, skin diseases are also common in the flood and post-flood periods of the study area. Regarding psychological health, the C.D. block Kandi demonstrates that the higher flood-prone block has the lowest phobia as flood is very common in the region but maximum shock due to the huge agricultural loss.

**Keywords** Riverine floods · Infrastructural vulnerability · Agrarian economy · Health issues · Social psychological problems

## 1 Introduction

Vulnerability is determined based on people's exposure to natural hazards and their level of social development. Recently, it has been advocated that strengthening local communities is a more efficient approach to minimizing vulnerability than creating infrastructure (Birkmann et al., 2011; Chinnasamy et al., 2021; Islam & Sarkar, 2020; Perdikaris, 2010; Wisner et al., 1994). Identifying a community's strengths and weaknesses in terms of knowledge distribution, social allocation, and welfare programs are central to the vulnerability assessment (Bhowmick, 2015; Wisner et al., 1994). Therefore, vulnerability is defined as "the characteristics of a person or group in terms of their capacity to anticipate, cope with, resist and recover from the impact of a natural hazard" (Wisner et al., 1994). This includes both the social and physical dimensions of a system (Vittal & Karmakar, 2019). The recent definition of vulnerability proposed by the Intergovernmental Panel on Climate Change (IPCC, 2014) includes climate variability and climate change in the definition and has given a broader perspective synergizing the recent issues related to climate change, variability, and also societal variables. However, the inclusion of social parameters in assessing vulnerability was first taken into consideration in the twentieth century. Before that, natural phenomena were considered the main factor for vulnerability assessment (Rufat et al., 2015).

Perdikaris (2010) classified vulnerability into five categories, viz., monetary vulnerability, economic vulnerability, social vulnerability, environmental vulnerability, and critical infrastructure vulnerability. Being one of the common measures of vulnerability, social vulnerability considers exposure to a natural system, demographic profile, household characteristics, education, and health status to calculate the final index (Karmakar et al., 2010; Laura et al., 2020; Vittal et al., 2020). The application of social vulnerability has been used extensively in Himalayan and sub-Himalayan regions (Dasgupta & Badola, 2020), coastal regions (Ahammed & Pandey, 2019; Gayen et al., 2022; Sahana et al., 2019), arid regions (Kar et al., 2018; Khetwani & Singh, 2020; Steinbach et al., 2016), and riverine floodplain region (Islam & Guchhait, 2015; Islam et al., 2016) of India and at national level (Karmakar et al., 2010; Vittal & Karmakar, 2019) as well. Improvement of socioeconomic indicators of local communities is emerging in India and reducing vulnerability (Karmakar et al., 2010). On the other hand, the increasing population density and unplanned growth of cities are acting in opposite directions.

Identification, measurement, and assessing the condition of the infrastructure of a region help to cope with adverse natural hazards that increase resilience and help to take proactive measures for risk management in a flood-affected region (Pant et al., 2016). Still, no clear definition of infrastructure has been made by the Government of India (GoI), but the national statistical commission in 2001 included railway, roads, bridges, airports, electricity, telecommunication networks, and pipelines for water, oil, canal, and sewage in the first stage of infrastructure. The infrastructure is identified as critical in the highly vulnerable region (Len et al., 2018; Pant et al., 2016). In other words, the regions with a high level of vulnerability and the infrastructure are the safeguards against natural hazards and destruction, which will fail the community to cope with the hazards. The issue has gained attention in recent times, and focus is being directed to supporting climate-resilient infrastructure (TERI, 2010) because it has been found that infrastructure development has a major role in reducing community vulnerability (Vittal et al., 2020). Notwithstanding, the construction of the infrastructures like the hospital, school, rehabilitation center, and roads should be on an elevated or dry-point area. Moreover, motor-boat facilities during flood and technological advancement may reduce rural people's vulnerability (Kumar et al., 2016).

IPCC (2021) stated about the changing climate due to anthropogenic stressors and is also concerned about the increasing community vulnerability. The marginalized, the poor, farmers, and fishing communities will be the most affected due to frequent natural hazards and disasters (Chinnasamy & Srivastava, 2021). Therefore, to gauge the vulnerability level, a divisive approach to natural hazards and social factors should be avoided because separating social aspects will generate an extra burden on natural hazards in assessing vulnerability (Birkmann et al., 2022). Flood has been considered one of the major natural hazards highly affecting livelihoods. Opinions of communities and researchers regarding the role of floods in shaping society and the economy have shifted from optimism to pessimism after floods started costing lives and wealth due to interventions by structural controls in the fluvial system (Mukhopadhyay & Let, 2014; Mukhopadhyay, 2010). The frequency of floods has increased in recent decades worldwide (Svetlana et al., 2015). In the vulnerability assessment framework, exposure, sensitivity, and coping capacity are the three major indices among which flooding due to proximity to the channel comes under biophysical characteristics and is considered as exposure (Porter et al., 2021). Previous studies demonstrate that floods have widespread effects on the economy, education, gender, and health and also control psychological behavior in the form of trauma (Gayen et al., 2022; Rufat et al., 2015). Since agricultural activities are concentrated in floodplain regions, the most affected economy is agriculture. Long-duration floods with high velocity have a large impact on crop damage (Wang et al., 2022). Coastal floods around the world also affect agricultural production due to the accumulation of salt in the land that causing economic loss to the farmers as lands are noncultivable for a long time (Gould et al., 2019). The effects of natural hazards on mental health can be direct or indirect, and prolonged exposure to a certain natural hazard may lead to mental block, posttraumatic stress disorder (PTSD), and traumatization (Cianconi et al., 2020). This aspect of natural hazards

needs a comprehensive study considering mental health as an important aspect of life.

India is severely affected by flood events almost every year, and the state of West Bengal, being located in the Ganga–Brahmaputra–Meghna Delt, portrays a higher severity of floods. Due to diversified physiographic conditions, West Bengal faces different types of floods in different regions. For example, the Himalayan and sub-Himalayan region faces flash flood (Chakraborty & Mukhopadhyay, 2015a, b; Gayen et al., 2022) while the western part is characterized by nontidal fluvial flood (Ghosh & Mistri, 2015) and the coastal part is affected of tidal floods (Bandyopadhyay et al., 2014; Rudra, 2014, 2018). Teesta, Torsa, Jaldhaka, Raidak in North Bengal and Pagla-Bansaloi, Dwarka-Brahmani, Mayurakshi-Babla, and Ajay in South Bengal are responsible for making 42.55% of the landmass, and 18 out of 23 districts are susceptible to flood events in West Bengal (Irrigation and waterways directorate, 2019). The Mayurakshi River Basin is a part of the Rarh Bengal that suffers from severe floods (irrigation and waterways directorate, 2014; Jha & Bairagya, 2013; Mukhopadhyay & Let, 2014; Roy, 2012). The average flood frequency in the last 20 years was measured as 9–12 times (Islam & Ghosh, 2021b). The major studies conducted in the region focused on geohydrometeorological effects on flood occurrence (Islam et al., 2022; Islam & Deb, 2020; Islam & Sarkar, 2020), and the other studies focus on the identification of the main drivers of flood risk emphasizing on community-based flood risk assessment (Islam & Ghosh, 2021a) and the economic transformation of the local communities induced by flood events (Islam & Ghosh, 2021b). Previous studies also show that developing countries need more studies related to rural floods, and more focus should be given to site-specific vulnerability assessment (Rehman et al., 2019). The Mayurakshi River Basin lacks studies related to social and infrastructural vulnerability with regard to flood events. Along with social factors, the assessment of infrastructure at risk will help the policymakers with long-term development plans by identifying the most crucial infrastructure for the local communities in the region. The present study aims to bridge the gaps identified in the existing literature and will focus on the issues such as: (1) to find out the nature of flood hazards in the study area, (2) to trace out the nature of agrarian decline due to flood hazards, and (3) to relate floods with the education and health and other infrastructural issues of the concerned areas.

## 2 Study Area

The Mayurakshi River travels 250 km from its source at Trikut Hill in Deoghar, Jharkhand, and is meeting with the Bhagirathi River at Narayanpur. The Mayurakshi Basin extends from 23°37'43" to 24°37'36"N and from 86°50'16" to 88°15'52"E, covering an area of 9596 km<sup>2</sup>. Nabagram, Khargram, Kandi, Burwan, and Bharatpur-I are the five C.D. blocks of Murshidabad Districts that make up the lower portion of the Mayurakshi River. Of the five C.D. blocks, Kandi is the most susceptible area to flooding (Mollah, 2016; Islam & Ghosh, 2021a). The region is

inundated every year by floods. For the present study, two municipality wards (Wards no. 8 and 13) and 43 villages have been selected using purposive sampling after conducting a pilot survey (Fig. 10.1).

The research location is situated in the Murshidabad district's *Rarh* plain, where the Mayurakshi–Dwarka and kuea River systems frequently cause flooding. Due to the feeble slope, the lower Mayurakshi River Basin has drainage congestion and regular floods (Islam & Ghosh, 2021b). Mayurakshi, Dwarka, Brahmani, and kuea are the main rivers to drain the water from the C.D block Kandi. Moreover, numerous spill channels and impoundments are spread over the region. The usual geographical features and outflow of rivers like the Dwarka–Brahmani and the kuea with the Mayurakshi River in a low-lying area of Hijal are what cause the intensity of the flood in this area. The mighty Bhagirathi River flows north to south; however, during the monsoon season, the Mayurakshi system finds it challenging to cross since the water level of the Bhagirathi also stays higher.

### 3 Database and Methodology

The present study has been carried out using a systematic methodology that starts with data collection and its processing for the assessment of the agrarian and socioeconomic vulnerability of the MRB (Fig. 10.2).

#### 3.1 Database

The study area has a homogeneous population and the primary data on the kind of flood, and its socioeconomic elements are collected by employing a statistically significant sample size ( $n$ ) for each village. The sample size was calculated based on the United Nations Framework Convention on Climate Change (UNFCCC, 2020) based on Eq. 10.1:

$$n \geq \frac{1.645^2 NV}{(1 - N)x0.1^2 + 1.645^2 V} \text{ and } V = \frac{p(1 - p)}{p^2} \quad (10.1)$$

where  $n$  denotes sample size;  $N$  is the total number of households in the villages as of the 2011 Census (Table 10.1);  $p$  denotes the proportion of households experiencing economic marginalization (loss of food crops and infrastructure devastation minus adaptive capacity) as a result of the flood of 2000 (Table 10.1), as determined by a pilot survey conducted in the field; 1.645 is for a needed level of 90% confidence; and 0.1 is for a level of 10% relative precision (Table 10.1).

Survey of India topographical maps (1:50,000) have been collected for the study area bearing the top sheet numbers 72 P/16, 78 D/4, 73 P/13, and 79 A/1. Moreover,

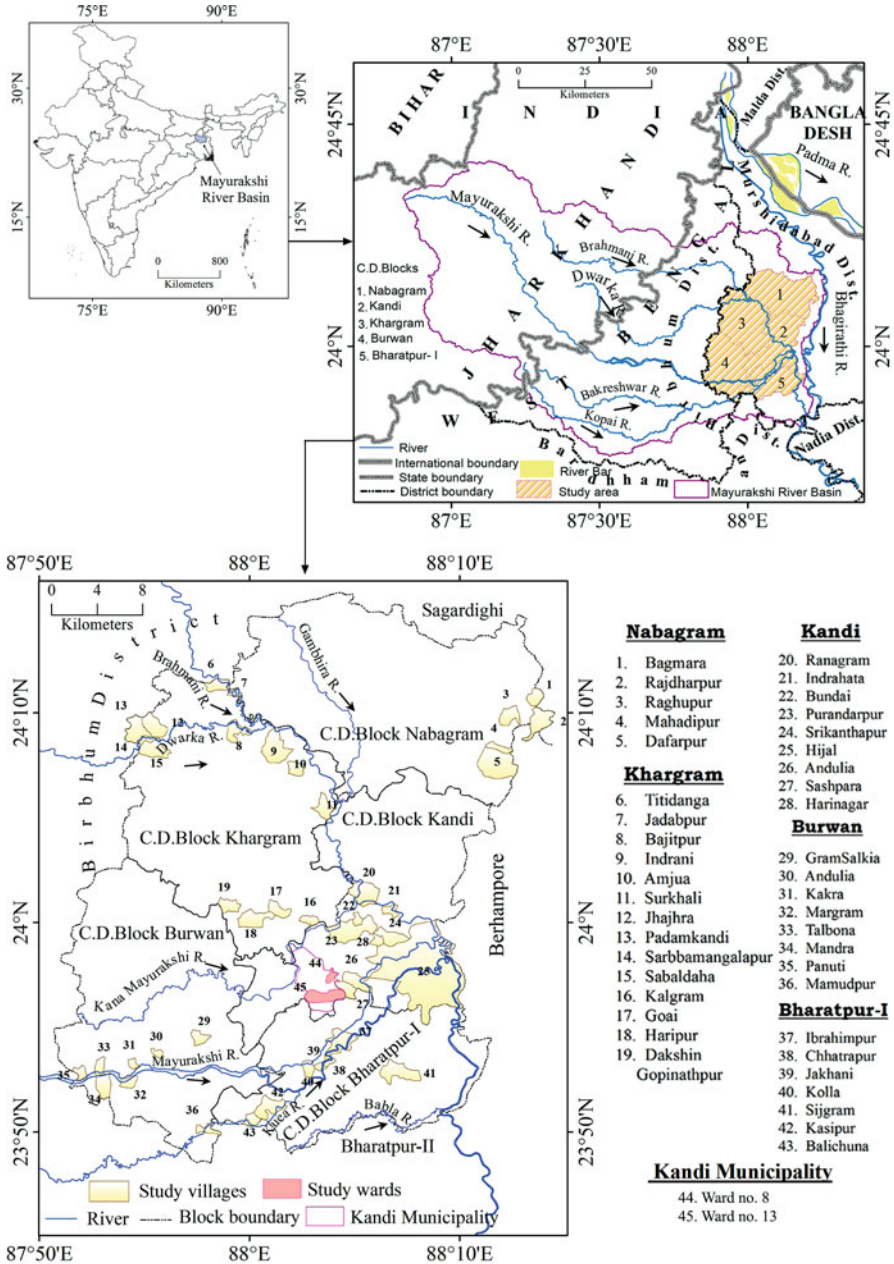


Fig. 10.1 Location of the Mayurakshi River basin and the study area

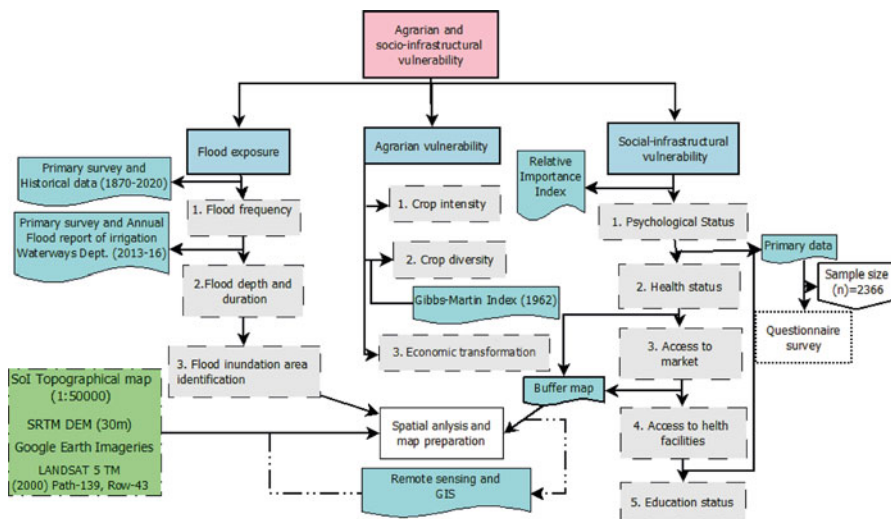


Fig. 10.2 Methodological flow chart adopted for the present investigation

Shuttle Radar Topography Mission Digital Elevation Model (SRTM DEM) 30 m and District Resource Maps of the Geological Survey of India have been used in the present context of the assessment of flood. Furthermore, the annual reports (2013, 2014, 2015, and 2016) of the Irrigation and Waterways Department, Govt. of West Bengal, District Census Handbook for Murshidabad (2011), and District Disaster Management Plan for Murshidabad (2016–17) are utilized for the present investigations.

### 3.2 Methodology

#### 3.2.1 Measuring Flood Hazard

Computation of flood hazards intensity has been executed with the aid of four components of flood hazards, i.e., flood frequency, flood depth, flood duration, and flooded area using annual reports of the Irrigation and Waterways Department, Government of West Bengal (2013–2016), Sanyal and Lu (2006), Landsat 5 TM (2000), and field observations (2017–2018) as well. The flood frequency concerning the whole basin has been computed from 1870 to 2020 whereas block-level flood hazards (flood frequency, depth, and duration) have also been measured for 20 years (1998–2017). The inundation area has been identified for the massive flood of 2000 using ArcGIS 10.4 software.



**Table 10.1** Representative households of each village and ward

C.D. blocks/ municipality	Villages/wards	Sample households	Total households (2011)
C.D. block Nabagram	Bagmara	43	427
	Rajdharpur	75	746
	Raghupur	46	459
	Mahadipur	17	167
	Dafarpur	123	1228
C.D. block Khargram	Tithidanga	43	433
	Jadabpur	18	184
	Bajitpur	8	82
	Indrani	189	1885
	Amjua	39	392
	Surkhali	80	801
	Jhajhra	18	175
	Padamkandi	60	603
	Sarbamangalapur	10	97
	Sabalaha	83	828
	Kalgram	40	401
	Goai	29	294
	Haripur	76	762
	Dakshin Gopinathpur	21	208
C.D. block Kandi	Ranagram	45	445
	Indrahata	51	505
	Bundai	39	389
	Purandarpur	111	1109
	Srikanthapur	88	881
	Hijal	271	2713
	Andulia-I*	52	521
	Sashpara	105	1045
Harinagar	27	269	
C.D. block Burwan	Gram Salkia	72	715
	Andulia-II*	12	116
	Kakra	10	98
	Margram	11	106
	Talbona	7	69
	Mandra	32	320
	Panuti	22	221
	Mamudpur	9	90
C.D. block Bharatpur I	Ibrahimpur	20	195
	Chhatrapur	11	108
	Jakhani	10	95
	Kolla	24	240
	Sijgram	119	1185

(continued)

**Table 10.1** (continued)

C.D. blocks/ municipality	Villages/wards	Sample households	Total households (2011)
	Kashipur	25	249
	Balichuna	8	75
Kandi municipality	Ward no. 8	73	757
	Ward no. 13	94	870
	<b>Total</b>	<b>2366</b>	<b>23,558</b>

Source: Computed from the Census of India, 2011 (\* Both having the same village name (Andulia) in the census and for the distinguishing purpose they have been renamed as Andulia-I and Andulia-II)

### 3.2.2 Measuring Flood Vulnerability

The social and infrastructural vulnerability has been measured with the help of the agricultural threat, health and psychological status of the villagers, and the impact of the flood on education, market, house condition, and transport. The agricultural threat is measured by the crop intensity, crop diversity and transferring the occupation from agriculture to other sectors, calculated from the field survey data 2017–2019, and the health and psychological status measured with the questionnaire survey 2017–2019. The data are collected regarding the pre-flood, flood, and post-flood conditions. The access to the health center during the flood is assessed by drawing the buffer from the village and ward geocenter and then plotting the health center on the map. Similarly, the availability of the market during flood has been assessed by creating the 1 km buffer from the geocenter of each village and ward and plotting the market location collected from the extensive field survey. The impact of the flood on education has been assessed by comparing the status of education field data of flood-affected households to the data of the District Census Handbook (2011). The road condition and the house condition have been portrayed as shown in the field photographs.

### 3.2.3 Cropping Intensity and Diversification

Cropping intensity (Ci) implies the degree of growing crops on a unit of land. This is used as a strategy to secure food for the growing population of a region. This may be computed using Eq. 10.2:

$$Ci = \frac{GCA}{NSA} \times 100 \quad (10.2)$$

where NSA stands for the net sown area and GCA stands for the gross cropped area.

A method of absorbing shocks in the agrarian economy is crop diversification. In the event of natural threats like floods or droughts, it may boost farmers' revenue and

lower the overall crop failure rate (Khanam et al., 2018). There is a movement in India to switch from conventional, unprofitable crops to more lucrative ones. In the study area, crop diversification is measured by the Gibbs–Martin (GM) index (1962) using Eq. 10.3:

$$GM = 1 - \frac{\sum x^2}{(\sum x)^2} \quad (10.3)$$

where  $x$  denotes the percentage of total cropped area accounted for by an individual crop.

### 3.2.4 Relative Importance Index

The relative importance index (RII) can be used to identify block-wise variations in perceptions of the local people to reveal the psychological traits regarding the fear, phobia, and shock scenario of a community. The algorithm to compute RII is mentioned using Eq. 10.4:

$$RII = \frac{\sum w}{AN} = \frac{1n_1 + 2n_2 + 3n_3 + 4n_4 + 5n_5 + 6n_6 + 7n_7 + 8n_8 + 9n_9 + 10n_{10}}{10N} \quad (10.4)$$

where “W” is the respondent’s weighting or rating of each element, which varies from 1 to 10, and “n1” denotes the number of respondents who gave the lowest rating (1), and “n10” denotes the highest rating (10). “A” stands for the greatest weight (10 in the study), and “N” stands for all of the samples combined.

### 3.2.5 Student’s T-Test

The student’s t-test has been used to test the significance of the coefficient of correlation ( $r$ ) based on the number of observations ( $N$ ). This is computed using Eq. 10.5 as per Das (1991):

$$t = \sqrt{\frac{r^2 (N - 2)}{1 - r^2}} \quad (10.5)$$

It is important to keep in mind that the null hypothesis is accepted for a degree of freedom at a selected significance level if the calculated value of “t” is larger than the tabulated value. The “t”-test has been used to examine the level of relevance between flood risk and economic vulnerability.

## 4 Results and Discussion

### 4.1 Nature of Flood

The historical accounts confirm that floods are annual, covering roughly 80% of the study area (Islam et al., 2022). The flood frequency, depth, duration, and flood inundation area of the study region vary from one C.D. block to another (Table 10.2). For example, C.D. block Kandi and Bharatpur-I are the most flood susceptible block. From 1870 to 2020, the flood frequency in the study area is gradually increasing (Fig. 10.3a). In the last 20 years, the villages of the C.D. block Kandi were affected by many flood events (9–15) while for Nabagram and Burwan, it is 8–10 times. The villages of the southeast portion of C.D. block Kandi (Hijal,

**Table 10.2** Spatial variation of flood frequency, depth, and duration in different C.D. Blocks

		Nabagram	Khargram	Kandi	Burwan	Bharatpur-I
Flood frequency	Average	9	10	12	9	11
	Range (highest to lowest)	10–8	11–8	15–9	10–8	13–9
	SD	0.84	0.85	2	0.93	1.29
	Skewness	–0.51	–0.43	0.48	0.00	0.00
	Standard error	0.37	0.23	0.67	0.33	0.49
Flood depth (m)	Average	0.91 (2.13)	1.28 (3.09)	1.35 (3.43)	0.53 (1.89)	1.73 (3.72)
	Range (highest to lowest)	1.46–0.57 (2.83–1.70)	2.89–0 (5.34–1.41)	2.44–0.32 (6.07–1.48)	1.24–0 (2.91–1.17)	2.32–1.01 (5.37–2.28)
	SD	0.35 (0.42)	0.78 (1.05)	0.74 (1.61)	0.45 (0.63)	0.39 (1.03)
	Skewness	1.10 (1.37)	0.47 (0.40)	0.06 (0.24)	0.29 (0.34)	–0.61 (0.31)
	Standard error	0.16 (0.19)	0.21 (0.28)	0.25 (0.54)	0.16 (0.22)	0.15 (0.39)
Flood duration (days)	Average	4.60 (20.20)	8.29 (22.29)	11.67 (40.22)	3.25 (15.38)	11.57 (30.29)
	Range (highest to lowest)	10–2 (26–16)	32–0 (67–14)	22–2 (80–11)	9–0 (45–7)	16–6 (41–18)
	SD	3.21 (4.49)	7.61 (13.22)	7.97 (24.27)	3.06 (12.22)	3.64 (9.71)
	Skewness	1.66 (0.61)	2.47 (3.41)	–0.13 (0.26)	0.92 (2.60)	–0.50 (0.13)
	Standard error	1.44 (2.01)	2.03 (3.53)	2.66 (8.09)	1.08 (4.32)	1.38 (3.67)

Source: Computed from the annual reports of Irrigation and Waterways Department, Govt. of West Bengal (2013–2016), Sanyal and Lu (2006), and field data (2017–2019); note: figures within parentheses denote the situation for agricultural land

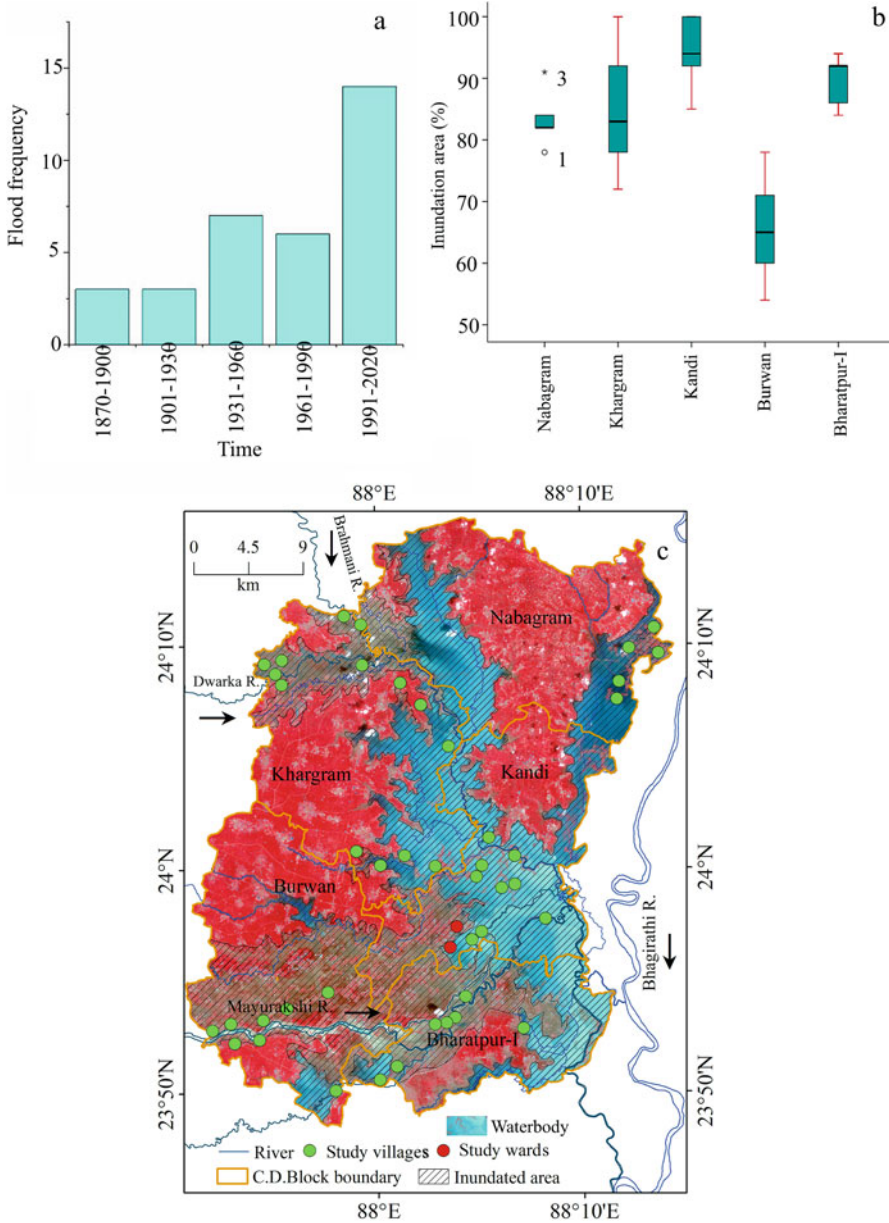


**Fig. 10.3** Nature and severity of flood hazards in the lower MRB. (a) Flood frequency during 1870–2020, (b) variation of flood inundation area across the selected C.D. blocks during 2000, and (c) spatiality in the flood inundation area during 2000

Sashpara, Srikantapur, and Andulia) are most flood prone due to the typical physiographic setup and drainage congestion of the area. Both Nabagram and Burwan are situated in the elevated portion, decreasing flood susceptibility. The average flood depth in the agricultural area ranges from 1.89 (Burwan) to 3.72 (Bharatpur-I) and in the settlement area from 0.53 (Burwan) to 1.73 (Bharatpur-I). In the C.D. block Kandi, both the flood duration and flood inundation are higher. Figure 10.3b, c depict that about 90% of the villages of Kandi block are flood inundated in the 2000 flood. Torrential rainfall, physical set-up, drainage congestion, and mostly the structural interventions, i.e., dams and barrages have been responsible for the flood characteristics. Regarding the study area, Massanjore dam and Tilpara barrage take an important role. As the study area is spread over 9596 km<sup>2</sup> area, spatial variation of flood hazard is not solely dependent on rainfall. Rather, the differential relief condition of villages and congestion of rivers due to the convergence of Hijuli, Banki, Kana Mayurakshi, Mayurakshi, Uttarason, Kuea, and Babla in the southeast portion of the study area are more responsible.

## 4.2 Threat to the Agricultural Economy

Cropping intensity is a measure of how intensively agriculture is practiced. The land is under strain from the large population, particularly in monsoon Asia. For this reason, farmers are keen to cultivate the land all year long. About 7% of the cropland in the study region is used for various crops, and double cropping dominates in the majority of the communities (more than 80 percent) (Fig. 10.4a). At the block level, all the C.D. blocks have 100% crop intensity during the *rabi* (winter) season while Kandi has the lowest cropping intensity (about 70%) during the *kharif* (monsoon) season. Moreover, Nabagram and Burwan have about 95% cropping intensity during the *kharif* season. In the C.D. block Kandi, the cropping intensity varies from 26.58 to 100 in the *kharif* season as the agricultural land of severe flood-prone villages (e.g. Andulia-I and Hijal of C.D. block Kandi) becomes inundated (Fig. 10.4b–d) and some villages (e.g. Srikantapur) do not cultivate in the monsoon to avoid the risk of crop damages due to sudden flood (Fig. 10.4e). Therefore, the reduction in crop intensity brought on by the flood stimulates the prompted diversification of the occupational structure.

Crop diversity is also recorded as higher during the *rabi* season and higher diversity found in Nabagram (0.57) and lower in Khargram (0.33) while in the *kharif* season crop specialization is mostly preferred by the farmers than the diversified cropping. Except for Nabagram (0.49), the rest of the blocks have crop diversification during *kharif* less than 0.2 with the lowest (0.08) found in Bharatpur-I. It is also noticed that the flood-affected villages ( $n = 19$ ), i.e., Indrani,

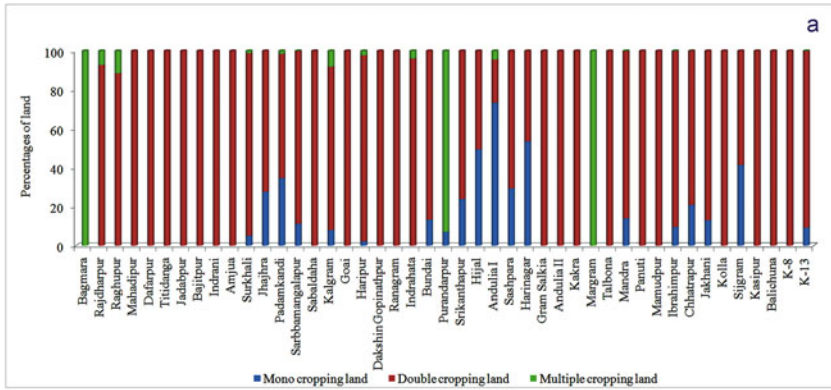


**Fig. 10.4** Cropping land and flood hazard: (a) distribution of cropping land, (b and c) inundated land in Andulia-I, (d) inundated land in Hijal, and (e) fallow land during monsoon in Srikanthapur. (Source: Field Survey, 2017–2019)

Hijal, and Sashpara, follow the crop specialization of rice during *kharif* season (Table 10.3). The flood hazard reduces the choice of crops for the farmers. It is observed that with the increasing flood depth, the GM index has fallen ( $r = -0.346$ ) because farmers in different communities have similar psychological profiles for growing traditional crops. Comparatively, lower flood-prone C.D. blocks like anagram scored higher GM index in all the three seasons (*rabi*, *kharif*, and *zaid*) while flood-prone blocks like Kandi and Bharatpur-I have a lower GM index for *kharif* seasons in monsoon.

Flood reduces crop diversity and intensity, paralyzing agriculture. On the other hand, supplying rich silt may improve agriculture. However, because the Mayurakshi system deposits coarse (coarse sand) sediments on the agricultural land,

**Table 10.3** Dynamics of agricultural pattern and occupational shifting

C.D. block	Season	Crop diversity		Crop intensity		Farmers shifted to other occupations <sup>a</sup>	
		Mean ± SD	Range	Mean ± SD	Range	Mean ± SD	Range (maximum to minimum)
Nabagram	<i>Rabi</i>	0.57 ± 0.06	0.49–0.64	100 ± 0	100–100	(7.67) ± 3.03	4.64–10.7
	<i>Kharif</i>	0.49 ± 0.09	0.36–0.61	96.26 ± 4.78	88.51–100		
	<i>Zaid</i>	0.22 ± 0.31	0–0.44	23.74 ± 38.38	7.22–100		
Khargram	<i>Rabi</i>	0.33 ± 0.27	0–0.69	100 ± 0	100–100	2.53 ± 6.71	16.67–(– 3.22)
	<i>Kharif</i>	0.2 ± 0.2	0–0.57	93.63 ± 10.79	65.29–100		
	<i>Zaid</i>	n/a	n/a	0.92 ± 2.1	0–8.06		
Kandi	<i>Rabi</i>	0.46 ± 0.11	0.29–0.61	100 ± 0	100–100	(11.12) ± 9.12	(24.57)– (–3.68)
	<i>Kharif</i>	0.19 ± 0.23	0–0.59	70.79 ± 23.37	26.58–100		
	<i>Zaid</i>	0.2 ± 0.35	0–0.61	11.24 ± 28.91	0–92.87		
Burwan	<i>Rabi</i>	0.45 ± 0.11	0.25–0.65	100 ± 0	100–100	(0.91) ± 0	0.91–0
	<i>Kharif</i>	0.15 ± 0.21	0–0.47	98.26 ± 4.62	86.05–100		
	<i>Zaid</i>	0.24 ± 0.34	0–0.48	14.24 ± 32.73	0–100		
Bharatpur I	<i>Rabi</i>	0.5 ± 0.78	0.38–0.64	100 ± 0	100–100	(10.52) ± 7.39	25–0
	<i>Kharif</i>	0.08 ± 0.19	0–0.51	87.85 ± 14.06	58.57–100		
	<i>Zaid</i>	n/a	n/a	n/a	n/a		

<sup>a</sup>Note that transformation from farmers to other occupations is denoted by positive and the reverse trend is marked as negative

the current study region does not enhance significant fertility following the flood. Additionally, because the dams retain the sediments in the reservoir, the agricultural area directly beneath the dams at Tilpara, Massanjore, and Bakreswar is devoided of any sediment. And the sediment-free water does not increase soil fertility. Hence, according to the local communities, the flood has become only a threat to them rather than a factor that is used to increase soil fertility. This results in agrarian distress, and it becomes acute especially when farmers and laborers are jobless for about one to one and half months during a flood. Thus, seasonal unemployment touches a limit of economic marginalization in the study area. Almost every village registered this type



of seasonal unemployment. Kandi shows the highest seasonal unemployment (IQR = 23, Med = 31), followed by Burwan and Khargram (IQR = 5, Med = 12, 28). This unemployment is a cyclic mechanism rather than a linear process. The lower income leads to agricultural poverty and reduces the capacity for buying agrarian inputs. As a result, the farmers are found to take high-interest loans from *mahajans* (persons who lend money at a high-interest rate) creating a debt trap for themselves.

However, when the harvest is reaped, the money they get from selling their produce is used to repay the previous loan. Moreover, the level of economic marginalization increases if a flood occurs before the crop matures. However, the general economic structure that has been shown in the study communities is not as bleak. This is simply because of the remittances that may back up utter agricultural failure. Remittances are therefore only a short-term fix, and the integration of the village economy with the foreign multiplier inside the agricultural system is what will ensure the local economic prosperity.

### 4.3 Impact on House Condition

The condition of the house portrays the socioeconomic status of a family. In some villages of the study area like Hijal, most of the people have two types of houses: (a) *khamarbadi* (farmhouse) and (b) *Basatbadi* (residential place). The *khamarbadi* is especially constructed for raising livestock and cultivating crops. Generally, these houses are located on the embankment or the elevated path between agricultural fields. On the other hand, some of the residential houses are on the embankments while others are located in low-lying areas. Therefore, houses become often vulnerable to flood attacks. It is mentioned that disaster intensity has also been measured by counting the number of houses damaged by the flood. The houses of the study villages are mainly *pucca* and a few are *katcha* constructed with mud, thatch, and clay pantiles (Fig. 10.5a–d). The *katcha* houses of the economically backward people are fragile to flood. Before the devastating flood of 2000, virtually, all the houses of study villages were *katcha*, which were washed away by the flood. Thus, the poor people became temporarily homeless, and some of them were fortunate to have been accommodated in the flood shelter while the rest were bound to take shelter under the trees. While describing the misery of the flood victims, Sultan (male, 46) said that “*before the colossal flood 2000, there was virtually no pucca house in our village. As a result, the severity of flood swept away almost every house, leaving the people under open sky. Some took shelter on the trees for couple of days while those who could not even afford that died.*” Similarly, another senior person of the study area shared his pathetic experience of 1963 flood. According to Jiyarul Haque (male, 76) “*during the flood of 1963 in our area, virtually all houses were smashed in few minutes following the cyclone like flood wave. People seeing the severity of flood cried and sat on the top of the demolished building.*”

Thus, having lost everything after the flood in 2000, the rate of labor migration started increasing especially in the Middle East countries. With the remittance from



**Fig. 10.5** Transformation of houses due to flood at Hijal: (a, b) represents the *kutcha* houses, and (c, d) *Pucca* house was constructed after the flood of 2000. (Source: Field Photographs, 2018)

the labor migrants, villagers constructed *pucca* houses (Fig. 10.5c, d). Moreover, some of them also got help from the government to build *pucca* houses under the scheme of Indira Awas Yojana (now Pradhan Mantri Awas Yojana). In the most flood-prone areas, all the houses are high from the ground (avg. 3 ft) so that in a small magnitude of flood the water cannot submerge the houses.

#### 4.4 Impact on Road and Transport

The transport system is often called the lifeline of a society. The mobility of the people and the movement of goods are determined by the connectivity and accessibility of the network (Rodrigue et al., 2016). The percentage of road space in a particular region is important. However, the physical condition of the road is more



**Fig. 10.6** Condition of the village road: (a) Typical *katcha* road during the monsoon and (b) breaching of the *pucca* road by flood. (Source: Field photographs, 2018)

important for mobility. In the study area, before the flood of 2000, almost all the village roads were *katcha*. Consequently, due to the flood of 2000, *katcha* roads were broken down. It is worth mentioning that Pradhan Mantri Gram Sadak Yojana, which was introduced in 2000, aimed at connecting the villages (with a minimum population of 500 persons) with the all-weather road to increase accessibility all throughout the year (PMGSY, 2015). Though most of the rural roads have been replaced by the *pucca* roads by this scheme, some village roads are still *katcha*. During the monsoon, the *katcha* roads become muddy and hence become inaccessible for cycles, bikes, or any type of vehicle (Fig. 10.6a).

Moreover, the *pucca* roads are frequently breached by the flood (Fig. 10.6b), which disrupts normal life by creating a lot of problems. Besides, small bridges connecting one village to another are also damaged due to floods. Similar conditions are reported for Bangladesh in 2004 due to the monsoon flood, which reduced the movement of the people (Rahman, 2014). Under these circumstances, boats become the only means of communication.

#### 4.5 Accessibility to Market

Society depends on the market for the requirements of necessary goods and services. A combination of goods and services from the market depends on the distance from the villages. A market is absent within a radius of 6 km of the village center for Bagmara, Raghupur, Rajdharpur, Mahadipur, Dafarpur of the C.D. block Nabagram, Surkhali of the C.D. block Khargram, and Mandra of the C.D. block Burwan (Fig. 10.7). In the study area, the location of the market during flood varies to a certain extent from one village to another. Therefore, these villages are mostly affected by floods regarding access to the market service. The people of Hijal village of the C.D. block Kandi and Padamkandi, Sarbamangalapur, Jhajhra, Sabaldaha of the C.D. block Khargram have to travel 4.5 km to access the market.

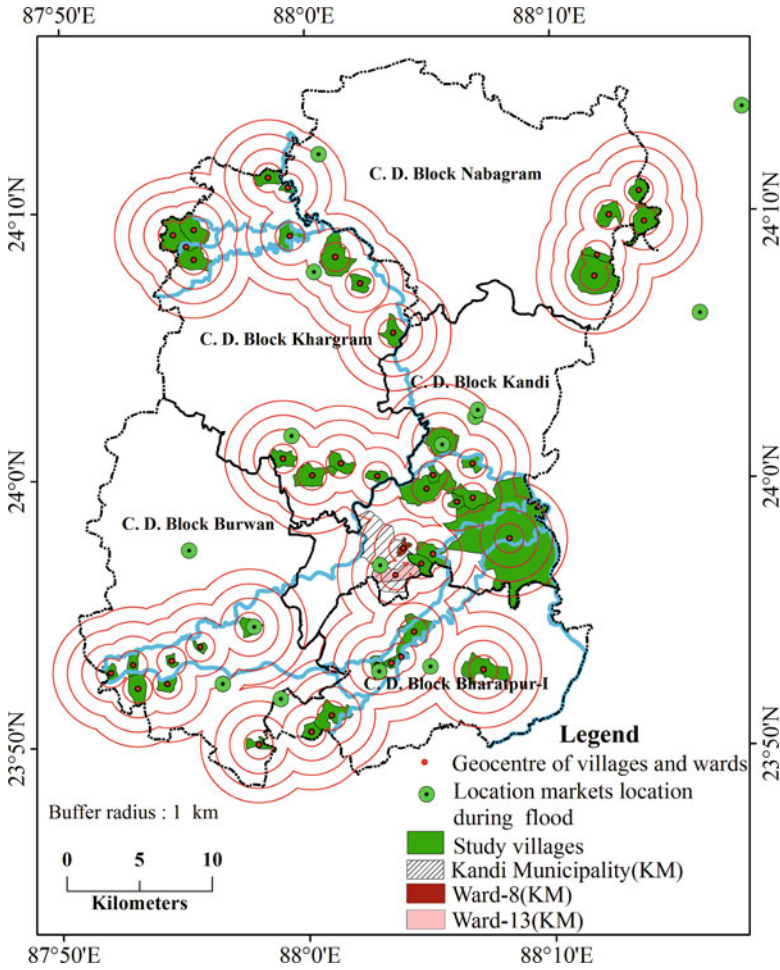


**Fig. 10.7** Location of markets in different buffer zones during the flood. (Source: Field Survey, 2017–2019)

In the C.D. block Bharatpur, all the study villages can access the market within 3 km of their village center. Ranagram village of the C.D. block Kandi, Gram Salkia of the C.D. block Burwan, and Kolla of the C.D. block Bharatpur-I have the market in close proximity to the village center. During the normal period (nonflood affected), 87.5% of households of Mahadipur, 95.24% of Bagmara, and 43.33% of Rajdharpur can avail of the market within a radius of 2 km from their village center. However, during flood cent percentage of households of these three villages have to travel about 5 km to reach the market. Similarly, all households of Jhajhra can access the market by travelling only about 5 km in normal conditions, which are extended to more than 10 km in flood periods. In the C.D. block Kandi, 69% of households of

Srikanthapur and 22% of households Purandarpur also travel more than 10 km during floods whereas all households of Ibrahimipur, Chattarpur, Kolla, Sijgram, Kasipur, and Balichuna of C.D. block Bharatpur-I, more than 84% of households of Indrani, about 97% of Sabaldaha, 98% of Kalgram, and 100% of the household of Dakshin Gopinathpur villages of C.D. block Khargram travel 5 km distance to reach the market. Throughout the flood period, the essential commodities are insufficient in the market. All the study villages of C.D. block Kandi are found to face difficulty to get essential commodities. However, other villages of the four study blocks can access almost all essential commodities in the market during the flood. But the price of the commodities is also high due to the higher transport cost and huge demand for the goods available in insufficient quantity. The flood victims face the music because they cannot afford the basic requirement due to higher prices (more than double) during flood episodes. The problem further aggravates when the shopkeeper did not agree to provide goods for lend. Besides, reaching the market often becomes difficult because during normal period people reach the market by cycling or by walking, but during flood, boat is the only medium to reach the market, and sometimes they have to expense more than 50 rupees 4 km distance to reach the market.

#### **4.6 Health Problems**

Flood has an immediate adverse effect on both physical and mental health. Flood is associated mainly with communicable diseases, which are mainly of two types: (a) waterborne disease and (b) vector-borne disease. In rural areas, waterborne diseases break out quickly because of the inadequacy of safe drinking water and sanitation problem. However, the entire health risk during flood depends on the availability of doctors, adequate supply of medicine, proper service from the nearby health center, access to safe drinking water, and good sewage system coupled with the proper transfer facility of patients to health centers. In the study area, more than 90% of people are affected by diarrhea. Besides, skin disease, typhoid, and dysentery are also common. The symptoms of diarrhea are frequent watery bowel motion, and it is an infectious disease and breaks out readily because of unsafe drinking water and contaminated food. In the study area, more than 99% of households are bound to use unsafe drinking water.

During the flood, 100% of households of all the study villages of C.D. block Nabagram; Surkhali, Sarbamangalapur, Kalgram, Goai, Haripur, and Dakshin Gopinathpur of C.D. Block Khargram; Ranagram, Indrahata, Bundai, and Purandarpur of C.D. block Kandi; Andulia-II, Kankra, Mandra, and Mamudpur of C.D. block Burwan; and Sijgram of C.D. block Bharatpur-I use tube well as the source of their drinking water (Fig. 10.8a). It is worth mentioning that the cent percent households of Panuti, 96% of Kasipur, 50% of Kolla, 43% of Sabaldaha, 38% of Jhanjra, 36% of Harinagar, and 33% of Chhatrapur use flood water as their drinking purpose while 81% of households of Indrani and 43% of Padamkandi use

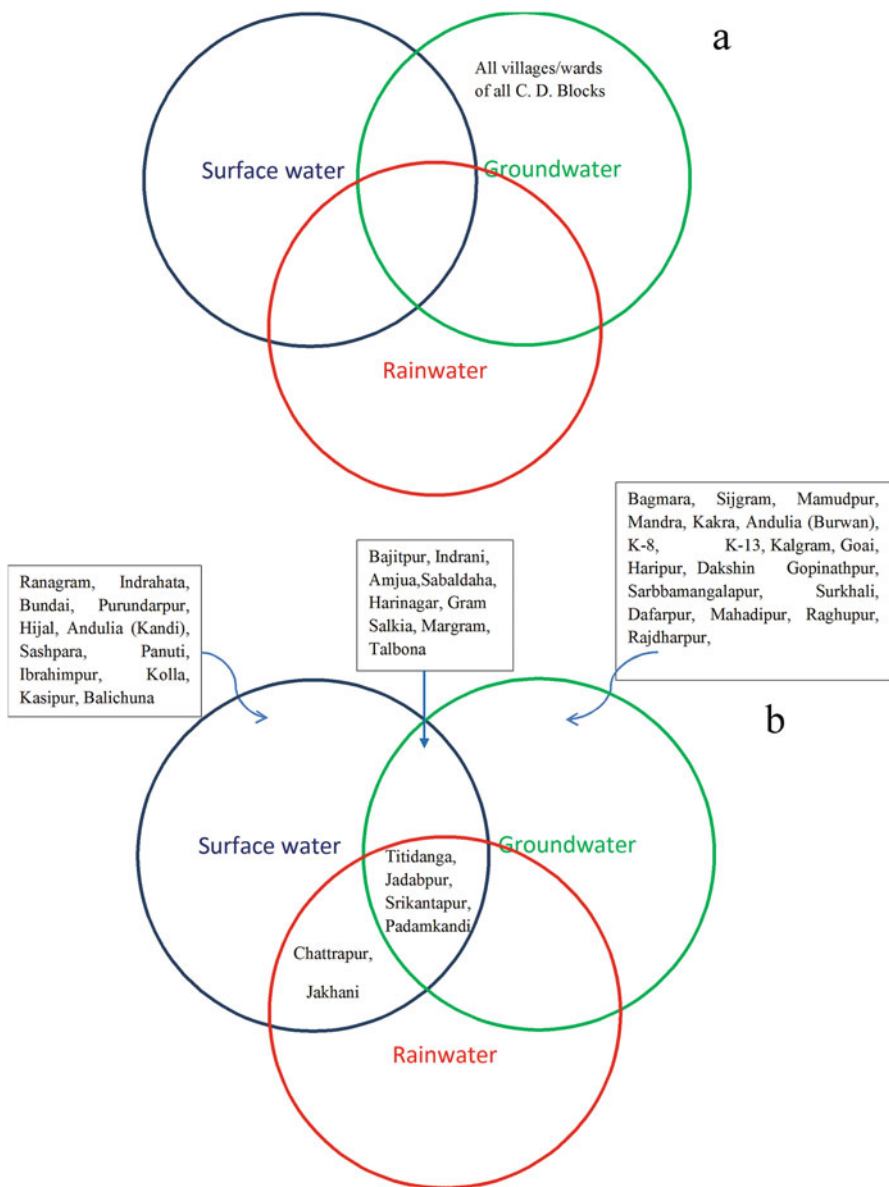


**Fig. 10.8** Sources of drinking water during (a) pre-flood and (b) flood in the study area. (Source: Field Survey, 2017–2019)

both flood and rainwater. Besides, all households of Sashpara, Andulia-I, Kolla, Kasipur, Balichuna, and 90% of Jakhani use flood water, and about 94% of the household of Indrani and 92% of Hijal use floodwater or rainwater (Fig. 10.8b). Only 18% of the household of Margram and 57% of Talbona use safe drinking

water. For this reason, diarrhea, cholera, and skin diseases are common in the study area (Table 10.4).

The village-wise investigation shows that the majority of the villages (e.g., Bagmara, Rajdharpur, Raghupur, Goai, Gram Salkia, Mandra, and Panuti) have 100% cases of diarrhea while few villages (e.g., Talbona) have only about 42% of people affected by diarrhea (Fig. 10.9).

Furthermore, skin diseases triggered by flood-contaminated water spread through infection. And this is aggravated in the post-flood period. From the survey in the study area, it is observed that doctors are not available during the flood. Besides, the inadequate supply of medicine further deteriorates the health conditions of the local people. During the flood, villagers even spend days without food, which deteriorated their health. After, Mohammad Asgar Ali (male,56) from Hijal, *“During flood of 2000 we were left with no food except eating uncooked rice wet in floodwater. When floodwater depth reduced, some cooked food reached us from village langarkhana through boat. Thus we suffered like anything during that time which cannot be expressed in language even”*. More than 95% of households do not have a proper sewage system at all. Almost all the village dwellers use *katcha* toilet and pit latrine before the flood. And during floods, their toilets and latrines go underwater, and it induces an unhygienic condition when the floodwater is mixed with the toilet, and ultimately it gives birth to different waterborne diseases.

Furthermore, flood triggers serious health issues for pregnant mother. It is difficult to avail the health facilities during this time. During the flood, they are often bound to use contaminated water for daily uses and unsafe drinking water, which leads to the spread of different waterborne diseases among pregnant mothers. These types of contaminants sometimes become fatal because the health centers are situated far away from the village as shown on the buffer map. There are some villages that do not have health center within a 3 km radius of the geocenter of the villages (Fig. 10.10). That’s why the main problem of the pregnant mother is to reach the health center for their checkup on time. This condition is aggravated especially for the *katcha* village road and deteriorating transport. During the flood, the indoor environment of the hospital is also unhealthy, and proper treatment is not available because most of the doctors are also out of the station. Some villages in the study area face the death of a mother during delivery. In Titidanga, Sarbamangalapur Jhajra, and Padamkandi villages, more than 50% families faced death during delivery. In the C.D. block Khargram, the death during delivery is high, but in the C.D. block Nabagram, there is not a single family facing it. Only Chhatrapur village from the C.D. block Bharatpur-I and Margram from the C.D. block Burwan faced death during delivery.

In the C.D. block Kandi Srikanthapur (4.49), Hijal (5.45), Andulia-I (2.5), and Sashpara (4) have a negligible percentage of death during delivery among the surveyed family.

**Table 10.4** Descriptive statistics of diseases

	Diarrhea	Cough	Skin disease	Cholera	Dysentery	Malaria	Typhoid	Dengue
Mean	87.77	6.99	16.52	8.20	0.05	0.02	1.00	0.32
Standard deviation	18.46	12.43	20.30	22.88	0.12	0.13	3.37	1.49
Kurtosis	1.35	5.56	0.40	7.17	8.87	45.00	23.81	19.99
Skewness	-1.57	2.35	1.19	2.91	2.89	6.71	4.59	4.59
Range	61.84	55.00	70.00	90.48	0.56	0.85	20.00	7.45
Minimum	38.16	0.00	0.00	0.00	0.00	0.00	0.00	0.00
Maximum	100.00	55.00	70.00	90.48	0.56	0.85	20.00	7.45

Source: Field Survey, 2017–2019



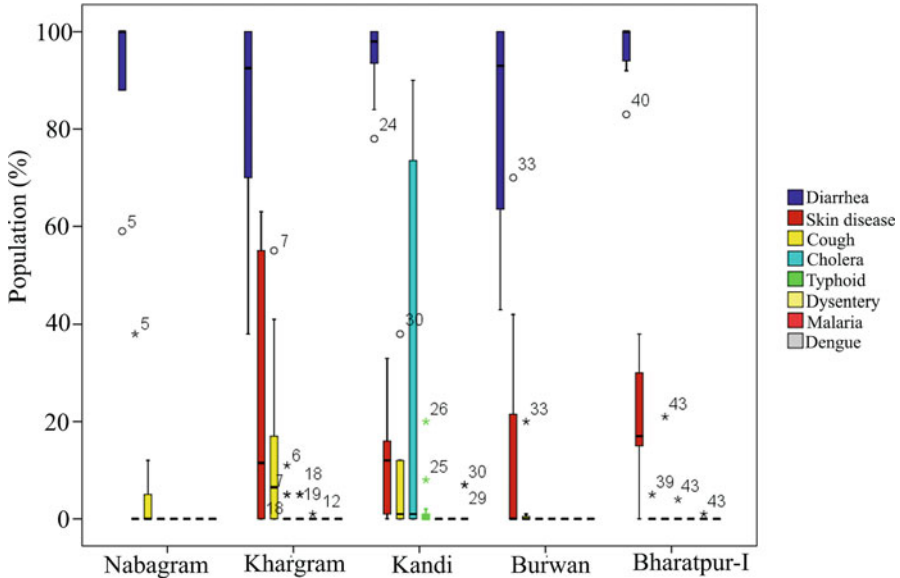
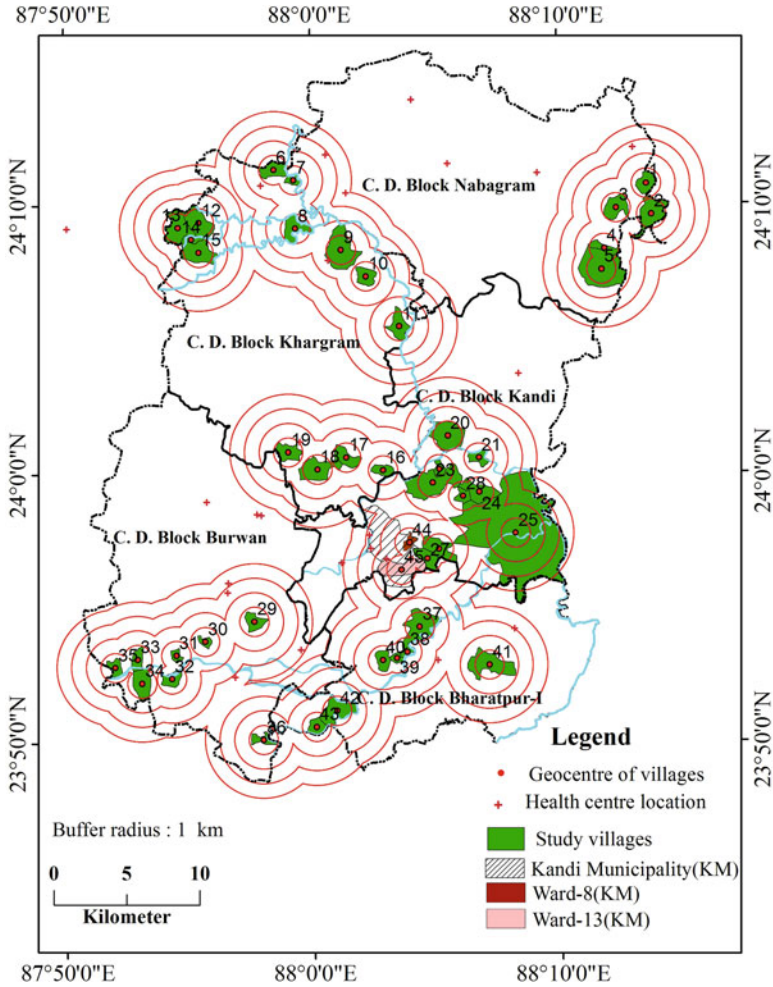


Fig. 10.9 Magnitude of different diseases in the study villages. (Source: Field Survey 2017–2019)

### 4.7 Education and Related Issues

The education system, the backbone of society, portrays the level of cultural attainments (Breen & Jonsson, 2005). Through education, people acquire knowledge of how to increase the coping capacity to live better with floods minimizing the adverse effects of flood vulnerability. Thus, education has an indirect correlation with the magnitude of vulnerability (Muttarak & Lutz, 2014). In the study area, more than 60% people of Mamudpur, Goai, Dafarpur, Talbona, Gram Salkia, Kakra, Bajitpur, Panuti, Rajdharpur, Mandra, Kalgram, Mahadipur, Padamkandi, Andulia-II, Surkhali, Indrahata, Ranagram, and Purandarpur did not attend school. School education is dependent on the nature and severity of the flood. Students’ attendance in school is directly related to the accessibility to reach school during the flood. The perception survey depicts that attendance falls sharply in tune with the flood. The maximum fall rate has been observed in the Bajitpur, Dafarpur, and Panuti villages while the minimum fall rate has been observed in the Chhatrapur, Ibrahimpur, Balichuna, Sarbamangalapur, and Indrani villages. During the flood, sending children to school is nothing but a luxury for them. The attendance of school students during the flood is very low, below 50%. Thus, it has been observed that the areas experiencing floods do not have an alternative source of income from outside and have a low literacy rate. For example, the literacy rate of the flood victim villages is far below the census villages of the C. D. blocks Nabagram, Khargram, and Burwan (Table 10.5).



**Fig. 10.10** Location of health centers in different buffer zones. (Source: State Bureau of Health Intelligence, Directorate of Health Services, 2015–2016)

However, receipt of remittance from the outside is a dominant control factor for literacy. The villages of the C.D. blocks Kandi and Bharatpur-I are mostly flood prone, and sample village literacy exceeds the total literacy of the block. This is due to the receipt of the remittance in flood-prone areas.

To find out any significant differences between the literacy rate of the sample villages and the total villages of each C.D. block, a student’s t-test has been performed using the field data and census data. For C.D. block Nabagram, the computed value of the t-test for total literacy is 3.98, and for male and female literacy values of t-test are 3.68 and 4.32, respectively, while the tabulated value is 2.78 for 4 degrees of freedom at a 95% confidence level. Therefore, the computed

**Table 10.5** Mean and SD of literacy rate in different study blocks

Name of the block	Mean (census)			Mean (sample)			SD (sample)			Number of villages (N)	
	Total	Male	Female	Total	Male	Female	Total	Male	Female	Total villages	Sample villages
Nabagram	70.83	76.44	64.98	42.87	48.43	36.37	15.71	17.03	14.81	118	5
Khargram	63.56	69.69	57.16	57.72	61.74	52.96	21.30	22.32	21.01	155	14
Kandi	65.13	71.66	58.25	65.31	69.86	59.70	23	20	27.10	93	9
Burwan	68.96	74.97	62.6	37.27	43.81	29.08	3.22	5.56	4.68	160	8
Bharatpur-I	62.93	67.94	57.57	79.86	80.52	78.84	13.10	15.17	12	92	7

Source: Field Survey, 2017–2019

value for total, male, and female literacy exceeds the tabulated value implying the significant differences in the percentages between literacy of the sample villages and total villages of C.D. block Nabagram (Table 10.6).

The computed t-test value for male literacy is lesser than female literacy, which indicates that across the villages and wards, female literacy varies more than that of the males. It may be reasoned that the spatial difference in literacy in this block may be due to variations in the flood character. About 60% area of this C.D. block is above 25 m altitude, and hence, maximum villages of this C.D. block are not flood prone. However, some villages are located in low-lying flood-prone areas. The average literacy of flood-prone villages, i.e., study villages, is lower, but other villages of this C.D. block have a higher literacy rate. In this block, a few persons are engaged in the international labor market. For example, Raghupurhas has about 2.5% labor migration while Dafarpur has only about 1%. Thus, these flood-prone villages do not receive huge remittances, which can give them courage for the expenses of educating their children. This ultimately makes remarkable differences between the literacy of the sample villages and total villages. In the C.D. block Khargram, the computed value for the t-test is 1.03 for total literacy while 1.33 and 0.75 for male and female literacy, respectively, against the tabulated value of 2.16 for 13 degrees of freedom at a 95% confidence level. The computed value for all kinds of literacy rates is lesser than the tabulated value, implying no significant differences between the sample village's literacy and the total village literacy of this C.D. block. All the villages of C.D. block Khargram are moderate to highly flood-prone. It is observed that five villages (Jadabpur, Bajitpur, Padamkandi, Sabaldaha, and Kalgram), which are less flood prone, attract no remittance while the rest of the more flood-prone sample villages receive remittances by sending their family members aboard. Thus, on the one hand, lower flood magnitude supports higher literacy by lesser socioeconomic marginalization, and on the other hand, higher flood magnitude supports education via remittances. This typical mechanism actually balances out the gap between the more flood-vulnerable and less flood-vulnerable areas. The C.D. block Kandi is the highest flood-prone block among all the study blocks. The computed t-test value for total, male, and female literacy are  $-0.02$ ,  $0.27$ , and  $-0.16$ , respectively, whereas the tabulated value of the t-test is 2.31 for 8 degrees of freedom at a 95% confidence level. The computed value for all kinds of literacy is far lesser than the tabulated value indicating no significant difference between the sample villages and total villages. All the villages of this C.D. block are flood prone, and the rate of labor migration to Arabian countries is higher than in other study blocks. The most flood-prone village in this C.D. block is Hijal, which has registered more than 10% labor migration. Besides, other villages like Srikanthapur, Andulia-I, Sashpara, and Harinagar are also highly flood-prone villages. These villages have recorded an average literacy rate of more than 80% because the rate of labor migration is high in these villages and thus receive a huge amount of remittances that help the villagers to increase their courage for the expense of children's education. This implies a strong positive relationship between the remittances and literacy rate among the flood-prone villages ( $r^2 = 0.67$ ). The field data indicates a picture of literacy level similar to that of the C.D. block

**Table 10.6** Student's t-test for detecting the difference between sample mean and population mean of literacy rate

Name of the C.D. Block	T value (computed)			T value (tabulated)	df	Significance level	Remarks	
	Total	Male	Female				Total	Male
Nabagram	3.977	3.676	4.316	2.776	4	0.05	Alt	Alt
Khargram	1.025	1.332	0.747	2.16	13	0.05	Null	Null
Kandi	-0.023	0.270	-0.161	2.306	8	0.05	Null	Null
Burwan	27.791	15.837	20.234	2.365	7	0.05	Alt	Alt
Bharatpur-I	-3.419	-2.193	-4.692	2.447	6	0.05	Alt	Alt

Source: Field Survey, 2017-2019

Nabagram. The computed t-test values for total, male, and female literacy are 27.79, 15.84, and 20.23, respectively, whereas the tabulated value is 2.37 for 7 degrees of freedom at a 95% confidence level. This portrays that the computed value for all types of literacy far exceeds the tabulated value (Table 10.6), which indicates that there are significant differences between the literacy of the sample villages and the census villages. About 85% area of this C.D. block is above 25 m of which 40% area is above 30 m. And the low-lying area, which is situated at the edges of Mayurakshi and Kana-Mayurakshi, is flood prone. Except Mamudpur, other study villages of this C.D. block do not receive any remittances, which increases the remarkable differences between the literacy rate of the sample and total villages. This may be because the sample villages are flood prone and do not receive remittances as well. Thus, the villagers are reluctant to incur more costs on the kid's education. This results in a lower level of literacy in the flood-victim villages. However, the other villages, which are not at all flood prone have a bright picture in education. This contrasts between the sample and census villages of the C.D. blocks. The last study block is Bharatpur-I, which experiences a totally different scenario from the rest of the C.D. blocks. The computed t-test values for total, male, and female literacy are -3.42, -2.19, and -4.69, respectively, while the tabulated value is 2.45 for 6 degrees of freedom at 95% confidence level, which implies that there is a significant difference between a sample and total village regarding total and female literacy. However, there is no significant difference in the male literacy rate. The most interesting observation of this C.D. block is that the total literacy of sample villages is far better than that of the total villages. About 50% of areas of these C.D. block are below 15 m altitudes while the rest are below 20 m altitudes. Besides, the three rivers (Kuye, Mayurakshi, and Babla) crisscross the block. All the villages of this C.D. block are moderately high to highly flood prone. However, labor migration is found only in some severely flood-prone villages, which indicates that the highly flood-prone sample villages receive remittances that help to increase their literacy rate.

#### **4.8 Sociopsychological Problems**

The psychological health of people related to their thoughts, feelings, and behavior is influenced by the surrounding conditions (Kahn, 1990). To cope with the situation, the behavioral pattern of people has changed (Carver et al., 1989). Moreover, social psychology is mostly controlled by environmental hazards like floods and river bank erosion (Smith et al., 2000; Islam & Guchhait, 2018). In this section, the impact of the flood on social psychology especially fear/phobia, physical and psychological stress, and shock has been examined. Fear and phobia are interlinked. According to Wilson (1996), "phobia involves the experience of persistent fear that is excessive and unreasonable". Fear and phobia are common in the pre-flood stage. Physical and psychological stress are observed during and post-flood periods while shock is a post-flood event. Regarding fear/phobia, there is sharp spatial variation across the

**Table 10.7** Descriptive statistics of fear/phobia, physical stress, psychological stress and shock

	Fear/ Phobia	Physical stress			Psychological stress			Shock
		Before flood	During flood	After flood	Before flood	During flood	After flood	
Mean	6.10	3.15	5.53	6.16	2.34	5.11	5.39	6.77
SD	0.62	0.16	0.34	0.28	0.10	0.23	0.26	0.52
Kurtosis	3.35	0.65	12.24	5.09	0.67	4.87	-0.15	-0.38
Skewness	-1.56	-0.63	-2.42	1.88	-0.7	-2.15	0.28	0.83
Range	3.06	0.78	2.35	1.61	0.47	1.06	1.26	1.98
Minimum	3.84	2.71	3.93	5.65	2.10	4.29	4.81	5.80
Maximum	6.91	3.5	6.28	7.27	2.58	5.36	6.08	7.79

Source: Field Survey, 2017–2019

villages and wards on a 10-point Likert scale. The minimum score for fear (3.84) has been registered for Ward 8 while the maximum by Kolla (6.9). The average score for fear is quite high (>6). It is quite natural because floods are annual and the people of the locality have an image of the devastating flood of 2000 and 1978, which indicates a feeling of fear and phobia, which they came to know about the impending flood. Regarding physical stress, there is a gradual increase in the average score from pre-flood to post-flood. The average physical stress in the pre-flood period has been recorded as 3.15, which has increased to 5.5 during the flood and ultimately reached the maximum score of about 6 in the post-flood period (Table 10.7).

It may be argued that during the flood, male members of the family are busy reaping their harvest to save it from the flood. Besides, they have to shoulder the duty of shifting household assets to a safer place and also relocating family members to the flood shelter camps, which magnifies their physical stress. Similarly, female members are busy taking care of their children and aged people and preparing the food. Moreover, in the post-flood period, physical stress reaches the maximum limit because male members of the society have to be responsible for reconstructing their damaged buildings while the females have to take the burden of rearranging household assets and nurturing kids and old people. Regarding psychological stress, a picture similar to that of physical stress has been observed. The most intriguing factor is the shock, which is maximum out of the fear, physical stress, psychological stress, and shock. This may be due to their obsessed thinking about the losses after the flood gets over. In other words, during and immediately after the flood, they are generally busy with their physical survival and have lesser scope to contemplate the losses of their belonging, but later on, when they think of their losses, they go in a pensive mood, and thus, shock increases.

The intensity of the perceptual assessment concerning the sociopsychological characteristics increases with RII value. The bar graphs (Fig. 10.11a–e) are indicating the values of RII while the error bar upon the bar graph shows the consistency of the opinion of the respondents, i.e., the shorter the error bar, the higher the consistency of opinion. Regarding the spatial variation of phobia across the different C.D. blocks, it is observed that phobia is comparatively lower for the C.D. block

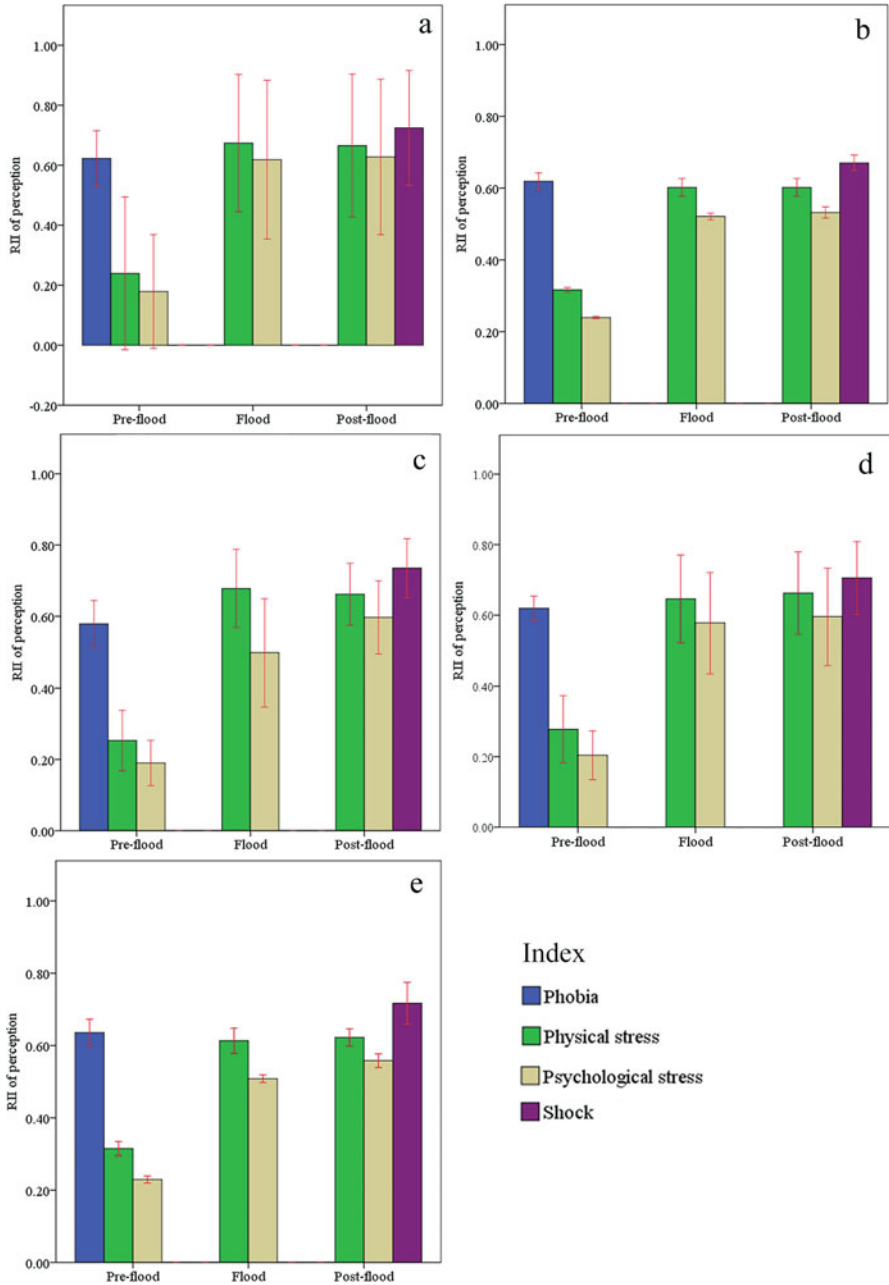


**Fig. 10.11** Level of fear/ phobia, physical stress, psychological stress, and shock before the flood, during the flood and after the flood: (a) C.D. Block Nabagram, (b) C.D. Block Khargram, (c) C. D. Block Kandi, (d) C.D. Block Burwan, and (e) C.D. Block Bharatpur-I. (Note: Error bars at 95% confidence limit) (Source: Field Survey, 2017–2019)



Kandi because this block is the most flood prone than others. Therefore, people are habituated to the annual flood. Moreover, they know if rainfall intensity becomes high during monsoon, a flood may occur, and they are mentally prepared for that. Regarding physical stress, the C.D. block Kandi tops the list followed by Bharatpur-I (Fig. 10.10a–e). This is due to the higher magnitude of flood in these two blocks inducing the people to toil in the field for reaping the crops and in the households for tying down the household assets. However, the consistency of the opinions is comparatively low in Kandi than Bharatpur-I because some villages in the C.D. block Kandi have huge marginalization due to floods than the others. Regarding psychological stress, C.D. block Nabagram portrays the maximum score. Though this block is comparatively less flood vulnerable, they are psychologically torn out because of the recipient of minimum remittance and dependence on agricultural income. The reverse scenario has been observed for the more flood-vulnerable block like Kandi where there is an alternative source of income from outside. However, shock is maximum for the C.D. block Kandi because of the huge agrarian loss. Besides, there is a variation of opinion across gender. Though there is no such variation regarding social psychology in the pre-flood and flood periods, it has been observed that women have more psychological stress in the post-flood period.

It may be reasoned that females have to play a pivotal role in running the family while the males have more physical stress in the post-flood period as they move out of their native place for sustaining their families by remittance. And they experience less psychological stress as they are not directly in front of their families.

## 5 Conclusions

The present study shows that flood is frequent in the study area with a grave consequence on the marginalization of the agricultural portfolio as depicted by the lowering of the cropping intensity, diversity, and productivity of the monsoon agriculture. Moreover, the *kutch*a houses collapsed during the monsoon period almost every year. The maximum loss in the house, road, and transport network was found during the colossal flood of 2000. After that event, the majority of the houses were upgraded to *pucca* houses either by the government (Pradhan Mantri Awas Yojana) or by taking loans from the banks. However, in the rural areas, many *kutch*a roads still exist, and vulnerable culverts and bamboo bridges tend to collapse during the floods. Furthermore, the study found that accessibility to the market falls remarkably during the flood season because of the threats to the transport networks. The issues of health like the outbreak of diseases and limited access to the health care units pose great challenges, especially for child and maternal health. Similarly, regarding literacy, flood propensity also plays a vital role. The general trend is that in the absence of a remittance economy, the higher the flood, the lesser the literacy. However, the trend reverses while remittances are received by the villages, i.e., higher remittances in the higher flood-prone areas and hence better literacy rate in

these areas. The study also found that fear/phobia is less among the flood-prone villagers; however, shock after the occurrence of a flood is really enormous. These typical study findings may help the various stakeholders to grasp the ground reality of the flood-prone villages in terms of the social and economic infrastructure and social psychological terrain. This will certainly help the local planners and people to get involved in participatory planning. However, in formulating a detailed plan for the reduction of infrastructural vulnerability, an in-depth assessment is needed in respect of the economic and ecological evaluation of the floods in a broader spatial and temporal framework.

## References

- Ahamed, B. K. K., & Pandey, A. C. (2019). Coastal social vulnerability and risk analysis for cyclone hazard along the Andhra Pradesh, East Coast of India. *KN – Journal of Cartography and Geographic Information*, 69(4), 285–303. <https://doi.org/10.1007/s42489-019-00029-9>
- Bandyopadhyay, S., Kar, N. S., & Das, S. (2014). *River systems and water resources of West Bengal: A review river systems and water resources of West Bengal: A review.*
- Bhowmick, P. K. (2015). *Livelihood vulnerability index analysis : An approach to study vulnerability in the context of Bihar. October 2018.* <https://doi.org/10.4102/jamba.v6i1.127>
- Birkmann, J., Krause, D., Setiadi, N. J., Suarez, D.-C., Welle, T., & Wolfertz, J. (2011). *World risk report: Focus governance and civil society* (pp. 1–74). Unu-Ehs. [http://www.preventionweb.net/files/21709\\_worldriskreport2011.pdf](http://www.preventionweb.net/files/21709_worldriskreport2011.pdf)
- Birkmann, J., Jamshed, A., McMillan, J. M., Feldmeyer, D., Totin, E., Solecki, W., Ibrahim, Z. Z., Roberts, D., Kerr, R. B., Poertner, H. O., Pelling, M., Djalante, R., Garschagen, M., Leal Filho, W., Guha-Sapir, D., & Alegría, A. (2022). Understanding human vulnerability to climate change: A global perspective on index validation for adaptation planning. *Science of the Total Environment*, 803, 150065. <https://doi.org/10.1016/j.scitotenv.2021.150065>
- Breen, R., & Jonsson, J. O. (2005). Inequality of opportunity in comparative perspective: Recent research on educational attainment and social mobility. *Annual Review of Sociology*, 31, 223–243.
- Carver, C. S., Scheier, M. F., & Weintraub, J. K. (1989). Assessing coping strategies: A theoretically based approach. *Journal of Personality and Social Psychology*, 56(2), 267.
- Chakraborty, S., & Mukhopadhyay, S. (2015a). An assessment on the nature of channel migration of River Diana of the sub-Himalayan West Bengal using field and GIS techniques. *Arabian Journal of Geosciences*, 8(8), 5649–5661. <https://doi.org/10.1007/s12517-014-1594-5>
- Chakraborty, S., & Mukhopadhyay, S. (2015b). Riverbank erosion and channel width adjustments across a meandering channel of North Bengal, India. *Earth Science India*, 8(3), 61–78. <https://doi.org/10.31870/esi.08.3.2015.5>
- Chinnasamy, P., & Srivastava, A. (2021). Revival of traditional Cascade Tanks for achieving climate resilience in Drylands of South India. *Frontiers in Water*, 3(April). <https://doi.org/10.3389/frwa.2021.639637>
- Chinnasamy, P., Maske, A. B., Honap, V., Chaudhary, S., & Agoramoorthy, G. (2021). Sustainable development of water resources in marginalised semi-arid regions of India: Case study of Dahod in Gujarat, India. *Natural Resources Forum*, 45(2), 105–119. <https://doi.org/10.1111/1477-8947.12217>
- Cianconi, P., Betò, S., & Janiri, L. (2020). The impact of climate change on mental health: A systematic descriptive review. *Frontiers in Psychiatry*, 11(March), 1–15. <https://doi.org/10.3389/fpsy.2020.00074>

- Das, N. G. (1991). *Statistical methods in commerce. Accountance and economics* (pp. 1–25). M. Das and Co.
- Dasgupta, S., & Badola, R. (2020). *Indicator-based assessment of resilience and vulnerability in the Indian Himalayan Region: A case study on socio-economy under different scenarios*. District Census Handbook. (2011). *Murshidabad District*. Directorate of Census operation. Accessed on 15 Mar 2019.
- Gayen, S., Villalta, I. V., & Haque, M. S. (2022). Flood risk assessment and its mapping in Purba Medinipur District, West Bengal, India. *Water*. <https://doi.org/10.3390/w14071049>
- Ghosh, S., & Mistri, B. (2015). Geographic concerns on flood climate and flood hydrology in monsoon-dominated Damodar River Basin, Eastern India. *Geography Journal*, 2015, 1–16. <https://doi.org/10.1155/2015/486740>
- Gould, I. J., Wright, I., Collison, M., Ruto, E., Bosworth, G., & Pearson, S. (2019). *Land Degrad Dev – 2020 – Gould – The impact of coastal flooding on agriculture A case-study of Lincolnshire United.pdf*. <https://doi.org/10.1002/ldr.3551>.
- IPCC. (2014). Climate change 2014: synthesis report. contribution of working Groups I, II, and III to the fifth assessment report of the. In *managing the risks of extreme events and disasters to advance climate change adaptation: Special report of the intergovernmental panel on climate change* (Vol. 9781107025). <https://doi.org/10.1017/CBO9781139177245.003>.
- IPCC. (2021). Climate change 2021 The physical science basis summary for policymakers working Group I contribution to the sixth assessment Report of the Intergovernmental Panel on Climate Change. In *Climate Change 2021: The Physical Science Basis*.
- Irrigation and Waterways Directorate. (2014). *Annual flood report*. Government of West Bengal, Jal Sampad Bhavan. Accessed on 15 Mar 2019.
- Islam, A., & Deb, S. (2020). Drainage basin morphometry and evaluating its role on flood-inducing capacity of tributary basins of Mayurakshi River. *SN Applied Sciences*. <https://doi.org/10.1007/s42452-020-2839-4>
- Islam, A., & Ghosh, S. (2021a). Community-Based Riverine Flood Risk Assessment and Evaluating Its Drivers: Evidence from Rarh Plains. In *Applied Spatial Analysis and Policy* (Issue 0123456789). Springer. <https://doi.org/10.1007/s12061-021-09384-5>.
- Islam, A., & Ghosh, S. (2021b). Economic transformation in the wake of flood: a case of the lower stretch of the Mayurakshi River Basin, India. In *Environment, development and sustainability* (Issue 0123456789). Springer. <https://doi.org/10.1007/s10668-021-01310-6>.
- Islam, A., & Guchhait, S. K. (2015). *Is severity of river bank erosion proportional to social vulnerability? A life and living through newer spectrum of geography*. January.
- Islam, A., & Guchhait, S. K. (2018). Analysis of social and psychological terrain of bank erosion victims: A study along the Bhagirathi River, West Bengal, India. *Chinese geographical science*, 28(6), 1009–1026.
- Islam, A., & Sarkar, B. (2020). Analysing flood history and simulating the nature of future floods using Gumbel method and Log-Pearson Type III: The case of the Mayurakshi River Basin, India. *Bulletin of Geography. Physical Geography Series*, 19(19), 43–69.
- Islam, M. S., Solaiman, M., Islam, M., Tusher, T., & Kabir, M. (2016). Impacts of flood on Char livelihoods and its adaptation techniques by the local people. *Bangladesh Journal of Scientific Research*, 28(2), 123–135. <https://doi.org/10.3329/bjsr.v28i2.26783>
- Islam, A., Ghosh, S., Deb, S., & Nandy, S. (2022). International journal of disaster risk reduction role of in-situ and ex-situ livelihood strategies for flood risk reduction: Evidence from the Mayurakshi River Basin, India. *International Journal of Disaster Risk Reduction*, 70(January), 102775. <https://doi.org/10.1016/j.ijdr.2021.102775>
- Jha, V. C., & Bairagya, H. (2013). Flood and flood plains of West Bengal, India: A comparative analysis. *Revista Georagauia*, 1, 1–10.
- Kahn, W. A. (1990). Psychological conditions of personal engagement and disengagement at work. *Academy of Management Journal*, 33(4), 692–724.

- Kar, S. K., Thomas, T., Singh, R. M., & Patel, L. (2018). Integrated assessment of drought vulnerability using indicators for Dhasan basin in Bundelkhand region, Madhya Pradesh, India. *Current Science*, 115(2), 338–346. <https://doi.org/10.18520/cs/v115/i2/338-346>
- Karmakar, S., Simonovic, S. P., Peck, A., & Black, J. (2010). An information system for risk-vulnerability assessment to flood. *Journal of Geographic Information System*, 02(03), 129–146. <https://doi.org/10.4236/JGIS.2010.23020>
- Khanam, R., Bhaduri, D., & Nayak, A. K. (2018). Crop diversification: An important way-out for doubling farmers' income. *Indian Farming*, 68, 31–32.
- Khetwani, S., & Singh, R. B. (2020). Drought vulnerability of Marathwada region, India: A spatial analysis. *GeoScape*, 14(2), 108–121. <https://doi.org/10.2478/geosc-2020-0010>
- Kumar, V., Cheng, S. Y. C., & Singh, A. K. (2016). Impact of flood on rural population and strategies for mitigation: A case study of Darbhanga District, Bihar State, India. *Contemporary Rural Social Work*, 8(1), 45–56.
- Laura, T.-G., Montserrat, F.-J., Maurici, R., & Eduardo, G.-M. (2020). Social vulnerability assessment for flood. *Water*, 12, 558.
- Len, N. L. S., Bolong, N., Roslee, R., Tongkul, F., Mirasa, A. K., & Ayog, J. L. (2018). Flood vulnerability of critical infrastructures – Review. *Malaysian Journal Geosciences*, 2(1), 34–37. <https://doi.org/10.26480/mjg.01.2018.34.37>
- Mollah, S. (2016). Assessment of flood vulnerability at village level for Kandi block of Murshidabad district, West Bengal. *Current Science*, 110, 81–86.
- Mukhopadhyay, S., & Let, S. (2014). Changing flood intensity zone of Dwarka river basin in eastern India. *Transactions of the Institute of Indian Geographers*, 36(1), 123–132.
- Mukhopadhyay, S. (2010). A geo-environmental assessment of flood dynamics in lower Ajoy River inducing sand splay problem in Eastern India. *Ethiopian Journal of Environmental Studies and Management*, 3(2), 96–110.
- Muttarak, R., & Lutz, W. (2014). Is education a key to reducing vulnerability to natural disasters and hence unavoidable climate change? *Ecology and Society*, 19(1), 1-8. [10.17491/ecgsi/0/v0i0/62893](https://doi.org/10.17491/ecgsi/0/v0i0/62893).
- Pant, R., Hall, J., Alderson, D., & Barr, S. (2016). *Critical infrastructure impact assessment due to flood exposure Critical infrastructure impact assessment due to flood exposure*. December. <https://doi.org/10.1111/jfr3.12288>.
- Perdikaris, J. (2010). Using multi-criteria analysis for undertaking vulnerability assessments of flood susceptible communities. *WIT Transactions on Ecology and the Environment*, 133, 35–45. <https://doi.org/10.2495/FRIAR100041>
- PMGSY. (2015). *District manual – Pradhan Mantri Gram Sadak Yojana*. Date of access: 10.06.2019. [https://darp.gov.in/sites/default/files/PMGSY\\_0.pdf](https://darp.gov.in/sites/default/files/PMGSY_0.pdf)
- Porter, J. R., Shu, E., Amodeo, M., Hsieh, H., Chu, Z., & Freeman, N. (2021). *Community flood impacts and infrastructure: examining national flood impacts using a high precision assessment tool in the United States*.
- Rahman, S. U. (2014). *Impacts of flood on the lives and livelihoods of people in Bangladesh: a case study of a village in Manikganj District*. BRAC University, Bangladesh.
- Rehman, S., Sahana, M., Hong, H., Sajjad, H., & Ahmed, B. B. (2019). A systematic review on approaches and methods used for flood vulnerability assessment: Framework for future research. *Natural Hazards, March*. <https://doi.org/10.1007/s11069-018-03567-z>
- Rodrigue, J. P., Comtois, C., & Slack, B. (2016). *The geography of transport systems*. Routledge.
- Roy, S. (2012). Spatial variation of floods in the lower Ajoy River Basin, West Bengal: A geo-hydrological analysis. *International Journal of Remote Sensing and GIS*, 1(2), 132–143.
- Rudra, K. (2014). Changing river courses in the western part of the Ganga-Brahmaputra delta. *Geomorphology*, 227, 87–100. <https://doi.org/10.1016/j.geomorph.2014.05.013>
- Rudra, K. (2018). *Geography of the physical environment rivers of the Ganga-Brahmaputra-Meghna delta a fluvial account of Bengal*. <http://www.springer.com/series/15117>

- Rufat, S., Tate, E., Burton, C. G., & Sayeed, A. (2015). Social vulnerability to floods: Review of case studies and implications for measurement. *International Journal of Disaster Risk Reduction*, 14, 470–486. <https://doi.org/10.1016/j.ijdrr.2015.09.013>
- Sahana, M., Rehman, S., Paul, A. K., & Sajjad, H. (2019). Assessing socio-economic vulnerability to climate change-induced disasters: Evidence from Sundarban Biosphere Reserve, India. *Geology, Ecology, and Landscapes*, 00(00), 1–13. <https://doi.org/10.1080/24749508.2019.1700670>
- Sanyal, J., & Lu, X. X. (2006). GIS-based flood hazard mapping at different administrative scales: A case study in Gangetic West Bengal, India. *Singapore Journal of Tropical Geography*, 27(2), 207–220. <https://doi.org/10.1111/j.1467-9493.2006.00254.x>
- Smith, B. W., Pargament, K. I., Brant, C., & Oliver, J. M. (2000). Noah revisited: Religious coping by church members and the impact of the 1993 Midwest flood. *Journal of Community Psychology*, 28(2), 169–186.
- Steinbach, D., Wood, R. G., Kaur, N., D'Errico, S., Choudhary, J., Sharma, S., Rahar, V., & Jhajharia, V. (2016). *Aligning social protection and climate resilience A case study of WBCIS and MGNREGA in Rajasthan* (Issue March). <https://doi.org/10.13140/RG.2.2.13883.03361>.
- Svetlana, D., Radovan, D., & Ján, D. (2015). The economic impact of floods and their importance in different regions of the world with emphasis on Europe. *Procedia Economics and Finance*, 34(15), 649–655. [https://doi.org/10.1016/S2212-5671\(15\)01681-0](https://doi.org/10.1016/S2212-5671(15)01681-0)
- Teri, T. E. & R. I. (2010). *Climate resilient infrastructure services case study brief: Panaji*.
- UNFCCC. (2020). Guidelines for sampling and surveys for CDM project activities and programme of activities. EB 69 Report Annex 5. [https://cdm.unfccc.int/Reference/Guidclarif/meth/meth\\_guid48.pdf](https://cdm.unfccc.int/Reference/Guidclarif/meth/meth_guid48.pdf). Accessed on 18 January 2021
- Vittal, H., & Karmakar, S. (2019). A comprehensive social vulnerability analysis at a national scale. In *Climate change signals and response* (pp. 163–176).
- Vittal, H., Karmakar, S., & Ghosh, S. (2020). *A comprehensive India-wide social vulnerability analysis: highlighting its influence on hydro-climatic risk A comprehensive India-wide social vulnerability analysis: highlighting its influence on hydro-climatic risk. x.*
- Wang, X., Liu, Z., & Chen, H. (2022). Investigating flood impact on crop production under a comprehensive and spatially explicit risk evaluation framework. *Agriculture (Switzerland)*, 12(4). <https://doi.org/10.3390/agriculture12040484>
- Wilson, R. R. (1996). Don't panic. In *Taking control of anxiety attacks*.
- Wisner, B., Blaikie, P., Cannon, T., & Davis, I. (1994). *At risk: Natural hazards, peoples vulnerability and disasters* (pp. 1–471). Routledge. <https://doi.org/10.4324/9780203714775>

# Chapter 11

## Contemporary and Future Flood Characteristics and Associated Environmental Impact: A Study of Ajay River Basin, India



Suvendu Roy 

**Abstract** Since 1956, a prominent transformation in flood characteristics of Ajay River Basin (ARB) has been observed in terms of area affected by the flood, the number of villages affected, breaching of the embankment, sand splay over agricultural land, soil nutrients, and crop productivity through different governmental reports, articles, and map. The projected climatic data by the World Resources Institute (WRI) on the depth of flood inundation up to 2080 have been analysed and found a significant rise in future flood height and areas affected by such floods at different flood return periods. In particular, about 0.5 m increase in inundation depth has been observed in 2080 at the 2-year return period, and a maximum rise of ~2 m in 2080 at the 500-year return period. The study also assessed the non-structural measures of flood control will be more effective than embankment-like structural measures for the lower region of ARB.

**Keywords** Ajay River Basin · Flood depth · Embankment · Sand-splay · Return period · Climate change

### 1 Introduction

Flood in the Ajay River Basin (ARB) is an inevitable phenomenon since the pre-historical period, and behaviour of the basin's flood has also been changed over time (Mukhopadhyay & Mukherjee, 2005; Mukhopadhyay, 2010). Ajay basin covers almost four percentage (~690 km<sup>2</sup>) of the total flood-prone area of West Bengal (~17,500 km<sup>2</sup>) (Roy, 2021), spatially which is concentrated on the downstream or lower region of the ARB, in particular below the Illambazar and after the confluence point of Hinglo tributary (Mukhopadhyay, 2010). Flood history of the ARB since the 1950s reveals that the major flooding years are 1956, 1959, 1970,

---

S. Roy (✉)

Department of Geography, Kalipada Ghosh Tarai Mahavidyalaya, Bagdogra, Darjeeling, India



**Fig. 11.1** A typical view of artificial embankment along the Ajay River near Bhedia

1971, 1973, 1978, 1984, 1995, 1999, 2000, 2005, and 2007, whereas, the most devastating experience has been observed in 1978, 1995, 1999, and 2000 (Mukhopadhyay, 2010). The economic strength of the basin area is predominantly depending on the different agricultural production, whereas, frequent floods are becoming a major problem for this region. Therefore, zamindari *bundhs* (embankments) were constructed to protect the fertile agricultural land and major settlements within the flood-prone areas (Majumdar, 1942; Mukhopadhyay, 2010). Recently, the Director of Irrigation and Waterways Department, Government of West Bengal, has made attempts to control the flood problem by repairing the old embankments and constructing new embankments, and about 10,400 km long embankment has been completed across the state (IWD-GoWB, 2019) (Fig. 11.1). In particular, a total of 136 km of embankment has been constructed along the Ajay River as of IWD-GoWB (2019), of which 81 km and 55 km are aligned along the right bank and left bank of the river, respectively (Roy, 2020).

Although, such engineering structures are failed to prevent the floods of this region and consequently welcome numerous new problems like altering channel geomorphology, increasing the flood frequency and duration of water-logged conditions particularly at the confluence zone of major tributaries, breaching of embankment and sand splay, soil fertility loss, etc. In this regard, eminent engineer Mr. S.C. Majumdar (1942) was warned about the long-term effect of embankment construction and told that the ‘construction of embankment as flood controlling measures would be like mortgaging the future generation’. The negative impacts of river regulation by embankment have been also ensured by Pethick and Orford (2013), Vlad et al. (2013), Rogers et al. (2013), and Chaudhuri et al. (2020). Rogers

et al. (2013) have estimated that the mean annual sedimentation rate ( $2.3 \text{ cm year}^{-1}$ ) in and around the embanked channel of the central Ganga-Brahmaputra delta is almost two times higher than natural inter-tidal channels of Sundarbans. Chaudhuri et al. (2020) have also ensured the statement with similar findings in addition to highlighting the negative impact of embankment-induced polder land on decreasing length of the tidal channels over time; in particular, about 59% fall in drainage network has been observed in 2013 than 2003. Vlad et al. (2013) have also listed the impact of embankment on increasing floodplain soil salinity, hydrological regime, changes in floodplain land use and significant alteration of the riverine biodiversity.

Globally, the behaviours of floods have drastically changed by changing climate, shifting land use/land cover change, water abstraction of trunk rivers, construction of dams and fragmentation of channels, and different river training programmes within the drainage basin (Habersack et al., 2015). Therefore, the basin-scale future prospect of floods is essential to understand, with the integration of past flood records for sustainable flood management based on non-structure measures instead of heavy river engineering. The primary objectives of this chapter are to evaluate the history of floods and related environmental problems in ARB and also to understand the future trends of floods in climate change scenarios up to 2080 based on modelled data archive.

## 2 Geographical Set-up of the Study Area

Ajay River (AR) is the right bank tributary of the Bhagirathi-Hooghly River (BHR) in West Bengal (WB), India. The river originates from the highlands of the Chhotanagpur plateau and meets with the BHR at Katwa (WB) after completing a run of  $\sim 299$  km over the three major geological units like high-grade metamorphic Archaean gneiss, semi-consolidated formation of Gondwana basin, and Quaternary sediments of marine-estuarine-fluviatile origin in the upper, middle, and lower sections of the basin, respectively (Niyogi, 1984, 1985). The area of the basin extends latitudinally from  $23^{\circ}25'N$  to  $24^{\circ}35'N$  and longitudinally from  $86^{\circ}15'E$  to  $88^{\circ}15'E$  and is enclosing an area of  $\sim 6050 \text{ km}^2$  within the three states of Eastern India, i.e. Jharkhand ( $\sim 53\%$ ), Bihar ( $\sim 6\%$ ), and West Bengal ( $\sim 41\%$ ) (Fig. 11.2). The basin area is also classified into upper and lower sections based on state boundary; in particular, the area under Jharkhand and Bihar is known as upper ARB, and the area under West Bengal is known as lower ARB. The major tributaries of ARB are Dakua (48 km), Parth (80 km), Jainti (87 km), Hinglow (180 km), Tumuni (192 km), Kunur (252 km), and Kundur (293 km), and the figures within first brackets are showing the distance of confluence point of respective tributaries from the source head of trunk river. The average annual discharge capacity of the river is about 2036 million  $\text{m}^3$  (Niyogi, 1984).

The range of the elevation varies from 335 m at the extreme western upland of the basin to 16 m at the confluence zone. Geomorphologically, the entire has been classified into three physiographic zone, namely, (a) dissected erosional plain with



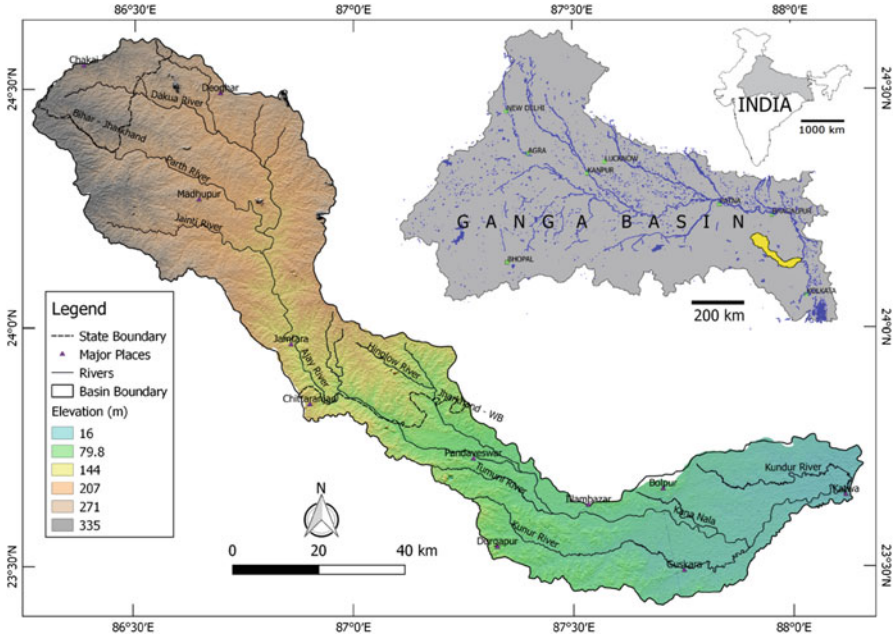


**Fig. 11.2** Location of the Ajay River Basin in the lower Ganga basin of India

monadnocks in the upper part of the basin, (b) erosional plain with broad swells and depression mainly over the Gondwana basin, and (c) riverine aggradation plain with extensively developed alluvial fans, which merge with the Bhagirathi delta proper (Niyogi, 1984). However, Bagchi and Mukherjee (1979) have classified the same in the name of as ‘plateau proper’ (>120 m), ‘plateau fringe’ (36–120 m), and ‘marginal plain’ (>36 m), respectively.

The primary climate of the basin is monsoon type, and 85% of rainfall occurs mainly during mid-June to October. The mean annual rainfall amount is 1380 mm with a mean annual temperature of 25.8° C (IMD, 2014). However, over the basin area, significant variation in rainfall amount has been observed annually as well as monthly. The type of soils and their texture over the basin are clearly associated with the lithological characteristics and pedogenic processes (Niyogi, 1985). Red-yellow and red soils with sandy loam to loamy texture have been observed on the Archaean gneiss and the areal coverage of these soil types is about 40% and 25%, respectively. The downstream area or lower basin area mainly covers by younger alluvial, older alluvial, and lateritic soils, which are about 6%, 19%, and 10% of the total basin area (Niyogi, 1985). The land use/land cover scenario of the basin reveals the intensive nature of human interference with 70–80% of agricultural land and up to 10% of agricultural waste at block level even in the uppermost areas. The basin area is covered by dry peninsula type of sal forest of only 9.9% on an average, which is temporally lost at a very high rate. The residential area has covered almost 5% of basin with six to seven major urban centres.

Administratively, the upper basin area comprises four districts of Jharkhand and a small section of Bihar, and LAB is composed of two districts of West Bengal. As per the Census of India (2011), the entire basin comes under a highly populated part of India, in particular, the districts (Jamui, 568 person/km<sup>2</sup>; Gridhi, 493 person/km<sup>2</sup>; Deogha, 602 person/km<sup>2</sup>; Jamtara, 437 person/km<sup>2</sup>) in the upper basin area are characterised with low population density in comparison with the districts (Bardhaman, 1099 person/km<sup>2</sup>, and Birbhum, 771 person/km<sup>2</sup>) of the lower part of the basin. The difference in topography and soil characteristics between the upper and lower sections of the basin might be the major cause behind this disparity.

### 3 Used Database and Methodology

To understand the contemporary as well as old flood characteristics, numerous literatures, reports, articles, and unpublished works have been studied and/or reviewed to collect secondary data regarding major flood years, magnitude, and damages. In particular, the annual flood reports from the Director of Irrigation and Waterways Department, Government of West Bengal, is one of the important sources of such flood data. A simple frequency method has been followed to analyse the trends of floods for the last 107 years, where the flood record has been categorised on a decadal basis since 1900. Mukhopadhyay (2010) initially summarised the major flooding years based on old reports and perception studies on the floodplain dwellers and also prepared the flood intensity map by overlapping layers of flood extend in different years. To get the values of channel geometry of Ajay and Kunur rivers, a geomorphic survey was done in 2012 along with some measurements using remote sensing data, e.g. DEM.

To assess the flood risk globally, the World Resources Institute (WRI) has developed a digital platform cum tool 'Aqueduct Floods' ([www.wri.org/data/aqueduct-floods-hazard-maps](http://www.wri.org/data/aqueduct-floods-hazard-maps)), a modelled raster data (spatial resolution ~0.80 km<sup>2</sup>) archive for empowering the researchers, planners, policymakers, and different stakeholders to understand the flood risk at present and in the future up to 2080 (Winsemius et al., 2013; Wrad et al., 2013, 2020). WRI performed the simulation using Global Flood Risk with IMAGE Scenarios (GLOFRIS) model (Winsemius et al., 2013) to assess the changing flood risk under climate change scenario. To analyse the flood hazard, an inundation map has been prepared to show the flood extend as well as depth of water at different return periods (2, 5, 10, 25, 50, 100, 250, 500, and 1000). With the help of hydrological model, PCRaster Global Water Balance (PCR-GLOBWB) (Sutanudjaja et al., 2018), WRI has also introduced the long-term simulations for the periods of 2030, 2050, and 2080 based on the simulation on available data for the period of 1960–1999 and presented as 2010 baseline data (Ward et al., 2020). To incorporate the future climate change, WRI also used the combination of a representative concentration pathway (RCP) (van Vuuren et al., 2011) for RCP4.5 and RCP8.5 scenario and ran different projection models of

different renowned organisations, e.g. Geophysical Fluid Dynamics (NOAA), Met Office Hadley Centre, etc.

For the present study, such database has been used to assess the flood risk of ARB in the future. In particular, flood inundation data for the years of 2010 (baseline), 2030, 2050, and 2080 at the return periods of 2, 10, 25, 50, 100, and 500 in the condition of RCP4.5 under the projection model of Geophysical Fluid Dynamics (NOAA) have been downloaded and analysed in geoinformatics platform.

## 4 Contemporary Flood Characteristics (1950s–2000s)

### 4.1 Trend in Flood Frequency During the Twentieth Century

In the last 107 years, a total of 17 major floods have been recorded over the lower ARB, which progressively increased over time (Table 11.1 and Fig. 11.3). The maximum number of floods (3) have been noticed during the decades of the 1970s and 1990s. Nevertheless, about 72% of flood events happened after 1956 only, and this year could be denoted as the period of separation between the embanked and the non-embanked basin. Therefore, such analysis reveals the role of embankments in increasing flood probability.

**Table 11.1** Decadal frequency of the major floods over the ARB since the beginning of the twentieth century

Range of time	Flood frequency		Cumulative flood frequency	
	Frequency	% of Frequency	Frequency	% of cumulative frequency
1900–1910	0	0	0	0
1911–1920	2	12	2	2
1921–1930	1	6	3	4
1931–1940	1	6	4	5
1941–1950	1	6	5	6
1951–1960	2	12	7	8
1961–1970	1	6	8	10
1971–1980	3	18	11	13
1981–1990	1	6	12	14
1991–2000	3	18	15	18
2001–2007	2	12	17	20
<b>Total</b>	<b>17</b>	<b>100</b>	<b>84</b>	<b>100</b>

Source: Flood Record Data, and Perception survey of local people, Mukhopadhyay (2010)

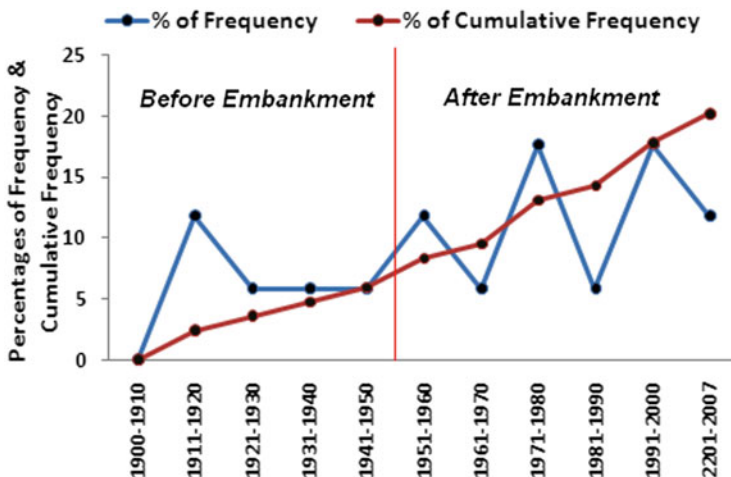


Fig. 11.3 Showing the frequency trend of major floods over ARB from 1900 to 2007

### 4.2 Spatial Extension of Flood over the Lower ARB

The spatial extension of the flood is confined along the narrow strip of the two banks at the western part of the lower ARB, but below the Illambazar up to Mangalkote, much wider areas are affected by the flood. The right bank of the river is more affected by floods than the left bank. The spatial extensions of flood-affected areas gradually increased from 1956 to 2007 (Figs. 11.4a, b). The flood intensity map is also revealing that over 60% of flood-affected areas are concentrated surrounding the embankment (Fig. 11.5). The significant role played by Kunur River Basin (KRB) in such distinguished distribution of flood areas could be perceived from the flood intensity map. The detailed geomorphic study by Roy and Mistri (2016) shows that the downstream decreasing trend of the channel carrying capacity and the rising trend of channel bed slope of Kunur River are playing crucial roles in creating havoc flood around the confluence zone of Ajay and Kunur rivers. In addition, the trend of the hydraulic gradient of groundwater is also towards the confluence zone, which is also helping to keep saturating the regional soil of this region and causing floods by generating maximum direct runoff (Roy & Mistri, 2016).

### 4.3 Trend in Flood-Affected Area Since 1956

The area affected by the flood has been significantly increased since 1956 even after the initiation of structural control of flood over the lower ARB in form of embankment construction (Table 11.2 and Fig. 11.6). Average ~ 33% of the lower ARB has been severely affected by flood in every major annual flood event, and the overall

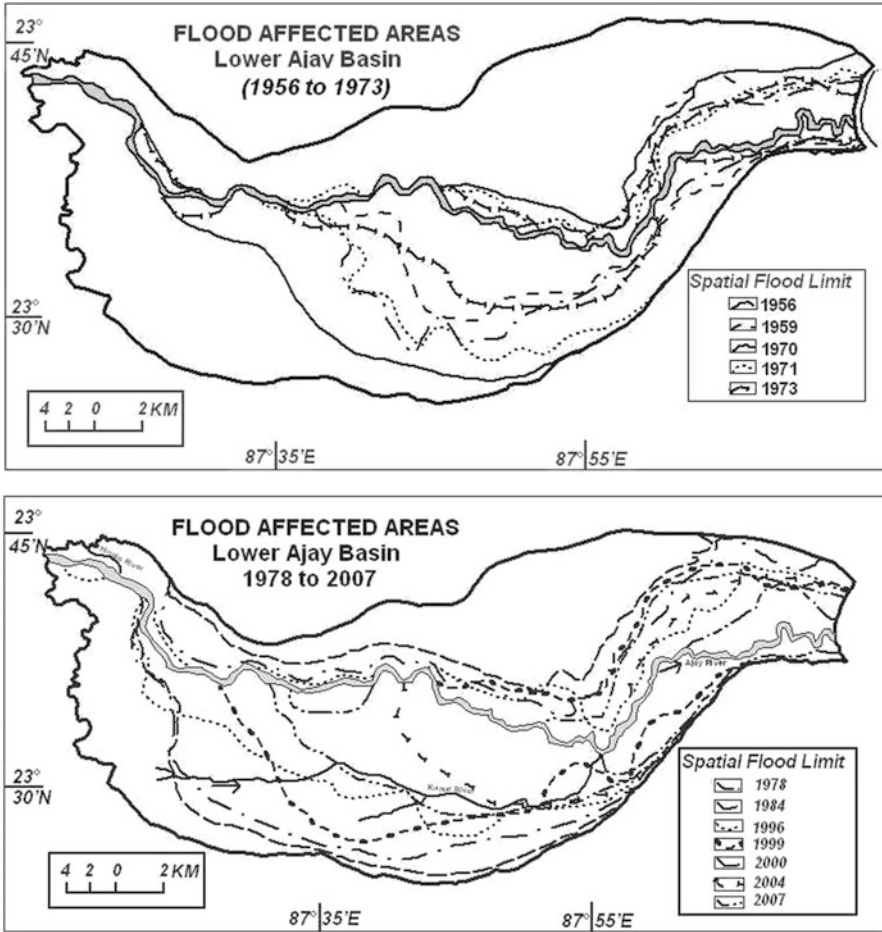


**Fig. 11.4** (a, b) Progressive change of flood-affected areas in lower ARB from 1956 to 2007. (Source: Mukhopadhyay, 2010)

trend of the flood-affected area is also rising. A noticeable amount of mouzas (village-level administrative units) also experienced the disaster by losing a huge amount of agricultural land by floodwater inundation and sand splay (Tables 11.2 and 11.3). Statistically, the number of mouza affected ( $r = 0.95, p < 0.1$ ) and area of sand splay ( $r = 0.79, p < 0.1$ ) are also positively correlated with the area of flood affected in the lower ARB at 99% level of significance. Breaching of the embankment is the main cause of sand splay across the lower ARB. Due to the poor structure and lack of maintenance of the existing embankment, breaching occurred on the side

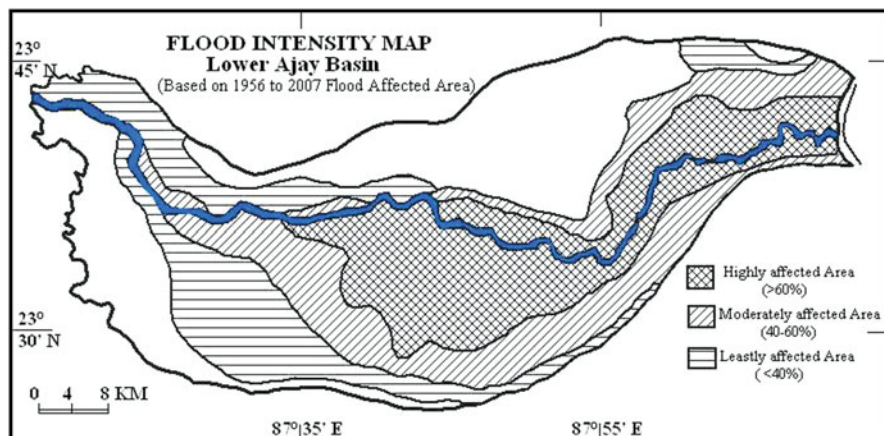


**Fig. 11.5** Flood intensity map in lower ARB. (Source: Mukhopadhyay, 2010)

**Table 11.2** Flood-affected area of the lower Ajay River Basin from 1956 to 2007

Year	Affected area (km <sup>2</sup> )	% of total lower basin area	Affected number of mouzas			Extent of sand splay in hectares	Maximum extension of sand splay from river embankment (distance in km)
			Entirely affected	Partially affected	Total		
1956	680.00	24.14	153	32	185	231.45	0.38
1959	584.34	20.74	120	27	147	269.63	0.38
1970	812.24	28.83	186	36	222	693.48	0.47
1971	642.71	22.81	130	31	161	762.11	0.78
1973	639.02	22.68	124	36	160	1193.2	1.12
1978	1680.00	59.64	307	67	374	3421.32	2.42
1984	305.72	10.85	78	20	98	865.55	0.68
1995	1380.82	48.99	227	49	276	1245.67	1.4
1999	1408.00	49.98	237	60	297	2567.23	2.12
2000	1488.00	52.82	263	106	369	3788.25	2.57
2006	764.23	27.12	152	46	198	2143.56	1.35
2007	972.79	34.53	214	79	293	2421.57	1.76

Source: Department of Irrigation and Waterways, Govt. of West Bengal (2001)

of the embankment at different places in the study area. The number of breaching points was also rapidly increasing downstream of the basin (Fig. 11.6). It is also confirmed that the breaching points are more concentrated on the right bank of the river and the numbers are also increased with time; in 1978 it is 12, in 1999, it is 22, in 2000, it is 25, and in 2005, it is 8 in number.

**Table 11.3** Sand splay cover and loss of cultivated land due to post-flood hazard

Name of the mouza	Area covered by sand splay (% of total area)	% of land loss to the total cultivated area	Name of the mouza	Area covered by sand splay (% of total area)	% of land loss to the total cultivated area
Bhedia	33.58	18.40	Itanda	42.43	39.89
Brahmandihi	21.66	32.00	Nabagram	16.43	30.7
Malocha	38.08	25.67	Natunhat	18.60	23.99
Maliara	44.03	21.52	Bira	17.30	24.82
Basudha	32.07	23.59	Narenga	20.32	29.84
Gitgram	58.92	30.80	Srikrishnapur	38.20	51.92
Natungram	36.74	44.66	Husainpur	48.25	26.66
Rasulpur	33.82	36.58	Vepura	44.46	40.00
Haripur	38.12	43.00	Pandura	21.39	17.08

Source: Burdwan and Birbhum Zilla Parishad Office and Handbooks (2001)

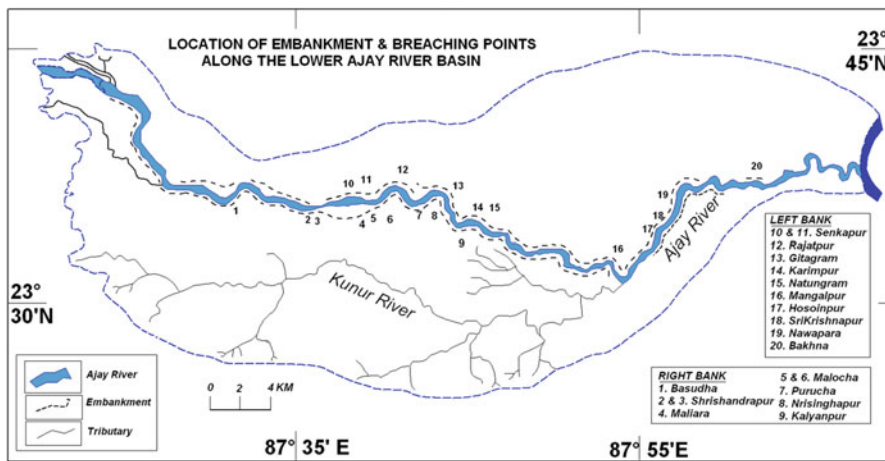


**Fig. 11.6** Location of breaching points along the right and left bank embankments of the lower ARB

### 4.4 Dominant Impact on Agriculture

The lower ARB is basically well known as an agricultural hub for producing rice, wheat, sugar cane, oilseeds, and potato as major crops with high productivity. It is estimated that 62.58% of the total land is used for cultivation of which 40.27% is irrigated and 22.31% is non-irrigated. Forested land occupies only 13.17% of the total area and is mostly concentrated on the right bank than the left bank (Mukhopadhyay, 2010). However, due to frequent floods, embankment breaching and sand splay significantly affect the agricultural system by losing cultivated area

**Table 11.4** Decreasing rate of rice production (kg/ha)

Name of the mouza	Before sand splay 1998	After sand splay 2000
		(marginal area)
Bhedia	3750	1500
Natungram	4000	750
Maliara	3000	800
Srikrishnapur	4500	1500
Narenga	3600	1312
Gomra	3375	500

Source: Mukhopadhyay (2010)

**Table 11.5** Nutrient status of the soil before and after flood of 2000

Name of the mouza	Ph		N <sub>2</sub> (kg/ha)		P <sub>2</sub> O <sub>5</sub> (kg/ha)		K <sub>2</sub> O (kg/ha)	
	Before	After	Before	After	Before	After	Before	After
Natungram	6.6	7.5	200	49.5	90	7.9	294	46
Gitgram	7.0	7.3	250	30.5	85	4.2	240	65
Maliara	7.1	7.1	280	39	21.2	4.2	316	59
Bhedia	6.9	6.9	330	26.4	45.5	3.6	305	72
Srikrishnapur	7.0	8.2	300	35	70	5.5	220	70

Source: Technical Report, Vol.7, Dept. of Soil Science, Palli Siksha Bhabana, Visva-Bharati

(Table 11.3), decreasing the productivity of rice (Table 11.4), and deteriorating soil fertility (Table 11.5). The agricultural land of riverside villages, like Bhedia, Brahamandihi, Malocha of Aushgram block; Kogram, Mangalkot, Halimpur of Mangalkot block and other different villages, have been seriously affected.

#### 4.5 Effect on the Channel Geomorphology

Generally, the alluvial river system follows the thumb rule of downstream widening of channel (Knighton, 1987; Leopold & Maddock, 1953) and increasing the degree of lateral connectivity (Wohl, 2017). However, an inverse scenario has been observed for the downstream section of the Ajay River might be for the installation of the embankment and related alteration of flow pattern. Table 11.6 shows the downstream decreasing trends of channel width and width-depth ratio, which reveals the poor lateral connectivity between floodplain and channel and causing threat to the river ecology (Wohl, 2017) (Fig. 11.7). However, depth of the channel has been increased towards down, which is indicating incision of channel below the Illambazar to contain enormous volume of upstream water because of the higher stream power as the average unit stream power is inversely correlated with the channel width (Baker & Costa, 1987). As a result, the possibility of bank erosion and embankment breaching has been increasing in the lower ARB. In addition, the presence of embankment also induces to rise of the river bed by gradual siltation of



**Table 11.6** Anomalies in channel geometry towards downstream of Ajay River

Cross-section site	Elevation (m)	Distance from confluence (km)	Channel width (w) (m)	Maximum depth (d) (m)	Width-depth ratio (w/d)
Pandaveswar	65	130.28	1026	11.89	86.29
Jaydeb Kenduli	59	111.00	719	10.51	68.41
Bankati	58	106.27	518	9.39	55.17
Ramchandrapur	50	85.12	345	8.58	40.21
Bhedia	44	77.08	473	7.02	67.38
Paligram	36	59.42	273	11.48	23.78
Kalyanpur	29	50.31	316	10.68	29.59
Kogram	27	44.34	221	11.78	18.76

Source: Roy and Mistri (2016)



**Fig. 11.7** Showing the contrast in channel width of Ajay River between near Pandaveswar (a) and Nabagram (b), ~130 km and ~6 km upstream reaches from the confluence, respectively

suspended sediment after restricting the spillover of floodwater over the floodplain area. Thereby, over time the channel area fails to accommodate the upcoming storm water and consequently increases the flood frequency as well as magnitude. Roy and Mistri (2016) have also observed that since 1956 the stage of discharge has also increased at different gauging stations of Ajay River.

## 5 Future Scenario of Flood Height and Affected Area (up to 2080)

The impact of climate change on increasing flood height has been clearly detected from the model data by WRI (Fig. 11.8). A gradual increase in the average flood height from 2010 to 2080 has been observed in every return period. The average increases in flood height for all the four periods (2010, 2030, 2050, 2080) show it is 0 m, 2.33 m, 4.93 m, 5.24 m, 5.79 m, and 6.35 m, for the return period of 2, 10, 25, 50, 100, and 500 years, respectively. In hydro-geomorphology, a 2-year return period is treated as the most probable as well as frequent flood level of a river system (Leopold et al., 1964), which is also increased by ~0.5 m in 2080. A maximum

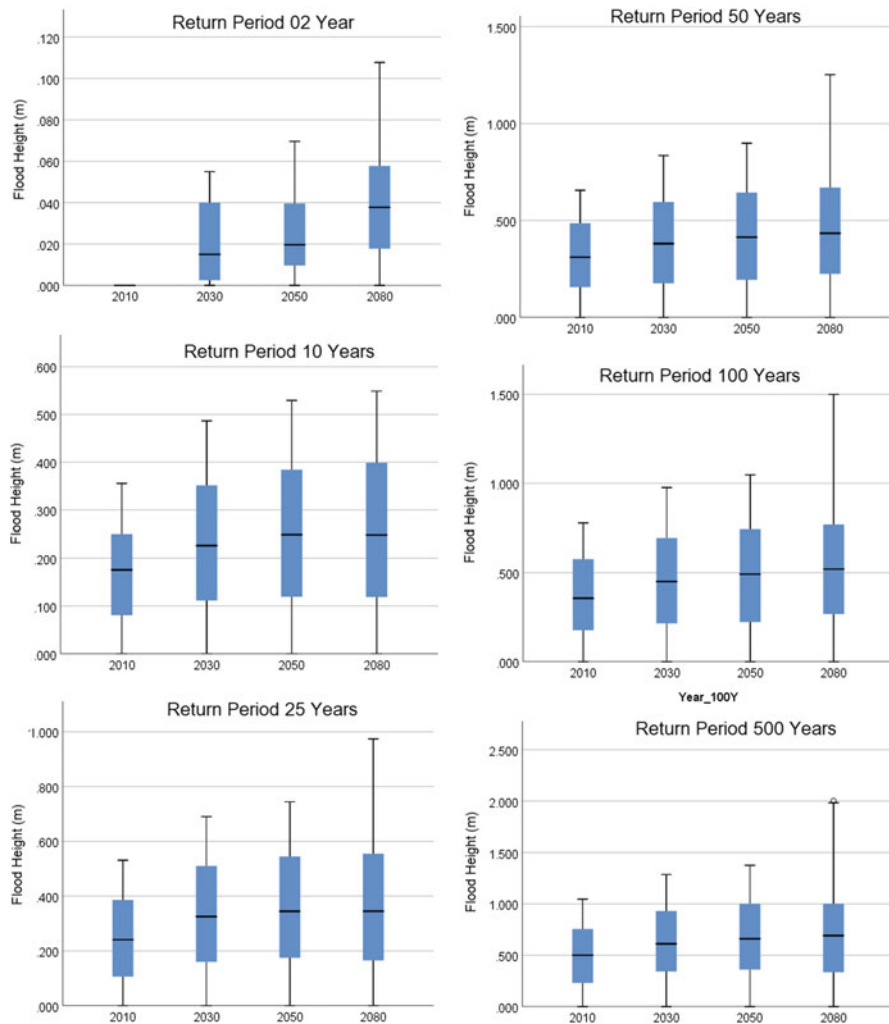


**Fig. 11.8** Changing future scenario of flood inundation depth (m) over the ARB at different return periods

possible increase of ~2 m in flood height has been observed in 2080 at the 500-year return period, which would be a devastating situation for the ARB. With increasing flood height over time, the area affected by the respective flood height is also enhanced in different return periods (Table 11.7). For example, the area covered by flood height of above 0.5 m is nil at the 2-year return period; however, it reached up to ~7 km<sup>2</sup> at the 500-year return period (Fig. 11.9). Previously, Dhar (2010) also projected a significant change in Ajay River’s flow pattern and soil moisture on four

**Table 11.7** Changes in the spatial coverage of basin area (in km<sup>2</sup> and percentage) at different flood heights in different return periods

Flood depth (m)	2010										2030										2050										2080									
	Area under varying flood heights (km <sup>2</sup> ) at different return periods										Area under varying flood heights (km <sup>2</sup> ) at different return periods										Area under varying flood heights (km <sup>2</sup> ) at different return periods										Area under varying flood heights (km <sup>2</sup> ) at different return periods									
	2	10	25	50	100	500	2	10	25	50	100	500	2	10	25	50	100	500	2	10	25	50	100	500	2	10	25	50	100	500										
0	6050	5728	5705	5683	5665	5622	5767	5713	5676	5654	5628	5586	5766	5707	5668	5642	5575	5575	5761	5704	5663	5641	5621	5571	5761	5704	5663	5641	5621	5571										
0.001–0.250		32	32	37	42	39	283	32	42	39	41	35	284	32	43	41	29	29	290	33	46	40	38	32	290	33	46	40	38	32										
0.251–0.500		290	31	35	32	41		306	32	39	45	42		31	32	39	43	43		31	35	42	43	46		31	35	42	43	46										
0.501–0.750			282	295	31	35			300	29	31	42		281	307	35	42	42		282	303	35	36	39		282	303	35	36	39										
0.751–1.000					281	31				288	306	33					36	36				293	36	43				290	31	43										
1.001–1.250						282						31					34	34					34	30				3	279	30										
1.251–1.500												282					292	292					292	284					3	284										
1.501–1.750																														2										
1.751–2.000																														3										



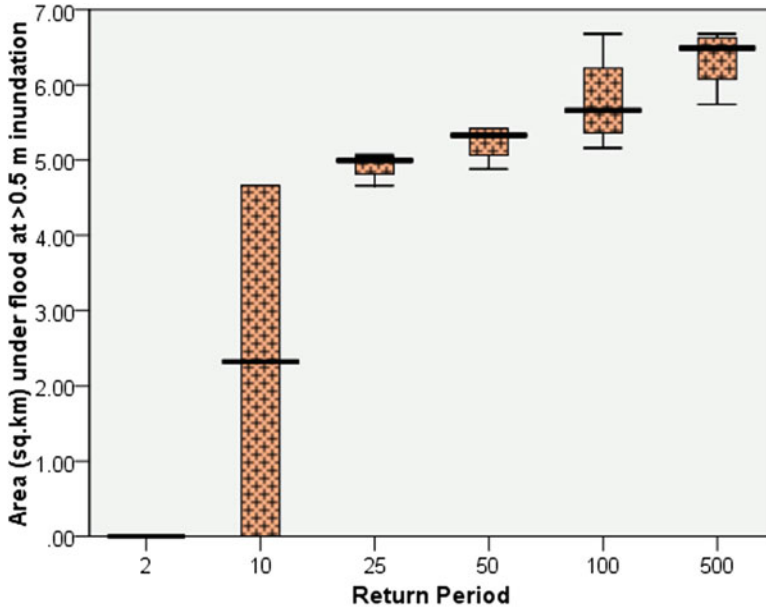


**Fig. 11.9** Increase in spatial coverage of flood with the inundation depth of more than 0.5-m flood height at different return periods

different sub-watersheds during 2040–2050 under the impact of future climate change through the modelling of projected data from the Hadley Centre for Climate Prediction (UK).

## 6 Concluding Remarks

The impact of floods on the ARB (particularly in the lower section) has been increased with time to the expansion of flood-affected areas, flood height, reduction of soil nutrients and crop productivity, the number of villages affected, etc., which is revealed from the previously documented data as well as from the recently available digital modelled data by WRI under the changing condition of climate. The negative effect on channel geomorphology is also prominent for the trunk river by altering channel width, depth, and width-depth ratio. In particular, the enhancement of such effects has been observed since 1956, which is the year of artificial embankment installation alongside the Ajay River in the downstream region. Therefore, instead of structural measures for flood control through artificial embankment along the river, non-structure measures like restoration of floodplain through afforestation, regulation on land use, flood-prone area delineation, timely flood forecasting and warning, and disaster prevention measures would be more effective for the ARB. The

projected data model is showing a prominent increase in flood inundation depth; in particular, about 0.5 m increase has been observed in 2080 at the 2-year return period, and a maximum rise of ~2 m in 2080 at the 500-year return period. Consequently, the area under floodwater is also positively increasing with rising inundation depth, although having some issues of underestimation of flood-affected areas in the modelled data in comparison with the previously documented data. Such anomaly may arise due to less information about present channel morphometry and the degree of connectivity of drainage network.

## References

- Bagchi, K., & Mukherjee, K. N. (1979). *Diagnostic survey of Rarh Bengal, part –I, morphology, drainage and flood: 1978*. Department of Geography, University of Calcutta.
- Baker, V. R., & Costa, J. E. (1987). Flood power. In L. Mayer & D. Nash (Eds.), *Catastrophic flooding* (pp. 1–21). Allen and Unwin.
- Census of India. (2011). Population Enumeration Data (Final Population). Access from [https://censusindia.gov.in/2011census/population\\_enumeration.html](https://censusindia.gov.in/2011census/population_enumeration.html) on 03/07/2019
- Chaudhuri, S., Chaudhuri, P., & Ghosh, R. (2020). The impact of embankments on the geomorphic and ecological evolution of the deltaic landscape of the indo-Bangladesh Sundarbans. In *River deltas – recent advances*. IntechOpen. <https://doi.org/10.5772/intechopen.94163>
- Dhar, S. (2010). Investigation into the effect of climate change for the Ajay River basin using hydroinformatics. *Journal of Management and Public Policy*, 2(1), 22–36.
- Habersack, H., Schober, B., & Hauer, C. (2015). Floodplain evaluation matrix (FEM): An interdisciplinary method for evaluating river floodplains in the context of integrated flood risk management. *Natural Hazards*, 75, 5–32. <https://doi.org/10.1007/s11069-013-0842-4>
- Indian Meteorological Department (IMD). (2014). *IMD District wise normal, Bardhaman*. Govt. of India.
- IWB-GoWB: Irrigation and Waterway Directorate-Govt. of West Bengal. (2019). Annual Flood Report for the Year 2016. In *Advance planning, project evaluation, and monitoring cell*. Jalsampad Bhavan.
- Knighton, A. D. (1987). *River channel adjustment – The downstream dimension* (pp. 95–128). River Channels: Environment and Process, Basil Blackwell, Oxford.
- Leopold, L. B., & Maddock, T. J. (1953). Hydraulic geometry of stream channels and some physiographic implications. *U. S. Geological Survey Professional Paper*, 252. 55 p.
- Leopold, L. B., Wolman, M. G., & Miller, J. P. (1964). *Fluvial processes and geomorphology* (1st ed.). Freeman.
- Majumdar, S. C. (1942). *Rivers of Bengal Delta* (pp. 16–22). Calcutta University.
- Mukhoopadhyay, S., & Mukherjee, M. (2005). *Hydrological characteristic of flood: A study in the lower Ajoy river, river floods: A socio technical approach* (pp. 51–58). ABC Publications.
- Mukhopadhyay, S. (2010). A geo-environmental assessment of flood dynamics in lower Ajoy River including sand splay problem in eastern India. *Ethiopian Journal of Environmental Studies and Management*, 3(2), 96–110.
- Niyogi, M. (1984). *Water resources of the Ajay Basin – A geographical – Hydrological study*. Ph. D. Thesis, Department of Geography, University of Calcutta.
- Niyogi, M. (1985). Ground water resource of the Ajay Basin. In S. P. Chatterjee (Ed.), *Geographical Mosaic- Professor K.G. Bagechi felicitation* (pp. 165–182). Manasi Press.
- Pethick, J., Julian, D., & Orford, J. D. (2013). Rapid rise in effective sea-level in Southwest Bangladesh: Its causes and contemporary rates. *Global and Planetary Change*, 111, 237–245.

- Rogers, K. G., Goodbred, S. L., Jr., & Mondal, D. R. (2013). Monsoon sedimentation on the 'abandoned' tide-influenced Ganges–Brahmaputra delta plain. *Estuarine, Coastal and Shelf Science*, *131*, 297–309.
- Roy, S. (2020). Anthro-geomorphological signatures over the Ajay River Basin. In B. Das, S. Ghosh, A. Islam, & S. Roy (Eds.), *Anthropogeomorphology of Bhagirathi-Hooghly River System in India (in press)*. CRC Press, Boca Raton. <https://doi.org/10.1201/9781003032373>
- Roy, S. (2021). Impact of linear transport infrastructure on fluvial connectivity across the catchments of West Bengal. *India. Geocarto International*, *37*, 5041. <https://doi.org/10.1080/10106049.2021.1903576>
- Roy, S., & Mistri, B. (2016). Flooding in the confluence zone of the Ajay and the Kunur Rivers, West Bengal: A Hydrogeomorphological assessment. *Journal of Indian Geomorphology*, *4*, 73–83.
- Sutanudjaja, E. H., van Beek, R., Wanders, N., Wada, Y., Bosmans, J. H. C., Drost, N., van der Ent, R. J., et al. (2018). PCR-GLOBWB 2: A 5 Arcmin global hydrological and water resources model. *Geoscientific Model Development*, *11*, 2429–2453. <https://doi.org/10.5194/gmd-11-2429-2018>
- van Vuuren, D.P.J., Edmonds, M., Kainuma, K., Riahi, A., Thomson, K., Hibbard, G.C., Hurtt, et al. (2011). The Representative Concentration Pathways: An Overview. *Climate Change*, *109*, 5–31. <https://doi.org/10.1007/s10584-011-0148-z>
- Vlad, L. M., Ilas, I., & Bartha, I. (2013). The effects of river regularization, embankment and draining on the ecology. *Present Environment and Sustainable Development*, *7*(1), 236–243.
- Ward, P. J., Jongman, B., Weiland, F. S., Bouwman, A., van Beek, R., Bierkens, M. F. P., Ligtoet, W., & Winsemius, H. C. (2013). Assessing flood risk at the global scale: Model setup, results, and sensitivity. *Environmental Research Letters*, *8*, 044019. <https://doi.org/10.1088/1748-9326/8/4/044019>
- Ward, P. J., Winsemius, H. C., Kuzma, S., Bierkens, M. F. P., Bouwman, A., de Moel, H., Díaz Loaiza, A., et al. (2020). *Aqueduct floods methodology. Technical note*. World Resources Institute. Retrieved from: [www.wri.org/publication/aqueduct-floods-methodology](http://www.wri.org/publication/aqueduct-floods-methodology), on 5th June 2022
- Winsemius, H. C., van Beek, L. P. H., Jongman, B., Ward, P. J., & Bouwman, A. (2013). A framework for Global River flood risk assessments. *Hydrology and Earth System Sciences*, *17*, 1871–1892. <https://doi.org/10.5194/hess-17-1871-2013>
- Wohl, E. (2017). Connectivity in rivers. *Progress in Physical Geography*, *41*(3), 345–362. <https://doi.org/10.1177/0309133317714972>

# Chapter 12

## Nature of Floods in the Khari River Basin, Eastern India



Subhankar Bera and Abhay Sankar Sahu

**Abstract** Floods over the deltaic land of Ganga-Brahmaputra-Meghna River system made a unique fluvial landscape. This flat anastomosing landscape is developed by overtopping and deposition of alluvium in their course and has diversity in flood nature from one to other river systems. The objective of this work is to discuss the flooded nature of the Khari River Basin (KRB) and areas of active flood that can be vulnerable to society. The KRB is a small right-hand tributary of the Bhagirathi-Hugli stream of the lower Ganga River system. Geomorphic parameters of basin and drainage networks have been used and analyzed in the GIS domain. High-surface runoff and seepage are the causes of peak flow during monsoon time which creates four to five times flood every year. Active floodplain of the Khari River is the regional geomorphic low surface discontinued by geomorphic highs where channels are more sinuous. Intensive flood and wider floodplain have been observed between Palumba and Randa village that is the result of high discharge by large tributaries, draining approximately 45% of the KRB area. Human intervention in form of longitudinal discontinuation of the floodplain has made artificial damming in the natural flow direction that intensifies the flood over this region. Though this waterlogged area is vulnerable for the floodtime crops, it helps in high yielding after the flood, and most settlements are located above the active floodplain.

**Keywords** Flood · River system · Basin morphology · Small river · Human intervention

### 1 Introduction

Flood is a geomorphic, meteorological, and hydrological process of a drainage basin in the plain land and in the deltaic part that alters the existing landforms. Though flood is a natural phenomenon, sometimes human activities are causes of floods. Flood is a major problem in the floodplains, areas that are often attractive for human

---

S. Bera (✉) · A. S. Sahu  
Department of Geography, University of Kalyani, Kalyani, West Bengal, India



developments, and in the period from 1970 to 2012, floods caused over one million deaths (WMO-World Meteorological Organization; <https://public.wmo.int/en/our-mandate/water/floods>, dated: 23/09/21). As reported by the WHO (World Health Organization), in between 1998 and 2017, more than 2 billion people have been affected by floods worldwide, and in the last 10 years, 80–90% of documented natural hazards are caused by floods, severe storms, and tropical cyclones ([https://www.who.int/health-topics/floods#tab=tab\\_1](https://www.who.int/health-topics/floods#tab=tab_1), dated: 23/09/2021). Among the continents, Asia faced the average highest numbers of flood events that continually increase in the last 65 years, and in the last decade, average of 60 major floods were reported every year (Sohoulande & Singh, 2016).

Over the Indian subcontinent, the significant increasing intensity and frequency of extreme precipitation events are potential to lead the flood events, though few recent studies in monsoon show a gradual decline circulation and precipitation amount over India (Ali et al., 2019). Frequent flooding of the Gangetic West Bengal is an inherent characteristic, particularly in the western part of the Bhagirathi-Hugli River. At present, ~42.55% of the total geographical area of this state is susceptible to flood (I & W. D., Govt. of W.B., Annual Flood Report, 2020). Floods in North Bengal are caused by rivers draining in the Himalayan parts. In South Bengal, mostly rivers like Ajay, Mayurakshi, Damodar, and Kangsabati are draining the Chotanagpur plateau and finally outfall into the Bhagirathi-Hugli River and carry a huge volume of water during the monsoon season or in an event of extreme precipitation that causes floods in the Deltaic Rarh Bengal (DRB). Thus, understanding flood nature became necessary for regional development. As flood is an event in the area of drainage basin, the study of drainage characteristics or drainage basin morphometry has become a pioneer of flood analysis that is helpful in flood risk control (Odiji et al., 2021; Leopold & Miller, 1956; Leopold & Maddock, 1953).

The flood of the DRB has widely been studied in different fields focusing on the large rivers which had developed devastating hazards for the society like floods at the lower part of the Mayurakshi, Ajay, Damodar, and Dwarakeswar River Basin (Islam & Barman, 2020; Pal et al., 2020; Islam & Sarkar, 2020; Mukhopadhyay, 2010; Malik & Pal, 2021; Ghoh & Guchhait, 2016; Singh et al., 2020). The interfluves of small river basins are paid less attention because of lack of data, though these rivers are also potentially vulnerable. The Khari River Basin (KRB), which is the focused area of this study, has no research work on the basin characteristics and flood. The KRB has been first explored by Bagchi and Mukherjee (1979) and Sen (1993) in terms of geomorphic analysis of this region and later on by Singh et al. (1998), Chakrabarti and Nag (2015), Roy & Sahu (2015), Roy and Bera (2018), and Barman et al. (2018), focusing on the aspects of regional tectonics and basin, and less importance has been given to understanding these interfluves of rivers' geomorphic process and flood nature. So, the objective of this work is to discuss the flood of the KRB and the role of the drainage basin morphometry and to prepare a map of the active floods areas that are vulnerable to society. This work also will help to understand the geomorphology and hydrological characteristics of West Bengal's small alluvial rivers.

## 2 Study Area

The KRB is a right-hand tributary drainage of the lower Ganga River system, draining an area of 1208 km<sup>2</sup> of the interfluvies of Ajay-Damodar Rivers of the Purba Bardhaman district, India. The Khari River is originating from the Panagarh lateritic upland (23°24'44.50"N, 87°31'58.56"E) at an altitude of ~58 meters (above MSL), near Maro village, and flows eastward ~212 km and joined with the Bhagirathi-Hugli River near the Kalna Town (23°16'4.67"N, 88°19'46.53"E) (Fig. 12.1a). Geographical extension of the studied KRB is 23°16'N to 23°32'N latitudes and 87°30'E to 88°18'E longitudes. The KRB drains the administrative area of Budbud, Galsi, Bhatar, Monteswar, Purbasthali, the northern part of Burdwan, the southern part of Katwa, and Mongalkote police stations.

Physiographically, the study basin comes under the eastern part of the “Rarh Bengal” (Bagchi & Mukherjee, 1979), and the surface geological formation of this region is mostly covered by quaternary alluviums (District resource map, GSI, 2001) (Fig. 12.1b). Geomorphologically, the KRB is an old deltaic part which belongs to the Damodar para-delta (Singh et al., 1998). Bagchi & Mukherjee (1979) divided the major relief characteristics of this area into three physiographical units that are marked by the counters of 18 m and 36 m, respectively (Roy & Sahu, 2015) (Fig. 12.1a). The climatic condition of the area is tropical wet and dry (aw) in

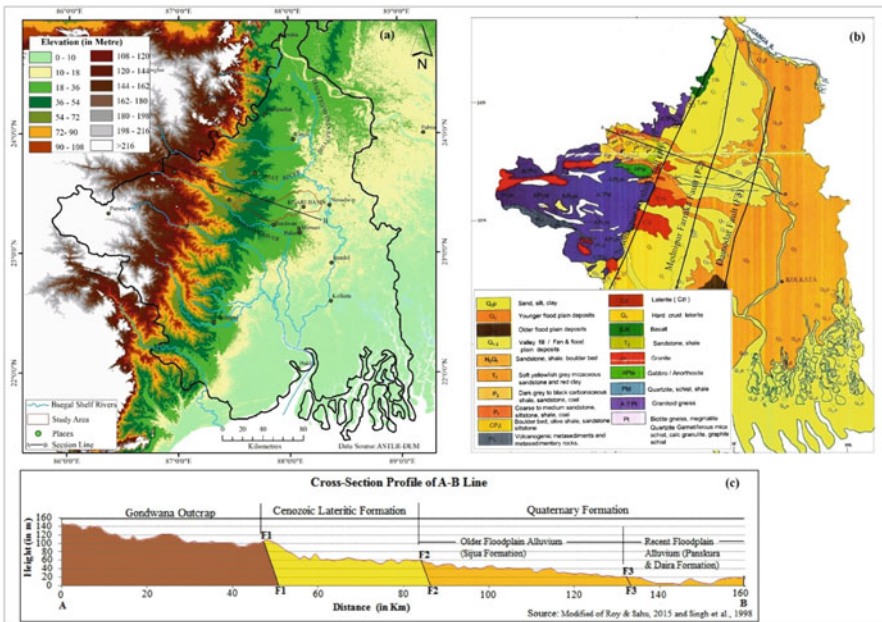


**Fig. 12.1** Location map of the study area. (a) Elevation map of the study area and the surroundings, (b) surface geology of the South West Bengal and study area with major faults, and (c) cross section of the surface geology along the A-B represents the surface slope and surface formation

types controlled by the seasonal migration of tropic of cancer (23°0.30'N). Mean annual temperature of the region is ~26.3 °C and receives more than 100 mm mean annual rainfall, and approximately 80% of the total precipitation goes on in the monsoon months with an average of 350 mm. Though the Khari River is mainly rain-fed, bankfull discharge is observed during the monsoon period or torrential rainfall of depression that developed floods.

### 3 Database and Methodology

The main data used in this work is ASTER Global DEM (Advance Spaceborne Thermal Emission and Reflection Radiometer, spatial resolution of 30 m), and heights that were obtained from the Survey of India topographical maps (79A/3& 79A/7 of 1:50,000 scale) have been used to develop the surface elevation map (SEM) in ArcGIS. Finally, the SEM database has been applied to compute the basin aerial and relief morphometric data by dividing the basin into 1 km<sup>2</sup> grids. The KRB drainage network (Fig. 12.2) has been digitized from the “aerial Bing map”(spatial resolution view of 0.30–0.33 m) through QGIS “OpenLayer Plug-in tool” and delineated after Strahler’s classification (1964), which were used for the analysis of linear morphometry of the basin. The KRB has also been delineated into 17 sub-basins and named as A to Q for the detailed analysis of flood potentiality (Fig. 12.2). The surface runoff dominates sub-basins D and N, Q has no tributary, and the paleochannels have dominated M. Therefore, these sub-basins themselves are areas of water logging. A total of 16 parameters (Table 12.1) have been used for the drainage network and basin morphometric analysis which are grouped into (a) linear parameters, (b) aerial parameters, and (iii) relief parameters. A correlation has been run between the 16 parameters to look at the association among them (Fig. 12.3).

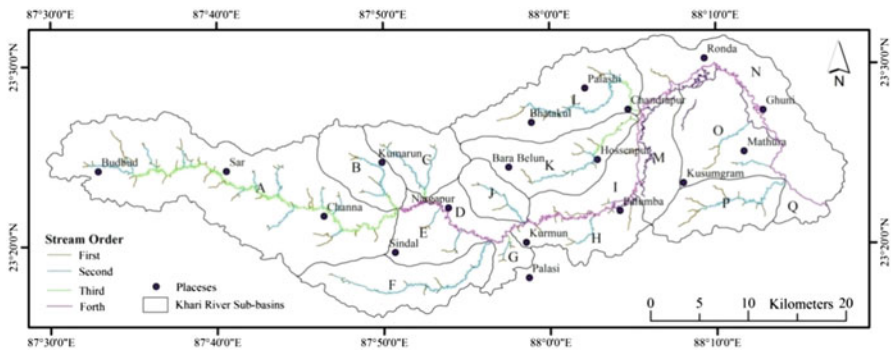


Fig. 12.2 KRB sub-basins and the drainage hierarchy

**Table 12.1** Morphometric parameters used to evaluate the KRB flood

Aspect of analysis	Morphometric parameters	Equation/formula	Followed by	Remarks
Linear aspect	Stream order (u)	Stream hierarchy	Strahler (1964)	The higher the order are, the more potential of hydraulic efficiency.
	Stream number (nu)	$N_u \frac{1}{4} N_{1p} N_{2p} \dots$ $N_n$	Horton (1945)	Comparative assessment of stream number shows surface runoff and channelized flow of water.
	Stream length ratio ( $S_{lr}$ )	$S_{lr} = L_u / L_{u-1}$	Horton (1945)	Shows the evolution of the geomorphic streams that can be related to hydraulic efficiency.
	Bifurcation ratio ( $R_b$ )	$R_b = N_u / N_{u-1}$	Schumm (1956)	$R_b$ normally ranges between 3.0 and 5.0 which indicate natural drainage system of homogenous surface, and the higher or lower values indicate the irregularities in drainage basin evolution with varied lithological and structural controls.
	Mean bifurcation ratio ( $B_R$ )	$B_R =$ average of $R_b$	Strahler (1957)	
	Stream gradient ratio ( $S_g$ )	$S_g = (a-b)/l$	Sreedevi et al., (2005)	Higher the $S_g$ is steep slope, and lower values of $S_g$ are gentle slope, which indicates the stream power and discharge potentiality of individual stream.
Aerial aspect	Stream frequency ( $S_f$ )	$S_f = \sum N_u / A$ (no./ $km^2$ )	Horton (1945)	Shows the flow concentration of unit area of watershed to runoff processes.
	Drainage density ( $D_d$ )	$D_d = \sum L_u / A$ ( $km/km^2$ )	Horton (1945)	Higher density is largely associated with floods in lower basin part.
	Form factor ( $F_f$ )	$F_f = A/L^2$	Horton (1945)	The value 0.786 is a circular basin, and lower values (<0.5) shows narrow and elongated watershed that are more vulnerable to flood.
	Elongation ratio ( $E_r$ )	$E_r = 1.128\sqrt{(A/L)}$	Schumm (1956)	Shows the shape of the basin, circular (0.9–1.0), oval (0.8–0.9), less elongated (0.7–0.8), elongated (0.5–0.7), and more elongated (<0.5) that are linked with runoff potentiality.
	Circularity ratio ( $C_r$ )	$C_r = 4\pi A/P^2$	Strahler (1957)	Identify the circularity of the basin. Lower values (<1) indicate elongated form and runoff generation.
	Compactness coefficient ( $C_c$ )	$C_c = 0.2821 P/A^{0.5}$	Gravelius (1914)	Is the ratio between the perimeter of the basin and the circumference of a circle; that area is equal to basin and used for inter-basin comparison.

(continued)

**Table 12.1** (continued)

Aspect of analysis	Morphometric parameters	Equation/formula	Followed by	Remarks
	Constant of channel maintenance ( $C_m$ )	$C_m = 1/D_d$	Schumm (1956)	Shows the dynamic equilibrium nature of basin and comprises an important channelized flow indicator.
	Length of overland flow ( $L_o$ )	$L_o = 1/2 D_d$	Horton (1945)	Shows the hydrological and physiographic condition of basins.
Relief aspect	Relative relief ( $R_r$ )	$R_r = B_r / L$	Schumm (1956)	Value $>0.5$ indicates high relative relief areas and $< 0.5$ shows low relative relief that are linked with basin surface slope.
	Absolute relief ( $A_r$ )	$A_r = H-h$	Schumm (1961)	Indicates the unit gradient distribution which helps to interpret runoff potentiality.

## 4 Result and Discussion

The KRB is an elongated fourth-order drainage basin of 1 fourth-order stream, 6 third-order stream, 33 second- order streams, and 157 first-order streams, and the width of the basin increases downstream from about 8.5 km to ~17 km. Though both sides of the trunk river are drained by an equal number of sub-basins, the number of left-side streams is almost double than the right side, and the gradient of the streams are steeper than the right side (Table 12.2). Total length of the stream is ~537 km with the drainage density of ~0.44 km/km<sup>2</sup>, where first, second, third, and fourth order contribute almost 27%, 36%, 17%, and 20%, respectively, of the total length. The total length and the area of the left-side drainage basins are also greater than the opposite side. Sub-basin variations of the stream order, number, and stream length are given in Table 12.2. Though these three have no direct relation in peak flood generation, it has a positive relation with surface runoff generation that developed flood (Nageswara Rao, 2020). The mean bifurcation ratio of the KRB is  $B_r = 5.42$ , that is, higher than any other small rivers draining at the Ajay-Damodar interfluves (Roy & Sahu, 2015), and  $B_r$  between first, second, second to third, and third to fourth orders are 4.80, 5.50, and 6.00, respectively. Sub-basins  $B_r$  ranges from 2 to 13 (Table 12.3). A negative exponential trend has been observed between the stream number and stream orders (Fig. 12.4), indicating the natural extension of the network (Horton, 1945). The left side basin area is drained by higher Nu and by the stream length that exhibits the area of potential for surface runoff (Resmi et al., 2019). The sub-basin A is draining by the highest Nu of 70 and  $L_u$  of ~154 km (Table 12.2). Sub-basins C, B, H, F, L, and K are draining by relatively higher Nu ( $>10$ ), and sub-basin O, I, G, J, P, and E are associated with the lower value of Nu ( $<10$ ) (Table 12.2). First- and second-order average stream lengths are very high in

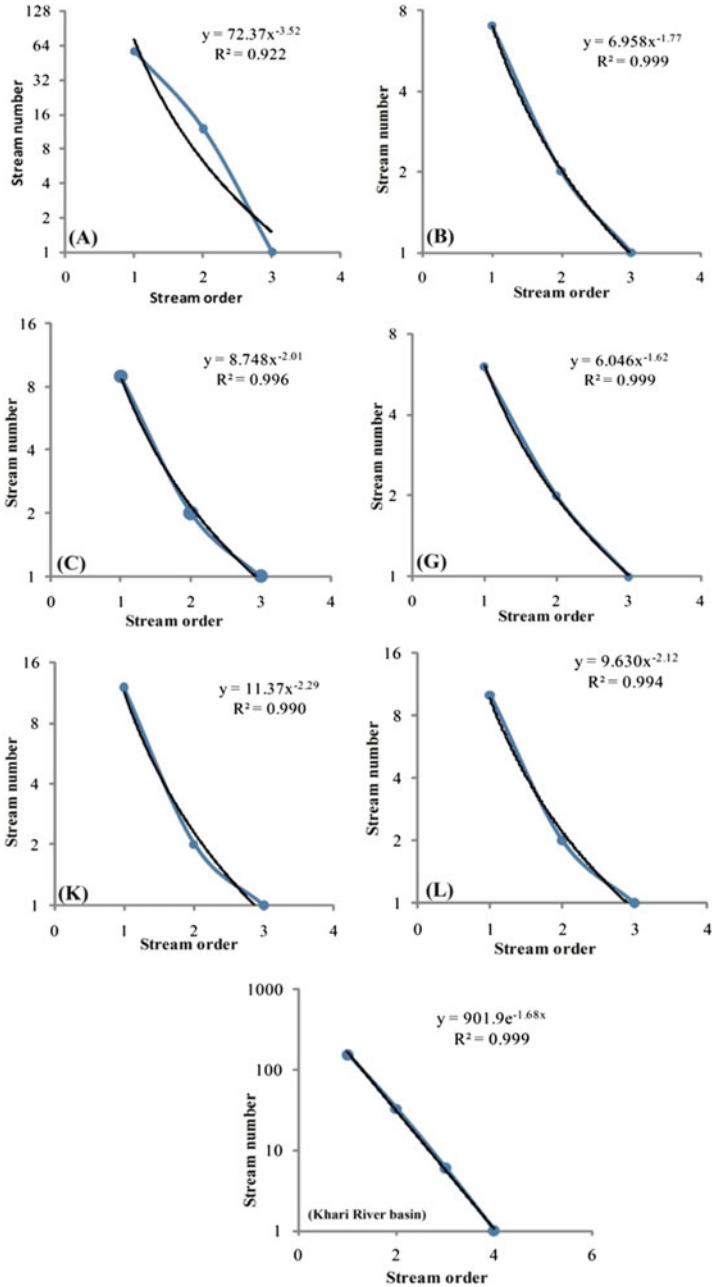


**Fig. 12.3** Semilogarithmic diagram of stream numbers versus stream orders of the KRB and sub-basins A, B, C, G, K, and L, respectively. Regression coefficient curve values are indicated

**Table 12.2** Basin properties of the KRB sub-basins

Sub-basin name ( <i>u</i> )	Total stream number of the order ( <i>N<sub>u</sub></i> )			A = Area of the basin (km <sup>2</sup> )	<i>L<sub>u</sub></i> = Total stream length of the order <i>u</i> (km)			L = Basin max length (km)	P = Perimeter (Km)	H = Maxelevation (m)	h = Minelevation (m)	a = Stream elevation at source (m)	b = Stream elevation at confluence (m)	l = Actual stream length (km)	Straight line stream length (km)	Average stream gradient (m/km)				
	1st	2nd	3rd		1st	2nd	3rd										Total			
<b>A</b>	3	57	12	1	70	295.34	45.56	40.52	67	153.06	34.96	106.40	73	27	58.70	29.50	47.63	32.54	0.613	
<b>B</b>	3	7	2	1	10	48.68	5.71	12.33	3.85	21.89	10.89	30.03	56	29	41.20	30.00	14.89	7.56	0.752	
<b>C</b>	3	9	2	1	12	51.53	3.80	16.28	2.39	22.47	9.86	31.41	45	25	38.00	26.20	12.42	7.03	0.95	
<b>D</b>	1	1	-	-	1	25.31	0.45	-	-	0.45	8.00	49.35	34	19	26.30	24.50	0.45	0.40	4.50	
<b>E</b>	2	6	2	-	8	41.59	4.41	6.9	-	11.31	7.75	40.31	36	20	30.4	20.6	5.9	2.9	1.16	
<b>F</b>	2	13	1	-	14	82.13	6.68	31.18	-	37.86	20.2	52.16	41	20	37.3	20	31.22	16.91	0.554	
<b>G</b>	3	6	2	1	9	16.55	3.27	2.64	1.22	7.13	6.75	23.43	29	20	27.9	21.6	4.24	2.83	1.48	
<b>H</b>	2	9	2	-	11	50.79	10.24	7.34	-	17.58	8.65	51.16	28	15	25.6	13.4	6.34	4.16	1.92	
<b>I</b>	2	5	1	-	6	41.65	8.19	0.69	-	8.88	12.5	53.32	25	13	15.3	13.2	1.69	1.31	1.24	
<b>J</b>	2	5	1	-	6	29.55	4.35	10.31	-	14.66	8.5	22.37	34	19	31	19.5	11.16	6.81	1.03	
<b>K</b>	3	12	2	1	15	78.7	11.52	13.98	9.1	34.6	17.71	45.29	33	13	26.6	12.5	23.76	12.95	0.593	
<b>L</b>	3	10	2	1	13	107.82	13.65	24.55	5.9	44.1	19.26	53.9	34	12	30.7	11.8	32.21	14.76	0.586	
<b>M</b>	-	-	-	-	-	48.24	-	-	-	12.25	-	40.3	20	12	-	-	-	-	-	-
<b>N</b>	1	1	-	-	1	120.66	3.5	-	-	3.5042	25.0	90.86	20	9	15.4	10.6	3.5	2.41	1.37	
<b>O</b>	2	4	2	-	6	96.45	6.39	10.87	-	17.26	12.1	52.89	16	8	17.6	9.4	7.67	6.8	1.07	
<b>P</b>	2	8	1	-	9	60.66	14.61	17.2	-	31.81	15.27	36.96	19	8	17.3	8	20.84	11.96	0.446	
<b>Q</b>	-	-	-	-	-	13.11	-	-	-	-	4.93	18.41	15	9	-	-	-	-	-	-

Based on: Computed by authors

Sub-basin in blue color is head water basin at the western side. The sub-basins highlighted in green color are draining the left side of the KRB, and the right-side sub-basins are marked by the brown color. Dotted in place of values are not applicable for respective parameters or basins

**Table 12.3** KRB sub-basins linear morphometric parameters

Sub-basin name	Stream order	Total stream number of u order				average stream length of order u (km)			Stream length ratio ( $S_{lr}$ )			Mean bifurcation ratio ( $B_R$ )	Stream gradient ratio ( $S_g$ )
		1st	2nd	3rd	Total	1st	2nd	3rd	1st to 2nd	2nd to 3rd	Average		
<b>A</b>	03	57	12	01	70	0.80	5.58	66.98	1.124	0.605	0.865	8.38	0.613
<b>B</b>	03	07	02	01	10	0.82	6.17	3.85	0.463	3.203	1.830	2.75	0.752
<b>C</b>	03	09	02	01	12	0.42	8.14	2.39	0.233	6.778	3.505	3.25	0.950
<b>E</b>	02	06	02	–	08	0.74	3.45	–	0.639	–	0.639	03	0.567
<b>F</b>	02	13	01	–	14	0.52	31.80	–	0.214	–	0.214	13	0.554
<b>G</b>	03	06	02	01	09	0.55	1.32	1.22	1.239	2.164	1.777	2.50	1.480
<b>H</b>	02	09	02	–	11	1.34	3.67	–	1.395	–	1.395	4.50	0.585
<b>I</b>	02	05	01	–	06	1.64	0.69	–	11.869	–	11.869	05	0.436
<b>J</b>	02	05	01	–	06	0.87	10.31	–	0.422	–	0.422	05	1.030
<b>K</b>	03	12	02	01	15	0.96	6.99	9.10	0.824	1.536	1.180	04	0.593
<b>L</b>	03	10	02	01	13	1.37	12.28	5.90	0.556	4.161	2.235	3.50	0.586
<b>O</b>	02	04	02	–	06	1.60	5.44	–	0.587	–	0.587	02	0.432
<b>P</b>	02	08	01	–	09	1.83	17.20	–	0.849	–	0.849	08	0.446

Based on: Computed by authors



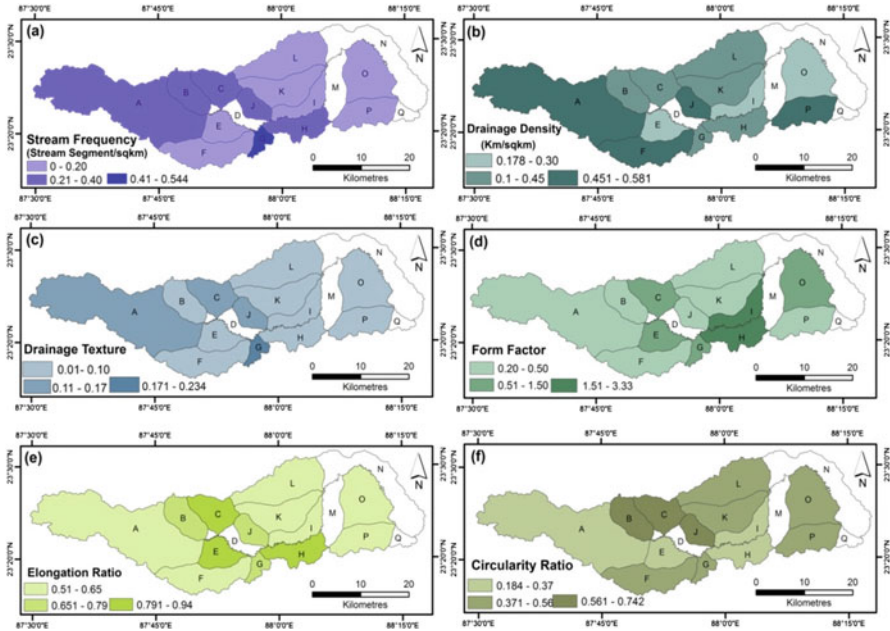


**Fig. 12.4** Sub-basin wise distributions of (a) stream frequency ( $S_f$ ), (b) drainage density ( $D_d$ ), (c) drainage texture ( $D_t$ ), (d) form factor ( $F_f$ ), (e) elongation ratio ( $E_r$ ), and (f) circularity ratio ( $C_r$ ) in the KRB

sub-basins K, H, J, I, P, O, L (>1 km) and in sub-basins J, F, C, L, P, K (>7 km), respectively (Table 12.2). Str values of the sub-basins P, J, L, and K are comparatively higher because of the relatively faster channel elongation process which causes the high stream gradient with channelized flow (Resmi et al., 2019) that shows diverseness between sub-basins gradient, different erosional stages, and potentiality for the surface-runoff generation. The  $B_R$  of the left-side sub-basins is comparatively high than right-side sub-basins (Table 12.3). These higher  $B_R$  and  $S_g$  of these downstream sub-basins also indicate the high discharge potentiality of tributaries to the Khari trunk stream, and high discharge into the trunk stream in the rainy season is a normal event that leads to floods over the region.

The KRB's maximum length is 82 km, and maximum width is approximately 22 km, i.e., the basin is almost 3.75 times longer, though the KRB is narrowly elongated ( $E_r = 0.48$  and  $F_f = 0.18$ ) and the basin is wider in its downstream. This is probably because of the relatively large sub-basins of the KRB draining in this part (Fig. 12.2). These sub-basins are joining with the trunk stream within a specific stretch, and their combined discharge makes the trunk stream overtopping in its floodplain. The sub-basins joining into this reach are also elongated in nature (Fig. 12.4d–f) indicating more surface runoff because the shape also controls the rate of flow at which it discharged into the trunk channels (Fenta et al., 2017). According to Thomas et al. (2012), elongated-shaped watersheds can be marked by a

flat hydrograph of longer duration with gentle rising and recession limbs. However, a more elongated watershed is more efficient in discharge of runoff; the hydrological response has also been affected by several factors like LULC, basin gradient, soil type, or rainfall intensity. The correlation shows that the  $F_f$  and  $E_r$  have  $C_c$ ,  $C_m$ , and  $L_o$  and also have a positive relationship with the relief aspects of the basin (Table 12.4).

The spatial variation of the  $S_f$ ,  $D_d$ , and  $D_t$  indicates the landscape dissection by the stream network along with the parameters of  $C_c$  and  $L_o$ . These are important linear variables that are related to the hydrological properties of the drainage system and help to predict the runoff and sediment yield (Fenta et al., 2017). The computed  $D_d$  of the KRB is 0.44 km/km<sup>2</sup> (Fig. 12.6d) and ranges between 0.18 and 0.58 km/km<sup>2</sup> (Fig. 12.4b). Though, the overall  $D_d$  is very low, sub-basins J, P, and A  $D_d$  values are relatively high ( $D_d > 0.5$ ), and sub-basins F, B, K, G, and C values are near to this (Fig. 12.4b). According to Ramalingam and Santhakumar (2001), the low  $D_d$  indicates less channelized flow which is a result of the higher infiltration rate caused by alluvium surface and higher-surface runoff. The  $S_f$  value of the KRB is ~0.17 no./km<sup>2</sup>, which ranges between 0.06 and 0.54 no./km<sup>2</sup> (Fig. 12.4a). Relatively moderate values of  $S_f$  have been observed at the middle part of the KRB which also indicates the possibility to generate surface runoff. Moreover, in sub-basin-wise analysis (Fig. 12.4a),  $S_f$  values are relatively higher in sub-basin C, B, J, K, P, and L indicating a high rate of channelized flow. Normally, when surface permeability decreases, runoff increases, and as a result of it, numbers of channels developed and thus tend to be relatively higher  $S_f$ . In the correlation matrix,  $S_f$ ,  $D_d$ , and  $D_t$  showed negative or very low positive correlation with other aerial and relief aspects (Table 12.4). Figure 12.5b shows the sub-basins draining the downstream part have much similarities.

The  $C_m$  and  $L_o$  are another two important aerial aspects from the hydrological perspective as proxy indicators of the dynamic equilibrium stage of the river basin (Schumm, 1956) and the length that water must travel before discharging into the channel, i.e., the greater the  $L_o$ , the greater is the possibility of infiltration and lesser the surface runoff (Horton, 1945). For the KRB, the calculated value of  $C_m$  and  $L_o$  are 2.27 and 0.262 km, respectively. And the sub-basins ranges  $C_m = 1.721$  to 5.617 and  $L_o = 0.861$  to 2.809, respectively (Fig. 12.5d). According to Ngapna et al. (2018), such values are normally associated with the low-energy surface and its hydrology controlled by a humid environment. Thomas et al. (2012) interpreted shorter  $L_o$  values as characteristics of areas with steeper basin gradient that generate high-surface runoff. Lower values of  $L_o$  for sub-basins A, F, J, and P indicate more surface-runoff generation and moderate values of  $L_o$  for sub-basins B, C, K, L, H, E, and G moderate type of surface-runoff generation (Fig. 12.5d). The correlation analysis showed  $L_o$  and  $C_m$  are statistically significant and positively correlated and have a significant inverse relationship between the  $D_t$  and  $D_d$ . So in sub-basins with lower drainage density,  $L_o$  is high which generates more surface runoff and that leads to the possibility of flood at the KRB downstream part.

To synthesize the hydraulic nature of landform and characteristic of the overland flow of the basin, quantitative investigation of the relief aspect is the base of this

**Table 12.4** Correlation matrix of selected morphometric parameters of the KRB sub-basins

	B <sub>r</sub>	S <sub>tr</sub>	S <sub>g</sub>	S <sub>f</sub>	D <sub>d</sub>	D <sub>t</sub>	F <sub>f</sub>	E <sub>r</sub>	C <sub>r</sub>	C <sub>c</sub>	C <sub>m</sub>	R <sub>r</sub>	A <sub>r</sub>	L <sub>o</sub>
B <sub>r</sub>	1													
S <sub>tr</sub>	-0.136	1												
S <sub>g</sub>	-0.299	-0.144	1											
S <sub>f</sub>	-0.155	-0.081	0.873 <sup>b</sup>	1										
D <sub>d</sub>	0.463	-0.445	0.364	0.312	1									
D <sub>t</sub>	0.016	-0.239	0.867 <sup>b</sup>	0.937 <sup>b</sup>	0.599 <sup>a</sup>	1								
F <sub>f</sub>	-0.190	0.778 <sup>b</sup>	-0.205	-0.059	-0.603 <sup>a</sup>	-0.293	1							
E <sub>r</sub>	-0.624 <sup>a</sup>	-0.183	0.071	-0.039	-0.505	-0.204	0.634 <sup>a</sup>	1						
C <sub>r</sub>	-0.158	-0.376	0.340	-0.046	0.517 <sup>a</sup>	0.152	-0.614 <sup>a</sup>	0.003	1					
C <sub>c</sub>	0.112	0.590 <sup>a</sup>	-0.330	0.003	-0.537	-0.203	0.811 <sup>b</sup>	0.015	-0.948 <sup>b</sup>	1				
C <sub>m</sub>	-0.396	0.421	-0.414	-0.401	-0.947 <sup>b</sup>	-0.620 <sup>a</sup>	0.536	0.453	-0.460	0.489	1			
R <sub>r</sub>	-0.339	0.581 <sup>a</sup>	0.213	0.193	-0.246	0.020	0.661 <sup>a</sup>	0.392	-0.088	0.300	0.108	1		
A <sub>r</sub>	-0.015	0.229	-0.314	-0.288	-0.105	-0.268	0.044	0.006	-0.137	0.145	0.098	0.336	1	
L <sub>o</sub>	-0.395	0.421	-0.414	-0.401	-0.947 <sup>b</sup>	-0.620 <sup>a</sup>	0.535	0.453	-0.460	0.489	1.000 <sup>b</sup>	0.108	0.098	1

Based on: Computed by authors

<sup>a</sup>Marks correlation is significant at the 0.05 level (2-tailed)

<sup>b</sup>Marks correlation is significant at the 0.01 level (2-tailed)

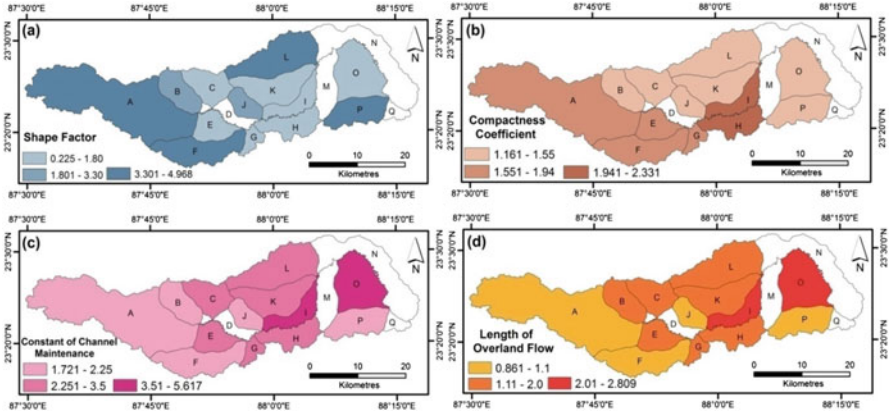
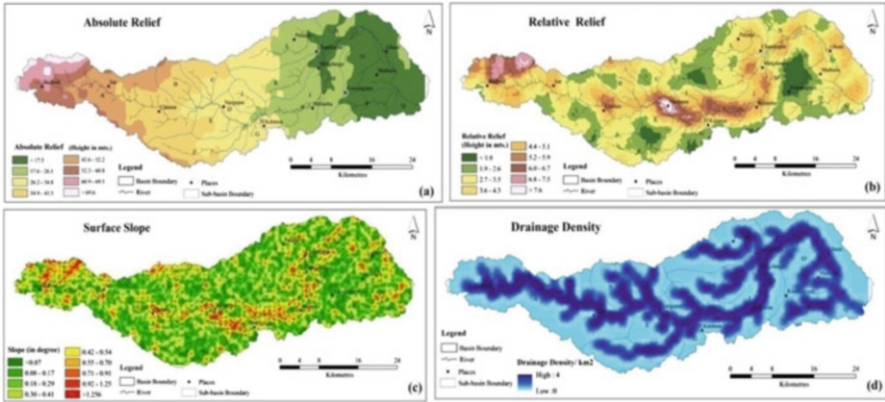


**Fig. 12.5** Sub-basin-wise distributions of (a) shape factor, (b) compactness coefficient ( $C_c$ ), (c) constant of channel maintenance ( $C_m$ ), (d) length of overland flow ( $L_o$ ) in the KRB



manifested as a high-surface runoff area (Fenta et al., 2017). The  $A_r$  and surface slope values are low at the eastern side of the basin, which is a relatively more flat surface and has less potential energy to generate surface runoff and has higher possibilities to stay water in this basin part (Fig. 12.6a).

The values of relative relief ( $R_r$ ) ranges between 1.1 m and 8.40 m (Fig. 12.6b) with basin average of 2.1 covering about half of the basin. Figure 12.6b shows that the downstream area is characterized by very low relief, in particular, sub-basins K, O, F, P, E, and L which are plain surfaces with alternative picks of high  $R_r$  along the Khari mainstream. The lower values of  $R_r$  for the KRB are associated with first and second-order streams at the irrespective upstream parts (Fig. 12.6b). An area of high  $R_r > 6.0$ , which has been marked at the NW corner of the KRB, is an area of the dissected lateritic surface, but the higher  $R_r$  along the trunk river course, particularly near the Channa village and downstream of Nargapur village, indicates that these parts are relatively lower and potentially active floodplain areas (Fig. 12.6b). Every year during the flood event, the surface runoff that has been generated at the upper area of the sub-basins is accumulating in these areas and submerged multiple times (Fig. 12.8a–c). The slope deformation along the riverbank in this part of the river course also reveals the flooded areas (Fig. 12.6c). Though the surface slope of the basin is eastward, due to trunk stream abrupt deflection toward the north near the Palumba village and its downstream circular flow, the floodplain in this area is bounded by two-side relatively high ground of potentially high-runoff areas (Figs. 12.6b and 12.7a). The low relative relief or geomorphic high of the Kusumgram area acts as a natural barrier of the floodwater flow toward the east,



**Fig. 12.7** Flood inundation and waterlogging areas of the KBR near (a, b) Channa village and downstream of Channa village, (c) downstream of Nargapur village, and (d) the left bank area between Malumba and Chandrapur village

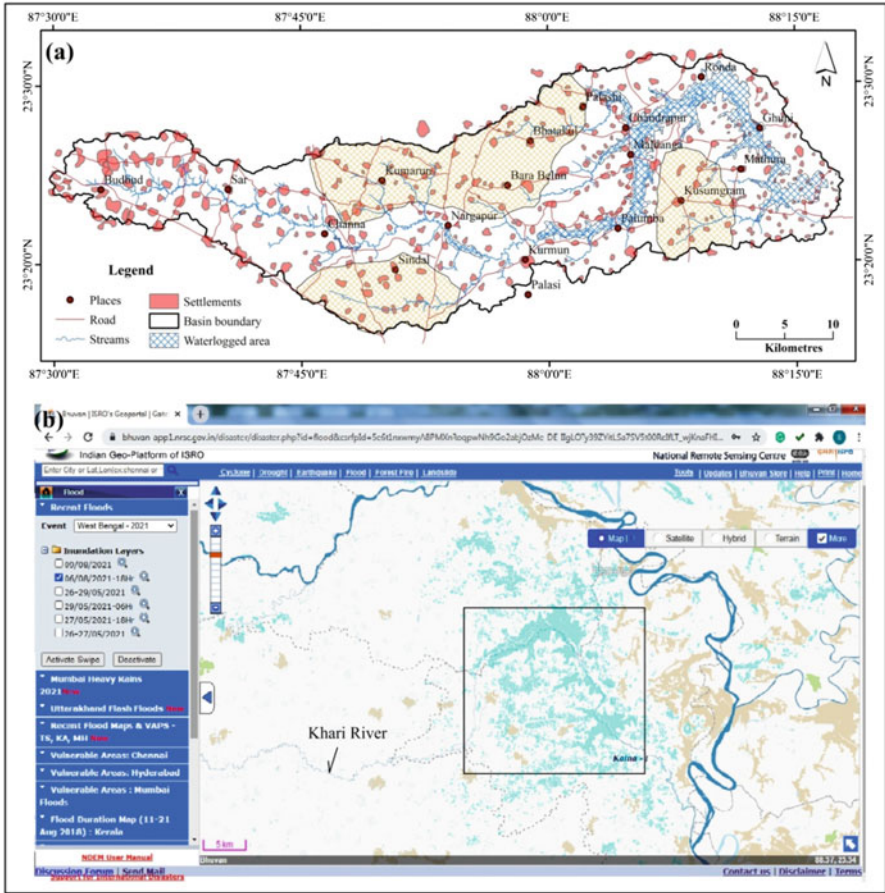


**Fig. 12.8** (a) Areas of flood waterlogged in the KRB along with the location of settlements areas and distribution of roads. The settlements are located away from the flood waterlogged areas. Marked areas by brown color lines are the areas of potential surface of runoff. (b) Flood inundation area of the lower KRB during the flood event on 06-08-2021 by a catastrophic rainfall (onscreen visualization of flood data by Bhuvan, Govt. of India)

and an extensive elongated submerged or waterlogged area evolved during the floodtime (Figs. 12.7a, b and 12.8d). It is an area of about 97 km<sup>2</sup> waterlogging. Human intervention in form of longitudinal discontinuation of the floodplain by roads intensifies the flood and waterlogging condition in this area. Though a number of roads were disconnected and damaged by floodwater, as settlements are located above the floodplain, no one settlement is affected by flood (Fig. 12.7a). Near the Channa and Nargapur village, approximately 0.62 km<sup>2</sup> and 3.0 km<sup>2</sup> area flooded along the river, respectively. In these areas, the settlements are also located away from the present floodplain and not vulnerable to flood submergence (Fig. 12.7a).

## 5 Conclusion

Flood in the KRB is a response to catastrophic rainfall, as it is mainly a seasonal river that generates high-surface runoff governed by morphometric parameters of the basin and drainage. Applied parameters indicate the different degrees of correlation among them and give an overall view of the hydraulic nature of the KRB. The nature of the relief aspects and surface-slope distribution show that active floodplain of the Khari River is the regional geomorphic low surface discontinued by geomorphic highs. KRB linear and aerial aspects reveals that the sub-basins J, L, K, O, P, and H are relatively high potential areas of surface runoff that drain approximately 45% of the total basin area. The combined discharge of these sub-basins into a particular reach of the lower Khari River between Palumba and Randavillage evolved the part as a flood basin. It is an elongated and circular waterlogged area bounded by two-side geomorphic high-surface areas. Another two active floodplain and waterlogged areas are developed near the Channa village and downstream of Nargapur village. Though these areas are potential for flood vulnerability and are submerged every year, as the settlements are located away from the present floodplain, the flood is not hazardous for the humans living in the basin. It will not be really possible to control flood frequency and situation in the lower part of the basin, but if we take a few constructive measures, flood vulnerability can be reduced, and for that we would recommend:

- (i) We can construct more capable underpass for floodwater in lateral roads that are blocking the flow of the surface runoff in floodplain area.
- (ii) As the flooded downstream area is relatively low-relief longitudinal basin, sedimentation is a common factor leading to the decreasing carrying capacity of the main channel than its middle part. So, to maintain its capacity, we need to rejuvenate the lower part.
- (iii) Another possible way is diverting the floodwater through the trunk stream of the sub-basin P, as source of this stream is near to the Khari main channel near the Palumba village that have to do by an artificial channel in a controlled way. Otherwise, the Khari segment between Palumba and Mahata village may dry out due to lack of water in channel.

**Acknowledgements** For this work, the authors would like to convey their gratitude to the Survey of India (SoI), the Geological Survey of India (GSI, Govt. of India), and USGS for maps and also to the software (ArcGIS, QGIS, and SPSS) manufacturers for making this beautiful software used in this work. The work is supported by the Kalyani University, Department of Geography. The authors would like to thank the editors and reviewers for their constructive queries, comments, and recommendations.

## References

- Ali, H., Modi, P., & Mishra, V. (2019). Increased flood risk in Indian sub-continent under the warming climate. *Weather and Climate Extremes*, 25, 100212. <https://doi.org/10.1016/j.wace.2019.100212>
- ASTER Global DEM (1arc). (n.d.). U.S. Geological Survey, <https://earthexplorer.usgs.gov/>
- Bagchi, K., & Mukherjee, K. N. (1979). *Diagnostic survey of Rarh Bengal, part -I, morphology, drainage and flood: 1978* (1st ed.). Department of Geography, University of Calcutta.
- Barman, S. D., Islam, A., Das, B. C., Mandal, S., & Pal, S. C. (2018). Imprints of new tectonism in the evolutionary record along the course of Khari River in Damodar fan delta of Lower Ganga basin. In B. C. Das, S. Ghosh, & A. Islam (Eds.), *Quaternary geomorphology in India – Case studies from the Lower Ganga basin* (pp. 105–126). Springer International Publishing. [https://doi.org/10.1007/978-3-319-90427-6\\_6](https://doi.org/10.1007/978-3-319-90427-6_6)
- Chakrabarti, P., & Nag, S. (2015). *Rivers of West Bengal: Changing scenario*. Department of Science and Technology, Government of West Bengal.
- Fenta, A. A., Yasuda, H., Shimizu, K., Haregeweyn, N., & Woldearegay, K. (2017). Quantitative analysis and implications of drainage morphometry of the Agula watershed in the semi-arid northern Ethiopia. *Applied Water Science*, 7, 3825–3840. <https://doi.org/10.1007/s13201-017-0534-4>
- Ghoh, S., & Guchhait, S. K. (2016). *Dam-induced changes in flood hydrology and flood frequency of tropical river: A study in Damodar River of West Bengal*. Arab J Geosci. <https://doi.org/10.1007/s12517-015-2046-6>
- Gravelius H (1914) Flusskunde. Goschen Verlagshan dlung Berlin. In: Zavoianu I (ed) Morphometry of drainage basins. Elsevier, Amsterdam
- Horton, R. E. (1945). Erosional development of streams and their drainage basins; hydrophysical approach to quantitative morphology. *Geological Society of America Bulletin*, 56(3), 275–370.
- Islam, A., & Deb Barman, S. (2020). Drainage basin morphometry and evaluating its role on flood-inducing capacity of tributary basins of Mayurakshi River, India. *SN Applied Sciences*, 2, 1087. <https://doi.org/10.1007/s42452-020-2839-4>
- Islam, A., & Sarkar, B. (2020). Analysing flood history and simulating the nature of future floods using Gumbel method and Log-Pearson type III: The case of the Mayurakshi River basin, India. *Bulletin of Geography. Physical Geography Series*, 19(1), 43–69. <https://doi.org/10.2478/bgeo-2020-0009>
- Leopold, L. B., & Maddock, T. (1953). *The hydraulic geometry of stream channels and some physiographic implications* (Vol. 252). US Government Printing Office.
- Leopold, L. B., & Miller, J. P. (1956). Ephemeral streams—Hydraulic factors and their relation to the drainage net. *U.S. Geological Survey*, 282, 1–37.
- Malik, S., & Pal, S. C. (2021). Potential flood frequency analysis and susceptibility mapping using CMIP5 of MIROC5 and HEC-RAS model: A case study of lower Dwarkeswar River, Eastern India. *SN Applied Sciences*, 3, 31. <https://doi.org/10.1007/s42452-020-04104-z>
- Mukhopadhyay, S. (2010). A geo-environmental assessment of flood dynamics in lower Ajoy River including sand splay problem in eastern India. *Ethiopian Journal of Environmental Studies and Management*, 3(2), 96–110.
- Nageswara Rao, K. (2020). Analysis of surface runoff potential in ungauged basin using basin parameters and SCS-CN method. *Applied Water Science*, 10, 47. <https://doi.org/10.1007/s13201-019-1129-z>
- Ngapna, M. N., Owona, S., Owono, F. M., Mpesse, J. E., Youmen, D., Lissom, J., Ondoa, J. M., & Ekodeck, G. E. (2018). Tectonic, lithology and climatic controls of morphometric parameters of the Edea – Eseka region (SW Cameroon, Central Africa): Implication on equatorial rivers and landforms. *Journal of Africal Earth Science*, 138, 219–232.
- Odiji, C. A., Aderoju, O. M., Eta, J. B., Shehu, I., Mai-Bukar, A., & Onuoha, H. (2021). Morphometric analysis and prioritization of upper Benue River watershed. *Northern Nigeria. Applied Water Science*, 11, 41. <https://doi.org/10.1007/s13201-021-01364-x>



- Pal, S., Mahato, S., & Bala, G. (2020). Hydro-geomorphic consequences of avulsion susceptible zones along lower Mayurakshi river of eastern India. *Remote Sensing Applications: Society and Environment*, 100425. <https://doi.org/10.1016/j.rsase.2020.100425>
- Ramalingam, M., & Santhakumar, A. R. (2001). Case study on artificial recharge using remote sensing and GIS. Retrieved from [www.GISdevelopment.net](http://www.GISdevelopment.net)
- Resmi, M. R., Babeesh, C., & Hema, A. (2019). Quantitative analysis of the drainage and morphometric characteristics of the Palar River basin, Southern Peninsular India; using bAd calculator (bearing azimuth and drainage) and GIS, *Geology, Ecology, and Landscapes*, 3:4, 295–307. <https://doi.org/10.1080/24749508.2018.1563750>
- Roy, S., & Bera, S. (2018). Geophysical control on the channel pattern adjustment in the Kunur River basin of Western part of lower Ganga Basin. In B. C. Das, S. Ghosh, & A. Islam (Eds.), *Quaternary geomorphology in India – Case studies from the lower ganga basin* (pp. 89–102). Springer International Publishing. [https://doi.org/10.1007/978-3-319-90427-6\\_5](https://doi.org/10.1007/978-3-319-90427-6_5)
- Roy, S., & Sahu, A. S. (2015). Quaternary tectonic control on channel morphology over sedimentary lowland: A case study in the Ajay-Damodar interfluvium of eastern India. *Geoscience Frontiers*, 6(6), 927–946. <https://doi.org/10.1016/j.gsf.2015.04.001>
- Schumm, S. A. (1956). Evolution of drainage systems and slope in badlands at Perth Amboy, New Jersey. *Geological Society of American Bulletin*, 67, 597–646.
- Sen, P. K. (1993). *Geomorphological analysis of drainage basin (an introduction to morphometry and hydrological parameters)*. The University of Burdwan.
- Singh, L. P., Parkash, B., & Singhvi, A. K. (1998). Evolution of the lower gangetic plain landforms and soils in West Bengal, India. *Catena*, 33, 75–104. [https://doi.org/10.1016/S0341-8162\(98\)00066-6](https://doi.org/10.1016/S0341-8162(98)00066-6)
- Singh, R. K., Vasanta Govind, K. V., Pasupuleti, S., & Nune, R. (2020). Hydrodynamic modeling for identifying flood vulnerability zones in lower Damodar River of eastern India. *Ain Shams Engineering Journal*, S2090447920300137. <https://doi.org/10.1016/j.asej.2020.01.01>
- Sohoulande, D. D. C., & Singh, V. P. (2016). Impact of climate change on the hydrologic cycle and implications for society. *Environment and Social Psychology*, 1(1), 36–49. <https://doi.org/10.18063/ESP.2016.01.002>
- Sreedevi, P. D., Subrahmanyam, K., & Ahmed, S. (2005). The significance of morphometric analysis for obtaining groundwater potential zones in a structurally controlled terrain. *Environmental geology*, 47, 412–420. <https://doi.org/10.1007/s00254-004-1166-1>
- Strahler, A. N. (1957). Quantitative analysis of watershed geomorphology. *American Geophysical Union, Transactions*, 38, 913–920. <https://doi.org/10.1029/TR038i006p00913>
- Strahler, A. N. (1964). Quantitative geomorphology of drainage basin and channel networks. In V. T. Chow (Ed.), *Handbook of applied hydrology* (pp. 4–76), New York, NY: McGraw Hill Book Co.
- Thomas, J., Joseph, S., Thrivikramji, K., Abe, G., & Kannan, N. (2012). Morphometrical analysis of two tropical mountain river basins of contrasting environmental settings, the southern Western Ghats, India. *Environmental Earth Sciences*, 66(8), 2353–2366. <https://doi.org/10.1007/s12665-011-1457-2>
- Topographical Map (79A/3 and 79A/7). (n.d.). Survey of India (SOI), Kolkata, India.

# Chapter 13

## Flood Risk Assessment and Numerical Modelling of Flood Simulation in the Damodar River Basin, Eastern India



Sandipan Ghosh  and Soumya Kundu

**Abstract** In the Damodar River Basin, the streamflow is scientifically controlled and regulated by the five large dams (viz., Panchet, Maithon, Konar, Tilaiya, and Tenughat) since the 1950s to manage irrigation water and floods in West Bengal, but currently, the water holding capacity of Damodar River and DVC (Damodar Valley Corporation) reservoirs (including Durgapur Barrage) is reduced due to siltation and lack of maintenance. For that reason, the recurrent flood events of each year, with minimum critical discharge of  $1651\text{--}1822\text{ m}^3\text{s}^{-1}$ , are triggered in the low-lying floodplains of Purba Bardhaman, Hooghly, and Howrah districts. The channels of lower Damodar basin (viz., Mundeswari and Damodar/Amta) are supposed to drain  $7079\text{ m}^3\text{s}^{-1}$  of water, but these are actually able to handle only  $2832\text{ m}^3\text{s}^{-1}$  of water during monsoon months. Nowadays, the government officials of West Bengal have blamed the flood regulation system of DVC, and they characterized this flood phenomenon as “man-made hazard.” Using advanced geospatial techniques, the present study tries to encompass the key factors of hydrometeorological floods and contemporary flood dynamics in the lower Damodar River Basin (Damodar fan-delta region of West Bengal), viz., analysis of flood-generated rainfall events, rainfall–runoff simulation, prediction of probable maximum flood, dam-included changes in flood hydrology, and 1D hydrodynamic flood model of steady and unsteady flow.

**Keywords** Flood frequency analysis · Curve number · 1D hydrodynamic model · Mann-Kendall test · Damodar River Basin · HEC-RAS

### 1 Introduction

Flood risk assessment (FRA) integrates two distinct parts: (a) estimating flood probability of certain return periods and the flood discharge of particular magnitude and (b) assessing the variable dimensions of flood risk, hydrogeomorphic

---

S. Ghosh (✉) · S. Kundu

Department of Geography, Chandrapur College, Purba Bardhaman, West Bengal, India

mechanisms of floods, flood controlling strategies, and real-time actions to be taken before during the floods (Hall & Penning-Rosewell, 2011). Floods are basically extreme hydrological phenomena, and it, generated by natural and anthropogenic causes, represents a classic example of the “pulsed type of disturbance” in the fluvial system (Kington, 2014). The term “flood” has a range of meanings, including (1) hydrological floods with different magnitude and inconstant flow frequency in connection with climate change; (2) floods as hazard and vulnerability, damaging, and livelihoods; and (3) consequences of floods on the components of environment and landscape change (Baker, 1994). A flood event may occur due to large streamflow magnitude as such as that the flow rate exceeds the capacity of the main channel at a location (i.e., the flow exceeds the bankfull discharge) or may occur for a lower streamflow rate when the flow happens at a time when the channel is fully or partially obstructed, as can occur with ice jam or as a result of debris flow in the channel (Burn et al., 2017). The floods of Indian rivers are very important hydrogeomorphic hazard, and the monsoon floods are inevitable and recurrence event because flooding is the natural mechanism (intensified by human activities) by which excess runoff water is discharged through channels, and occasionally it overflows in the floodplains (Kale, 2003; Sinha et al., 2012). In West Bengal, floods are natural as well as man-made hazards which cause considerable damages, particularly in the populated areas of lower Damodar River Basin. The main concern is economic impacts of floods (triggering poverty at village level) including costs due to loss of, or damage to, property, infrastructure damage or destruction, loss of crops and livestock, and lost wages and productivity due to more disruptions.

The flood account of Damodar River, hydrometeorology, nature of annual monsoon floods, structural measures of flood mitigation, changing flood dynamics and floodplain morphology, fluvial aggradation and degradation, dam-controlled environmental flow, role of human on flood hydrology and geomorphology, and impact of flood in agrarian society were previously studied and discussed in details by Glass (1924), Kirk (1950), Pramanik and Rao (1952), Bagchi (1977), Saha (1979), Sen (1985), Roy and Mazumdar (2007), Majumder et al. (2010a), Bhattacharya (2011), Ghosh (2011), Choudhury (2012), Lahiri-Dutt (2012), Lahiri-Dutt and Samanta (2013), Bera and Mistri (2014), Rajbanshi (2015), Ghosh and Mistri (2015), Ghosh and Guchhait (2016), Verma et al. (2017), Das et al. (2017), Chattopadhyay et al. (2020), Mahata and Maiti (2020), Ghosh and Illahi (2020), Ghosh et al. (2021, 2022a), and Hoque et al. (2022). Before dam construction, the floods were very violent in nature (exceeding  $18,000 \text{ m}^3 \text{ s}^{-1}$  peak flow) and devastating in this funnel-shaped basin, damaging economic assets and livelihood to a large extent, and it was renowned as the “Sorrow of Bengal.” In the 1950s, the DVC (Damodar Valley Corporation) had been introduced the first multipurpose river valley project of India to boost up the regional economy of eastern India and to manage annual flood peaks. Carrying more than 75 years of legacy the DVC has partly achieved the objectives of planning, but the lower segment of the Damodar River (two bifurcated branches – Mundaswari and Damodar/Amta channel) is still vulnerable to recurrent flood hazard during peak monsoon rainfall or tropical depression. At present, elevated embankments and large dams have progressively altered the morphology and

hydrology of the fluvial system to a great extent, and the problems of ecological degradation, water pollution, water security, downstream flood hazard, reservoir siltation, drainage congestion, degradation of palaeochannels or spill channels (i.e., floodways of fan-delta), and declining carrying capacity of channel (accommodating diminutive bankfull discharge) are the key issues.

The assessment of flood hydrological dynamics and risk is an essential part of water resource management, especially in a dam-controlled river. Flood forecasting model, a tool of FRA, only makes sense if its results reach as many of the affected people as possible in a suitable form (Sharma et al., 2022). At present, the application of flood and river analysis software and machine learning process in the field of flood hydrology and river flow simulation/hydrodynamic model is a popular practice to develop better flood management at spatial scale (Correia et al., 1998; Leandro et al., 2009; Albano et al., 2017; Mojaddadi et al., 2017; Teng et al., 2017; Sharma et al., 2022). The HEC-RAS (Hydrologic Engineering Center's River Analysis System) developed by the US Army Corps of Engineers is a toolkit (an open-source software, <https://www.hec.usace.army.mil/software/hecras/>) of hydrologists and river scientists that allows the user to perform one-dimensional steady flow, one- and two-dimensional unsteady flow calculations, sediment transport/mobile bed computations, and water temperature/water quality modelling (Goodarzi & Eslamain, 2022). The application of HEC-RAS software for flood simulation and floodplain inundation was successfully executed by Horritt and Bates (2002), Merwade et al. (2008), Gibson et al. (2010), Pender and Neelz (2011), Sarhadi et al. (2012), Khattak et al. (2016), Dasallas et al. (2019), Kumar et al. (2019), Farooq et al. (2019), Ongdas et al. (2020), Pathan and Agnihotri (2020), Mawasha (2021), and Rana and Suryanarayana (2021). In numerous studies, HEC-RAS one-dimensional (1D) or two-dimensional (2D) hydrodynamic models are used to simulate flood flows, environmental flows, spatial coverage of floodplain inundation, flood depth, sediment transport along channel, flow velocity in respect of variable discharge, culvert flow design, spatial variability of water quality, and scour phenomenon at bridge piers (Tate & Maidment, 1999; Goodell, 2005; Knebl et al., 2005; Lee et al., 2006; Parsa et al., 2013; Mawasha, 2021). Alongside the floods of Indian rivers (viz., Krishna, Yamuna, Teesta, Mahanadi, Dwarkeswar, Bhagirathi-Hooghly etc.) and unsteady flow simulation were assessed using the hydrodynamic models of HEC-RAS (Mandal & Chakrabarty, 2016; Kumar et al., 2017; Patel et al., 2017; Surwase et al., 2020; Pathan & Agnihotri, 2020; Jagadesh & Veni, 2021; Malik & Pal, 2021; Rana & Suryanarayana, 2021; Ghosh et al., 2022b). It is essential to mention that in the Damodar River the hydraulic routing of extreme floods, 1D/2D flood simulation, 1D-2D coupled LISFLOOD-FP model, and TELEMAC-2D model were analyzed by Sanyal et al. (2013, 2014a, b), Sanyal (2017), and Singh et al. (2020, 2021).

These studies already show that the HEC-RAS software makes it possible to determine how high the water surface will be in the floodplain during specific discharge and which areas are affected by it (Goodarzi & Eslamain, 2022). The study of an inundation area (an area of land subject to flooding) and the evaluation of its water surface level are the most important part of each flood risk management

project (Ogras & Onen, 2020). For floodplain modelling and visualization of input or output data, HEC-RAS is designed in order to model the hydrologic engineering properties of river flow and to import/export data to ArcGIS platform to facilitate the decision-making (Ogras & Onen, 2020). To improve the flood management system of riparian terrain, the utmost vital tool of HEC-RAS software is to check the magnitude of flood risk and vulnerability of flood-prone region, determining the critical floodplain boundaries of maximum flood flow. As the river floodplain zoning maps provide valuable hydrologic information, such as flow area, frictional loss, Froude number, hydraulic conveyance, critical hydraulic depth, flood depth, and area of flood prevention in flood zones, it is decisive to place the maps in the first step of flood management (ShahiriParsa et al., 2016). Observing the potentiality of HEC-RAS, the present study aims to assess the dam-induced changes in the occurrence of extreme floods, floodplain inundation during unsteady flows, and the associated floodplain risk of variable return period discharge (2-year, 5-year, 10-year, 25-year, 50-year, and 100-year floods) in the lower part of Damodar River Basin. Heavy rainstorm event of monsoon climate, runoff yield of different terrain (hard rock or alluvium), and flash floods have inevitable in situ uncertainty with a physical open system, but if the current estimates of flood flow or bankfull discharge or carrying capacity of Damodar River can be deduced, then an idea of flood risk can be derived with some statistical perception.

## 2 Geographical Settings of Study Area

The Damodar River Basin (DRB) covers a basin area of 23,370 km<sup>2</sup> in Jharkhand and West Bengal. Its latitudinal extension ranges from 23° to 23° 22' 10" N, and the longitudinal extension ranges from 87°28'23" to 88°01'00" E. The 541-km-long stretch of Damodar starts its journey from the Khamarpat Hill (altitude 1062 m from mean sea level) of Chandwa, Palamu district (Jharkhand). The main tributaries of upper catchment are Barakar, Konar, Gobai, Jamuniya, Haharo, Garhi, Bhera, and Uttala. Below the Durgapur Barrage, the River receives the last tributary, named Sali. Following almost linear channel pattern (eastern ward slope), the river takes a sharp 90 southward turn at Palla (24 km east of Bardhaman town). At Paikpara, Jamalpur the main river bifurcates into two distributaries (Mundeswari at west and Damodar/Amta channel at east), and the Amta channel joins the Bhagirathi-Hooghly River at Falta, Howrah (48.3 km south of Kolkata). From the elbow of 90 turn several spill channels and palaeochannels (old distributaries of Damodar) are observed showing the topographic signature of fan-delta formation (prograding towards east and southeast direction) and palaeofloodways of monsoon months. Below the bifurcation point both channels, Mundeswari and Damodar/Amta channel, is confined within embankments, but bankfull discharge and monsoonal overflow make this floodplain or active fan-delta a flood-prone region of West Bengal which includes agriculturally dominated blocks of Pursura, Tarakeswar, Khanakul I and II, Jangipara, Udaynarayanpur, and Amta I and II. The main hydrologic concern

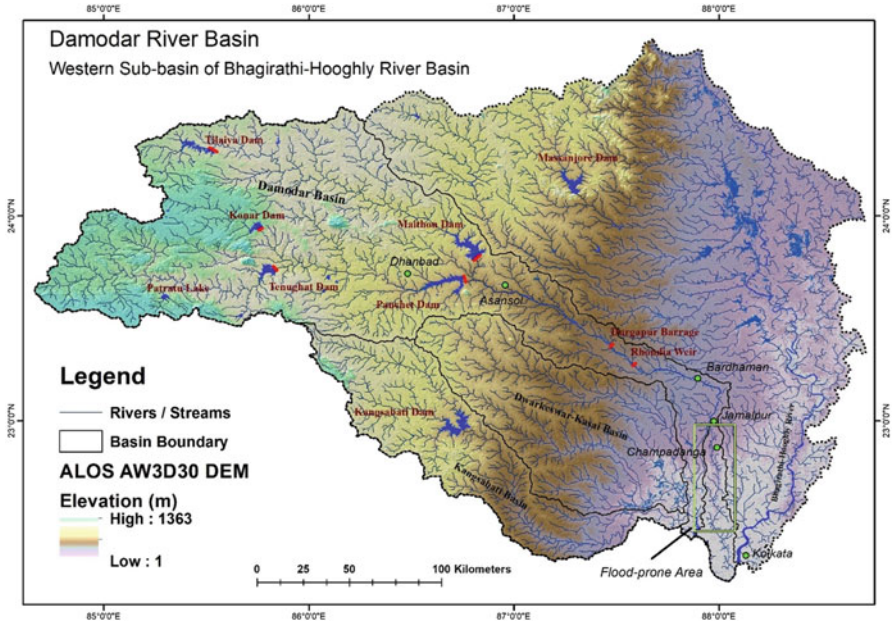


**Fig. 13.1** Location map of Damodar River Basin (including sites of dams, barrage, and weir) on ALOS AW3D30 DEM, along with associated western sub-basins of Bhagirathi-Hooghly River System

is the lower fluvial system of Damodar River which extends from 22° 35' 42" to 23° 09' 30" N and 87° 51' 08" to 88° 00' 31" E.

The DRB (Fig. 13.1) is located in the topographic transitional zone (break of slope) of the Chhotangapur Plateau (west) and the Bengal Basin (east), following three major south-north trend basement faults – (1) Chhotanagpur Foothill fault, (2) Pingla Fault, and (3) Khandagosh-Garhmayna fault (Ghosh & Guchhait, 2015; Mahata & Maiti, 2019). In the upper part of Damodar, the slope is 1.86 m km<sup>-1</sup> for the first 241 km, and for the next 167 km, it is 0.57 m km<sup>-1</sup>, and in the lower part, it is only 0.16 m km<sup>-1</sup> (Mahata & Maiti, 2019). The upper part of the basin (upstream of Durgapur) is covered mainly by granite and gneiss of the Archean, Gondwana sandstone and shale, and Recent channel alluvium, whereas the lower part (downstream of Durgapur) is characterized by the deposits of tertiary sediments, Early-Late Pleistocene laterites and Late Pleistocene – Recent alluvium (Mahata & Maiti, 2019). Since Oligocene (34–23 Ma BP), influenced by several marine transgression and regression periods, the vast load of plateau sediments was deposited by the fluvial system of Damodar, and it filled up the western shelf zone of the Bengal Basin in the subaerial and subaqueous tropical palaeoenvironment (Mahata & Maiti, 2019). By process of avulsing channels, sheet flow and debris flow the total fan-delta of Damodar (below Panagrah, Paschim Bardhaman) prograded into the shallow marine condition of the Bengal Basin. Downstream of Panagrah, the topography of lower Damodar River is subdivided into three distinct fan-deltaic

parts – (1) Early Pleistocene to Late Pleistocene Panagarh fan-delta (trending east), (2) Late Pleistocene to Early Holocene Memari fan-delta (trending southeast), and (3) Late Holocene to Recent active fan-delta (trending south) (Acharyya & Shah, 2007; Mahata & Maiti, 2019) (Fig. 13.1).

The most significant part of the basin is large-scale modification of channels by installing large dams, and to understand the anthropogenic impact on fluvial system, the DRB is a practical example from India. Perceived in 1945, following the model of the Tennessee Valley Authority (TVA), the Damodar Valley Corporation (DVC) was designed in 1948 under the guidance of Dr. Meghnad Saha and W.L. Voorduin who had been provided the total framework of multipurpose Damodar Valley Project, named “Preliminary Memorandum on the Unified Development of the Damodar River.” DVC was aimed to integrate the people, water, cropland, and mineral resources in a single thread of sustainable development with a holistic approach (Kirk, 1950; Saha, 1979). Firstly, it was decided to build eight large dams at eight sites, viz., (1) Tilaiya, Maithon, and Balpahari dams on the Barakar River; (2) Bokaro dam on Bokaro River; (3) Konar on Konar River; and (4) Aiyer, Bermo, and Panchet on Damodar River (Chandra, 2003). Finally, DVC decided to build only four dams at first phase, viz., Tilaiya (1953), Konar (1955), Maithon (1957), and Panchet (1959) (Table 13.1). After that, in 1974 one more reservoir, Tenughat, on the Damodar River was built. The Durgapur Barrage, built in 1955, is one of the important river impoundments because it finally releases incoming excess runoff water which has potentiality to flood in the lower floodplain of Damodar. Eight large dams would be able to reduce peak discharge of  $28,321 \text{ m}^3 \text{ s}^{-1}$  (resulting from a rainstorm of 50.8 cm at the upper catchment) to  $7080 \text{ m}^3 \text{ s}^{-1}$  at Rhondia, having total flood reserve of 6500 million  $\text{m}^3$ , but five dams only provide a maximum storage capacity of 3591 million  $\text{m}^3$  (Bhattacharya, 2011). Now DVC flood-controlling system provides a flood benefit of only 162.56 mm of surface runoff to the lower part of the basin, in place of 452 mm as advocated by the committee (Ghosh & Guchhait, 2016). Living on the active floodplain of Damodar and its structural modifications for protection against floods and for utilization of regional resources and wealth has aggravated the problem of hydrological risk factor to inundation (Table 13.1).

### 3 Methodology

The present study incorporates selected quantitative methods and techniques used in flood hydrology which deals with hydrometeorological aspects of flood, alluvial channel dynamics, flood routing and flood stage identification, hydraulic and engineering dimensions of floods, holistic flood risk assessment, and integrated flood management. Alongside, the methods of fluvial hydrology (Ward, 1978; Garde, 2006) include estimation of channel planforms and geometric dimensions (viz., width, depth, slope, sinuosity, sediment, channel roughness, etc.) and river hydraulics (viz., flow pattern, regime, hydrograph, and discharge anomalies). Along with

**Table 13.1** Overview and salient features of the dams in the Damodar River Basin

Dams/barrage River	Tenughat Damodar	Konar	Tilaiya Barakar	Maithon Barakar	Panchet Damodar	Durgapur Barrage
Inauguration year	1974	1955	1953	1957	1959	1955
Location	23°44' N 85°55' E	23°43' N 85°30' E	24°19' N 85°31' E	23°78' N 86°81' E	23°40' N 86°44' E	24°06' N 86°13' E
Catchment area (km <sup>2</sup> )	3393	997	984	6293	10,966	19,555
Dam height (m)	55.0	57.6	30.18	56.08	47.85	—
Annual runoff (m <sup>3</sup> )	2,450,000,000	555,070,000	431,720,000	2,614,990,000	4,539,230,000	—
Total dead storage (m <sup>3</sup> )	160,960,000	34,400,000	74,780,000	93,170,000	119,140,000	—
Spillway design discharge (m <sup>3</sup> s <sup>-1</sup> )	15,990	6796	1348	13,592	16,608	—
Minimum annual flow (m <sup>3</sup> s <sup>-1</sup> )	69.83	13.63	10.37	81.5	135.87	168.03
Environmental flow (m <sup>3</sup> s <sup>-1</sup> ) Q50 7-days	39.17	22.59	22.05	62.88	71.25	193.81

Source: Verma et al. (2015)



the techniques of flood prediction and modelling, the aim of flood hydrologic assessment is providing assistance and preliminary information to manage active floodplain zones and vulnerable flooded areas with the help of 1D or 2D hydrodynamic model and advanced geo-spatial tools.

### 3.1 Data Collection

The primary spatial information of study area was mostly collected from the topographical sheets (73 M/7, M/11, M/12, M/15, M/16, N/13, and 19 A/4) of SOI (Survey of India). The topographic and hydrological information of DRB were collected from the book, entitled “The Planning Atlas of the Damodar Valley Region,” which was written by Chatterjee (1969). The up-to-date daily rainfall, gauge data, and reservoir discharge data were retrieved from the official website (<https://www.wbiwd.gov.in/>) of IWD (Irrigation and Waterways Department, Government of West Bengal). In this study the main river gauge data (gauge level in metre) was collected for the four IWD monitoring stations – (1) Rhondia (23° 22' 56" N, 87° 29' 35" E), (2) Edilpur (23° 13' 40" N, 87° 49' 12" E), (3) Jamalpur (23° 02' 39" N, 87° 58' 56" E), (4) Champadanga (22° 50' 24" N, 87° 58' 12" E), and (5) Harinkhola (22° 50' 22" N, 87° 54' 16" E) (Fig. 13.2). The daily IWD reservoir discharge data were collected for the Durgapur Barrage (23° 38' 35" N, 87° 18' 11" E). The historical flood data and annual peak flow data of the DRB were collected from the research paper of Glass (1924), annual flood report of IWD (1959 and 2000), the books of Bhattacharya (2011) and Rudra (2018), and the research papers of Das et al. (2017) and Majumder et al. (2010b). The basin map of Damodar was prepared from the data repository of HydroSHEDS (Hydrological data and maps based on Shuttle Elevation Derivating at multiple scale). HydroRIVERS has been extracted from the gridded HydroSHEDS core layers at 15 arc-second resolution. The surface geology, lineaments, drainage, and other geomorphic information and thematic maps were retrieved from the web portal of the Geological Survey of India ([www.bhukosh.gsi.gov.in](http://www.bhukosh.gsi.gov.in)). Monthly and annual rainfall data were retrieved from the CHRS (Center for Hydrometeorology and Remote Sensing) data portal ([www.chrs.eng.uci.edu](http://www.chrs.eng.uci.edu)) which provided gridded precipitation data of resolution  $0.04^\circ \times 0.04^\circ$  ( $4 \times 4$  km). The rainfall data belongs to PERSIANN (Precipitation Estimation from Remotely Sensed Information using Artificial Neural Networks) CCS (Cloud Classification System) algorithm, which relates to variable threshold cloud segmentation (Nguyen et al., 2019). Alongside, another  $0.25^\circ \times 0.25^\circ$  resolution gridded rainfall data was collected from the official website of the Indian Meteorological Department ([www.imdpune.gov.in](http://www.imdpune.gov.in)). The land use and land cover (LULC) information were collected from the web portal of ESRI 2020 Land Cover Downloader (<https://www.arcgis.com/home/item.html?id=fc92d38533d440078f17678ebc20e8e2#overview>) where the analysis was done using the Sentinel – 10 m resolution imagery (2017–2021). The ALOS Global Digital Surface Model (AW3D30) digital elevation data of 30 m resolution was collected from the web portal of Open Topography. The

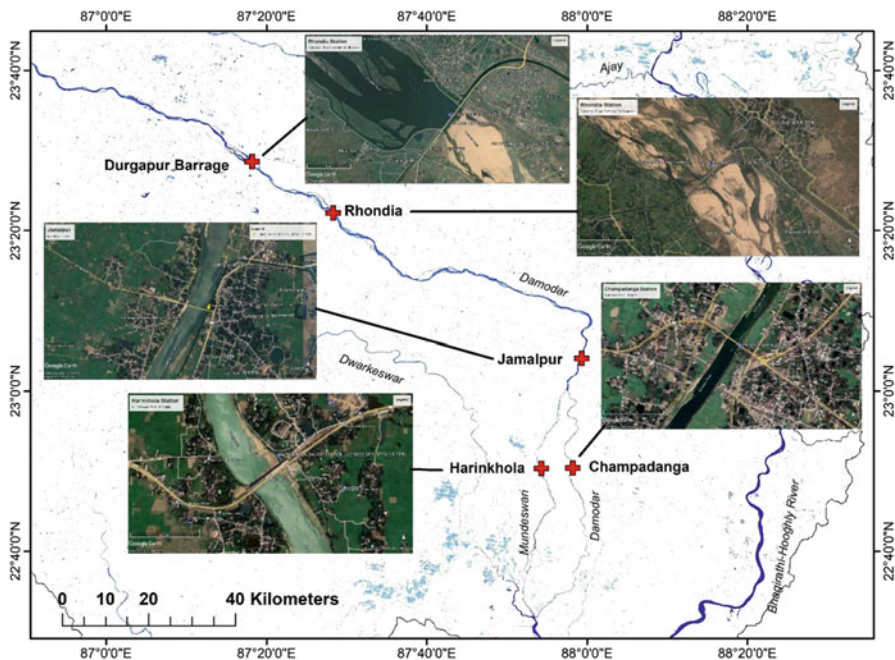


**Fig. 13.2** Important sites of river gauge stations and Durgapur Barrage in the lower Damodar River Basin (West Bengal)

Japan Aerospace Exploration Agency (JAXA) releases the global digital surface model (DSM) dataset of AW3D30 with a horizontal resolution of 30-meter mesh (1 arcsec). The dataset of surface water occurrence (SWO) was gathered from the web portal ([www.global-surface-water.appspot.com/download](http://www.global-surface-water.appspot.com/download)) of the Joint Research Centre's Global Surface Water Dataset (1984–2020) which was prepared to analyse the seasonal occurrence of inundated areas and permanent water bodies. National level hydrological modelling framework (National Remote Sensing Centre, Hyderabad) provides the database of evapotranspiration, surface runoff, and soil moisture on a daily basin of 5.5 km grid resolution in India ([www.bhuvan.nrsc.gov.in/nhp](http://www.bhuvan.nrsc.gov.in/nhp)). In this study, all databases are analysed and spatially mapped in the ERDAS Imagine 2014, ArcGIS 10.4, HEC-RAS 6.2, and XLSTAT (Table 13.2).

## 4 Methods

### 4.1 Basics of 1D-Hydrodynamic Model

One-dimensional (1D) hydrodynamic model in flood simulation assumes that the phenomenon of peak streamflow can be defined satisfactorily as unsteady or steady

**Table 13.2** Important sources of secondary database

Sl. no.	Data	Provider	Web portal
1	Daily rainfall, gauge data, and reservoir discharge	Irrigation and Waterways Department, Government of West Bengal	<a href="http://www.wbiwd.gov.in/">www.wbiwd.gov.in/</a>
2	Hydrological data and maps	HydroSHEDS	<a href="http://www.hydrosheds.org/page/hydrobasins">www.hydrosheds.org/page/hydrobasins</a>
3	Surface geology, lineaments, drainage, and other geomorphic information	Geological Survey of India	<a href="http://www.bhukosh.gsi.gov.in">www.bhukosh.gsi.gov.in</a>
4	Monthly and annual rainfall data	Center for Hydrometeorology and Remote Sensing	<a href="http://www.chrs.eng.uci.edu">www.chrs.eng.uci.edu</a>
5	Land use and land cover	Environmental Systems Research Institute	<a href="https://www.arcgis.com/home/item.html?id=fc92d38533d440078f17678ebc20e8e2#overview">https://www.arcgis.com/home/item.html?id=fc92d38533d440078f17678ebc20e8e2#overview</a>
6	Digital elevation model data	Japan Aerospace Exploration Agency	<a href="https://portal.opentopography.org/raster?opentopoID=OTALOS.112016.4326.2">https://portal.opentopography.org/raster?opentopoID=OTALOS.112016.4326.2</a>
7	Dataset of surface water occurrence	Joint Research Centre's Global Surface Water Dataset	<a href="http://www.global-surface-water.appspot.com/download">www.global-surface-water.appspot.com/download</a>
8	Global hydrologic soil groups database	National Aeronautics and Space Administration	<a href="https://catalog.data.gov/dataset/global-hydrologic-soil-groups-hysogs250m-for-curve-number-based-runoff-modeling">https://catalog.data.gov/dataset/global-hydrologic-soil-groups-hysogs250m-for-curve-number-based-runoff-modeling</a>
9	Database of evapotranspiration, surface runoff, soil moisture	National Remote Sensing Centre	<a href="http://www.bhuvan.nrsc.gov.in/nhp">www.bhuvan.nrsc.gov.in/nhp</a>

flow (with certain geometry and boundary conditions of channel) in a space of single dimension. 1D flood model was elaborated and applied by numerous workers (Horritt & Bates, 2002; Merwade et al., 2008; Leondro et al., 2009; Pender & Neelz, 2011; Betsholtz & Nordlof, 2017; Dasallas et al., 2019). 1D- hydrodynamic model is based on the Bernoulli (energy equation) and Saint-Venant equations (mass and moment conservation) for steady and unsteady flows in open channels, respectively. Betsholtz and Nordlof (2017) mentioned the following assumptions behind 1D flood simulation:

- The fluid is incompressible. Where the density of fluid is constant, the volume should be proportional to the mass.
- It is assumed that the water flows follow a longitudinal direction.
- In pressure distribution along a channel, the hydrostatic and vertical accelerations are overlooked.
- Vertical variations in flow and velocity are ignored.
- The water depth is much lower than the wave lengths.
- The average channel bed slope is small.

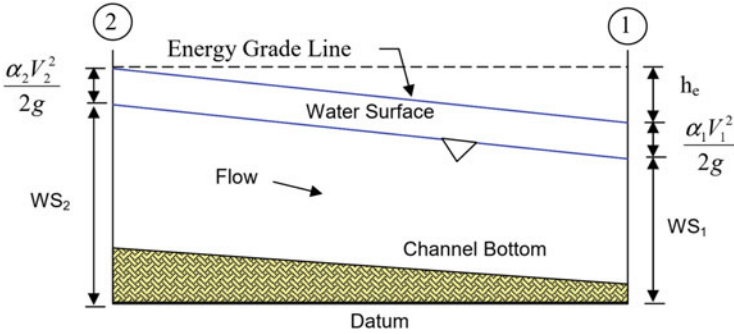


**Fig. 13.3** A schematic diagram of 1D hydrodynamic model (where  $\alpha_1$  and  $\alpha_2$  = velocity weighting coefficients;  $V_1$  and  $V_2$  = average velocity;  $g$  = gravitational acceleration;  $h_e$  = energy head loss;  $WS_1$  and  $WS_2$  = water surface elevation)

- Manning’s equation estimates the value of bed friction for the steady flow condition.
- The flow is the continuous function of the velocity and the water surface elevation  $H$ .

To simplify the calculation, the computing system of HEC-RAS assumes a horizontal water surface at each cross-section normal to the direction of flow such that the momentum exchange between the channel and the floodplain boundaries can be neglected (Dasallas et al., 2019). Kumar et al. (2017) and Dasallas et al. (2019) mentioned the following derivatives of 1D model (Fig. 13.3):

$$Y_2 + Z_2 + \frac{\alpha_2 V_2^2}{2g} = Y_1 + Z_1 + \frac{\alpha_1 V_1^2}{2g} + h_e \tag{13.1}$$

where  $Y_1$  and  $Y_2$  = flow depth of water (m),  $Z_1$  and  $Z_2$  = elevation of the main channel inverts (m),  $V_1$  and  $V_2$  = average velocity ( $m\ s^{-1}$ ),  $\alpha_1$  and  $\alpha_2$  = velocity weighting coefficients,  $g$  = gravitational acceleration ( $m\ s^{-2}$ ), and  $h_e$  = energy head loss (m).

De Saint Venant (1871) derived the following equations which is now used in HEC-RAS (Stelling & Verway, 2005; Fan et al., 2017):

$$\frac{\partial A_t}{\partial t} + \frac{\partial Q}{\partial x} = q_{lat} \tag{13.2}$$

$$\frac{1}{gA} \left\{ \frac{\partial Q}{\partial t} + \frac{\partial}{\partial x} \left( \frac{Q^2}{A} \right) \right\} + \frac{\partial \zeta}{\partial x} + \frac{Q|Q|}{K^2} = 0 \tag{13.3}$$

where  $A_t$  = cross-sectional area ( $m^2$ ),  $t$  = time (s),  $Q$  = discharge ( $m^3\ s^{-1}$ ),  $x$  = position along the channel axis (m),  $q_{lat}$  = lateral discharge per unit length of channel ( $m^2\ s^{-1}$ ),  $A$  = flow-conveying cross-sectional area ( $m^2$ ),  $\zeta$  = water level

above a selected horizontal reference plane (m), and  $K$  = channel conveyance ( $\text{m}^3 \text{s}^{-1}$ ). In its simplest form, Eq. (13.3) may be reduced to the familiar steady flow conveyance relationship

$$Q = K\sqrt{I} \quad (13.4)$$

with the conveyance  $K$  expressed as

$$K = CA\sqrt{R} \text{ or } K = \frac{1}{n}AR^{2/3} \quad (13.5)$$

where  $K$  is a function of Chezy resistance coefficient, hydraulic radius, cross-sectional area, and Manning's friction coefficient.

The set of Eqs. (13.2) and (13.4) forms the so-called *kinematic wave approximation* for flood propagation, which, after substitution of (13.4) into (13.2) and neglecting the lateral flow term, can be further simplified to the form

$$\frac{\partial Q}{\partial t} + c \frac{\partial Q}{\partial x} = 0 \quad (13.6)$$

with a flood wave celerity  $c$  ( $\text{m s}^{-1}$ ) expressed as

$$c = \frac{1}{b_s} \frac{dQ}{dh} \quad (13.7)$$

## 4.2 Steps in Flood Inundation Model of HEC-RAS

The HEC-RAS 6.2 version software includes extreme number of hydrologic applications, mainly (1) steady and unsteady flow modelling, (2) analysis of both subcritical and supercritical flow regimes, (3) design of culvert and bridge, (4) bridge scour computation, (5) analysis of floodplain and channel area encroachment, (6) multiple profile computations, (7) sediment transport/movable bed modelling, (8) reservoir and spillway analysis, (9) X-Y-Z (pseudo 3D) graphics of the river system, (10) levee overtopping, etc. (Hicks & Peacock, 2005; Stelling & Verway, 2005; Merwade et al., 2008; Pramanik et al., 2010; Sarhadi et al., 2012; Sanyal et al., 2014b; Kumar et al., 2017; Patel et al., 2017; Teng et al., 2017; Pathan & Agnihotri, 2020; Singh et al., 2020). The goal of the flood inundation modelling is to evaluate the possible flood extent in a river reach using the basic functions of RAS Mapper in HEC-RAS to create a 1D model of a river system. To assist the decision makers or planners, the thematic maps of 1D hydrodynamic model is very significant to recognize the inundated areas of different flow regimes for mitigating floods, protection of cropland and settlements, and adapting flood-controlling measures in

reality. Flood inundation mapping needs high-resolution DEM (digital elevation model) or DTM (digital terrain model) database to maintain accuracy at field scale, and comparing the DEM of water with the DEM of ground the area of flooding is determined at all points where the water surface is above the ground surface (Merwade et al., 2008). The details of workflow and modeler application guide can be found in the technical document of US Army Corps of Engineers (2020). In this study the following steps are taken to execute 1D hydraulic model for flood inundation mapping (Merwade et al., 2008; Kumar et al., 2019):

1. Design steady flow (e.g., 2-year, 5-year, 15-year, and 25-year flood) is firstly estimated using a calibrated popular hydrologic model (log-Pearson Type III distribution), and an unsteady flow database is collected from the daily discharge data of a gauge station for a specific period.
2. The requirement of channel geometric data includes width, elevation, shape, length, location, geomorphic shape, boundary condition (Manning's coefficient), and slope. River floodplain data (digitizing main and tributary mid-channel part, left-right banks, channel confluence/bifurcation junction, and floodplain span) is firstly needed. The consecutive maximum numbers of downstream cross-sections (covering boundary of floodplain) are developed, creating river transects in DEM or DTM.
3. Step 1 (design steady or unsteady flow) and step 2 (channel geometry) are then processed in HEC-RAS to deduce water surface elevations (WSE) along the channel. Other hydraulic parameters are obtained by calibration.
4. The DEM is subtracted from the water surface to obtain a water-depth map. The area with positive values in the water-depth map gives the flood inundation map of different design flows.
5. Other main outputs of HEC-RAS modelling water velocity of design flows, flow area, cross-sectional view of WSE, and energy grade line slope.

### 4.3 Risk and Flood Frequency Analysis

For any hydrologic design, the estimation of risk and reliability is very essential task, and the hydrological risk can be used to fix the return period for a given design life, reflecting level of risk (Vogel & Castellarin, 2017). The probability of flood occurrence in any one year (event) is  $p = 1/T$ , and the probability of  $x$  occurrences in  $n$  years is  $B(n, p)$ . According to Vogel and Castellarin (2017), "the probability (at least one incidence in  $n$  events) is called risk which is defined as the probability that one or more events will exceed a given magnitude within a specified binomial distribution."

$$\text{Risk} = 1 - (1 - 1/T)^n \quad (13.8)$$

$$\text{Reliability} = (1 - p)^n = (1 - 1/T)^n \tag{13.9}$$

Nearly in all series of natural floods, the log-Pearson Type III (LPT3) distribution (similar to normal or Gaussian distribution) is applied as a commonly used frequency distribution for annual peak streamflow. The mean in LPT3 distribution is approximately equal to the logarithm of the 2-year peak discharge. The standard deviation is the slope of the line, and the skew is shown by the curvature of the line. The probability density function (PDF) of log-Pearson Type III distributed random variable is given by Rao and Hamed (2019):

$$f(x) = \frac{1}{\alpha x \Gamma(\beta)} \left[ \frac{\log(x) - \gamma}{\alpha} \right]^{\beta - 1} e^{-\left\{ \frac{\log(x) - \gamma}{\alpha} \right\}} \tag{13.10}$$

where  $f(x)$  = the probability density function,  $x$  = the variable in a Pearson III distribution (range  $\gamma < x < \infty$ ),  $\alpha$  and  $\beta$  = distribution location and scale parameters, and  $\Gamma$  = gamma function.

The distribution function of LPT3 distribution is given by the following equation (Rao & Hamed, 2000):

$$f(x) = \frac{1}{\alpha x \Gamma(\beta)} \int_0^x \frac{1}{x} \left[ \frac{\log(x) - \gamma}{\alpha} \right]^{\beta - 1} e^{-\left\{ \frac{\log(x) - \gamma}{\alpha} \right\}} dx \tag{13.11}$$

If  $y = \frac{\log(x) - \gamma}{\alpha}$  is substituted in equation, then we can get the equation

$$f(x) = \frac{1}{\Gamma(\beta)} \int_0^y \frac{1}{x} [y]^{\beta - 1} e^{-y} dy \tag{13.12}$$

In general form, the LPT3 distribution can be written as

$$Q_{LPT} = Q_{avg} + K_T S_l \tag{13.13}$$

where  $Q_{LPT}$  = logarithm of predicted discharge, at return period  $T$ ,  $Q_{avg}$  = average of annual peak discharge logarithms,  $K_T$  = a function of return period (frequency factor) and skew coefficient, and  $S_l$  = the standard deviation of logarithms of annual peak discharge.  $K_T$  can be written as

$$K_T = \frac{2}{C_S} \left[ \left\{ \frac{C_S}{6} \left( u - \frac{C_S}{6} \right) + 1 \right\}^3 - 1 \right], C_S > 0 \tag{13.14}$$

where  $u$  is the standard normal variate corresponding to a probability on non-exceedance of  $P = 1 - 1/T$  and  $C_S$  is skew coefficient.

#### 4.4 Other Hydrological Estimates

Daily runoff ( $Q_{\text{Run}}$ ) of the ungauged basin can be calculated using NRCS-CN (Natural Resource Conservation Service Curve Number) method. Surface runoff for a particular rainstorm event is controlled by spatial pattern of land use–land cover (LULC) and hydrologic soil groups (HSG) which produce unique curve number (0–100) for a grid or a basin. An area-weighted average curve number is used for the entire catchment of Damodar to study the runoff effectively. The quantitative expressions of NRCS-CN method (Zade et al., 2005; Viji et al., 2015) can be written as

$$Q_{\text{Run}} = (\text{Rainfall} - 0.3 S_t)^2 / (\text{Rainfall} + 0.7 S_t) \quad (13.15)$$

$$S_t = 25,400 / \text{CN} - 254 \quad (13.16)$$

where  $S_t$  is potential maximum retention or recharge capacity after runoff begins (after 5 days antecedent rainfall condition).

In this study, the empirical formulae of flood peak potential ( $Q_{\text{fpp}}$ ) are used to assess the probable maximum discharge of Damodar River, taking upper catchment basin area (19,920 km<sup>2</sup>) from the Rhondia gauge station. Alongside, other hydrological estimates and indices related to flood hydrology are given in Table 13.3. It is needed to mention that two nonparametric methods (Mann-Kendall and Sen's slope estimator) were used to detect the significant trends of annual rainfall and annual peak discharge. The Mann-Kendall statistical test (M-K Test) and Sen's slope (Kamal & Pachauri, 2019; Saikia & Konwar, 2020) are used here to quantify the significance of trends in hydrometeorological time series (viz., annual rainfall and annual peak discharge). Positive values of Kendall  $T$  (tau) indicate increasing trends,

**Table 13.3** Important quantitative indices of flood hydrology

Sl. no.	Empirical formula and index	References
1	Dickens formula: $Q_{\text{flood}} = C_D A^{3/4}$ , where $Q_{\text{flood}}$ = estimated maximum flood peak (m <sup>3</sup> s <sup>-1</sup> ), $C_D$ = Dickens constant (range: 6–30), and $A$ = catchment area (km <sup>2</sup> )	Raghunath (2006)
2	Inglis formula: $Q_{\text{flood}} = 124 A / (A + 10.4)^{0.5}$	Raghunath (2006)
3	World envelope curve: $Q_{\text{flood}} = 3010 A / (277 + A)^{0.78}$	Subramanya (2013)
4	Indian envelope curve: $Q_{\text{flood}} = 4897 A^{0.19}$	Rakhecha and Singh (2017)
5	$C_v = \sigma / X_{\text{mean}}$ , where $C_v$ = coefficient of variation, $X_{\text{mean}}$ = mean annual peak discharge, and $\sigma$ = standard deviation	Raghunath (2006)
6	$C_s = \Sigma(X_i - X_{\text{mean}})^3 / (n-1) \sigma^3$ ; $C_s$ = coefficient of skew, $X_i$ = each observation of annual peak discharge, and $n$ = number of observations	Raghunath (2006)
7	$C_f = X_{\text{mean}} A^{0.8} / 2.14$ ; $C_f$ = coefficient of flood	Raghunath (2006)



while negative  $T$  values show decreasing trends. In this study, significance levels  $\alpha = 0.01$  and  $\alpha = 0.05$  were used. At the 5% significance level, the null hypothesis of no trend is rejected if  $|T| > 1.96$  and rejected if  $|T| > 2.576$  at the 1% significance level. Alongside estimating statistically significant range of peak discharge, the confidence interval ( $CI$ ) at 99% significance is applied here:

$$CI = X_{\text{mean}} - 3\sigma/\sqrt{n} \text{ to } X_{\text{mean}} + 3\sigma/\sqrt{n} \quad (13.17)$$

## 5 Results

### 5.1 Analysis of Flood Climate

The terms “flood climate” (Hayden, 1988) and “flood hydroclimatology” (Hirschboeck, 1988) include detail focus on the regional climate and atmospheric activity which promotes recurrent flood condition in connection with changing climate of the regions. Tropical climate, including monsoon climate of India, has high potentiality of torrential rainfall within a short period, which can instigate massive flood flows of Indian rivers. The flood climate of India can be designated as  $Tszo$  type (Hayden, 1988) in which barotropy ( $T$ ), seasonal basis ( $s$ ), intertropical convergence zone, ( $z$ ) and organized convective activity at synoptic scale ( $o$ ) are key determinants (Ghosh, 2013). The rainfall maps (Fig. 13.4) of DRB and associated basins (1990–2020) express that trend of mean annual rainfall increases from west to east direction and the maximum annual rainfall of the eastern basin varies from 1662 to 1977 mm (minimum annual rainfall of western basin: 790–1309 mm). In monsoon months (June–October), the rivers experience floods annually after a spell of heavy rainfall (150–300 mm within 3–4 days) because this amount of rainfall yields a gigantic volume of runoff in respect of catchment’s physical characteristics. Today’s climate is occurring in an atmosphere that’s been made warmer, wetter/humid and more energetic. Due to global warming input of more heat energy to atmosphere promotes more moisture in the air. It is learned that for every degree of warming, the atmosphere can hold around 7% more moisture (Climate Signals, 2022), and more rainfall comes in short with intense downpours, which has increased the risk of flash floods in India. The 2010 report by the Ministry of Environment and Forests, Government of India stated that India’s average temperature has risen by around 0.7 °C during 1901–2018. Due to climate change the summer monsoon precipitation (June–September) over India has also weakened by around 6% from 1951 to 2015 with notable decrease of annual rainfall (but increase of extreme rainfall event for a short period) over the Indo-Gangetic Plains (Sahoo & Bhaskaran, 2016). Interestingly, in the world, the number of rainy days is declining, while intense rainfall events of 10–15 cm per day are escalating (Chattopadhyay et al., 2020). This means that more amount of water is pouring downs in lesser time, and it creates maximum

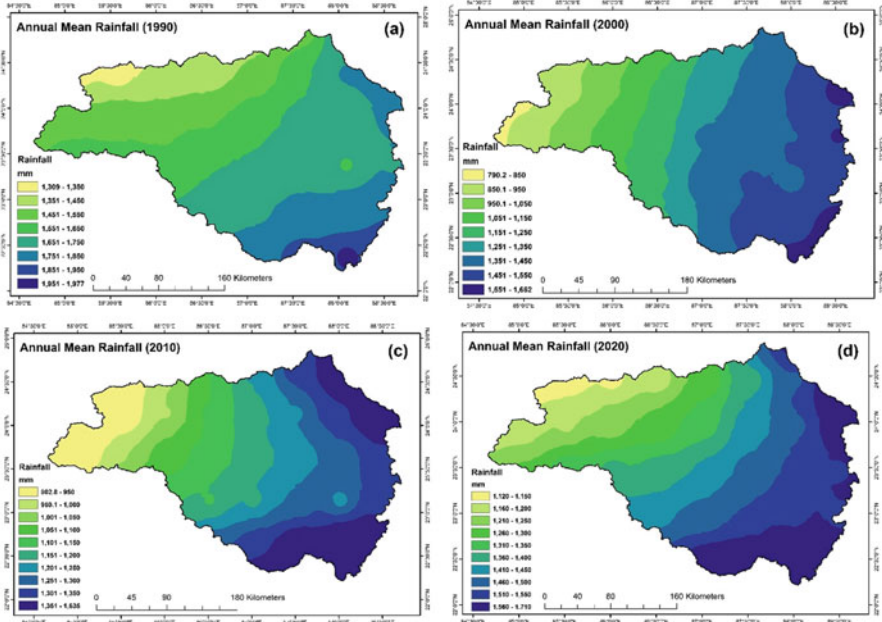


**Fig. 13.4** Areal distribution of mean annual rainfall (decreasing trend from west to east) in 1990 (a), 2000 (b), 2010 (c), and 2020 (d) over the Damodar River Basin and other associated basins

level of flood risk in the tropical region. In a nutshell, climate change has extreme impacts in India: (a) rise in average temperature, (b) trend of no rain for long period, (c) sudden burst of excessive heavy rainfall, and (d) occurrence of extreme weather hazard, like flash floods of Himalayas and monsoon floods of Ganga and Brahmaputra Basins.

Alongside, the tropical depressions and cyclones are another factor of heaviest rainfall and flood in India. The lower Ganga basin, including DRB, experiences west-north-westwards tracks of depressions and cyclones from the head of the Bay of Bengal to the Chhotangapur Plateau, causing heavy rainstorms and downpours throughout the region of West Bengal and Jharkhand. Tropical cyclone activity (development of depression and cyclonic storm) during late monsoon period shows an upward trend and also exhibits El Nino Southern Oscillation (ENSO) of 2–5 years’ time scale over the Bay of Bengal (Sahoo & Bhaskaran, 2016). Track of cyclone and depression is very much linked to occasional extreme floods of DRB, because in many cases (viz., floods of October 1978, June 1981, September 2000, September 2009, August 2016, and May 2021), the path of cyclonic activity moved from downstream to upstream direction (southeast to northwest) along the entire basin. In between 1986 and 1995, the track was mostly northward and then westward from the Bay of Bengal, and it covered the DRB and its associated basins. During 2006–2015, most cyclones moved northward. A key fact of DRB is that during cyclonic rainfall (moving southeast to northwest), the lower basin (West Bengal) is

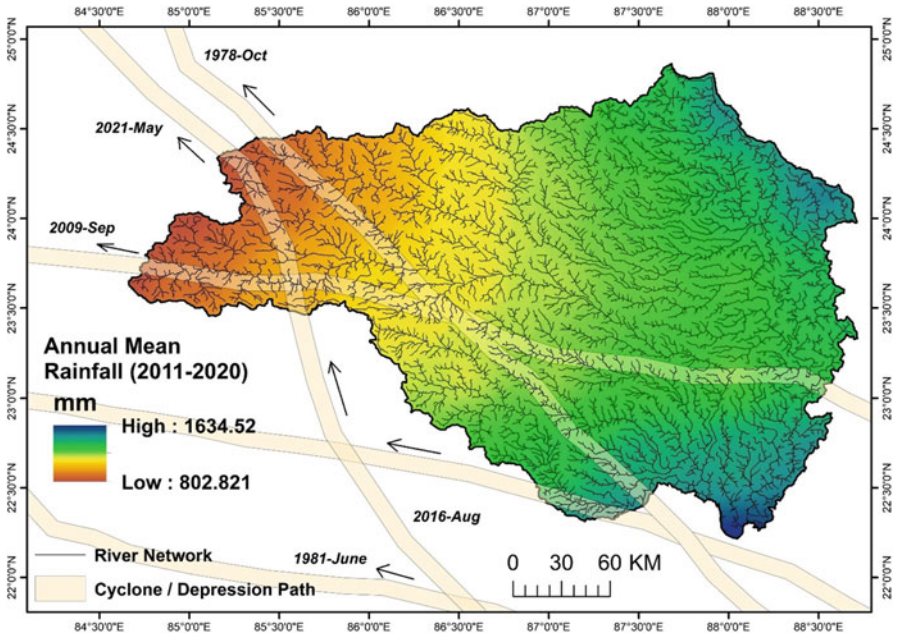


**Fig. 13.5** Tracks of tropical cyclones and depressions over the rainfall region of Damodar River Basin

already saturated with high moisture, and alongside when the cyclone reaches at the upper basin (Jharkhand), the region also experiences heavy rainfall (110–230 mm in 3–4 days) due to high topographic lift (>600 m from mean sea level) causing the excessive concentrations of runoff (later flood flow) in the fluvial system of Damodar and Barakar (Fig. 13.5).

W.W. Hunter (1876), in his Statistical Account of Bengal, described Damodar floods as *harka ban* (flash flood) having floodplain inundation depth of 1.5 m in the lower basin. Floods in the DRB have been presented as an aberrant and unpredicted behavior of the river, making “river training,” “river control,” “taming,” and “harvesting” of it very problematic and of then critical for a decade (Majumder et al., 2010b). In documentation, the great floods of Damodar were almost recurrent phenomena at past – 1770, 1855, 1866, 1873–1874, 1875–1876, 1884–1885, 1891–1892, 1897, 1900, 1907, 1913, 1927, 1930, 1935, 1943, 1959, 1978, 2000, 2011, 2016, and 2021 (Majumder et al., 2010b). Bardhaman town and its adjoining region were completely flooded in 1770, 1855, 1913, and 1943 having discharge of more than  $16,000 \text{ m}^3 \text{ s}^{-1}$ . To save the land from flood, the embankment was stated to build between 1866 and 1873 under the leadership of Maharaja Kirti Chand of Bardhaman. After independence of India, the flood hydrology of the Damodar catchment was getting more importance in view of India’s first multipurpose river valley project being undertaken in the basin adapting the model of Tennessee Valley Authority (TVA). The extensive studies of Glass (1924), Kirk (1950), Pramanik and

**Table 13.4** Historical record of seven rainstorms and resulting flood flows in the Damodar River at Raniganj

Sl. no.	Date of occurrence of rainstorm	No. of days rainfall	Date of occurrence of floods	Mean rainfall (mm)	Mean discharge ( $\text{m}^3\text{s}^{-1}$ )	Peak discharge ( $\text{m}^3\text{s}^{-1}$ )
1	28th Aug–31st Aug, 1909	4	31st Oct–1st Sept	116.84	5017	10,109
2	5th Aug–10th Aug, 1913	5	6th Aug–14th Aug	299.72	5663	18,406
3	21th Sep–7th Oct, 1916	6	22nd Sep–28th Sep	162.56	3879	11,128
4	1st Oct–25th Sep, 1916	5	2nd Oct–9th Oct	119.38	2832	6711
5	29th Jul–2nd Aug, 1917	5	30th Jul–4th Aug	243.84	4814	8070
6	30th Sep–7th Oct, 1917	8	1st Oct–12th Oct	248.92	4106	10,902
7	29th Oct–31st Oct, 1917	3	30th Nov–1st Nov	68.58	3398	6050

Rao (1952), Chatterjee (1967), Bhalla (1969), Sinha and Rao (1985), and Bhattacharya (2011) made few conclusions regarding the unique characteristics of flood climate in the DRB:

1. Key driver of each miserable flood is the torrential rainfall over the upper catchment. Total mean rainfall on the whole catchment producing floods generally varies from 76.2 mm in 3 days to a maximum of about 304.8 mm in 6 days. It is assumed that a maximum extreme rainfall of 508 mm in the first half of the monsoon season and 127 mm in the latter half with runoff coefficient of 90%.
2. An intensive rainstorm giving more than 330.2 mm of mean rainfall over the upper catchment may occur once in about 65 years and one giving more than 381 mm once in about 120 years. A storm giving 457.2 mm rainfall in 6 days of which 330.2 mm may fall in 3 days and 177.8 mm in a day may be assumed as the maximum that is likely to occur over the upper catchment.
3. A rainstorm magnitude equal to or greater than 304.8 mm occurs once in 100 years and greater than 355.6 mm in 250 years. Further, a storm rainfall giving 411.48 mm is likely to be equaled or exceeded only once in 1000 years. Between 1891 and 1980, 1 day maximum rainfall recorded as 124.71 mm and 7 days maximum rainfall recorded as 312.93 mm in the DRB.

Pre-dam historical data and analysis (Glass, 1924; Pramanik & Rao, 1952) is very much needed to understand and predict the flood condition. The following lessons are learnt from the past records (Table 13.4):

1. The maximum recorded 3-day rainfall was about 254 mm at pre-dam period. That rate of rainfall for the Damodar catchment of 18,648  $\text{km}^2$  work out to an average rate of peak discharge 18,264  $\text{m}^3\text{s}^{-1}$  at Raniganj.

2. High discharge at Rhondia (exceeding  $5663 \text{ m}^3\text{s}^{-1}$ ) on any date is very highly correlated with the rainfall recorded on the date and the preceding 2 days. It is formulated a regression trendline between rainfall ( $R$ , inches) of July to October with the corresponding seasonal flow ( $D$ , cusec) expressed during pre-dam period:  $D = 0.65 R - 8.68$ .
3. Discharge of the Damodar River at Rhondia on any day is very much correlated with the following: (a) rainfall of preceding day (0.73), (b) rainfall of preceding 2 days (0.80), and (c) rainfall of preceding day and discharge of preceding day (0.82). Two linear relationships are established: (a)  $D = 4.35 (R_{-1} + R_{-2}) + 0.9703$  and (b)  $D = 71.70 R_{-1} + 14.6787$ .
4. From 1909 to 1917 it was observed that 3–8 days continuous mean rainfall of 68.58–299.72 mm produced a peak flood discharge range of 6060–18,406  $\text{m}^3\text{s}^{-1}$  at Raniganj (table).

It was estimated that Damodar catchment received monsoon rainfall (June–October) of 855.57–1043.55 mm and Barakar catchment received monsoon rainfall of 840.54–1079.81 mm annually (Ghosh & Mistri, 2015). In between 1950 and 2000, the Jharkhand division of DRB received mean annual rainfall of 1091 mm, and the part of West Bengal receives 1167 mm. CHRS data of 2001–2020 period shows that mean normal annual rainfall of upper catchment ranges in between 1219 mm (western part) and 1923 mm (eastern part), reflecting an increasing trend of annual rainfall than previous (Fig. 13.6a). Rainfall trends in the DRB over the period of 46 years (1970–2015) reflect summer monsoon rainfall accounting for around 80% of total rainfall and increasing rainfall trend in post-monsoon season (Chattopadhyay et al., 2020). Total DRB receives quite same annual rainfall in between 1970 and 2015, and it is increasing from past record, reflecting high chance of flood risk: (1) Damodar catchment – 1298 mm (14.4–18.3% positive change); (2) Barakar catchment – 1267 mm (11.7–19.1% positive change); and (3) lower Damodar catchment – 1339 mm (12.1–16.6% positive change). Mann-Kendall test and Sen's slope reveal a significant increasing trend in annual rainfall: (1) 1.64–3.78  $\text{mm year}^{-1}$  in the Barakar catchment, (2) 0.85–2.32  $\text{mm year}^{-1}$  in the Damodar catchment, and (3) 0.46–4.80  $\text{mm year}^{-1}$  in the lower Damodar catchment (Table 13.5).

Now, the analysis is concentrated on the post-dam records of flood events which reflect the spatial concentration of 3–4 days flood producing rainfall and the resultant peak discharge at Rhondia. The mean annual rainfall (2001–2020) of the upper catchment varies from 1219 to 1923 mm (Fig. 13.6a) which is exceptionally extortionate, signifying high moisture laden basin area. Four distinct maps of flood events are taken into consideration to depict the moisture condition over the upper catchment during short period of heavy rainfall:

- Seven days (17th–23rd September, 2000) continuous rainfall of 34–290 mm was received in the Damodar and Barakar catchment due to tropical depression (Fig. 13.6b). The most intense rainfall of 251–290 mm was recorded around the Panchet and Maithon reservoirs. That period of cumulative rainfall generated maximum peak discharge of  $6387 \text{ m}^3 \text{ s}^{-1}$  at Rhondia on 23rd September, 2000.

**Fig. 13.6** Spatial distribution of rainfall over the upper catchment of Damodar: (a) mean normal rainfall distribution of period 2001–2020 in the upper catchment of Damodar, showing west–east increasing trend, (b) an event of maximum 290 mm rainfall (September, 2000) generated streamflow of  $6387 \text{ m}^3 \text{ s}^{-1}$ , (c) an event of maximum 268 mm rainfall (September, 2006) generated streamflow of  $7035 \text{ m}^3 \text{ s}^{-1}$ , (d) an event of maximum 203 mm rainfall (September, 2007) generated streamflow of  $8883 \text{ m}^3 \text{ s}^{-1}$ , and (e) an event of maximum 235 mm rainfall (August, 2011) generated streamflow of  $5211 \text{ m}^3 \text{ s}^{-1}$

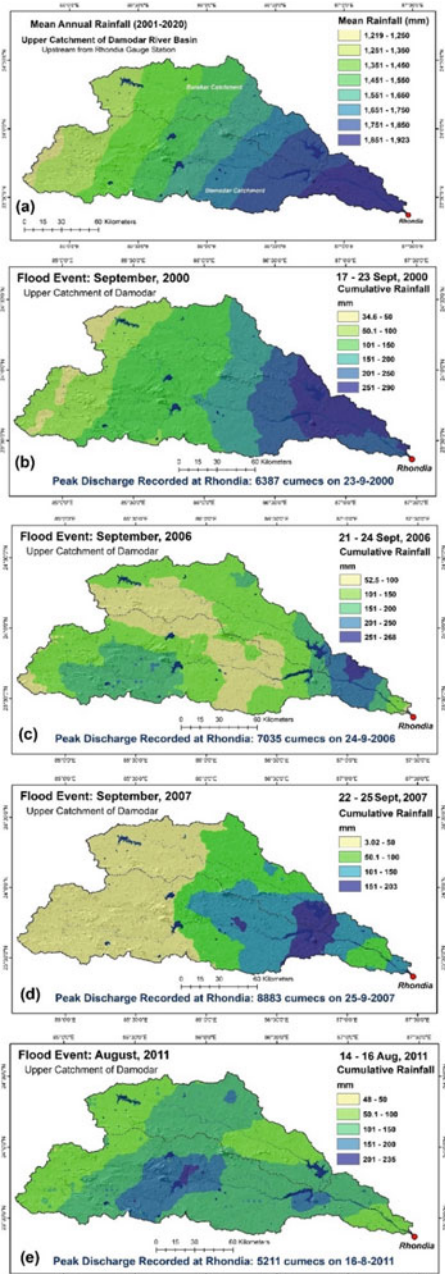


**Table 13.5** Summary of rainfall record (1970–2015), M-K Test, and Sen's slope in the DRB

Catchment	Station	Mean annual rainfall (mm)	SD	CV (%)	M-K Test Z value	Trend	Sen's slope (mm year <sup>-1</sup> )
Barakar	Maithon	1272	204	16	1.36	+	1.64
	Tilaiya	1273	198	16	0.98	+	1.56
	Barkisuriya	1280	203	16	1.43	+	3.78
	Barhi	1243	190	15	1.40	+	2.65
Damodar	Panchet	1307	189	15	1.05	+	2.32
	Sindri	1305	191	15	0.68	+	0.85
	Bokaro	1283	191	15	0.96	+	1.87
	Hazaribagh	1302	190	15	0.77	+	1.35
Lower Damodar	Asansol	1336	236	18	0.33	+	0.46
	Durgapur	1338	237	18	0.68	+	1.42
	Bardhaman	1340	235	17	0.71	+	3.75
	Uluberia	1342	235	17	0.81	+	4.8

Data source: Chattopadhyay et al. (2020)

SD standard deviation, CV coefficient of variation

- Four days (21st–24th September, 2006) rainfall varied from 52.5 to 268 mm, and the Damodar catchment received alone cumulative rainfall of 201–268 mm (Fig. 13.6c). After DVC flow regulation on 24th September, 2006, the recorded peak discharge was 7035 m<sup>3</sup>s<sup>-1</sup>.
- Four days period (22nd–25th September, 2007) of 50–203 mm rainfall (Fig. 13.6d) generated maximum peak discharge of 8883 m<sup>3</sup>s<sup>-1</sup> at Rhondia. The region around Panchet and Maithon reservoirs contributed more than 151 mm rainfall within 4 days.
- From 14th to 16th August, 2011, the upper catchment received rainfall of 48–235 mm (Fig. 13.6e), and more than 101 mm rainfall was recorded over the Damodar catchment within 3 days. During that rainfall event, the Durgapur Barrage was compelled to release maximum peak discharge of 5211 m<sup>3</sup>s<sup>-1</sup> on 16th August, 2011.

Finally, an exponential relationship between peak discharge ( $Q_{\text{peak}}$ ) and 3–4 days cumulative rainfall of upper catchment ( $R_{\text{cum}}$ ) is established on the basis of post-dam flood records:

$$Q_{\text{peak}} = 2213.1e^{0.0038 R_{\text{cum}}} (R^2 = 0.6838) \quad (13.18)$$

From this empirical relationship a forecast of flood-generating rainfall is developed for 2-year, 10-year, 50-year, and 100-year floods (design flood developed using log-Pearson Type III distribution) in the DRB:

1. 2-year flood (3254 m<sup>3</sup>s<sup>-1</sup>): 205 mm rainfall
2. 10-year flood (6676 m<sup>3</sup>s<sup>-1</sup>): 304 mm rainfall
3. 50-year flood (9417 m<sup>3</sup>s<sup>-1</sup>): 360 mm rainfall
4. 100-year flood (11,969 m<sup>3</sup>s<sup>-1</sup>): 412 mm rainfall.

### 5.2 Impact of Dam on Hydrological Variability

Few significant studies (Glass, 1924; Bhattacharya, 2011, Ghosh & Mistri, 2015; Ghosh & Guchhait, 2016; Karim & De, 2019; Singh et al., 2019) revealed the dam-induced changes in annual hydrograph, streamflow, and maximum flood discharge of the Damodar River. Here, a number of important hydrologic observations are presented to know the flood hydrological variability of a dam-controlled river. Annual hydrograph (Fig. 13.7a) of pre-dam (1934–1957) and post-dam (1958–2015) shows a marked shifting of peak monsoon flow from August to

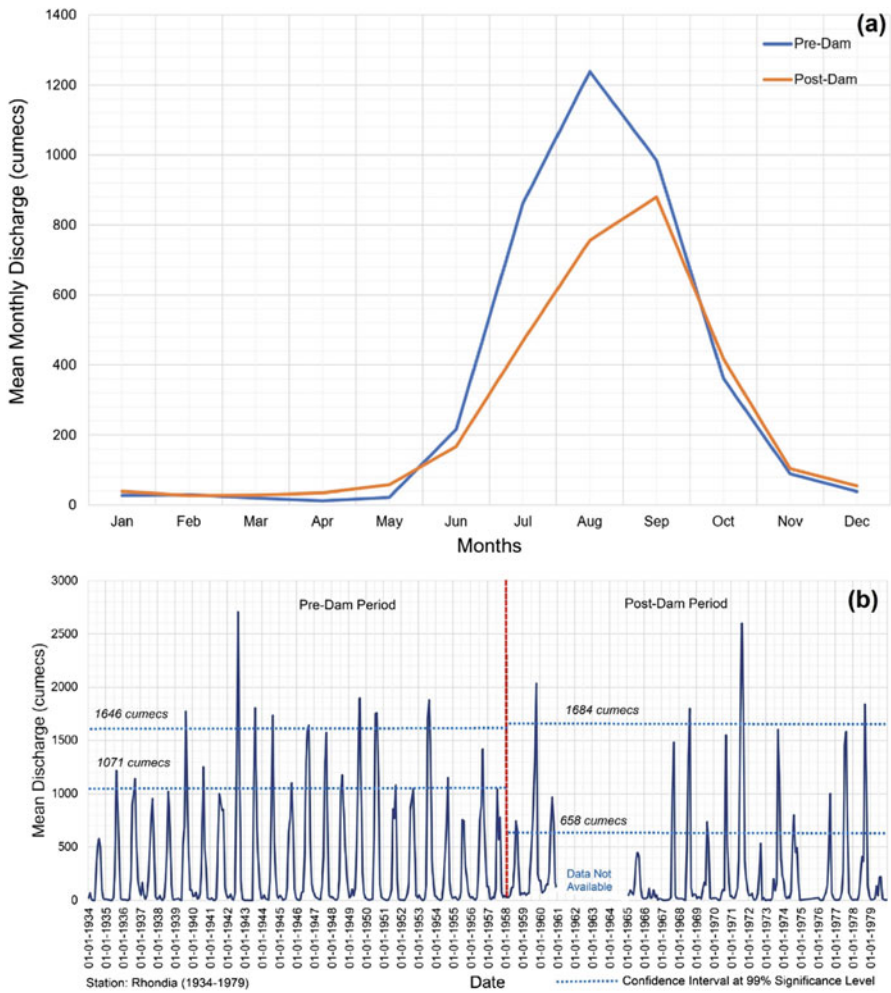


**Fig. 13.7** (a) Annual hydrograph of pre-dam and post-dam period based on mean monthly discharge and (b) marked variability of mean discharge during pre-dam and post-dam period, delimiting confidence intervals of discharge



September due to flow regulation of DVC dams. To maintain flood storage of first half monsoon, the DVC dams are now compelled to release excess water during 2nd half of monsoon. It also reflects the changing period of flood occurrence: (1) pre-dam maximum likelihood of flood event was August, and (2) post-dam maximum likelihood of flood event is September. Due to dam-controlled flow regulation, the average monthly peak flow is now reduced up to 28.94% from the previous natural condition (decreased from 1238 to 879  $\text{m}^3\text{s}^{-1}$ ). Mean monthly discharge of Damodar River was regulated by DVC dams since 1958. Pre-dam pre-monsoon base flow was near about 12.16  $\text{m}^3\text{s}^{-1}$ , but dam regulation has maintained a base flow of 34.41  $\text{m}^3\text{s}^{-1}$  (Fig. 13.7b). Under natural condition, the mean monsoon peak discharge was greater than 1500  $\text{m}^3\text{s}^{-1}$  in a number of cases, but that value has reduced significantly in post-dam period.

In natural condition, the Damodar River had high potentiality to cause violent flood flow. Between 1934 and 1948, the highest recorded average peak discharge was 14,767  $\text{m}^3\text{s}^{-1}$  on 10 October, 1941 (Fig. 13.8a). Another peak discharge of 18,123  $\text{m}^3\text{s}^{-1}$  was recorded on 12th August, 1935. Pramanik and Rao (1952) estimated that in the pre-dam period, a maximum discharge of 28,317  $\text{m}^3\text{s}^{-1}$  could be likely exceeded once in about 850 years. From 1823 to 1942, 12 times the peak discharge of flood events reached beyond 10,000  $\text{m}^3\text{s}^{-1}$  and during 5 times the river experienced discharge beyond 17,000  $\text{m}^3\text{s}^{-1}$ . A significant variation of annual peak discharge time series is observed. Since 1823, 13 times the annual peak discharge or extreme flood flow crossed 10,000  $\text{m}^3\text{s}^{-1}$  in the Damodar River, reflecting violent nature of flood. In pre-dam period (1933–1957), calculated *CI* (at 99% significance level) varied from 6055 to 10,459  $\text{m}^3\text{s}^{-1}$  (range – 4404  $\text{m}^3\text{s}^{-1}$ ) which is considered an exceptional high flow as compared to present condition (Fig. 13.8b). Since 1958, the DVC dams have effectively reduced *CI* which now ranges between 2790 and 4511  $\text{m}^3\text{s}^{-1}$  (range – 1721  $\text{m}^3\text{s}^{-1}$ ), reducing the maximum likelihood flood flow up to 53.92–56.87% in the river. Importantly the post-dam time series shows a positive growth trend (1958–1978 and 1979–2015) which matches with increasing trend of annual rainfall in the DRB since 1970 (as discussed in pervious section). M-K test is performed on two separate time series ( $N = 21$  and  $N = 37$ ), separated on the basis of maximum 1978 flood flow (10,919  $\text{m}^3\text{s}^{-1}$ ); Kendall tau (0.1238 and 0.2012) shows significant (rejecting null hypothesis and accepting alternative hypothesis, i.e., slope is not zero at 0.05 significance level) but weak time series trend (Table 13.6). The positive *Z* value, 0.75492 and 1.7395. expresses an increasing trend of annual peak discharge with time. Sen's slope of two time periods is expressed as: (i) 44.487  $\text{m}^3\text{s}^{-1}$  per year (1958–1978) and (ii) 46.639  $\text{m}^3\text{s}^{-1}$  per year (1979–2015).

Apart from the annual peak discharge analysis, NRCS-CN output exhibits the spatial variability of curve number (*CN*) and surface runoff depth in the selected flood events of 2000 and 2006 to portray the regions of maximum water concentration (or excess water coming from which areas in the upstream watershed of Panchet and Maithon dams). The runoff curve number (i.e., *CN* is an empirical parameter used for predicting direct runoff during a rainfall event) is primary guided by the HSG and LULC which are mapped in the upper catchment of Damodar. GIS analysis suggests that a maximum area of 17,011  $\text{km}^2$  (85.39% of total upper

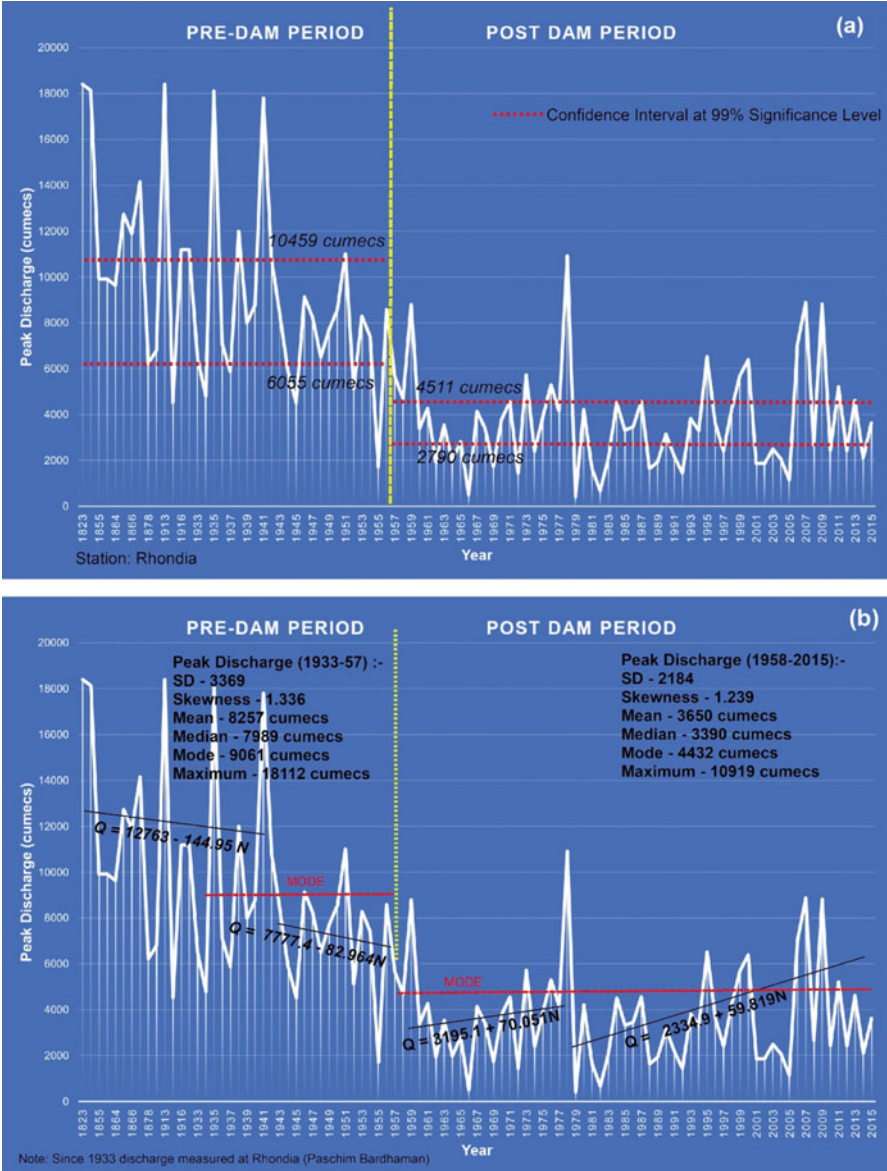


**Fig. 13.8** (a) Erraticism between natural annual peak flow regime and dam-induced changes in annual peak flow, delimiting marked variation of confidence intervals, and (b) observed trends of annual peak flow during pre- (decreasing) and post-dam period (increasing), including variations of hydrological statistics

**Table 13.6** M-K test and Sen's slope analysis for post-dam annual peak discharge time series

Parameters	Time period (1958–1978)	Time period (1979–2015)	Remarks
$N$	21	37	Rejecting null hypothesis and accepting alternative hypothesis, i.e., slope is not zero at 0.05 significance level, an increasing trend (+) in time series of post-dam period
$Z$	0.7549	1.7395	
$p$ -value	0.4503	0.0819	
$S$	26	134	
Var $S$	1096.66	5846	
Tau	0.1238	0.2012	
Sen's slope	44.487	46.639	
Sen's slope at 95% confidence interval	– 104.545–226.000	– 6.166–110.863	

catchment area) is categorized as HSG  $C$  (viz., loam, sandy clay loam, silt loam, clay loam, and silty clay loam soil textures), and other categories are HSG  $D$  (463 km<sup>2</sup>), HSG  $C/D$  (319 km<sup>2</sup>), and  $D/D$  (56 km<sup>2</sup>). In the catchment, an area of 4948 km<sup>2</sup> (24.84% of total upper catchment area) is designated as natural vegetation and forest cover, and the area of cropland and seasonal fallow land covers 9702 km<sup>2</sup> (48.71% of total area). Alongside, other LULC classes are designated as waterbodies/rivers (525 km<sup>2</sup>), grassland (40 km<sup>2</sup>), scrub/shrub/bushes (2178 km<sup>2</sup>), flooded vegetation (34 km<sup>2</sup>), bare land (42 km<sup>2</sup>), and built-up/settlement (2493 km<sup>2</sup>), respectively. Using Python programming in ArcGIS 10.4, the weighted  $CN$  (0–100) is derived for the upper catchment from the raster database of HSG and LULC. The mean weighted  $CN$  of the catchment is 78.57 which signifies quite high runoff potentiality of the hard rock terrain. The  $CN$  map reflects the maximum coverage of range 51–75, followed by range 76–100 (Fig. 13.9a). The runoff maps of rainfall events of September, 2000 and September, 2006 exhibit the following findings:

- *First case:* The total rainfall, during 13–23 September, 2000, varied widely from 34 to 290 mm (Fig. 13.9b), and it had maximum record (>201 mm) around the adjoining parts of Panchet and Maithon dams. For that amount of 7 days cumulative rainfall that parts of catchment yielded potentially 151–200 mm runoff, having extreme concentration of 201–282 mm runoff at selected pockets. That amount of runoff on a vast region accumulated in the DVC reservoirs, and finally, the dams were compelled to release excess water at the rate of maximum 6387 m<sup>3</sup>s<sup>-1</sup> on 23 September, 2000 in the Damodar River, inundating the lower valleys of Purba Bardhaman, Hooghly, and Howrah districts.
- *Second case:* The 4 days total rainfall, from 21 to 24 September, 2006, ranged between 52.5 and 268 mm (Fig. 13.9c), and the torrential rainfall of >151 mm was observed in the hilly tract of Damodar catchment and downstream of Panchet and Maithon dams. That amount of heavy rainfall yielded a runoff range of 10–207 mm, having extreme concentration (>101 mm) around those parts. As a result, on 24 September, 2006, the recorded maximum discharge of Damodar was 7035 m<sup>3</sup>s<sup>-1</sup>, causing havoc flood in the low-lying floodplains of Hooghly and Howrah.

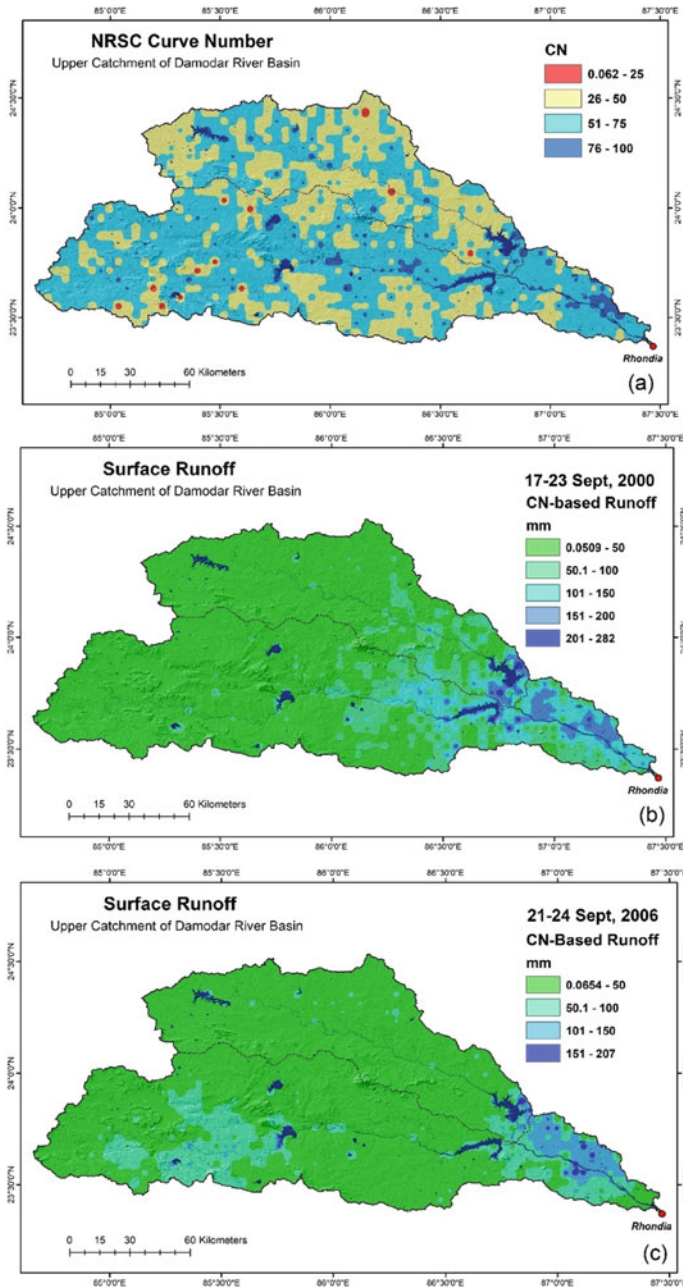


**Fig. 13.9** (a) An important and useful map of weighted NRCS curve numbers developed for the upper catchment of Damodar (including basin area of Barakar River), (b) spatial extent of CN-derived potential runoff (50–282 mm) during the flood event of 17–23 September 2000, and (c) spatial extent of potential runoff (50–207 mm) during the flood event of 21th–24 September 2006

### 5.3 Flood Frequency and Hydrological Risk

The empirical formulae of predicting maximum flood peaks (Table 13.1) have yielded variable results for the Damodar River (considering 19,920 km<sup>2</sup> of catchment area from Rhondia gauge station): (i) Dickens result – 23,474 m<sup>3</sup>s<sup>-1</sup>; (ii) Inglis result – 17,455 m<sup>3</sup>s<sup>-1</sup>; (iii) world envelope curve result – 26,286 m<sup>3</sup>s<sup>-1</sup>; and (iv) envelope curve of Rakhecha and Singh result – 32,121 m<sup>3</sup>s<sup>-1</sup>. The maximum recorded flood peak in pre-dam period was 18,406 m<sup>3</sup>s<sup>-1</sup> (1913), and in post-dam period it was 10,919 m<sup>3</sup>s<sup>-1</sup> (1978). So, the observed value is very much close to the result of Inglis empirical formula. In this study, two different time series (annual peak discharge of pre-dam and post-dam) of two stations (Rhondia and Harinkhola) are taken into consideration for flood frequency analysis (FFA). From the pre-dam (1933–1957) and post-dam (1958–2015) database of Rhondia station, it is estimated that in pre-dam period, i.e., natural condition, there are a greater number of floods above the mean peak discharge (7413 m<sup>3</sup>s<sup>-1</sup>) than the post-dam period mean (3650 m<sup>3</sup>s<sup>-1</sup>). The curve which fits the annual peak flood discharge data on a log-log paper will not be a symmetrical curve, but a skew curve which unsymmetrical, i.e., points do not lie on the straight line but the line bends off. The general slope of this curve is given by the coefficient of variation ( $C_v$ ), and the departure from the straight line is given by the coefficient of skew ( $C_s$ ). In pre-dam period the smaller value of  $C_v$  (0.312) indicates occurrence of floods in same magnitude, but large  $C_v$  (0.592) of post-dam period reflects a range in the magnitude of floods due to dam control. The coefficient of flood ( $C_f$ ) indicates the general magnitude of the floods above one unit in the particular river; it fixes the height of the nonlinear curve above the base. In pre-dam period  $C_f$  was extremely huge, i.e., 5.767, but after dam construction it reduces to 2.855, decreasing (49.50%) the flood curve height significantly.

Distribution of annual peak discharge fits well log-Pearson Type III (LPT3) distribution, as significant in Goodness-of-Fit test, in the case of DRB. The output shows very less deviation of LPT3 predicted flow ( $Q_{\text{pred}}$ ) in respect of observed flow ( $Q_{\text{obs}}$ ), fitting a linear relationship of  $Q_{\text{pred}} = 88.515 + 0.9758 Q_{\text{obs}}$  ( $R^2 = 0.9757$ ). The hydrological risk, associated with FFA, is assessed here in terms of reoccurrence interval and exceedance of probability measures. The results of FFA exhibit a notable predictability of flood design in respect of pre-dam (1933–1957) and post-dam (1958–2015) probability distribution. The key statistical findings are mentioned as follows:

1. There is a reduction (up to 55.79%) of mean annual peak discharge ( $Q_{\text{peak}}$ ) or flood flow from pre-dam to post-dam period due to the regulated control of DVC dams during the monsoon months. The weighted skewness ( $C_w$ ) of pre-dam period is  $-0.51074$  which was transformed to very high, i.e., 2.234, during post-dam period, signifying high range between flood magnitude. Another LPT3 derived parameter is coefficient of skewness ( $C_s$ ) which is exceptionally very high (3.6962) during pre-dam period, but after dam construction due to flow regulation and flood reserve of reservoirs  $C_s$  reduces to  $-0.757$ . Kurtosis of

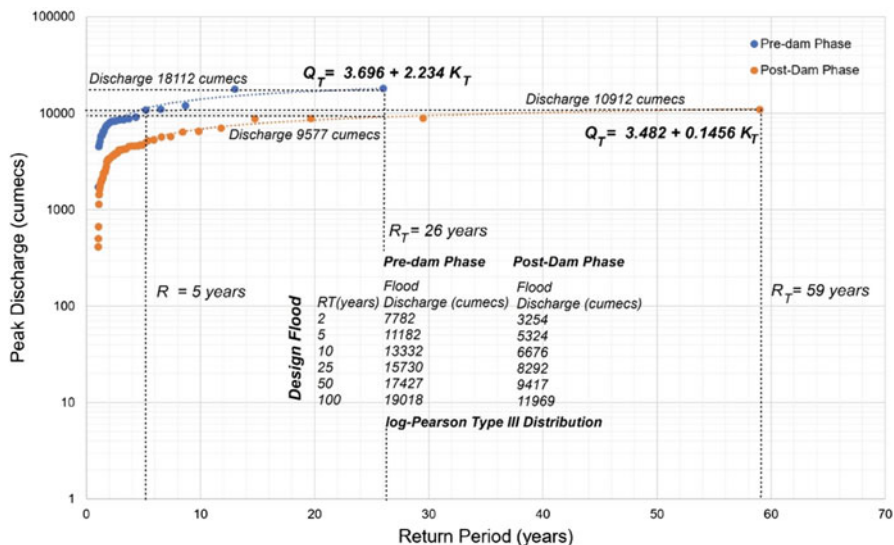


**Fig. 13.10** Variability of LPT3 flood frequency distribution in pre- and post-dam period, showing estimated changes in design floods and return periods

pre-dam period is 1.776 which changed to 2.625 in post-dam period. In both cases, kurtosis reflects a fat-tailed distribution (leptokurtic), having very high skewness and high degree of peakedness of the flood frequency distribution with high probability of extreme outlier values (i.e., maximum likelihood of flood events).

- LPT3 shows that the annual peak discharge of less than  $5658 \text{ m}^3\text{s}^{-1}$  (during pre-dam period) occurs with an exceedance probability of greater than 80%, but in post-dam period the 80% exceedance probability of flood occurrence is reduced to only  $1897 \text{ m}^3\text{s}^{-1}$  in the Damodar River. It is noteworthy to mention that an extreme peak flow of  $10,919 \text{ m}^3\text{s}^{-1}$  (observed in 1978) can be occurred having only 1.69% chance (in any one year) at present condition and that flow had 19.34% probability of occurrence during pre-dam period (Fig. 13.10).
- Recurrence interval or return period ( $R_T$ ) provides the estimated interval between events of a similar size or intensity of flood. In pre-dam period, a flood flow of  $18,112 \text{ m}^3\text{s}^{-1}$  (observed in 1935) has 26 years  $R_T$ , and it has 3.846% chance of being exceeded in any one year. The pre-dam flow of  $4514 \text{ m}^3\text{s}^{-1}$  has only  $R_T$  of 1.08 years (almost regular event), having 92.30% chance of being exceeded in any one year. A 100-year flood, a flood event that has 1% probability or 1 in 100 chances of being equalled or exceeded in any given year, is estimated about  $19,018 \text{ m}^3\text{s}^{-1}$ . Alongside, FFA estimates the 2-year flood was  $7782 \text{ m}^3\text{s}^{-1}$  having 50% chance of occurrence in one of given years. It shows the propensity of past furious floods with a maximum likelihood of occurrence in the DRB. For that

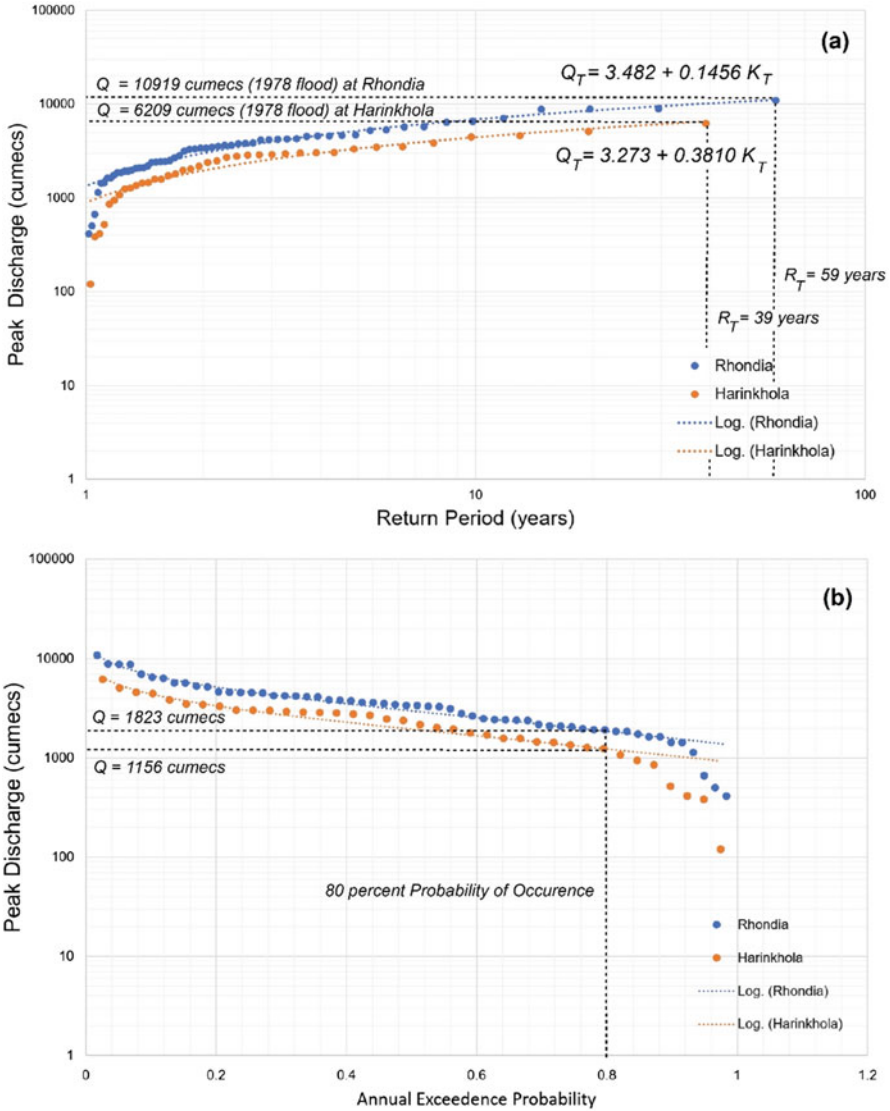


**Fig. 13.11** (a) Dam-controlled LPT3 distributions of annual peak discharge in relation to return period at Rhondia (Damodar River) and at Harinkhola (Mundeswari River) and (b) comparative analysis of variability in annual exceedance probability of peak discharge at two river gauge stations

reason, the DVC had a prime objective to control the abnormal extreme flow under a critical level in the lower Damodar River.

4. The flood regulation system of DVC dams has turned the hydrological regime to a large extent. Now, a maximum flood flow of  $10,919 \text{ m}^3\text{s}^{-1}$  has  $R_T$  of 59 years, and it has only 1.604% chance of being exceeded in any one year (Fig. 13.11a).

At present, annual peak discharge of 1443–1434  $\text{m}^3\text{s}^{-1}$  has 1.11–1.09 years  $R_T$ , and it has 89–91% chance of occurrence in any one year. The 100-year flood of post-dam period is estimated about 11,969  $\text{m}^3\text{s}^{-1}$  (reduction of 37.06% from the pre-dam 100-year flood flow), which has only 1% chance of occurrence in one of given year (i.e., 1 in 100 years). The 2-year flood (50% probability of occurrence) is estimated about 3234  $\text{m}^3\text{s}^{-1}$ , (reduction of 58.44% from the pre-dam 2-year flood flow).

5. FFA at Harinkhola gauge station (1978–2015) reflects the extreme downstream flood flow condition of the Mundeswari River (western bifurcated channel of main Damodar River). The 100-year flood at this station is near about 8058  $\text{m}^3\text{s}^{-1}$ , and the estimated 2-year flood is 2045  $\text{m}^3\text{s}^{-1}$ . The observed maximum flood flow is 6208  $\text{m}^3\text{s}^{-1}$  (observed in 1978) which has 39 years  $R_T$ , having 2.6% chance of occurrence in one of the given years. It is observed that there is 80% probability to encounter peak discharge of 1156–1183  $\text{m}^3\text{s}^{-1}$  in the lower Damodar River (Fig. 13.11b).

#### 5.4 1D Flood Simulation of Unsteady and Steady Flow

“Steady flow” refers to conditions that do not change with time. Mathematically, steady flow implies that  $(\partial h/\partial t) = 0$ ,  $(\partial V/\partial t) = 0$ , and  $(\partial Q/\partial t) = 0$ . “Uniform flow” refers to conditions that do not change with space. Unsteady flow equations in open channels with friction define kinematic and dynamic waves. The model is performed on two bifurcated channels of the main Damodar River, viz., Mundeswari River and Damodar/Amta River (Fig. 13.12). In the first case, a database of unsteady flow (observed at Durgapur Barrage) is used in 1D flood simulation. A current low-magnitude flood wave (1410–1811  $\text{m}^3\text{s}^{-1}$ ) occurred during June 2021, and a hydrological simulation of discharge and gauge height was retrieved from IWD web database to understand the current flow regime at spatial scale in the platform of HEC-RAS 6.2 version. The hydrograph of early monsoon rainfall shows an escalation of base flow (nearer to 400  $\text{m}^3\text{s}^{-1}$ ) to 1811  $\text{m}^3\text{s}^{-1}$  at a sudden due to release of excess water from the Durgapur Barrage (1 June–6 July 2021) (Fig. 13.13a). The unsteady flow got momentum from 18 June 2021 (846  $\text{m}^3\text{s}^{-1}$ ) and it reached peak on 22 June 2021, and then it gradually reduced to 487  $\text{m}^3\text{s}^{-1}$  on 6 July 2021. A strong relationship between streamflow or daily discharge ( $Q_{un}$ ) and station gauge height ( $G_h$ ) was observed at Jamalpur and Champadanga gauge stations. With a high coefficient of determination, the stage-gauge height curve of Damodar River followed a power regression positive trend (Fig. 13.13b, c):

- At Jamalpur gauge station:  $G_h = 9.4998 Q_{un}^{0.094}$
- At Champadanga gauge station:  $G_h = 3.6743 Q_{un}^{0.1705}$

A flood management strategy is deduced from the empirical relationship. From this relationship an estimate of bankfull discharge (critical flow level for downstream



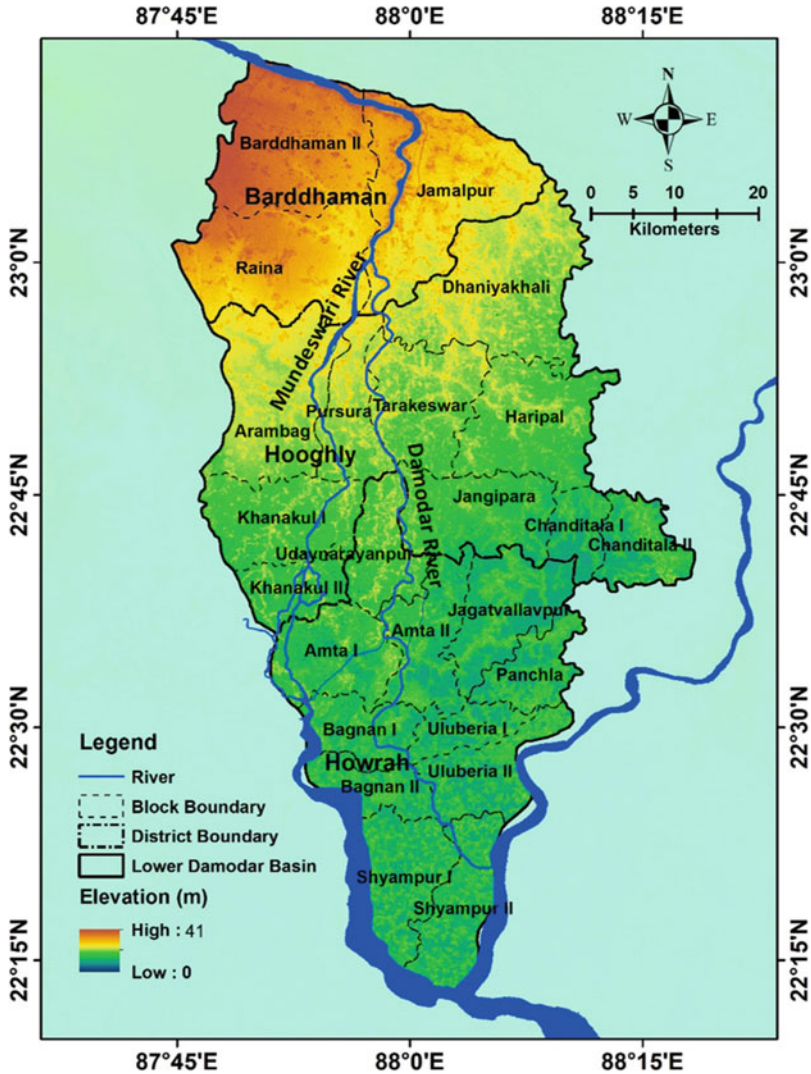


**Fig. 13.12** Flood prone channels of lower Damodar River Basin (considered in HEC-RAS 1D hydrodynamic model) on the terrain of 0–41 m elevation, covering the administrative blocks of Purba Bardhaman, Hooghly, and Howrah districts (West Bengal)

inundation or overbank flow) can be established on the basis of danger level (DL) and extreme danger level (EDL) gauge heights at two stations. Alongside, the estimated bankfull discharge ( $Q_{\text{bank}}$ ) reflects the present carrying capacity of channel (Table 13.7). Jamalpur gauge station is a vital location for flood prediction because from this site the main river is bifurcated into Munderwari channel and Damodar/Amda channel. At this site,  $Q_{\text{bank}}$  of DL (23.24 m from msl) and EDL

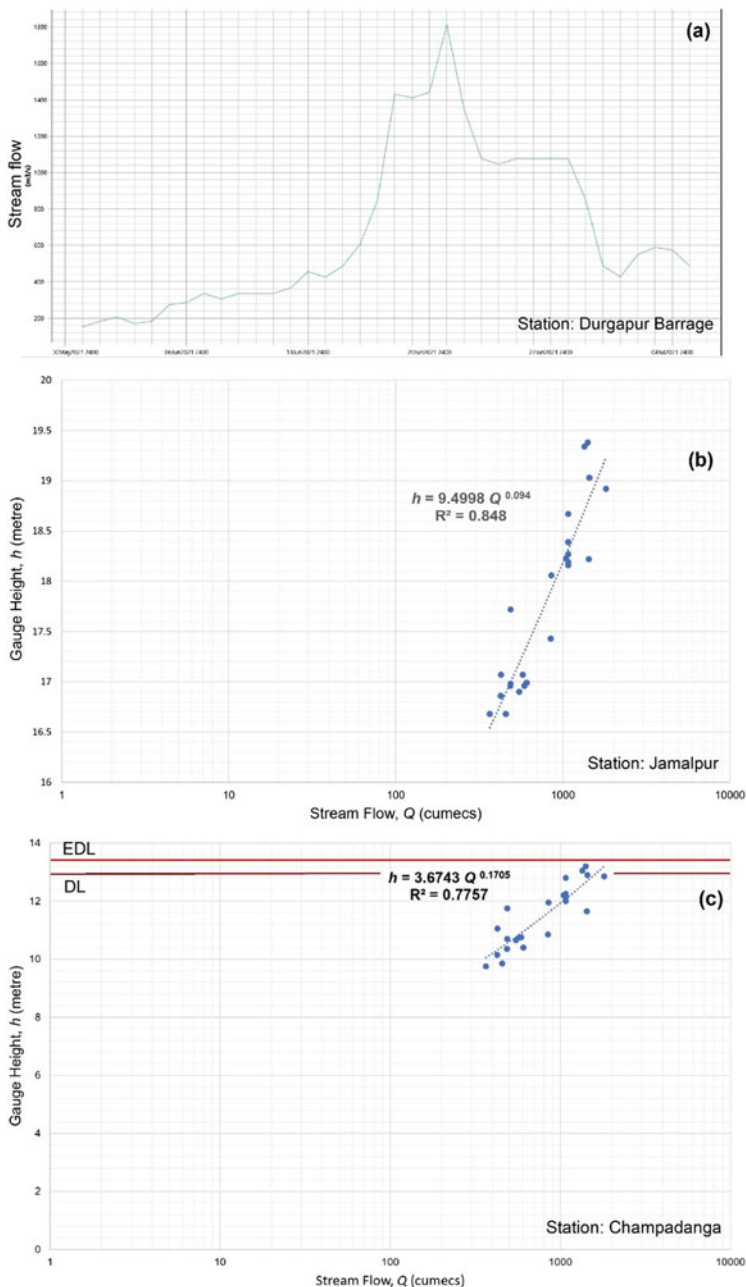


**Fig. 13.13** (a) Schematic hydrograph of period 1 June–6 July 2021 observed at the Durgapur Barrage, (b) stage-streamflow rating curve at Jamalpur gauge station, and (c) stage-streamflow rating curve at Champadanga gauge station

**Table 13.7** HEC-RAS estimated present critical bankfull discharge in the Mundeswari and Damodar channel

Parameters	Jamalpur gauge station	Champadanga gauge station	Harinkhola gauge station
Danger level (DL)	23.24 m	12.9 m	12.8 m
Extreme danger level (EDL)	23.54 m	13.5 m	13.41 m
Bankfull discharge at DL	$3198 \text{ m}^3\text{s}^{-1}$	$1353 \text{ m}^3\text{s}^{-1}$	$1518 \text{ m}^3\text{s}^{-1}$
Bankfull discharge at EDL	$3326 \text{ m}^3\text{s}^{-1}$	$1651 \text{ m}^3\text{s}^{-1}$	$1822 \text{ m}^3\text{s}^{-1}$

Note: Elevation of DL or EDL measured from mean sea level

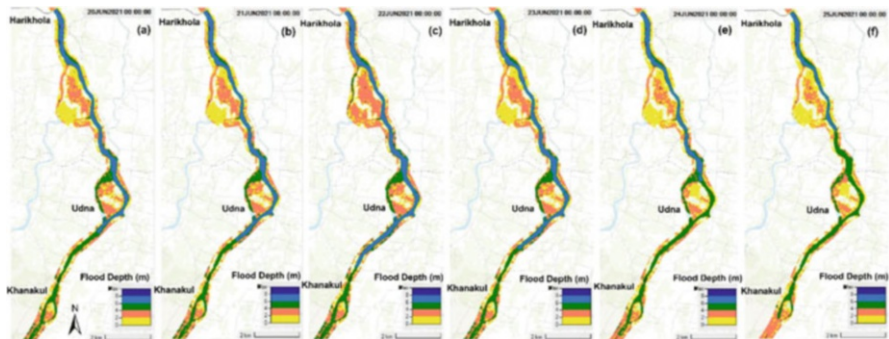


**Fig. 13.14** HEC-RAS 1D floodplain inundation modelling output maps (a–f) of Mundeswari River (between Harinkhola and Khanakul) based on unsteady flow simulation (20–25 June 2021), noticing observed maximum discharge ( $1811 \text{ m}^3\text{s}^{-1}$ ) on 22nd June, 2021

(23.54 m from msl) are  $3198 \text{ m}^3\text{s}^{-1}$  and  $3326 \text{ m}^3\text{s}^{-1}$ , respectively. The peak flow at Champadanga gauge station determines the flood condition of Hooghly and Howrah districts. At this site,  $Q_{\text{bank}}$  of DL (12.9 m from msl) and EDL (13.5 m from msl) are  $1353 \text{ m}^3\text{s}^{-1}$  and  $1651 \text{ m}^3\text{s}^{-1}$ , respectively. So, from this critical bankfull flow database, the DVC and IWD should regulate the flood flow or peak discharge (maintaining flow under critical level) to save the floodplains from a long period of inundation. During the unsteady flow of June–July 2021 the streamflow did not cross the bank at Jamalpur, but it overtopped the bank DL from 20–24 June 2021 ( $>1410 \text{ m}^3\text{s}^{-1}$ ) at Champadanga, signifying the low carrying capacity of Amta channel and downstream vulnerability of flood.

1D flood simulation of HEC-RAS exhibits the floodplain inundation depths during a period of unsteady flow at downstream of Harinkhola gauge station ( $22^\circ 50'22.38'' \text{ N}$ ,  $87^\circ 54'15.75'' \text{ E}$ ). From the maps (Fig. 13.14) it is observed that in the floodplain of Mundeswari, the maximum flood depth of certain discharge (20–25 June 2021) varies from 1 to 8 m in the active channel area and the adjoining floodplain. On 22 June 2021 the region around Harinkhola, Udna, and Khanakul experienced inundation depth of greater than 3 m for the discharge of  $1811 \text{ m}^3\text{s}^{-1}$

**Table 13.8** HEC-RAS derived hydrologic statistics (unsteady flow) of the cross-sections along Mundeswari River and Damodar/Amta River

Hydrologic parameters	Mundeswari River		Damodar/Amta River	
	Upstream cross-section	Downstream cross-section	Upstream cross-section	Downstream cross-section
Total flow in channel area	1685.02 m <sup>3</sup> s <sup>-1</sup>	1457.07 m <sup>3</sup> s <sup>-1</sup>	1378.12 m <sup>3</sup> s <sup>-1</sup>	1081.22 m <sup>3</sup> s <sup>-1</sup>
Flow area	1056.88 m <sup>2</sup>	548.11 m <sup>2</sup>	687.86 m <sup>2</sup>	478.91 m <sup>2</sup>
EG elevation	18.78 m	14.69 m	18.45 m	16.13 m
WS elevation	18.65 m	14.35 m	18.28 m	15.91 m
EG slope	0.00440 m m <sup>-1</sup>	0.002270 m m <sup>-1</sup>	0.000471 m m <sup>-1</sup>	0.000750 m m <sup>-1</sup>
Minimum main channel elevation	13.00 m	9.00 m	12.00 m	11.00 m
Top width	199.2 m	163.14 m	268.97 m	214.92 m
Average velocity	1.55 m s <sup>-1</sup>	2.66 m s <sup>-1</sup>	1.68 m s <sup>-1</sup>	1.99 m s <sup>-1</sup>
Hydraulic depth in channel	5.31 m	3.36 m	5.81 m	4.91 m
Wetted perimeter	199.35 m	164.43 m	118.50 m	97.68 m
Shear	22.87 N m <sup>-2</sup>	74.26 N m <sup>-2</sup>	26.83 N m <sup>-2</sup>	81.37 N m <sup>-2</sup>
Stream power	36.47 N m s <sup>-1</sup>	197.29 N m s <sup>-1</sup>	53.75 N m s <sup>-1</sup>	36.47 N m s <sup>-1</sup>
Froude number	0.214	0.461	0.221	0.285

EG energy grade, WS water surface

which had crossed the bankfull discharge of DL and EDL (Table 13.5). The most critical level of bankfull discharge is 1518 m<sup>3</sup>s<sup>-1</sup> at downstream of Harinkhola. The hydrological estimates of downstream and upstream cross-sections reveal in Table 13.8. At upstream cross-section near Gotan, the channel can accommodate maximum flow of 1685 m<sup>3</sup>s<sup>-1</sup> and the flow area is 1057 m<sup>2</sup>, but at downstream cross-section near Khanakul region, the flow area is reduced to 548.11 m<sup>2</sup> (48.15% reduction from upstream), and total flow along cross-section is maximum 1457 m<sup>3</sup>s<sup>-1</sup> (13.53% reduction from upstream). Energy grade slope of downstream cross-section is 0.002270 m m<sup>-1</sup> which is nearer to 0.00440 m m<sup>-1</sup> at upstream (almost double than downstream). For the certain maximum flow, the downstream stream power can reach up to 197.29 N m s<sup>-1</sup> (velocity of 2.66 m s<sup>-1</sup>), having shear stress of 74.26 N m<sup>-2</sup>, but it is relatively smaller in the case of upstream. The Froude number ( $F_r$ ) of two cross-sections (0.214–0.461) exhibits subcritical flow of lower energy state (slow/tranquil flow regime) during the observed flood event.

In the steady flow 1D flood modelling the post-dam LPT3 designed potential discharges of 2-year  $R_T$  flood (3254 m<sup>3</sup>s<sup>-1</sup>), 5-year  $R_T$  flood (5324 m<sup>3</sup>s<sup>-1</sup>), 10-year  $R_T$  flood (6676 m<sup>3</sup>s<sup>-1</sup>), and 25-year  $R_T$  flood (8292 m<sup>3</sup>s<sup>-1</sup>) are taken into consideration to observe the spatial extent of floodplain inundation along the Mundeswari River. From the maps (Fig. 13.15) it is observed that maximum part of active channel area (38.84 km) can experience a flood depth of 4–8 m in 2-year flood, with floodplain inundation depth of less than 4 m at some parts of Khanakul. During

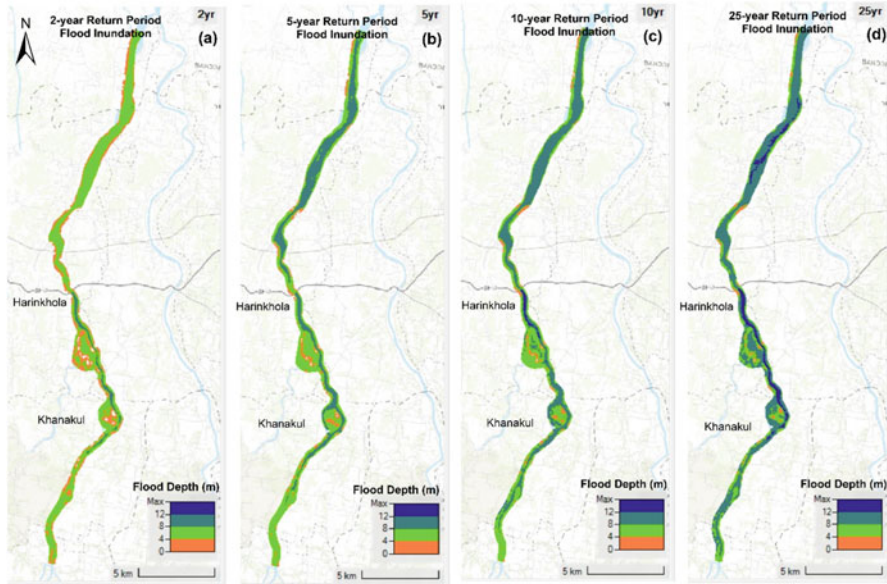


**Fig. 13.15** HEC-RAS 1D model derived potential floodplain inundation maps (a–d) of Mundeswari River based on steady flow simulation (LPT3 distribution designed 2-year, 5-year, 10-year, and 25-year flood discharge), noticing flood depth of over 12 m during 25-year flood of  $8292 \text{ m}^3\text{s}^{-1}$

5-year and 10-year flood event, the depth can reach 4–12 m from the bifurcation point to Khanakul, and it has maximum chance of overbank flow crossing the embankments of Khanakul region. In a 25-year flood, the total channel and active floodplain area can experience flood depth of beyond 8 m, and in between Harinkhola and Khanakul, the depth can exceed 12 m, recognizing the critical site of embankment failure and flood vulnerability (exceeding EDL and EDL).

In the 1D flood model of unsteady flow, the downstream section (Damodar/Amta channel) of Champadanga gauge station ( $22^{\circ}50'22.92'' \text{ N}$ ,  $87^{\circ}58'11.75'' \text{ E}$ ) shows marked variation of flood depths (1–8 m) for the streamflow simulation during 1 June–6 July 2021. On 20 June, 2021, due to flow rate of  $1410 \text{ m}^3\text{s}^{-1}$ , the flood depth varied from 1 to 4 m below Udaynarayan region, and the active channel part experienced greater than 6 m deep water (Fig. 13.16). On 22nd June, 2021 the flow rate reached up to  $1811 \text{ m}^3\text{s}^{-1}$  and the flood depth exceeded 6 m near Rajbalhat region, and at the downstream of Udaynarayanpur, the depth touched 2–6 m range, across the embanked floodplain. The observed discharge from 20th to 25th June, 2021 had crossed the bankfull limit of DL and EDI (Table 13.5), and the vast region of Joynagar and Udaynaryanpur was flooded. At upstream cross-section near Jamdara, the channel can accommodate maximum flow of  $1378 \text{ m}^3\text{s}^{-1}$  and the flow area is  $687 \text{ m}^2$ , but at downstream cross-section near Udaynarayanpur region, the flow area is recued to  $478 \text{ m}^2$  (30.42% reduction from upstream), and total flow along cross-section is maximum  $1081 \text{ m}^3\text{s}^{-1}$  (21.55% reduction from upstream)

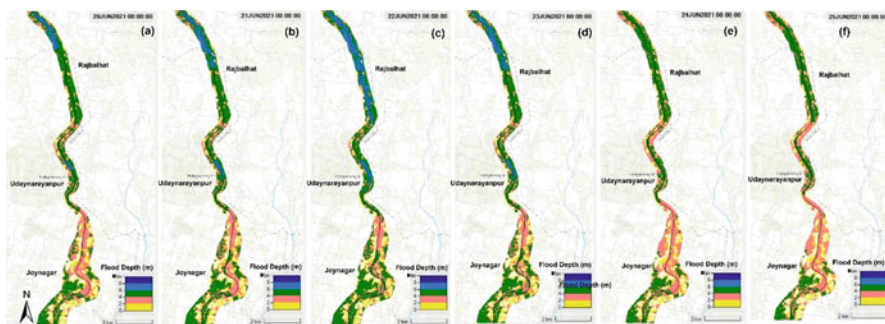


**Fig. 13.16** Thematic flood depth maps (a–f) of Damodar/Amta Channel (between Rajbalhat and Udaynaryanpur) using HEC-RAS 1D floodplain inundation modelling on unsteady flow simulation (20th–25th June, 2021)

(Table 13.6). Energy grade slope of downstream cross-section is  $0.000471 \text{ m m}^{-1}$  which is nearer to  $0.000750 \text{ m m}^{-1}$  at upstream. The downstream stream power can reach up to  $81.37 \text{ N m s}^{-1}$  (velocity of  $1.99 \text{ m s}^{-1}$ ), having shear stress of  $36.47 \text{ N m}^{-2}$ , but it is relatively higher in case of upstream. The Froude number ( $F_r$ ) of two cross-sections (0.221–0.285) exhibits subcritical flow of lower energy state during the observed flood event of 1st June–6th July, 2021.

In steady flow 1D hydrodynamic model, the Damodar/Amta channel (49.26 m stretch) can experience devastating flood because all LPT3-designed potential discharges of 2-year, 5-year, 10-year, and 25-year flood can exceed the bankfull limit of Champadanga gauge station (Fig. 13.17). In a 2-year flood ( $3254 \text{ m}^3 \text{ s}^{-1}$ ), the maximum floodplain inundation depth can range from 6 to 8 m from the bifurcation point to Udaynaryanpur. During 5-year and 10-year floods, the depth of flood water can exceed 8 m at downstream of Champadanga. The flood depth can reach beyond 10 m during a 25-year flood along the 34.40 km stretch of Damodar channel. The most vulnerable site of embankment failure and overbank flow is stretch between Rajbalhat and Udaynaryanpur where the flood depth can cross 10 m limit for the discharge of  $1811 \text{ m}^3 \text{ s}^{-1}$ .

## 6 Discussion

The DVC has now completed 75 years in 2022, and the authority has experienced a number of success (mainly irrigation water supply and flood control) as well as failure (mainly river metamorphosis and downstream recurrent flood), but it is worthwhile to mention that the prime objective of DVC was to make the Damodar Valley as an Eden of economic potentiality or “Valles Opima” of India (Kirk, 1950) which was partly achieved. The DVC dams and flood regulation system are now not able to manage sudden peak monsoonal flow to save the floodplains of lower DRB (mainly Purba Bardhaman, Hooghly, and Howrah districts). During late monsoon

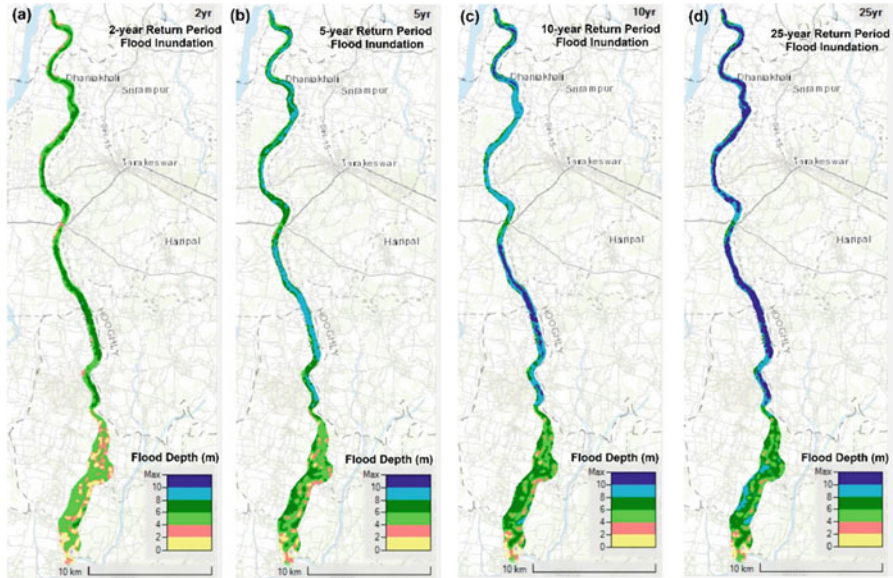


**Fig. 13.17** HEC-RAS 1D model derived potential floodplain inundation maps (a–d) of Damodar/Amta Channel based on steady flow simulation (LPT3 distribution designed 2-year, 5-year, 10-year, and 25-year flood discharge), observing flood depth of greater than 12 m during a 25-year flood ( $8292 \text{ m}^3\text{s}^{-1}$ )

consecutive torrential rainfall from the tropical depressions or cyclones, the last two terminal dams, Panchet and Maithon, are compelled to release excess water (less capacity of flood storage due to siltation) which recurrently turns into nightmare for the inhabitants of the Damodar fan-delta floodplains. The funnel-shaped basin size, with a wide upper catchment and a narrow bottle-neck location at downstream, has potentiality of phenomenal increase in peak discharge in the lower Damodar River. The DVC dams have successfully reduced the flood heights, i.e., furious peak discharge of greater than  $12,000 \text{ m}^3\text{s}^{-1}$  with short duration, but now the flood peaks are decreased significantly, except flood of September, 1978 ( $10,919 \text{ m}^3\text{s}^{-1}$ ), and the duration of inundation period becomes large. Preliminary report suggested to build eight large dams to moderate maximum peak discharge of  $28,000 \text{ m}^3\text{s}^{-1}$ – $7079 \text{ m}^3\text{s}^{-1}$  at Rhondia gauge station, but now five dams (including Tenughat Dam) only provide flood storage of 3591 million  $\text{m}^3$  which was only 55% of storage capacity as mentioned in the report. Therefore, the present flood regulation system of DVC does not have full capability to regulate exceptional peak discharge of 100-year flood ( $11,969 \text{ m}^3\text{s}^{-1}$ ).

In the trans-Damodar area of fan-delta (i.e., Late Quaternary – Recent floodplains of Mundeswari and Amta channels), the floods are encountered in each year, and it is mainly caused by the drainage congestion in the channels, tidal influence at outlet, and increasing siltation which promotes reduction of flow area in the active channel part. Hydrometeorological observations exhibit that in late monsoon month

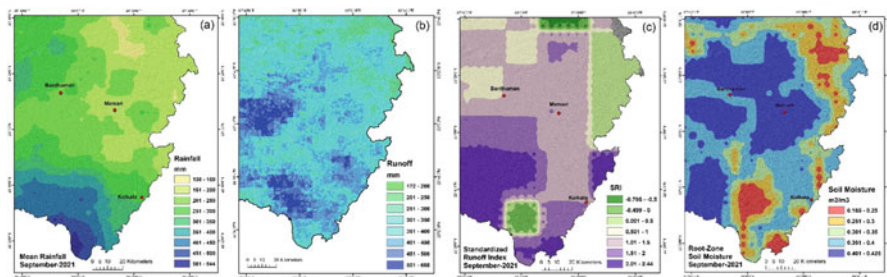


**Fig. 13.18** Hydrometeorological maps of the Damodar fan-delta (covering floodplains of Mundeswari and Damodar/Amta channel) – (a) spatial concentration of monsoon rainfall (September 2021), (b) mean runoff potential of monsoon months based on NRCS-CN method, (c) Standard Runoff Index (SRI) map of September 2021 (SRI > 0 means surplus runoff water) and (d) Root-Zone Soil Moisture map of September 2021 (RZSM > 0.40 means excess soil moisture)

(September–October, 2021), the fan-delta region receives more than 251 mm monthly rainfall, reaching high root zone moisture at maximum level ( $0.351\text{--}0.425\text{ m}^3/\text{m}^3$ ) and high standardized runoff index ( $1.51\text{--}2.44$ ) in the active floodplains (Fig. 13.18). During that time, the region does not capacity to absorb excessive water coming from high flood discharge (due to 3–4 days rainstorm in the upper catchment), and then, the inundation of floodplains for longer period was an inevitable condition. In addition, the Quaternary floodplains of Damodar fan-delta region have high potentiality of surface runoff in a range of 172–608 mm during the monsoon months, and the free flow is hampered due to tidal inflow from the Bhagirathi-Hooghly River. The miserable flood situation is aggravated by adding of excess water from the DVC canals by breaches, tail discharge, and over toping. The further analysis suggests some following suggestions to improve the flood management strategies of DRB:

- Intense short spells (usually 3–4 days) of extreme rainfall ( $150\text{--}290\text{ mm}$ ) are now very common in each year due to aggravation of extreme climatic events in response to global climate change. A rainstorm magnitude equal to or greater than  $304.8\text{ mm}$  may occur once in 100 years. This study has estimated the probable maximum rainfall for a given magnitude of flood: (a) 2-year flood ( $3254\text{ m}^3\text{s}^{-1}$ ) rainfall, 205 mm; (b) 10-year flood ( $6676\text{ m}^3\text{s}^{-1}$ ) rainfall, 304 mm; (c) 50-year flood ( $9417\text{ m}^3\text{s}^{-1}$ ) rainfall, 360 mm; and (d) 100-year flood ( $11,969\text{ m}^3\text{s}^{-1}$ ) rainfall, 412 mm. Therefore, from the early precise prediction of heavy rainfall (now given by Indian Meteorological Department), the DVC authority can regulate the flows in all reservoirs to reduce the peak flow under  $7079\text{ m}^3\text{s}^{-1}$  at Rhondia or at the Durgapur Barrage. In this case, a good coordination between DVC and IWD is needed to act on real-time flood forecast for the sake of inhabitants living in the low-lying floodplains of Hooghly and Howrah districts.
- Reduction of reservoirs' flood storage capacity, due to excessive siltation, is another problem in the DRB. The Maithon and Panchet reservoirs have lost



significant amount of overall storage capacity, viz., 27.4% in Maithon and 15.9% in Panchet, respectively. The sedimentation rates of the reservoirs are depicted as follows: (a) Konar,  $1748 \text{ m}^3 \text{ km}^{-2} \text{ year}^{-1}$ ; (b) Maithon,  $1076 \text{ m}^3 \text{ km}^{-2} \text{ year}^{-1}$ ; (c) Panchet,  $631 \text{ m}^3 \text{ km}^{-2} \text{ year}^{-1}$ ; (d) Tenughat,  $716 \text{ m}^3 \text{ km}^{-2} \text{ year}^{-1}$ ; and (e) Tilaiya,  $2792 \text{ m}^3 \text{ km}^{-2} \text{ year}^{-1}$  (Ghosh et al., 2022a). The sedimentation rate can be managed by installing small check dams in the gullies or streams of upper catchments. Regular dredging of the reservoirs is very much needed to increase the functional longevity of dams and to check flood risk.

- HEC-RAS 1D hydrodynamic model reveals that present carrying capacity (i.e., critical limit of overbank flow) of Mundeswari and Damodar/Amta channel is near about  $1518\text{--}1822 \text{ m}^3 \text{ s}^{-1}$  and  $1353\text{--}1651 \text{ m}^3 \text{ s}^{-1}$ , respectively. It is predicted the floodplain inundation region (flood depth of 1–12 m) in respect to 2-year, 5-year, 10-year, and 25-year flood. The most vulnerable sites of embankment failure and overbank flow are the 27 km long Damodar/Amta channel from Rajbalhat to Udaynarayanpur and 19 km long Mundeswari channel from Udna to Khanakul. If the HEC-RAS 1D model database is calibrated and validated with actual field result or SAR (synthetic aperture radar) flood dataset, the floodplain inundation prediction can be done precisely for a certain streamflow in the river valleys of Hooghly and Howrah districts.
- Finally, the Damdoar fan-delta region should be saved from drainage congestion during the monsoon months. Construction of marginal embankments, settlements, railways, and dense network of roads have aggravated the miserable flood situation (Fig. 13.19a). Embankments serve the purpose of preventions of floods for the time being but tend to create more problems later. Behind the embankments vested interests grow up encroaching into the active floodplain of the river. Development of additional settlements, roads, and cropland, around the active floodplains, hinders the flow paths of overbank discharge, and it transforms the palaeochannels of Damodar to abandoned channels permanently. It is suggested that if the palaeochannels or abandoned channels are linked with main river, Mundeswari and Damodar/Amta, through sluice gates, then the peak monsoon flow can be distributed along those channels during floods to reduce the rate of peak discharge in main river (downstream of Harinkhola and Champadanga) and to save the low-lying floodplains from recurrent inundation (Fig. 13.19b).

## 7 Conclusion

Seven decades (completed 75 years) have passed since the partial implementation of the DVC project. The life span of the reservoirs is also coming to an end, and the effectiveness of flood-controlling system is declining. The benefit that was found in the first episode, the level of evil in the next episode is surpassing the inhabitants of lower Damodar valley. The DVC should start to think about the alternative plan to mitigate excess streamflow through construction of another dam or preparation of

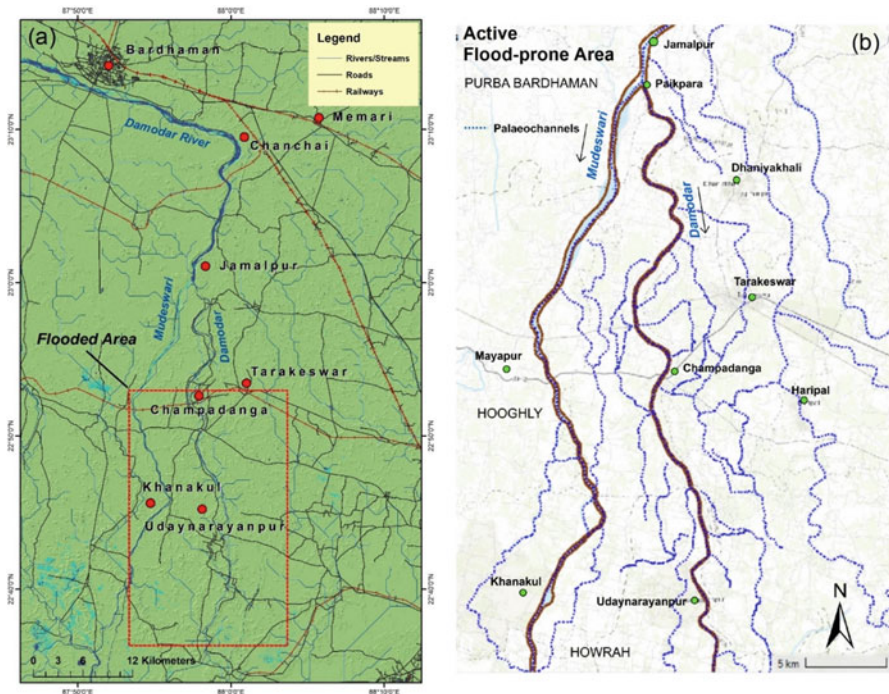


**Fig. 13.19** (a) Dense network of roads and railways in the floodplain of Damodar fan-delta region, promoting drainage congestion and (b) downstream palaeochannels and abandoned channels of Mundeswari and Damodar/Amta channel, having the option of reconnecting with the main river through sluice gates

numerous check dams at upstream. The need of dredging is an immediate task to extend the life span of reservoirs. Alongside the IWD should maintain coordination with DVC during the release of flood water. Alternatively, IWD may think about the rejuvenation of palaeochannels, connecting the old and abandoned courses of Damodar and Mundeswari with the main channel for evenly distribution of the excess streamflow during flood. The current study provides an outlook on the probable maximum rainfall in connection with expected flood discharge and the spatial dimension of the floodplain inundation model, which can be applied to reduce flood risk. The future research need to develop a real-time geospatial model of rainfall – streamflow simulation to predict peak discharge for a certain rainfall and the probable region of inundation or overbank flow. Another application of 1D/2D hydrodynamic model is now needed to calculate the flooded areas of different land use categories for estimating the monetary loss and economic vulnerability.

## References

- Acharyya, S. K., & Shah, B. A. (2007). Arsenic-contaminated groundwater from parts of Damodar fan-delta and west of Bhagirathi River, West Bengal, India: Influence of fluvial geomorphology and Quaternary morphostratigraphy. *Environmental Geology*, 52, 489–501. <https://doi.org/10.1007/s00254-006-0482-z>
- Albano, R., Mancusi, L., Sole, A., & Adamowski, J. (2017). Flood risk: A collaborative, free and open-source software for flood risk analysis. *Geomatics, Natural Hazards and Risk*, 8(2), 1812–1832. <https://doi.org/10.1080/19475705.2017.1388854>
- Bagchi, K. G. (1977). The Damodar Valley and its impact on the region. In A. G. Noble & A. Rudra (Eds.), *Indian urbanization and planning: Vehicles of modernization*. Tata McGraw-Hill Publishing Co. Ltd.
- Baker, V. R. (1994). Geomorphological understanding of floods. *Geomorphology*, 10, 139–156.
- Bera, S., & Mistri, B. (2014). Flood in the lower Damodar Basin and channel morphology: A case study at the bifurcation zone into Damodar and Mundeswari River, West Bengal. *International Journal of Geology, Earth and Environmental Sciences*, 4(2), 172–181.
- Betscholtz, A., & Nordlof, B. (2017). *Potentials and limitations of 1D, 2D and coupled 1D-2D flood modelling in HEC-RAS*. Division of Water Resource Engineering, Lund University. <https://lup.lub.lu.se/student-papers/record/8904721/file/8904723.pdf>
- Bhalla, D. N. (1969). The Damodar Valley Corporation: A study of the transplantation of foreign administrative institutions into India. Doctoral thesis, Radboud University Nijmegen. <https://repository.ubn.ru.nl/handle/2066/148493>
- Bhattacharya, K. (2011). *The Lower Damodar River, India: Understanding the Human Role in Changing Fluvial Environment*. Springer, Dordrecht. <https://doi.org/10.1007/978-94-007-0467-1>.
- Burn, D. H., Castellarin, A., & Kjeldsen, T. R. (2017). Floods. In V. P. Singh (Ed.), *Handbook of applied hydrology* (pp. 75-1–75-7). McGraw Hill.
- Chandra, S. (2003). *Integrated flood management case study India: Flood management – Damodar River Basin*. WMO/GWP Associated Programme on Flood Management. [http://www.floodmanagement.info/publications/casestudies/cs\\_india\\_full.pdf](http://www.floodmanagement.info/publications/casestudies/cs_india_full.pdf)
- Chatterjee, S. P. (1967). *Damodar Valley planning Atlas*. NATMO.
- Chatterjee, S. P. (1969). *The planning atlas of the amodar Valley region*. International Geological Congress, Calcutta
- Chattopadhyay, S., Acharya, R., & Sen, A. K. (2020). Analysis of rainfall trends in Damodar valley area. *VayuMandal*, 46(2), 61–72.
- Choudhury, S. (2012). Damodar Valley Corporation, the missed opportunity. *Journal of Infrastructural Development*, 3(2), 117–226. <https://doi.org/10.1177/097493061100300202>
- Climate Signals. (2022). *Atmospheric moisture increase*. <https://www.climate-signals.org/climate-signals/atmospheric-moisture-increase#:~:text=A%20warmer%20atmosphere%20holds%20more,mores%20moisture%20as%20it%20warms>
- Correia, F. N., Rego, F. C., Saraiva, M. D. G., & Ramos, I. (1998). Coupling GIS with hydrologic and hydraulic flood modelling. *Water Resources Management*, 12, 229–249.
- Das, B., Pal, S. C., & Malik, S. (2017). Assessment of flood hazard in a riverine tract between Damodar and Dwarkeswar River, Hugli District, West Bengal, India. *Spatial Information Research*, 26, 91–101.
- Dasallas, L., Kim, Y., & An, H. (2019). Case study of HEC-RAS 1D-2D coupling simulation: 2002 Baeksan flood event in Korea. *Water*, 11, 2048. <https://doi.org/10.3390/w11102048>
- De Saint Venant, B. (1871). Theorie du mouvement non-permanent ´ des eaux avec application aux crues des rivieres et a l’introduction des marees dans leur lit. *Comptes Rendus de l’Acad’emie des Sciences*, 73, 148–154, 237–240.
- Fan, Y., Ao, T., Yu, H., Huang, G., & Li, X. (2017). A coupled 1D-2D hydrodynamic model for urban flood inundation. *Advances in Meteorology*, 2017, Article ID 2819308. <https://doi.org/10.1155/2017/2819308Advncns>

- Farooq, M., Shafique, M., & Khattak, M. S. (2019). Flood hazard assessment and mapping of River Swat using HEC-RAS 2D model and high-resolution 12-m TanDEM-X DEM (World DEM). *Natural Hazards*, 97, 477–492.
- Garde, R. J. (2006). *River morphology*. New Age International.
- Ghosh, S. (2011). Hydrological changes and their impact on fluvial environment of the lower Damodar Basin over a period of fifty years of damming The Mighty Damodar River in Eastern India. *Procedia – Social and Behavioral Sciences*, 19, 511–519.
- Ghosh, S. (2013). *Flood hydrology and risk assessment: Flood study in a dam-controlled river of India*. Lambert Academic Publishing.
- Ghosh, S., & Guchhait, S. K. (2015). Characterization and evolution of primary and secondary laterites in northwestern Bengal Basin, West Bengal, India. *Journal of Palaeogeography*, 4(2), 203–230. <https://doi.org/10.3724/SP.J.1261.2015.00074>
- Ghosh, S., & Guchhait, S. K. (2016). Dam-induced changes in flood hydrology and flood frequency of tropical river: A study in Damodar River of West Bengal, India. *Arabian Journal of Geosciences*, 9(2), 1–26. <https://doi.org/10.1007/s12517-015-2046-6>
- Ghosh, S., & Illahi, A. (2020). Responses of fluvial forms and processes to human actions in the Damodar River Basin. In B. Das et al. (Eds.), *Anthropogeomorphology of Bhagirathi-Hooghly River system in India* (pp. 213–251). CRC Press.
- Ghosh, S., & Mistri, B. (2015). Geographic concerns on flood climate and flood hydrology in monsoon-dominated Damodar River Basin, Eastern India. *Geography Journal*, 2015, 1. <https://doi.org/10.1155/2015/486740>
- Ghosh, P. K., Mukhopadhyay, R., & Jana, N. C. (2021). Quantitative analysis of drainage basin parameters towards better management of Damodar River, Eastern India. *Journal Geological Society of India*, 97, 711–734.
- Ghosh, S., Hoque, M. M., Saha, U. D., & Islam, A. (2022a). Assessment of dam-induced changes in ecogeomorphological behaviour and fluvial functionality in the Damodar River, West Bengal, India. *Journal of Water Supply: Research and Technology-Aqua*, 71, 722. <https://doi.org/10.2166/aqua.2022.003>
- Ghosh, A., Roy, M. B., & Roy, P. K. (2022b). Evaluating the performance of MIKE NAM model on rainfall-runoff in lower Gangetic floodplain, West Bengal, India. *Modelling Earth Systems and Environment*, 168, 4001. <https://doi.org/10.1007/s40808-021-01347-6>
- Gibson, S., Pak, J., & Fleming, M. (2010, August 23–27). *Modeling watershed and riverine sediment processes with HEC-HMS and HEC-RAS*. Watershed Management Conference. [https://doi.org/10.1061/41143\(394\)120](https://doi.org/10.1061/41143(394)120)
- Glass, E. L. (1924). Floods of the Damodar River and rainstorms producing them. *Minutes Proc*, 217, 333–346.
- Goodarzi, M., & Eslamain, S. (2022). Riverine and flood modeling software. In S. Eslamain & F. Eslamain (Eds.), *Flood handbook analysis and modelling* (pp. 353–368). CRC Press.
- Goodell, C. R. (2005, May 15–19). *Dam break modeling for tandem reservoirs—A case study using HEC-RAS and HEC-HMS*. World Water and Environmental Resources Congress. [https://doi.org/10.1061/40792\(173\)402](https://doi.org/10.1061/40792(173)402)
- Hall, J. W., & Penning-Rosewell, E. C. (2011). Setting the scene for flood risk management. In J. W. Hall & E. C. Penning-Rosewell (Eds.), *Flood risk science and management* (pp. 3–16). Wiley. <https://doi.org/10.1002/9781444324846.ch1>
- Hayden, B. P. (1988). Flood climates. In V. R. Baker, R. C. Kochel, & P. C. Patton (Eds.), *Flood geomorphology* (pp. 13–27). Wiley.
- Hicks, F. E., & Peacock, T. (2005). Suitability of HEC-RAS for flood forecasting. *Canadian Water Resources Journal*, 30(2), 159–174. <https://doi.org/10.4296/cwrj3002159>
- Hirschboeck, K. K. (1988). Flood hydroclimatology. In V. R. Baker, R. C. Kochel, & P. C. Patton (Eds.), *Flood geomorphology* (pp. 27–50). Wiley.
- Hoque, M. M., Islam, A., & Ghosh, S. (2022). Environmental flow in the context of dams and development with special reference to the Damodar Valley Project, India: A review. *Sustainable Water Resources Management*, 8, 62. <https://doi.org/10.1007/s40899-022-00646-9>

- Horritt, M. S., & Bates, P. D. (2002). Evaluation of 1D and 2D numerical models for predicting river flood inundation. *Journal of Hydrology*, 268, 87–99.
- Hunter, W. W. (1876). *A statistical account of Bengal – Vol. 4*. Trubner & Co.
- Jagadesh, B., & Veni, K. K. (2021). Floodplain modelling of Krishna lower basin using ArcGIS, HEC-GeoRAS and HEC-RAS. *IOP Conference Series: Materials Science and Engineering*, 1112, 012024. <https://doi.org/10.1088/1757-899X/1112/1/012024>
- Kale, V. S. (2003). Geomorphic effects of floods in Indian Rivers. *Natural Hazards*, 28, 65–84.
- Kamal, N., & Pachauri, S. (2019). Mann-Kendall, and Sen's slope estimators for precipitation trend analysis in North-Eastern states of India. *International Journal of Computer Applications*, 177(11), 7–16.
- Karim, S., & De, S. K. (2019). Impact of dam on river discharge: A study on the Damodar River, Jharkhand. *Journal of Indian Geomorphology*, 6, 116–124.
- Khattak, M. S., Anwar, F., Saeed, T. V., Sharif, M., Sheraz, K., & Ahmed, A. (2016). Floodplain mapping using HEC-RAS and ArcGIS: A case study of Kabul River. *Arabian Journal for Science and Engineering*, 41, 1375–1390.
- Kinghton, D. (2014). *Fluvial forms and processes*. Routledge.
- Kirk, V. (1950). The Damodar Valley “Valles Opima”. *Geographical Review*, 40(3), 415–443. <https://doi.org/10.2307/211218>
- Knebl, M., Yang, Z. L., Hutchison, K., & Maidment, D. (2005). Regional scale flood modeling using NEXRAD rainfall, GIS, and HEC-HMS/RAS: A case study for the San Antonio River Basin Summer 2002 storm event. *Journal of Environmental Management*, 75(4), 325–336. <https://doi.org/10.1016/j.jenvman.2004.11.024>
- Kumar, N., Lal, D., Sherring, A., & Issac, R. K. (2017). Applicability of HEC-RAS and GFMS tool for 1D water surface elevation/flood modelling of the river: A case study of River Yamuna at Allahabad (Sangam), India. *Modelling Earth Systems and Environment*, 3, 1463–1475. <https://doi.org/10.1007/s40808-017-0390-0>
- Kumar, N., Kumar, M., Sherrig, A., Suryavanshi, S., Ahmad, A., & Lal, D. (2019). Applicability of HEC-RAS 2D and GFMS for flood extent mapping: A case study of Sangam area, Prayagraj, India. *Modelling Earth Systems and Environment*, 6, 397–405.
- Lahiri-Dutt, K. (2012). Large dams and changes in an agrarian society: Gendering the impacts of Damodar Valley Corporation in eastern India. *Water Alternatives*, 5(2), 529–542.
- Lahiri-Dutt, K., & Samanta, G. (2013). *Dancing with the river*. Yale University Press. <https://doi.org/10.12987/9780300189575>
- Leandro, J., Chen, A. S., Djordjević, S. & Savić, D. A. (2009). Comparison of 1D/1D and 1D/2D coupled (Sewer/Surface) hydraulic models for urban flood simulation. *Journal of Hydraulic Engineering* 135(6), 495–504. [https://doi.org/10.1061/\(ASCE\)HY.1943-7900.0000037](https://doi.org/10.1061/(ASCE)HY.1943-7900.0000037)
- Lee, K. T., Ho, Y. H., & Chyan, Y. J. (2006). Bridge blockage and overbank flow simulations using HEC-RAS in the Keelung River during the 2001 Nari typhoon. *Journal of Hydraulic Engineering*, 132(3), 319–323. [https://doi.org/10.1061/\(ASCE\)0733-9429\(2006\)132:3\(319\)](https://doi.org/10.1061/(ASCE)0733-9429(2006)132:3(319))
- Mahata, H. K., & Maiti, R. (2019). Evolution of Damodar fan delta in the western Bengal Basin, West Bengal. *Journal of Geological Society of India*, 93, 645–656.
- Mahata, H. K., & Maiti, R. (2020). Alluvial fan flooding in Lower Damodar Basin, West Bengal. *Geographical Review of India*, 82(1), 1–16.
- Majumder, M., Barman, R. N., Roy, P., Jana, B. K. & Mazumder, A. (2010a). Estimation of reservoir discharge with the help of clustered neurogenetic algorithm. In: Jana, B., Majumder, M. (eds) *Impact of climate change on natural resource management*. Springer, Dordrecht.
- Majumder, M., Roy, P., & Mazumdar, A. (2010b). An introduction and current trends of Damodar and Rupnarayan river system. In B. Jana & M. Majumder (Eds.), *Impact of climate change on natural resource management* (pp. 461–486). Springer.
- Malik, S., & Pal, S. C. (2021). Potential flood frequency analysis and susceptibility mapping using CMIP5 of MIROC5 and HEC-RAS model: A case study of lower Dwarkeswar River, Eastern India. *SN Applied Sciences*, 3, 31. <https://doi.org/10.1007/s42452-020-04104-z>

- Mandal, S. P., & Chakrabarty, A. (2016). Flash flood risk assessment for upper Teesta River basin: Using the hydrological modelling system (HEC-HMS) software. *Modeling Earth Systems and Environment*, 2, 59. <https://doi.org/10.1007/s40808-016-0110-1>
- Mawasha, T. S. (2021). Combined 1D modelling with HEC-RAS for delineation floodplain area: A case study of Hennops River in the Centurion Area. *American Journal of Mathematical and Computer Modelling*, 6(4), 55–62.
- Merwade, V., Olivera, F., Araabi, M., & Edleman, S. (2008). Uncertainty in flood inundation mapping: Current issues and future directions. *Journal of Hydraulic Engineering*, 13(7), 608. [https://doi.org/10.1061/\(ASCE\)1084-0699\(2008\)13:7\(608\)](https://doi.org/10.1061/(ASCE)1084-0699(2008)13:7(608))
- Mojaddadi, H., Pradhan, B., Nampak, H., Ahmad, N., & Ghazali, A. H. (2017). Ensemble machine-learning-based geospatial approach for flood risk assessment using multi-sensor remote sensing data and GIS. *Geomatics, Natural Hazards and Risk*, 8(2), 1080–1102.
- Nguyen, P., Shearer, E. J., Tran, H., Ombadi, M., Hayatbini, N., Palacios, T., Huynh, P., Braithwaite, D., Updegraff, G., Hsu, K., Kuligowski, B., Logan, W. S., & Sorooshian, S. (2019). The CHRS Data Portal, an easily accessible public repository for PERSIANN global satellite precipitation data. *Nature Scientific Data*, 6, Article number: 180296. <https://doi.org/10.1038/sdata.2018.296>
- Ogras, S., & Onen, F. (2020). Flood analysis with HEC-RAS: A case study of Tigris River. *Advances in Civil Engineering*, Article ID 6131982. <https://doi.org/10.1155/2020/6131982>
- Ongdas, N., Akiyanova, F., Karakulov, Y., Muratbayeva, A., & Zinabdin, N. (2020). Application of HEC-RAS (2D) for flood hazard maps generation for Yesil (Ishim) river in Kazakhstan. *Water*, 12, 2672. <https://doi.org/10.3390/w12102672>
- Parsa, A. S., Heydari, M., Sadeghian, M. S., & Moharrampour, M. (2013). Flood zoning simulation by HEC-RAS model (Case Study: Johor River-Kota Tinggi Region). *Journal of River Engineering*, 1(1), 6. <https://doi.org/10.5281/zenodo.18264>
- Patel, D. P., Ramirez, J. A., Srivastava, P. K., Bray, M., & Han, D. (2017). Assessment of flood inundation mapping of Surat city by coupled 1D/2D hydrodynamic modelling: A case application of the new HEC-RAS 5. *Natural Hazards*, 89, 93–130.
- Pathan, A. I., & Agnihotri, P. G. (2020). Application of new HEC-RAS version 5 1D hydrodynamic flood modelling with special reference through geospatial techniques: A case of River Purna of Navsari, Gujarat, India. *Modelling Earth Systems and Environment*, 7, 1133–1144. <https://doi.org/10.1007/s40808-020-00961-0>
- Pender, G., & Neelz, S. (2011). Flood inundation modelling to support flood risk management. In G. Pender & H. Faulkner (Eds.), *Flood risk science and management* (pp. 324–257). Blackwell Publishing Ltd.
- Pramanik, N., Panda, R. K., & Sen, D. (2010). One dimensional hydrodynamic modelling of river flow using DEX extracted river cross-sections. *Water Resources Management*, 24, 835–852. <https://doi.org/10.1007/s11269-009-9474-6>
- Pramanik, S. K., & Rao, K. N. (1952). Hydrometeorology of the Damodar catchment. *Indian Journal of Meteorology & Geophysics*, 3(2), 429–431.
- Raghunath, H. M. (2006). *Hydrology – Principles, analysis and design*. New Age International Publishers.
- Rajbanshi, J. (2015). Rainfall distribution and its spatial and temporal variability over Damodar Basin under climate change scenario (1901–2002). *IOSR Journal of Environmental Sciences, Toxicology and Food Technology*, 9(9), 95–104.
- Rakhecha, P. R., & Singh, V. P. (2017). Enveloping curves for the highest floods of river basins in India. *International Journal of Hydrology*, 1(3), 79–84.
- Rana, V. K., & Suryanarayana, T. M. V. (2021). Estimation of flood influencing characteristics of watershed and their impact on flooding in data-scare region. *Annals of GIS*, 27(4), 397–418.
- Rao, A. R., & Hamed, K. H. (2000). *Flood frequency analysis*. CRC Press, Boca Raton. <https://doi.org/10.1201/9780429128813>
- Rao, A. R., & Hamed, K. H. (2019). *Flood frequency analysis*. CRC Press.

- Roy, P. K., & Mazumdar, A. (2007). Study on hydrology and drought in the flood region of Damodar River Basin. *Journal of Geological Society of India*, 69(5), 1011–1019.
- Rudra, K. (2018). *Rivers of the Ganga-Brahmaputra-Meghna Delta*. Springer Nature.
- Saha, S. K. (1979). River-basin planning in the Damodar Valley of India. *Geographical Review*, 69(3), 273–287.
- Sahoo, B., & Bhaskaran, P. K. (2016). Assessment on historical cyclone tracks in the Bay of Bengal, east coast of India. *International Journal of Climatology*, 36(1), 95–109.
- Saikia, P., & Konwar, K. (2020). Analysis of changes in groundwater levels using Mann-Kendall and Sen's slope estimator in Kamrup (M) District, Assam. In R. Sarkar (Ed.), *Geography in the 21st century: Emerging issues and the way forward* (pp. 357–368). Namya Press.
- Sanyal, J. (2017). Uncertainty in levee heights and its effect on the spatial pattern of flood hazard in a floodplain. *Hydrological Sciences*, 62(9), 1483–1498. <https://doi.org/10.1080/02626667.2017.1334887>
- Sanyal, J., Carbonneau, P., & Densmore, A. L. (2013). Hydraulic routing of extreme floods in a large ungauged river and the estimation of associated uncertainties: A case study of the Damodar River, India. *Natural Hazards*, 66, 1153–1171. <https://doi.org/10.1007/s11069-012-0540-7>
- Sanyal, J., Densmore, A. L., & Carbonneau, P. (2014a). Analysing the effect of land use – Land cover changes at sub-catchment levels on downstream flood peaks: A semi-distributed modelling approach with sparse data. *Catena*, 118, 28–40. <https://doi.org/10.1016/j.catena.2014.01.015>
- Sanyal, J., Carbonneau, P., & Densmore, A. L. (2014b). Low-cost inundation modelling of the reach scale with sparse data in the lower Damodar River Basin, India. *Hydrological Sciences*, 59(12), 2086–2102. <https://doi.org/10.1080/02626667.2014.884718>
- Sarhadi, A., Soltani, S., & Modares, R. (2012). Probabilistic flood inundation mapping of ungauged rivers: Linking GIS techniques and frequency analysis. *Journal of Hydrology*, 458–459, 68–86.
- Sen, P. K. (1985). The genesis of floods in the Lower Damodar catchment. In P. K. Sen (Ed.), *The concepts and methods in geography* (pp. 71–85). The University of Burdwan.
- ShahiriParsa, A., Noori, M., Heydari, M., & Rashidi, M. (2016). Floodplain zoning simulation by using HEC-RAS and CCHE2D models in the Sungai Maka River. *Air, Soil and Water Research*, 9, 55–62.
- Sharma, P., Patil, P., & Eslamain, S. (2022). Flood forecasting time series or flood frequency analysis? In S. Eslamain & F. Eslamain (Eds.), *Flood handbook analysis and modelling* (pp. 131–150). CRC Press.
- Singh, R. K., Villuri, V. G. K., & Pasupuleti, S. (2019). Assessment of parameters and preparation of hydrodynamic model for lower Dmaodar Basin using geomatic techniques. *Masum*, 70(4), 815–824.
- Singh, R. K., Villuri, V. G. K., Pasupuleti, S., & Nune, R. (2020). Hydrodynamic modeling for identifying flood vulnerability zones in lower Damodar River of eastern India. *Ain Shams Engineering Journal*, 11(4), 1035–1046. <https://doi.org/10.1016/j.asej.2020.01.011>
- Singh, R. K., Soni, A., Kumar, S., Pasupuleti, S., & Gobind, V. (2021). Zonation of flood prone areas by an integrated framework of a hydrodynamic model and ANN. *Water Supply*, 21(1), 80–97. <https://doi.org/10.2166/ws.2020.252>
- Sinha, B., & Rao, P. R. (1985). A study for optimum utilization of the Damodar water resources. *Sadhana*, 8, 273–290. <https://doi.org/10.1007/BF02811290>
- Sinha, R., Latrubesse, E. M., & Nanson, G. C. (2012). Quaternary fluvial systems of tropics: Major issues and status of research. *Palaeogeography, Palaeoclimatology, Palaeoecology*, 356–357, 1–15.
- Stelling, G. S., & Verway, A. (2005). Numerical flood simulation. In M. G. Anderson (Ed.), *Encyclopaedia of hydrological sciences* (pp. 1–14). Wiley. <https://doi.org/10.1002/0470848944.hsa025a>
- Subramanya, K. (2013). *Engineering hydrology*. Tata McGraw Hill.

- Surwase, T., Manjusree, P., Sachin Prakash, S., & Kuntla, S. (2020). Development of algorithms for evaluating performance of flood simulation models with satellite-derived flood. *H<sub>2</sub>Open Journal*, 3(1), 222–235. <https://doi.org/10.2166/h2oj.2020.117>
- Tate, E. C., & Maidment, D. R. (1999). *Floodplain mapping using HEC-RAS and ArcView GIS*. University of Texas.
- Teng, J., Jakeman, A. J., Vaze, J., Croke, B. F. W., Dutta, D., & Kim, S. (2017). Flood inundation modelling: A review of methods, recent advances and uncertainty analysis. *Environmental Modelling and Software*, 90, 201–216.
- United States Army Corps of Engineers. (2020). *HEC-RAS River Analysis System. HEC-RAS hydraulic reference manual version 6.0 Beta*. US Army Corps of Engineers Hydrologic Engineering Center. <https://www.hec.usace.army.mil/confluence/rasdocs/ras1dtechref/latest>
- Verma, R. K., Murthy, S., & Tiwary, R. K. (2015). Assessment of environmental flows for various sub-watersheds of Damodar River Basin using different hydrological methods. *International Journal of Waste Resources*, 5(4). <https://doi.org/10.4172/2252-5211.1000182>
- Verma, R. K., Murthy, S., Verma, S., & Misgra, S. K. (2017). Design flow duration curves of environmental flows estimation in Damodar River Basin, India. *Applied Water Sciences*, 7, 1283–1293.
- Viji, R., Prasanna, P. R., & Ilangovan, R. (2015). GIS based SCS – CN method for estimating runoff in Kundahpalam Watershed, Nilgries District, Tamilnadu. *Earth Sciences Research Journal*, 19(1), 59–64.
- Vogel, R. M., & Castellarin, A. (2017). Risk, reliability, and return periods and hydrologic design. In V. P. Singh (Ed.), *Handbook of applied hydrology* (pp. 78-1–78-10). McGraw-Hill Education.
- Ward, R. C. (1978). *Floods: A geographical perspective*. Macmillan.
- Zade, M., Ray, S. S., Dutta, S., & Panigrahy, S. (2005). Analysis of runoff pattern for all major basins of India derived using remote sensing data. *Current Science*, 88(8), 1301–1305.



# Chapter 14

## An Account of the Flood History in the Ghatal Region of West Bengal, India



Sayoni Mondal and Priyank Pravin Patel

**Abstract** Floods, being the most common natural disaster, affect millions of people worldwide. Out of 3290 lakh hectare (3,290,000 km<sup>2</sup>) land area in India, 40 million hectares have been declared as flood prone, with an annual average of 75 lakh hectares being affected, either directly or indirectly. West Bengal is considered as one of the most flood-prone states in India, with its southern portion being severely affected by floods annually. Although natural factors are probably the usual causes of floods, the Silabati (also called Silai) River basin, near its mouth in the vicinity of Ghatal town of Paschim Medinipur district, experiences annual flooding partly due to its regional setting within the subdued Bengal fan, while much of the inundation here occurs due to direct anthropogenic interventions into the channel and the floodplain. The various natural and anthropogenic causes of flooding in the region have been explained in this study with a special emphasis on the embankment circuits of the area that make the river flow constrained, thereby causing siltation and rising of the river bed with resultant flooding. An analysis of the extent, recurrence and duration of flooding in the region has also been done to highlight the severity of the event and the annual suffering of the resident communities in the region. The formulation of the Ghatal Master Plan in the region has not been much of a success, with non-structural mitigation measures being a viable means to reduce floods in the region.

**Keywords** Flood · Inundation · Ghatal Master Plan · Embankment circuit · Anthropogenic intervention

---

S. Mondal · P. P. Patel (✉)

Department of Geography, Presidency University, Kolkata, India

e-mail: [priyank.geog@presiuniv.ac.in](mailto:priyank.geog@presiuniv.ac.in)

## 1 Introduction

Floods have been identified as the single most harmful natural disaster affecting economies worldwide (Borrows & Bruin, 2006). Annually, about 170 million people get afflicted by floods (Das, 2019), with the United Nations reporting that nearly 2.3 billion people were affected, with 157,000 recorded deaths due to flooding, from 1995 to 2015 (Hoque et al., 2019). Out of 3290 lakh hectare (3,290,000 km<sup>2</sup>) land area in India, 40 million hectares have been declared as flood prone, with an annual average of 75 lakh hectares being affected, either directly or indirectly (Gangwar, 2013). Their causative natural factors comprise of catchment hydrology and physiography-related attributes like the general elevation and slope of the region, soil type, precipitation received and land-use pattern, all of which determine the susceptibility level of a region to floods (Blistanova et al., 2016; Sahana & Patel, 2019). Although the average frequency of flood events is 2.33 years (Leopold et al., 1964), such events have severely increased in recent years due to global issues like climate change, rapid urbanisation and poor river management programmes (Das, 2019). Floods have also occurred due to marked land cover/use changes within river corridors (cf. Banerji & Patel, 2019) due to faulty agricultural practices and the resultant siltation of active channels consequent upon their degradation, which have been progressively constrained by embankments to enable infrastructural development (Mondal et al., 2016; Patel et al., 2020; Sahana et al., 2020). Big floods can potentially set back development goals and hamper economic development in any region (Patel & Dasgupta, 2009), and thus flood hazard preparedness and management has been the most obvious way of combating such disasters (Behanzin et al., 2015).

## 2 Locational Setting and Causes of Flood in the Ghatal Region

West Bengal is one of the most flood-prone states in India, with almost 42% of its geographical area being affected by floods every year. Ghatal Block in Paschim Medinipur District is one of the most flood-affected regions of the state, experiencing annual flooding (Mitra & De, 2016). This region is part of the Bengal Basin and resembles a subdued fan system that is characterised by palaeo-deltas, which merge with the oldest part of the Ganga delta further east (Kar & Das, 2020). As such, the Silai River (also called Silabati River) in this section shows a sudden decline in its channel gradient, which is also reflected in the river's high sinuosity and thereby its marked erosion of its banks in its middle and lower courses (Naskar & Patel, 2019).

From a hydrological viewpoint, watersheds like the Silai (that are situated in transition zones straddling both plateau fringes and alluvial plains) are sensitive to short-duration high-intensity rainfall events and land-use changes and show a more pronounced effect of overland flow in causing floods (Sahoo & Sivaramakrishnan,

2014). The average elevation in the lower part of the Silai basin ranges between 9 and 11 m, while it is even less near the river's mouth further to the south-east, where it is just 4–5 m around the confluence of the Silai with the Darakeswar. This lowland landscape enables annual water stagnation during the monsoon, which is exacerbated by voluminous run-off from the upland tracts of the Silai and tidal ingress into the Rupnarayan that retards floodwater outflow. The critical physiographic location of the block forms a closed area surrounded by rivers on all sides, with the Silai and the Old Cossye in the south and south-east, respectively, and the Darakeswar and its tributary, the Jhumi, in the north and north-east (Mitra & De, 2016). Ghatal Block gets inundated two to three times in a single monsoon, and a little excess rainfall compared to the normal scenario creates a flood-like situation.

### 3 Disrupted Rivers and Embankments

Ghatal Block is further criss-crossed by a number of smaller tributaries and distributaries of the Silai, which join/rejoin the main river and drain a significant amount of its discharge during the monsoon (Fig. 14.1). The Ketia Khal, a distributary of the Silai, emerges from the main channel near Nischintapur village. It flows almost parallel to the main channel for a considerable distance before the off-take of the Katan Khal (a human-made canal) from it. Both these channels join the main Silai further downstream, near Surajnagar. The Ketia carries almost 80% of the monsoonal flow of the main channel. The Parang, Tamal, Kubai, Donai and Buriganga are some of the notable right bank tributaries of the Silai that augment its total discharge, which ultimately accumulates near Ghatal town, causing floods. A small distributary of the Old Cossye River, the Kanki Khal, also links up with the main Silai during heavy rains when the main Kangsabati channel overflows and contributes additional discharge (WAPCOS Limited, 2009). Similar conditions prevail on the left bank of the channel, where the Darakeswar and Jhumi join the Silai to form the Rupnarayan, downstream of Ghatal town.

Within the above locational and topographic setting, the mean annual rainfall of 153–155 cm between June and September often causes floods (Fig. 14.2), with meander shifting induced bank erosion occurring concurrently (Pal, 2014). The situation is worsened by the haphazard network of high embankments along these channels (Kar & Das, 2020) that restrict channel-floodplain connectivity. These were constructed to safeguard valuable agricultural lands from flood spills (Kar & Das, 2020) but were hardly built taking the morphological, hydraulic and geotechnical attributes of the rivers into consideration (Pal, 2014). The ensuing siltation of the river bed due to in-stream deposition of the considerable sediment volume derived via soil loss from the upstream areas has caused the river to rise and flow on a more elevated level than the surrounding region (i.e. through convex floodplains, which are typical of any deltaic lowlands), with multiple instances of embankment breaching and bank overtopping causing sustained floods and waterlogging in the region as the excess water cannot easily drain back to the channel and gets stagnated

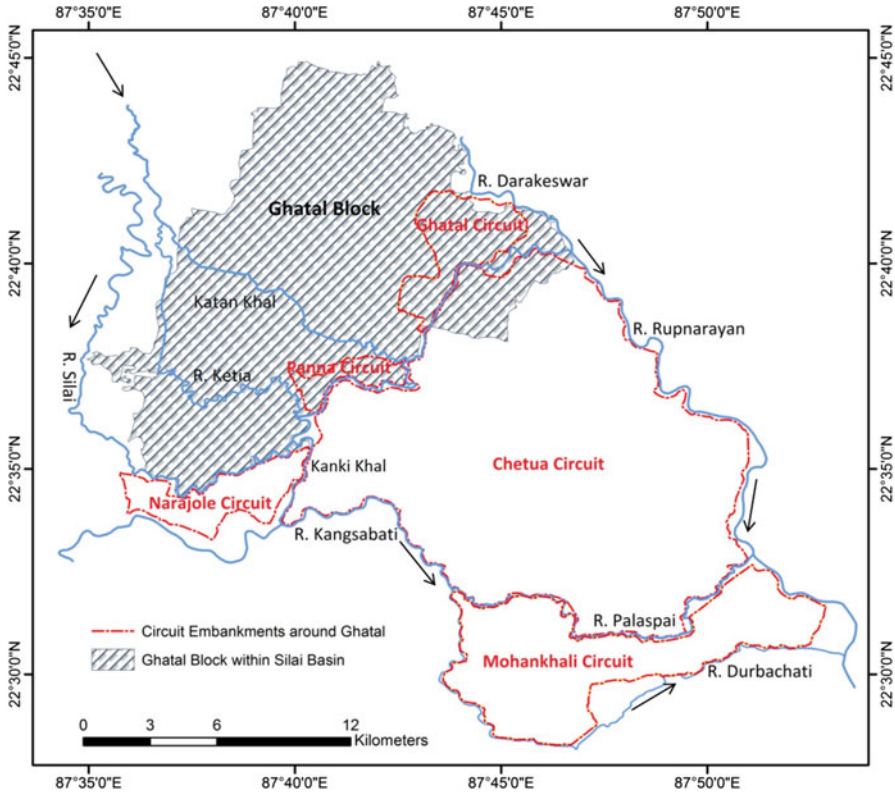


**Fig. 14.1** Location of Ghatal Block, with its drainage system and embankment circuits

for around 2–3 months (Das & Bandyopadhyay, 2015). An increase in the impervious urbanised area in the lower Silai basin from 14.2 km<sup>2</sup> in 1971 to 25.6 km<sup>2</sup> in 2005 to almost 37.5 km<sup>2</sup> in 2014 has also feasibly contributed towards greater run-off (Pal, 2014).

A number of embankment circuits are still present in the region, such as the abandoned Ghatal and Panna circuit on the left bank of the river, whereas the functional Chetua circuit and the abandoned Narajole circuit are on the right flank. These abandoned circuits are locally called *Chatal* and are a quite levelled strip of land that serve as the main transport route during the monsoon when they are used as flood causeways as the main roads get submerged. The functional Chetua circuit embankment on the right bank protects that side from inundation and thus diverts the overflowing discharge onto the left bank where the abandoned circuits are usually unable to restrict such high flows within the Silai-Darakeswar interfluve (Kar & Das, 2020). Further explanations of the other causes and effects of floods in this region have been documented by Dolui and Ghosh (2013).

Along with embankment breaches, riverbank erosion has been another cause of concern in the lower reaches. Non-cohesive bank materials initiate rotational



**Fig. 14.2** Flood inundation in and around Ghatal town (a) Ghatal municipality office, (b) Ghatal bridge, (c) inundated land near the Bhasapool (wooden bridge across the river) and (d) houses built on bamboo poles/canes to raise their height above the water surface). (Source: Ghatal Municipality)

failures, while slab or block failures are prominent in regions having cohesive banks (Pal, 2014). Bank toe scouring and undercutting increase bank steepness, which further triggers bank erosion and instability in regions buffeted by the greater hydraulic force of floodwaters. The thalweg orientation and the location of depositional sandbars affect the severity of riverbank erosion in the region, along with the low gradient and high sinuosity of the channel in the lower course (Pal, 2014). A viable proposal for mitigating the above and also reducing the possible severity of the occurring floods has been proper river channel and riparian zone management using nature-based principles such as live vegetation buffers (Mondal & Patel, 2018) and complete hydromorphological assessments of the river network (Mondal & Patel, 2022).

#### 4 Documenting the Near-Annual Flood Phenomenon in Ghatal

The Ghatal Master Plan (GMP), which was formulated in 1976 with the noble objective of restoring the economic, social and commercial viability of the region, identified 1270 km<sup>2</sup> area out of the total area of 1659 km<sup>2</sup> of the GMP as flood prone, with the most affected central, eastern and southern parts covering an area of

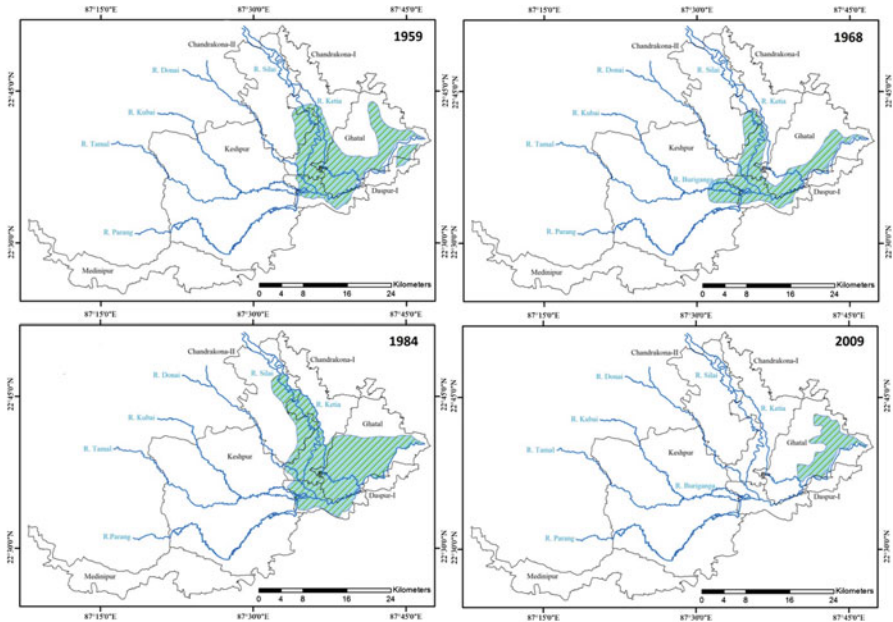


**Fig. 14.3** Historical flood inundation extent maps of the lower Silai basin area around Ghatal. (Source: Ghatal Municipality)

793 km<sup>2</sup> and being spread across Chandrakona-I, Chandrakona-II, Daspur-I and Ghatal Blocks (WAPCOS Limited, 2009). Almost the entire lower course of the Silabati River, mostly in the vicinity of Banka, Khirpai, Rashikganj, Surajnagar and the towns of Chandrakona and Ghatal, gets inundated annually, and historical flood maps have been used to identify such zones (Fig. 14.3). The flood situation in Ghatal town is even more grim, with 12 out of its 17 wards being declared as fully flood prone, most of which are located on the left bank.

The inundation history and flood depth in the area reveal the degree of devastation caused (Table 14.1). Daspur-I Block, which is affected by floods each year, recorded an annual crop damage worth approximately Rs. 4.12 crores in 2011 alone (Mal & Mandal, 2013). The GMP had an initial plan of multipurpose flood management strategies like construction of new embankments on the left bank of the Silai from Banka to Bandar for a length of 42 km, resuscitation of existing streams and palaeochannels, construction of new river sluices, augmenting the river carrying capacity, framing regulations and flood proofing for floodplain development and improvement of the overall drainage network in the region. However, over time, this overambitious project has taken a go-slow attitude, with the result that the misery and distress of the resident community continues to prevail and may increase in the coming years.

A detailed picture of the socio-economic vulnerability of the region to floods has been portrayed by Sahoo and Sivaramakrishnan (2014), highlighting the various

**Table 14.1** Inundation and damages caused due to flooding in Ghatal Block

Year of flood	Inundation for more than a month		Inundation for more than 15 days		Total damage (Lakh rupees)
	Area submerged (km <sup>2</sup> )	Flood depth (m)	Area submerged (km <sup>2</sup> )	Flood depth (m)	
1959	100.0	2.0	184	1.5	Not available
1967	100.0	2.5	69.3	1.5	Not available
1968	350.0	2.5	307.64	2.0	Not available
1973	208.0	3.0	150	2.0	247.64
1974	61.0	3.0	102.83	2.0	191.85
1975	104.0	2.5	110	2.0	309.50
1976	55.17	2.5	108	2.0	52.79
1977	100.0	3.5	130	2.0	1361.92
1978	710.0	3.5	356	2.0	5174.19
1999	78.39.0	3.0	100	2.0	8585.34
2000	80.0	3.0	120.85	2.0	16313.09
2007	232.5	3.0	400	2.0	49923.05
2013	200.0	3.0	125	2.0	4515.70
2015	700.0	3.5	330	2.0	10000.0

Source: Ghatal Municipality

flood adaptability measures and coping strategies of the local residents. With floods being an annual event in the region and about 65% of the population getting affected at least once every year, the local cultivation pattern has also undergone changes, with people shifting to *rabi* crops for sustenance and avoiding *kharif* crops. Almost 70% of the residents are directly or indirectly dependent on agriculture, and most plots are intensively cultivated following a double-cropping pattern for vegetables during winter. Since the majority of the area remains waterlogged even after the monsoon, inhabitants temporarily resort to pisciculture during that period (Sahoo & Sivaramakrishnan, 2014). Local household adaptation measures followed here include raising the house plinth levels, using landfill materials to raise the floor base, building stairs up to the raised floor level from the ground (Pater, 2018) and constructing homes on strong pillars to allow complete security and protection from higher flood events (cf. NOAA, 2012).

Comprehensive flood management therefore requires detailed information regarding all aspects of flooding, i.e. hydrological, physiographical, geotechnical, economic, social as well as political (Tehrany et al., 2014; Mondal & Patel, 2021). With forecasting and early warning being the only strategy to reduce its ill effects, flood management programmes should aim to identify areas that are more susceptible to flooding so that early warning can significantly reduce the chaos caused (Sahana & Patel, 2019). Here, the flood-susceptible zones were identified using the flood extent maps obtained from the European Commission Joint Research Centre's Global Surface Water dataset (Pekel et al., 2016) that accurately identifies the flood-affected tracts in the region.

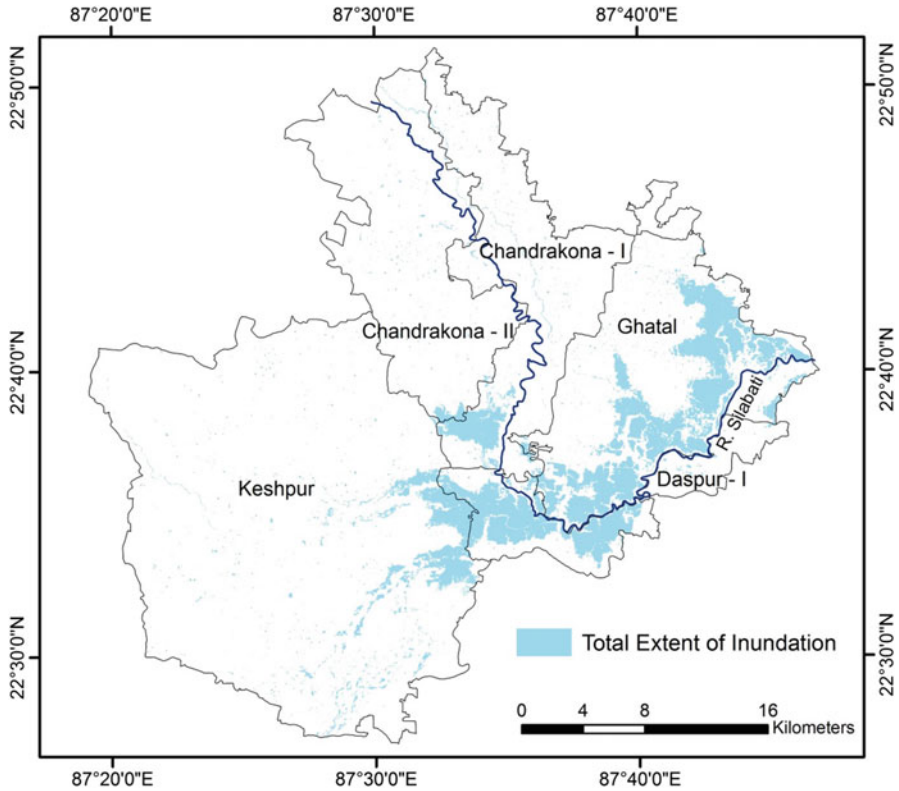


**Fig. 14.4** Flood inundation extent in the downstream section of the Silai River (1985–2020). (Source: Global Surface Water dataset (see Pekel et al., 2016, for details))

Almost the entirety of Ghatal Block on the left bank of the Silai is flood prone (Fig. 14.4), with the right bank being far less affected due to the presence of the Chetua circuit embankment along the southern part of Daspur-I Block, which also covers parts of Keshpur Block. Similar patterns have been captured in the Google Earth imagery showing more or less exact inundation extents that occurred in the 2009 flood which devastated the region quite severely (see Fig. 14.8). While the flood recurrence map shows the frequency with which water gets stranded in the extreme low-lying parts of the region, explaining the inter-annual variability in the presence of water (Fig. 14.5), the flood seasonality map (Fig. 14.6) shows the duration for which water usually stagnates herein, and this in turn determines the temporal change in land use and occupation structure as this stranded, sediment-free water enables pisciculture as the only means of sustenance in the aftermath of floods. Much of the region on the left bank receives at least a month of inundation, with low-lying zones experiencing water accumulating for longer duration. Another parameter of utmost importance here is the flood transition map (Fig. 14.7), which depicts the change in seasonality of the three main water classes (viz. permanent water, seasonal



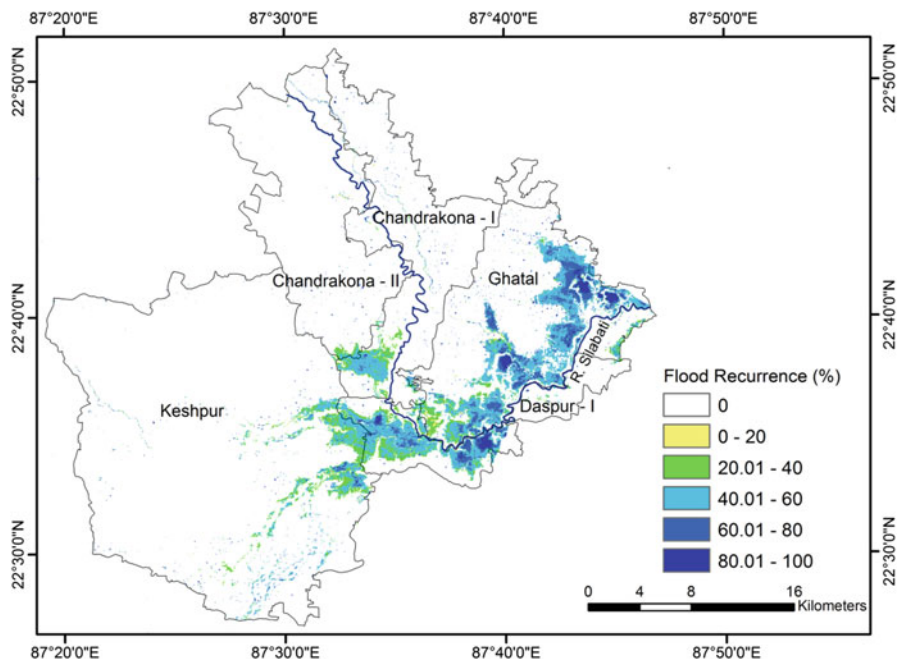


**Fig. 14.5** Percentage of flood recurrence in the flood-affected region (1985–2020). (Source: Global Surface Water dataset (see Pekel et al., 2016, for details))

water and no water) in the region. Although no new parcel of land has been declared as permanently flood affected in the region in the examined time frame of this dataset (1985–2016 and extended up to 2020), the percentage of seasonal water coverage has increased, with new seasonal water surfaces cropping up and indicating a conversion of land into seasonal water and also conversion of water back into land surfaces, which denotes continued inundation depending on the severity of the monsoon.

Therefore, it is apparent that although the GMP had been prepared in accordance with the flooding issues prevalent in the region, such occurrences continue unabated, with attendant riverbank erosion. The lack of a secure and long-term flood management strategy still remains a problem, and questions on sustainable strategies to create resilience among such communities are seldom addressed in any flood management plan (Pater, 2018). The overemphasis on structural mitigation methods (river embankments and riprap boulders) has in many instances led to scenarios where these techniques have drastically failed, putting the efficacy of structural methods (given their high cost and adverse ecological impacts) under scrutiny. Quite recently, with the central policy on flood mitigation shifting from controlling to managing floods (NITI Aayog, 2021; PTI, 2021), non-structural methods (using live vegetation buffers to arrest high flood velocities) have been attempted,

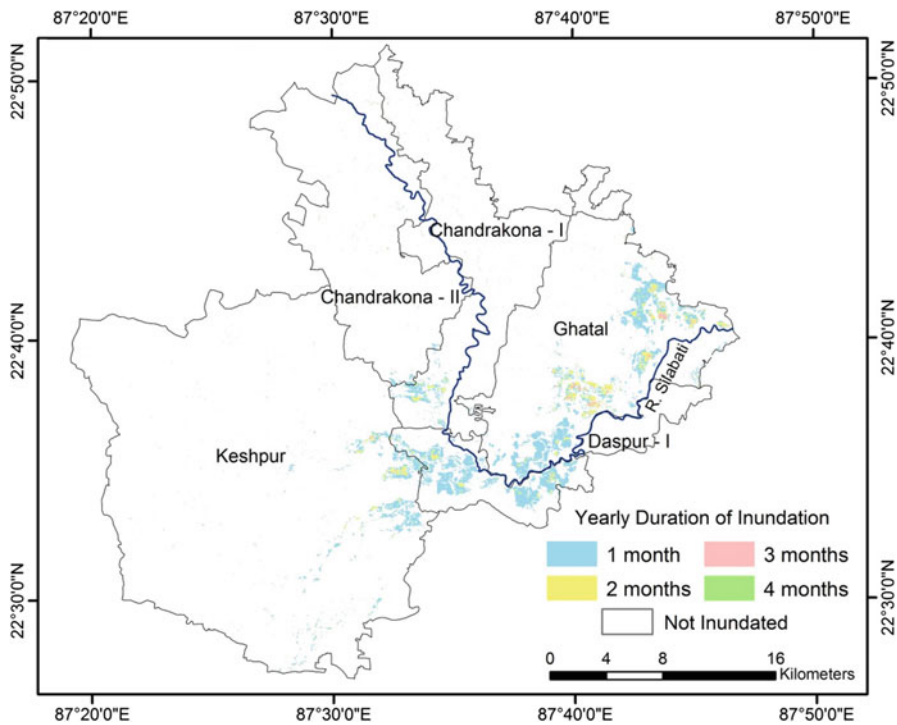


**Fig. 14.6** Yearly inundation duration in the flood-affected reaches (1985–2020). (Source: Global Surface Water dataset (see Pekel et al., 2016, for details))

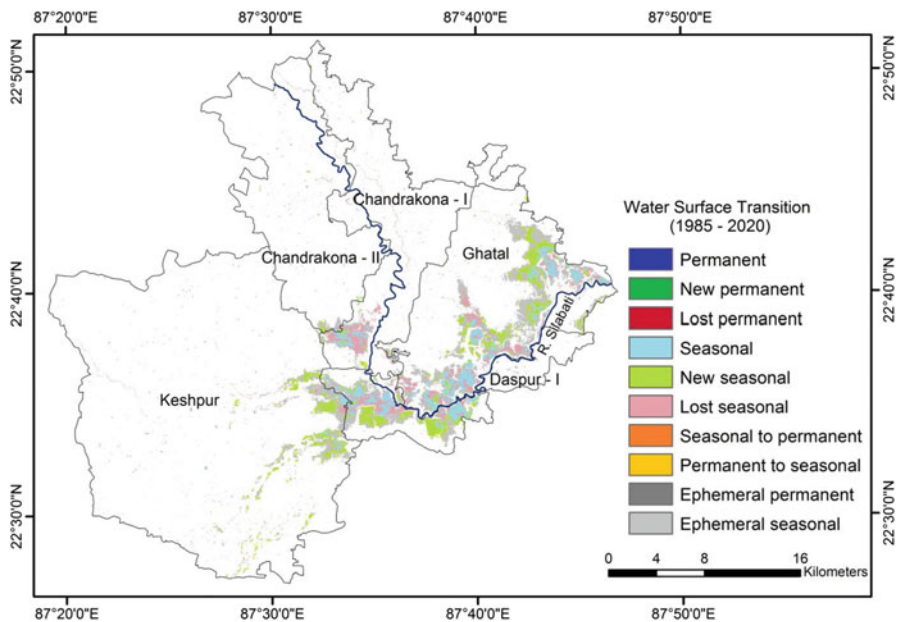


**Fig. 14.7** Water surface transition from one land use class to another in flooded areas (1985–2020). (Source: Global Surface Water dataset (see Pekel et al., 2016, for details))



**Fig. 14.8** Floodwaters of the Silai inundating Ghatal town and the western flank of the river. (Source: Google Earth, Image date: 13th September, 2009)

although on a piecemeal basis to control and abate the problems of flooding and riverbank erosion in the region (e.g. Mondal & Patel, 2020).

## 5 Conclusion

The Ghatal flood is a near-annual phenomena that has been in play for decades. Possibly there are no viable solutions to completely eradicate its occurrence given the low-lying nature of the local topography and the region's almost saucer-like situation, with multiple rivers draining into this region along all sides. The principal inundation is caused by the rise in the waters of the Silai and its distributaries, but this is augmented by the inflow of waters from distributaries of the Kangsabati to the south and from the Darakeswar in the north. Furthermore, the tidal effect of the Rupnarayan, into which the Silai drains, can retard its outflow and enable/prolong inundation. However, this natural situation has been markedly exacerbated by the construction of multiple embankments, which have dissociated the river from its floodplain and thus taken away those locations (primarily wetlands) that once could have accommodated overflows along the channel throughout the lower course of the river. This leads to a greater volume of water reaching the mouth area of the Silai, with the consequent inundation. Alongside the flood effect, riverbank erosion and collapse are common occurrences in this stretch, with regular embankment breaching. Nature-based solutions (using live vegetation buffers and proper zoning of the riparian corridor) have been proposed to mitigate this to an extent, and these measures need to be explored and adapted further herein, given the historical failure of only the structural measure-based approach that have been adopted so far for this purpose.

**Acknowledgements** This research has been funded by the Department of Science and Technology and Biotechnology, Government of West Bengal. The grant was awarded to Priyank Pravin Patel. The UGC-SRF Award of Sayoni Mondal is also acknowledged.

## References

- Banerji, D., & Patel, P. P. (2019). Morphological aspects of the Bakreshwar River Corridor, West Bengal, India. In B. Das, S. Ghosh, & A. Islam (Eds.), *Advances in micro geomorphology of lower Ganga Basin – Part I: Fluvial geomorphology* (pp. 155–189). Springer. [https://doi.org/10.1007/978-3-319-90427-6\\_9](https://doi.org/10.1007/978-3-319-90427-6_9)
- Behanzin, I. D., Thiel, M., Szarzynski, J., & Boko, M. (2015). GIS-based mapping of flood vulnerability and risk in the Benin Niger River Valley. *International Journal of Geomatics and Geosciences*, 3(6), 1653–1669.
- Blistanova, M., Zelenakova, M., Blistan, P., & Ferencz, V. (2016). Assessment of flood vulnerability in Bodva river basin, Slovakia. *Acta Montanistica Slovaca*, 21(1), 19–28.
- Borrows, P., & Bruin, D. (2006). The management of riverine flood risk. *Irrigation and Drainage*, 55(S1), 151–157.
- Das, S. (2019). Geospatial mapping of flood susceptibility and hydro-geomorphic response to the floods in Ulhas basin, India. *Remote Sensing Applications: Society and Environment*, 14, 60–74.
- Das, B., & Bandyopadhyaya, A. (2015). Flood risk reduction of Rupnarayan River, towards disaster management— A case study at Bandar of Ghatal Block in Gangetic Delta. *Journal of Geography and Natural Disasters*, 5(1), 135.
- Dolui, G., & Ghosh, S. (2013). Flood and its effects: A case study of Ghatal Block, Paschim Medinipur, West Bengal. *International Journal of Science and Research*, 2(11), 248–252.
- Gangwar, S. (2013). Flood vulnerability in India: A remote sensing and GIS approach for warning, mitigation and management. *International Journal of Environmental Science: Development and Monitoring*, 4(2), 77–79.
- Hoque, M. A., Tasfia, S., Ahmed, N., & Pradhan, B. (2019). Assessing spatial flood vulnerability at Kalapara Upazila in Bangladesh using an analytical hierarchy process. *Sensors*, 19, 1302.
- Kar, N. S., & Das, S. (2020). Flood-Prone Ghatal Region, India: A study on post-‘Phailin’ inundations of 2013. In S. Bandyopadhyaya, H. Magsi, S. Sen, & T. P. Dentinho (Eds.), *Water management in South Asia: Socio-economic, infrastructural, environmental and institutional aspects* (pp. 69–89). Springer.
- Leopold, L. B., Wolman, M. G., & Miller, J. P. (1964). *Fluvial processes in geomorphology*. Freeman.
- Mal, S., & Mandal, S. (2013). An analysis of the public perception on flood control assessment of Daspur-I Block of Paschim Medinipur District in West Bengal, India. *International Journal of Current Research*, 5(4), 969–972.
- Mitra, P., & De, I. (2016). Flood prediction modelling of Ghatal Block (West Bengal). *International Journal of Advanced Research in Computer Science Engineering and Information Technology*, 6(1), 1075–1078.
- Mondal, S., & Patel, P. P. (2018). Examining the utility of river restoration approaches for flood mitigation and channel stability enhancement: A recent review. *Environmental Earth Sciences*, 77, 195. <https://doi.org/10.1007/s12665-018-7381-y>
- Mondal, S., & Patel, P. P. (2020). Implementing Vetiver grass-based riverbank protection programmes in rural West Bengal, India. *Natural Hazards*, 103, 1051–1076.
- Mondal, S., & Patel, P. P. (2021). Mapping, measuring and modelling common fluvial hazards in Riparian Zones: A brief review of relevant concepts and methods. In P. K. Shit, H. R. Pourghasemi, G. S. Bhunia, P. Das, & A. Narsimha (Eds.), *Geospatial technology for environmental hazards* (pp. 353–389). Springer. [https://doi.org/10.1007/978-3-030-75197-5\\_16](https://doi.org/10.1007/978-3-030-75197-5_16)

- Mondal, S., & Patel, P. P. (2022). Incorporating hydromorphological assessments in the fluvial geomorphology domain for transitioning towards Restorative River science – Context, concepts and criteria. In A. Islam, P. Das, S. Ghosh, A. Mukhopadhyay, G. A. Das, & A. K. Singh (Eds.), *Fluvial systems in the anthropocene -process, response and modelling* (pp. 43–75). Springer: [https://doi.org/10.1007/978-3-031-11181-5\\_4](https://doi.org/10.1007/978-3-031-11181-5_4)
- Mondal, S., Sarkar, A., & Patel, P. P. (2016). Causes of drainage congestion in the Moyna Block, Purba Medinipur, West Bengal. In D. K. Mondol (Ed.), *Application of geospatial technology for sustainable development* (pp. 1–9). University of North Bengal, India, North Bengal University Press.
- Naskar, R., & Patel, P. P. (2019). Stream classification & historical shifting of middle stretch of the Shilabati River at Garbeta. *Asian Studies, XXXVI*(1&2), 1–16. Netaji Institute of Asian Studies.
- NITI Aayog. (2021). Report of the committee constituted for formulation of strategy for flood management works in entire country and river management activities and works related to border areas (2021–2026).
- NOAA. (2012). *Calcutta/Alipore climate normals 1971–1990*. National Oceanic and Atmospheric Administration. Available at: <ftp://ftp.atdd.noaa.gov/pub/GCOS/WMO-Normals/RA-II/IN/42807.TXT>. Viewed 14 Dec 2021.
- Pal, S. K. (2014). A geomorphological study on regular flood of lower Silabati River Basin and its impact on the arable land. *International Journal of Interdisciplinary and Multidisciplinary Research, 1*(1), 28–52.
- Patel, P. P., & Dasgupta, R. (2009). Flood induced land use change in the Dulung River Valley, West Bengal. In R. B. Singh, S. D. D. Roy, H. D. D. K. Samuel, V. D. Singh, & G. D. Biji (Eds.), *Geoinformatics for monitoring and modelling land-use, bio-diversity and climate change – Contribution towards international year of planet Earth* (Vol. 1, pp. 103–123). NMCC Publication.
- Patel, P. P., Mondal, S., & Prasad, R. (2020). Modifications of the geomorphic diversity by anthropogenic interventions in the Silabati River Basin. In B. C. Das, S. Ghosh, A. Islam, & S. Roy (Eds.), *Anthropogeomorphology of Bhagirathi-Hooghly River system in India* (pp. 331–356). Routledge.
- Pater, B. (2018). *Self-dependent health care for Flood-Prone Ghatal Area*. Available at <https://repository.tudelft.nl/islandora/object/uuid:c2783fe0-4b86-4a88-803c2d43a708119a/datastream/OBJ1/download>. Viewed 15 Dec 2021.
- Pekel, J., Cottam, A., Gorelick, N., & Belward, A. S. (2016). High-resolution mapping of global surface water and its long-term changes. *Nature, 540*, 418–422.
- PTI. (2021, March 8). Non-structural measures should be given priority for flood management: Report. *Financial Express*.
- Sahana, M., & Patel, P. P. (2019). A comparison of frequency ratio and fuzzy logic models for flood susceptibility assessment of the lower Kosi River Basin in India. *Environmental Earth Sciences, 78*, 289.
- Sahana, M., Rihan, M., Deb, S., Patel, P. P., Ahmad, W. S., & Imdad, K. (2020). Detecting the facets of anthropogenic interventions on the palaeochannels of Saraswati and Jamuna. In B. C. Das, S. Ghosh, A. Islam, & S. Roy (Eds.), *Anthropogeomorphology of Bhagirathi-Hooghly River system in India* (pp. 469–490). Routledge.
- Sahoo, P. M., & Sivaramakrishnan, L. (2014). Vulnerability of flood prone communities in the lower reaches of Shilai River– Ghatal Block, Paschim Medinipur District, West Bengal, India. *International Journal of Development Research, 4*(7), 1393–1400.
- Tehrany, M. S., Lee, M. J., Pradhan, B., Jebur, M. N., & Lee, S. (2014). Flood susceptibility mapping using integrated bivariate and multivariate statistical models. *Environmental Earth Sciences, 72*, 4001–4015.
- WAPCOS Limited. (2009). *Master plan and DPR for Ghatal area, draft final report*. International Consultants in Water Resources, Power and Infrastructure Development.

## Chapter 15

# A Baseline Study on Silaboti River Shifting, Flood, and Its Impact on Livelihood at Ghatal, Paschim Medinipur District, West Bengal



Sudip Bera, Riya Samanta, and Nilanjana Das Chatterjee

**Abstract** Climate change has increased hazardous events associated with tropical cyclones, which ultimately increased the intensity of other extreme events such as flooding and associated impacts. This event has increased the vulnerability of low-lying areas, deltas, coasts, and islands in many parts of the world including Indian subcontinent. Floods and water-related disasters and their associated problems are the most common natural calamity in most parts of West Bengal. The flood is frequently occurring in every year in many low-lying areas of West Bengal. The existing study has been completed with the use of geospatial technology both remote sensing (RS) and GIS environment in Pratappur village, Ghatal Block, Paschim Medinipur district. This study aims toward the shifting nature of river course and assessment of flood vulnerability zones in the study area. The position of Silaboti River has affected more this area. The depth of riverbed is low to hold huge discharge, especially during monsoon. The area is characterized by low-lying land. People inhabited in this area are habituated and adopted with the occurrence of two or three times flood situation in a year. A devastating flood happened in 2017 due to breaching of Chetua circuit embankment at Pratappur, located at the left bank of Silaboti River. This event inundated 93.27 km<sup>2</sup> of area and stayed for 45 days.

**Keywords** Shifting of river course · Flood vulnerability · RS& GIS technique · Silaboti river · Ghatal block

## 1 Introduction

India with its million rivers suffered from devastating flood throughout the year (Ganguly & De, 2015). Floods are caused due to intense storm precipitation, basin overflow, and sometime physiographic location of river basin and intervention of

---

S. Bera · R. Samanta · N. Das Chatterjee (✉)

Department of Geography, Vidyasagar University, Midnapore, West Bengal, India

e-mail: [nilanjana\\_vu@mail.vidyasagar.ac.in](mailto:nilanjana_vu@mail.vidyasagar.ac.in)

people. River channels are very dynamic in nature, changing their morphology, i.e., shape, size, and sediment load, etc. Generally we put more emphasis on nonstructural measures of flood management and control than structural measures. These measures include flood forecasting, floodplain zoning, and inundation mapping. Floods are actual problem in West Bengal. This problem makes people's lives miserable. Critical physiographic condition of river is an important cause of flood. With the passage of time, the frequency and intensity of floods in the Ghatal subdivision have significantly increased (Dolui & Ghosh, 2013). However, man-made causes are now more responsible for floods than natural causes. The main natural causes for river flooding are high-intensity rainfall within short period of time, the meandering course of the river, large floodplains, break of slopes along the long profiles of rivers, etc. (Singh, 1991). During the monsoon season, floods occur in the Purba Medinipur and parts of Burdwan districts of West Bengal due to excess water release from the many reservoirs. Especially Damodar, Kangsavati, Mundeshwari, Dwarkeshwar, and Shilabati Rivers are prone to floods. Floods are observed in other rivers also. The Ghatal floods become a major issue not only in West Bengal but also in India. Flood in Ghatal not only affect the environment but also break down the economic structure and weaken the people economically.

Remote sensing has developed as an important tool in the study of floods, particularly with its capacity to provide near-real-time data of the study area, enabling preparation of maps of inundated areas and assessment of damages. Flood is a perennial phenomenon (Dandapat & Panda, 2017) where flow rate is very fast than the natural flow of the river water (Bhadra et al., 2011). Plenty of researches have been conducted using remote sensing and GIS techniques (Jain & Sinha, 2003; Sankhua et al., 2005; Jain et al., 2005; Prasad et al., 2006). Remote-sensing technologies are excellent tools in the mapping of the spatial distribution of disaster-related data within a relatively short period of time. Applications of using data from satellites to predict weather-related disastrous phenomena, such as extreme rainfall, are widely known and frequently utilized. Satellite data can be used before, during, and after a disaster, for prevention, monitoring, mitigation, and relief operations, respectively. Areas, mainly agriculture land and vegetable crops affected by flooding, are typically large in size. It has been demonstrated that using satellite data for flood mapping becomes economically advantageous with respect to ground survey for a large area. Though floods are disruptive events and the occurrences of floods cannot be prevented which they are actually natural features of a river system and their role in replenishing, the floodplain cannot be ignored. The main aims of the study are (i) to study the nature of shifting of river Silaboti (selected part), (ii) to assess flood vulnerability zones and their causes, and (iii) to assess flood damage in the selected part.

## 2 Materials and Methods

### 2.1 About Experiment Site

Geographically, the experiment site, Ghatal block, is a devastating flood-affected area of Paschim Medinipur district as well as West Bengal in eastern India (Mitra & De, 2014). Not only Paschim Medinipur but also Purba Medinipur district is one of the flood-affected areas of West Bengal. Ghatal block (selected part) lies between  $22^{\circ}40'43.93''\text{N}$  to  $22^{\circ}32'49.43''\text{N}$  latitude and  $87^{\circ}43'04.74''\text{E}$  to  $87^{\circ}51'39.77''\text{E}$  longitude. Ghatal is located in the lower basin of the Silaboti River and upper part of Rupnarayan River (Fig. 15.1). The study area extends over  $139\text{ km}^2$  area. The average height of the study area (selected part of Ghatal) is 3–16 m. The area is highly flood prone due to low elevation. Basically, this area is most suitable for agriculture, but 2–3 month most of the agricultural land is inundated due to flood probably three to five times in a year (Kar & Das, 2020). The climate is moderate throughout the year. The drainage system of Ghatal block is good. Silaboti is the main river in this block. This river is situated at the northern most portions of this study area; it is also the border of Ghatal block and Hooghly district also. The Chandraswar Khal is flowing from southeast to south direction to join with Rupnarayan River in the upper catchment region. Dwarakeswar River join with Silaboti River from the left side with huge amount of water in the monsoon time. The study area has a very low to gentle slope, so in this region more deposition of sand, silt, etc. is accumulated. Therefore, this part of Silaboti River has very high runoff during the monsoon season mainly June to August. During monsoon season, the Silaboti River is known for its rapid flood discharge in low-lying Ghatal areas. The study area is flooded by the Silaboti River during this season. These rivers are most important for agricultural production in this block. On the other hand, the other side of Silaboti flood is it increases the fertility of the soil and helps to produce agricultural produce like rice, potato, and other vegetables which are the main livelihood of the people. The most effected villages are Pratappur, Harisinghpur, Harishpur, Shripur, Khanjapur, Ratnaswarbati, Gopmahal, Monohorpur, Shyamsundarpur, Jotkanusamgor, Sagarapur, Basudevput, and Sagarapur. The people of the Ghatal block as well as villages basically receive their capital by producing agricultural crops, like paddy, potato, wheat, jute vegetables, nut, etc.

### 2.2 Database, Methodology, and Sampling

The present research used both primary and secondary data. The primary data have been collected from door-to-door household survey, cross section, and sediment sample collected from the study area. Secondary data is also important to assess flood impact. Rainfall and water gauge height data were collected from Ghatal irrigation and waterway department. Satellite image was used for measuring current



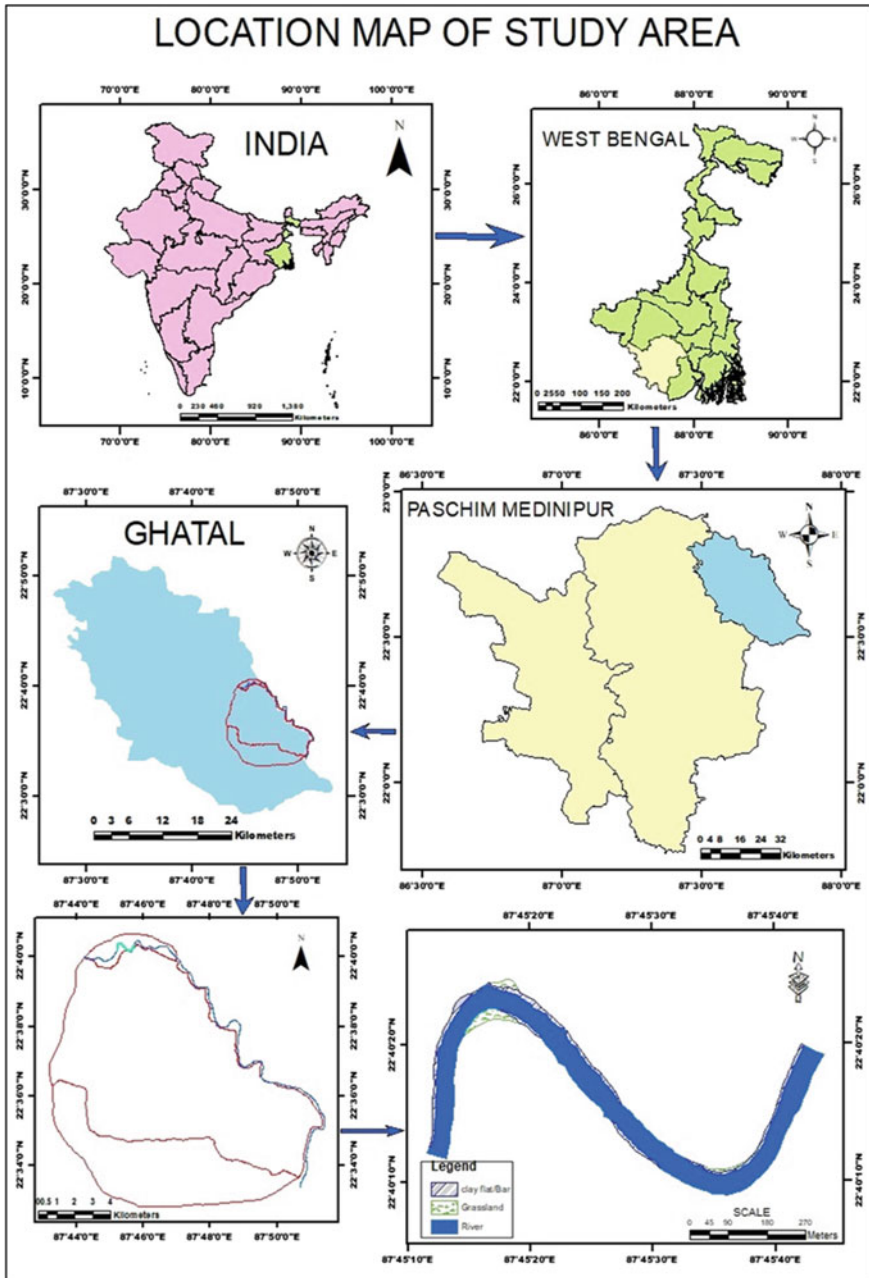
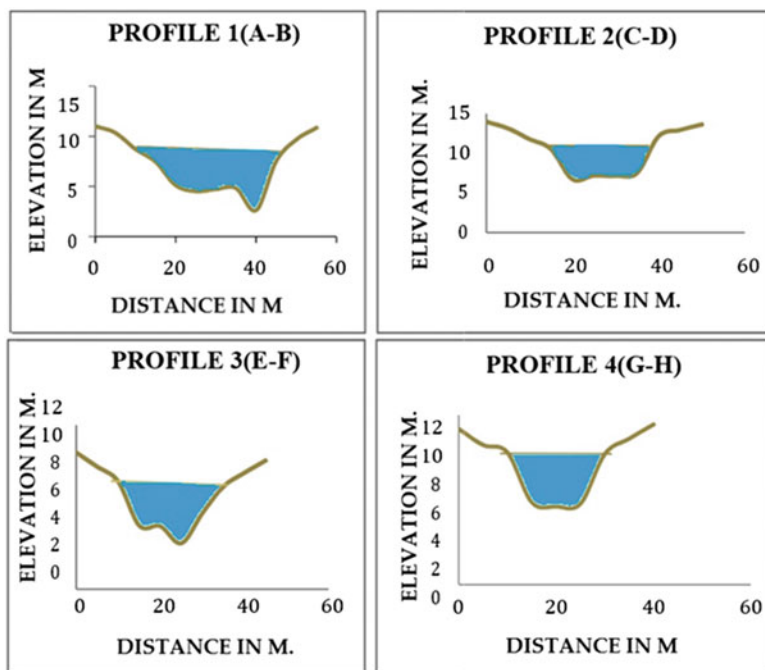


Fig. 15.1 Location of the study area



**Fig. 15.2** Cross section

situation in this area which was collected (USGC earth explore) from <https://earthexplorer.usgs.gov/>. Four cross-section lines (Fig. 15.2) were taken along the Silaboti lower basin of the Silaboti River, to examine the channel shifting and causes of flood in Ghatal (selected part) and assess the effects of the flood in human life and their livelihood pattern. Information on inundation prone area were collected from the Irrigation and Waterways Department of Ghatal, and flood inundation map was made. For the questionnaire survey, eight areas of five villages were chosen that were frequently under risk of flood inundation. We conducted randomly selected household for interviews about flood. In each village, we conducted about ten household interviews to randomize different location. Fifty household samples and 43 farmer's household interviews and 65 people for residential area were covered. The agricultural damage assessment required  $35.33 \text{ km}^2$  as the actual area of rain-fed paddy fields out of  $96.34 \text{ km}^2$  area which is passively dependent on irrigation of Silaboti River. Finally, the data from satellite image 2017 is imported into ArcGIS (Mitra, 2015) and ERDAS 9.1 to prepare a flood map (Sanyal & Lu, 2005; Bhadra et al., 2011). Most of the researchers have used analytic hierarchy process (AHP) weighting approach and GIS technique (Sarif et al., 2021) for identification of flood-prone area (Saaty, 1980; Wang et al., 2011; Siddayao et al., 2014; Pham et al., 2021; Vojtek et al., 2021).

## 2.3 Cross Section

Cross section is an important parameter for analyzing the flood situation in a river. To understand the nature of channel shapes and channel patterns, a total of four cross sections of the Silaboti River have been taken (Fig. 15.2). Using a leveling instrument, staff readings have been collected and plotted for the Silaboti River (Maity & Maiti, 2017). The benchmark is 10.5 m. near Ghatal SDO office, used as standard for the calculation of reduced levels at all the stations (Fig. 15.3). Cross-sectional area and width-depth relation have been estimated by the collected data in the study area. Slope of the riverbed is calculated by the equation (Stark, 2006).

$$\theta = \tan^{-1} r/h$$

where  $\theta$  = the riverbed slope,  $r$  = difference of reduced level at the first and last points, and  $h$  = the horizontal distance between same two points. The slope of the river is  $0^{\circ}4.89''$ .

Sinuosity index (SI) is computed following the equations:

$$SI = \text{Channel Length} / \text{Wave Length (Leopold and Wolman 1957)}.$$

There are several methods to calculate sinuosity index (SI) of river channel. In this study we have used Leopold and Wolman (1957) method. If the value of SI is greater than 1.05, the channel is indicated as sinuous, meandering if greater than 1.5, meandering and braided if the value is greater than 1.3, and anastomosing if value is greater than 2.0 (Morisawa, 1985). The sinuosity index (SI) of the river (selected part) by using this method is 1.636. This value is indicated that the selected portion of the river is meander in nature. The slope and length of both sides of the cross sections are from the thalweg position. Depending on the channel's form, the velocity distribution changes (Morisawa, 1962). The velocity gradients are greater along the bed than at the banks where the channel is wide and shallow (Maity & Maiti, 2017). Turbulence has a significant impact on the mechanics of river flow, i.e., the combination of secondary movements with the water's main downstream flow (Morisawa, 1962). In case of Silaboti, in the study area, such phenomena are present.

## 3 Results and Analysis

### 3.1 Shifting of River Course

In case of river shifting the river flow showing in the selected study area, the river course is shifting in different times in the year 2003 in the western part, the position of thalweg is shifted to the southeastern part, and its cause is embankment erosion (Fig. 15.4). The selected study area has two meanders; the first one in the western

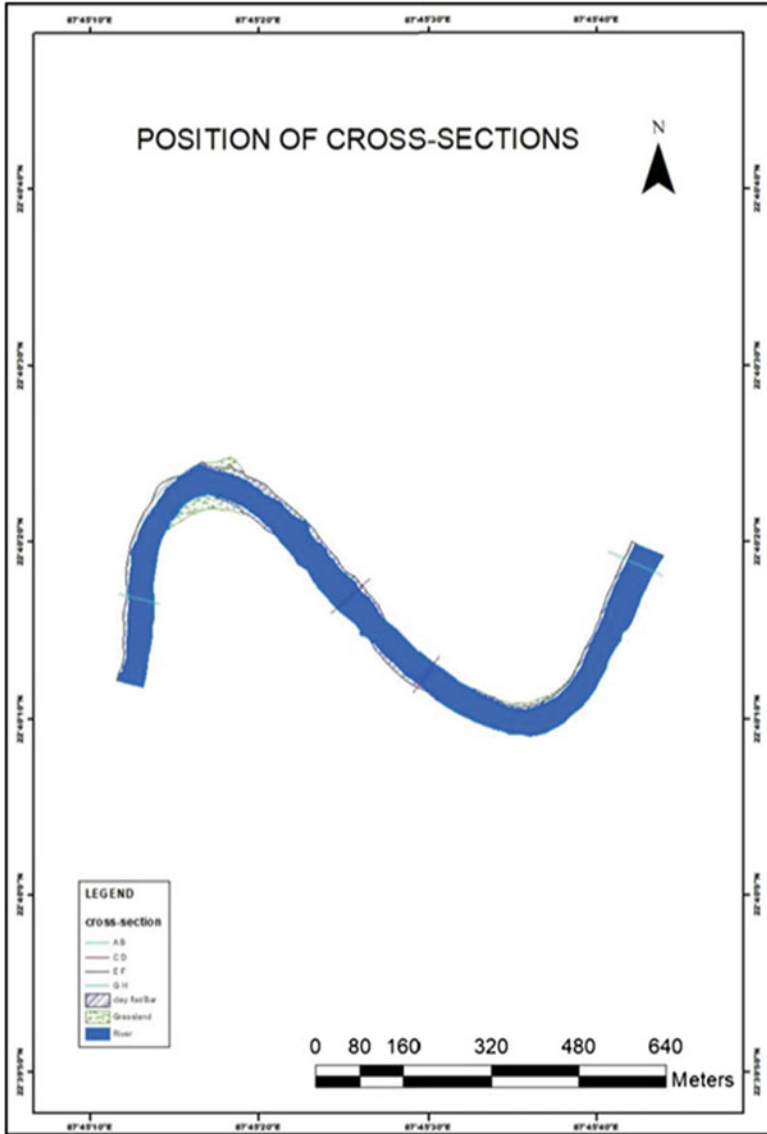
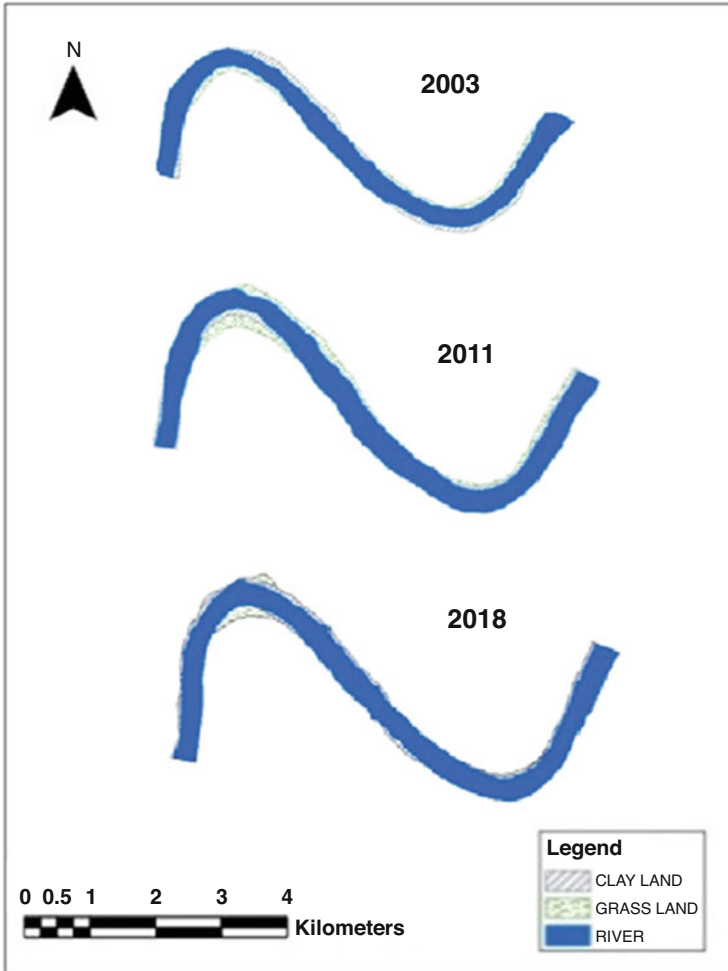


Fig. 15.3 Position of cross section

side is mostly eroding its embankment and cutting the point bar. Southeastern part is also eroded, but it is lesser because here is an embankment which is protected by bolder, and this embankment is the main road connected to the Pratappur village and its nearby villages with the Ghatal town. The shifting of river position in this area might be one of the causes of more flood vulnerability (Liang et al., 2017) as a whole area. The position and depth of riverbed of Silaboti River caused more effects in this



**Fig. 15.4** Shifting of river Course

area. The bed is shallow to hold a huge discharge. The change detection and discharge of the river are shown in Fig. 15.5.

### 3.2 *Width-Depth Ratio*

Width-depth ratio is one of the significant variables to understand the channel form of the river. The width-depth ratio changes continuously to adjust with the discharge and slope of the bed. Having large width-depth ratio is more efficient to transport bed load by shear on the bottom of the stream (Maity & Maiti, 2017). In the study area,

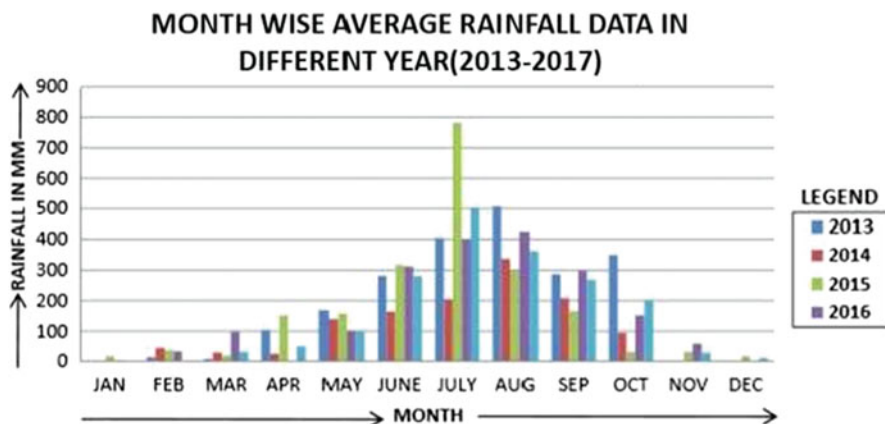


Fig. 15.5 Average discharge

width-depth ratio is less; near profile G-H is 10, but width-depth ratio in the middle portion of the channel profile E-F and C-D is 11.25 and 14.25, respectively. Similarly, the width-depth ratio of the profile A-B is 15. River discharge, rock type, slope, type of load being transported, type of sediment at the channel’s perimeter, and rock uplift rate have all been shown to control river width and width-depth ratio (Schumm, 1960).

### 3.3 Meandering of a Stream

Channel pattern is usually characterized by the ratio of stream length to valley length (stream sinuosity). The value of sinuosity index ( $SI = 1.636$ ) denotes the nature of the channel of the river. Sinuosity index indicates the braided pattern of the channel with the value of  $SI$  1.636 (Susware et al., 2021). The sinuosity index in this study’s analysis of the entire lower section of the Silaboti River shows the river is braided. However, very gentle to almost flat are the main characteristics of the gradient of the riverbed.

### 3.4 Catchment Size

Dwarakeswar and Silaboti Rivers meet at Bandar, and then they flow toward the southeast direction, and the combined flow is named as Rupnarayan. However, in monsoon season, two rivers carry large amount of water from their tributary and source point. After that, they meet near Bandar, and the water is overflowing, and a

large area is used to be inundated underwater because the catchment size of the river is not enough here to hold large amount of water (Das et al., 2020).

### 3.5 Catchment Shape

Catchment shape is an important indicator of flood. Catchment shape of Silaboti and Dwarakeswar is different in different locations. The actual width of the Silaboti and Dwarakeswar Rivers is 50 m in some locations, but it is 80 m for Rupnarayan, where two rivers meet. The average width of Rupnarayan River is 66.66 m. The tidal effect is one of the important causes for increasing volume of water as well as increasing the extra width of the Rupnarayan River at the meeting point of two rivers (Das et al., 2020). This sudden widening of width of the river causes flow separation leading to increased sedimentation and causing flood (Fig. 15.6). The selected study area comes under monsoon climate. And climate is one of the main controlling factors of flood in the study area. Therefore, the maximum rainfall occurs in this time is >90% of annual rainfall. Thus huge amount of rainfall and water released from different dams like, DVC, created enormous amount of discharge which could not pass through small channels, and the entire area comes under the flooded condition.

### 3.6 Critical Drainage Pattern

Physiography of drainage pattern is very critical in Ghatal Block. The present study area at Pratappur village is most affected because the Silaboti River meets with Darakeswar River in this village at Bandar (Rudra, 2008) with its huge discharge (Fig. 15.7).

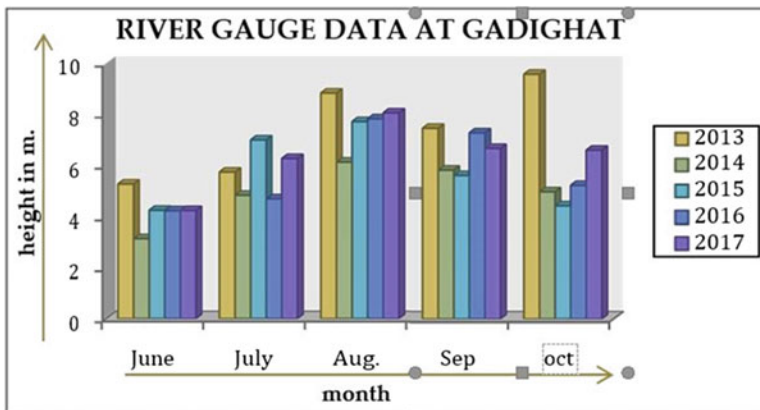


Fig. 15.6 River Gauge data

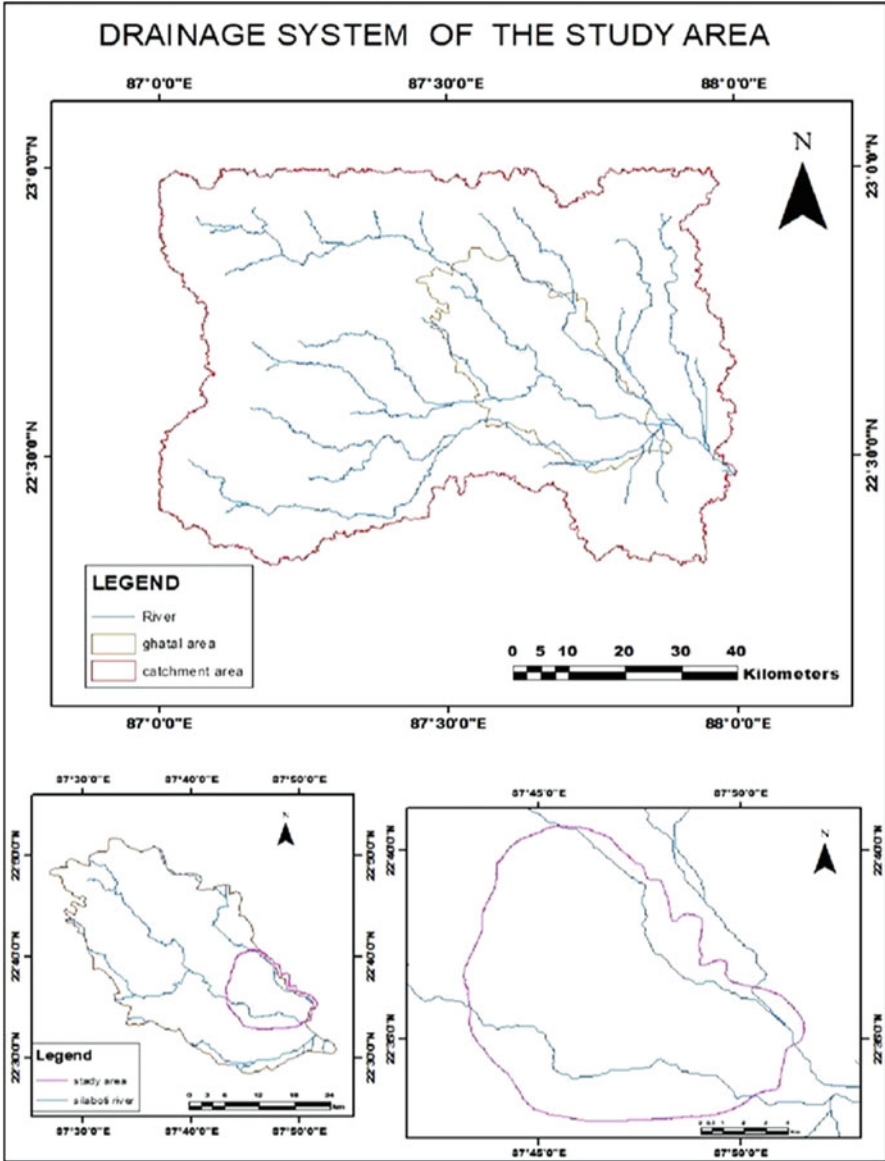


Fig. 15.7 Change detection of river course

## 4 Discussion

Flood is one of the most frequent natural disasters in the world in present-day scenario. Not only India but also West Bengal faces this devastating problem every year. Ghatal Block has also faced almost every year in varying degrees.



Most of the year floods occur in four to five times. The flood is most effective environmental events of Ghatal subdivision which is one of the flood-prone areas in West Bengal (Dolui & Ghosh, 2013). The floods in Ghatal have taken a place on the map of India. In the eighteenth century, floods occur due to a huge volume of water flow through the Silaboti River of sufficient depth. During the British period in the nineteenth century, major floods occurred in 1867, 1877, 1885, and 1896. After that unusual high flood occurred in 1913–1914 causing serious loss of life and property, damage to standing crops, seeds, and houses. In 1956, 1959, 1970, 1971, 1973, 1978, 1984, 1995, 1999, 2000, and 2007, major floods have been recorded in those years (Mukhopadhyay & Dasgupta, 2010). A devastating flood occurred in 2017 which inundated 93.27 km<sup>2</sup> areas for 45 days. It happened due to breaching of Chetua circuit embankment at Pratap Pur left bank of Silaboti at 22°66′69″ N and 87°75′79″ E. This is the most devastating flood till now. It spreads over 139 km<sup>2</sup> area. According to census 2011, a total of 116,408 persons with a density of 837/km<sup>2</sup>. in this area was affected by this flood. Many villages along the river were once important trading centers. But these settlements have lost their significance due to the occurring of the frequent floods in this area. If we go through the river pattern at Ghatal, the block is divided into three parts, namely, interfluves of Sankari and Darakeswar River, interfluves of Sankari and Rupnarayan River, and interfluves of Silaboti and Sankari River. Ghatal town is situated in the interfluves of Silaboti and Rupnarayan River (Fig. 15.8). Excessive monsoonal rainfall from July to September and additional discharge water from Mukutmanipur and DVC reservoir are mainly responsible for flooding in this block. Floodwater can seriously disrupt the public and private transport by cutting off roads and railway lines, as well as total communication system like telephone communication which is also damaged by this flood. Floods disrupt the normal drainage systems in this area, and serious health hazard occurred due to sewage spills.

#### **4.1 Effect on People**

After the flood the NGO and government take some initiative and rescue people by speedboat, and in most vulnerable areas, speedboats fail to rescue the affected people who suffer badly. Most of the people were shifted from the devastating flood zone about 1264 people was affected and 81 people was sifted by the rescue operation team during the 2017 flood event in the study area (Fig. 15.9).

#### **4.2 Effect on Agricultural Products**

Ghatal Block is agriculturally developed. Most of the people are engaged in agricultural activities. Agricultural land is an essential resource for the people who are living in the study area, especially those who live on the total agricultural production

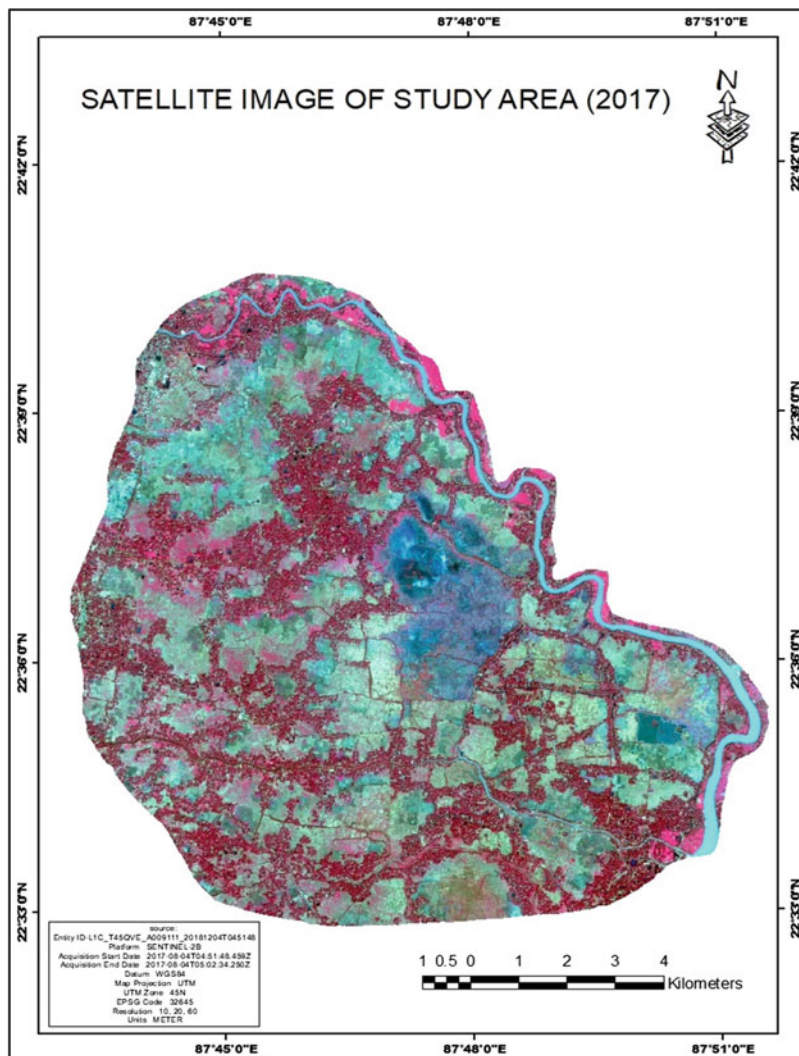
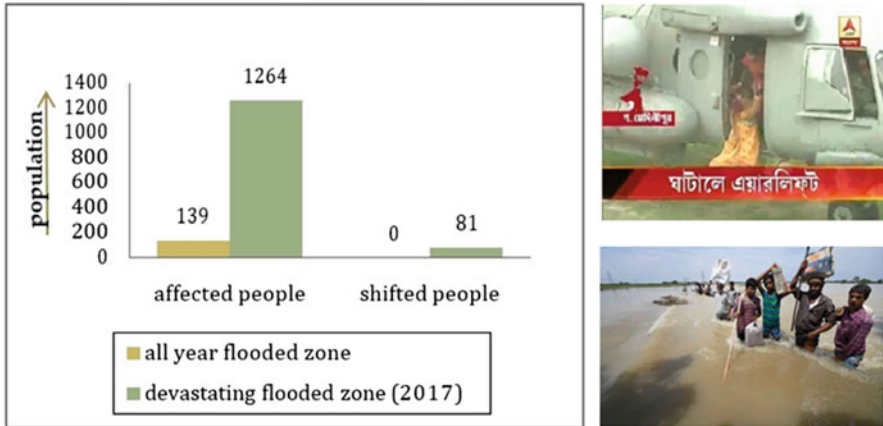


Fig. 15.8 Open source image to show flood situation in the study area

of that particular land and the labor force engaged in that occupation. The poor people had less amount of agricultural land to support their family. About 62% of the total population live on agriculture. Agriculture lands are inundated by floodwater, and all crops have been damaged in this area. Farmers were asked about the flood depth, duration, and any damage or loss of paddies (Win et al., 2018). Rain-fed paddies are usually cultivated with a deepwater rice variety in the low-lying flood-plains along the Silaboti River to take advantage of this flood-prone land.



**Fig. 15.9** Effect on people

### 4.3 Road Damage

The flood has significant impact on the physical infrastructure such as road. This study illustrates that the frequent flood in this study area has resulted in various destructions on major physical infrastructures especially road infrastructure. When floodwater hits the roads, it causes more damage to the road materials. Structural deterioration of the road resulted in huge expenses for immediate and long-term maintenance of roadways. However, it is also monitored that the frequencies of flooding in various districts are directly related to the amount of rainfall and affect most of the road network. During this time, the major state highways Ghatal-Chandrakona and Ghatal-Medinipur routes were completely unusable. However, the main causes of road damage can be highlighted as the failure of the substandard or the road foundation, so it is important that research in future should be focused on this part of the road communication systems in the area as well as in this district (Fig. 15.10).

### 4.4 Effect on Household Damage

In this study, for residential and agricultural area, both direct and indirect damages were taken into account. For the purpose of assessing residential flood damage, three damage types were taken into consideration: (1) house damage, (2) in-house damage, and (3) income loss or economic damage (Win et al., 2018). House damage included the repair/rebuild costs for damaged or destroyed buildings. It also considered the cost of building new houses to replace the houses that were completely lost due to embankment breaching at Pratappur village and the cost of repair of the exterior of the building's appurtenances which were damaged by the flood. In-house

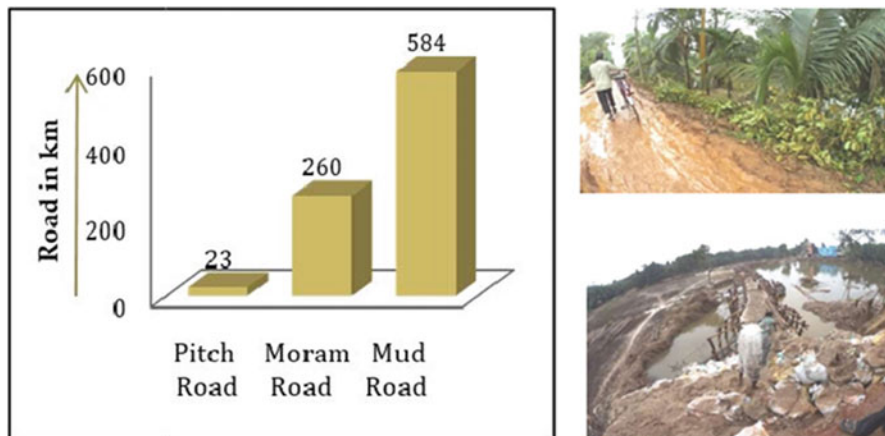


Fig. 15.10 Road damage

damage included costs associated with damage to or loss of, furniture (Win et al., 2018), toilet, clothes, appliances, kitchen utilities, food grain, animals, and other household goods. Income loss was the only indirect damage that was observed in this study and can be defined as the sum of income loss due to flooding. In addition, three type damage estimates have been recorded. Households were asked to record the depth of the flooding on their yards during the 2017 flood event. During a flood, the majority of the houses was submerged and damaged. Most of the houses were partly damaged. The households were asked to estimate the total value of their houses and their in-house belongings, as well as their annual household incomes (Win et al., 2018). The results of this household survey were used as a ratio of the value of the loss to the total cost of the household to estimate the loss rate of each household (Fig. 15.11).

#### 4.5 Effect on Health

Health hazard is a serious problem during flood. Floodwater may have high levels of raw sewage or other hazardous substances. Early symptoms from exposure to contaminated floodwater may include stomach upset, intestinal problems, cholera, dysentery, headache, and other flu-like discomfort. Anyone experiencing these and any other problems should immediately seek medical attention. Many people suffer from stomach ailments during floods mainly due to waterborne diseases especially children. Many people may die without treatment as there is no chance of treatment at this time. During floods, there is a severe shortage of drinking water as all the wells or tube wells run out of water. The incidence of flies and mosquitoes is also high during this time. Many elderly people and children also drowned during the floods. Many houses were destroyed, and many people and cattle died. Mosquitoes

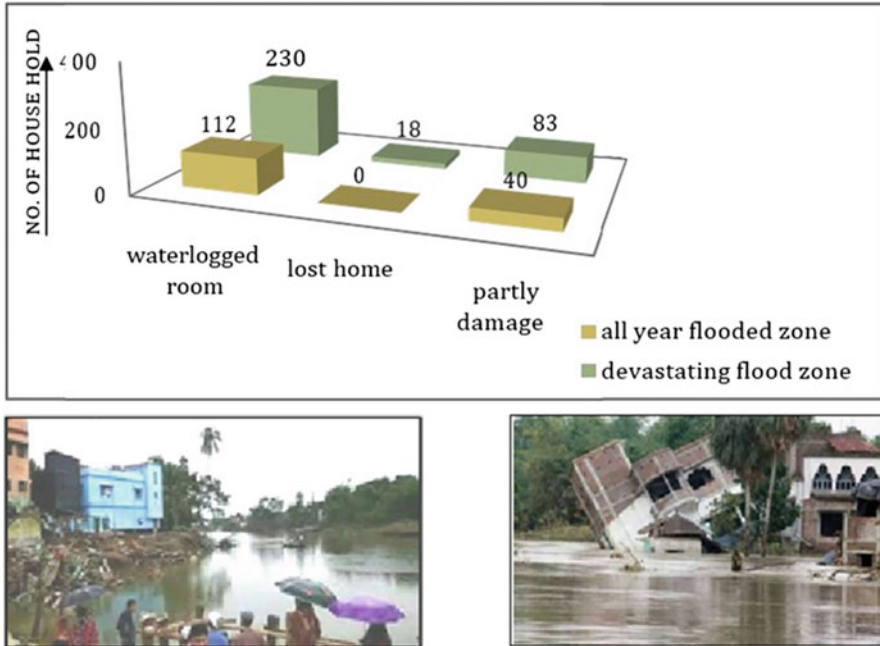


Fig. 15.11 House damage

can sharply increase after a flood, due to the sudden availability of standing water which is suitable for breeding even very small amounts of water. Flooding affects people in a multitude of ways. People suffer stress on multiple fronts, not just as flooding occurs, but also in the anticipatory period preceding a flood and during the cleanup and recovery phase. Flooding can damage properties, destroy homes, create financial burden, and cause emotional hardship.

#### 4.6 Effect on Soil pH

Soil pH is a measure of the acidity and alkalinity in soils. Liming had less impact on the pH value of the flooded soil; however the amount of  $\text{CaCO}_3$  applied to the unflooded soil caused those pH values to rise. pH levels range from 0 to 14, with 7 being neutral, below 7 acidic, and above 7 alkaline (Fig. 15.12). The optimal pH range for most plants is between 5.5 and 7.0; however, many plants have adapted to thrive at pH values outside this range. An acid is defined as a substance that tends to release hydrogen ions ( $\text{H}^+$ ). Conversely, a base is defined as a substance that releases hydroxyl ions. All acids contain hydrogen ions, and the strength of the acid depends upon the degrees of ionization (release of hydrogen ions) of the acid. The more hydrogen ions there are in the soil exchange complex related to the basic ions (Ca,

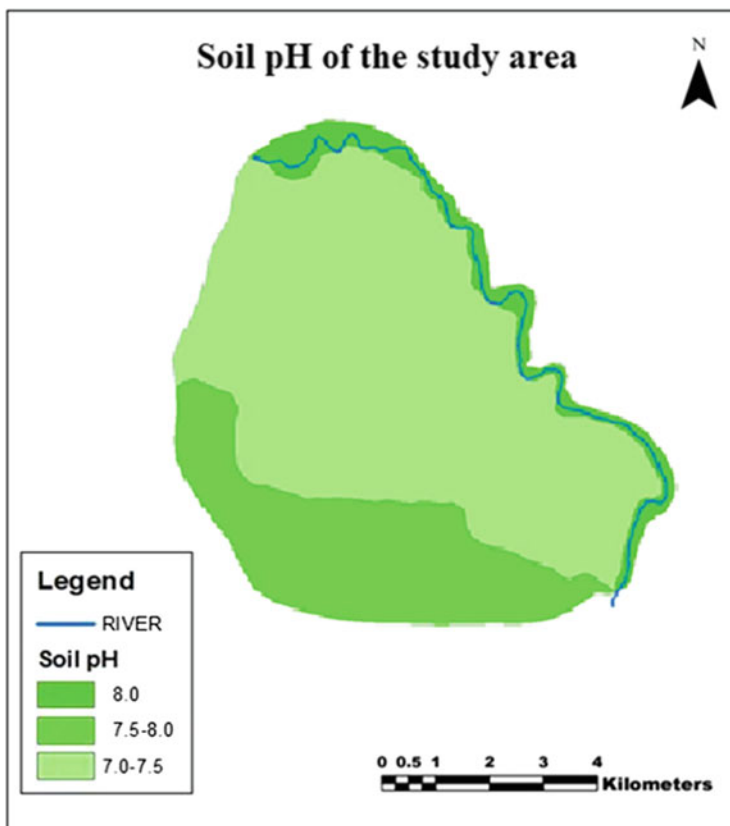


Fig. 15.12 Soil pH

Mg, K), the higher the acidity of the soil. The desirable pH range for optimum plant growth varies among crops. While some crops grow best in the 6.0–7.0 range, others grow well under slightly acidic conditions. Soil properties that influence the need for and response to lime may vary by region. Knowledge of the soil and the crop is important in managing soil pH for the best crop performance. Soils become acidic when basic elements such as calcium, magnesium, sodium, and potassium held by soil colloids are replaced by hydrogen ions. Soils formed under conditions of high annual rainfall are more acidic than soils formed under more arid conditions. Our study area Ghatal (selected part) is under alluvial type of soil. Due to deposition of river sediment, the soil is so fertile for agriculture. Most of the land produces paddy and potato, and some of area produced vegetable. The study area is divided into three flood zones (Fig. 15.13). First zone is all year-flood zone, and pH of this zone is 7.5–8.0. Second zone is devastating flood zone, and pH of this zone is 7.0–7.5, and third is no-flood zone, where pH is 8.0. So, all the land is suitable for different types of agriculture and cultivation of vegetation. Apart from agriculture, Ghatal Block is also well developed for vegetable cultivation which is mainly cultivated on

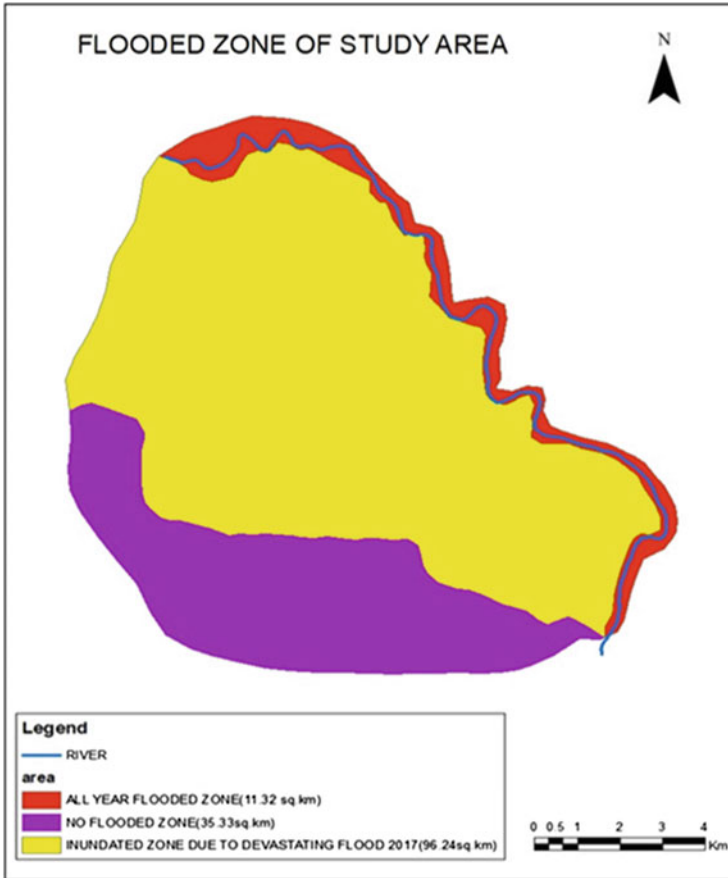


Fig. 15.13 Flood zone

floodplain silt soils in riverine areas. However, Ni, Zn, and Cu contents were marginally higher where the flood sediment depth was more than 5 cm.

## 5 Conclusion

Ghatal flood is an undeviating problem. Many people suffer from this problem. The flood of Ghatal is a long-standing problem in the combined flow of Silaboti, Kangsabati, and Darakeswar Rivers. The floods at Pratappur on the banks of the Silaboti ruin livelihood of the people of riverine areas. The loss includes not only life and property, but it also has instant and long-term effects. For instance, floods can affect human health by causing man and animal death, disease transmission, physical injury, malnutrition, and loss of morale. Similarly, floods can affect the agricultural

sector by destroying crops and livelihoods, homes, and infrastructure. Flooding affects people in a multitude of ways. The Irrigation and Waterways Department (I & WD) of the Government of West Bengal has already taken up development works in some major reaches of the river. However, the progress is not up to the mark, and there is no comprehensive project to solve the problem.

**Acknowledgements** The authors would like to thank the students and staffs of Department of Geography, Vidyasagar University, and grateful to Departmental Soil Laboratory for giving consent for different experiments.

## References

- Bhadra, A., Choudhury, S., & Kar, D. (2011). Flood hazard mapping in Dikrong basin of Arunachal Pradesh (India). *World Academy of Science, Engineering and Technology*, 60, 1614–1619.
- Dandapat, K., & Panda, G. K. (2017). Flood hazard assessment at block level and its management strategy in Paschim Medinipur District, West Bengal, India. *IOSR Journal of Humanities and Social Science*, 22(6), 7–14.
- Das, U., Bajpai, R., & Chakraborty, D. (2020). River regulation and associated geo-environmental problems: A case study of lower reaches of Shilabati river basin, West Bengal, India. *International Journal of Ecology and Environmental Sciences*, 2, 233–240.
- Dolui, G., & Ghosh, S. (2013). Flood and its effects: A case study of Ghatal Block, Paschim Medinipur, West Bengal. *International Journal of Science and Research*, 2(11), 248–252.
- Ganguly, K., & De, S. K. (2015). Spatio-temporal analysis of flood and identification -1 /offlood hazard zone of west tripura district, tripura, india using integrated geospatial technique, *Hill Geographer* Vol . XXXI: 1 (2015) / ISSN 0970-5023
- Jain, V., & Sinha, R. (2003). Geomorphological manifestations of the flood hazard: A remote sensing-based approach. *Geocarto International*, 18(4), 51–60.
- Jain, S. K., Singh, R. D., Jain, M. K., & Lohani, A. K. (2005). Delineation of flood-prone areas using remote sensing techniques. *Water Resources Management*, 19(4), 333–347.
- Kar, N. S., & Das, S. (2020). Flood-prone Ghatal region, India: A study on post-‘Phailin’ Inundations of 2013. In *Water management in South Asia* (pp. 69–89). Springer.
- Leopold, L. B., & Wolman, M. G. (1957). *River channel patterns: Braided, meandering, and straight*. US Government Printing Office.
- Liang, D., Du, H., Gui, Q., Su, T., & Chen, Z. (2017, March). Risk assessment for regional flood disaster in Hubei Province based on GIS. In *2017 2nd International Symposium on Advances in Electrical, Electronics and Computer Engineering (ISAECE 2017)* (pp. 167–172). Atlantis Press.
- Maity, S. K., & Maiti, R. K. (2017). *Sedimentation in the Rupnarayan River: Volume 1: Hydro-dynamic processes under a tidal system*. Springer.
- Mitra, S. (2015). Shifting courses of Ganga River, it causes and resultant hazards of Manikchak Block, Malda District, West Bengal. *International Journal of Humanities and Social Science Studies*, Volume-II, Issue-I, 348–350.
- Mitra, P., & De, I. (2014). *Flood prediction monitoring of Ghatal Block*. ISR Jarnal and Publications.
- Morisawa, M. E. (1962). Quantitative geomorphology of some watersheds in the Appalachian Plateau. *Geological Society of America Bulletin*, 73(9), 1025–1046.
- Morisawa, M. (1985). *Streams: Their dynamics and morphology*. McGraw Hill.
- Mukhopadhyay, S. C., & Dasgupta, A. (2010). *River dynamic of West Bengal: Physical aspects*. Prayash.



- Pham, B. T., Luu, C., Van Dao, D., Van Phong, T., Nguyen, H. D., Van Le, H., & Prakash, I. (2021). Flood risk assessment using deep learning integrated with multi-criteria decision analysis. *Knowledge-Based Systems*, 219, 106899.
- Prasad, A. K., Vinay Kumar, K., Singh, S., & Singh, R. P. (2006). Potentiality of multi-sensor satellite data in mapping flood hazard. *Journal of the Indian Society of Remote Sensing*, 34(3), 219–231.
- Rudra, K. (2008). *BanglarNadikatha* (in Bengali). Sahitya Samsad.
- Saaty, T. L. (1980). *The analytic hierarchy process*. McGraw-Hill.
- Sankhua et al. (2005). Use of remote sensing and ANN in assessment of erosion activities in Majuli, the world's largest river island. *International Journal of Remote Sensing*, 26, pp. 4445–4454
- Schumm, S. A (1960). The Shape of Alluvial Channels in Relation to Sediment Type: Erosion and Sedimentation in a Semiarid Environment (Geological Survey Professional Paper 352-B), Published by Government Printing Office, Washington, D.C.
- Sanyal, J., & Lu, X. X. (2005). Remote sensing and GIS-based flood vulnerability assessment of human settlements: A case study of Gangetic West Bengal, India. *Hydrological Processes: An International Journal*, 19(18), 3699–3716.
- Sarif, M. N., Siddiqui, L., Islam, M. S., Parveen, N., & Saha, M. (2021). Evolution of river course and morphometric features of the river Ganga: A case study of up and downstream of Farakka Barrage. *International Soil and Water Conservation Research*, 9(4), 578–590.
- Siddayao, G. P., Valdez, S. E., & Fernandez, P. L. (2014). Analytic Hierarchy Process (AHP) in spatial modeling for floodplain risk assessment. *International Journal of Machine Learning and Computing*, 4(5), 450.
- Singh, S. (1991). Environmental geography, PrayagPustak Bhavan, Allhabad, India. | 11. *The Frame* (20 August 2013). <http://blogs.sacbee.com/photos/2011/06/the-monsoon-season-begins-in-i.html>
- Stark, C. P. (2006). A self-regulating model of bedrock river channel geometry. *Geophysical Research Letters*, 33(4), 1–5. <https://doi.org/10.1029/2005GL023193>
- Susware, N. K., Sapkale, J. B., Susware, V. N., & Gavhane, S. K. (2021). Linkages between sinuosity index and flood sustainability: A study of Morna River (Maharashtra), India. *Current World Environment*, 16(2). <https://doi.org/10.12944/CWE.16.2.28>
- Vojtek, M., Vojteková, J., Costache, R., Pham, Q. B., Lee, S., Arshad, A., et al. (2021). Comparison of multi-criteria-analytical hierarchy process and machine learning-boosted tree models for regional flood susceptibility mapping: A case study from Slovakia. *Geomatics, Natural Hazards and Risk*, 12(1), 1153–1180.
- Wang, Y., Li, Z., Tang, Z., & Zeng, G. (2011). A GIS-based spatial multi-criteria approach for flood risk assessment in the Dongting Lake Region, Hunan, Central China. *Water Resources Management*, 25(13), 3465–3484.
- Win, S., Zin, W. W., Kawasaki, A., & San, Z. M. L. T. (2018). Establishment of flood damage function models: A case study in the Bago River Basin, Myanmar. *International Journal of Disaster Risk Reduction*, 28, 688–700.

# Chapter 16

## Future Floods in the Brahmaputra River Basin Based on Multi-model Ensemble of CMIP6 Projections



Md. Khalequzzaman, Badrul Masud, Zahidul Islam, Sarfaraz Alam,  
and Md. Mostafa Ali

**Abstract** The Brahmaputra River frequently floods large areas in Bangladesh and northeast India during the annual monsoon rains with devastating consequences. The intensity and duration of these flood events may increase as the climate warms. We incorporated the CMIP6 data to project the basin-scale changes in mean annual precipitation using three Shared Socioeconomic Pathways (SSPs). We analyzed the tail behavior of projected precipitation to estimate the probability of future extreme precipitation in the basin. Moreover, we projected the future peak streamflow that will result due to global warming by 1, 1.5, 2, and 2.5 °C. Our results show an increase in the ensemble mean annual precipitation by 7.48%, 8.01%, and 19.37% under SSP126, SSP245, and SSP585, respectively, during the 2071–2100 period as compared to the 1981–2010 historic period. The basin will experience more intense precipitation compared to the historic period. Based on the SSP585 and 1.5-degree warming, the peak discharge at Bahadurabad, Bangladesh, will potentially increase by 39%, resulting in an increase in flood risk in Bangladesh. Collaboration among co-riparian countries in the basin will be essential for optimal utilization of water resources and for minimizing future damage caused by increased flooding.

---

M. Khalequzzaman (✉)

Department of Environmental, Geographical, and Geological Sciences, Commonwealth University of Pennsylvania, Lock Haven, PA, USA

e-mail: [mkhalequ@lockhaven.edu](mailto:mkhalequ@lockhaven.edu)

B. Masud

Ministry of Environment, Government of Saskatchewan, Regina, SK, Canada

Z. Islam

Department of Environment and Protected Areas, Government of Alberta, Edmonton, AB, Canada

S. Alam

Department of Geophysics, Stanford University, Stanford, CA, USA

M. Mostafa Ali

Department of Water Resources Engineering, Bangladesh University of Engineering and Technology, Dhaka, Bangladesh

**Keywords** Brahmaputra River · Extreme precipitation · Flood risk · CMIP6 · SSP · Climate change

## 1 Introduction

The Brahmaputra is the fourth-largest river in the world in terms of annual discharge (Jungclauss et al., 2007). Being a sub-basin of the Ganges-Brahmaputra-Meghna basin, the Brahmaputra River Basin (BRB) plays a key role in the socio-economic development of over 131 million people living in the basin countries: China, Bhutan, India, and Bangladesh (Barua et al., 2019, Alam et al., 2021). The river frequently floods large areas in Bangladesh and northeast India during the annual monsoon rains with devastating consequences (Rao et al., 2020). Over the last few decades, the basin experienced major floods in 1954, 1974, 1987, 1988, 1993, 2004, 2007, 2008, 2010, 2012, 2016, 2017, and 2019 (Khalequzzaman, 1994, 2020; Hossain et al., 2019). Damage to property and loss of lives due to flooding have increased in recent years. For example, the flood in 1998, which displaced ~30 million people and caused ~1000 deaths (DMB, 1998), inundated 69% of Bangladesh (Mirza, 2003). The number of major floods that covered more than 35% of the land area in Bangladesh has increased from 1 in 32 years during the 1954–1986 period to 5 in the following 20 years during 1987–2007 (Dasgupta et al., 2011). In the Brahmaputra River, the number of years when the total annual flow exceeded 120 billion cubic meters has increased from 10 during 25 years between 1955 and 1980 to 18 during the following 25 years between 1981 and 2005 (Ray et al., 2015). In order to minimize the damage caused by such devastating floods, it is imperative to understand the changing patterns of floods in space and time for the BRB. This study uses the most up-to-date data available in the public domain on projected global warming and precipitation changes due to climate change that have the potential to impact future floods in the BRB basin.

The intensity and duration of flood events can potentially change as the climate warms. Climate change-induced temperature warming will likely increase precipitation in the basin and may shift the snow melting time in the headwaters. (Alam et al., 2021). Extreme precipitation is also expected to increase in the future (Immerzeel, 2008). Since the basin is susceptible to flooding, any substantial changes in precipitation and streamflow, especially in the wet season, can lead to increased flood risk. An increase in flooding is the most important change risk in northern and eastern India, adjoining Nepal, and Bangladesh (Sharma & Sharma, 2008).

Numerous studies reported that climate change-induced warming will influence the magnitude and intensity of precipitation, river discharge, and flood extent in the BRB (Ahmed et al., 2021; Dutta et al., 2020). Scientific evidence shows that most glaciers are retreating in South Asia's Hindu Kush Himalayan region, including the ones that feed the Brahmaputra River discharge (National Research Council, 2012). Ding et al. (2006) found that the retreat of glaciers in this region is related to the increasing temperature. Yao et al. (2008) suggested that the glacial retreat increased

more than 5.5% of river runoff from the plateau. Such observations align with broader scientific evidence of glacial retreat in the eastern and central Himalayas, including those feeding the Brahmaputra (National Research Council, 2012). On the other hand, Ge et al. (2004) observed that precipitation in the upper BRB shows an overall increasing trend, with the most remarkable increasing trend in spring, no significant change in fall and winter, and a decreasing trend in summer. Haque et al. (2021) concluded that compared to the historic baseline years, the mean annual temperature, amount of precipitation, discharge, and sediment yield in the BRB will likely increase in the 2030s (30 years during 2011–2040), 2050s (30 years during 2041–2070), and 2080s (30 years during 2071–2100). The implication of such changes has been quantified in several studies (e.g., Haque et al., 2021; Ghosh & Dutta, 2011, 2012; Alam et al., 2016, 2021). Climate change is likely to increase the peak flow of the Brahmaputra River by about 28% (Ghosh & Dutta, 2011). Change in monthly flow for August is likely to rise by 4, 5, and 8% for the years 2020s, 2050s, and 2080s, respectively (Paul, 2014). Alam et al. (2016) investigated the sensitivity of long-term discharge (mean and maximum of 30-year period) of the BRB to climate change and found that changes in discharge are correlated with changes in precipitation and temperature. Climate models predict an intensified monsoon and higher flood risk with global warming (Alam et al., 2021; Ray et al., 2015). In summary, earlier studies agree that climate change will change river discharge volume and seasonality in the BRB, with a higher impact during the latter part of the century (2080s).

Since global warming and potential changes in precipitation patterns will play a key role in the hydrologic responses of the BRB, it is crucial to analyze the extreme precipitation in the basin based on the most updated Global Circulation Model (GCM) projections. In particular, the new Intergovernmental Panel on Climate Change (IPCC) scenarios using the Coupled Model Intercomparison Project phase 6 (CMIP6) data incorporated the effect of changes in socio-economic projection and political environment in addition to global warming (Meinshausen et al., 2020). The probability estimation of extreme precipitation depends on the tail behavior of the distribution that models extreme events. The tail behavior is described by the shape parameter of the extreme value distribution (Coles, 2001). A heavy tail (the shape parameter is greater than zero) implies a higher probability of more frequent extreme events (Serinaldi & Kilsby, 2014).

The future peak streamflow based on projected precipitation and global warming can be useful to assess flood risk. These will help in developing an improved prediction of monsoon flooding which is an essential part of BRB management and could reduce loss of life and minimize the economic damage in the basin. With that in mind, there are three distinct objectives of this study: (a) analyze the basin-scale changes in mean annual precipitation for the future periods, (b) analyze the tail behavior of projected precipitation in the basin under various IPCC scenarios, and c) project the future peak streamflow of the basin based on CMIP6 precipitation and projected climate change that will result in global warming by 1, 1.5, 2, and 2.5 degrees.

We chose to calculate the discharges and corresponding river stages in Brahmaputra River at Bahadurabad, Bangladesh using 1, 1.5, 2, and 2.5 °C of global warming for the following reasons. First, as per the IPCC Sixth Assessment Report, the likely range of total human-caused global surface temperature increase from 1850–1900 to 2010–2019 is 0.8 °C to 1.3 °C, with the best estimate of 1.07 °C (IPCC, 2021). Second, the Paris Agreement, a legally binding international treaty on climate change, was adopted by 196 countries at COP 21 held in Paris on December 12, 2015, to limit global warming to well below 2 °C, preferably to 1.5 °C, compared to preindustrial levels (UNFCCC, 2021). Third, the IPCC (2021) predicted that 1.5 °C global warming is likely to occur between 2030 and 2052. Fourth, although it is desirable to limit global warming well below 2 °C, the current actions and policies promised and practiced by most countries in the world through Nationally Determined Contributions (NDC) are not enough to reach the desired goal. The Climate Action Tracker (CAT), an independent scientific research group that analyzes the progress in tackling climate change, concluded that the average global temperature will likely increase by 2.7 °C by the end of the century (CAT, 2021). To be consistent with our calculation of discharges and river stages for each 0.5 °C increase, we have used 2.5 °C along with 1, 1.5, and 2 °C.

Several studies determined the future flow in the BRB at Bahadurabad using different GCMs and RCMs (Gain et al., 2011; Ghosh & Dutta, 2011; Pravettoni, 2015). Those studies used precipitation data for shorter periods. For example, Pravettoni (2015) used the precipitation data for 1983–2010, and Gain et al. (2011) used a discharge-weighted ensemble based on the inputs from the 12 General Circulation Models (GCMs) that are older than the CMIP6. The degree of knowledge about the impact of climate change on future precipitation events under various SSPs has improved since the last CMIP5 data (IPCC, 2021).

We calculated future extreme flows and corresponding river stages that will cause flooding in the BRB using the most up-to-date precipitation data generated by the CMIP6. Our study is the first of its kind to use the CMIP6 data to determine the changes in the future stream flows and river stages that are calculated using a field-based rating curve at Bahadurabad in the BRB.

## 2 Study Area

The BRB, the mainstream of which originates from the Tibetan Plateau, is the largest trans-Himalayan river basin, occupies 580,000 km<sup>2</sup> area, and encompasses parts of the territory, ecosystems, people, economies, and politics of China (50.5% of the basin area), Bhutan (7.8%), India (33.6%), and Bangladesh (8.1%) (see Fig. 16.1). The BRB is characterized by three distinct physiographic zones, namely, the Tibetan Plateau (elevation is greater than 3500 m) in the western and northern parts of the basin, the Himalayan belt (elevation ranges between 100 m and 3500 m), and the piedmont-floodplain zone (elevation is less than 100 m). These three zones occupy about 44.4, 28.6, and 27% of the basin area, respectively (Immerzeel, 2008).

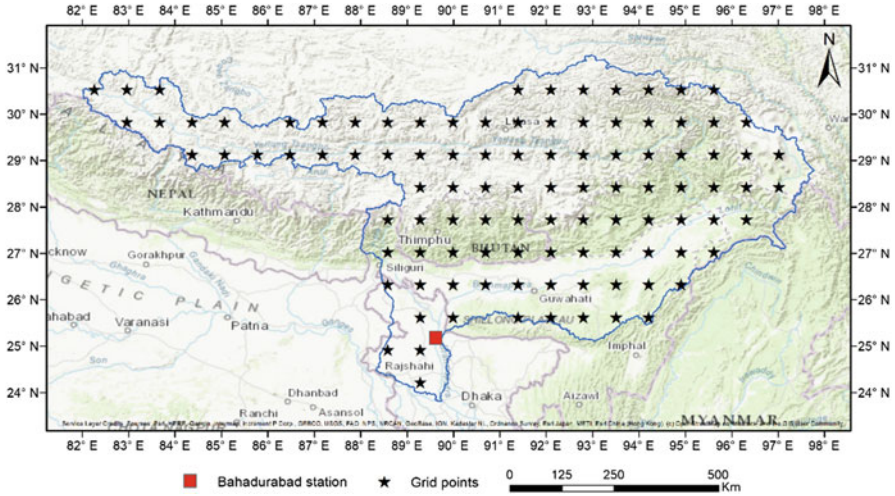


**Fig. 16.1** A map of the Brahmaputra River Basin. The star symbols show CMIP6 precipitation grid locations, and the red square indicates the Bahadurabad hydrometric station

The basin’s climate is monsoon (May–September) driven, and 60–70% of the annual precipitation is received during the monsoon period. However, the upstream flow is generated by groundwater and glacial/snowmelt (Barua et al., 2019). The Brahmaputra basin receives an annual average 1,100 mm of precipitation (Immerzeel, 2008). The precipitation is high in the southern (downstream) part and is low in the northern part (upstream) of the basin. Duration and the total amount of precipitation have changed between 1951–1980 and 1981–2007 in the basin. The major changes occurred in the southern part of the basin where both duration and amount of precipitation events have increased during recent years (Pravettoni, 2015). The annual average streamflow of BRB is ~21,250 m<sup>3</sup>/s at the Bahadurabad station (located near the downstream end, see Fig. 16.1). The streamflow during the dry season (December–May) and wet season (June–November) indicated strong seasonality having the flow 7,565 m<sup>3</sup>/s for the earlier and 30,840 m<sup>3</sup>/s for the later season (Alam et al., 2021).

### 3 Data and Methods

We acquired daily precipitation outputs from nine GCMs used in CMIP6 historical and future experiments. These nine GCMs were chosen based on data availability for the study area. In addition, these nine GCMs reproduced the historic precipitation data for the BRB that closely matched the recorded historic precipitation values of 1,100 mm/year (Pravettoni, 2015). Table 16.1 shows a description of the GCMs selected for this study. The historical experiments include data from 1950 to 2014,

**Table 16.1** List of GCMs selected for the study

GCM	Host institute	Resolution (km)	Reference
ACCESS-CM2	CSIRO-ARCCSS (Australia)	250	Bi et al. (2020)
ACCESS-ESM1	CSIRO (Australia)	250	Ziehn et al. (2020)
CAMS-CSM1-0	Chinese Academy of Meteorological Sciences	100	Rong et al. (2019)
EC-Earth3-Veg	EC-Earth Consortium	100	Döscher et al. (2021)
EC-Earth3-Veg-LR	EC-Earth Consortium	250	Döscher et al. (2021)
KACE-1-0-G	Korea Meteorological Administration	250	Byun et al. (2019)
MIROC6	JAMSTEC, NIES, AORI, U. of Tokyo (Japan)	250	Tatebe et al. (2019) and Hajima et al. (2020)
MPI-ESM1-2-HR	MPI (Germany)	100	Jungclaus et al. (2007)
MRI-ESM2-0	MRI (Japan)	100	Yukimoto et al. (2019a, b)

and the future experiments include data from 2015 to 2100. We used three Shared Socio-economic Pathways (SSPs), namely, SSP126, SSP245, and SSP585 (Bottinger & Kasang, 2021; Riahi et al., 2021). As included in the sixth IPCC report (IPCC AR6), compared to the previously used Representative Concentration Pathways (RCPs), the new SSPs have been improved to a great extent. The SSPs represent various socio-economic developments and atmospheric greenhouse gas concentration pathways (Meinshausen et al., 2020). These are (1) SSP126, a sustainable future pathway, low mitigation and adaptation challenge; (2) SSP245, an intermediate challenge for mitigation and adaptation, and (3) SSP585, fossil-fuel development, greenhouse gas emission through the twenty-first century, and mitigation challenges dominate. We have used these three scenarios to highlight the differences in three distinct pathways that range from the best to worst possible outcomes for the planet in the future.

We used a rating curve to estimate corresponding river stages for calculating the future streamflow of the Brahmaputra River at Bahadurabad station (see Fig. 16.2). The rating curve is developed by Bangladesh Water Development Board and is currently operational to forecast flood stages in Bangladesh (Sarder Udoy Raihan, Sub-divisional Engineer, Flood Forecasting and Warning Centre, Bangladesh Water Development Board; personal communication).

The methodology used in this study is as follows:

**Step 1:** The daily precipitation data for the historical and climate change period of the 2080s from nine GCMs and three SSPs were downloaded from the CMIP6 database. The resolution of the GCMs ranges from 100 to 250 km. Therefore, GCMs were regridded at 100 km grid spacing using spline interpolation

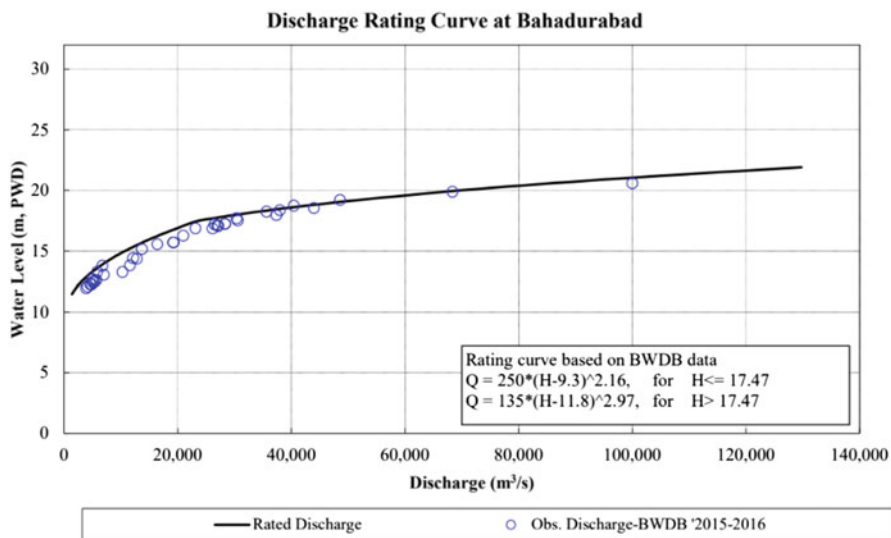


**Fig. 16.2** Rating curve of the Brahmaputra River at Bahadurabad station (Sarder Udoj Raihan, Sub-divisional Engineer, Flood Forecasting and Warning Centre, Bangladesh Water Development Board; personal communication)

technique before the multi-model analysis was carried out on the 103 grid locations as shown in Fig. 16.1.

- Step 2: The peak over threshold (POT) approach was used to sample the extreme precipitation events. The 90th percentile (P90) was considered to define the threshold value above which peaks are sampled. We employed the likelihood ratio test to choose the optimum threshold and used the extremal index to ensure the independence of exceedances (Masud et al., 2021). The generalized Pareto distribution (GPD) was fitted for these extreme events to analyze the tail behavior.
- Step 3: The behavior of precipitation extremes is described by modeling the tails of the GPD distribution. The tail index of the fitted GPD distribution was calculated and compared between the climate normal period (30 years from 1981 to 2010) and the climate change period of 2080s. A heavy-tailed distribution generates more frequent and severe extremes compared to a light-tailed distribution.
- Step 4: The basin-scale mean precipitation changes ( $\Delta P\%$ ) for the 2080s were calculated with reference to the climate normal period. Then, four static temperature changes ( $\Delta T$ ) for the 2080s with respect to a climate normal period were set (1, 1.5, 2, and 2.5 °C) to consider the target global warming.
- Step 5: The annual peak discharge ( $Q_{Max}$  (m<sup>3</sup>/s)) of the Brahmaputra River at Bahadurabad for the 2080s was estimated using the established multivariable regression equation developed by Alam et al. (2021):



$$Q_{\text{Max}} = 47,110 + 2655 * \Delta T + 731 * \Delta P$$

where  $\Delta T$  is the changes in mean temperature ( $^{\circ}\text{C}$ ) and  $\Delta P$  is the changes in mean precipitation (%) from the climate normal period at the basin scale. We have used the above equation to calculate the maximum flow, as opposed to the minimum and mean flow, because we are interested in extreme precipitation events that will result in flooding in the future.

Step 6: Finally, the corresponding river stages for calculated discharge values from Step 5 were determined using a rating curve developed by Bangladesh Water Development Board for the Brahmaputra River at Bahadurabad. The river stage values that exceed the flooding stage of the river were analyzed to assess the future flood risk for the Brahmaputra River at the Bahadurabad location in Bangladesh.

## 4 Results and Discussion

### 4.1 Changes in Basin-Scale Precipitation

Figure 16.3 shows the simulated basin-scale mean annual precipitation for the historical (1950–2014) and future (2015–2100) periods based on nine GCMs and three SSPs. The blue-shaded band zone shows the range of historical precipitation, and the orange-shaded zone shows the range of future precipitation based on these scenarios. The thin lines indicate simulated precipitation for various GCMs and SSPs, whereas the bold lines indicate the ensemble mean. A careful observation of the plots reveals that there exists a great number of uncertainties in simulated

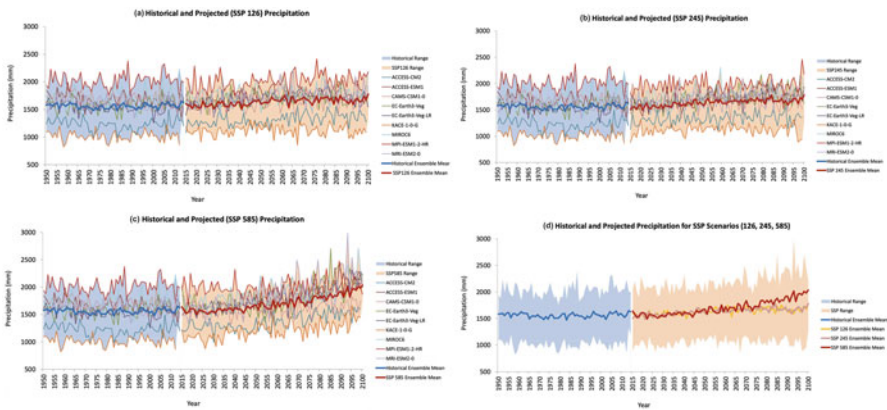


**Fig. 16.3** Historical (1950–2014) and projected (2015–2100) basin-scale mean annual precipitation in the Brahmaputra River Basin based on nine GCMs and three SSPs

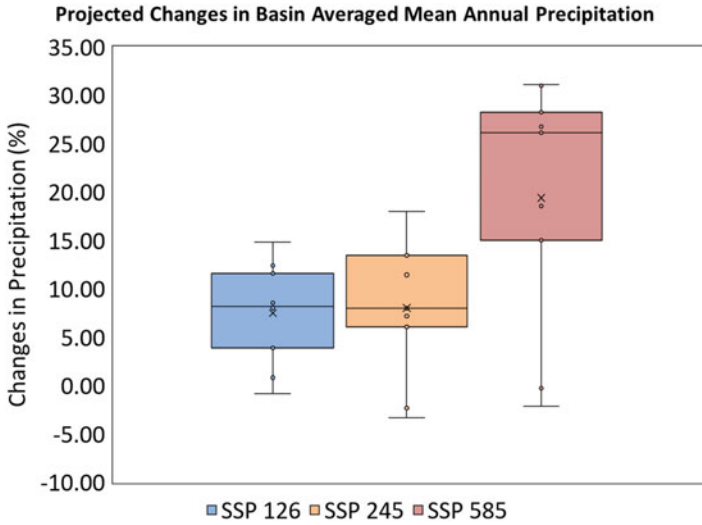


**Fig. 16.4** Boxplots of basin-scale mean annual precipitation changes for the 2080s compared to the climate normal period of 1981–2010 based on nine GCMs and three SSPs. The cross marks demonstrate the ensemble mean of the projected changes in precipitation

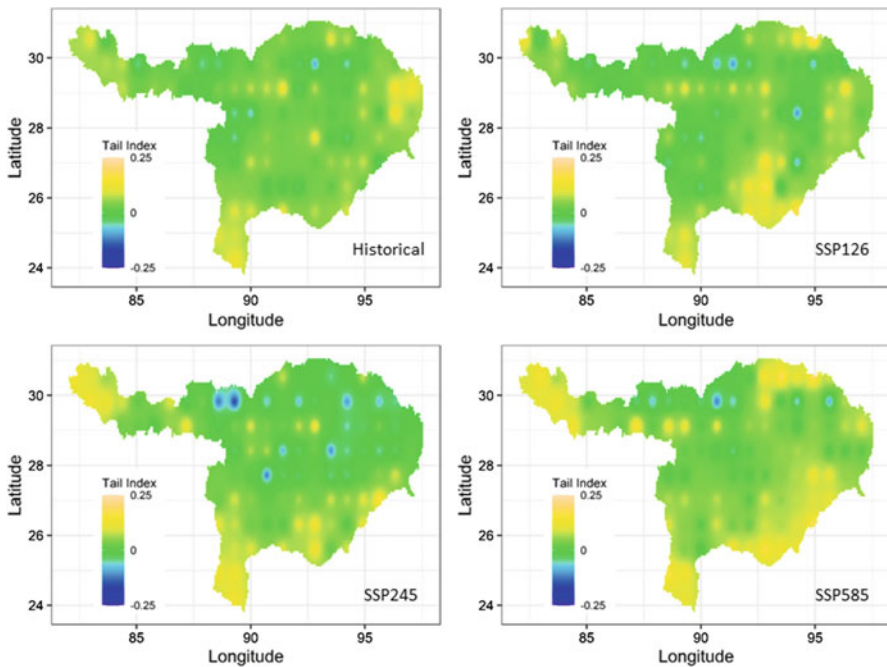
precipitation in historical and future scenarios. The SSP126 and SSP245 demonstrate a mild increase in basin-scale mean annual precipitation, whereas the SSP585 results in a higher increase in mean annual precipitation for future periods.

Figure 16.4 shows boxplots of basin-scale precipitation changes for the 2080s compared to the climate normal period based on the nine GCMs and the three SSPs. As expected, the interquartile ranges of projected precipitation, which is a measure of uncertainties associated with the projections, grow as we move to the distant future. The cross marks demonstrate the ensemble mean of the projected changes in precipitation. The percentage changes in basin-scale mean annual precipitation for the 2080s compared to the climate normal period for the SSP126 range from 0.85% to 14.84% with an ensemble mean of 7.48% (Fig. 16.4). The GCM ACCESS-CM2 projected the highest increase (14.84%), and the CAMS-CSM1-0 projected a slight decrease (−0.85%) in mean annual precipitation (Fig. 16.3a). The percentage changes in basin-scale mean annual precipitation for the 2080s compared to the climate normal period for the SSP245 range from −3.31% to 18.01% with an ensemble mean of 8.01% (Fig. 16.4). The EC-Earth3-Veg-LR projected the highest increase (18.01%), and the CAMS-CSM1-0 projected a significant decrease (−3.31%) in mean annual precipitation (Fig. 16.3b). The percentage changes in basin-scale mean annual precipitation for the 2080s compared to the climate normal period for the SSP 585 range from −2.13% to 31.12% with an ensemble mean of 19.37% (Fig. 16.4). The MRI-ESM2-0 projected the highest increase (31.12%), and the CAMS-CSM1-0 projected a considerable decrease (−2.13%) in mean annual precipitation (Fig. 16.3c). These results are generally in agreement with previous

studies (Almazroui et al., 2020; Caesar et al., 2015). As shown in Fig. 16.3d, all SSPs (SSP126, SSP245, SSP585) project a moderate increase in basin-scale precipitation in the early to mid-twenty-first century (2015–2050). The projected changes in precipitation in the near decades are not very sensitive to the emission pathways as the radiative forcing is very similar during this time. From 2050 onwards, SSP585 projects a significant increase in mean annual precipitation, and SSP126 and SSP245 show a moderate increase. Ensemble mean of the mean annual precipitation in 2080s is almost similar for SSP126 and SSP245, indicating that higher precipitation change is only expected in the worst scenario (SSP585) that will result from high warming and low mitigation measures in the future.

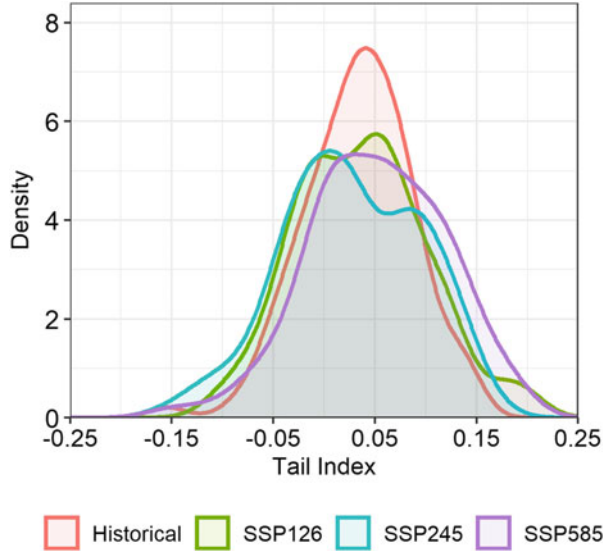
## 4.2 Tail Behavior of Extreme Precipitation Events

Figure 16.5 shows the tail index (shape parameter of GPD distribution) for historical and three future climate change scenarios (SSPs) based on the ensemble mean of nine GCMs. The tail indices determined for precipitation extremes show that by the 2080s, the BRB will experience more intense precipitation events under various SSPs as compared to the historic period. The extreme precipitation will increase



**Fig. 16.5** Tail index (shape parameter of GPD distribution) for historical and three future climate change scenarios (SSPs)

**Fig. 16.6** Kernel density plot (a non-parametric probability density function plot) of the tail index



under all SSPs. The reason behind the increase in extreme precipitation is attributed to enhance tropical convective precipitation in this region (Ge et al., 2021). Such an increase will likely be observed in the upstream part of the basin in the Tibetan Plateau and the downstream part of the basin in Bangladesh.

Figure 16.6 shows the kernel density plot (a nonparametric probability density function plot) of the tail index. A density plot is a representation of the unknown distribution of a numeric variable and a smoothed version of the commonly used histogram. The tail index clearly shows that extreme precipitation will increase in the future (positive values of tail index and right side of the density curves), and floods are likely to occur due to such extreme heavy precipitation (Chen & Zhai, 2013) although changes in antecedent soil moisture, storm extent, and snowmelt will pose a grand challenge for such a cause-effect relationship (Sharma et al., 2018).

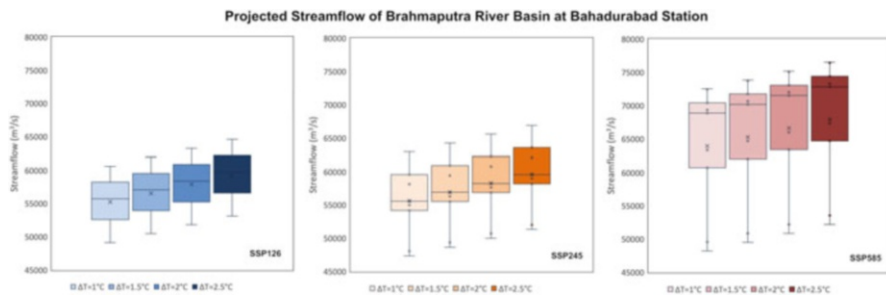
### 4.3 Future Peak Streamflow and River Stage

Table 16.2 shows the estimated peak discharge of the Brahmaputra River at Bahadurabad based on the projected changes in precipitation from nine GCMs and three SSPs and four target temperature changes (1, 1.5, 2, and 2.5 °C) in the 2080s. Figure 16.7 shows a Boxplot representation of these projected streamflows. The corresponding river stages are shown in Fig. 16.8. The cross marks in Figs. 16.7 and 16.8 demonstrate the ensemble mean of the projected streamflow and stages, respectively.

The baseline (climate normal period) maximum streamflow of the Brahmaputra River at Bahadurabad is 47,110 m<sup>3</sup>/s (Alam et al., 2021). Note: this peak streamflow

**Table 16.2** Projected future (2080s) peak discharges of the Brahmaputra River at Bahadurabad based on precipitation changes projected by nine GCMs and three SSPs and four target temperature changes

GCMs	$\Delta P\%$	SSP126 ( $\Delta T$ )				SSP245 ( $\Delta T$ )				SSP585 ( $\Delta T$ )			
		1 °C	1.5 °C	2 °C	2.5 °C	1 °C	1.5 °C	2 °C	2.5 °C	1 °C	1.5 °C	2 °C	2.5 °C
ACCESS-CM2	14.84	60613	61941	63268	64596	59597	60924	62252	63579	68844	70172	71499	72827
ACCESS-ESM1	8.17	55737	57065	58392	59720	54202	55530	56857	58185	63332	64660	65987	67315
CAMS-CSM1-0	-0.85	49144	50471	51799	53126	47345	48673	50000	51328	48208	49535	50863	52190
EC-Earth3-Veg	8.01	55620	56948	58275	59603	59772	61100	62427	63755	72411	73739	75066	76394
EC-Earth3-Veg-LR	12.39	58822	60150	61477	62805	62930	64258	65585	66913	70416	71743	73071	74398
KACE-1-0-G	8.53	56000	57328	58655	59983	55584	56911	58239	59566	69327	70654	71982	73309
MIROC6	3.88	52601	53929	55256	56584	54992	56319	57647	58974	60715	62043	63370	64698
MPI-ESM1-2-HR	0.8	50350	51677	53005	54332	48062	49389	50717	52044	49560	50888	52215	53543
MRI-ESM2-0	11.56	58215	59543	60870	62198	58113	59441	60768	62096	72514	73841	75169	76496
Ensemble mean	7.48	55234	56561	57889	59216	55622	56949	58277	59604	63925	65253	66580	67908
Increase from climate normal (%)		17	20	23	26	18	21	24	27	36	39	41	44



**Fig. 16.7** Projected future (2080s) peak discharge of the Brahmaputra River at Bahadurabad based on precipitation changes projected by nine GCMs and three SSPs and four target temperature changes. The cross marks demonstrate the ensemble mean

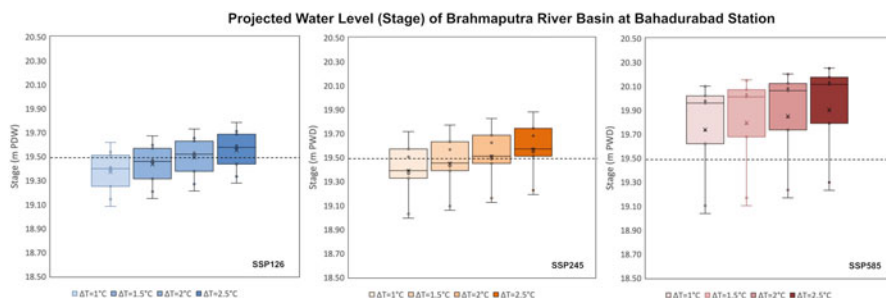


**Fig. 16.8** Projected future (2080s) peak stage of the Brahmaputra River at Bahadurabad based on precipitation changes projected by nine GCMs and three SSPs and four target temperature changes. The cross marks demonstrate the ensemble mean. The dotted line indicates the current danger level (flood stage) for the Brahmaputra River at Bahadurabad, Bangladesh

does not represent the instantaneous peak flow over the climate normal period rather represents maximum discharge averaged over the climate normal period. The corresponding river stage at Bahadurabad, as derived from the rating curve, is 18.98 m Public Works Datum (PWD).

It was found that for all SSPs, the projected maximum discharge, and corresponding river stage increase linearly with the target warming scenarios. This aligns with the results from Alam et al. (2016, 2021). For SSP126, an increase of 1-, 1.5-, 2- and 2.5-degree in basin-scale temperature in the 2080s will potentially increase the maximum streamflow at the Bahadurabad location by 17%, 20%, 23%, and 26%, respectively (ensemble mean). For SSP245, an increase of 1, 1.5, 2, and 2.5 degree in basin-scale temperature in the 2080s will potentially increase the maximum streamflow at the Bahadurabad location by 18%, 21%, 24%, and 27%, respectively. For SSP585, an increase of 1, 1.5, 2, and 2.5 degree in basin-scale temperature in the 2080s will potentially increase the maximum streamflow at the Bahadurabad location by 36%, 39%, 41%, and 44%, respectively. We found that the projected maximum discharge in the 2080s for SSPs is relatively higher than those

estimated using CMIP5 scenarios by Alam et al. (2021). Alam et al. (2021) showed maximum discharge will increase by 16% (median) for ensemble scenarios. However, we find maximum discharge increase is even higher for a relatively optimistic scenario (SSP126) and a 1-degree increase in temperature.

Because of the nonlinear relationship between streamflow and stage, the percentage changes in river stage compared to the baseline stage of 18.98 m PWD range between 2.06% and 4.87% for various target temperature and SSPs. For SSP126, a 1-, 1.5-, 2-, and 2.5-degree increase in basin-scale temperature in the 2080s will potentially increase the maximum river stage at the Bahadurabad location by 2.06%, 2.39%, 2.70%, and 3.01%, respectively (ensemble mean). For SSP245, a 1-, 1.5-, 2-, and 2.5-degree increase in basin-scale temperature in the 2080s will potentially increase the maximum river stage at the Bahadurabad location by 2.14%, 2.46%, 2.78%, and 3.09%, respectively. For SSP585, a 1-, 1.5-, 2-, and 2.5-degree increase in basin-scale temperature in the 2080s will potentially increase the maximum river stage at the Bahadurabad location by 4%, 4.30%, 4.59%, and 4.87%, respectively. According to the Flood Forecasting and Warning Centre, Bangladesh Water Development Board (<http://www.ffwc.gov.bd/>), the Flood Danger Level (FDL) at Bahadurabad is 19.50 m PWD, and the recorded Highest Water Level (HWL) at Bahadurabad is 21.16 m PWD. Our analysis shows that for the SSP126, the projected river stage (ensemble mean) exceeds the FDL for a 2.5-degree increase in basin-scale temperature in the 2080s. For SSP245, the projected river stage exceeds the FDL for a 2-degree and 2.5-degree increase in basin-scale temperature in the 2080s. For the SSP585, the projected river stage exceeds the FDL for all warming scenarios. However, it should be noted that this projected river stage only demonstrates the mean value of the maximum river stage for the 2080s, not the instantaneous river stage.

The results of our study have several practical implications. First, the changes in the amount of extreme precipitation in the future under all three scenarios will have direct implications in terms of the availability of water resources in the BRB. If managed properly at the basin-scale through integrated water resources management involving all co-riparian countries, such an increase in water resources can be utilized to augment flow during lean season and can be harnessed for multipurpose uses. Second, such an increase in water availability will result in untimely flooding that will have to be managed to reduce the damage to property and ecosystems. Third, increased flooding propensity will cause damage to crops, life, and livelihood in the BRB. The existing flood control and mitigation efforts will have to be retrofitted to tackle additional flood depth, duration, and frequency. Fifth, collaboration among co-riparian countries in the BRB will be essential for optimal utilization of water resources and for minimizing future damage caused by increased severe flooding in the BRB.

## 5 Conclusions

1. The ensemble mean of the percentage changes in basin-scale mean annual precipitation for the 2080s compared to the climate normal period of 1981–2010 for the SSP126, SSP245, and SSP585 are 7.48%, 8.01%, and 19.37%. All future scenarios project a moderate increase in basin-scale precipitation in the early to mid-twenty-first century (2015–2050). From 2050 onwards, SSP585 projects a significant increase in mean annual precipitation, and SSP126 and SSP245 show a moderate increase. The uncertainties associated with the projections grow as we move to the distant future.
2. The tail index determined for precipitation extremes shows that by the 2080s the BRB will experience more intense precipitation under various SSPs as compared to the historic period. The extreme precipitation will increase under all SSPs.
3. The ensemble mean of percentage changes in peak discharge at Bahadurabad is higher for higher warming scenarios. Based on SSP585 and 1.5-degree warming, the peak discharge will potentially increase by 39% which will increase the flood risk in Bangladesh.

Considering the complex topography of the study region, further downscaling is recommended before using them to quantify the climate change impact assessments on natural and built systems. Fine-scale processes are known to influence the regional distribution of precipitation changes. Therefore, the use of high-resolution climate scenarios as generated by Regional Climate Models is also recommended.

**Acknowledgments** The authors would like to thank Sarder Udo Raihan, Sub-divisional Engineer, Flood Forecasting and Warning Centre, and Bangladesh Water Development Board for providing data and information. Dr. Loretta Dickson of Commonwealth University of Pennsylvania reviewed an earlier version of the manuscript and provided valuable suggestions that helped improve the quality of this paper.

**Disclaimer** The author's role in this research is as a freelance researcher. This research study is not part of any Alberta Environment and Protected Areas project.

## References

- Ahmed, I. A., Shahfahad, Dutta, D. K., et al. (2021). Implications of changes in temperature and precipitation on the discharge of Brahmaputra River in the urban watershed of Guwahati, India. *Environmental Monitoring and Assessment*, 193, 518. <https://doi.org/10.1007/s10661-021-09284-8>
- Alam, S., Ali, M. M., & Islam, Z. (2016). Future streamflow of Brahmaputra river basin under synthetic climate change scenarios. *Journal of Hydrologic Engineering*. [https://doi.org/10.1061/\(ASCE\)HE.1943-5584.0001435](https://doi.org/10.1061/(ASCE)HE.1943-5584.0001435)
- Alam, S., Ali, M. M., Rahaman, A. Z., & Islam, Z. (2021). Multi-model ensemble projection of mean and extreme streamflow of Brahmaputra river basin under the impact of climate change. *Journal of Water and Climate Change*. <https://doi.org/10.2166/wcc.2021.286>



- Almazroui, M., Saeed, S., Saeed, F., Islam, M. N., & Ismail, M. (2020). Projections of precipitation and temperature over the South Asian Countries in CMIP6. *Earth Systems and Environment*, 4, 297–320.
- Barua, A., Deka, A., Gulati, V., Vij, S., Liao, X., & Qaddumi, H. M. (2019). Re-interpreting cooperation in transboundary waters: Bringing experience from the Brahmaputra basin. *Water*, 11(12), 22. <https://doi.org/10.3390/w11122589>
- BBC News. (2008, September 4). *Assam towns threatened by floods*. Accessed 8 Sept 2008.
- Bi, D., Dix, M., Marsland, S., O'Farrell, S., Sullivan, A., Bodman, R., Law, R., Harman, I., Sribnovsky, J., Rashid, H. A., Dobrohotoff, P., Mackallah, C., Yan, H., Hirst, A., Savita, A., Dias, F. B., Woodhouse, M., Fiedler, R., & Heerdegen, A. (2020). Configuration and spin-up of ACCESS-CM2, the new generation Australian Community Climate and Earth System Simulator Coupled Model. *Journal of Southern Hemisphere Earth Systems Science*, 70, 225–251. <https://doi.org/10.1071/ES19040>
- Bottinger, M., & Kasang, D. (2021). *The SSP scenarios*, DKRZ, Deutsches Klimarechenzentrum. <https://www.dkrz.de/en/communication/climate-simulations/cmip6-en/the-ssp-scenarios>. Accessed 16 Dec 2021.
- Byun, Y.-H., Lim, Y.-J., Sung, H. M., Kim, J., Sun, M., & Kim, B.-H. (2019). *NIMS-KMA KACE1.0-G model output prepared for CMIP6 CMIP amip*. Earth System Grid Federation. <https://doi.org/10.22033/ESGF/CMIP6.8350>
- Caesar, J., Janes, T., Lindsay, A., & Bhaskaran, B. (2015). *Temperature and precipitation projections over Bangladesh and the upstream Ganges*. Environ Sci Process Impacts. <https://doi.org/10.1039/c4em00650j>
- CAT. (2021). *State of Climate Action 2021*. <https://climateactiontracker.org/>. Accessed 29 Dec 2021.
- Chen, Y., & Zhai, P. (2013). Persistent extreme precipitation events in China during 1951–2010. *Climate Research*, 57, 143–155.
- Coles, S. (2001). *An introduction to statistical modeling of extreme values* (Springer Series in Statistics). Springer. ISBN:978-1-84996-874-4.
- Crueger, T., Fast, I., Fiedler, S., Hagemann, S., Hohenegger, C., Jahns, T., Kloster, S., Kinne, S., Lasslop, G., Kornblueh, L., Marotzke, J., Matei, D., Meraner, K., Mikolajewicz, U., Modali, K., Müller, W., Nabel, J., Notz, D., Peters-von Gehlen, K., Pincus, R., Pohlmann, H., Pongratz, J., Rast, S., Schmidt, H., Schnur, R., Schulzweida, U., Six, K., Stevens, B., Voigt, A., & Roeckner, E. (2019). MPI-M MPI-ESM1.2-HR model output prepared for CMIP6 CMIP historical, Version 20190710. *Earth System Grid Federation [data set]*. <https://doi.org/10.22033/ESGF/CMIP6.6594>
- Dasgupta, S., Huq, M., Khan, Z. H., Sohel Masud, M., Ahmed, M. M., Mukherjee, N., & Pandey, K. (2011). Climate proofing infrastructure in Bangladesh: The incremental cost of limiting future flood damage. *The Journal of Environment & Development*, 20, 167–190.
- Ding, Y., Liu, S., Li, J., & Shangguan, D. (2006). The retreat of glaciers in response to recent climate warming in Western China. *Annals of Glaciology*, 43(43), 97–105.
- DMB. (1998). *Report on Bangladesh flood 1998 (chronology, damages and response)* (p. 73). Disaster Management Bureau.
- Döscher, R., Acosta, M., Alessandri, A., Anthoni, P., Arneth, A., Arsouze, T., Bergmann, T., Bernadello, R., Bousetta, S., Caron, L.-P., Carver, G., Castrillo, M., Catalano, F., Cvijanovic, I., Davini, P., Dekker, E., Doblas-Reyes, F. J., Docquier, D., Echevarria, P., Fladrich, U., Fuentes-Franco, R., Gröger, M., Hardenberg, J., Hieronymus, J., Karami, M. P., Keskinen, J.-P., Koenigk, T., Makkonen, R., Massonnet, F., Ménégoz, M., Miller, P. A., Moreno-Chamarro, E., Nieradzic, L., van Noije, T., Nolan, P., O'Donnell, D., Ollinaho, P., van den Oord, G., Ortega, P., Prims, O. T., Ramos, A., Reerink, T., Rousset, C., Ruprich-Robert, Y., Le Sager, P., Schmith, T., Schrödner, R., Serva, F., Sicardi, V., Sloth Madsen, M., Smith, B., Tian, T., Tourigny, E., Uotila, P., Vancoppenolle, M., Wang, S., Wårlind, D., Willén, U., Wyser, K., Yang, S., Yepes-Arbós, X., & Zhang, Q. (2021). The EC-Earth3 earth system model for the climate model intercomparison project 6. *Geoscientific Model Development Discussion*. <https://doi.org/10.5194/gmd-2020-446>

- Dutta, P., Hinge, G., Marak, J. D. K., & Sarma, A. K. (2020). Future climate and its impact on streamflow: A case study of the Brahmaputra River basin. *Modeling Earth Systems and Environment*, 1, 3. <https://doi.org/10.1007/s40808-020-01022-2>
- Gain, A. K., Imerzzel, W. W., Sperna-Weiland, F. C., & Bierkens, M. F. P. (2011). Impacts of climate change on the stream flow of lower Brahmaputra: trends in high and low flow based on discharge-weighted ensemble modelling. *Hydrology and Earth System Sciences Discussions*, 8(1), 365–390.
- Ge, Z. X., Wang, H. R., Cao, L. Q., & Wang, X. L. (2004). The change characteristics and correlativity of precipitation and air temperature in Tibet region. *Sci. Meteorol. Sin.*, 24(4), 468–473.
- Ge, F., Zhu, S., Luo, H., Zhi, X., & Wang, H. (2021). Future changes in precipitation extremes over Southeast Asia: insights from CMIP6 multi-model ensemble. *Environmental Research Letters*, 16(2).
- Ghosh, S., & Dutta, S. (2011). *Impact of climate and land use changes on vulnerability of the Brahmaputra Basin* (p. 364). Geospatial World Forum.
- Ghosh, S., & Dutta, S. (2012). Impact of climate change on flood characteristics of Brahmaputra basin using a macro-scale distributed hydrological model. *Journal of Earth System Science*, 121(3), 337–357.
- Hajima, T., Watanabe, M., Yamamoto, A., Tatebe, H., Noguchi, M. A., Abe, M., Ohgaito, R., Ito, A., Yamazaki, D., Okajima, H., Ito, A., Takata, K., Ogochi, K., Watanabe, S., & Kawamiya, M. (2020). Development of the MIROC-ES2L Earth system model and the evaluation of biogeochemical processes and feedbacks. *Geoscientific Model Development*, 13, 2197–2244. <https://doi.org/10.5194/gmd-13-2197-2020>
- Haque, S., Ali, M. M., Islam, A. K. M. S., & Khan, J. U. (2021). Changes in sediment load and flow of poorly gauged Brahmaputra basin under an extreme climate scenario. *Journal of Water and Climate Change*, 12(3), 937–954.
- Hossain, S., Cloke, H. L., Ficchi, A., Turner, A. G., & Stephens, E. M. (2019). Hydrometeorological drivers of the 2017 flood in the Brahmaputra basin in Bangladesh. *Hydrology & Earth Systems Science Discussion*. <https://doi.org/10.5194/hess-2019-286>
- Immerzeel, W. (2008). Historical trends and future predictions of climate variability in the Brahmaputra basin. *International Journal of Climatology: A Journal of the Royal Meteorological Society*, 28(2), 243–254.
- International Federation of Red Cross and Red Crescent Societies. (2008, September 8). *India floods information bulletin number six*. Published on ReliefWeb. Accessed 8 Sept 2008.
- IPCC. (2021). Summary for policymakers. In V. Masson-Delmotte, P. Zhai, A. Pirani, S. L. Connors, C. Péan, S. Berger, N. Caud, Y. Chen, L. Goldfarb, M. I. Gomis, M. Huang, K. Leitzell, E. Lonnoy, J. B. R. Matthews, T. K. Maycock, T. Waterfield, O. Yelekçi, R. Yu, & B. Zhou (Eds.), *Climate Change 2021: The physical science basis. Contribution of Working Group I to the sixth assessment report of the Intergovernmental Panel on Climate Change*.
- Jungclaus, J., Bittner, M., Wieners, K.-H., Wachsmann, F., Schupfner, M., Legutke, S., Giorgetta, M., Reick, C., Gayler, V., Haak, H., de Vrese, P., Raddatz, T., Esch, M., Mauritsen, T., von Storch, J.-S., Behrens, J., Brovkin, V., Claussen, M., Kamal-Heickman, S., Derry, L. A., Stöcker, J. R., & Duncan, C. C. (2007). A simple predictive tool for lower Brahmaputra River Basin Monsoon Flooding. *Earth Interactions*, 11(21).
- Khalequzzaman, M. (1994). Recent floods in Bangladesh: Possible causes and solutions. *Natural Hazards*, 9, 65–80.
- Khalequzzaman, M. (2020). Underlying causes of the early flood in haor region. *Journal of Bangladesh Studies*, 20(2), 41–51.
- Masud, B., Cui, Q., Ammar, M. E., Bonsal, B. R., Islam, Z., & Faramarzi, M. (2021). Means and extremes: evaluation of a CMIP6 multi-model ensemble in reproducing historical climate characteristics across Alberta, Canada. *Water*, 13, 737. <https://doi.org/10.3390/w13050737>
- Meinshausen, M., Nicholls, Z. R., Lewis, J., Gidden, M. J., Vogel, E., Freund, M., Beyerle, U., Gessner, C., Nauels, A., Bauer, N., & Canadell, J. G. (2020). The shared socio-economic

- pathway (SSP) greenhouse gas concentrations and their extensions to 2500. *Geoscientific Model Development*, 13(8), 3571–3605.
- Mirza, M. M. Q. (2003). Three recent extreme floods in Bangladesh: A hydro-meteorological analysis. *Natural Hazards*, 28, 35–64.
- National Research Council. (2012). *Himalayan glaciers: Climate change, water resources, and water security*.
- Paul, S. (2014). Assessment of change in future flow of Brahmaputra basin applying SWAT model using multi-member ensemble climate data. MSc. Thesis, Bangladesh University of Engineering and Technology, Dhaka, Bangladesh. <http://lib.buet.ac.bd:8080/xmlui/handle/123456789/642>
- Pravettoni, R. (2015). *The Himalayan climate and water atlas*. GRID Arendal (a UNEP partner). <https://www.grida.no/resources/6686>. Accessed 16 Dec 2021.
- Rao, M. P., Cook, E. R., Cook, B. I., et al. (2020). Seven centuries of reconstructed Brahmaputra River discharge demonstrate underestimated high discharge and flood hazard frequency. *Nature Communications*, 11, 6017. <https://doi.org/10.1038/s41467-020-19795-6>
- Ray, P. A., Yang, Y. E., Wi, S., Khalil, A., Chatikavanij, V., & Brown, C. (2015). Room for improvement: Hydro-climatic challenges to poverty-reducing development of the Brahmaputra River basin. *Environmental Science and Policy, Elsevier*, 18. <https://doi.org/10.1016/j.envsci.2015.06.015>
- Riah, K., van Vuuren, D. P., Kriegler, E., O'Neill, B., & Rogelj, J. (2021). *International Committee on New Integrated Climate Change Assessment Scenarios (ICONICS)*.
- Rong, X. Y., Li, J., & Chen, H. M. (2019). Introduction of CAMS-CSM model and its participation in CMIP6. *Climate Change Research*, 6. <https://doi.org/10.12006/j.issn.1673-1719.2019.186>
- Serinaldi, F., & Kilsby, C. G. (2014). Rainfall extremes: Toward reconciliation after the battle of distributions. *Water Resources Research*, 50, 336–352.
- Sharma, B. R., & Sharma, D. (2008). *Impact of climate change on water resources and glacier melt and potential adaptations for Indian agriculture*. Keynote address at 33rd Indian Agricultural Universities Association Vice Chancellors' annual convention on "Climate Change and Its Effect on Agriculture", December 4–5, 2008, Anand, Gujrat, India.
- Sharma, A., Wasko, C., & Lettenmaier, D. P. (2018). If precipitation extremes are increasing, why aren't floods? *Water Resources Research*, 54(11), 8545–8551.
- Tatebe, H., Ogura, T., Nitta, T., Komuro, Y., Ogochi, K., Takemura, T., Sudo, K., Sekiguchi, M., Abe, M., Saito, F., Chikira, M., Watanabe, S., Mori, M., Hirota, N., Kawatani, Y., Mochizuki, T., Yoshimura, K., Takata, K., O'ishi, R., Yamazaki, D., Suzuki, T., Kurogi, M., Kataoka, T., Watanabe, M., & Kimoto, M. (2019). Description and basic evaluation of simulated mean state, internal variability, and climate sensitivity in MIROC6. *Geoscientific Model Development*, 12, 2727–2765. <https://doi.org/10.5194/gmd-12-2727-2019>
- UNFCCC. (2021). *The Paris Agreement*. <https://unfccc.int/process-and-meetings/the-paris-agreement/the-paris-agreement>. Accessed 29 Dec 2021.
- Yao, T. D., Pu, J., Lu, A., Wang, Y., & Wu, W. (2008). Glaciers significantly retreating in the Qinghai-Tibetan Plateau. *Scientist*, 2008(03), 72.
- Yukimoto, S., Koshiro, T., Kawai, H., Oshima, N., Yoshida, K., Urakawa, S., Tsujino, H., Deushi, M., Tanaka, T., Hosaka, M., Yoshimura, H., Shindo, E., Mizuta, R., Ishii, M., Obata, A., & Adachi, Y. (2019a). MRI MRI-ESM2.0 model output prepared for CMIP6 CMIP historical, Version 20190222. *Earth System Grid Federation [data set]*. <https://doi.org/10.22033/ESGF/CMIP6.6842>
- Yukimoto, S., Koshiro, T., Kawai, H., Oshima, N., Yoshida, K., Urakawa, S., Tsujino, H., Deushi, M., Tanaka, T., Hosaka, M., Yoshimura, H., Shindo, E., Mizuta, R., Ishii, M., Obata, A., & Adachi, Y. (2019b). MRI MRI-ESM2.0 model output prepared for CMIP6 ScenarioMIP, Version 20191108. *Earth System Grid Federation [data set]*. <https://doi.org/10.22033/ESGF/CMIP6.638>
- Ziehn, T., Chamberlain, M. A., Law, R. M., Lenton, A., Bodman, R. W., Dix, M., Stevens, L., Wang, Y.-P., & Srbinovsky, J. (2020). The Australian Earth System Model: ACCESS-ESM1.5. *Journal of Southern Hemisphere Earth Systems Science*, 70, 193–214. <https://doi.org/10.1071/ES19035>

# Chapter 17

## Assessment of Flood Risk in the Brahmaputra-Jamuna Floodplain, Bangladesh



Md. Serajul Islam and Nazmun Nahar

**Abstract** The old Brahmaputra river is one of the most contributing rivers to flooding in Bangladesh. Assessment of flood risk for this country is indispensable to save lives and properties. The underlying objective of this study is to contribute to the flood management system in the country. Shortest objective involves assessment of flood risk of the Brahmaputra-Jamuna Floodplain. To reach the goal some variables have been taken into consideration as land elevation, hydrology, river distance, population density and settlement, and coping capacity of the local people. From the analyzed result, it is found that among the 23 upazila, 6 are very highly hazardous, 7 are highly, 11 are medium, and 12 are low hazardous area, whereas 5 upazila are found moderately vulnerable, while 14 are medium and 5 are found having low vulnerability. The combined results of hazard and vulnerability demonstrate that uniform flood risk does not exist into the whole area. Some parts of the area are identified as high-risk zones, some are moderate risk zones, and others are risk-free or low-risk zones. Flood intensity and duration of the area are controlled mainly by the hydrological and topographical characteristics of the catchment area. The effect of river morphology and dynamics and precipitation trends of the area were found fluctuating with season. Coping strategies and options of the local residents were found to be poor and inadequate and are mainly based on indigenous knowledge. Almost all of the people found were not afraid of flood, and they take it as a routine problem that happens almost every year. Notwithstanding the need for greater sophistication, it is likely that, the flood protection, mitigation, and risk assessment model have been developed and expected to acknowledge the problem and considered here to successfully deal the flood problems of the study area. Moreover, the suggested models to analyze the risk of flood should be considered rudimentary and are presented solely to illustrate the concept.

**Keywords** Flood risk · Hazard · Vulnerability assessment · Risk model

---

M. Serajul Islam (✉) · N. Nahar

Department of Geography and Environment, University of Dhaka, Dhaka, Bangladesh

## 1 Introduction

Bangladesh is a land of rivers with numerous complex river system, three of the world's largest rivers, the Ganga, the Padma, and the Meghna. Almost all the stream flows through Bangladesh originated from the upstream catchment in India, Nepal, Bhutan, and China. Peak flow of these rivers mainly depends on the annual rainfall in the catchment area mainly located outside the boundary of the country Bangladesh (Rahman, 1996). The delta plain of the [Ganges \(Padma\)](#), [Brahmaputra \(Jamuna\)](#), and [Meghna Rivers](#) and their tributaries occupy 79% of the country. Four uplifted blocks (including the Madhupur and Barind tracts in the center and northwest) occupy 9%, and steep hill ranges up to approximately 1000 m (3300 ft) high occupy 12% in the southeast (the [Chittagong Hill Tracts](#)) and in the northeast (Wikipedia, 2022). Flooding in Bangladesh is caused by several factors. These include huge amount of inflows from upstream catchment, low floodplain gradients, cyclonic storms, drainage congestion in older floodplain areas, effects of confluence of the major rivers, and siltation in dry seasons (Rahman, 1996). Once every 10 years roughly one-third of the country gets severely affected by floods, while in catastrophic years such as 1988, 1998, 2004, and 2007, more than 60% of the country was inundated that is area of approximately 100,000 km<sup>2</sup> for duration of nearly 3 months (CEGIS, 2010). The increase volume of rainfall caused by climate change during the past decades has intensified the flood problem in Bangladesh (Mirza et al., 2003). The population expected to be hardest hit by flood disaster is the poor people who lack adequate means to take protective measures and who also have very little capacity to cope with the loss of property and income (IPCC, 2001). Since the mid-1990s, the concept of social vulnerability is used to describe and analyze the exposure and coping mechanisms of groups and individual to environmental risk, primarily in the context of climate change and flooding hazards in developing countries (e. g., Blaikie et al., 1994) in which Bangladesh is included. The study area (Brahmaputra-Jamuna Floodplain) is one of the most flood-prone areas of Bangladesh where almost every year flood takes place and the people of the area living with vulnerability of this natural hazard. Till to date a few scientific studies have so far been done of this hazardous environmental disaster of Bangladesh. But no specific study on flood risk assessment of the Brahmaputra-Jamuna Floodplain is found. Flood risk assessment and identification of vulnerabilities are now a worldwide requirement. Now time claims the assessment of flood risk of the area for the safety and security of lives and properties. The present study endeavored to assess flood risk in the Brahmaputra-Jamuna Floodplain using variables from social, economic, and environment aspects. Furthermore, coping strategies of communities have also been studied.

## 2 Overview of the Study Area (Brahmaputra-Jamuna Floodplain)

This study takes a vast area for the general consideration of flood risk assessment. In view of the large-scale approach, it is important to define subregions for the details study which allows taking a case study in the Brahmaputra-Jamuna Floodplain located only in the geographical unit of Bangladesh. Old Brahmaputra floodplain: A remarkable change in the course of the Brahmaputra took place in 1787. In that year, the river shifted from a course around the eastern edge to the western side of the Madhupur tract. This new portion of the Brahmaputra is named the Jamuna. The old course (Old Brahmaputra) between Bahadurabad and Bhairab shrank through silting into a small seasonal channel only two kilometers broad. The old river had already built up fair high levels on either side over which the present river rarely spills. The Old Brahmaputra floodplain stretching from the southwestern corner of the Garo Hills along the eastern rim of the Madhupur tract down to the Meghna river exhibits a gentle morphology composed of broad ridges and depressions. The latter is usually flooded to a depth of more than 1 m, whereas the ridges are subject to shallow flooding only in the monsoon. Jamuna (Young Brahmaputra) Floodplain is an alternative name used for the mighty Brahmaputra river, because the Jamuna channel is comparatively new, and this course must be clearly distinguished from that of the older one. Before 1787, the Brahmaputra's course swung east to follow the course of the present Old Brahmaputra. In that year, apparently, a severe flood had the effect of turning the course southward along the Jenai and Konai rivers to form the broad, braided Jamuna channel. The change in course seems to have been completed by 1830 (Fig. 17.1).

The Brahmaputra-Jamuna floodplain again could be subdivided into the Bangali-Karatoya floodplain, the Jamuna-Dhaleshwari floodplain, and diyaras and chars. The right bank of the Jamuna was once a part of the Tista floodplain, and now through the Bangali distributary of the Jamuna, it is a part of the bigger floodplain. Several distributaries of the Jamuna flow through the left bank floodplain, of which the Dhaleshwari is by far the largest; this floodplain is subclassed as the Jamuna-Dhaleshwari floodplain (Rob & Serajul, 2007). The southern part of this subregion was once a part of the Ganges floodplain. Along the Brahmaputra-Jamuna, as along the Ganges, there are many diyaras and chars. In fact, there are more of them along this channel than in any other river in Bangladesh. There is a continuous line of chars from where this river enters Bangladesh to the off-take point of the Dhaleshwari. Both banks are punctuated by a profusion of diyaras. The soil and topography of chars and diyaras vary considerably. Some of the largest ones have point bars and swales. The elevation between the lowest and the highest points of these accretions may be as much as 5 m. The difference between them and the higher levees on either bank can be up to 6 m. Some of the ridges are shallowly flooded, but most of the ridges and all the basins of this floodplain region are flooded more than 0.91 m deep for about four months (mid-June to mid-October) during the monsoon.

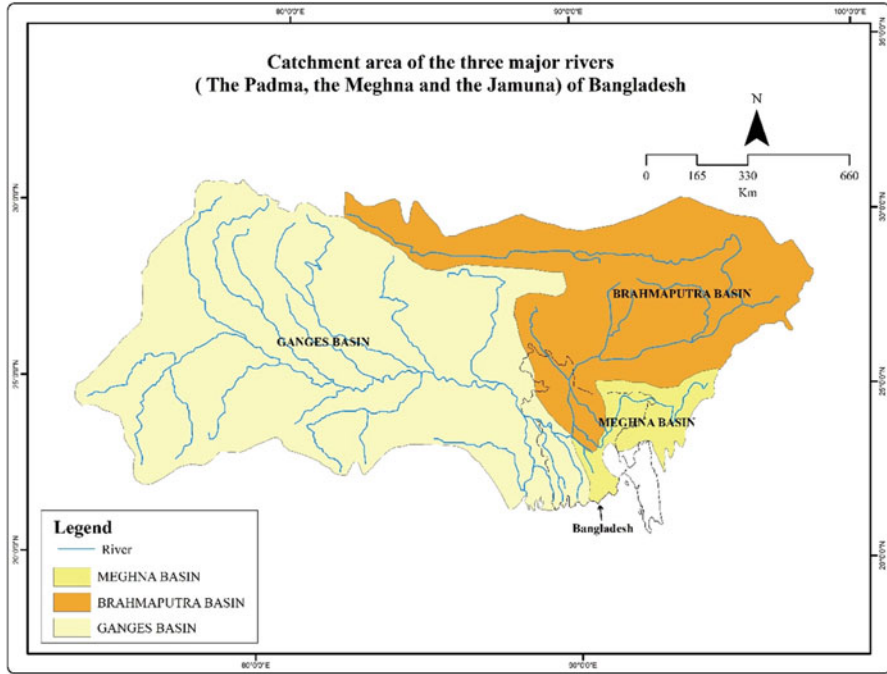


**Fig. 17.1** Catchment area of the three major rivers (the Padma, the Meghna, and the Jamuna) of Bangladesh. (Source: Self developed based on Joint River Commission of Bangladesh)

### 3 Methods and Materials of the Study

Methods of analysis of flood risk of the study area include three main steps. These are (1) determination of probability of flooding, (2) simulation of flood characteristics, and (3) assessment of the consequence. In this study risk estimate has been done fully probabilistic analysis in which all possible loads in the flood system, the resistance of the system, flood patterns, possible breaches, and their consequences are included. Such an approach would require a numerical elaboration and very large number of simulations. However, a simplified approach has been chosen in this study. A limited number of flood scenarios has been selected and elaborated. Furthermore, some parameters have also been taken into consideration to assess flood vulnerability. These are hydrological analysis of the concerned river(s), analysis of topographical situation, analysis of settlement pattern, and revealing the coping strategies of the local people.

For the purpose of hydrological analysis of the study area, secondary data and information from BWDB, IWM, and IWFM have been collected and analyzed. Variations of the water level, discharge, river width, and distance from river have been given emphasis. To assess flood vulnerability, topographic analysis, changing nature of flood, settlement pattern, and coping strategies of the local people of the

study area have been analyzed in detailed. To analyze topography of the study area, relevant data from LANDSAT-7 (GLOVIC, USGS) were used. For the purpose of exposing (revealing) the coping strategy of the local people, questionnaire survey was conducted. Field observation, participatory survey, and focus group discussion (FGD) were also made.

### 3.1 Stages of Investigation

The study involves multistage analytical methods of analysis those shown in the Table 17.1.

#### 3.1.1 Collection and Analysis of Secondary Data

Secondary data (flood data, elevation data, population, settlement data, etc.) and other relevant information were gathered from different authentic sources. These are SRTM (Shuttle Radar Topographic Mission) data and SPARRSO (Space Research and Remote Sensing Organization) Satellite Imageries; LANDSAT-7, USGS, and CEGIS maps were collected and analyzed. Meteorological and climatological data were collected from meteorological office, Dhaka for various climatic data from 1949 to 2011. Hydrological data were collected from the Bangladesh Water Development Board (BWDB), Dhaka to understand the spatiotemporal configuration of inundation and to reveal the extent of flood levels in different year of the study area. The river station (hydrological gauge reaching point) Bahadurabad at Jamuna river

**Table 17.1** Stages of investigation and purposes

Stages	Investigation	Purpose	Remarks
Study area selection	The whole country Bangladesh considered to assess flood risk. Hence Brahmaputra-Jamuna Floodplain has been selected as study area	Identification of the specific study area	Shown in the map
Secondary data collection	Hydrological data, settlement coverage, population density, elevation and river distance data	Collection of published and unpublished data and information	Literature survey
Primary data collection	Education, economic strength, indigenous knowledge, relief system, awareness	Questionnaire survey and field observation	Coping capacity analysis
Preparation of maps and diagrams	GIS-based maps, tables, and diagrams	Pictorial and graphical presentation	Computer-based work
Analysis of findings	Analysis and description	Analysis using appropriate techniques	Writings and presentation

Source: Self developed



has been given emphasis for analysis purpose. Analyzed data and information are presented through different statistical and graphical methods. Old and new maps and hydrological charts were also collected and analyzed. Among those flood vulnerable maps of Bangladesh, normally flooded area map of Bangladesh, inundated areas in different years prepared by BWDB, IWM, and IWFM are noteworthy. Books, reports, articles, and thesis prepared by different authorities and scholars are also collected and analyzed. FAP reports and research-based published and unpublished articles were also extensively used in this purpose. Both pictorial and mathematical procedures have been adopted to interpret the water level of the Brahmaputra-Jamuna river system. It includes the analysis of maximum, minimum, and average water level as well as discharge. It also include the frequency and probability analysis of flood in analyzing the flood hazard of the study area for a long period (1949–2001).

### **3.1.2 Questionnaire Survey and Field Observation**

In order to generate primary data involving flood adjustment and risk assessment, some scientific questionnaires were prepared. Among these questionnaires for flood affected people and expertise opinions are important ones. Samples for questionnaire survey were selected from the flood-affected people from the study area (Vij, Brahmaputra–Jamuna Basin) of different categories. Samples were selected purposively covering all the affected areas so that they could represent flood affected people from all categories.

The detail investigation regarding human adjustment to flood was undertaken in 2015 along the Brahmaputra and Jamuna River Bank during the month of May to August. In the study area, a total number of 300 households were interviewed. The survey had two broad sections: (a) flood situation as a hazard as perceived by the people, damage caused by it, and the local level mechanism to adjust with this hazard and (b) socio-economic condition of the respondent's vis-à-vis incidence of flood in the study area. During the survey period, an extensive field visit was undertaken in the whole region in order to understand the overall flood situation. Besides, interviews were taken with local leader and teacher, on the issues related to flood in their respective areas. Information thus drawn had lent qualitative support to those obtained through questionnaire survey. Focus group discussion and participatory survey were also made to collect primary data and information while visiting (as a part of field observation) the study area for the purpose of conducting survey. Telephonic survey with the aristocrat people of the study area was also conducted to understand the policy of flood mitigation both existing and near future.

### **3.1.3 Preparation of Maps**

To prepare maps of the study area (Brahmaputra-Jamuna Floodplain) like upazilawise elevation maps, settlement maps, contour maps, flood hazard map,

flood vulnerability map, etc., digital elevation model (DEM) data were used from Earth Explorer and then converted to SRTM. Downloaded images were processed to identify the boundary of the study area and subdivided (of the study area) using Raster Clipping Methods (RCP). Aoi files (from shape files) were used to subset the image, and elevation maps of the divided units were prepared using geo-processing tools. In order to prepare settlement maps (of all the units of the study area) digitized shape of LGED and Google Earth were used. Arc-info and Arc-view software were used to prepare the maps.

### 3.1.4 Analysis of Findings Using Appropriate Statistical Techniques

In the present study some advanced quantitative techniques were used. In order to find out the complex and intricate interrelationship between various climatological and hydrological parameters like rainfall, discharge of water, flood stages and seasonality, duration of flood, water level, frequency of occurrence of flood, etc., statistical methods like multivariate factor analysis and correlations analysis were used. In this stage a computer-based ANOVA program and SPSS programs were used. For the graphical presentation of the data and information MS Word, MS Excel, and MS Power Point software were utilized. Appropriate graphic/matrix was also applied using GIS technology for the representation of different data (Fig. 17.2).

## 4 Hazard Assessment (Hazard Index Identification)

In a land unit, flooding of different depths and duration may occur. So, it is essential to estimate the mean hazard index (MHI) for each land unit. The MHI was calculated separately for depth and duration considering the percentage of land under each category. According to the Hydrological Process (John Wiley & Sons, Ltd. 2005), the MHI is furnished by the following equation:

$$\left\{ \sum_{i=1}^n (\text{HI})_i A_i \right\} / \sum_{i=1}^n A_i$$

where

(HI) = hazard index of land area  $A_i$  of hazard category

$n$  = is the total number of land areas in the land unit.

Hazard index for the study area in analyzing the depth and duration of flooding is shown Tables 17.2 and 17.3.

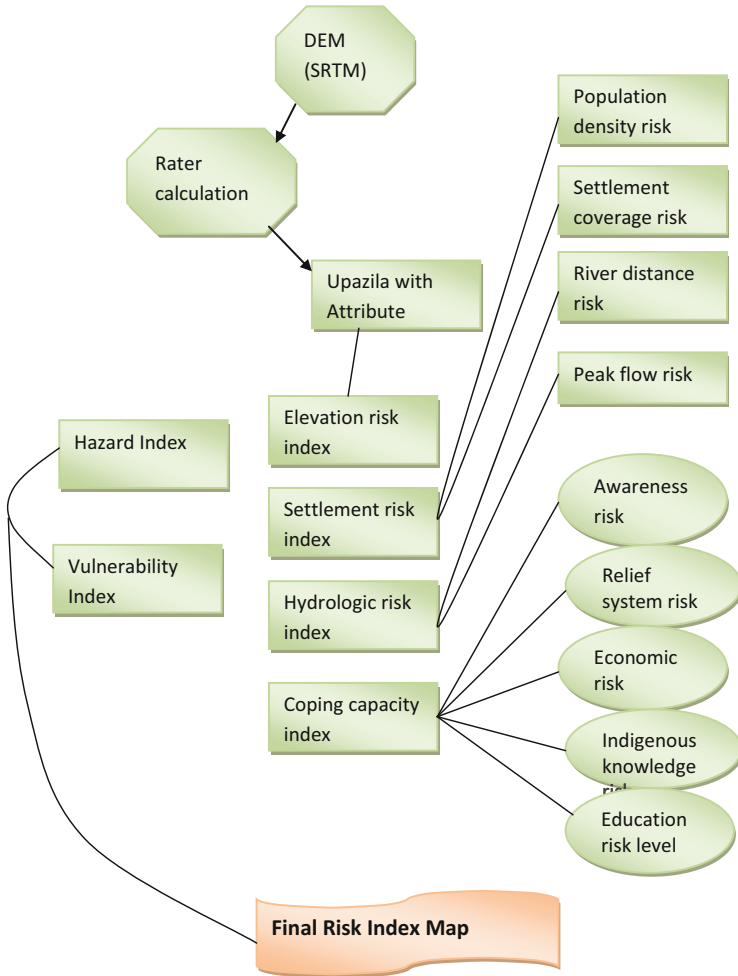


**Fig. 17.2** Flow chart of the image processing and preparation of maps. (Source: Self developed)

**Table 17.2** Hazard index for depth of flooding

Depth ( <i>D</i> ) of flooding (m)	Flood depth category	Hazard category	Hazard index	
			Alternative 1	Alternative 2
$0 < D \leq 0.6$	1	Low	1	2
$0.6 < D \leq 1.0$	2	Medium	2	3
$1.0 < D \leq 3.5$	3	High	3	4
$3.5 < D$	4	Very high	4	5

Source: Based on Tawatchai Tingsanchali, Wiley & Sons Ltd. 2005

**Table 17.3** Hazard index for duration of flooding

Duration of flooding	Duration category	Hazard category	Hazard index	
			Alternative 1	Alternative 2
Short	1	Low	1	0
Medium	2	Medium	2	1
Long	3	High	3	2
Very long	4	Very high	4	3

Source: Based on Tawatchai Tingsanchali, Wiley & Sons Ltd. 2005

#### 4.1 General Hazard Index

According to the abovementioned index of hazard, the whole area was taken into consideration in respect of all parameters deliberated in this study. Each of the upazila of the study area brought under analysis of hazard identification in respect of elevation, settlement, and water volume is categorized as follows (Table 17.4).

Hazard index for 19 units of the study area (upazila-wise) was calculated separately based on elevation, settlement, depth of water, and duration of flooding. In considering the intensity of flood of the study area, a hazard map has been prepared (Fig. 17.3).

The above hazard map shows that maximum parts of the study are found moderately hazardous. A major portion in the southwestern part especially Tangail, Kalihati, Bhuapur, Nagarpur, and Gopalpur are highly hazardous.

### 5 Vulnerability Assessment

Upazilawise vulnerability index shows that among the 19 units (upazila) of land Gopalpur, Bhuapur, Delduar, Kalihati, Tangail, and Islampur area are moderately high vulnerable. Among the other upazilas Trisal, Bhaluka, and Gafargaon are low vulnerable, and the others upazila are found medium vulnerable (Table 17.5).

The study uses the vulnerability definition of International Strategy for Disaster Reduction; it is “a set of conditions and processes resulting from physical, social, environmental, and economic factors, which increase the susceptibility of a community to the impact of hazards.” Another vulnerability definition adopted by IPCC (McCarthy et al., 2001) – namely, vulnerability of an entity is a function exposure, sensitivity, and adaptive capacity, which in turn are defined as exposure, sensitivity, and adaptive capacity. The following schematic diagram illustrates this approach (Figs. 17.4 and 17.5).

**Table 17.4** Upazilawise hazard index and hazard category of the study area

Sl. no.	Name of the upazila	Area (km <sup>2</sup> )	Percentage	Hazard index	Hazard category	Comments
1.	Basail	157.78	2.48	4	Very high	Whole area
2.	Delduar	184.54	2.90	3	High	Whole area
1.3.	Ghatail	451.30	7.10	1	Low	Middle and eastern part
				2	Medium	Western and middle part
4.	Gopalpur	193.37	3.04	1	Low	Whole area
1.5.	Kalihati	301.22	4.74	2	Medium	Western part
				3	High	Eastern part
1.6.	Madhupur	500.67	7.87	1	Low	Northeastern part
				2	Medium	Southwestern part
1.7.	Mirzapur	373.89	5.88	1	Low	Northeastern part
				4	Very high	Western and southern part
1.8.	Sakhipur	429.63	6.75	3	High	Western part with a few exception
				1	Low	North, south, and eastern part
1.9.	Tangail Sadar	334.26	5.25	2	Medium	Rest of the area
				3	High	Eastern part
1.10.	Bhaluka	444.05	6.99	2	Medium	Rest of the area
				4	Very high	Northeastern region-partly
1.11.	Gafargaon	401.16	6.30	4	Very high	Southern and middle portion of the upazila
				3	High	Northeastern part
1.12.	Muktagacha	314.71	4.94	1	Low	Northern part
				2	Medium	A few portion of south and southeastern part
1.13.	Phulbari	402.41	6.32	1	Low	Western part
				2	Medium	Middle-eastern part
1.14.	Trisal	338.98	5.32	2	Medium	Northern part
				3	High	Middle-southern part
15.	Jamalpur Sadar	489.56	7.70	1	Low	Whole area
16.	Madargonj	225.38	3.54	1	Low	Whole area
17.	Melandaha	239.65	3.77	1	Low	Whole area
1.18.	Sharishabari	263.48	4.14	1	Low	Maximum of the upazila
				2	Medium	A little portion of southern part
1.19.	Kaliakair	314.14	4.93	2	Medium	Middle western part
				4	Very high	Southwestern
20.	Bhuapur			3	High	Whole area

(continued)

**Table 17.4** (continued)

Sl. no.	Name of the upazila	Area (km <sup>2</sup> )	Percentage	Hazard index	Hazard category	Comments
21.	Nagarpur			4	Very high	Whole area
22.	Gazipur			1	Low	Whole area
23.	Sreepur			2	Medium	Whole area
	Total	6360.18	100%			

Source: Prepared based on hazard index

### ***5.1 Analytical Model of Socioeconomic Vulnerability to Flood Risk***

The analytical “model” of socioeconomic vulnerability to flood risk exposure in our case study is shown. Central to the concept of vulnerability are, as mentioned, the exposure to risk and the adaptive capacity to risk (Fig. 17.6).

### ***5.2 Coping Strategies: Adaptation and Mitigation***

Adaptation and mitigation strategy are important to reduce the losses and damages of flood. Coping strategy of the local people is furnished below as Fig. 17.7.

### ***5.3 Local Knowledge System***

Local knowledge system observed an integrated arrangement of knowledge, practice, process, and capacity of the local people which brings result on the natural hazards especially in flooding. Observed mitigation and adaptation processes have direct effect on their level of security and community resilience building. Observed local knowledge system of the study is described in Fig. 17.8 as below.

### ***5.4 Use of Indigenous Knowledge***

People of the study area are supposed to use indigenous knowledge in their occupation and daily life. Strategies are used to safe their live and households. They used to safe their shelter and to protect crops and live stocks. It varies upon the educational qualification of the affected people. Some of them are found well prepared in coping practices, and some of them are moderately conscious about flood hazard. Occupation of the people also has a great influence to make them well prepared in

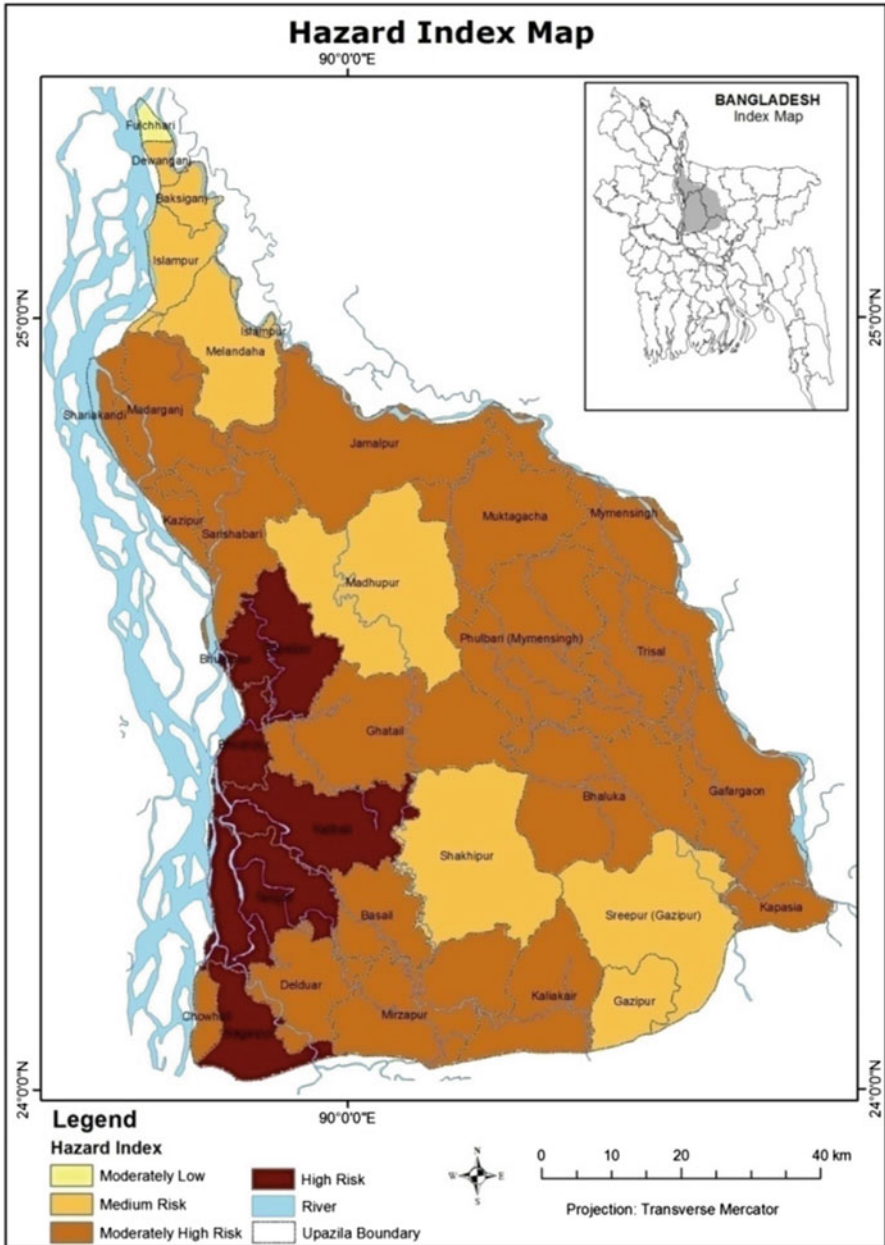
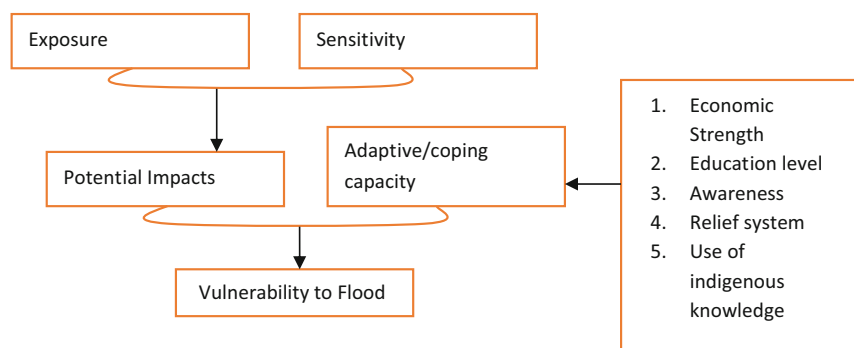


Fig. 17.3 Flood hazard map for the Brahmaputra-Jamuna River basin. (Source: Produced as of Arc GIS model)

**Table 17.5** Upazila-wise vulnerability index

Name of upazila	Level of vulnerability	Name of upazila	Level of vulnerability
Basail	Medium	Gafargaon	Low
Nagarpur	Moderately high	Muktagacha	Medium
Ghatail	Medium	Fulbari	Medium
Gopalpur	Moderately high	Trisal	Low
Kalihati	Moderately high	Jamalpur Sadar	Medium
Madhupur	Medium	Madargonj	Medium
Mirzapur	Medium	Melandaha	Medium
Sakhipur	Medium	Sharishabari	Medium
Tangail Sadar	Medium	Kaliakair	Medium
Bhaluka	Low	Bhuapur	Moderately high
Gazipur	Medium	Delduar	Moderately high
Sreepur	Low		

Source: Self prepared based on collected and analyzed data



**Fig. 17.4** Conceptualization of vulnerability to flood. (Source: Developed after Fuzzy Inference System)

copied practice. Indigenous flood prevention and coping strategies are presented below (Fig. 17.9).

Moreover, the local people of the study area take some measures to cope with floods like dry food reserves, household preparation, taking steps to protect live-stock, crop production, removal of assets, preservation of seeds, taking shelter to the nearby flood free area or flood shelter centers, taking children and aged people to the safer areas, collecting pure drinking water and medicine, changing food habit and reduce food consumption, changing occupation, cooperation with local people and receiving relief from the government and nongovernmental organization (NGO), changing the mode of transportation, loan, household repairing, searching of jobs, crop diversification, crops strategies and process, using battery- or oil-operated electronics, etc.



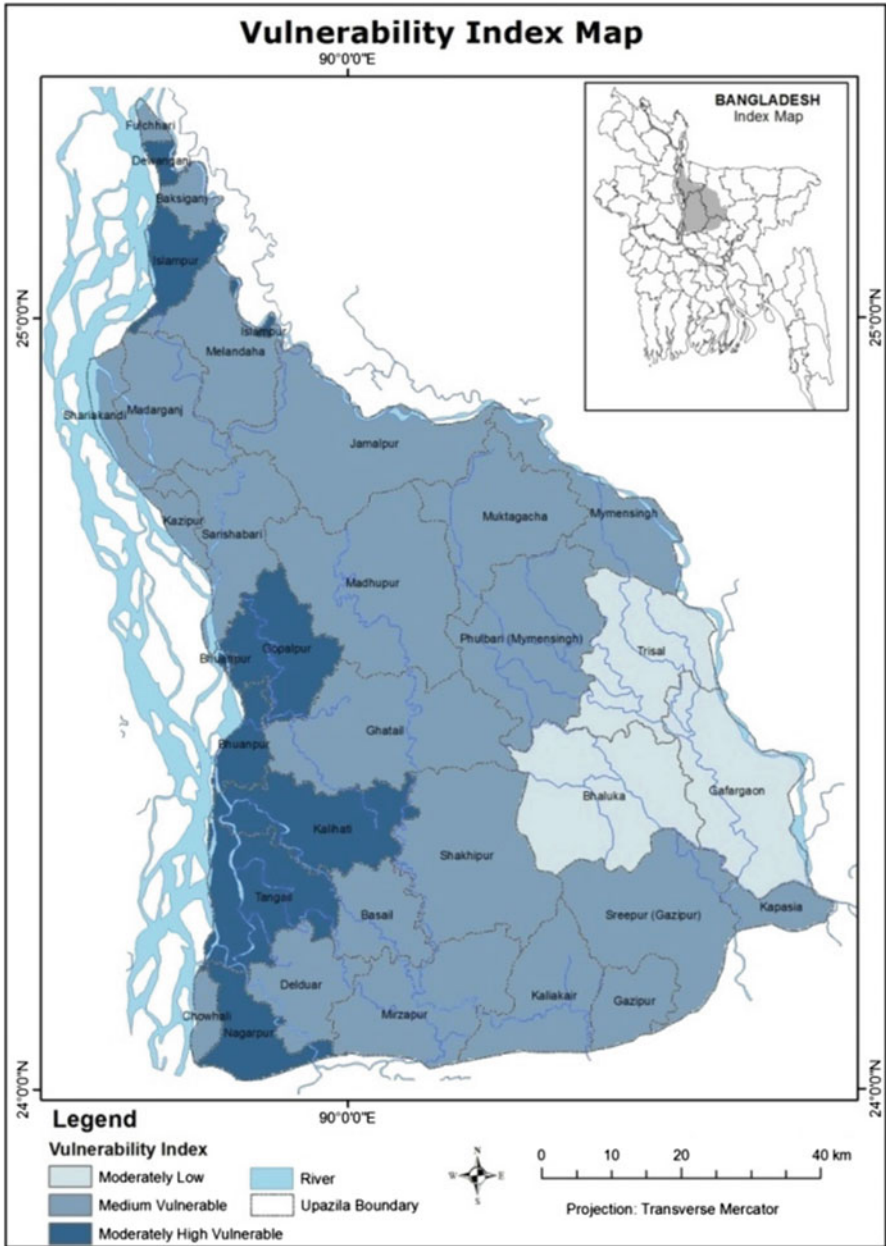


Fig. 17.5 Vulnerability map of the study area. (Source: Prepared on the basis of vulnerability index)

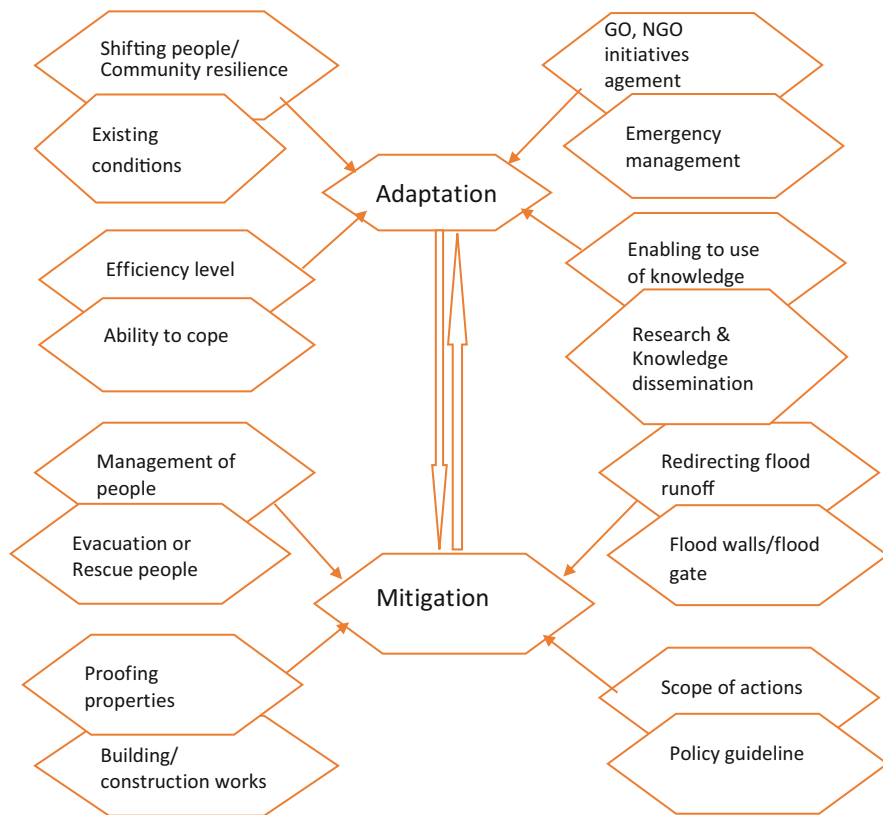


Fig. 17.6 Analytical model of socioeconomic vulnerability to flood risk. (Source: Self prepared)

## 6 Risk Assessment Through GIS-Based Model

Proposed model is prepared for risk assessment of the Brahmaputra-Jamuna Floodplain. Four variables, topographic conditions, hydrological situation, settlement scenarios, and coping strategies of the local people, have been taken into consideration to build up the prepared model. Each of the abovementioned variables was elaborately discussed to reveal the actual scenarios of the study area in related field.

It reflects the decision-maker’s own interpretation of the likelihood of being exposed to the conditions propagating risk. Keeping this in mind, the variables of the model have been furnished and analysis was done. Risk includes hazard and vulnerability of a particular area. In this model hazard and vulnerability index have been prepared considering all the variables. In that case topography, hydrology, population settlement, population coverage, and coping strategies of the people of the study area were analyzed in detailed. Each variable of the model has been described in validating the model (Fig. 17.10).

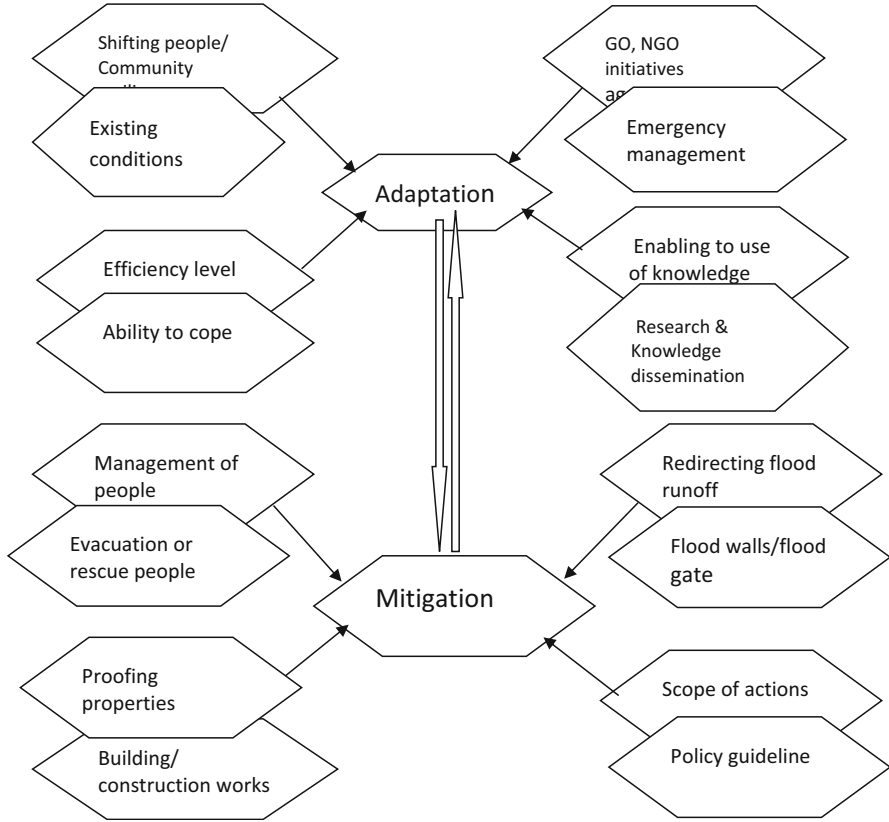


Fig. 17.7 Coping strategies of the local people. (Source: Self developed)

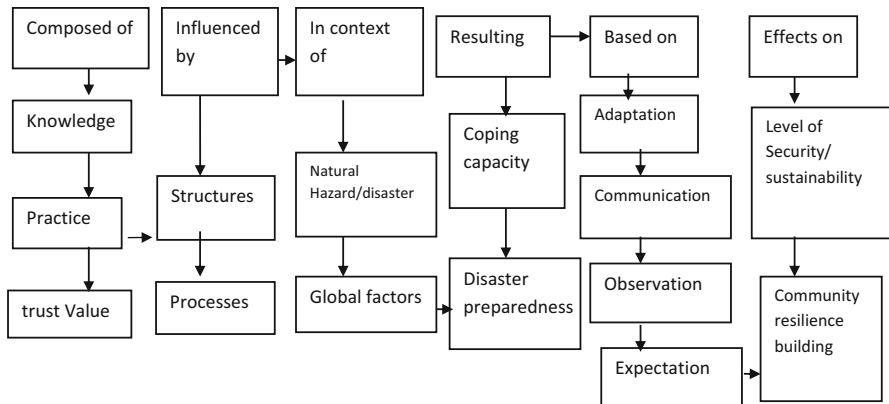


Fig. 17.8 Observed knowledge system of the study area

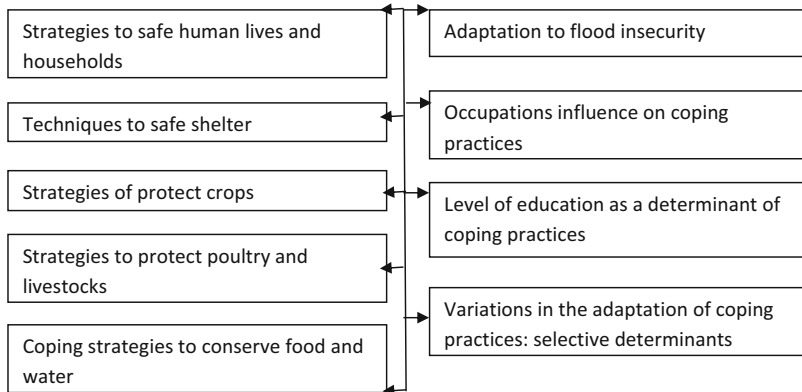


Fig. 17.9 Indigenous flood prevention and coping strategies

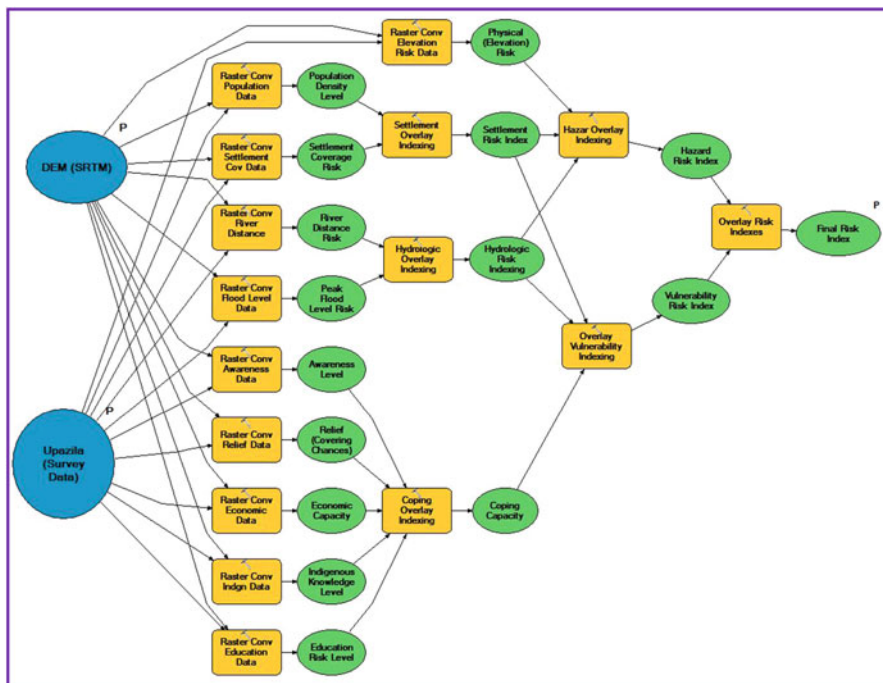


Fig. 17.10 GIS-based proposed model developed for risk assessment of the Brahmaputra-Jamuna Floodplain. (Source: Self developed)

Data and information used in this model are given below in tabulating form. The contribution of each variable in assessing flood risk in the study area has been considered both qualitative and quantitative aspects. Qualitative risk assessment is

used more frequently in analyzing coping strategies of the local people of the study area. Depending on the result of the analysis, flood hazard index has been prepared, and flood vulnerability of the study area were determined. The role of the variables of flood risk assessment of the Brahmaputra-Jamuna Floodplain is explained below:

### ***6.1 Model Specification and Validation***

In the past, flood management has considered on providing protection against floods through technocratic measures such as storm surge barriers and dike (Aerts and droogers. 2004). Later fueled by the knowledge that the abovementioned measures will be much more expensive, it is also established that the probability of flooding can never be reduced to zero. Considering the phenomenon, it was observed that flood risk assessment could be the first step in reducing flood risk. There is currently in international shift towards an integrated system of flood risk assessment (De Bruijn, 2005). In this context flood risk defined as the probability of flooding multiplied by the potential consequence such as economic damages or losses of lives (Smith & Greenway, 1984). The proposed model has been developed in an integrated approach of variables; those have direct influence on occurrence of flood and strategies of coping with floods in the study area.

### ***6.2 Major Findings***

1. The flood history of Bangladesh shows that the study area is one of the most flood-prone area with some few exceptions due to topographic conditions. All major historic floods inundated the area partly and sometimes catastrophically.
2. Topographically the area consists some flood-free zone and some areas are highly risky zone. The lowest hazard zones are located in the middle and northern parts of the study area which have higher ground elevation. The high and very high hazard zones are located in the southern and southeastern part of the study area, while the highest hazard zones are located in the southwestern part which are topographically low and adjacent to the mighty river Jamuna.
3. Most of the time the area is being inundated due to high discharge of river water coming from the upstream catchment area.
4. Local government and the people of the study area have the intention on how effective flood mitigation procedures could be adopted and can reduce the risk as a landform of downstream but felt upset as there is a need of a bold decision from the central government level.
5. Vulnerability index shows that among the 19 units (upazila) of land Mirzapur, Delduar, Kalihati, Tangail, and Islampur area are highly vulnerable. The other upazilas Gopalpur, Phulbari, Bhaluka, Gafargaon, Kaliakair, Trisal, and Kapasia are found highly vulnerable. The rest of the land units are moderately vulnerable

of which Jamalpur, Muktagaccha, Sarishabari, and Melandaha are found low vulnerable.

6. People of the study area are familiar to flood and habituated to cope with the same, but it is observed that coping capacity of the local people is not at satisfactory level.
7. In the period of flooding, local people suffer mainly lack of food including pure water, medical services, communication problem, residential problem, and waterborne diseases. Relief and economic assistance served ever past seemed insufficient to the local people. Security and sanitation problems are also mentioned as major problems during the flood time.
8. Flood protection activities both from the government and from the side of local people have been found in the study area.
9. Most of the time people of the study area depend on their fate in protecting their agricultural product. Quick pass of flood water or resistant of flood water to enter the crop field felt a new concept to the local people.
10. Flood damages road agriculture field and creates riverbank erosion an ongoing problem in this area. Suffering of poor people causes to change their occupation.
11. Flood shelter centers are not found available in the high vulnerable part of the study area which cause the flood-affected people to suffer more. Recently some initiatives have been taken to protect the affected people and to save agricultural crops giving emphasis to the most affected areas. Flood forecasting and warning system, construction of embankment and sluice gate, etc. could be mentioned as approved initiatives.
12. People are highly resilient and self-reliant, and they have a number of coping strategies.
13. The greatest area of concern is that the flood will push large numbers of the poorest families deeper into poverty.
14. Urgent response actions are still required in some areas in terms of bulk food relief and supplementary feeding for vulnerable groups, support to housing rehabilitation and sanitation, and emergency healthcare interventions.
15. Employment generation, whether through food/cash for work or support and widespread provision of affordable credit will be essential for recovery from the floods.

### **6.3 Recommendations and Conclusions**

Based on the lesson learned from this research, it is felt that the role of scientific principles for the flood risk assessment should be enhanced by following the concept of appropriate scientific methods; the need-based flood controlling measures could be taken. Any excessively complex method should not be enhanced which may make too hard to employ to the user. Quantitative relationship between flow velocity and flood damage should be established, and a sound and appropriate scientific risk assessment model should be applied. Geophysical politics and bold political decision are required because of the fact that including the main river (Jamuna) of the

study area, 54 rivers originate and locate outside Bangladesh, mainly in India and Nepal. Hence if we want to stop flood, identifying the level of risk and measures of adaptation and mitigation should be given emphasis to reduce the losses and damages of the study area as well as the country. International cooperation is required to implement the International River Laws. A twin track approach is needed for community-based training, relief, and rehabilitation activities to solve the flood problem.

The lack of flood controlling measures is a critical problem because Bangladesh has an agrarian economy dependent on water. At different times and in an unpredictable manner, flood has too much water. The intricate network of alluvial rivers carries a huge annual discharge and sediment load, causing channel shifting and bank erosion. Withdrawals in upstream areas seriously affect socioeconomic growth, the environment, and the ecology. The habitat of fish, which is a major source of protein for the rural poor, is under threat from the increasing conversion of land to agricultural use. Inland navigation is hindered by blockages in the river delta. Meanwhile, the need for pure water is increasing along with the salinization of the coastal belt and the degradation of ecosystems. The study area is included in one of the most vulnerable parts of Bangladesh comprising the basin of the river Brahmaputra and Jamuna. The southern part of the study area is found more vulnerable to flooding as topographically lower than northern and middle part. Almost every year the vulnerable part is being inundated and considered as a hazardous part of the basin. This study endeavored to assess the risk estimating the challenges related to flood events of the study area analyzing past and future events. Focus has been given to determining acceptable risk assessment through the developed model as stated above.

## References

- Blaikie, P., Cannon, T., Davis, I., & Wisber, B. (1994). *At risk: Natural hazards, vulnerability, and disasters*. Rutledge, London, UK.
- CEGIS (2010). CEGIS Annual Flood Report, 2010, Bangladesh.
- De Bruijn, K. M. (2005). *Resilience and flood risk management: A systems approach applied to Lowland rivers*. Delft University of Technology, Delft, NL.
- McCarthy, J. J., et al. (2001). *Climate change 2001: Impacts, adaptation, and vulnerability: Scenario of the 21st century*. IPCC, Cambridge.
- Mirza, M. M. Q., Warrick, R. A., & Ericksen N. J. (2003). The implications of climate change on floods of the Ganges, Brahmaputra, and Meghna rivers in Bangladesh. *Climatic Change*, 57, 287–318.
- Smith, D. I., & Greenway, M. A. (1984). *Urban flood damage: The assessment of tangible effects in Australia*. Australian National University.
- Rahman, A. (1996). Peoples' perception and response to flooding: The Bangladesh experience. *Journal of Contingencies and Crisis Management*, 4(4), 198–207.
- Wikipedia (2022). [https://en.wikipedia.org/wiki/Floods\\_in\\_Bangladesh](https://en.wikipedia.org/wiki/Floods_in_Bangladesh)

# Chapter 18

## Characteristics of Flood in the Meghna River Basin Within Bangladesh



M. Shahidul Islam and Afrin Sharabony

**Abstract** Meghna is the third largest river in Bangladesh, and its basin is primarily flooded by torrential rain-fed water coming from Assam, India and also from local rainfall. Within Bangladesh, the Meghna catchment area is divided into upper Meghna and lower Meghna basin. The hilly portion in the north and north-west of the upper Meghna basin is characterised by flash flood nearly in every year and usually in the months of May and June (early monsoon flood). The second peak appears as regular riverine flood during the June–July period and inundates a greater portion of the Meghna floodplain. The flood in the lower Meghna basin is fluvio-tidal in nature and highly driven by south-western monsoon winds. The flood of this year (2022) is also catastrophic in nature, showing two peaks: the first peaks (May) of flash floods have created huge damages in the hilly areas of Sylhet and Sunamganj, and during the second peak (June), a greater portion of the basin remains deeply inundated, and all communication remains cut-off with the capital. Like other previous flood, the flood of 2022 also shows that excessive rainfall in the Indian portion of the catchment is the main cause of unusual flooding in the Meghna basin. The flood management of this region is thus requiring timely flood forecasting and accurate risk assessment. It is thus urgent need of regional cooperation among the co-riparian countries. The major area of cooperation includes real-time data sharing, sharing information on flood forecasting, exchange of knowledge and technology and collaborative research. It shows that the flood problem issue of this region is technical in nature, but its solution is largely political. All concerned countries thus need to be politically committed to resolve the problem and to reduce the suffering of millions of people of this region.

---

M. S. Islam (✉)

Department of Geography and Environment, University of Dhaka, Dhaka, Bangladesh  
e-mail: [shahidul.geoenv@du.ac.bd](mailto:shahidul.geoenv@du.ac.bd)

A. Sharabony

Research Intern, Coastal Research Unit (CRU), Department of Geography and Environment,  
University of Dhaka, Dhaka, Bangladesh



**Keywords** Meghna basin · Flash flood · Backwater effect · Regional cooperation

## 1 Introduction

Bangladesh is situated in a unique location in the Indian subcontinent, and this location has led the country susceptible to regular annual flooding. Ganges-Brahmaputra and Meghna (GBM) are three major rivers crossing through the country, and combine flow finally discharges into the Bay of Bengal. The sediment carried by the GBM rivers system has formed one of the largest delta systems of the world – the GBM delta – which covers about 80% area of Bangladesh. Meghna is the third largest river in Bangladesh which is primary rain fed, and its basin contains 29 subbasins (Mohammed et al., 2018). Average flow of GBM rivers 1,009,000 million m<sup>3</sup> and sediment more than 1 bill tons (Mahmud et al., 2020; FFWC, 2021). This river basin experiences early flash flooding in the hilly areas and regular riverine flooding in the floodplain areas almost in every year. However, in some years, this flash flood and riverine flood become catastrophic in nature, as has been experienced in this year (2022). The severity and inundation scale of this exceptional flooding is site depended and largely been controlled by hydro-meteorological inputs. Excessive rainfall in the entire Meghna catchment area is the main cause of such catastrophic nature of floods. This chapter is an attempt to evaluate the nature and characteristic of flood in the Meghna basin area within Bangladesh, with special attention to flood of 2022.

## 2 Meghna River Course

The Meghna River is originated from the rainiest part of Shillong Plateau in Assam state of India. Travelling 400-km Barak as main source, it enters Bangladesh at Amalshid in Sylhet district and bifurcates into Surma in the north and Kushiya in the south (Fig. 18.1). The Surma on its right bank receives tributaries originated from the Khasi and Jaintia hills. Due to steep hill slopes and heavy rainfall, all the tributaries are subject to annual flash floods. Kushiya on the other hand, on its left bank, receives flows from tributaries, such as the Monu, Gumti and Khowai rivers originating from Tripura, India, and are the sources of flash flood in this southern part of the catchment, although less violent than that of the north. The lowlands and haors in between Surma and Kushiya rivers are unique basin-shaped geomorphology, being deeply flooded and are the immense source of biodiversity. The floodplain in between is also characterised by meandering channels and many abandoned river courses. Surma and Kushiya rivers finally rejoined near Bhairab Bazar and take the name as Meghna, until it joins the Ganges (Padma) near

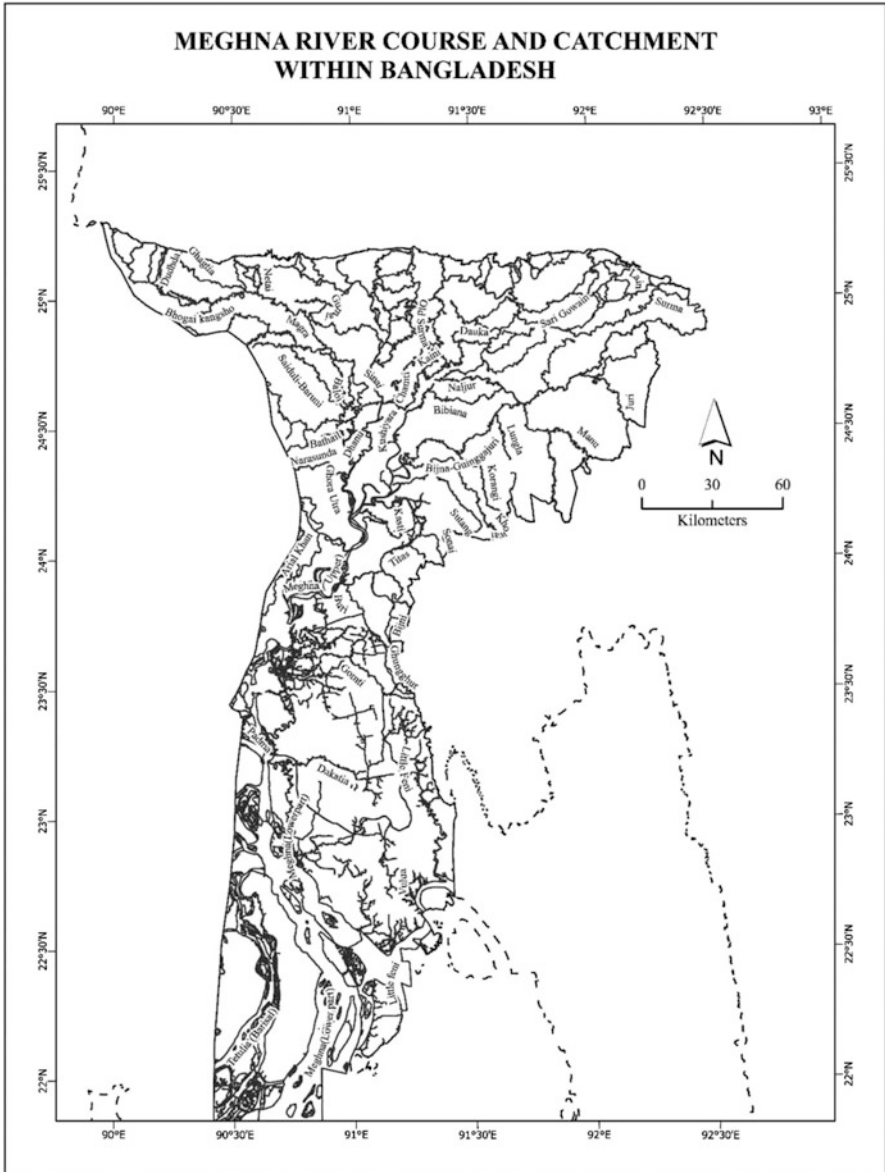


**Fig. 18.1** Rivers of Bangladesh showing Meghna River course and catchment. (Source: Banglapedia, 2021)

Chandpur (Fig. 18.1). The catchment up-Chandpur is widely known as upper Meghna River in Bangladesh. Upper Meghna River also receives hilly streams originating from the Meghalaya and Assam of India. The catchment below Chandpur down until the estuary is the lower Meghna basin, which is fluvio-tidal in nature.

### 3 Meghna River Catchment

The total area of the GBM catchment is 1.6 million km<sup>2</sup> of which only 7.5% is within Bangladesh and remaining 92.5% lies outside the country (India, China, Nepal and Bhutan). Among these three river basins, the Meghna River catchment is the smallest one and occupies about 65,000 km<sup>2</sup> of which 43% belongs to Bangladesh, occupying 24% of the territory (Masood & Takeuchi, 2016) (Fig. 18.2). It comprises fertile alluvial lowland, has formed extensive plain land mass and support 170 million people (Paszkowski et al., 2021).

The upper Meghna River (UMR) catchment is located in the world's highest rainfall regime with an average precipitation of 5800 mm y<sup>-1</sup>. The morphology of the upper Meghna River basin is distinctive in nature and can be characterised by the presence of alluvial ridge, natural levee, back swamps, depression (haor), abandoned channels, oxbow lakes and extensive non-tidal plain lands.

The lower Meghna River (LMR) starts from the confluences with the Padma River at Chandpur and finally flows into the Bay of Bengal. It is one of the largest rivers of the world and at its mouth receives the combine flow from three mighty rivers, the Ganges, Brahmaputra and upper Meghna. The lower Meghna River is tidal in nature, which has profound influence on delta morphology. This portion of Meghna River is highly dynamic and experiences significant morphological changes, either by erosion or accretion. There are numerous islands in this portion of river course, which are subject to regular bankline shifting.

In lower Meghna River basin, tide is the predominant force to shape up the morphology of the floodplain. Major geomorphological features are the mud flats and tidal floodplain, with distinctive spatial variation in their nature and fluvio-dynamic characteristics. Enormous water and sediment supply from the GBM system has led to rapid morphological changes of the lower Meghna River (LMR) basin, including significance impact on natural environment and social-cultural settings. This highly dynamic LMR basin experiences intense hydro-morpho-ecological changes and the fertile soil, which supports farmers to engage in agricultural activities and fishermen to fishing.

The Himalayan and Burma Arcs are the two sources of water and sediment supply, which are being carried by the GBM river system to shape up the morphology of GBM delta. The LMR basin shows high seasonal variation in sediment and water discharge. The annual average water discharge of the LMR is 34,600 m<sup>3</sup>s<sup>-1</sup> and mean annual flood discharge rate of 97,000 m<sup>3</sup>s<sup>-1</sup> (Sarker & Thorne, 2009), and the tidal rage is 4 m (Allison et al., 2003).

The lower Meghna floodplain is characterised by plain land of less than 5 m above MSL and very gentle slope. Both banks of LMR occupy Holocene sediments of deltaic and tide-dominated plain land. The floodplain along the left banks of the Meghna River is slightly elevated due to tectonic cause and shows gradual eastward rising up of its elevation (Bakr, 1977).

### MEGHNA RIVER CATCHMENT (Including Flood Station)

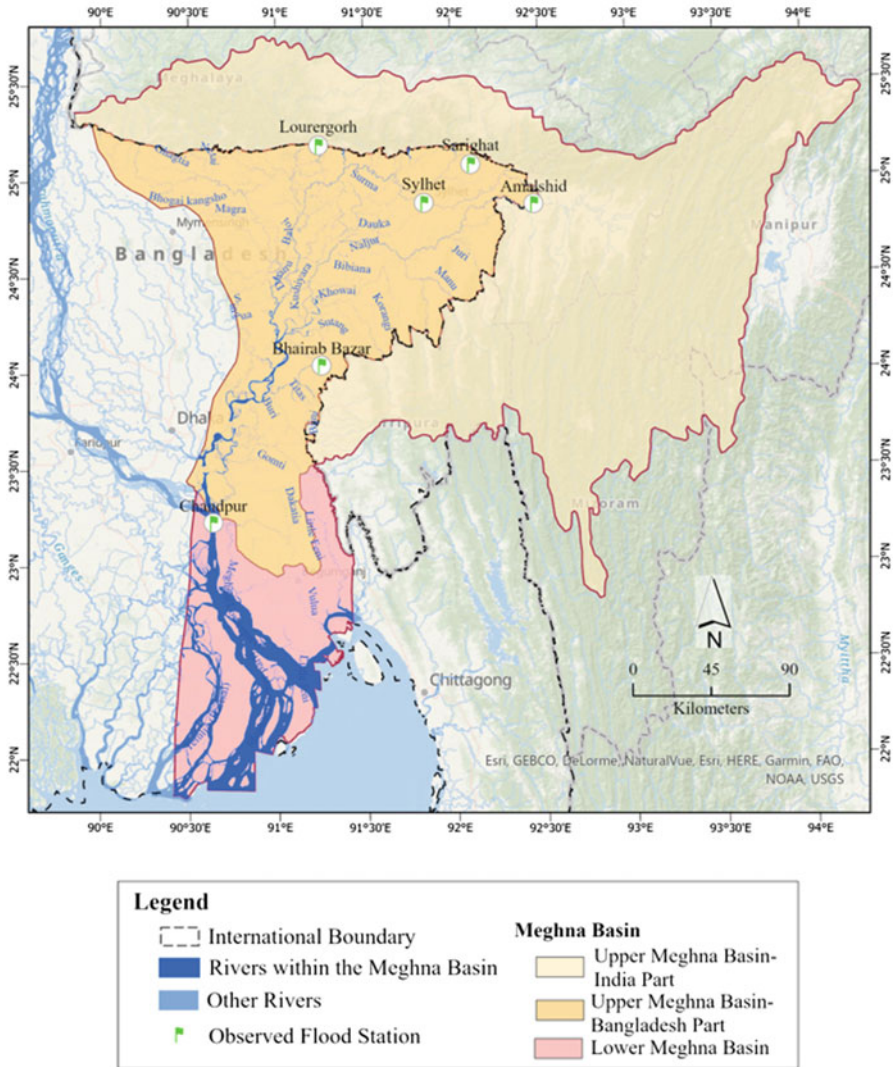


Fig. 18.2 Meghna River catchment area. (Source: IUCN, 2018)

In the lower Meghna River, the freshwater flow from upstream is halted and reduced naturally and by human interventions, particularly from the Ganges and Brahmaputra sources in the west. As consequence the lower reach of the Meghna basin is predominantly under strong tidal effects. Tide generated in the south-west and south-east of the bay finally finds its way toward the Meghna estuary, where the

tidal amplitude rises up to 4–6 m, particularly during the monsoon spring tide. Tide along Bangladesh coast propagates up to 100 km inland. Tide-dominated coastal flooding is well noticed in the south central and eastern part of the coast than the west. In the lower Meghna reach, the flood is thus fluvio-tidal in nature. However, unlike the south-west, the LMR receives proportionately more freshwater and remains relatively fresh throughout the year, showing comparatively a lower salinity intrusion and salinity remains largely unchanged despite immense tidal effect. In this part of the Meghna river there remains a balance between fresh water influx and relative tide level rise.

## 4 Flood Characteristics of Meghna River

In hydrological regime, flood is defined as a sudden peak of river discharge to overflow the riverbanks and inundate the floodplain for a certain period of a year. It could be a regular inundation, without any loss of properties and such floods are desirable. It could also be beyond the expectation level, crossing the danger level and destroying live and properties for a short span of time varied from a few days to a few weeks. On an average the annual flood inundates 20% of the country, including a greater portion of Meghna floodplain. However, some year the flood become catastrophic in nature, inundating larger portion of the floodplain than it is expected. Some of the major flooding years covering more than 25% of the country are shown in Table 18.1. Figure 18.3 shows the hydrographs of floods of Meghna River of the severe flooding years 1998, 2017 and 2020 at three different stations within the catchment.

Flood in a river basin may result from various causes, of which some important causes are heavy torrential rainfall, channel hydraulics and backwater effects from tidal amplitudes. Floods in Bangladesh are usually classified into four categories: flash flood, regular riverine flood, tidal flood and cyclone-induced storm surges. Flood discharge data for Brahmaputra-Jamuna Ganges-Padma and Meghna Rivers are collected by BWDB at Bahadurabad Ghat, Harding Bridge and Bhairab Bazar, respectively. The combined flow of Brhamaputra-Jamuna and Ganges is measured at

**Table 18.1** Year-wise flood-affected area in Bangladesh

Year	Flood-affected area		Year	Flood-affected area	
	km <sup>2</sup>	%		km <sup>2</sup>	%
1955	50,500	34	2004	55,000	38
1969	41,400	28	2007	62,300	42
1970	42,400	29	2015	47,200	32
1974	52,600	36	2016	48,675	33
1987	57,300	39	2017	61,979	42
1988	89,970	61	2019	45,747	31
1998	100,250	68	2020	59,028	40

Source: FFWC (2021)

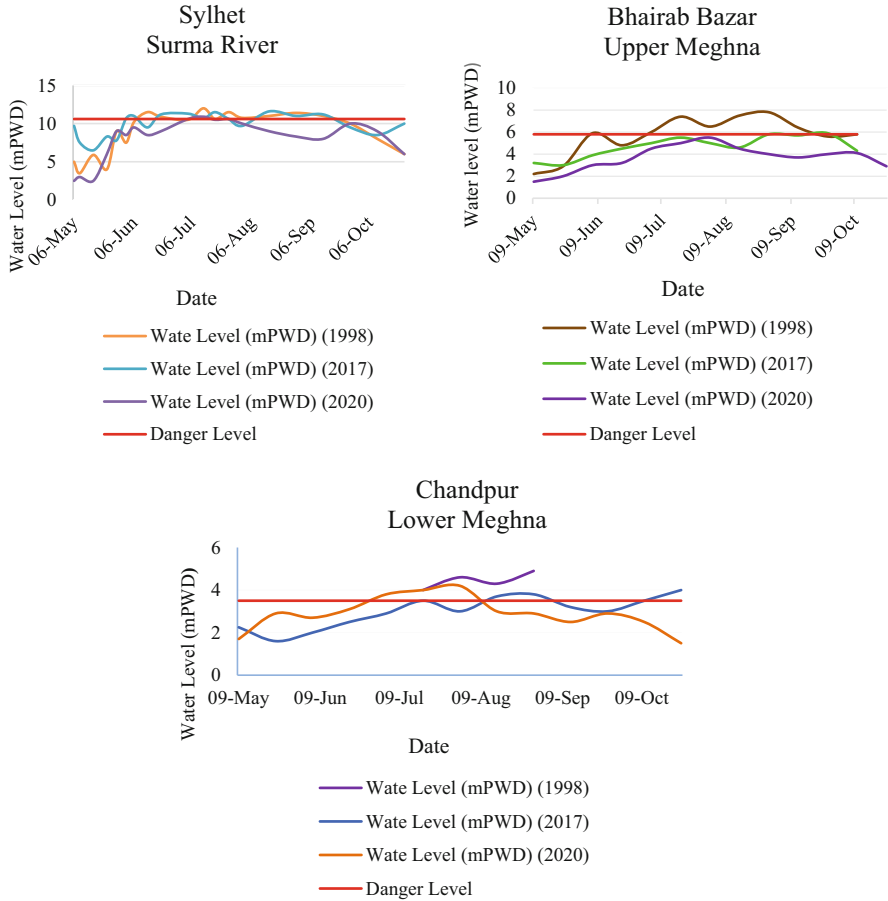


**Fig. 18.3** Hydrograph of extreme flood years in Meghna basin. (Date Source: FFWC, 2022)

Baruria and Brahmaputra-Jamuna and Ganges-Padma is recorded at Mawa. Combined discharge data of Brahmaputra-Jamuna, Ganges-Padma and Meghna are collected at Chandpur.

Flood in Meghna River basin incorporates all the above categories, with regional and spatial disparity. In the upper part of the basin within Bangladesh, due to the presence of small hillocks, relative steep slope of the ground, narrow and small river types and excessive torrential rainfall are characterised by flash flood, particularly in the onset of monsoon period. Local rainfall in the upstream hilly areas flows downward without any further delay and produces the flash flood in Bangladesh territory. There is a difference of timing of flood peaks among three major rivers, which is because of the variation of rain pouring in the catchments and difference of travelling time of water flows from the upstream. In a normal year, the upper Meghna River receives first flood peak in the 3<sup>rd</sup> or 4<sup>th</sup> week of May, and second

peak occurs closed to the second peak of Brahmaputra River. Synchronising the peaks of all major rivers is rare, and in such case, the flood level becomes severe in nature. The occurrence of the peak floods of Meghna River, when coincides with the peaks of the Ganges and Brahmaputra flood, the extension, depth and duration of flood at lower Meghna basin become severe. It is further intensified when effects coincide with the high tide and backwater effect. Backwater effect is an important cause of flooding in the Meghna course, particularly in the LMR, as was observed in 1997 and 1988. During that flood the water at Bhairab Bazar station remained above danger level for consecutive 68 days (Mirza et al., 2003). Mirza et al. (1998) also have given the illustration of such flood synchronising and tidal impact of flood amplification during the 1987 flood.

It is believed that the flow of upstream water is halted at the Meghna mouth due to dynamic action of the Bay of Bengal. The bay appears to work as a barrier wall of water due to south-west monsoon wind, tidal amplitude and occasionally cyclonic depressions. South-west monsoon piles up water in the north-east corner of the bay, particularly in the Meghna estuary, and intensifies the flood inundation. Meghna mouth is the drainage route of the Ganges-Brahmaputra-Meghna water flow. Water congestion at Meghna mouth scales up the tidal inundation, particularly during the spring tidal stage. The unprotected area outside the embankment becomes more vulnerable due to tidal flooding.

However, there do not exist reliable observational evidences of backwater effect of flood in Bangladesh. Ali (1995) has shown that it is the monsoon wind that has impact to hold up floodwater in the Meghna mouth. The inflow and outflow of floodwater through the month largely depend on strength balance between the freshwater discharge and south-west monsoon wind.

#### ***4.1 Meghna River Flood 2020***

Severe flood was caused by the upper Meghna River systems in 2020 which affected low-lying lands of northern and north-western regions of Bangladesh. Flood affected 40% of the country in 2020. In October 2020, in the Meghna basin, out of 28 rainfall monitoring stations, 21 stations recorded more rainfall than the normal of the month. The basin received 34.39% more rainfall than monthly normal during the month (FFWC, 2021) (Table 18.2). Due to this flood, 635 schools were damaged in Sylhet in 2020 (Iqbal & Rahman, 2020). Nearly 1.3 million homes were damaged, hundreds of thousands of people were marooned, and hundreds died ([www.bbc.com](http://www.bbc.com)). The Government of Bangladesh has allocated total 8210 metric tons of rice, and each district received 200 metric tons of rice ([reliefweb.int](http://reliefweb.int)). Figure 18.4 shows the DEM of the Meghna basin, and the flood inundation of the Meghna basins area is shown in Fig. 18.5. The water levels at three stations (Sylhet, Bhairab Bazar and Chandpur) of monsoon flood of 2020 are shown in Fig.18.6.

During the monsoon 2020, out of 29 water level (WL) stations, the flow was above the danger level in 17 stations, which were in coexistence with local monsoon

**Table 18.2** Monsoon rainfall statistics of 2020 in Meghna basin

Month	Meghna basin
May	-11.34%
June	7.39%
July	10.49%
August	-35.07%
September	32.89%
October	45.65%

Source: FFWC (2021)

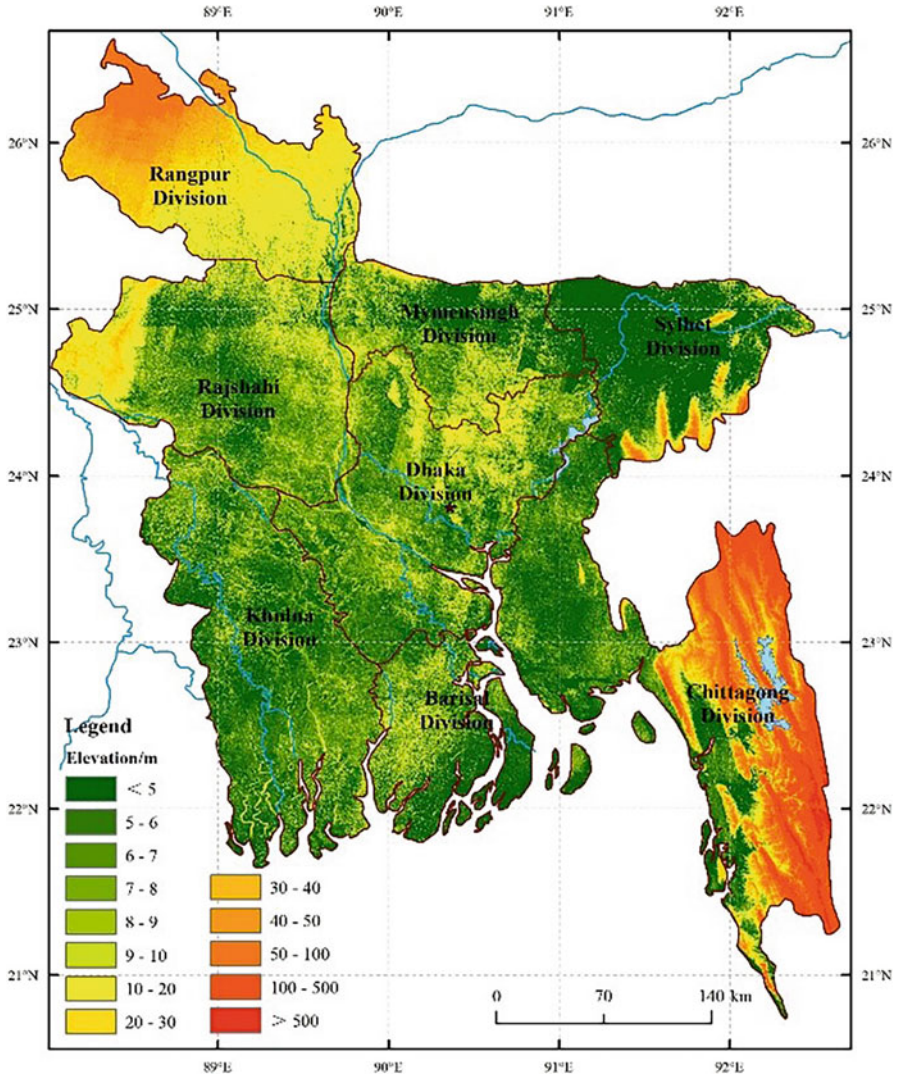


**Fig. 18.4** DEM of Meghna basin. Source: (Jiang et al., 2021)



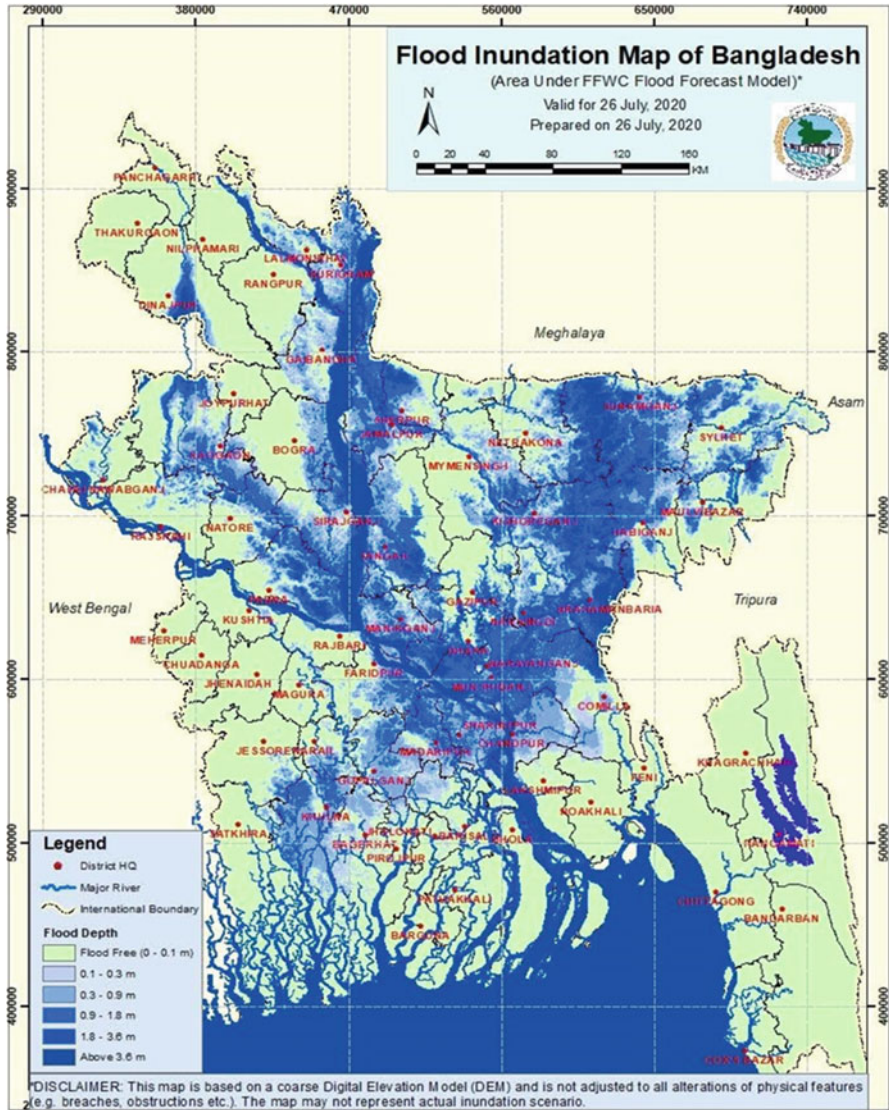


Fig. 18.5 Flood 2020 (26 June) inundation of Meghna basin. (Source: FFWC, 2021)

rainfall intensity. In Meghna basin there are 19 rainfall stations of which in 9 stations received 7.23% more rainfall than normal in June 2020 (FFWC, 2021). The basin received 10.21% more rainfall in July, 2020, which was 29.08% more than normal in September. Because of rainfall intensity, there were two peaks of monsoon flood in the Meghna basin, which occurred during June–July and late September for period of 26 days. Because of backwater affect and tidal influence, the flood prolonged for a period of 40 days at lower Meghna regime (FFWC, 2021).

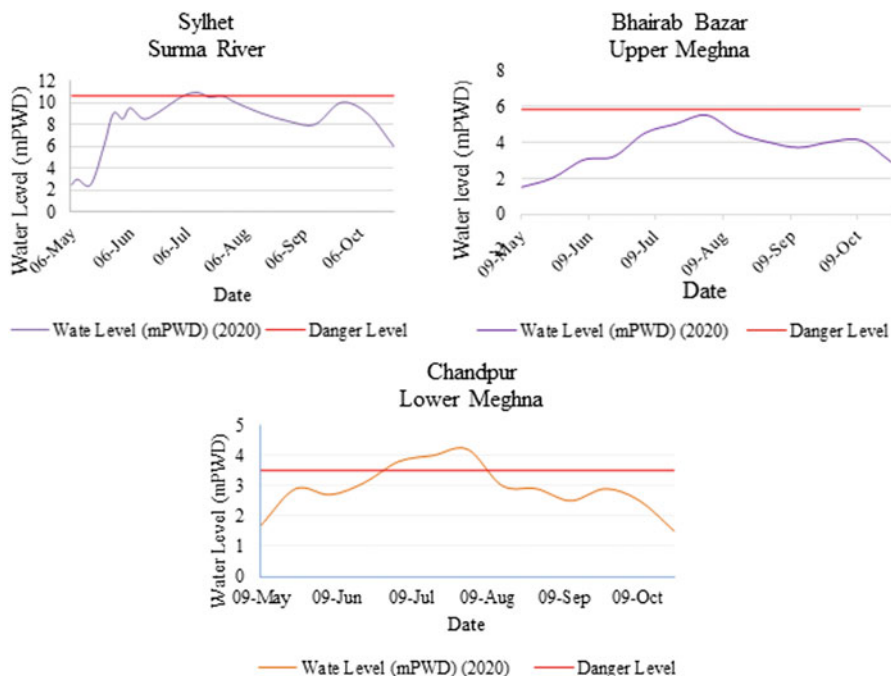


Fig. 18.6 Hydrograph of Meghna basin in 2020. (Source: FFWC, 2021)

In the upstream region, the monsoon 2020 flood characteristic was distinctive. That year the basin had experienced severe incidents of flash flood with multiple peaks, which affected the the basin very badly. It shows at least five to seven fluctuations crossing the danger level at different points of the Surma River flows, starting from May 2020. Some of the important peaks occurred in 3rd of June (for 1 day), 25th of June to 4th of July (for 9 days) and 9th–24th of July (14 days), mostly covering the Surma and Kushyara catchment area. Due to tidal water effect, the floodwater coming from the upstream Meghna during June and July period was blocked at Chandpur point, which also led to intensified flood events. Sunamganj, Nterokona, Sylhet, Brahmanbaria and Chandpur regions experience fold of short to moderate in duration. The Kushyara river also showed similar fluctuation lasting from 3 to 6 days throughout the monsoon.

### 4.2 Meghna River Flood 2022

The flood of 2022 is a typical one to understand the flood characteristics of the Meghna River basin. It shows two flood peaks: one is per monsoon (mid-May) flash flooding event, and another one is monsoon (mid-June) riverine flooding event (Fig. 18.7). The pre-monsoon peaks of stronger flash flood hit north-eastern region

of Bangladesh which is more severe than the floods in last two decades. Extensive flash flooding has affected 4 million people, and nearly 13 upazillas have been flooded including Kanaighat, Gowainghat, Companyganj, Jaintapur, Zakiganj, Sylhet Sadar, Fenchuganj and many more (Islamic Relief Bangladesh, 2022). According to FFWC, among 39 rivers of the north-eastern part of the country, in 33 rivers, water level has risen, and 4 rivers have exceeded their danger level including Surma, Kushiyara, Jadukata and Sarigowain (Prothom Alo, 2022).

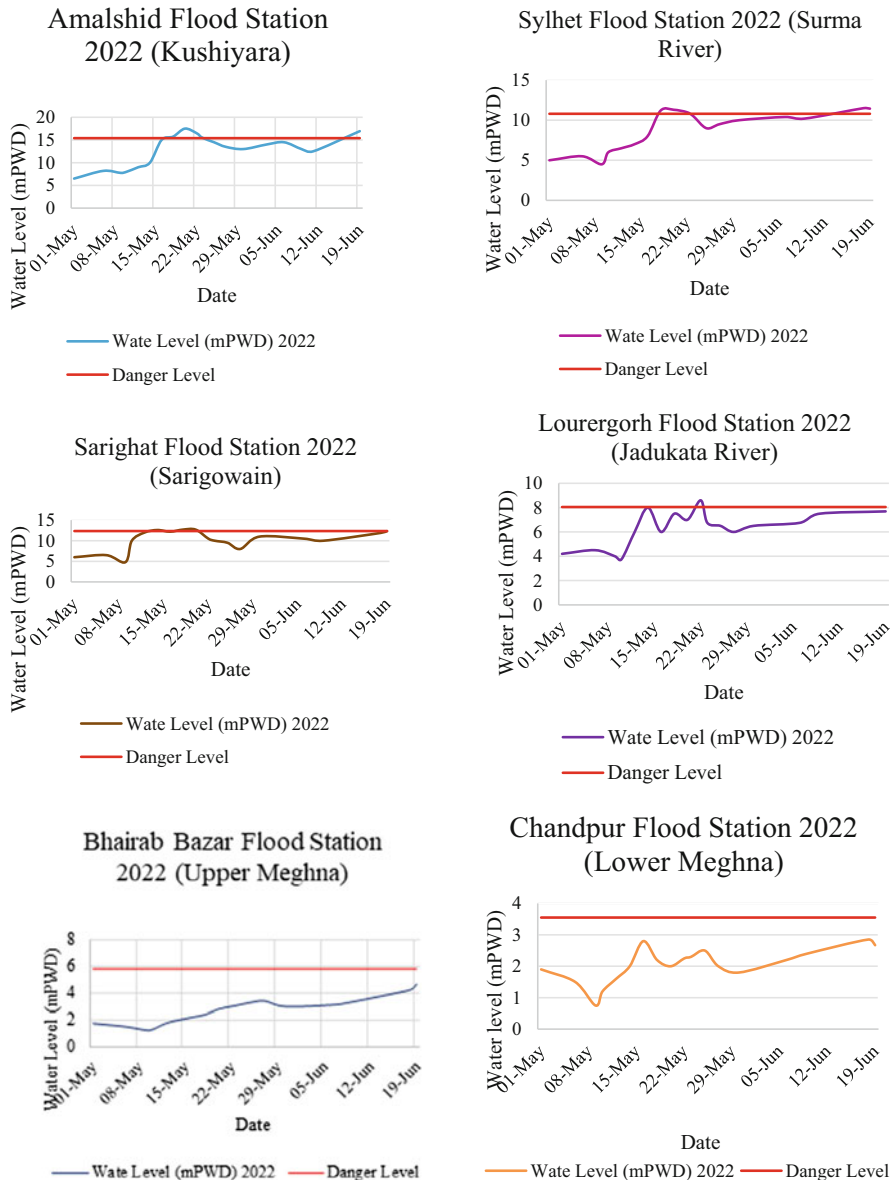


Fig. 18.7 Hydrograph of Meghna basin (2022). (Source: FFWC, 2022)

Seventypercent of Sylhet district and about 60% of neighbouring Sunamganj have been submerged (AFP, 2022).

The second peak of monsoon flood hit the upper Meghna basin due to excessive rainfall in the upstream catchment. It has been reported that on 17th of June only in 24 h, 972-mm rainfall was recorded in Cherrapunji (Assam, India) (Prothom Alo, 2022). As consequence of that, most parts of Sunamganj and Sylhet district become severely inundated. Local rainfall is also high in Sylhet region. Sylhet metropolitan areas have been inundated this time, and greater Sylhet division has broken all previous records of flood inundation and damages. About 90% of the low-lying areas of the division is under water and isolated from the country.

One of the characteristics of the flood of Bangladesh is that it moved from Meghna basin to Brahmaputra basin, and the first peak of Barahmaputra coincided with the second peak of the Meghna flood, as has been observed in 2022 (Prothom Alo, 2022).

Transport system and power stations have been drowned in Sylhet and Sunamganj, and as a result around 0.15 million families were cut off from power supply (UNICEF, 2022). At least 3000 ha of rice paddy fields have been damaged by the flooding. Around 873 educational institutions in Sylhet have been shut down due to the flood crisis. People are suffering from diarrhoea, respiratory infection and skin diseases (The Daily Star, 2022).

The flood has inundated about 1137 ha of agricultural land, and 205 km<sup>2</sup> area has been inundated. About 69,165 people of 10 unions have been affected by this flash flood in Goainghat upazila of Sylhet district (IFRC, 2022).

## 5 Floodplain Morphology

Based on hydrology and physiographic condition, Bangladesh is divided into 30 agro-ecological zones, (AEZ) of which six zones – middle Meghna River floodplain, lower Meghna River floodplain, young Meghna River floodplain, old Meghna River floodplain, eastern Surma-Kushiyara floodplain and Sylhet basin – cover the Meghna floodplain morphology (Table 18.3). These AEZs include distinctive geomorphic units, including back swamps, haors, abundant channels, oxbow lakes, tidal flats and char lands. Based on inundation depth of these AEZs, there exists four categories of floods: shallow flood, when flood depth is less than 1 m and natural levee remains above flood level; moderate flood, when flood depth varies between 1 and 2 m; deep flood when flood depth exceed 2 m and all levees are submerged; and highly deep flood, when the low-lying floodplains and back swamp remain under more than 3 m water depth in Meghna basin area, and one-third of the flooded area is the deeply flood zone and can be characterised by a portion of permanent water bodies throughout the year, such as the haor areas of Sylhet district.

**Table 18.3** Agro-ecological zones of Meghna basin

SL	Region	Sub-region	Area (km <sup>2</sup> )	Location
1.	Arial Beel	Arial Beel	144	Dhaka, Munshiganj
2.	Middle Meghna River Floodplain	Middle Meghna River Floodplain	1555	Kishoreganj, Brahmanbaria, Comilla, Chandpur, Narsindi and Narayanganj
3.	Lower Meghna River Floodplain	(a) Calcareous, flood protected; (b) Calcareous, unembanked; (c) Noncalcareous, flood protected; (d) Noncalcareous, unembanked	909	Chandpur, Lakshmipur and Noakhali districts
4.	Young Meghna Estuarine Floodplain	(a) Nonsaline; Central Bhola; (b) Nonsaline; Meghna Estuary Charland; (c) Nonsaline; North Bhola; (d) Saline; Central Bhola; (e) Saline; Noakhali, Hatiya and Meghna Estuary; (f) Saline; Sandwip and South Bhola	9269	Chittagong, Feni, Noakhali, Lakshmipur, Bhola, Barisal, Patuakhali and Barguna districts
5.	Eastern Surma-Kushiyara Floodplain	Eastern Surma-Kushiyara Floodplain	4622	Sylhet, Moulvi Bazar, Sunamganj and Habiganj districts
6.	Sylhet Basin	(a) Central and Southern; (b) Northern; (c) Western	4573	Sunamganj, Habiganj, Netrokona, Kishoreganj and Brahmanbaria
7.	Old Meghna Estuarine Floodplain	(a) Dhaka-Narayanganj-Demra Project Aiea; (b) High; Old Meghna Estuarine Floodplain; (c) Low: Daudkandi-Habiganj; (d) Low: Dhaka- Shariatpur-Barisal; (e) Low: Eastern Kishoreganj; (f) Low: Gopalganj Beels margins; (g) Low: Habiganj-North Brahmanbaria; (h) Low: Titas Floodplain; (i) Medium Low; (j) Very poorly drained: Laksham-Begumganj	7740	Kishoreganj, Habiganj, Brahmanbaria, Comilla, Chandpur, Feni, Noakhali, Lakshmipur, Narsindi, Narayanganj, Dhaka. Sariatpur, Madaripur, Gopalganj and Barisal districts

Source: FAO (1988) and Rahman et al. (2019)

Within Bangladesh, the topography of Meghna basin is relatively flat and low lying, except a few hillocks in the north and east. The floodplain morphology of the basin is being continuously changing due to rapid siltation, accretion and erosion.

## 5.1 *Sedimentation*

The Himalayan and Burma Arcs are the two sources of water and sediment supply, which are being carried by the GBM river system to shape up the morphology of GBM delta. This part of the sedimentation pulse is supposed to be affected by past mega-seismic events (Brammer, 2014). Regular sediment supply, seasonal fluctuation of sediment influx and earthquake-driven sudden sediment pulses collectively lead to the modification of river morphology.

Datta and Subramanian (1997) have shown that fine to very fine sand grains occupy more than 76% of total grain composition. The remaining portion is dominated by silt and clay. In case of Meghna River, the bed sediment is well sorted than other major rivers. All the bed sediments are positively skewed indicating the domination of finer particles. The suspended particles are finer in case of Meghna than those of Jamuna River.

Wilson and Goodbred (2015) have shown that about one-third of total load of 1 billion tons of sediment is being retained in the Meghna estuary and it is the main source of land formation in the central part of the coast. The LMR is characterised by seasonal fluctuation of sediment flux ranging from  $0.8 \text{ g l}^{-1}$  to  $9 \text{ g l}^{-1}$ .

Sediment flux in the coastal belt is seriously been disrupted by constructing polders in the coastal belt, particularly in the south-west. During the 1960s aiming to increase agricultural outputs by halting saline water influx into the floodplain, massive polderisation programme was undertaken, which finally not only halted saline water but also the sediment influx into the floodplain. In the central part of the coast, particularly in LMR basin, such type of human interventions are minimum, although many other interventions, such as char development project, Muhuri irrigation project and coastal afforestation project, have been implemented. All these projects are somehow related to the sediment budget and sediment accumulation rate in the lower Meghna basin area.

Siltation is one of the most striking oceanographic features of the continental shelf zone of the northern Bay of Bengal. Due to high sediment accumulation in the Meghna estuary, the navigation becomes a serious problem, across the Meghna River mouth. Roy and Islam (2016) have shown that in the Meghna estuary of less than 5-m water depth, the turbidity is very high and reveals the suspended sediment concentration of  $1.9 \text{ g l}^{-1}$ , which is more than  $2 \text{ g l}^{-1}$  near the shore and is not significant ( $<0.3 \text{ g l}^{-1}$ ) beyond the 10-m water depth. Due to season of low water discharge from the river network, this turbidity is mainly triggered by the bottom sediment re-suspension induced by the action of tide and wave energy.

## 5.2 *Riverbank Erosion*

Riverbank erosion is one of the major disasters in Bangladesh. It creates direct and indirect sufferings of 1 million people annually and loss of their properties. It is one

of the major causes of rural-urban migration. It is estimated that in three decades more than 100,000 ha of land has been lost and 800,000 people have been displaced due to riverbank erosion in Bangladesh (Sarker & Thorne, 2009). The long-term sustainability and economic stability of the people have been threatened due to instability of the riverbanks.

Active tectonic settings of the Meghna catchment, due to its location in between Himalayan and Burmese Arcs, are one of the main causes of higher erosion rates in the right bank of lower Meghna River compare to its left bank, which leads to westward shifting of lower Meghna course (Mahmud et al., 2020). The westward shifting of Brahmaputra River to its present course along the present Jamuna is widely documented, and it has its long-lasting impact on 20–30 km westward avulsion of the Meghna River course (Sarker et al., 2011). Present-day Titas might be a remnant of old Meghna River. Widening of the LMR is also associated with bankline shifting and channel equilibrium. Changes in annual run-off and existences of frequent extreme flooding events lead to channel widening to keep the hydraulic equilibrium of the LMR. Expansion of existing chars and emergence of new chars also related to excessive erosion on both sides of the river.

Riverbank stability of the Meghna River is also related to the textural composition of grain sizes in the riverbanks. LMR banks mostly composed of weakly consolidated, stratified fine-grained particles of varying coherent of recent origin. They are easily subject to bank-line failure and lead to enormous damage of fertile lands and displacement of people. Seasonal fluctuations of river discharge are also the leading force to bankline instability and hydraulic changes of river geometry. The discharge of the LMR varies less than  $10,000 \text{ m}^3 \text{ s}^{-1}$  during the dry season to more than  $50,000\text{--}100,000 \text{ m}^3 \text{ s}^{-1}$  during the monsoon (Wilson & Goodbred, 2015). Extreme flooding events, (as observed in 1987, 1988, 2004, 2007 and 2020) might have sudden and remarkable instability and period shifting of banklines of the LMR.

Due to wave action and tidal affect, the morphology of the lower Meghna basin may alter significantly. The Meghna River at Chandpur has historically been experiencing enormous bankline erosion, and over the last five decades, it has been found that the left bank is continuously receding.

## 6 Climate Change Impact

Most climate mode shows that under projected climate change scenarios, the intensity of rainfall in Meghna basin will increase. Mirza et al. (2003) have shown that at  $2^\circ\text{C}$  temperature rise of the mean peak discharge of the Meghna River will increase by 19.9%, with an increase of current peak discharge of  $14,060 \text{ m}^3 \text{ s}^{-1}$  to  $19,861 \text{ m}^3 \text{ s}^{-1}$ . Under  $4^\circ\text{C}$  and  $6^\circ\text{C}$  global temperature rise, the projected peak discharges would be  $20,940 \text{ m}^3 \text{ s}^{-1}$  and  $22,470 \text{ m}^3 \text{ s}^{-1}$ , respectively.

Mohammed et al. (2018) in another model-based study have shown that the flood magnitude in Meghna River basin would be more severe in the future due to global climate change. They have projected that at temperature rise of  $1.5^\circ\text{C}$ ,  $2^\circ\text{C}$  and  $4^\circ\text{C}$

in 100 years return period, the flood intensity of Meghna basin will increase by 15%, 38% and 81%, respectively, which is much higher than that projected for the Ganges and Brahmaputra basin. It is most likely that the combined high flow events of GBM river and also individually for Meghna River will increase in future. They have shown that annual discharge of the Meghna basin increases linearly with basin-wise increase of precipitation. Similar alarming projections are found by a number of studies for greater South Asian region (Mishra & Lilhari, 2016; Turner & Annamalai, 2012, Immerzeel, 2008).

Kamal (2013) also has shown that anticipated climate change likely to have significant impact of flood intensity of lower Meghna River, with significant seasonal variability. The peak flow may increase by 4.5–39.1% during the monsoon, with a decrease of 4.1–26.9% during the dry season, indicating a high seasonality due to climate change impact.

Water and sediment supply in the Meghna catchment is largely been affected by climate change. Kamal (2013) has shown that due to climate change, the peak flow of the GBM river may increase up to 39.1% during monsoon and may decrease up to 26.9% during dry season by the end of this century. Such a projection would lead Bangladesh, particularly the Meghna basin, more vulnerable of intensified monsoon flood inundation in one hand and during dry period to prolonged drought on the other hand.

## **6.1 Hydrological Impact**

Due to its geographical location, the Meghna basin experiences water-induced hydro-meteorological disaster at regular intervals. Climate change will tremendously affect the local hydrological cycle, which would intensify the occurrence of water-induced disasters. Rivers of the upper Meghna basin are comparatively the smallest, steep and relatively flashy. These flashy rain-fed streams might invite localised short-duration flooding event more frequent and more intensified under the changing climatic condition in the future. The intensity, duration and extent of such flash flood might have significant effect on local topography, hydrology and water resources.

The hydrological impact of climate change in the Meghna River basin is well apparent. It shows spatio-temporal variations of rainfall intensity and run-off, which would be more visual in the future. Climate change would intensify the precipitation and run-off, particularly in the north-eastern part of Bangladesh, which mostly occupies the Meghna River basin. It is projected that in the near future the precipitation and run-off in this region would increase by 30% (Masood & Takeuchi, 2016). The flood inundation would be higher due to lower ground elevation compare to upstream part of the Meghna basin, which is the main source of rain water. Therefore, there is more likely of occurrence of frequent and intensified flash flood in the north-eastern hilly regions of Bangladesh in the future.



## 6.2 Cyclonic Impact

Bay of Bengal is the breeding ground of cyclonic depression, many of which turned to storm surges before landfalling along the coastal belt of Bangladesh. Record from all previous major cyclone shows that because of the funnel shape of the estuary, the common pathway of cyclone movement and landfalls is across the Meghna estuary (Fig. 18.8). It has been found that due to shallow continental shelf, the surge is amplified while travelling the lower Meghna valley and creates massive destruction. In case of cyclonic events, this area also being inundated and submerged by storm water surges for a couple of hours, creating huge casualties and loss of properties, as had been experienced in 1970 and 1991 cyclones, when more than 500,000 and 143,000 people were killed, respectively (Hossain & Mullick, 2020) (Table 18.4).

In terms of extent and duration, the storm surge-induced floods are different than those of riverine floods but of severe effects on coastal region. Rahman et al. (2019) in their model study have shown that under the climate change-induced projected sea-level scenarios, the inundation level due to storm surges in the Meghna estuary would increase in the future and would affect the livelihood of about 9 million people. Rahman et al. (2015) have shown that due to climate change the upstream river flows as well the severity and intensity of cyclone-induced storm surges will increase in the future, leading more coastal people, particularly along the Meghna estuary and lower Meghna basin, vulnerable to suffering. The subsidence and river bed sedimentation will intensify the flooding problem (Islam et al., 2002; Goodbred et al., 2003; Rahman et al., 2015). Polders across the coastal belt play an important role to reduce storm surge effects, but the people outside the polders, in case of polder failure, and people inside the polders become highly vulnerable to storm surge-induced flooding.

## 7 Ecosystem Services of Meghna Floodplain

Floodplain ecosystem provides employment opportunity and livelihood to local people through providing goods and services. They act as a source of safety net and a way to poverty alleviation of poor people. Ecosystem services of Meghna floodplain offer the opportunity for the rich people to accumulate more resources and area of tourism and recreation. It provides alternative livelihood for the poor people. Farmers and fishermen are two important folks directly dependent on floodplain ecosystem services. However, the efficiency of ecosystem service-based livelihood and poverty-alleviation efforts depends on how local people get access to the nature-based solution. Meghna floodplains, particularly the low-lying hoar areas, are the rice and fish treasure of the country, supporting direct or indirect livelihood for 20 million people.

Fertile soil, freshwater, nutrients, tidal force and sediment inputs are some of the common nature-based components to explore ecosystem services in the Meghna

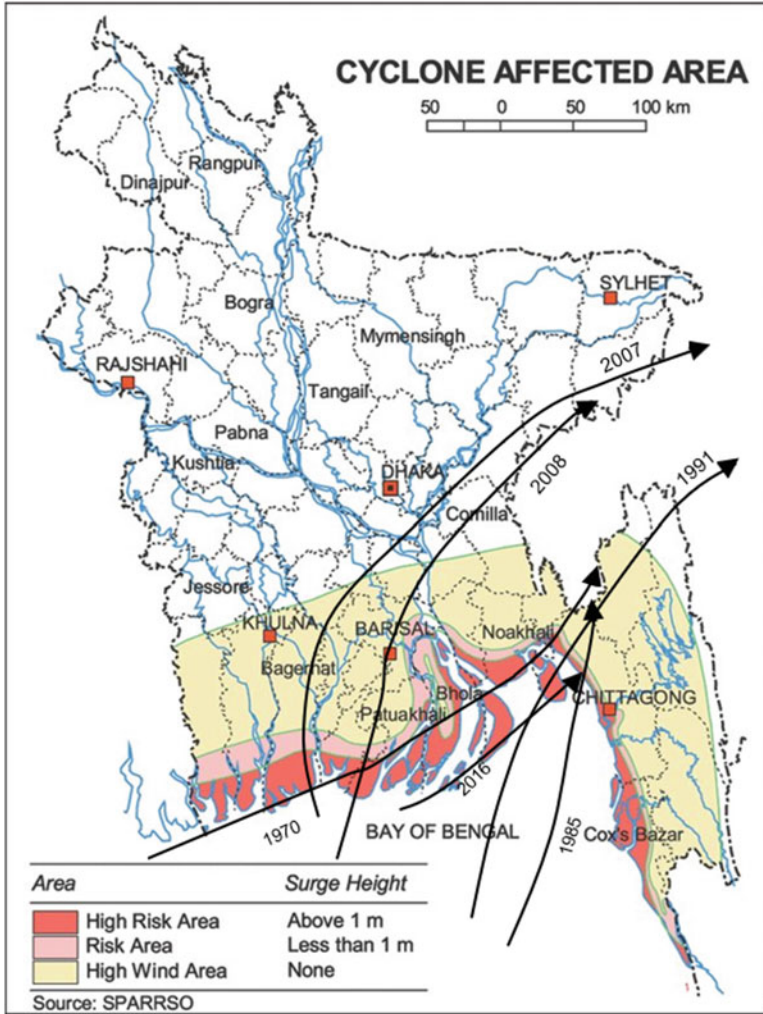


Fig. 18.8 Cyclone paths of previous cyclones. (Source: SPARRSO; Rahman et al., 2019)

basin. They provide ideal condition for fertile and resourceful ecosystem. The most common benefit from this fertile ecosystem is to provide productive agriculture, fisheries and navigation, which proved safety net for local poor people. The reliance ecosystem services of the Meghna floodplain remain important for poverty prevention and poverty alleviation. It addresses nearly all the major goals of the SDGs, particularly goals 1, 2, 3, 4 and 15.

The ecosystem services of the basin area is interconnected and interdependent, and there remains a significant trade-off between different ecosystem services, such as the conflicts between agriculture and fishing, as commonly noticed in the haor and

**Table 18.4** Cyclone passing through Meghna basin (Hossain & Mullick, 2020)

Year	Date	Wind speed (km/h)	Affected area	Deaths
1970	12 November	223	Khulna, Chattogram coast (landfall at Hatia)	500,000
1985	25 May	154	Noakhali, Cox's Bazar coast (landfall at Sandwip)	11,069
1991	29 April	225	Patuakhali-Cox's Bazar coast (landfall north of Chattogram)	143,000
1997	19 May	225	Coastal belt of Bangladesh	126
2007	15 November	215	Coastal belt of Bangladesh	3363
2008	8 May	85	Coastal belt of Bangladesh	3500
2016	19 May	110	Chittagong	26

low-lying areas. Upper Meghna River basin includes about 4000 km<sup>2</sup> haor areas, which become deeply flooded during the monsoon. The economy of local people is hindered by flood damages nearly in every year. It is one of the major source causes of local poverty and threat to local economy. However, the opportunity of nature-based solution is also immense in the haor area, which can be harnessed sustainably and in harmony with nature. Imparting the local harsh natural condition, it is possible to improvise local agricultural product, fisheries, livestock, forestry and many other nature-based solutions.

Similarly, agriculture and shrimp farming, fish larva collection and biodiversity conservation in the floodplain and coastal area are in conflicts. Converting of agricultural land and forest coverage into shrimp farming is an important challenge to nature-based solution and source of ecosystem services, as commonly noticed in the lower Meghna tidal floodplain areas.

Another important challenge to floodplain ecosystem services is the transformation and mobility of services and access to the nature-based resources. Social structure and policy tools are the mechanisms to ensure rural poor people to ensure their access to ecosystem service available in Meghna floodplain areas. The ownership of land and water resources is also a challenge. Community access to publicly own nature-based domain, such as beel, haor, river and wetland services, to ensure ecosystem services needs to be available for rural poor people. The social mechanism of how people perceive their presence to common nature-based services in the floodplain area is an important element of ecosystem services and nature-based solution. In Meghna floodplain region despite highly productive ecological system, poverty persistence and nature-based solution yet need more attention to connect.

## 8 Floodplain Economy

The Ganges, Brahmaputra-Jamuna, Teesta and Meghna Rivers are the lifeline of millions of around 500 million people of South Asia. They cover a catchment area of about 175 million ha and supply water for agriculture, fishing, industry, navigation,

industrial and household activities. The source of water of these rivers are either ice meeting in Himalayan region, torrential rainfall in the catchment area or cyclonic events.

Seasonal flooding is a blessing to farmers in one hand and disastrous to the other hand. Soil fertility in the floodplain is improved due to seasonal inundation, which invites people to settle in the floodplains and engage themselves in agricultural activities with hope of good harvest. However, unusual floods can be disastrous, and people living the low-lying floodplains are always under the threat of losing their harvest. In lower Meghna basin, the fertile soil and unique topography are contributory to the economy by providing water for agriculture, fisheries, navigation and biodiversity conservation. The floodplain of lower Meghna River provides ecosystem services for agricultural production, fishing and ecological nourishment.

Compare to Ganges and Brahmaputra basin, the proportionate of Meghna basin within Bangladesh is higher (43%). The area inside Bangladesh territory is relatively flat, has formed extensive floodplain and is the rice and fishing ground of the country. The boro rice production during the dry season and fish catch during the monsoon are two important economic activities of the local people and driving sources of national economy. The basin produces 16% of total rice production (Quddus, 1970) and supports the livelihood of 20 million people. The annual production of boro at this region is about 3 million metric tons, which accounts 12% of total annual rice production. However, this important agricultural bowl of the country is being affected by pre-monsoon (April–May) and monsoon (June–September) flood nearly in every year, causing damages of people's livelihood. The agriculture and standing crop of this area is frequently affected by advances of floods and flash flood events, as has been observed this year (2022).

It is projected that in the near future the precipitation and run-off in this region would increase by 30% (Masood & Takeuchi, 2016). This would intensify flash flood in this region, which would destroy agricultural products and fisheries. To protect the standing crops from climate change-induced intensified flash flood incident, it is necessary to take protective steps before harvesting and supporting farmers with adaptable crop varieties.

The lower Meghna River is the prime fishing location in Bangladesh and is an important source to fill the national demand. However, the catch in an estuary and river mouth largely depends of seasonal variation of tide, local weather condition and flood intensity. Rising tide level created lateral expansion of flood inundation and more waterlogging, whereas low tide created navigation problems to the fishermen. The fish catches at the Meghna River estuary, which is an important sector of local employment and economy, are largely of naturally determinant and seasonally controlled. During the monsoon, due to bad weather condition, the catch is very often jeopardised, and local fishermen have to take shelter to a safer place, suspending their catches.

## 9 Flood Management

It has been mentioned earlier that the Meghna basin area is highly vulnerable to annual flooding. The top priority of flood management in this region is, thus, to reduce the damages of standing crops and ensure the food security. Effective flood management requires timely flood forecasting and accurate risk assessment. It can help the decision-makers to take appropriate mitigation measures. Hydrological modelling can help to take appropriate flood adaptation and mitigation measure. However, appropriate application of hydrological modelling in Meghna basin is difficult because 60% of the basin area is located outside Bangladesh. Without accurate rainfall data of upper catchment area and water flows data of upstream rivers, the flood simulation model is not reliable and dependable. Climate change-induced regional hydro-climatological changes remain another challenge to flood modelling. Moreover, the massive human interventions in the catchment, particularly the completed and proposed cross-dams and water controlling measures in the upstream areas make the flood situation in Meghna basin uncertain and unmanageable. It is, thus, necessary to adapt basin-wise management strategies and measures.

Basin-wise flood management requires the reduction flood intensity, reduction of flood damage, ensuring food security, ensuring poverty alleviation, promoting local economy and conserving basin environment. As much of the basin lies outside Bangladesh, it is thus not realistic to manage flood and water resources of Meghna River and make any flood management plan success by Bangladesh alone. Due to increasing seasonal and annual variation of river flow, most of which is rain fed from upstream and climate change driven; it is difficult to manage flood and water resources of Meghna River singly by Bangladesh. Climate change-induced impact of Meghna basin is expected to be more prominent in the future and requires cooperation among co-riparian countries. It requires sharing and cooperation in aspects of flood management among the concerned countries. Both flood and drought can be managed with regional cooperation among the co-riparian countries. To achieve that long-term basin-wise planning and sustainable water resource management, plan is prerequisite. There is also a requirement of a good coordination between the academia, practitioners, professionals, bureaucrats and politicians of the concern countries.

The enhancement of end-to-end early warning system should be an area of urgent need. Transboundary cooperation among and within the South Asian countries, which includes around 10% of world population, requires international cooperation. The major area of cooperation includes real-time data sharing, sharing information on flood forecasting, exchange of knowledge and technology and collaborative research. All riparian countries, such as Bangladesh, India, China, Nepal and Bhutan, require adopting basin-based approach to address flood and water resource-related issues. It can be done under an umbrella of hydro-meteorological services. Regional cooperation on hydro-meteorological issues will enhance regional economic and political stability and towards the achievement of nearly all targets of SDG-6.

## 10 Conclusions

Flood, floodplain ecology and livelihood of local people are closely links in Bangladesh. In Meghna River basin, rice and fish are two important nature-based resources, which supports national economy and significantly contribute to national GDP. However, unusual and unexpected flood in the basin is a threat to the lives and livelihood of people. The local economy of Meghna basin improvise local economy due to existence of harsh natural environment, such as in haor areas and coastal areas. Such areas are very poorly connected to the city centres, and due to poor communication of urban economics, access to industrial and service sectors is very negligible. Employment opportunities in industries and poor access to urban facilities lead local people to depend more on nature-based solution for their lives and livelihoods. In the Meghna basin, one of the worst accesses to Dhaka City, people cannot find their works in the capital or nearby cities and are forced to live in poverty with nature at home. Any disruption of natural ecosystem services and nature-based solution either by unusual flood or by drought in dry season is a threat to their livelihood and source of poverty. However, in order to create employment opportunities and promote local economy, it is necessary to mitigate flood damage and improvise nature-based solution at grassroot level.

## References

- AFP. (2022). *Millions marooned as worst floods in 20 years ravage Bangladesh*. Dawn. <https://www.dawn.com/news/1691051>, May 23, 2022.
- Ali, A. (1995). A numerical investigation into the back water effect on flood water in the Meghna River in Bangladesh due to the south-west monsoon wind. *Estuarine, Coastal and Shelf Science*, 41(6), 689–704. <https://doi.org/10.1006/ecss.1995.0084>
- Allison, M. A., Khan, S. R., Goodbred, S. L., Jr., & Kuehl, S. A. (2003). Stratigraphic evolution of the late Holocene Ganges–Brahmaputra lower delta plain. *Sedimentary Geology*, 155(3–4), 317–342. [https://doi.org/10.1016/s0037-0738\(02\)00185-9](https://doi.org/10.1016/s0037-0738(02)00185-9)
- Bakr, A. (1977). *Quaternary geomorphic evolution of the Brahmanbaria-Noakhali area, Comilla and Noakhali districts*. Geological Survey of Bangladesh.
- Banglapedia. (2021). *Banglapedia*. Asiatic Society of Bangladesh. <https://en.banglapedia.org/index.php/River>
- Brammer, H. (2014). Bangladesh's dynamic coastal regions and sea-level rise. *Climate Risk Management*, 1, 51–62. <https://doi.org/10.1016/j.crm.2013.10.001>
- Daily Star. (2022). *The Daily Star*. <https://www.thedailystar.net/youth/education/news/873-schools-colleges-closed-due-nonstop-rain-sylhet-sunamganj-3027081>, 19 May 2022.
- Datta, D. K., & Subramanian, V. (1997). Texture and mineralogy of sediments from the Ganges–Brahmaputra–Meghna River system in the Bengal Basin, Bangladesh and their environmental implications. *Environmental Geology*, 30(3–4), 181–188. <https://doi.org/10.1007/s002540050145>
- Egairé Humphrey, L. (Ed.). (2012). *Surma-Meghna River System*. Claud Press.
- EU. (2022). [https://www.eeas.europa.eu/delegations/bangladesh/european-union-brings-relief-those-affected-flash-floods-north-eastern\\_en?s=164](https://www.eeas.europa.eu/delegations/bangladesh/european-union-brings-relief-those-affected-flash-floods-north-eastern_en?s=164), 8 June, 2022.

- FFWC. (2021). *Annual flood report*. <http://www.ffwc.gov.bd/images/annual20.pdf>. Flood Forecasting and Warning Centre.
- FFWC. (2022). *Flood forecasting and warning centre*. BWDB, Bangladesh. Retrieved June 20, 2022, from <http://www.ffwc.gov.bd>
- Goodbred, S. L., Jr., Kuehl, S. A., Steckler, M. S., Maminul, H., & Sarker. (2003). Controls on facies distribution and stratigraphic preservation in the Ganges–Brahmaputra delta sequence. *Sedimentary Geology*, 155(2003), 301–316.
- Hossain, I., & Mullick, A. (2020). Cyclone and Bangladesh: A historical and environmental overview from 1582 to 2020. *International Medical Journal*, 25, 2595–2614.
- IFRC. (2022). <https://www.ifrc.org/press-release/bangladesh-severe-flooding-puts-more-4-million-people-risk-food-insecurity-and>, 18 June, 2022.
- Immerzeel, W. (2008). Historical trends and future predictions of climate variability in the Brahmaputra basin. *International Journal of Climatology: A Journal of the Royal Meteorological Society*, 28(2), 243–254. <https://doi.org/10.1002/joc.1528>
- Iqbal, J., & Raham, K. S. (2020). *Bangladesh monsoon floods 2020 -coordinated preliminary impact and needs assessment*. (Unpublished).
- Islam, M. R., Begum, S. F., Yamaguchi, Y., & Ogawa, K. (2002). Distribution of suspended sediment in the coastal sea off the Ganges–Brahmaputra River mouth: Observation from TM data. *Journal of Marine Systems*, 32(2002), 307–321.
- Islamic Relief Bangladesh. (2022). <https://islamicrelief.org.bd/response-to-flash-flood-in-north-eastern-region-of-bangladesh2022/>, 7 June, 2022.
- IUCN, BRIDGE and OXFAM. (2018). *Opportunities for benefit sharing in the Meghna Basin, Bangladesh and India*. [https://www.iucn.org/sites/dev/files/content/documents/2018/meghna\\_profile.pdf](https://www.iucn.org/sites/dev/files/content/documents/2018/meghna_profile.pdf)
- Jiang, L., Wu, S., Liu, Y., & Yang, C. (2021). Grain security assessment in Bangladesh based on supply-demand balance analysis. *PloS One*, 16(5), e0252187. <https://doi.org/10.1371/journal.pone.0252187>
- Kamal, R. (2013). Response of river flow regime to various climate change scenarios in Ganges–Brahmaputra–Meghna basin. *Journal of Water Resources and Ocean Science*, 2(2), 15. <https://doi.org/10.11648/j.wros.20130202.12>
- Mahmud, M. I., Mia, A. J., Islam, M. A., Peas, M. H., Farazi, A. H., & Akhter, S. H. (2020). Assessing bank dynamics of the Lower Meghna River in Bangladesh: An integrated GIS-DSAS approach. *Arabian Journal of Geosciences*, 13(14). <https://doi.org/10.1007/s12517-020-05514-4>
- Masood, M., & Takeuchi, K. (2016). Climate change impacts and its implications on future water resource management in the Meghna Basin. *Futures*, 78–79, 1–18. <https://doi.org/10.1016/j.futures.2016.03.001>
- Mirza, M. Q., Warrick, R. A., Ericksen, N. J., & Kenny, G. J. (1998). Trends and persistence in precipitation in the Ganges, Brahmaputra and Meghna river basins. *Journal Des Sciences Hydrologiques [Hydrological Sciences Journal]*, 43(6), 845–858. <https://doi.org/10.1080/02626669809492182>
- Mirza, M. M. Q., Warrick, R. A., & Ericksen, N. J. (2003). *Climatic Change*, 57(3), 287–318. <https://doi.org/10.1023/a:1022825915791>
- Mishra, V., & Lilhare, R. (2016). Hydrologic sensitivity of Indian sub-continental river basins to climate change. *Global and Planetary Change*, 139, 78–96. <https://doi.org/10.1016/j.gloplacha.2016.01.003>
- Mohammed, K., Islam, A. K. M. S., Islam, G. M. T., Alfieri, L., Khan, M. J. U., Bala, S. K., & Das, M. K. (2018). Future floods in Bangladesh under 1.5°C, 2°C, and 4°C global warming scenarios. *Journal of Hydrologic Engineering*, 23(12), 04018050. [https://doi.org/10.1061/\(asce\)he.1943-5584.0001705](https://doi.org/10.1061/(asce)he.1943-5584.0001705)
- Paszkowski, A., Goodbred, S., Jr., Borgomeo, E., Khan, M. S. A., & Hall, J. W. (2021). Geomorphic change in the Ganges–Brahmaputra–Meghna delta. *Nature Reviews Earth & Environment*, 2(11), 763–780. <https://doi.org/10.1038/s43017-021-00213-4>

- Prothom Alo. (2022). Retrieved June 18, 2022, from <https://en.prothomalo.com/topic/Flood>
- Quddus, M. A. (1970). Crop production growth in different agro-ecological zones of Bangladesh. *Journal of the Bangladesh Agricultural University*, 7(2), 351–360. <https://doi.org/10.3329/jbau.v7i2.4746>
- Rahman, M. M., Haque, A., Nicholls, R. J., Jisan, M. A., Nihal, F., Ahmed, I., & Lazar, A. N. (2015). *Storm surge flooding in the Ganges-Brahmaputra-Meghna Delta: Present and future scenarios*. In E-proceedings of the 36th IAHR World Congress 28 June – 3 July, 2015, The Hague, the Netherlands.
- Rahman, S., Islam, A. K. M. S., Saha, P., Tazkia, A. R., Krien, Y., Durand, F., Testut, L., Islam, G. M. T., & Bala, S. K. (2019). Projected changes of inundation of cyclonic storms in the Ganges–Brahmaputra–Meghna delta of Bangladesh due to SLR by 2100. *Journal of Earth System Science*, 128, 145. <https://doi.org/10.1007/s12040-019-1184-8>
- Sarker, M. H., & Thorne, C. R. (2009). Morphological response of the Brahmaputra–Padma–lower Meghna river system to the Assam earthquake of 1950. In *Braided Rivers* (pp. 289–310). Blackwell Publishing Ltd.
- Sarker, M. H., Akter, J., & Noor, F. (2011). Sediment dispersal processes and management in coping with climate change in the Meghna Estuary, Bangladesh. In *Proceedings of the ICCE workshop* (Vol. 349, pp. 1–16). IAHS Publication.
- Turner, A. G., & Annamalai, H. (2012). Climate change and the South Asian summer monsoon. *Nature Climate Change*, 2(8), 587–595. <https://doi.org/10.1038/nclimate1495>
- UNDP and FAO. (1988). *Land resources appraisal of Bangladesh for agricultural report no. 2* (pp. 212–221). Agro-Ecological Region of Bangladesh. United Nations Development Program in Food and Agriculture Organization.
- UNICEF. (2022). Retrieved June 18, 2022, from <https://reliefweb.int/report/bangladesh/over-15-million-children-risk-devastating-floods-hit-bangladesh-unicef>
- Wilson, C. A., & Goodbred, S. L., Jr. (2015). Construction and maintenance of the Ganges-Brahmaputra-Meghna delta: Linking process, morphology, and stratigraphy. *Annual Review of Marine Science*, 7(1), 67–88. <https://doi.org/10.1146/annurev-marine-010213-135032>



# Chapter 19

## Flooding and Floodplain Management Around Dhaka City: A Case of Buriganga and Shitalakhya Rivers



Asib Ahmed and Md. Shamim Hossain

**Abstract** The geographical location of the Buriganga and the Shitalakhya Rivers bears importance in the context of flooding in and around a megacity like Dhaka. Therefore, this chapter analyzes the flooding and floodplain management of Buriganga and Shitalakhya. The present study is based on primary and secondary data and followed qualitative research method. Flood hits every year in the Buriganga and the Shitalakhya with varying degree of nature and magnitude. Since 1954, major floods in the years 1955, 1970, 1974, 1980, 1987, 1988, 1998, 2004, 2007, and 2017 largely impacted on the floodplains of Buriganga and Shitalakhya. However, the concerned authority has been taken several structural interventions (e.g., embankment, flood shelter center, highways and railways, maintenance of river, floodwall, retention pond, etc.) and nonstructural measures (e.g., flood forecasting and warning (this is structural measure), flood proofing, etc.) for managing floods in the floodplain areas of the rivers. This chapter is useful for flood managers, researchers, and local people in identifying the nature of flood and management interventions in the Buriganga and Shitalakhya river basins.

**Keywords** Dhaka City · Buriganga · Flooding · Floodplain management · Shitalakhya

## 1 Introduction

Bangladesh is a flood-prone country. Every year, flood hits in the country with different nature and magnitude. There are several reasons for regular flooding in Bangladesh such as geographical location, huge amount of monsoon rainfall (i.e.,

---

A. Ahmed (✉)

Department of Geography and Environment, University of Dhaka, Dhaka, Bangladesh  
e-mail: [asib01geo@du.ac.bd](mailto:asib01geo@du.ac.bd)

M. S. Hossain

Department of Geography and Environmental Science, Begum Rokeya University, Rangpur, Bangladesh

about 80%), high precipitation (i.e., 2300 mm annually on average), huge number of rivers (i.e., 230 rivers with 57 trans-boundary rivers), lower riparian country, and physiography of the country (i.e., 80% floodplain area) (BWDB, 2019; MoDMR, 2014; Parvin et al., 2018). However, there are five rivers flowing across Dhaka and its surrounding areas that include the Buriganga in the south, Turag in the west, Tongi in the north, the Lakhya in the east, and the Balu in the southeast (Masuya et al., 2015). Flood visits in Buriganga and Shitalakhya almost every year with varying degree of nature and magnitude. Hence, nearby areas of these two rivers remain underwater up to 5–15 feet during monsoon season. Floods are causing direct and indirect damages to the crops (e.g., especially rainy season crops), ecology, environment, and people in the floodplain areas of Buriganga and Shitalakhya.

## 2 Study Area

The Buriganga River is flowing from the southwestern side of Dhaka City and meets at the confluence of Padma (Ganges) and upper Meghna (Fig. 19.1). The average depth of the river is about 7.6 m, and the maximum depth is 18 m. Its average width is 400 m, and average length is 27 km (Chowdhury, 2021; Kibria et al., 2015; Majumder, 2009). The Buriganga River is a tributary of the Dhaleswari River which falls into the Meghna River. At the western side, a small river Turag falls into the Buriganga in the northern part of the Dhaka City area. The main sources of water of the Buriganga River come through the Turag River along with local runoffs. The upstream of the Buriganga was formerly a branch of the Dhaleswari River and contributed substantially to the flow of the Dhaleswari (SWMC, 1996). However, the upper part of the Buriganga has already been silted up to Chhaglakandi point. The downstream junction varies from time to time in response to the changes of the Dhaleswari River. The downstream junction is currently at about 3.22 km southwest of Fatullah (Chowdhury, 2021). One of the branches of the Ganges River flowed into the Bay of Bengal through the Dhaleswari River which, over time, changed its course and eventually lost its connection with the primary flow of the Ganges River and was renamed as Buriganga (Old Ganges) (Majumdar, 1971).

The Shitalakhya River is a distributary of the Brahmaputra River. The river in its earlier stages flows to the southwest direction and then east of the city of Narayanganj, until it merges with the Dhaleswari near Kalagachhiya (Fig. 19.1). The river is nearly 110 km long and 300 m wide. Maximum depth of the river is 21 m, and average depth is 10 m (Murshed, 2012). The river flows through Gazipur district forming its border with Narsingdi for some distance and then through Narayanganj district. Shitalakhya is a branch of the Brahmaputra and bifurcates into two courses, affecting the flow of water in the Shitalakhya. The main flow of the Brahmaputra waters is through the Jamuna channel. After tracing a curve round the Garo Hills on the west, it took a sharp turn in the southeast direction near Dewanganj and, then passing by Jamalpur and Mymensingh, threw off the Shitalakhya branch and flowed through the eastern side of Dhaka district and fell into the Dhaleswari.

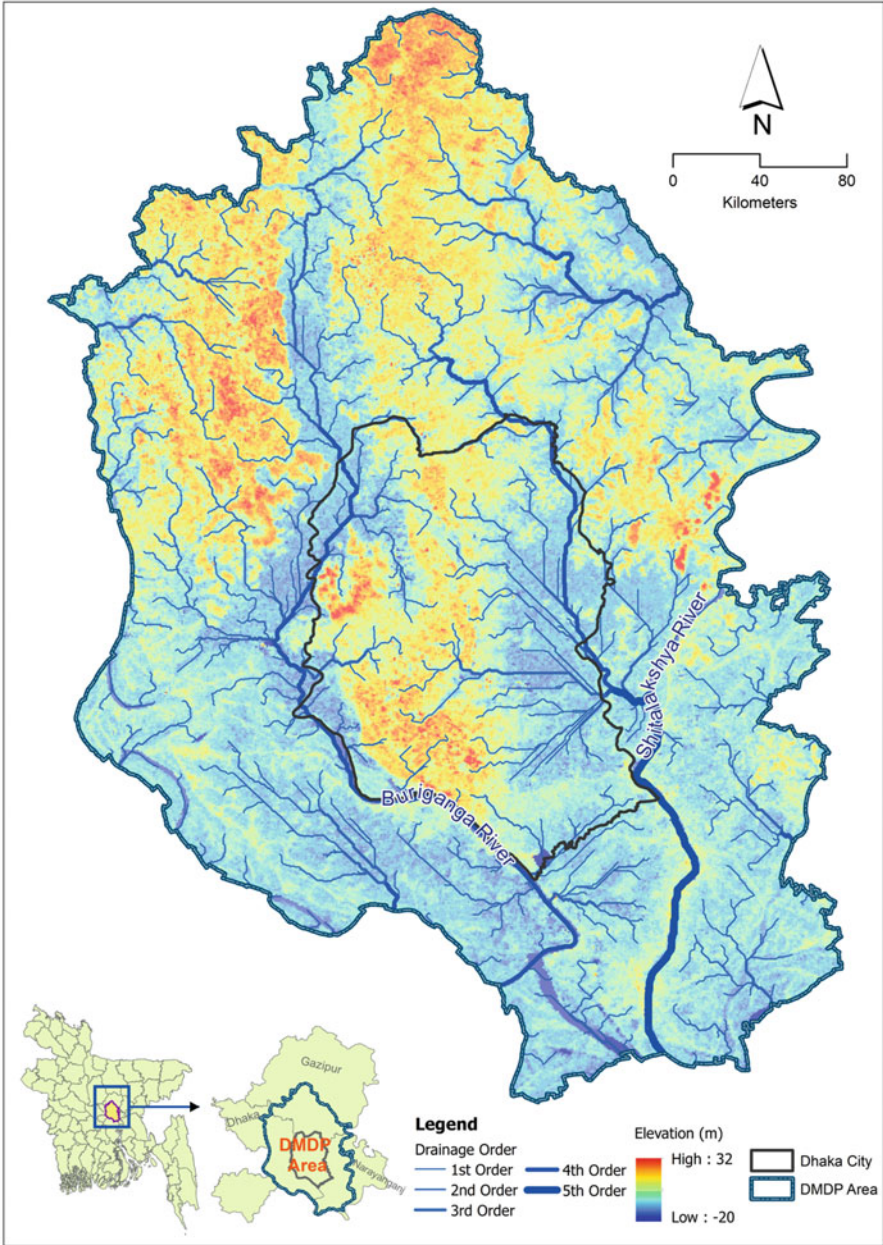


**Fig. 19.1** The drainage network around Dhaka City covering Dhaka Metropolitan Development Plan (DMDP) area. The location of Buriganga and the Shitalakshya Rivers in the network embrace the city from west and east sides, respectively. (Source: Authors, 2022)

The Shitalakhya runs almost parallel to the Brahmaputra and joined the Dhaleswari after passing by Narayanganj (Majumdar, 1971).

### 3 Historical Perspective of Floods

The flood of 1988 posed a great threat to the Buriganga and Shitalakhya river basins. At the time of 1988 flood, level of water overran the top of the Dhaka Narayanganj and Demra (DND) embankment. In 1988, the water level of Buriganga was 7.58 m PWD at the Mill Barrack station (Islam et al., 2020). However, based on duration as well as magnitude, the flood 1998 was incomparable to the previous highest floods (Saleh et al., 1998). The highest flood level at the Shitalakhya riverside was 6.49 m PWD (Public Works Datum) during 1998 floods. Elsewhere, designed upper pump limit was 5.79 m PWD. The high water level above pump limit continued for 44 days (Munshi & Amin, 2008).

### 4 Materials and Methods

This chapter follows qualitative research method. The study conducted five focus group discussions (FGDs) in the study area where each group consists of five local people including both male and female. Moreover, ten key informants' interview (KIIs) have been taken to validate the responses obtained from the FGDs. Of them, there were three academicians, three local people who have lifelong experiences on flooding in the area, and four other key informants from relevant organizations (i.e., Bangladesh Water Development Board (BWDB), Disaster Management Bureau (DMB), Department of Disaster Management (DDM), and Ministry of Disaster Management and Relief-MoDMF). Present study also uses secondary data that were collected from different reports of BWDB, DMB, DDM, MoDMF, and the Government of People's Republic of Bangladesh for the analysis of historical perspectives of floods and the nature and magnitude of floods. Besides, data from the Office of Emergency Preparedness, Executive Office of the President of the United States (OEP-EOP, 1972), have been used. Furthermore, a number of literatures have been reviewed for collecting reliable data and information for further analysis of the chapter.

### 5 Nature and Magnitude of Floods

Floods are very common phenomena in Buriganga and Shitalakhya Rivers (Fig. 19.2). Almost every year flood hits these rivers. However, the nature and magnitude of floods vary for different years. Table 19.1 represents the water level

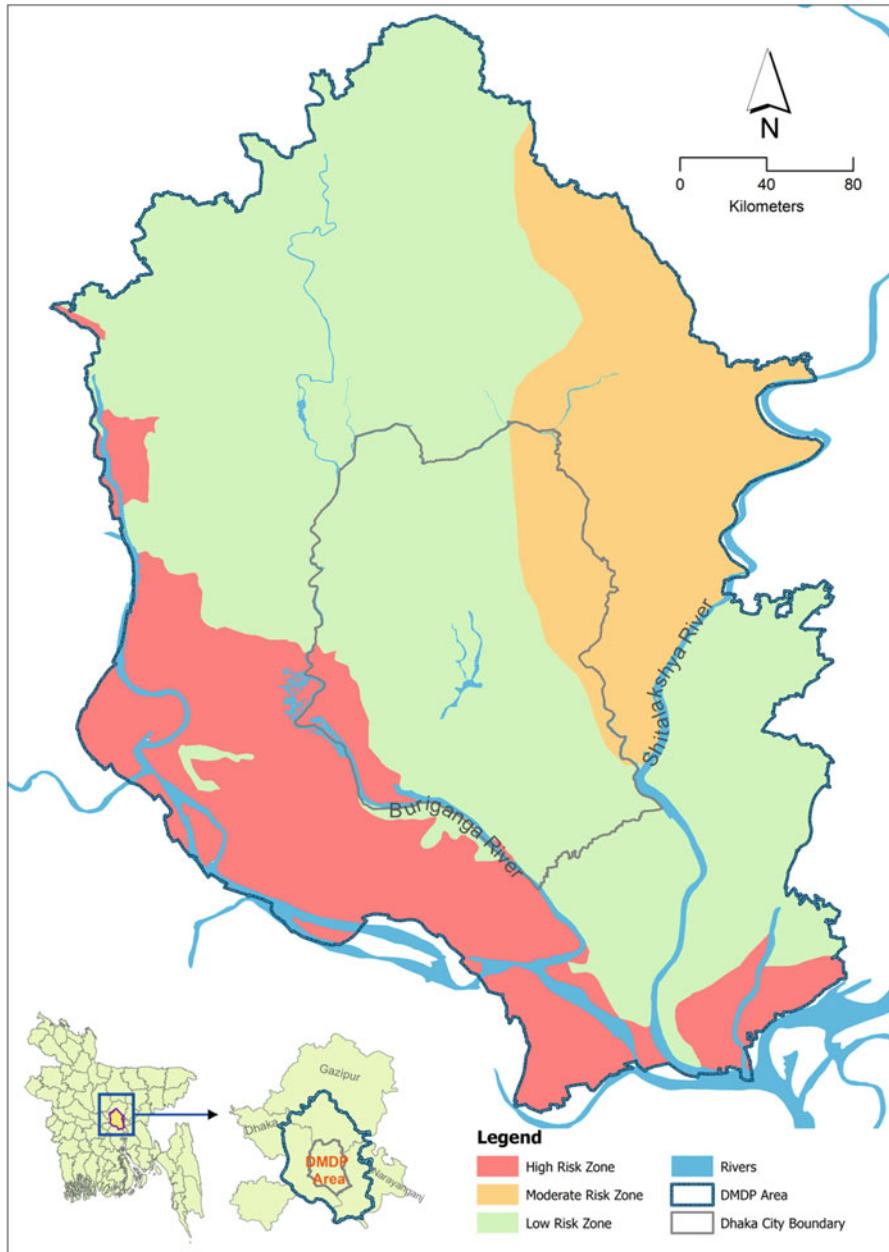


**Fig. 19.2** Flood risk zonation surroundings the Buriganga and the Shitalakshya river. (Source: Authors, 2022)

**Table 19.1** Water level of some floods at the Buriganga and Shitalakhya River from 2015 to 2019

River	Station	Previously recorded maximum (m)	Danger level (m)	Peak of the year (m)				
				2019	2018	2017	2016	2015
Buriganga	Dhaka	7.58	6.00	4.9	4.64	5.22	5.21	5.2
Shitalakhya	Narayanganj	6.93	5.50	5.33	4.95	5.74	5.82	5.6

Source: BWDB (2015, 2016, 2018, 2019)

at the Buriganga and the Shitalakhya Rivers from 2015 to 2019. It is observed that the water level during the last 5 years at the Buriganga River near Dhaka station did not cross the danger level. However, different scenarios are observed at the Shitalakhya near Narayanganj station. Except 2018 and 2019, the water level at Shitalakhya River crossed danger level for every year.

## 6 Drivers and Causes of Floods

### 6.1 Natural Forces

There are a number of natural reasons for occurring floods in the surrounding area of Buriganga and Shitalakhya. The key causes are over rainfall, low topography, and flat slope of the river basin along with some other causes that include the following issues:

***The Geographic Location and Climatic Pattern*** Bangladesh is situated at the bottom of the Himalayas. The highest mountain range in the world is also the highest precipitation zone in the world. This precipitation, i.e., rainfall, is caused by the control of the southwest monsoon. Moreover, the utmost rainfall area in the world, for example, Cherrapunji, is also lying a few kilometers northeast of the Bangladesh boundary. An increased amount of local rainfall results flood every year in and around the Buriganga and the Shitalakhya (BWDB, 2019). Moreover, yearly rainfall (i.e., 2085 millimeters) and monthly rainfall of Dhaka and its beyond accelerate the situation of flooding in and around the Buriganga and the Shitalakhya. The monthly average rainfall of Dhaka is ranging from 8 mm in January (the driest month) to 375 mm in July (the wettest month) (BMD, 2022).

***The Junction of Three Prime Rivers Together with the Ganges, the Brahmaputra, and the Meghna (GBM)*** The runoff from their enormous catchment (about 1.72 million km<sup>2</sup>) passes by a small area. About 8% of these catchments stays inside Bangladesh. At the monsoon season, the large volume of water entering Bangladesh from upstream is higher than the capacity of the rivers to discharge into the Bay of Bengal. Therefore, every year floods are occurring in Bangladesh including the Buriganga and the Shitalakhya floodplain areas (BWDB, 2019).

**Table 19.2** Sedimentation status of the Buriganga and Shitalakhya Rivers

River	Sediment grain size d <sub>50</sub> [mm]	Sediment concentration [mg/l]
Burigana (1989–2000)	0.116	377
Shitalakhya (1985, 1989, 1995, 1999, 2000)	0.166	547

Source: JICA (2000) and Hossain et al. (2014)

**Coincide of Flood Peaks** The coincidence of flood peaks for three principal rivers which include the Ganges, the Brahmaputra, and the Meghna occurred between a 14-day period, resulting in an abrupt increase in the level of water across all rivers of Bangladesh (GoB and UNDP, 1989; Brammer, 1990). This affects the Buriganga and the Shitalakhya causing floods in the area (Khalequzzaman, 1994).

**Sedimentation** The larger-grained sediments are deposited near the source area on the river beds due to higher settling velocity, forming sandbars. Continuous sedimentation decreases the gradient of a river. Low gradient and high sedimentation are responsible for aggradation of riverbed (Table 19.2). Riverbed aggradation reduces the water-carrying capacity of the river, resulting them to overflow their banks and contribute to flooding in and around the Buriganga and the Shitalakhya river basin (Khalequzzaman, 1994).

## 6.2 Anthropogenic Factors

Along with natural causes, there are many anthropogenic reasons which are responsible for occurring floods in the Buriganga and the Shitalakhya including:

**Unplanned Urbanization and Industrialization** Unplanned urbanization and industrialization are mainly responsible for urban flooding and bring lots of suffering to the stakeholders. Both area of Buriganga and Shitalakhya are occupied by urbanization and industrialization (Munshi & Amin, 2008). For example, the capital of Bangladesh stands on the Buriganga River. People of Dhaka City dump their residential garbage as well as industrial wastes into the Buriganga River. On the other side, the jute mills and other large industries including the world largest Adamjee Jute Mills (presently known as Adamjee Export Processing Zone) of the country are located on the riverside of Shitalakhya. There are more than 20 jute mills along the riverside of Shitalakhya. These jute mills throw the solid wastes of jute (e.g., dry leaves, dry sticks, etc. which cannot be used as fiber) into the river. Thus the Shitalakhya River is dying due to enormous discharge of solid waste from the garments and jute mills. As a result, both the rivers are dying because of dumping of wastes from houses and industries. Hence, floods are occurring in the Buriganga and the Shitalakhya frequently.

***Land Grabbing and Development Activities*** Some people have encroached internal *khals*, canals, and even significant portions of riversides. They set up new homesteads, industries, markets, shops, brickfields, filling stations, cinema hall, and so on. There are some land developer companies continuing landfilling in these areas. Moreover, some governmental departments including RAJUK (the capital development authority), DIT, WASA (Water Supply and Sewerage Authority), and Road and Highways Department had encroached large portion of agricultural lands for development purposes (Munshi & Amin, 2008). For instance, in the southern portion of Buriganga River, RAJUK commenced a residential project on an area of about 381 acres. Further, about 3000 square kilometers of natural water bodies have already disappeared by the development of housing on the southern part of Buriganga riverbank. This rapid and excessive development around the Buriganga aggravated the urban flooding problem in and around Dhaka (Khalequzzaman, 1994; Rahman, 2010).

***Construction of Embankments*** Surrounding areas of the rivers are protected by heightened roads cum embankment like a triangle. As a result, lands are used in unplanned and unregulated ways for construction of roads and highways, homesteads, industries, market, institutions, and other development purposes in the floodplain resulting obstructions of water flow (Munshi & Amin, 2008). To save Dhaka, Narayanganj, and Demra from the two mighty rivers Buriganga, and Shitalakhya, respectively, the Government of Bangladesh constructed a dam popularly known as DND dam. Dhaka (on the side of Buriganga), Narayanganj (on the side of Shitalakhya), and Demra (DND) enclosed by the embankment. Taking advantages from embankment, different types of infrastructures have been developed. At the one hand, stagnant water is blocked by unplanned and unregulated infrastructures; on the other hand, canal within the DND is encroached by the local people. So, drainage through the canal also hampered. Hence, most of the time of a year, this area is underwater. As a result, during monsoon season heavy rainfall accelerates the flooding problem of the study area.

***High Population Density*** Because of the existence of two prominent cities (i.e., Dhaka City and Narayanganj City), the floodplain areas of the Buriganga and the Shitalakhya are overpopulated. Overpopulation creates extra pressure on the land, and, hence, vacant land areas of the riversides of Buriganga and Shitalakhya are transformed to infrastructure development such as houses, industries, etc.

## **7 Impact of Floods on Physical Environment**

From geomorphological point of view, the Buriganga and the Shitalakhya Rivers are dynamic. The frequent occurrences of flood change the geomorphological settings of the Buriganga and Shitalakhya floodplain areas (Table 19.3) along with other relevant factors such as the slope of the river valleys, the sediment properties, and the large number of sediment supply (Hossain et al., 2014).



**Table 19.3** Hydro-geomorphological changes on the rivers around Dhaka

River	Changes in riverbed elevation	Changes in top width [m/year]	Left/right bank line change [m/year]
Buriganga (1989–2009)	−6.3 to −16.2	7.3–12.4	LB: 1.7–5.8 RB: 1.3–6.8
Shitalakhya (1985, 1989, 1995, 1999, 2009)	−0.4 to −14.1	3.3–9.67	LB: 0.125–6.6 RB: 0.04–7.3

Source: JICA (2000) and Hossain et al. (2014)

## 8 Human Dimensions

### 8.1 Flood Vulnerabilities

The field survey shows that flood is a regular phenomenon in Buriganga and Shitalakhya causing several impacts on human beings. Flood brings different types of vulnerabilities including social, economic, physical, structural, agricultural, and psychological for both men, women, and children in the study area. As a result, the people's lives have been hampered. Often people and livestock are injured and even killed. The condition of health deteriorates and spread waterborne diseases. Moreover, floods damage the roads and bridges, and thus the communication system deteriorates. Normal living arrangements are disrupted as normal communication is interrupted.

It is evident from the field survey that frequent floods increase the trends of migration and displacement in the study area. For this reason, cluster settlements are more common in Dhaka and Narayanganj districts. Moreover, it is seen that flood-affected families have been suffering from mental health problems. Losing family members, especially children, they become mentally disturbed. Additionally, they suffer mental health problems for long periods of time because of losing home, resources, as well as livelihood. The field study indicates that about 25% people of a flood-affected area suffered from physical injuries. On the other hand, about 85% people of a flood-affected area suffered from various diseases such as diarrhea, cholera, typhoid, and skin rashes. Shortage of food has been identified as a severe problem during flood, causing malnutrition. Moreover, scarcity of clothes, fuel wood, and sanitation are some common problems during flood in the area.

### 8.2 Life and Livelihood

Areas around Buriganga and Shitalakhya have experienced a few major floods in the years 1954, 1955, 1970, 1974, 1980, 1987, 1988, 1998, 2004, and 2007. During the floods of 1995, Buriganga was overflowed, and around 80% of Dhaka was inundated (EPWAPDA, 1964). Among the floods, 1988 flood had catastrophic effects. About 150 people died, and about 2.2 million people were affected by the flood in 1988

(Barua & van Ast, 2011; Huq & Alam, 2003). About 50% area of greater Dhaka was flooded (JICK, 1990) which caused 6–12 million USD worth of damages (Jahan, 2000). The 1988 flood costs about 4000 million BDT for 400,000 residential building and about 400 million BDT for 14,000 public institutions (Alam & Rabbani, 2007). On the other hand, the 1998 flood was the most severe according to extent and duration. It was also caused by the flow of river water. Dhaka and its surrounding areas were inundated for more than 2 months (Huq & Alam, 2003). Floods created health hazards, economic loss, and property damage in the areas. Moreover, waterlogging in the floodplain areas caused problems for roads, railways, communication lines, house, and institution (Barua & van Ast, 2011). During the 1988 flood, DND project also faced severe breaching threat from the river flows and was damaged by leakage, seepage, and piping developed in the road cum embankment (Munshi & Amin, 2008).

The field survey identified that people who reside along the Buriganga and Shitalakhya Rivers faced severe problems by the recent flood occurred in 2020. The water level of these rivers crossed the danger level at some points during 2020 flood and flooded the low-lying areas (e.g., Fatullah of Narayanganj, Dohar of Dhaka) along the riverside. Moreover, some infrastructures including houses, roads, and business establishments have been damaged by the incurred floodwater. Alongside, the DND area goes underwater, causing lots of suffering to the people. Approximately 1000 houses of the study area have been inundated by the recent flood. Most of the houses remained inundated for a week. Affected people lost their cattle, poultry, and other belongings of the houses.

### **8.3 Coping Strategies**

The field survey revealed that living with flood in the area is prerequisite for the inhabitants. To cope with floods in the study area, people have developed some strategies. People make high platform where they can take place during flood. They try to make house wall made with flood-resistant elements such as bricks or concrete. Few people take shelter on the dam with their cattle, and others move their friend's or relative's house.

## **9 Management of Floods**

Flood is a crucial part of Buriganga and Shitalakhya floodplain areas. Therefore, to protect surrounding people of Buriganga and Shitalakhya, different flood management measures including flood prevention, control, and mitigation efforts have been taken by the Government of Bangladesh entitled to DND project in 1962 (BWDB, 1984; Munshi & Amin, 2008). Concerned authorities have taken several measures for the management of flood followed by structural approach and nonstructural

approach. Moreover, some policies and their implementation at local level also are reflected in the area for managing flood.

## 9.1 Structural Measures

Bangladesh followed structural measures by the implementing of flood control projects since the 1960s after the great flood of 1963. There are some structural measures for controlling flood in and around Buriganga and Shitalakhya.

**Embankment or Cordon Approach** An embankment was made in 1962 to protect Dhaka, Narayanganj, and Demra (DND) from adjoining Buriganga and Shitalakhya Rivers (Islam, 1998). The DND project provides flood protection, drainage, and irrigation facilities to 5870 hectares of land (Islam, 2003). Moreover, about 30 kilometers of earthen embankment along the Tongi canal, Turag River, and Buriganga River was made to protect floods in the area (Chowdhury et al., 1998).

**Highways and Railways** Highways and railways have been raised above flood level in the area. For example, Dhaka-Narayanganj-Demra is bounded and protected from flood by embankment cum pitch road. On the other hand, small portion of DND project (i.e., bankside of Buriganga and Shitalakhya), from Haziganj to Chasara (Narayanganj), is embankment cum railway line for flood management in the area (Munshi & Amin, 2008).

**Floodwall** A floodwall was constructed in 1988 (i.e., after the 1988 flood) from Buriganga to Fatullah which ranges from 7.6 m to 8.0 m with its road elevation being about 7.0 m. Further, from Demra to Haziganj along the Shitalakhya River, the top of the floodwall ranges from 7.5 m to 8.1 m with the road elevation being about 7.0 m (Munshi & Amin, 2008).

**Retention Pond** There are some natural water bodies around the Buriganga and the Shitalakhya which serve as retention ponds. These retention ponds can hold huge amount of floodwater in time of need (Munshi & Amin, 2008).

## 9.2 Nonstructural Measures

Some nonstructural approaches are also followed for the management of floods in the study area. The field study identified that there are some nonstructural measures taken for controlling flood in and around Buriganga and Shitalakhya. Bangladesh Water Development Board (BWDB) has started flood forecasting and warning in 1972. There are some flood shelter centers established in some school building in the area. Moreover, people took some flood-proofing measures such as rebuilding their used material (e.g., raising homesteads, schools, market places, etc.) to prevent or minimize damages from future floods.

**Table 19.4** Different types of flood action plans for Dhaka and its beyond

Number of flood action plans	Name of flood action plans
8A	Greater Dhaka protection project
8B	Dhaka integrated Flood protection project
9B	Meghna River Bank protection project

Source: Parvin et al. (2018)

### 9.3 Policy Issues and Local-Level Implementation

Different institutions are working for the management of flood and water around Dhaka. There are more than ten organizations of different ministries are responsible for the flood protection of Bangladesh including Dhaka and its surrounding areas (Haq, 2006; Khorshed, 2003). Moreover, a number of flood action plans (Table 19.4) have been adopted for Dhaka and its beyond to lay the foundation for a long-term program to acquire a sustainable solution to the flood problem and to create a sound environment for economic growth and social development. These flood action plans are directly or indirectly related to Buriganga and Shitalakhya Rivers' flood management.

## 10 Response to Floods

Different organs of the government (i.e., ministries, local governments) and some non-governmental organizations (NGOs) are trying to respond in flood management in the study area. Considering the emergency preparedness plan for flood in Bangladesh from June 2013, there are few organizations working on flood management. First of all, Department of Disaster Management (DDM) contributes to dissemination of all information on natural disasters including flood information at community level, flood preparedness, awareness building, etc. Moreover, Water Resources Planning Organization is working on water resources management. The Bangladesh Water Development Board (BWDB) is working on feasibility studies, implementation, operation, and maintenance of flood management projects. Besides, BWDB works on flood forecasting and warning services. Local Government Engineering Department (LGED) is engaged in the construction, repairing, and maintenance of local government infrastructures like roads, small bridges, culverts, and water control structures. Local government institutions take part in implementation, operation, and maintenance of small-scale flood management projects, flood information dissemination, relief, and rehabilitation of flood victims (Parvin et al., 2018). Moreover, Directorate of Relief, Bangladesh Armed Forces (Army, Navy, and Air Force), and non-governmental organizations (NGOs) are working on relief distribution, rehabilitation programs, as well as reconstruction activities. Furthermore, these organizations are providing lifesaving food and medical care, safe drinking

water, and temporary shelter. They coordinate and initiate disaster drills and training programs and other preparedness measures in the study area.

## 11 Conclusion and Way Forward

The field survey suggests that for better management of flood in and around the Buriganga and the Shitalakhya, the following measures should be taken. Bangladesh Water Development Board (BWDB) is monitoring the level of water. However, other characteristics such as sedimentation, water quality, filling up of river, and ecosystem behavior should also be added to the measurement scheme. Moreover, well-developed geographical information system (GIS) and remote sensing (RS) system have to set up for visualizing many different factors which influence the river system in the area. Technical measures need to be implemented in the area to recover the encroached portions of the rivers. To save Shitalakhya and Buriganga, awareness should be raised among the stakeholders to make them understand that mindless disposal of wastes is harmful for the river and the environment around it. Awareness campaigns need to be carried out on the bank of the river as well as in print and electronic media to sensitize people. Political influences on the bank of the river must be tackled with an iron hand by the government. Land grabbing, sand extraction, silt extraction, and extortion by local politicians must be stopped in the area.

The field study suggests that government should urgently organize the effective drainage system inside the DND dam as well as proper maintenance of DND dams. Coordination among different ministries and different organs of the government, for example, BWDB, Local Government Engineering Department (LGED), Ministry of Water Resources (MoWR), Roads and Highway Development, etc., should be well developed. Periodic dredging of Buriganga, Shitalakhya, and canals of the area should be conducted. Moreover, people who reside along the low-lying areas of riverside should be shifted slowly for mitigating severe damage from the incurred floods.

## References

- Alam, M., & Rabbani, M. G. (2007). Vulnerabilities and responses to climate change for Dhaka. *Environment and Urbanization*, 79(1), 81–97.
- Barua, S., & van Ast, J. A. (2011). Towards interactive flood management in Dhaka, Bangladesh. *Water Policy*, 13(5), 693–716.
- BMD (Bangladesh Meteorological Department). (2022). *Weather database of Bangladesh meteorological department*. Ministry of Defense.
- Brammer, H. (1990). Floods in Bangladesh: Geographical background to the 1987 and 1988 floods. *The Geographical Journal*, 156(1), 12–22.

- BWDB. (1984). *Socio-economic evaluation report 1984*. Bangladesh Water Development Board, Ministry of Water Resources.
- BWDB. (2015). *Annual flood report 2015*. Bangladesh Water Development Board, Ministry of Water Resources. Retrieved from <http://ffwc.gov.bd/>, retrieved on August 4, 2021
- BWDB. (2016). *Annual flood report 2016*. Bangladesh Water Development Board, Ministry of Water Resources. Retrieved from <http://ffwc.gov.bd/>, retrieved on August 4, 2021
- BWDB. (2018). *Annual flood report 2018*. Bangladesh Water Development Board, Ministry of Water Resources. Retrieved from <http://ffwc.gov.bd/>, retrieved on August 4, 2021
- BWDB. (2019). *Annual flood report 2019*. Bangladesh Water Development Board, Ministry of Water Resources. Retrieved from <http://ffwc.gov.bd/>, retrieved on August 4, 2021
- Chowdhury, S.Q. (2021). *Buriganga River*. Retrieved from <https://en.banglapedia.org>, retrieved on July 26, 2021.
- Chowdhury, J. U., Rahman, R., Bala, S. K., & Islam, A. K. M. S. (1998). Impact of 1998 flood on Dhaka City and performance of flood control works. Report November 2008. In *Institute of flood control and drainage research*. Bangladesh University of Engineering and Technology.
- EPWAPDA (East Pakistan Water and Development Authority). (1964). *Master plan, main report: vol 1*. International Engineering Company.
- GoB (Government of Bangladesh) and UNDP (United Nations Development Programs). (1989). *A flood policy for Bangladesh*. Mott MacDonald International. p6.
- Haq, K. A. (2006). In C. Tortajada, O. Varis, J. Lundqvist, & A. K. Biswas (Eds.), *Water management in Dhaka. Water management for large cities* (pp. 107–127). Routledge.
- Hossain, S., Rahman, M., Nusrat, F., Rahman, R., & Anisha, N. F. (2014). Effects of climate change on river morphology in Bangladesh and a morphological assessment of Sitalakhyariver. *Journal of River Research Institute (RRI)*, 1, 1–13.
- Huq, S., & Alam, M. (2003). Flood management and vulnerability of Dhaka City. In *Building Safer Cities: The future of disaster risk, disaster risk management Series*. In A. Kreimer, M. Arnold, & A. Carlin (Eds.), *The World Bank* (pp. 121–135).
- Islam, N. (1998). *Alternative approaches to flood control: The case of Bangladesh*. Department of Economics, Emory University.
- Islam, N. (2003). *Environmental impact assessment due to the urbanization of Dhaka-Narayanganj*. Demra (DND) Project Area.
- Islam, M. R., Mondal, M. S., & Biswas, S. (2020). *Historical flood inundation studies at several important locations of Dhaka city under Dhaka mass rapid transit development project line*. ICCESD.
- Jahan, S. (2000). Coping with flood: the experience of the people of Dhaka during the 1998 flood disaster. *Australian Journal of Emergency Management, Spring*, 16–20.
- JICA. (1990). *Updating study on storm water drainage system improvement project in Dhaka city*. Japan International Cooperation Agency.
- JICA. (2000). *Baseline information study of the Dhaka combined flood control cum eastern bypass road project*. Final Report. Volume I – Main Report. March 2000. JICA for BWDB.
- Khalequzzaman, M. D. (1994). Recent floods in Bangladesh: Possible causes and solutions. *Natural Hazards*, 9(1), 65–80.
- Khorshed, A. (2003). *Cleanup of the Buriganga River: Integrating the environment into decision making*. PhD Thesis, Murdoch University.
- Kibria, M. G., Kadir, M. N., & Alam, S. (2015). *Buriganga river pollution: Its causes and impacts* (pp. 323–328). International Conference on Recent Innovation in Civil Engineering for Sustainable Development.
- Majumdar, R. C. (1971). *History of ancient Bengal* (pp. 3–4). Tulsi Prakashani. ISBN 81-89118-01-3.
- Majumder, A. (2009). *Bangladesh river pollution threatens millions*. Retrieved from [https://en.wikipedia.org/wiki/Buriganga\\_River](https://en.wikipedia.org/wiki/Buriganga_River), retrieved on July 25, 2021

- Masuya, A., Dewan, A., & Corner, R. J. (2015). Population evacuation: evaluating spatial distribution of flood shelters and vulnerable residential units in Dhaka with geographic information systems. *Natural Hazards*, 78(3), 1859–1882.
- MoDMR. (2014). *Flood response preparedness plan of Bangladesh, June*, Department of Disaster Management, Ministry of Disaster Management and Relief. Government of People's Republic of Bangladesh.
- Munshi, M., & Amin, R. (2008). *Flood disaster mitigation in DND: Land use perspective*. Doctoral Dissertation, BRAC University.
- Murshed, M. M. (2012). Shitalakhya river. In S. Islam & A. J. Ahmed (Eds.), *Banglapedia: National Encyclopedia of Bangladesh (Seconded)*. Asiatic Society of Bangladesh.
- OEP-EOP (Office of Emergency Preparedness, Executive Office of the President of the United States). (1972). *Disaster Preparedness: Report to Congress*. US Government Printing Office.
- Parvin, G. A., Rahman, R., Fujita, K., & Shaw, R. (2018). Overview of flood management actions and policy planning in Bangladesh. *International Journal of Public Policy*, 14(5/6), 423–443. Geophysical Union, 73 pp.
- Rahman, M. A. (2010). Dhaka in danger. *The Daily Star*. Retrieved from <http://www.thedailystar.net>, on October 15, 2021
- Saleh, A., Ahmed, S., Mirjahan, M., Rahman, M., Salehin, M., & Mondal, M. (1998). *Performance evaluation of FCD/FCDI projects during the 1998 flood*. *Engineering Concerns of Flood, Institute of Flood Control and Drainage Research* (pp. 253–266). BUET.
- SWMC (Surface Water Modeling Centre). (1996). *Water quality modeling of the Buriganga-Lakhya river system*. Calibration Report, July 1996.

## Chapter 20

# Floods of Jalangi and Mathabhanga-Churni Rivers, Indo-Bangladesh



Balai Chandra Das , Sanat Das , and Biplab Sarkar 

**Abstract** Floods of Jalangi and Mathabhanga-Churni Rivers along with the floods of Bhagirathi River played a key role in the delta-building processes of Nadia and Murshidabad districts. Floods of these rivers have boosted the health of soils and water bodies of the region. Floods have also a significant effect on the productivity of soils and water bodies. Events of (1) neotectonics and subsequent eastward tilting of the Bengal basin, (2) eastward flight of the Padma River leaving behind its distributaries, (3) formation of huge sandbars at the oftakes of these rivers restricting the entrance of water from the Padma, and (4) post-Farakka lowering of the water level of the Padma River in comparison to bed level of these distributaries have changed the flood scenario significantly. Now there is no flood like before, except for the deluge of 2000. However, the evil effects of normal floods have been multiplied as the side effect of several structural or hardware solutions against floods. Living with floods is suggested.

## 1 Introduction

People have come to perceive floods as disasters in terms of loss of lives and damage to property (Khan, 2011). This perception is due to the partial glance at floods and not assessing them holistically. A flood is nothing but a huge pileup of water resources surpassing the managing capacity (Yadav & Ibrar, 2022). To escape from the unmanageable volume of floodwater, people have altered the flow of rivers but with occasionally disastrous consequences (Ray et al., 2019). Though floods may be devastating to population centers, they have always been integral to nature's

---

B. C. Das (✉)

Department of Geography, Krishnagar Government College, Nadia, West Bengal, India

S. Das

Department of Geography, Adamas University, Kolkata, India

B. Sarkar

Department of Geography, Aliah University, Kolkata, India



renewal process, providing many long-term positive effects (Sahrawat, 1998; Cookey & Ukpong, 2018; Duong et al., 2019; Mandal et al., 2021). Flooding for several weeks makes soil chemical fertility regime stable (Sahrawat, 1998). Cookey and Ukpong (2018) found that the rural economy becomes benefited from flooding. Duong et al. (2019) from their experimental study conclude that flooding benefits the maintenance and restoration of native wetland plant communities. Bengal delta originated from the deposition of a huge quantum of silt carried down by the Ganga-Brahmaputra river system (Allison, 1998a, b; Kuehl et al., 2005). And the delta reached its present elevation due to depositing of silts during several frequent inundations (Majumder, 1941; Goodbred, 1999). The creation of numerous floodplain wetlands (oxbow lakes, abandoned channels, and backswamps) is inseparable from the delta-building processes (Das et al., 2020a). During inundation, floods renew those wetlands by supplying nutrient-rich silts and water for both aquatic plants and animals (Loucks & Beek, 2017). The flood-carried silt is distributed and deposited over a vast tract of the floodplain, replenishing nutrients in topsoil and making agriculture more profitable (Tang et al., 2014). Many population centers of the present world depend primarily on groundwater for agricultural, industrial, drinking, and other domestic uses. In flood-inundated areas, waters are absorbed into the ground and percolated downward to recharge underground aquifers. These underground aquifers supply water in wells, lakes, and rivers, especially during lean months. The silt-laden floodwaters deposit their silt load on vast low-lying wetlands (Islam, 2016). During lean months, the reverse flow of silt-free clear waters into rivers not only maintains the ecological flow of the channel but also increases stream power to carry downriver the loose slur from the bed. This reverse flow of silt-free spill waters enables the rivers to keep their channel's self-maintenance mechanism (Majumder, 1941).

Jalangi and Churni are two of the three Nadia Rivers that have not only built up the land of the region but also raised its level to its present elevation. Floods of these rivers had made lands of Nadia fertile and productive, lakes rich in plants and animal communities (Mandal et al., 2021), and rivers rich in fish. Annual floods of these two rivers have been the key factors behind the prosperity of agriculture and fish production in this area. However, the flooding capacity of the rivers has long decreased, and the region has been deprived of the blessings of floods (Das, 2013). Why and how did these two important distributaries of the Padma River lose their flood power? What are the consequences of flood inferiority upon hydrogeomorphology of the catchment? What is the impact of flood inferiority on resources? How are these impulses from changes in flow behavior absorbed by other natural and anthropogenic variables of the system? The present chapter illuminates all these issues.

## 2 Regional Settings

The area is geologically a product of riverine silt (Chakraborty, 1970) of recent age (Majumder, 1978) completely obscuring the subsurface geology of the area (Sen & Sen, 1989). Jalangi formation took place during the period from Upper Paleocene to Lower Paleocene (Dasgupta, 1997). The geographic extent of the Jalangi-Churni basin is 23°07'18.21" N to 24°25'54.4" N and 88°15'36.05" E to 88°54'58.84" E and covers an area of 5319.58 km<sup>2</sup> (Fig. 20.1). The highest elevation of the area is 45 m (Fig. 20.2) at the Suti II block of the district of Murshidabad, and the lowest elevation is 6.0 m at Swarupganj of CD Block Nabadwip of Nadia district. The region is comprised mainly of fluvisols. Jalangi-Churni basin drains an area of 5319.58 km<sup>2</sup>. Out of the total area, more than half (3716.86 km<sup>2</sup>) of the region, from north to south, is occupied by calcaric gleysols. The second-largest area (1040.34 km<sup>2</sup>) to the west of the basin is covered by orthic luvisols. Calcaric fluvisols to the northeast cover an area of 429.864 km<sup>2</sup>. The smallest area of 132.52 km<sup>2</sup> of eutric fluvisols is in the southern part of the basin (<https://www.fao.org/soils-portal> and <https://www.fao.org/soils-portal/data-hub/en/> retrieved on 15th May 2022).

Jalangi and Churni river basins are deltaic monotonous plains interspersed with rivers, spills, palaeochannels, oxbow lakes, and meander scars (Sarkar et al., 2022). The lowest elevation of 6 m. is recorded at Hulor Ghat (Mayapur ghat), opposite Swarupganj (Bagchi, 1978) in the Nabadwip block of Nadia district. The general slope is from north to south.

Jalangi is a moribund river of 233 km (Das & Bhattacharya, 2020) in the Bengal delta. The river is simultaneously a distributary of the Padma River and a tributary of the Bhagirathi River. The reach of 9.1 km from abandoned offtake at Char Madhubona near Gopalpur (Ghat) to the Sialmari-Jalangi confluence at Kupila is erased from the map of the region and 41.9 km from Sialmari River-Jalangi River confluence to Bhairab River-Jalangi River confluence at Moktarpur, though traceable but dead at present (Das & Bhattacharya, 2020). The reach downstream to the Bhairab-Jalangi confluence up to Jalangi-Bhagirathi confluence at Swarupganj (182 km) is being maintained by the base flow of seepage water, contribution of the Bhairab River, and other spills during a few months of the rainy season. The catchment area of the Jalangi river system is 2832 km<sup>2</sup> (Das & Bhattacharya, 2020).

During the British colonial rule in Bengal, Bhagirathi, Jalangi, and Mathabhanga Rivers were known as "Nadia Rivers" (Hunter, 1877; Garrett, 1910) or "Kishnaghur Group of Rivers" (Fergusson, 1912). Although these three rivers were grouped and named after Nadia or Krishnagar, Mathabhanga found its path crossing and recrossing the international Indo-Bangladesh (Sarkar et al., 2020) border. The Mathabhanga River bifurcates in Ichamati and Churni near Majdiya. From offtake to the point of bifurcation at Pabakhali near Majdiya, the length of the river is 196.40 km. Ichamati, the left branch, follows a tortuous course toward the south to find its path to the Kalindi-Raimangal outfall into the Bay of Bengal. Churni River, the right branch of the river Mathabhanga, takes a south-easterly course and runs

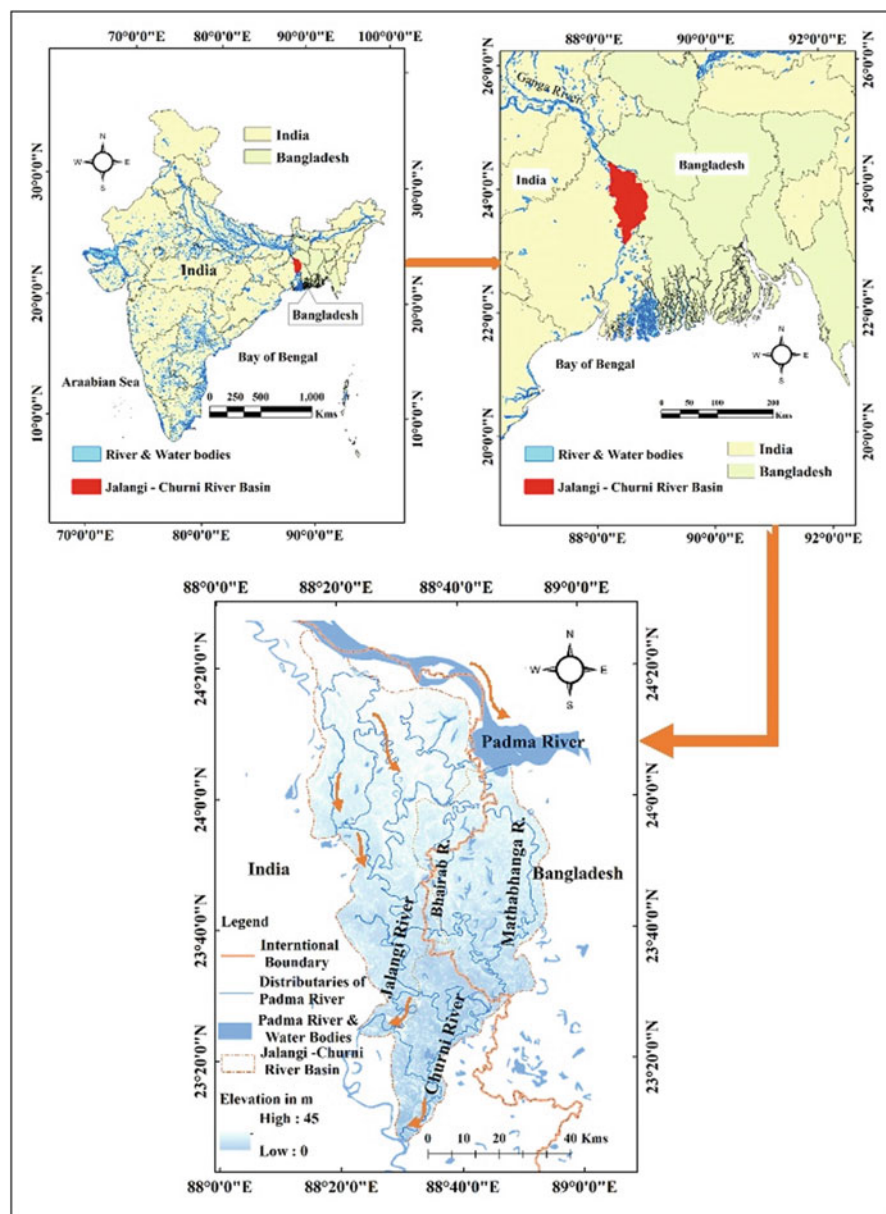


Fig. 20.1 Location of Jalangi-Churni basin

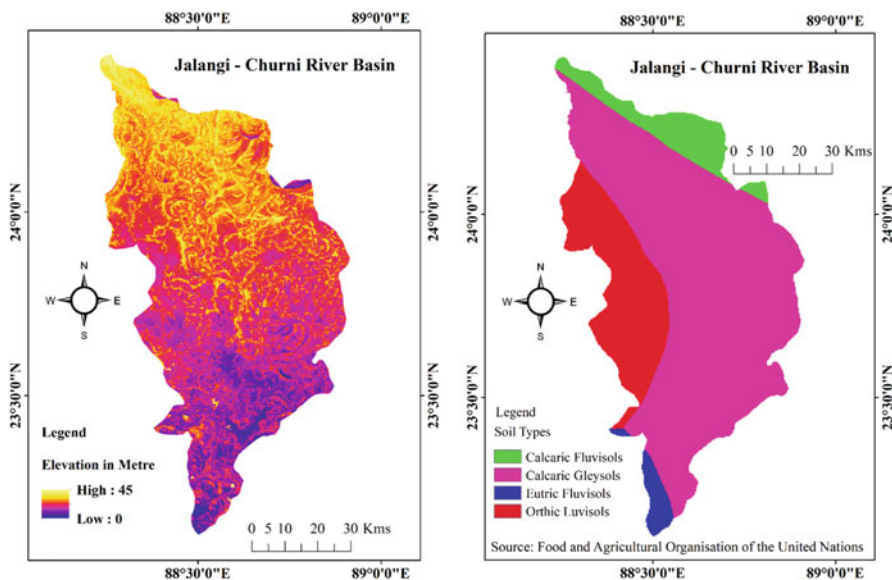


Fig. 20.2 Relief and soil of Jalangi-Churni basin

56 km (Sarkar & Islam, 2019) by Shibnibas, Hanskhali, Aranghata, Ranaghat to fall into the river Bhagirathi near Shibpur (Sarkar & Islam, 2019). The total length of the river Mathabhanga-Churni is 252.40 km. The catchment area of the Mathabhanga-Churni River is 2585 km<sup>2</sup> having a perimeter of about 295.30 km.

The general slope of the region is from North North-West to South South-East. Following the general slope, distributaries of the river Padma and spills carry flood water from Padma and Bhagirathi-Hooghly to South South-East. Flood water of Padma overtops the banks and finds its path through Gobra Nala, Suti River, Bhairab River, and Sialmari River toward south to outfall into the Jalangi River (Fig. 20.3). When the flood overtops the left bank of the river Bhagirathi, water moves eastward and amalgamates with floods of Jalangi, via Gobra Nala, Suti River, and some other minor spills like Kalma Khal, Sahebnagar Khal, etc. from Kalantar tract. As the Jalangi River surpasses its banks, floodwater finds its paths downstream to the southwest and through different spills like Choto Bhairab, Kesto-Raiyer Khal, Saraswati Khal, Chandpur-Kukradaha Khal, etc. toward south and southeast to be amalgamated with the floods of the Churni River. Floods of the river Padma get their way through the Mathabhanga River via Churni to Hooghly River. A portion of the Jalangi floods passes through the Choto Bhairab River at Karimpur and runs through Meherpur of Bangladesh to fall finally into the Mathabhanga River at Subalpur in Bangladesh. The portion of Padma floods, getting its way through Mathabhanga River, spills through Ichhamati and Churni to North 24 Parganas and Nadia, respectively.

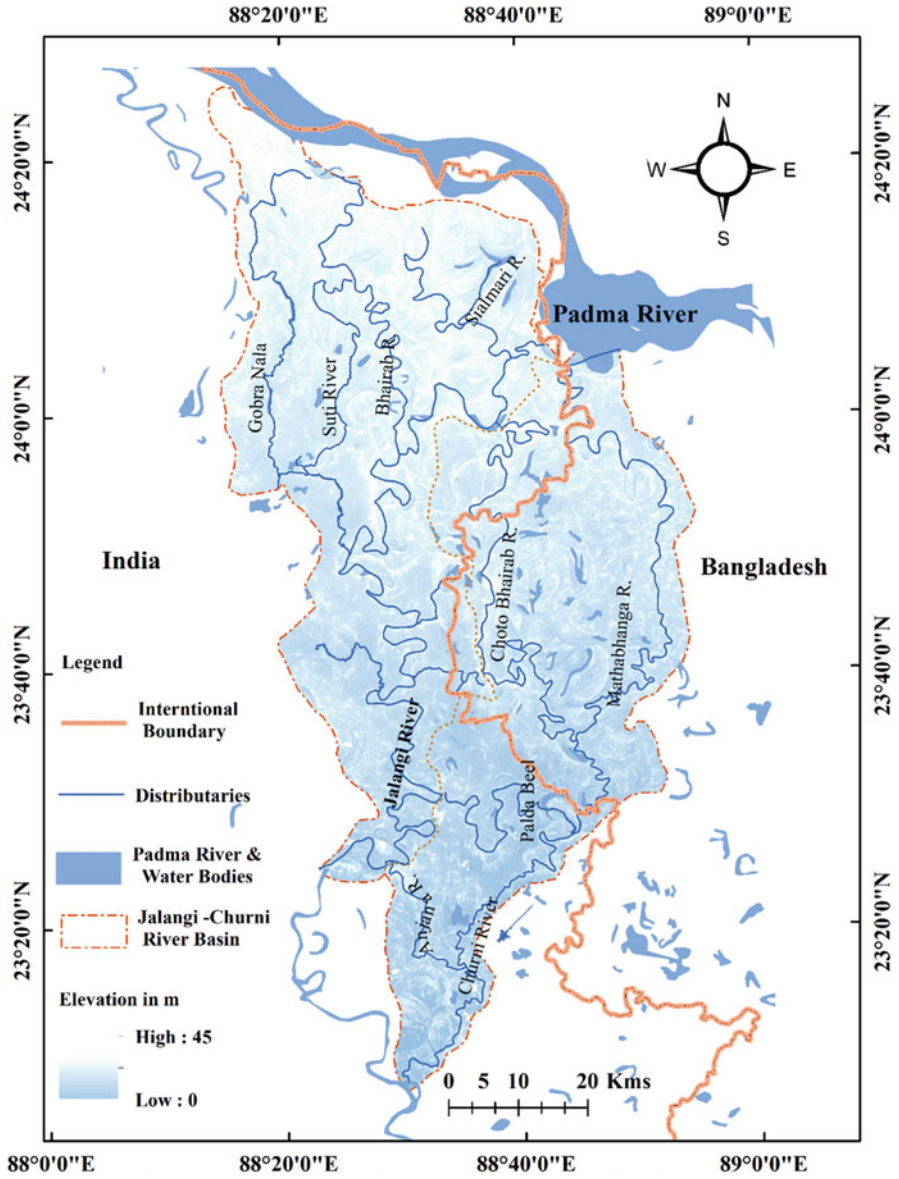


Fig. 20.3 Rivers and spills for flood flow in Jalangi-Churni basin

### 3 Historical Perspective

Flood is one of the key processes of the delta-building mechanism. Floods give maturity to an immature delta raising its elevation well above sea level. Therefore, it seems logically mathematic that since the inception of the Jalangi and the Churni, these two rivers inundated their catchment area several times to raise their elevation to their present level. The exact date of origin of these two rivers is not known. Jalangi was first mapped in 1660 by Van-den-Brouck. From regional literature of Gaudiya Vaishnavism, the possible earlier existence of the Jalangi River during the fifteenth century was noted (Das, 2013). Therefore, it is expected that the Bhagirathi-Jalangi interfluvium had been flooded several times since the fifteenth century. But the flood record of the region is not so old. Chaudhury (2004) mentioned devastating floods of 1747, 1770, 1801, 1820, 1823, 1838, 1857, 1859, 1867, 1871, 1885, 1887, 1900, 1906, 1911, 1912, 1913, 1922, 1928, 1938, 1939, 1956, 1978, 1987, 1992, 1999, and 2000 in and around Nabadwip, and these floods have significantly change the geographical setup of the town Nabadwip. The Bhagirathi River has shifted its course from the west of the town Nabadwip to the east and separated the town Nabadwip from the rest part of the district (Das, 2013). Reaks (1919) reported that high floods on many occasions have inundated the district of Nadia. A severe flood of 1801 was followed by floods of 1823, which lasted for 2 months. Inundation took place in 1838, 1856, 1867, 1870, and 1871. In 1871, discharge of floodwaters through breach of Laltakuri embankment was 40,000 cusecs (Reaks, 1919). Floodwaters inundating 321 square miles of Murshidabad amalgamated with water floods of Jalangi and Mathabhanga. Floods during 1874, 1889, 1890, and 1907 (Reaks, 1919) breached the Laltakuri embankment, and floodwater reached Jalangi catchment through Gobra Nala via the Kalantar area (Reaks, 1919).

Regarding the millennium flood of 2000, a government report (IWD, 2000) stated that during the second spell of heavy rain (September 17, 2000 to second week of October 2000), nine districts (viz., Nirbhum, Bardhaman, Nadia, Murshidabad, Howrah, Hooghly, Malda, Midnapur, and North 24 Parganas) in the basin of Bhagirathi-Hooghly River system faced severe devastating flood. Due to unprecedented heavy rains from September 17, 2000, to September 22, 2000, coupled with cyclonic depression in the Chota Nagpur Plateau in Bihar, “this flood had surpassed all previous records in wideness and virulence” (IWD, 2000). The record of incessant rainfall during the week was as follows (Table 20.1):

Due to these heavy rains pickup barrages of the Mayurakshi reservoir system flunked out, and the Massanjore dam exceeded its capacity. All the rivers overtopped their banks and breached embankments, roads, and rails. The communication system collapsed. “When the Bhagirathi flood entered the Jalangi outfall point, the Jalangi basin itself had already been experiencing high rainfall in its basin area. The Jalangi basin situation had become worse with the addition of this Bhagirathi flood spill” (IWD, 2000). Gauge height at Swarupganj rose by 2.76 m above the extreme danger level (EDL) of 9.05 m. As the receding flood of the Bhagirathi river system was passing through Nadia district and as Padma floods were spilling through

**Table 20.1** Rainfall records of different river basins during floods of 2000

Period	Basin	Total rainfall in mm
17.09.2000 to 21.09.2000	Pagla-Bansloi, Brahmani, Dwaraka	1165
17.09.2000 to 21.09.2000	Mayurakshi basin system catchment above Massanjore dam	1004
17.09.2000 to 21.09.2000	Catchment between Massanjore dam and Tilpara barrage	1153
17.09.2000 to 21.09.2000	Catchment between Tilpara barrage and outfall at Babla River	596
17.09.2000 to 21.09.2000	Ajay basin system	396
17.09.2000 to 21.09.2000	Jalangi system	793
17.09.2000 to 21.09.2000	Rain gauge station at Maithon	572.40
17.09.2000 to 21.09.2000	Rain gauge station at Panchet	375.80
17.09.2000 to 21.09.2000	Rain gauge station at Durgapur	129.30

Source: IWD (2000)

Mathabhanga and Jalangi, Krishnagar and Nabadwip towns including all the blocks were inundated. Drainage congestion in Nadia continued for 1.5 months.

The combined floodwater of Bhagirathi-Jalangi added with the flood spill of Ajay River crossed the basin boundary of the Churni River which was already rising high due to the flood discharge of Mathabhanga from Bangladesh. Even at the time of the falling level of upper basins, due to adverse conditions at outfalls, the level of Jalangi, Churni, and Ichhamati kept rising. The flood of 2000 inundated 3731 km<sup>2</sup> area of the district (IWD, 2000).

In 2005, the flood level (8.42 m) of the Jalangi River was even below the danger level of 8.44 m at Swarupganj (IWD, 2005). The highest flood level (HFL) of the river Churni was 5.96 m, much below the DL of 7.53 m and EDL of 8.14 m. In 2019, the flood level (8.73 m) of the Jalangi River at Swarupganj was 0.29 m above DL. Mathabhanga-Churni did never reach its DL in the year 2019 (IWD, 2019) (Fig. 20.4).

The highest discharge of 109,678 cusecs in 1914 through the Jalangi River at Punditpur (Panditpur) was reported by Hirst (1916). In 1890, the highest discharge of the river was 100,000 cusecs (Williams, 1919). The discharge of 1917, shown in the figure (Fig. 20.4), is average value. During the last quarter of the twentieth century, the discharge of the river declined very sharply.

The record of flood discharge during the last 100 years shows a decreasing trend (Fig. 20.4). After the Farakka Barrage came into operation in 1975, the discharge of the Jalangi and Churni Rivers also decreased significantly except for the flood year 2000. Why this happened is discussed under the section drivers of the flood.

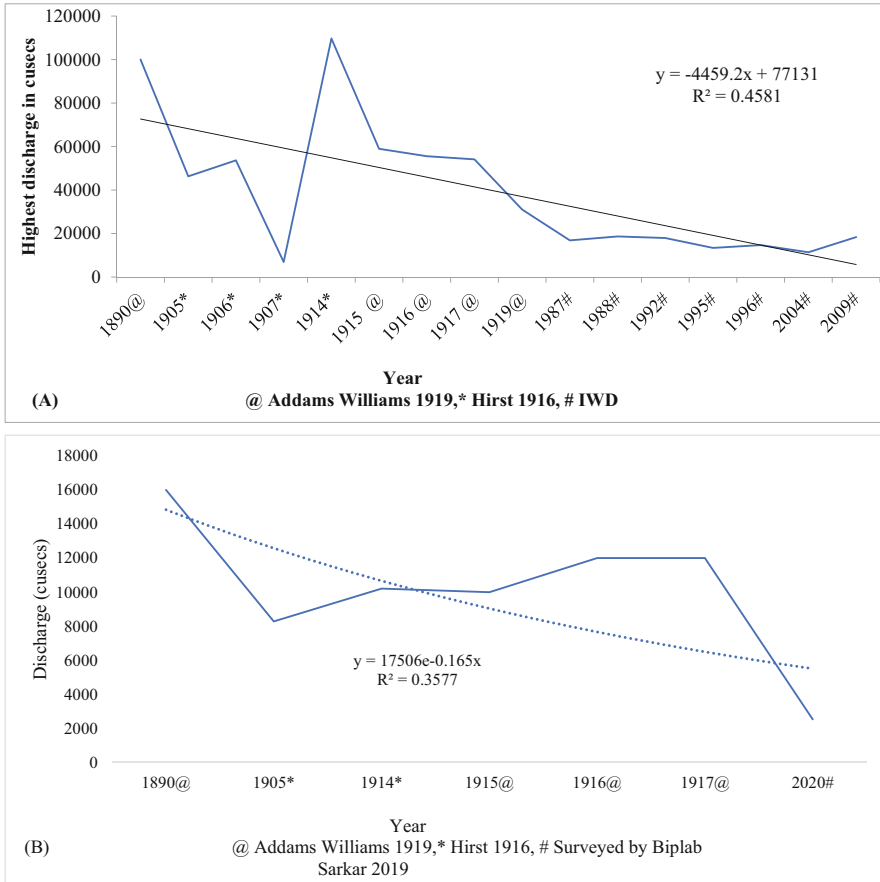


**Fig. 20.4** Decreasing trend in the discharge of the river (a) Jalangi at Swarupganj and (b) Churni at Hanskhali. Data sources are mentioned in the figure

### 4 Materials and Methods

The data used in this study were collected from various sources. Shuttle Radar Topography Mission (SRTM) with 30 m resolution (2014) was used in this study and downloaded from the USGS EarthExplorer website. Google Maps were also used for demarcating Jalangi-Churni river basin and rivers within the study area. Basin boundaries were digitized on Google Earth maps with use of ArcMap software. Shapefile of inland water bodies and boundary of countries’ spills channels were downloaded from the DIVA-GIS (<https://www.diva-gis.org>). The highest flood level (HFL) data and rainfall data were collected from the Department of Irrigation and Waterways, Government of West Bengal.

The elevation is an important factor for flood-prone area mapping, and disparities in elevation have effects on climate characteristics (Natarajan et al., 2021).



Universally available data from the USGS EarthExplorer Shuttle Radar Topography Mission (SRTM, 2014) was used for the digital elevation model. This model was created using the ArcGIS spatial analysis tool. The soil type map was prepared by the Food and Agriculture Organization of the United Nations in the year 1974 (<https://www.fao.org/soils-portal>). The flood-prone area (1990–2010) was measured by the use of HFL (highest flood level) in this basin area. Flood-prone areas are calculated by using the raster calculator in the spatial analyst tool in ArcMap.

We used literature (Williams, 1919; Hirst, 1916) published during the colonial rule in Bengal for collecting data especially related to channel hydraulics. Data on river hydraulics for the post-independence period were collected from different published literature and government documents (IWD, 2000, 2005, 2019) and unpublished government records (IWD). To analyze available data, we used statistical techniques [Coefficient of Correlation ( $R^2$ ), regression equation ( $y = a + bx$ )], graphical methods (maps, bar diagrams, time series line graphs, scatter plots, photographs), and tools of mathematics (simple arithmetics).

## 5 Nature and Magnitude of Floods

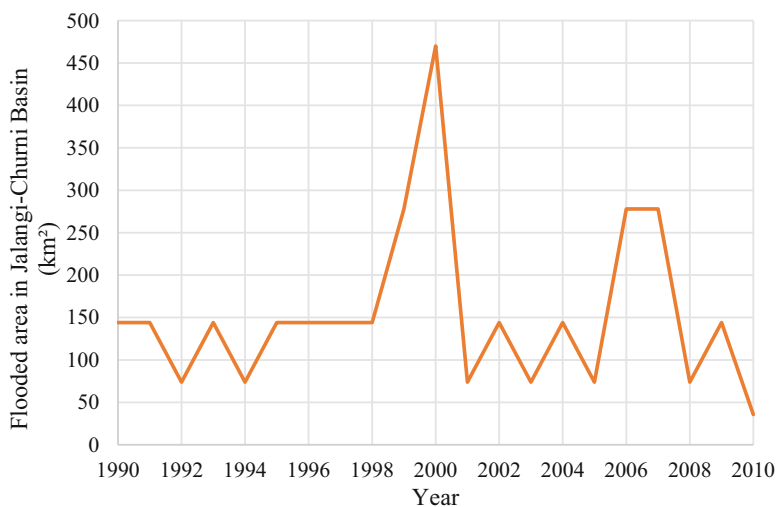
Floods of the Jalangi-Churni basin are fluvial, and neither tidal nor flash floods have any impact on them. They occur due to overtopping of the river-banks by water. This happens generally because of heavy rains in the basin concerned and upper catchments of rivers connected with the Jalangi-Churni system via the Padma and Bhagirathi-Hooghly system. We have estimated the flooded area of the basin for 20 years from 1990 to 2010. It was found that except for the millennium deluge of 2000, flooded areas of the basin are not so much (below 150 km<sup>2</sup>). This is <0.028% of the total basin area. And this flooded area is adjacent to the Jalangi-Bhagirathi confluence and Churni-Hooghly confluence. The part of CD blocks of Nabadwip, Krishnagar I and II, Shantipur, and Ranaghat I, adjacent to the Bhagirathi-Hooghly River and the Jalangi-Bhagirathi confluence and Churni-Hooghly confluence, experiences floods.

Table 20.2 and Fig. 20.5 show the flooded area computed by the authors. Therefore, it can be concluded that except for a very low-frequency high-magnitude deluge (e.g., floods of 2000), the Jalangi-Churni basins are less affected by floods. During the flood of 2000, the highest gauge height (17.71 m) of Bhairab at Akhriganj did not exceed the DL (18.44 m) or EDL (19.05 m). But at Swarupganj, the highest gauge height (11.72 m) exceeded both DL (8.44 m) and EDL (9.05 m). At Hanskhali on Churni, the highest gauge reading in 2000 was 10.50 m which was well above the DL (7.53 m) and EDL (8.14 m) (IWD, 2000).

**Table 20.2** Temporal variation in rainfall and flooded area from 1990 to 2010

Year	Flooded area (sq. km)	Rainfall (mm)
1990	144.08	1977.80
1991	144.08	1675.40
1992	73.79	1185.10
1993	144.08	1689.40
1994	73.79	1198.40
1995	144.08	1876.20
1996	144.08	1552.00
1997	144.08	1757.20
1998	144.08	1653.60
1999	277.99	1801.20
2000	470.00	2362.30
2001	73.79	1850.20
2002	144.08	1623.30
2003	73.79	1665.80
2004	144.08	1596.00
2005	73.79	1270.80
2006	277.99	1349.40
2007	277.99	2198.20
2008	73.79	1655.60
2009	144.08	1483.80
2010	35.67	–

Source: Rainfall data was collected from IWD, 2019 and flooded area calculated by authors using spatial analyst tool in ArcGIS

**Fig. 20.5** Temporal variation of the flooded area in the Jalangi-Churni basin

## 6 Drivers of Floods

### 6.1 Natural Forcing

#### 6.1.1 Magnitude of Rainfall

Quantum and intensity of rainfall is the prime driver of the floods in the Jalangi-Churni basin which is best proved by the occurrence of floods in August–September, during the last phase of the rainy season. During July–August, not only do the rivers reach their bank full stages, but groundwater of the adjacent fields of the basin rises near the surface, and soils become saturated prohibiting further infiltration. At this phase, heavy rains of high intensity surpass the carrying capacity of the rivers and overtop banks to cause floods. We have applied a correlation coefficient between the amount of rainfall and the area inundated from 1990 to 2010 and found a positive relationship (Fig. 20.6) which suggests control of precipitation over the flood magnitude of the area.

#### 6.1.2 Very Low Slope and Tortuous Course

The slope of the Jalangi River was reported as 2.7" per mile or 0.00426% (Reaks, 1919). In this calculation, Reaks (1919) considered the length of the Bhairab-Jalangi from Akhriganj to Swarupganj 140 miles. Therefore, the difference in elevation between Akhriganj and Swarupganj is 378" or 9.6 m. At present (in 2022), the length of the river course between Akhriganj and Swarupganj is 260.25 km. Therefore, the slope at present is only 0.0037%.

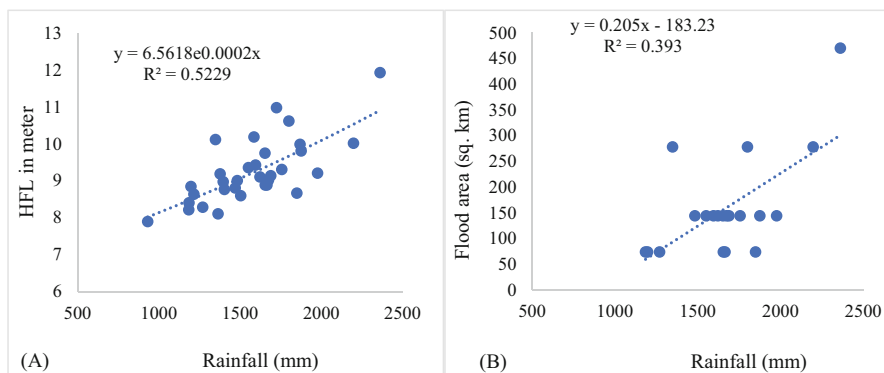


**Fig. 20.6** Positive correlation between (a) magnitude of rainfall and highest flood level (HFL), and Jalangi River at Swarupganj (b) magnitude of rainfall and flooded area indicates the controls of precipitation over flood magnitude of Jalangi-Churni basin

The slope of the Mathabhanga-Churni Rivers, as reported, is 3.6" per mile, i.e., 0.005682%, slightly higher than the slope of the Jalangi River. These negligible slopes of the rivers create obstacles to the hasty flow of the water through the channel causing flow congestion and banks to overtop and inundate the area.

### **6.1.3 Decayed Channel Retarding Hasty Pass of Floodwater**

Several factors like neotectonics and eastward shifting of feeder river, the Padma, and consequent detachment of the distributaries from Padma (Sarkar et al., 2020), in bed siltation (Majumder, 1941), Farakka Barrage, and consequent lowering of Padma water level in respect to the bed level of Jalangi and Mathabhanga (Das & Bhattacharya, 2020; Sarkar et al., 2020) caused deterioration and decay of the river channels. Decayed channels cannot carry silt charge within their beds, and as a result of which, silting in beds reduces channel capacity. As a result, during heavy rains, the river banks of Jalangi and Mathabhanga overtop and inundate neighboring areas.

## **6.2 Anthropogenic Factors**

### **6.2.1 Discharge from Reservoirs**

Regulated discharge of water from reservoir also has important controls over flood magnitude of downstream basin (Ayalew et al., 2013). Sometimes this regulated discharge from the reservoir is voluntary, while in some other situations when reservoir pressure threatens the structure, it becomes involuntary or forced. In most cases of severe floods, discharge from reservoirs becomes involuntary because of potential threats to reservoir structures. That is why rational management of reservoirs is essential for flood management (Valdes & Marco, 1995; López-Moreno et al., 2002). However, for the cause of floods in the Jalangi-Churni basin, regulated discharge from Panchet and Tilpara barrages do significant control. The discharges from barrages raise the gauge of the Bhagirathi River and surpass the banks' height. This flood finds its course eastward overtopping the left bank of the Bhagirathi River and runs through the Jalangi and then Churni basin. Moreover, raising the level of Bhagirathi-Hooghly makes an obstacle to the outfall of the Jalangi and Churni Rivers exaggerating the flood situation. We tried to link the magnitude of regulated discharge from reservoirs and floods. For this purpose, we used discharge data of the Tilpara Barrage to scatter plots with an inundated area of the Jalangi-Churni basin and found a significant bearing of involuntary regulated discharge on floods (Fig. 20.7).

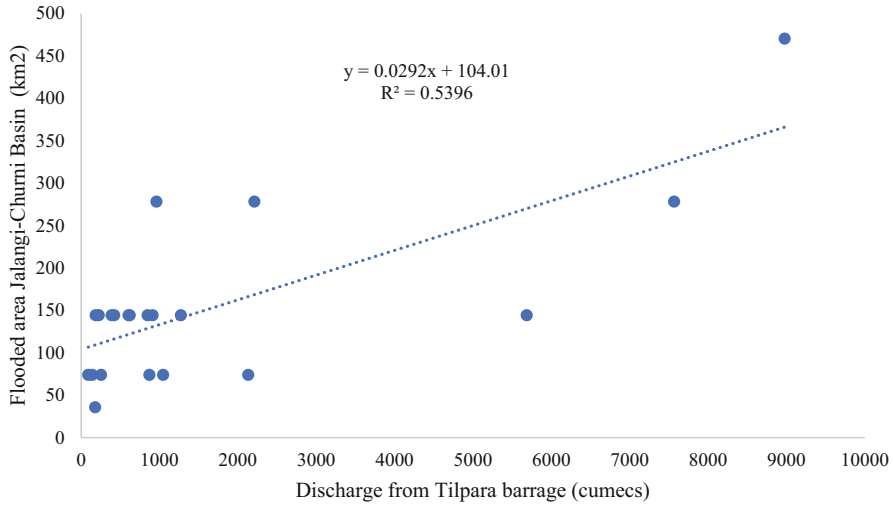


**Fig. 20.7** Correlation between regulated discharge and flooded area of Jalangi-Churni basin

### 6.2.2 Impact of Land Use and Land Cover (LULC)

Impacts of land use–land cover change and urbanization on flooding are studied well (Abdulkareem et al., 2018; Burby & French, 1981; Hussein et al., 2020; Roy & Sahu, 2016; Zope et al., 2016). Changes in LULC, especially deforestation (Islam et al., 2021), agriculture (Tu et al., 2005), and urbanization (Hollis, 1975), reduce infiltration, enhance silt charge, runoff and discharge, reduce channel capacity, and eventually cause floods. Jalangi-Churni basin is a densely populated agricultural area almost devoid of extensive forests. All these trigger floodings. Moreover, high population pressure compelled people to make settlements in low-lying flood-prone areas. This also exaggerates flood impacts. The rapid increase of built-up area or urbanization in the Jalangi basin is also portrayed in the table, while LULC in the Churni basin is portrayed in Fig. 20.8 (Table 20.3).

### 6.3 Why Don't Jalangi-Churni Flood as Before

Many rivers in the Bengal delta are facing the problems of remarkable reduction in discharge due to climate change, neotectonics, construction of dams, and overexploitation of water (Sarkar & Islam, 2020).

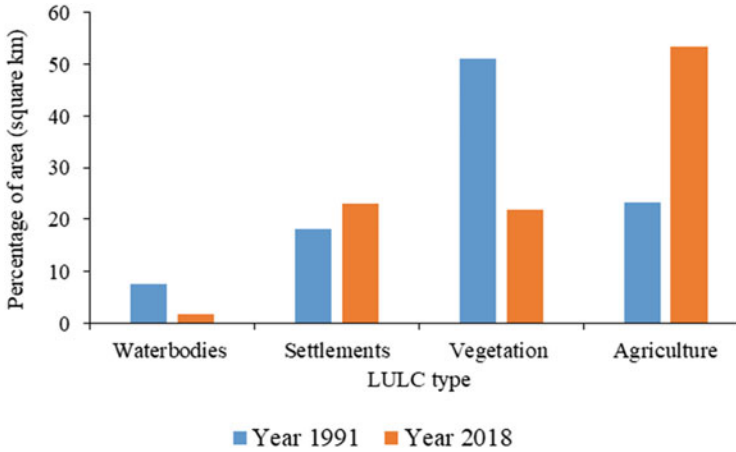


**Fig. 20.8** LULC change in Mathabhanga-Churni basin. (Sarkar et al., 2020)

**Table 20.3** Decadal changes in LULC from 2005–2006 to 2015–2016 in Jalangi basin

LULC type	2005–2006 (area in km <sup>2</sup> )	%	2015–2016 (area in km <sup>2</sup> )	%
Deciduous forest	5.82	0.21	3.62	0.13
Inland water body	20.64	0.73	19.53	0.69
Mining	5.96	0.21	7.89	0.28
Lake/ponds/reservoir	11.43	0.41	10.82	0.38
River	70.59	2.51	64.64	2.30
Fallow land	0.11	0.00	0.19	0.01
Scrub forest	0.27	0.01	0.34	0.01
Plantation	0.74	0.03	0.19	0.01
Forest plantation	1.18	0.04	1.40	0.05
Urban	17.72	0.63	22.45	0.80
Rural	608.35	21.61	624.85	22.19
Cropland	2072.52	73.62	2059.41	73.15
Total	2815.33	100.00	2815.33	100.00

Das and Bhattacharya (2020)

### 6.3.1 Neotectonics and Deterioration of Distributaries

The neotectonic jerks in the Bengal basin have altered the channel behavior of the Ganga-Brahmaputra basin to a great degree (Islam & Sarkar, 2020). Neotectonic events have made the deltaic Bengal tilted towards the east (Kuehl et al., 1997; Allison & Kepple, 2001; Kuehl et al., 2005; Parua, 2010; Chapman & Rudra, 2015). As a result, the Ganga-Padma system shifted eastward, and as a result, sandbars of considerable size blocked offtakes of distributaries. And Bhairab, Jalangi, and Mathabhanga Rivers have been beheaded from their feeder river, the Padma, and

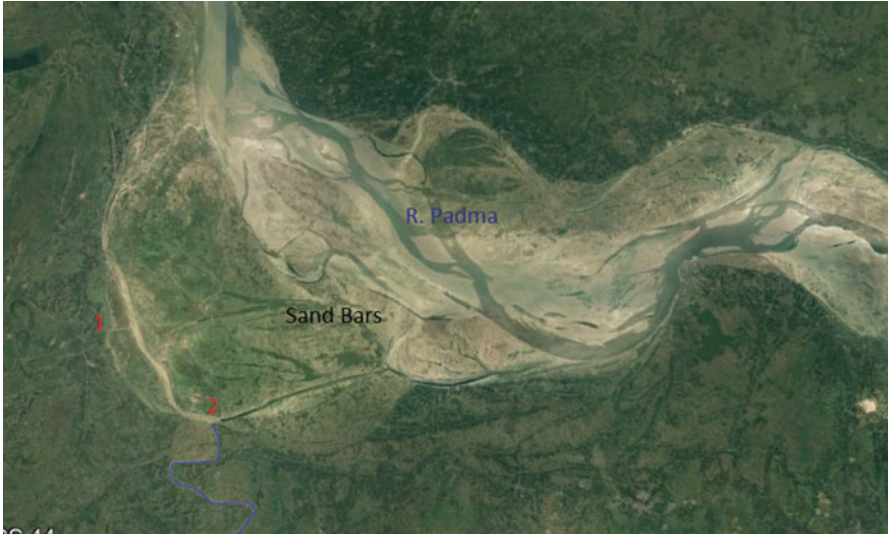


**Fig. 20.9** Due to the eastward shifting of the Padma River and deposition of sandbars at offtakes, (1) Jalangi and (2) Mathabhanga River have been detached from the feeder river, the Padma. As a result, they don't get supply to flood their basins.

decayed gradually. Nowadays, the offtake of the Jalangi River is detached from the Padma permanently. Connections of the Bhairab River and the Mathabhanga-Churni with the Padma are episodic.

In the last few decades, the pace of separation between Padma and distributaries has been multiplied which is imprinted in sedimentary records and fluvial architecture. The gradual separation of the Bhairab and Mathabhanga-Churni Rivers from the Padma River (Fig. 20.9) is a response to the deposition of sediment in between them. That is why Jalangi-Churni is being deprived of their supply from the Padma River and is unable to flood as before.

### 6.3.2 Delta-Forming Processes and River Shifting

Changes in the course of rivers are an inseparable part of the delta-building mechanism. The deltaic rivers are at a loss to find a perceptible slope (Bagchi, 1978), and as a result, they deposit a lion's share of their silt load within the bed and on the bank and a little portion deposited on low-lying flood plains behind levee (Majumder, 1941). As a result, after a long period, the rivers flow on elevated beds of higher levels than in surrounding low-lying areas. During high floods, when the threshold is reached, rivers find new courses through lower areas breaching levees (Rudra, 2010a). This oscillation of rivers, over several cycles, is the key process of delta building. However, due to huge sedimentation within the channel, the beds of these distributaries are raised well above the water level of Padma. As a result, water from

the Padma cannot enter into Bhairab-Jalangi and Mathabhanga-Churni. So, Jalangi and Mathabhanga-Churni remain active only for a few days a year (Das & Bhattacharya, 2020; Sarkar et al., 2020) and cannot flood as before the tract over which they flow.

### **6.3.3 Reduction in Rainfall**

It is reported that the overall amount of precipitation over the Indian subcontinent has been reduced. The Ministry of Earth Sciences' first-ever [climate change assessment](#) for the Indian region, released in 2020, said that monsoon rainfall had [declined by around 6% from 1951 to 2015](#), with notable decreases over the Indo-Gangetic Plains and the Western Ghats (Krishnan et al., 2020). Therefore, due to decreased rainfall, it is obvious that the overall flow of the river Ganges has declined to feed its distributaries as before. That is why the Jalangi-Churni is getting a lesser and lesser volume of water from the Padma and is not doing flood as before.

### **6.3.4 Reduced Flow of the Padma River**

The maximum discharge of the river Ganges has shown a negative trend at almost all the sites. Data on discharge and sediment load of the Ganges for monsoon months have also revealed declining trends at most of the gauging sites (Zakwan & Ahmad, 2021). Ganga River basin model and WIS report and documentation (GRBM and WIS & RD, 2018) have revealed that there is a decreasing gradient in water availability in the plain from west to east. So, having decreased flow, the river Ganges no more supplies its distributaries as before, and Jalangi-Churni, having a lesser volume of water from the Padma, cannot flood as before.

### **6.3.5 Farakka Barrage**

In addition to decreasing monsoon precipitation in the Indian subcontinent, the declined flow of the Ganges and Farakka Barrage also caused a reduction in downstream flow and a lowering of gauge height at the offtakes of Jalangi and Mathabhanga-Churni (Sarkar et al., 2021). As a result, having a lower water level of Padma than the bed level of offtakes of Jalangi and Mathabhanga-Churni, water cannot enter the rivers (Das & Bhattacharya, 2020). So, the Farakka Barrage also impacts badly the flooding capacity of the Jalangi and Churnia Rivers before.



## 7 Impact of Floods

### 7.1 Flood and Hydrogeomorphology

The Jalangi River had been beheaded at its offtake at Jalangi in the latter half of the nineteenth century. Since then, the river is being fed by the Bhairab River which joins the former river at Char Moktarpur (Das & Bhattacharya, 2020). The upstream of the Jalangi River from offtake to Bhairab confluence has deteriorated to such an extent that it either does not exist or does exist as a relict channel or wetland. The reach of 9.1 km from the abandoned offtake at Char Madhubona near Gopalpur (Ghat) to the Sialmari-Jalangi confluence at Kopila is erased from the map of the region (Das & Bhattacharya, 2020). The rest 41.9 km of upper reach from Sialmari-Jalangi confluence to Bhairab-Jalangi confluence at Moktarpur is, though, traceable but dead at present (Das & Bhattacharya, 2020). As the offtake is closed, so, no significant hydrogeomorphological dynamicity is recorded in the reach for a long time (Fig. 20.10). This reach of the river remains covered year-round by hyacinth.

Middle reach from Bhairab-Jalangi confluence to Suti-Jalangi confluence along with down reach from Suti-Jalangi confluence to Swarupganj continues flowing during year-round either being fed by Bhairab and Suti in rainy season or by seepage water from the basin. Bank erosion and bankline shifting, though not so severe, are found in these reaches (Fig. 20.11). Due to lack of discharge as before, Panditpur meander loop at the doorstep to neck cut-off is still waiting for about a century.

### 7.2 Flood and Floodplain Characteristics

Floodplains of the Jalangi-Churni basin are very gently undulated monotonous flat land and interspersed with oxbow lakes, relict channels, swamps, *beels*, and meander scars. Flooding of the rivers not only has raised the general level of the basin but also



**Fig. 20.10** (a) Bank erosion in middle reach and, (b) hyacinth-covered channel and cross-bandh at Karimpur-Bakshipur Ghat on the upper reach of Jalangi River

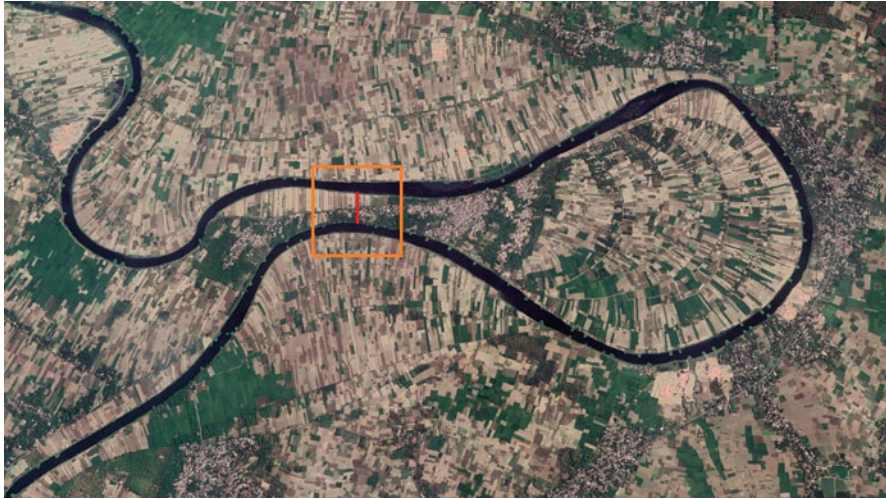


**Fig. 20.11** Due to lack of flow, the Panditpur loop of Jalangi River waiting for a century for its neck of 223 m wide (marked as a red line in the orange box) to be cut off (Retrieved on 03.03.2022)

kept numerous water bodies ecologically active and environmentally fit. In the years, when floodwater enters these oxbow lakes, relict channels, swamps, and *beels*, these water bodies get recharged with fresh silts and water. As a result, these watery depressions are gradually losing their depths. But in recent years they remain deprived.

### 7.3 Flood and Resource Appraisal

No doubt flood causes colossal loss of life and other resources in the region concerned. The cases of human death in West Bengal during the flood of 2000 were 1320 persons (IWD, 2000). The resource loss in the flood of 2000 is listed below (Table 20.4).

Other than deluges like 2000, floods of the Jalangi-Churni basin do very little in terms of life and property loss. A part of Nabadwip block, especially low-lying areas of Nabadwip town, inundates regularly. Cropped areas of other villages along the Bhagirathi-Hooghly River also become inundated. But these are not the only face of floods. Along with these evils, floods do well for a man and his environment. A flood is the excess of water resources that annually recharges the groundwater table. It raises low-lying areas depositing huge silts carried with them. Flood also augments soil fertility depositing nutrient-rich silts on lands. Moreover, wetland flora and aquatic fauna get a booster in floodwaters. There is a significant role of floods in wetland in health and productivity.

**Table 20.4** Loss in flood 2000

Sl. No.	Item	Magnitude of loss
1.	Total length/no. of breaches occurred	221.73 km/ 786 Nos.
2.	Total damaged length of embankments	601 km/ 41 Nos.
3.	Total damaged length of protective works	145.65 km
4.	Total no. of sluices damaged	481
5.	Total inundated areas	23,971 km <sup>2</sup>
6.	Total cropped area affected	19,200 km <sup>2</sup>
7.	Total population affected	2,18,00000
8.	Total loss of human life	1320
9.	Total missing persons	154
10.	Total houses damaged	21,94,000
11.	Total no. of blocks affected	117
12.	Total no. of municipalities affected	68
13.	Total damaged length of state highway (SH) and district road in 8 districts	1009.20 km
14.	Total damaged length of national highway (NH) in 8 districts	789 km + 19 structures
15.	Total damaged length of roads other than NH, SH, and district roads in 8 districts	2763.40 km
16.	No. of the hospitals affected in the 8 districts	30
17.	No. of health centers, subcenters, and office buildings affected in 8 districts	1270
18.	No. of death and missing buffalos and cattle in 8 districts	28,829
19.	No. of death and missing goats and sheep in 8 districts	68,223
20.	Total no. of poultry affected	207,636

Source: IWD (2000)

## 8 Management of Floods

### 8.1 Structural Approach (Hardware Solution)

At present, there is 10,550 km. embankments along the banks of rivers (Rudra, 2010b) of West Bengal, out of which more than 60% were inherited from the zamindars or landlords (Basu, 2002). Embanking floodplains in the Jalangi-Churni basin is an age-old practice against floods. During the seventeenth century, Raja Rudra Ray of the Nadia Raj family was patronized for the construction and maintenance of flood embankments. Raja Rudra Ray initiated a road from Krishnagar to Shantipur (Mallick, 1911). Several other railways, national highways, state highways, and district roads are there in the Jalangi-Churni basin aimed against floods. Details of embankments in the Jalangi basin as of 2020 are given in Chap. 12 of Anthropogeomorphology of the Bhagirathi-Hooghly River System in India (Das et al., 2020b). River embankments and railway embankments have contributed in a significant way to the occurrences of floods (Ghosh, 2018). Mr. H. Bell, the then collector of the district of Nadia, in letter No. 75, dated January 14, 1868, also opined

being inclined in the same direction. He wrote, *It is generally thought that the railway embankment impeded the flow of the water, and so retarded the subsidence of the inundation. This I consider to be altogether a mistake* (Inglis, 1909). However, Jalangi-Churni, as they do not do havoc regarding floods, are not regulated rivers at all.

## **8.2 Nonstructural Approach (Software Solution)**

In normal situations (except floods like 2000), floods in the rural area of the Jalangi-Churni basin affect agriculture. Though this part of deltaic Bengal had its variety of crops and methods of cultivation in normal flood situations, for profit-maximization motive, farmers cultivate a high-yielding variety of crops which are vulnerable to even normal floods. Therefore, selection of crops and their variety, cropping pattern, etc. directed to the principles adaptive to local flood situations are suggested.

## **9 Response to Floods**

### **9.1 Initiatives of the Communities, Government and NGOs**

District Disaster Management and Civil Defence Section of Nadia has its disaster management committee (<https://wbxpress.com/files/2021/05/Nadia.pdf>). Along with vulnerability mapping, they have pre- and post-flood mitigation policies. Different departments of government assisted by NGOs being equipped with helipads, flood shelters, airdropping sites, do's and don'ts directives, evacuation and shelter management plans, etc. work together in flood mitigation. Blockwise vulnerability mapping has been prepared. A list of flood shelters, boat owners, trained divers, ambulances, well diggers, tube well mechanics, electricians, NGOs, heritage buildings, private health centers, etc. have been prepared for every Gram Panchayat (GP).

### **9.2 Way Forward**

Structural mitigation strategy, especially the blockage of spills of drainage, by the feeder canal and by roads and railways with inadequate culverts and bridges, made flooding more sudden, less predictable, deeper, and longer-lasting than would otherwise be the case (Chapman & Rudra, 2007). Adapting locally suitable land-use patterns and lifestyles for living with floods is recommended widely (Cuny, 1991; Haskoning, 2003; Hazarika, 2006; Mishra, 2001; Pegu, 2018; Shaw, 1989; Zaman, 1993).

## 10 Conclusion

Jalangi-Churni basin does not get flooded to such magnitude as before. This is mainly because of the tilting of the Bengal basin and subsequent eastward shifting of the Padma River. And finally, the Jalangi-Churni Rivers became detached from the feeder river the Padma. Huge sandbars at the offtake of the distributaries made irreparable obstacles to entering water into distributaries from the Padma. Moreover, the lowering of the water level of the river Padma downstream to the Farakka Barrage exacerbated the problem of water not entering the Jalangi and Mathabhanga-Churni Rivers from the Padma. However, the evil effects of normal floods become multiplied by several structural or hardware solutions against floods. Rather living with the flood is recommended.

## References

- Abdulkareem, J. H., Sulaiman, W. N. A., Pradhan, B., & Jamil, N. R. (2018). Relationship between design floods and land use land cover (LULC) changes in a tropical complex catchment. *Arabian Journal of Geosciences*, 11(14), 1–17.
- Allison, M. A. (1998a). Geologic framework and environmental status of the Ganges–Brahmaputra delta. *Journal of Coastal Research*, 14, 826–837.
- Allison, M. A. (1998b). Historical changes in the Ganges–Brahmaputra delta front. *Journal of Coastal Research*, 14, 1269–1275.
- Allison, M., & Kepple, E. (2001). Modern sediment supply to the lower delta plain of the Ganges Brahmaputra River in Bangladesh. *Geo-Marine Letters*, 21(2), 66–74.
- Ayalew, T. B., Krajewski, W. F., & Mantilla, R. (2013). Exploring the effect of reservoir storage on peak discharge frequency. *Journal of Hydrologic Engineering*, 18(12), 1697–1708.
- Bagchi, K. (1978). Diagnostic Survey Of Deltaic West Bengal, A Research And Development Project, Department of Geography, Calcutta University.
- Basu, P. K. (2002). Seminar on flood & drainage problem of rivers of West Bengal, Calcutta Mathematical Society, Kolkata, pp. 1–5.
- Burby, R. J., & French, S. P. (1981). Coping with floods: The land use management paradox. *Journal of the American Planning Association*, 47(3), 289–300.
- Chakroborty, S. C. (1970). In A. B. Chatterjee et al. (Eds.), *Some consideration on the evolution of the physiography of West Bengal* (p. 28). Presidency College.
- Chapman, G. P., & Rudra, K. (2015). *Time streams: history and rivers in Bengal. Occasional Paper*. Centre for Archaeological Studies and Training, Kolkata
- Chapman, G. P., & Rudra, K. (2007). Water as foe, water as friend: lessons from Bengal's millennium flood. *Journal of South Asian Development*, 2(1), 19–49.
- Chaudhury, J. (2004). *Sri Chaitanyadev O Samakalin Nabadwip*. Nabadwip Puratattva Parishad. Nadia, p. 9.
- Cookey, A. T., & Ukpong, I. E. (2018). Adaptation strategies and benefits of flooding in the rural communities of Rivers state. *Nigeria. International Journal of Social Sciences*, 12(1), 63–73.
- Cuny, F. C. (1991). Living with floods: Alternatives for riverine flood mitigation. *Land Use Policy*, 8(4), 331–342.
- Das, B. C. (2013). *Changes and deterioration of the course of river jalangi and its impact on the people living on its banks*. Ph.D. Thesis. University of Calcutta. 14.03.2013.

- Das, B. C., & Bhattacharya, S. (2020). The Jalangi: A story of killing of a dying river. In Das et al. (Eds.), *Anthropogeomorphology of Bhagirathi-Hooghly river system in India*. Taylor & Francis Group. ISBN (eBook) 9781003032373. <https://doi.org/10.1201/9781003032373>
- Das, B. C., Islam, A., & Biswas, B. (2020a). Morphometry as tool to trace out the genealogy of oxbow Lake. *Environmental Earth Sciences*. ISSN: 1866-6280 (print), 79, 137. 1866-6299 (web). <https://doi.org/10.1007/s12665-020-8854-3>
- Das, B. C., Ghosh, S., Islam, A., Roy, S. (2020b). *Anthropogeomorphology of Bhagirathi-Hooghly River System in India*. ISBN 9780367557270. Taylor & Francis Group. <https://doi.org/10.1201/9781003032373>
- Dasgupta, A. B. (1997). Geology of the Bengal Basin. *Indian Journal of Geology*, 69(2), 161–176.
- Duong, A., Greet, J., Walsh, C. J., & Sammonds, M. J. (2019). Managed flooding can augment the benefits of natural flooding for native wetland vegetation. *Restoration Ecology*, 27(1), 38–45.
- Fergusson, J. (1912). On recent changes in the Delta of the Ganges, Bengal Secretariat Press, Calcutta, ed Biswas, K. R. 2001, Rivers of Bengal, (p. 184, 205). Quarterly Journal of the Geological Society of London, XIX, 1863.
- Garrett, J. H. E. (1910). Bengal District Gazetteer, Nadia, Bengal Secretariat Book Depot, reprinted in 2001, p. 14, 15, 26
- Ghosh, T. (2018). Floods and people, colonial North Bengal, 1871–1922. *Studies in People's History*, 5(1), 170.
- Goodbred, S. L., Jr. (1999). *Sediment dispersal and sequence development along a tectonically active margin: Late quaternary evolution of the Ganges-Brahmaputra River delta*. The College of William and Mary.
- GRBM and WIS & RD. (2018). <http://cwc.gov.in/sites/default/files/ganga-river-basin-model-and-wis-report-and-documentation.pdf>
- Haskoning, R. (2003). *Controlling or living with floods in Bangladesh*. Toward an interdisciplinary and integrated approach to agricultural drainage.
- Hazarika, S. (2006). Living intelligently with floods. *Background Paper*, 5.
- Hirst, F. C. (1916). *Report on the Nadia Rivers*, 1915. Bengal Secretariat Book Department.
- Hollis, G. E. (1975). The effect of urbanization on floods of different recurrence interval. *Water Resources Research*, 11(3), 431–435.
- Hunter, W. W. (1877). A Statistical Account of Bengal, Vol-II, D.K. Publishing House, Delhi, p. 25.
- Hussein, K., Alkaabi, K., Ghebreyesus, D., Liaqat, M. U., & Sharif, H. O. (2020). Land use/land cover change along the Eastern Coast of the UAE and its impact on flooding risk. *Geomatics, Natural Hazards and Risk*, 11(1), 112–130.
- Inglis, W. A. (1909). *The canals and flood banks of Bengal* (p. 507). The Bengal Secretariate Press. Calcutta. Government.
- Islam, S. N. (2016). Deltaic floodplains development and wetland ecosystems management in the Ganges–Brahmaputra–Meghna Rivers Delta in Bangladesh. *Sustain. Water Resour Manag*, 2, 237–256. <https://doi.org/10.1007/s40899-016-0047-6>
- Islam, A., Das, B. C., Mahammad, S., Ghosh, P., Deb Barman, S., & Sarkar, B. (2021). Deforestation and its impact on sediment flux and channel morphodynamics of the Brahmani River Basin, India. In Shit et al. (Eds.), *Forest Resources Resilience and Conflicts* (pp. 377–416). Elsevier Inc. <https://doi.org/10.1016/B978-0-12-822931-6.00029-0>. ISBN: 978-0-12-822931-6.
- IWD. (2019). Annual flood report for the year 2019. Advance Planning, Project Evaluation; Monitoring Cell Jalasampad Bhavan, Salt Lake Kolkata – 7000 091. Accessed on December 20, 2021.
- IWD. (2005). Annual flood report for the year 2005. Advance Planning, Project Evaluation; Monitoring Cell Jalasampad Bhavan, Salt Lake Kolkata – 7000 091. Accessed on December 20, 2021.
- IWD. (2000). Annual flood report for the year 2000. Advance Planning, Project Evaluation; Monitoring Cell Jalasampad Bhavan, Salt Lake Kolkata – 7000 091. Accessed on December 20, 2021.

- Khan, A. N. (2011). Analysis of flood causes and associated socio-economic damages in the Hindukush region. *Natural Hazards*, 59(3), 1239–1260.
- Krishnan, R., Sanjay, J., Gnanaseelan, C., Mujumdar, M., Kulkarni, A., & Chakraborty, S. (2020). *Assessment of climate change over the Indian region: A report of the ministry of earth sciences (MOES), Government of India* (p. 226). Springer Nature.
- Kuehl, S. A., Levy, B. M., Moore, W. S., & Allison, M. A. (1997). Subaqueous delta of the Ganges-Brahmaputra river system. *Marine Geology*, 144(1–3), 81–96
- Kuehl, S. A., Allison, M. A., Goodbred, S. L., & Kudrass, H. E. R. M. A. N. N. (2005). The Ganges-Brahmaputra Delta. *Special Publication-SEPM*, 83, 413.
- López-Moreno, J. I., Beguería, S., & García-Ruiz, J. M. (2002). Influence of the Yesa reservoir on floods of the Aragón River, central Spanish Pyrenees. *Hydrology and Earth System Sciences*, 6(4), 753–762.
- Loucks, D. P., & Beek, E. V. (2017). Water resources planning and management: An overview. *Water resource systems planning and management*, 1–49.
- Majumder, S. C. (1941). In K. R. Biswas (Ed.), *Rivers of the Bengal Delta, 2001* (pp. 17–54). Rivers of Bengal, Department of Higher Education, Govt. of West Bengal.
- Majumder, D. (1978). *West Bengal District Gazetters Nadia*. Govt. of West Bengal, India, p. 5–16.
- Mallick, K. (1911). Nadia Kahini, (in Bengali), Ranaghat, edited by Roy Mohit (1997), Kumudnath Mallick, Nadia Kahini, Pustak Bipani, Calcutta, pp. 32–34, 19–21, 121, 231–233, 299, 229, 322, 338.
- Mandal, M. H., Roy, A., & Siddique, G. (2021). Spatial dynamics in people-wetland association: An assessment of rural dependency on ecosystem services extended by Purbasthali wetland, West Bengal. *Environment, Development, and Sustainability*, 23(7), 10831–10852.
- Mishra, D. K. (2001). Living with floods: People's perspective. *Economic and Political Weekly*, 2756–2761.
- Natarajan, L., Usha, T., Gowrappan, M., Kasthuri, B. P., Moorthy, P., & Chokkalingam, L. (2021). Flood susceptibility analysis in Chennai corporation using frequency ratio model. *Journal of the Indian Society of Remote Sensing*, 49, 1533. <https://doi.org/10.1007/s12524-021-01331-8>
- Parua, P. K. (2010). *The Ganga: water use in the Indian subcontinent* (Vol. 64). Springer Science & Business Media.
- Pegu, T. (2018). 'Living with floods': An analysis of floods adaptation of Mising community—A case study of Jiadhhal River. In *Development and Disaster Management* (pp. 259–279). Palgrave Macmillan.
- Ray, K., Pandey, P., Pandey, C., Dimri, A. P., & Kishore, K. (2019). On the recent floods in India. *Current Science*, 117(2), 204–218.
- Reaks, H. G. (1919). Report on the Physical and Hydraulic Characteristics of the Rivers of The Delta. In *Report on the Hooghly river and its head-waters* (pp. 87–107). Vol-I, The Bengal Secretariat Book Depot, Calcutta, 1919, In Biswas (2001), Rivers of Bengal, Vol-II, Govt. of West Bengal.
- Roy, S., & Sahu, A. S. (2016). Effect of land cover on channel form adjustment of headwater streams in a lateritic belt of West Bengal (India). *International Soil and Water Conservation Research*, 4(4), 267–277.
- Rudra, K. (2010a). Dynamics of the Ganga in West Bengal, India (1764–2007)—implications for sciencepolicy interaction. *Quaternary International* 227, 161–169.
- Rudra, K. (2010b). *Banglar Nadikatha*. Sahitya Sangshad, Kolkata.
- Sahrawat, K. Á. (1998). Flooding soil: A great equalizer of diversity in soil chemical fertility. *Oryza*, 35, 300–305.
- Sarkar, B., & Islam, A. (2019). Assessing the suitability of water for irrigation using major physical parameters and ion chemistry: a study of the Churni River, India. *Arabian Journal of Geosciences*, 12(20), 637.
- Sarkar, B., Islam, A., & Das, B. C. (2020). Anthro- footprints on Churni River: A river of stolen water. In Das et al. (Eds.), *Anthropogeomorphology of Bhagirathi-Hooghly River system in*

- India. Taylor & Francis Group. ISBN (eBook) 9781003032373. <https://doi.org/10.1201/9781003032373>
- Sarkar, B., & Islam, A. (2020). Drivers of water pollution and evaluating its ecological stress with special reference to macrovertebrates (fish community structure): a case of Churni River, India. *Environmental Monitoring and Assessment*, 192(1), 45.
- Sarkar, B., Islam, A., & Das, B. C. (2021). Role of declining discharge and water pollution on habitat suitability of fish community in the Mathabhanga-Churni River, India. *Journal of Cleaner Production*. 326, 129426. ISSN 0959-6526. <https://doi.org/10.1016/j.jclepro.2021.129426>
- Sarkar, B., Islam, A., & Datta, D. (2022). Characterising topophilic behaviour in the wake of river decay and pollution through structural equation modelling. *Environment, Development and Sustainability*, 1–32.
- Sen, S., & Sen, J. (1989). *Evolution of rural settlements in West Bengal, 1850–1985: A case study*. Daya Books.
- Shaw, R. (1989). Living with floods in Bangladesh. *Anthropology Today*, 5(1), 11–13.
- Tang, Q., Bao, Y., He, X., Zhou, H., Cao, Z., Gao, P., et al. (2014). Sedimentation and associated trace metal enrichment in the riparian zone of the Three Gorges Reservoir, China. *Science of the Total Environment*, 479, 258–266.
- Tu, M., Hall, M. J., de Laat, P. J., & de Wit, M. J. (2005). Extreme floods in the Meuse river over the past century: aggravated by land-use changes? *Physics and Chemistry of the Earth, Parts A/B/C*, 30(4–5), 267–276.
- Valdes, J. B., & Marco, J. B. (1995). *Managing reservoirs for flood control* (pp. 1–13). Proceedings of the US–Italy Research Workshop on the Hydrometeorology, Impacts, and Management of Extreme Floods, Perugia, Italy.
- Williams, C. A. (1919). *History of the Rivers in the Gangetic Delta, 1750–1918*. Bengal Secretariat Press.
- Yadav, V., & Ibrar, Z. (2022). Relationship of water stress and flood damage for sustainable development. *Water Resources Management*, 36(4), 1323–1338.
- Zakwan, M., & Ahmad, Z. (2021). Analysis of sediment and discharge ratings of Ganga River, India. *Arabian Journal of Geosciences*, 14(19), 1–15.
- Zaman, M. Q. (1993). Rivers of life: Living with floods in Bangladesh. *Asian Survey*, 33(10), 985–996.
- Zope, P. E., Eldho, T. I., & Jothiprakash, V. (2016). Impacts of land use–land cover change and urbanization on flooding: A case study of Oshiwara River Basin in Mumbai, India. *Catena*, 145, 142–154.



# Chapter 21

## Geospatial Assessment of Fluvial Dynamics and Associated Flood Vulnerability in the Bhagirathi-Hugli Sub-basin in West Bengal, India



Biraj Kanti Mondal , Tanmoy Basu , Rima Das, Sanjib Mahata, and Ming-An Lee

**Abstract** The present study inquires about the dynamicity of the river processes and associated flood vulnerabilities of the Bhagirathi-Hugli River, particularly in the upper catchment area of the river. The geospatial techniques for analyzing the meandering, sinuosity, and other geometric features of the main channel of the Bhagirathi-Hugli River and the morphometric description of the sub-basin accentuate the dynamicity of fluvial processes. The image processing techniques have been employed to measure normalized difference vegetation index (NDVI), modified normalized difference water index (MNDWI), normalized difference built-up index (NDBI), Z-score (standard scores of annual rainfall), and rainfall erosivity index and analyze them as the major factors of flood vulnerability using the geospatial platform. A composite flood vulnerability index has been formulated to identify the potential flood risk zones in the study districts. The rainfall data of 2000 and 2015 of the study area have been collected to analyze the standardized rainfall. The maps of standardized rainfall have been compared with the surface flow raster of the year 2000 and 2015. The factors of terrain and streamflow also have an impact on flood frequency and intensity; those predict the normalized difference flood index by multiple linear regression model. The major consequences of flood hazards of the Bhagirathi-Hugli sub-basin have been identified in the northeastern and southwestern portions of Murshidabad district, northern and mid-portions of Nadia district, and eastern part of Purba Bardhaman district under the Bhagirathi-Hugli sub-basin

---

B. K. Mondal (✉) · S. Mahata

Department of Geography, Netaji Subhas Open University, Kolkata, West Bengal, India

T. Basu

Department of Geography, Katwa College, Katwa, West Bengal, India

R. Das

Department of Geography, Bhangar Mahavidyalaya, Bhangar, West Bengal, India

M.-A. Lee

Department of Environmental Biology Fisheries Science, National Taiwan Ocean University, Keelung, Taiwan

area. However, diverse factors and mechanisms in controlling flood have been analyzed aiming to formulate integrated flood management plans. To eradicate the severe flood hazard risks and minimize its vulnerability, integrated flood management program needs to be implemented with community participation, preparedness, resilience, and capacity building in the study area.

**Keywords** Flood hazard · Fluvial processes · Flood vulnerability · Bhagirathi-Hugli sub-basin · Geospatial techniques

## 1 Introduction

Flood is primarily considered a natural disaster throughout the world causing life and property damage (Demir & Kisi, 2016, p. 1). Along with the physical factors, human-induced activities have also influenced the occurrence of floods, and thereby the devastation of natural and human resources (Danumah et al., 2016, p. 2) has been observed. The flood hazard characterized by the intensity and probability of high river flows depends on the physical processes (Merz et al., 2010, p. 509). Several fluvial factors and their dynamicity determine flood occurrences. Morphometric parameters expound the “form and structure” of the basins of the drainage networks (Biswas et al., 2014, p. 1). The morphometric parameters like *drainage network*, *basin geometry*, *drainage texture*, and *relief characteristics* govern the severity, intensity, and vulnerability of flood hazards (Biswas et al., 2014, p. 5). The Bhagirathi-Hugli River, the main tributary of the Ganges River, belongs to the lower Ganga plains in India (Nandargi & Shelar, 2018). The Bhagirathi-Hugli River, a major river system in West Bengal of India, has experienced the frequent occurrence of flood hazards. According to Samal et al. (2014, p. 46), significant floods in this river system had been observed occurring in recent decades (1956, 1959, 1978, 1995, 1999, and 2000). During these floods, Bhagirathi-Hugli, the main river, and its eastern tributaries like Jalangi, Churni, Mathabhanga, and Bhairab, afford a huge amount of water along with its western tributaries like Damodar and Ajay rivers (Rudra, 2018). During “the past 30 years,” the Ganga River caused major and minor floods throughout its catchment areas of Uttarakhand, Bihar (Nandargi & Shelar, 2018, p. 35), and West Bengal. Generally, floods caused by precipitation from the Bay of Bengal depressions include the peak flood of record (Jha & Bairagya, 2013, p. 1). The districts like Murshidabad, Nadia, Purba Bardhaman, Hugli, Howrah, parts of North and South 24 Parganas, Paschim, and Purba Medinipur have been affected by the “river” and “coastal” type of floods situated in the Bhagirathi-Hugli sub-basin in West Bengal (Jha & Bairagya, 2013, pp. 3, 8). Several causes of floods had been determined in India, like the “downstream impacts of dam construction” which reflect the lowered flood peak magnitudes and marked reductions in sediment load (Das et al., 2020, p. 28). Likewise, the unusually concentrated rainfall caused by the cloudburst is the major cause of flood in West Bengal (Das et al., 2020, p. 31). According to Ghosh et al. (2020, p.1), the “geomorphic change” of the river caused by riverbank erosion, meandering, and “illegal sand mining” triggered the floods

during the rainy season in West Bengal. Moreover, “extensive deforestation” in the “upper catchment” of the Damodar River is also a significant factor in flood occurrences in West Bengal (Das et al., 2020, p. 24). Another cause of flood is riverbank erosion and deposition of eroded materials under the riverbed which decrease the navigability and water holding capacity of the river. Based on the studies by Mollah (2016), Dutta (2022), and Misra and Roy (2019), parts of Murshidabad, Nadia, and Purba Bardhaman districts are affected by riverbank erosion of Bhagirathi-Hugli, respectively. Jha and Bairagya (2013, p. 8) opined that the flood of 2000 was almost comparable to flood of 1978 in West Bengal in terms of loss of property and life. The planning strategies have been extensively focused to implement actions plans such as construction, restoration, or improvement of drainage channels to mitigate flood hazards in West Bengal (Nath et al., 2008, p. 859).

The present study accomplishes the review of the literature to understand the dynamicity of the Bhagirathi-Hugli River, its factors, and extension of flood hazards in the study area. This Bhagirathi-Hugli River is the western branch of the Ganga and flows more than 500 km through West Bengal (Rudra, 2018, p. 77). The recent flood phenomena have been occurring due to rising water levels caused by “drainage congestion” at the outlets of the Bhagirathi-Hugli River and its tributaries (Rudra, 2018, p. 83). Based on the study of Islam (2020, p. 149), Bhagirathi River has shifted 224 m on average (1990–2004) and 115 m (2004–2014) in the lower Gangetic delta in West Bengal. The high discharge rate from 2005 to 2010 was a major cause of floods in Bhagirathi-Hugli near Katwa and Jalangi near its confluence with Bhagirathi near Mayapur, Nabadwip (Islam, 2020, p. 153). Channel morphology has been changed dynamically along with the river course of Bhagirathi-Hugli. Several changes of meandering have been followed from 1955 to 2011 in the Bhagirathi-Hugli River near its confluence with Ajay and Jalangi (Pal, 2016, p. 6). According to Pal (2016, p. 10), meandering and channel shifting are associated with high flood occurrences and settlement disruption along the channel of the Bhagirathi-Hugli River in West Bengal. Saha and Praneeth (2016, p. 1654) postulated that flood results widespread damage to agriculture, residences and public utilities, and amount to the loss of billions of dollars each year in addition to the loss of human as well as animal lives in regional and global perspectives. According to Saha and Praneeth (2016, 1654), West Bengal has a flood-prone area of 37,600 km<sup>2</sup>. To study the flood hazard, the application of the geographical information system has been adopted by Sanyal and Lu (2003). Looking into the regional extent of flood in the selected areas of Murshidabad, Nadia, and Purba Bardhaman districts, it shows that eastern and western parts of Murshidabad district (Mollah, 2013, p. 393), Bhagirathi-Jalangi confluence near Mayapur, Nabadwip with the imprint of several riverbank shifting (Mallick, 2016), and eastern part of Purba Bardhaman district (Katwa, Ketugram, Purbasthali, and Kalna; Misra, 2018) are extensively vulnerable to flood. Riverbank morphology has been changed with its morphometric techniques such as “sinuosity index,” “meander belt,” and “meander cutoff” (Das et al., 2014, p. 285). Das, Adak, and Samanta (2014, p. 299) also mentioned that major changes in bank line shifting of Bhagirathi-Hugli River have been identified in the “left bank

toward east” and “right bank toward west” from the Krishnagar side to Nabadwip in Nadia district. The main causes of the floods of Bhagirathi-Hugli River along the eastern blocks of Bardhaman district (undivided) have been identified by Pal (2021, p. 237) such as excessive rainfall in a short period, high discharge of water with a decrease of the width of the lower catchment of the river, lower capacity of the river to carry excess water, and anthropogenic interference alongside the riverbank. Pal (2021, p. 243) also stated that “frequent flooding affects the livelihood pattern of the local people.” To mitigate flood hazards, several integrative attempts like “diversion” and “development” of river channels along with plantations alongside riverbanks are needed (Pal, 2021, p. 241).

The previous literature reflects the analysis of flood susceptibility and its spatio-temporal extension in the Bhagirathi-Hugli plain of West Bengal. The studies integrated the dominant factors of flood occurrences. The present study attempts to identify the significant fluvial and morphometric factors of this river network system, which influence flood occurrences in the district-level areas (Murshidabad, Nadia, and Purba Bardhaman districts) of West Bengal. Besides, the novelty of the present study is that it focuses on the dynamicity by concentrating on the meandering, sinuosity, and shifting and the relationship between normalized difference flood index and its predictors of the Bhagirathi-Hugli sub-basin. Some specific and integrated geospatial techniques have been adopted to prominently identify the flood hazard vulnerability zones and to analyze the risks in the study area aiming at sustainable management.

## 2 Objectives

The foremost objectives of the present study are as follows:

1. To identify the major morphometric factors of the river basin that influenced the flood hazard in the Bhagirathi-Hugli sub-basin.
2. To delineate the flood hazard vulnerability zones belonging to the study area, especially in the Murshidabad, Nadia, and Purba Bardhaman districts of West Bengal.
3. To access the recent flood incidence in the study area of West Bengal in 2015.

## 3 Materials and Methods

### 3.1 Study Area

Bhagirathi-Hugli sub-basin is a major river basin in West Bengal extending from 21° 39' to 26°56' north latitudes and 86°07' to 89°28' east longitudes (Rehman et al., 2022, p. 3). The Bhagirathi-Hugli River is flowing more than 200 km on its sub-basin consisting of the parts of Murshidabad, Nadia, and Purba Bardhaman

districts of West Bengal with the confluence of its major tributaries Jalangi and Churni rivers. The present study has been completed mainly on the three major districts comprising a significant part of the Bhagirathi-Hugli River, namely, Murshidabad, Nadia, and Purba Bardhaman (Fig. 21.1). According to the GIS analysis concurred in the current study, the total area of the river basin is 14499.74 km<sup>2</sup> spread in the aforesaid districts. The river covers its longest path in Nadia district among the three study districts. “Three major river basins of the southern West Bengal state, namely, the Bhagirathi-Hugli Jalangi, and Churni, comprise the study area designated as Gangetic West Bengal” (Sanyal & Lu, 2006, p. 208). Bhagirathi River is flowing from Farakka (Murshidabad) to Nabadwip (Nadia) over Katwa (Purba Bardhaman). The Bhagirathi River is named as Hugli near Swarupganj, Nabadwip from the confluence of river Jalangi and flowing toward south. Churni River confluent with Bhagirathi near Payradanga, Ranaghat (Nadia). Physiographically, the study area has been situated in the floodplain areas where slopes decline from north to south and west to east. Several meanderings have been identified along with oxbow lake alongside the main river and its tributaries. The Bhagirathi River has distributed its flow from the river Ganges near Farakka in Murshidabad district (Rudra, 2018). It extends its pathway from Murshidabad to the boundary of Purba Bardhaman and Nadia. Jalangi River has a confluence in Bhagirathi near Nabadwip and named the main river course named as Hugli toward the south (Rudra, 2018). The overall basin area of this river in the study districts is situated in a tropical monsoon climatic region dominated by seasonal rainfall and excessive surface flow during heavy rainfall caused by deep depression in the monsoon season.

In describing the Bhagirathi-Hugli River system, Rudra (2018, p. 80) mentioned that the distributaries of Ganga River on its right bank are burring with rivers Jalangi, Mathabhanga, and Churni which are the main eastern tributaries of Bhagirathi-Hugli River in West Bengal. In this river system, the seasonally variable discharge and unconsolidated quaternary sediment layers composing the bank governed the formation of intricate meandering (Rudra, 2018, p. 80). Jha and Bairagya (2013, p. 7) found that presently 42.3% area of West Bengal is susceptible to flood. Murshidabad, Nadia, and Burdwan (former) districts have 534,100, 390,000, and 70,000 hectares flood-prone area, respectively. Mollah (2016) identified the causes of flood in Murshidabad district in the year 2000. The main causes of this flood were the overflow of discharged water from the dams in the rivers of this district, erosion of the riverbank, and heavy rainfall during late September (p. 108). The flood had affected most of the C.D. Blocks of Murshidabad district including Suti I, Raghunathganj II, Bhagwangola II, Khargram, Jalangi, Kandi, Naoda, and Bharatpur I (pp. 109, 110, 111). Dutta (2022, p. 114) studied that the floodplain of Nadia district had been developing due to the sediment deposition of Bhagirathi-Hugli River in the entire region. According to Dutta (2022), the influential factors of changes in the floodplain of Nadia including Nakashipara were heavy discharge in the duration of a large amount of rainfall, severity of riverbank erosion, and frequent shifting of river channels. Misra and Roy (2019, p. 3) observed several changes in the riverbank of the Bhagirathi-Hugli River in Purba Bardhaman district including

the impact of floods, riverbank erosion, and sedimentation, and changes in land use and land cover due to the shifting of the river. From 1970 to 2016, the sedimentation process was dominant in Katwa and Ketugram areas, whereas the erosional process was observed in Purbasthali and Kalna (p. 3).

The three districts have been selected in the present study comprising several flood occurrences with their devastating impacts in recent decades. Besides, fluvial dynamicity correlated with various morphometric parameters of the drainage basin has been under consideration in the focus of the study and selection of the study area.

### **3.2 Database**

The study has been conducted using secondary databases (2000 and 2015) in the study area. Participants' observations have been assisted to trace out the outline of the occurrence of flood in 2015. The relevant remotely sensed (RS) satellite data have been collected from USGS (United States Geological Survey) and NRSC (National Remote Sensing Centre) websites. Geospatial techniques and statistical methods have been employed for data analysis, mapping, and representation. Available databases are mentioned in the following table (Table 21.1). A general methodological framework has been illustrated in Fig. 21.2. A total of 18 indicators have been selected to formulate the composite flood vulnerability index. The indicators have been selected on the basis of five broader categories— terrain analysis, drainage basin and river characteristics, normalized differential spectral indices, and rainfall effectivity. The selection of indicators and justification for compositing flood vulnerability index has been mentioned in the Table 21.2.

### **3.3 Delineation of Drainage Basins**

The specific stream network and drainage basin have been delineated based on the following procedures using digital elevation model (DEM) data. After successful extraction of the flow direction raster, the drainage basin has been delineated using a specific algorithm. To create the stream network, the flow accumulation raster has been extracted from the flow direction map, and then the stream raster has been converted into a polyline to acquire the specific stream network. Raster classes of flow accumulation are greater than 5000. In these processes, SRTM-DEM (Shuttle Radar Topography Mission-Digital Elevation Model) (USGS, 2000) data are used for the districts of Murshidabad, Nadia, and Purba Bardhaman. Moreover, the ordering of streams has been prepared using a stream raster and flow direction raster using Strahler's method (Strahler, 1964). It is the measure of the position of a stream in the hierarchy (Leopold, 1994). The total number of the streams (Nu) (Horton, 1945) and the total length of the streams in km (Lu) (Strahler, 1964) have been calculated for each stream order (Strahler, 1964). Figure 21.3 shows the extraction of

drainage basins, DEM, and streamflow raster. The bifurcation ratio and mean bifurcation ratio have been calculated using the following formula:

$$R_b = N_u / N_u + 1 \quad (\text{Horton, 1945}) \quad (21.1)$$

where

$R_b$  is the bifurcation ratio;

$N_u$  is the number of streams of any given order;

$N_{u+1}$  is the number in the next higher order. The mean bifurcation ratio ( $R_{bm}$ ) (Strahler, 1957) is derived as the average of the bifurcation ratios of all orders. The total area of delineated drainage basins has been overlapped on 10 by 10 grids. After extraction total of 54 points is found with their coordinates. Geometric and other features of the drainage basin and river channels have been analyzed using the following parameters, i.e., basin length, basin area, basin perimeter, basin circulatory ratio, elongation ratio, form factor, sinuosity index, stream length ratio, drainage density, drainage texture, compactness coefficient, and shape factor. The details of measurements of each parameter have been mentioned in Table 21.2.

### 3.4 DEM and Raster Analyses

Remote sensing and GIS analyses for determining flood vulnerability and occurrences have been focused on by the studies of the researchers. According to Biswas et al. (2014, p. 1), the morphometric properties of a drainage basin are quantitative attributes of the landscape that are derived from the terrain or elevation surface and drainage network within a drainage basin. Besides, Biswas et al. (2014) emphasized the relationship between “surface morphometry” and “subsurface geology” in Supin river basin, Uttarakhand, in India. These parameters such as “basin geometry,” “drainage texture,” “relief” characteristics, and “hypsometry” have been analyzed by Biswas et al. (2014). Sanyal and Lu (2006) studied “flood frequency mapping” of “flood hazard mapping” based on selected variables of regional development in the Gangetic West Bengal. The flood hazard map of the blocks alongside Jalangi River showed a “very high occurrence of flood” in 1991–2000 (Sanyal & Lu, 2006, p. 214). Sanyal and Lu (2005) used the Landsat ETM+ (Enhanced Thematic Mapper Plus) satellite imageries of the year 2000 to build up access to the vulnerability of floods in Gangetic West Bengal. The flood-prone areas along the Bhagirathi-Hugli are under a “very high water discharge” and “high-depth” zone of water during the flood (Sanyal & Lu, 2005, p. 3707). Sanyal and Lu (2003) integrated the factors of flood hazard into mapping to prepare “a composite index” of “an additive model” in Gangetic West Bengal. In this process, Sanyal and Lu (2003) recognized that the principle of assigning weightage to the variables is very crucial in this entire process of hazard mapping. Furthermore, the unit-free indicators have been used to build up the composite index using mean and standard deviation (Sanyal & Lu, 2003).

The present study emphasizes the extent and impact of physical factors related to river basin geometry, fluvial dynamics, and basin morphometry. The factors associated with linear, aerial, and relief aspects of river basin morphometry are considered in this study. In this aspect, the digital elevation model has been adopted to analyze the drainage network and basin features and raster analysis for formulating normalized differential spectral indices. Standardization of annual rainfall (2015) of the selected sites has been interpolated using GIS (geographical information system) techniques to extract the grid-point-wise value of the standardized score of annual rainfall. The following indicators have been used to identify the flood vulnerability in the study area (Table 21.2).

### 3.5 Formulation of Composite Flood Vulnerability Index

The factor analysis (principal component analysis, PCA) of the 18 selected indicators of the flood vulnerability has been employed by the composite indices method to bring out the composite flood vulnerability index using the standardized predicted factor scores.

Min-max normalization method (Nardo et al., 2009; Joint Research Centre-European Commission, 2008) has been applied to normalize the indicators.

$$x' = \frac{x - \min(x)}{\max(x) - \min(x)} \quad (21.2)$$

where  $x$  is the indicator.

For the composite factor analysis, the following formula (PCA, Pearson, 1901) has been used as:

$$P_1 = \sum a_{j1} XZ_j \text{ or } P_1 = a_{11} \cdot Z_1 + a_{21} \cdot Z_2 + \dots + a_{n1} \cdot Z_n \quad (21.3)$$

where,

$P_1$  denotes the composite flood vulnerability index; the first factor denotes the factor loading of the “ $j$ ”th variable and 1 indicates the factor number that is the first factor vector of factor loadings.

While the  $Z_j$  denotes the standardized value of the “ $j$ ”th variable, which is expressed as:

$$Z_d = \frac{X_j - X_m}{\delta_j} \quad (21.4)$$

where,  $X_j$  denotes the original value of “ $j$ ”th variable,  $X_m$  denotes the mean (simple arithmetic mean) of “ $j$ ”th variable, and  $\delta_j$  denotes the standard deviation of “ $j$ ”th variable. This method has been applied also to calculate the standardized scores (Z-score) of monthly rainfall (January–December, 2000 and 2015).



In this aspect, the mean and standard deviation are calculated. Standard error mean (SEM) has been estimated by using the sample SD (s) in place of the unknown  $\sigma$  (Carlin & Doyle, 2000).

Finally, mean composite factor scores have been calculated using the standardized factor scores extracted from PCA.

$$\begin{aligned} &\text{Mean Composite Factor Scores} \\ &= \frac{\text{Factor}_1 + \text{Factor}_2 + \text{Factor}_3 \cdots + \text{Factor}_n}{\text{Total number of factors}} \end{aligned} \tag{21.5}$$

where,  $n$  is the factor.

### 3.6 Autocorrelation and Regression Analysis

In the present study, a multiple linear regression model has been employed to predict the marginal effects of the selected factors of flood vulnerability. Furthermore, autocorrelation values are extracted in the regression model to validate the nature of autocorrelation among independent variables and the justification of the regression model. Besides the coefficient of determinants, analysis of variance (ANOVA), marginal effect analysis of the population mean, and significance test have been adopted during the analysis of the multiple linear regression model.

The formula of multiple linear regression model (Uyanik & Güler, 2013, p. 235) is based on Pearson (1897, 1914), which is:

$$Y = \beta_0 + \beta_1 X_1 + \dots + \beta_n X_n + e_t \tag{21.6}$$

where

$Y$  is dependent variable (here, normalized difference flood index 3 or NDFI3).

$X_j$  is independent variable.

$\beta_j$  is parameter

$e_t$  is error.

Here the correlation coefficient ( $r$ ) and coefficient of determinants ( $r^2$ ) values are calculated using the Pearsonian formula.

The formula of “ $R$ ” (multiple correlation coefficient) (Pearson, 1897; Pearson, 1914) is:

$$R = \sqrt{\frac{[(r \cdot yx_1)^2 + (r \cdot yx_2)^2] - (2 \times r \cdot yx_1 \times r \cdot yx_2 \times r \cdot x_1x_2)}{1 - (r \cdot x_1x_2)^2}} \tag{21.7}$$

where

$R$  is the value of the correlation coefficient  
 $x_1$  is one independent variable  
 $x_2$  is another independent variable  
 $y$  is the dependent variable

Autocorrelation has been determined using the “Durbin-Watson test” (Durbin & Watson, 1971) with 99% and 95% confidence intervals (Farebrother, 1980). The formula of the Durbin-Watson test is adopted by Holt and Refenes (1998, p. 60) is:

$$d = \frac{\sum_{t=2}^n (\hat{e}_t - \hat{e}_{t-1})^2}{\sum_{t=1}^n (\hat{e}_t)^2} \tag{21.8}$$

where

$d$  = Durbin and Watson statistic (DW statistic)  
 $e_t$  = error term

To identify the  $f$ -statistics, ANOVA has been run using the following formula.

The “ $F$ ” value in the  $j$ th “one-way ANOVA” (Fisher, 1934) is calculated through the following formula:

$$F = \frac{\text{Explained variance}}{\text{Unexplained variance}} \tag{21.9}$$

$$\text{or, } F = \frac{\text{Between-group variability}}{\text{Within-group variability}} \tag{21.10}$$

The “explained variance or “between-group variability” is

$$\sum_{i=1}^k ni (\bar{Y}_i - \bar{Y})^2 / (K - 1) \tag{21.11}$$

where,

$\bar{Y}_i$  denotes the sample mean in the  $i$ th group  
 $ni$  is the number of observations in the  $i$ th group  
 $\bar{Y}$  denotes the overall mean of the data and  
 $K$  denotes the number of groups

The “unexplained variance” or “within-group variability” is

$$\sum_{i=1}^n \cdot \sum_{j=1}^{ni} (Y_{ij} - \bar{Y}_i.)^2 / (N - K) \tag{21.12}$$

where

$Y_{ij}$  is the observation in the  $i$ th out of  $K$  groups and  $N$  is the overall sample size.

This  $F$ -statistic follows the  $F$ -distribution with  $K-1, N-K$  degree of freedom under the null hypothesis.

For testing the hypotheses, independent samples *t*-test or Student's *t*-test has been used.

The formula of Student's *t*-test (Student, 1908) is:

$$t = \frac{m - \mu}{s/\sqrt{n}} \quad (21.13)$$

where

*t* is the *t*-score in Student's *t*-distribution

*m* is the arithmetic mean

$\mu$  is the theoretical value

*s* is the standard deviation

*n* is the size of the variable set

In the study, the degree of freedom is (*n*-1) and confidence intervals are 95% and 99%.

## 4 Results and Discussions

### 4.1 *Fluvial Dynamics and Characteristics of the Bhagirathi-Hugli River Basin*

Fluvial dynamicity is associated with the changes of river courses, its geometric and morphometric heterogeneity. Pal et al. (2016, p. 4) identified a several meanderings cutoff in the river course of Bhagirathi-Hugli in West Bengal. Ghosh et al. (2020, p. 9) analyzed that river "sinuosity," "width" and "migration" of river channel, its "radius," and "curvature" expeditiously change with the increase of "peak discharge" of river water. Mandal et al. (2016) analyzed that Bhagirathi River was shifted toward its right bank in 2000. The river channel had shifted also due to a large amount of deposition in the right bank from 2000 to 2015 in Murshidabad district (Mandal et al., 2016). The dynamic changes of the river channel of Bhagirathi-Hugli in Nadia district have been observed by Das et al. (2014, p. 286). Eastward shifting of river courses has been observed during 1977 to 2000 near Nabadwip in Nadia district (Das et al., 2014, p. 286). The squandering and acquiring of land areas by the shifting of Bhagirathi-Hugli River in Katwa block of Bardhaman was 3.94 km<sup>2</sup> and 2.08 km<sup>2</sup>, respectively (Misra, 2018, p. 487). The scenarios of land loss and land gain in Purbasthali blocks were 20.66 km<sup>2</sup>. and 22.23 km<sup>2</sup>, respectively (Misra, 2018, p. 488) where in Kalna block these were 1.84 km<sup>2</sup> and 3.55 km<sup>2</sup>, respectively (Misra, 2018, p. 489). The present study also depicts the nature of dynamicity of Bhagirathi-Hugli River along the study areas of Murshidabad, Nadia, and Purba Bardhaman districts. The drainage texture, meandering length, and sinuosity index have been increased from 0.93 to 0.96, 336.79 km to 342.00 km and 1.59 to 1.79, respectively, from 2000 to 2015. The eastern side banks of the Bhagirathi-Hugli

River had been decayed more than the western side banks, and the river is gradually shifting from west to east (2000–2015).

The total length of the Bhagirathi-Hugli River in West Bengal is 260 km. A major portion of the river has been measured in Nadia and Murshidabad districts. Drainage density varies with the length of each stream order and the basin area included in the basin of each district. The highest drainage density has been in Murshidabad district followed by Nadia and Purba Bardhaman, among the three districts. The mean bifurcation ratio ( $>3$ ) indicates the greater probability of flooding in the study area. The area and perimeter of each of the basins included in the three districts are 5381.14 km<sup>2</sup>, 3903.46 km<sup>2</sup>, 5215.14 km<sup>2</sup>, and 538.97 km, 578.98 km, and 526.96 km, respectively. The ratio of drainage length is measured high in the first two orders than in the second and third order that indicate an early stage of geomorphic maturity of the river basin area. The drainage texture, meandering length, and sinuosity index of the total basin area are 0.93, 336.79 km, and 1.59, respectively, indicating that the river basin consists of greater surface flow with highly meandering features. The basin included in Murshidabad, Nadia, and Purba Bardhaman indicates the circulatory ratio as 0.233, 0.146, and 0.236, whereas the elongation ratios are 0.153, 0.121, and 0.154, respectively. The form factor has been measured as 0.0185, 0.012, and 0.0187 in the basins included in Murshidabad, Nadia, and Purba Bardhaman districts. Based on the values of the circulatory ratio, elongation ratio, and form factor, the Bhagirathi-Hugli River basin has the nonhomogeneous type of rocks; it is more elongated with less efficient runoff discharge and consists of extended shape factor in the study area. Figure 21.4 shows the various cross-section types in the three selected sites, Murshidabad, Nadia, and Purba Bardhaman, respectively. The cross-section line from Farakka to the southern part of the Nadia district shows a curvature profile of the river basin area (Fig. 21.4). Satellite images show a highly meandering situation and oxbow lakes along with the confluence of Jalangi and Churni with Bhagirathi-Hugli (Fig. 21.5) which signifies a greater probability of bank erosion on the side banks of the rivers.

## ***4.2 Factors of Flood Occurrences and Flood Vulnerability Index***

Being a flood-prone zone of West Bengal, the study area has been influenced by several factors of occurrence of flood incidences. The present study focuses on 18 factors related to rainfall situation, drainage basin morphometry, stream features, and other normalized differential spectral indices. Based on the analysis of the year 2000, the mean annual rainfall of Murshidabad, Nadia, and Purba Bardhaman was 113.21 mm, 156.87 mm, and 108.37 mm. A large amount of rainfall in the study area within June, July, August, and September had extended the discharge of water from dams and overflow situation. Standardized scores of annual rainfall are higher in the middle portion of Nadia district where the rainfall erosivity is also high (Figs. 21.6

and 21.8). The overall situation of the selected factors of flood occurrences in the study area has been discussed here (Figs. 21.7 and 21.8). The elevation varies from 0 to 80 m which is higher on the western side of Purba Bardhaman and lower in the south of Nadia districts. The slope varies from 0% to 12.86% where the direction of aspect is mostly flat (-1) and slope change from north to south and west to east. The ruggedness values are not too high but increasing from south to north and east to west of the study area. The flow length is high (1.27 km) near the main river channel, and flow distance is also increasing from the main and subsequent river channels along the boundary of the three districts to the northern part of Murshidabad, the northwestern part of Nadia, and the northwestern part of Purba Bardhaman district. Highly sink flow has been followed in the Nadia and Purba Bardhaman districts where the flow length density is high in Murshidabad and part of the boundary of Nadia and Purba Bardhaman (near Nabadwip). The normalized difference spectral indices, such as NDVI, MNDWI, NDBI, NDFI3; normalized difference turbidity index (NDTI), normalized difference soil index (NDSI); and the other indices like topographic wetness index (TWI) and sediment transport index (STI) show a varied situation in the study area. The normalized difference flood index varies from -0.68 to 0.99 which is higher in the parts of Murshidabad and Nadia district and becomes lower in the western part of Purba Bardhaman. The highest standard deviation and standard error of mean have been calculated respective to sink flow and flow length of the drainage basin and streams among the indicators (Table 21.3). The principal components as a first factor are slope, flow direction, sink flow, flow length, MNDWI, NDBI, NDFI3, NDTI, NDSI, TWI, TRI, STI, and Z-score of annual rainfall (Table 21.4). Figure 21.9 shows the spatial distribution of the composite flood vulnerability index and mean composite flood vulnerability index, respectively, based on the discussed factors. The value of very low CFVI is -8.0 to -5.8 followed by low (-5.7 to -3.7), moderate (-3.6 to -1.5), high (-1.4 to -0.67), and very high (0.68 to 2.80) values of that index (Table 21.4). The very low flood vulnerability exists nearer the tri-junction boundary of the three districts, the northwestern boundary of Murshidabad, and the northeastern boundary of Nadia. The very high flood vulnerability exists mostly on a larger part of the middle to the south of Nadia and Purba Bardhaman district and scattered in Murshidabad district. The northern parts of Nadia and Purba Bardhaman and a large portion of Murshidabad show high flood vulnerability. The maps (in Fig. 21.9) show the overlapping situation of NDFI3 and Z-score of annual rainfall, respectively, on the composite flood vulnerability index, that is, mostly the areas of higher values of NDFI3 and Z-score of annual rainfall show high flood vulnerability.

Based on the above discussion, it is summarized that the Bhagirathi-Hugli River basin in Murshidabad, Nadia, and Purba Bardhaman districts have nearly very high to high flood vulnerability. The topographic and drainage conditions vary along the main river, and its tributaries show a greater probability of a flood in the riverbank areas where the flow length and flow length density are high and the distance to the stream is low. Besides, a large amount of rainfall with its erosivity and a high normalized difference flood index influence the higher probability of a flood in the study area. Based on the participants' observation and raster analysis, it is revealed

that a large portion of Nadia and Murshidabad districts and a part of Purba Bardhaman district is under the deforestation condition (NDVI is low) where the turbidity and sediment transport is high in the river channels that increase the riverbank erosion along with the decrease of the navigability of the rivers Bhagirathi-Hugli, Jalangi, and Churni. In this situation during the high and intensive rainfall situation, the rivers fail to flow the excessive waters discharged from the check dams which frequently increases a highly intensive flood situation in the inhabited areas (high NDBI) in the study area.

### 4.3 Relationship Between NDFI and Its Predictors

The normalized difference flood index is high in the parts of the study area where flood vulnerability is also high. Here, in the study, 18 factors have been selected based on the principal component analysis (a total of 18 factors cumulatively explain 71.59% of the total variance). The predictors establish a high correlation with the dependent variable (NDFI3,  $r$  value is 0.974). The independent variables highly predict the NDFI3 (94.8%,  $r$  square is 0.948). The autocorrelation value extracted from the multiple linear regression model is nearer to 2 (value is 2.417). This value is significant at 0.05% and 0.1% significance levels. The Durbin-Watson value falls between 1.5 and 2.5, which is relatively normal with nearly no autocorrelation among the predictors (Table 21.5). The  $f$ -value is significant at a 0.05% significance level ( $f < 0.001$ ) which indicates a significantly less variation of means among the predictors (Table 21.5). Variance of inflation (VIF) values for all of the predictors are less than 10. The beta values of the unstandardized coefficient of the predictors and significance values have been mentioned in Table 21.5. One unit change of relief increases 0.02 unit of NDFI3 followed by the slope (increase 0.014 unit of NDFI3), flow direction (increase 0.000356 unit of NDFI3), sink flow (increase 0.000000424 unit of NDFI3), flow length (decrease 0.026 unit of NDFI3), MNDWI (increase 0.891 unit of NDFI3), NDTI (decrease 1.000008 unit of NDFI3), TWI (increase 0.008 unit of NDFI3), TRI (increase 0.042 unit of NDFI3), STI (increase 0.001 unit of NDFI3), Z-score (annual rainfall, decrease 0.025 unit of NDFI3), and REI (increase 0.000232 unit of NDFI3). The highest positive influential predictor is MNDWI. Respective to the study area, the modified normalized difference water index is higher along the river channel of Bhagirathi-Hugli and its tributaries which increases the possibility of flood occurrences. Based on the analysis, relief, flow direction, MNDWI, NDTI, and REI indicate a significant relationship among the variables where  $p < 0.05$  is in the case of MNDWI, NDTI, and REI and  $p < 0.1$  is in the case of relief and flow direction. Intensive rainfall extends the erosivity of soil which influences the decrease of negligibility and excessive water holding capacity of the river channel in the study area causing an increase in flood vulnerabilities and occurrences. Figure 21.10 shows the graphical plots of ZPR and ZRE (multiple linear regression model).

#### ***4.4 Major Flood Incidence in 2015 and Outline of Flood Management***

In the recent decades (2011–2021), a major flood has been occurring in 2015 in the study area. According to the annual flood report (Irrigation and Waterways Department, 2015, p. 3), a total of 111 blocks had been affected by “flood and tidal inundation” in 2015 in West Bengal. The “alluvial and deltaic plain” consisted annual average rainfall of 1650 mm this year (p. 3). Thirty-seven thousand five hundred forty-two sq. km areas of the state had affected by the flood. Along the river channel of the Bhagirathi-Hugli sub-basin, flood had been occurring in mainly 2537 km<sup>2</sup> of Murshidabad, Nadia, and the eastern part of Purba Bardhaman district by the “Bhairab-Jalangi-Sealmari group of rivers” and “the Mathabhanga-Churni-Ichamati system of rivers” (p. 5, and 6). The rainfall records (Fig. 21.6) show that the annual rainfall of Murshidabad district was 1152.18 mm, followed by Nadia (1781.66 mm), and Purba Bardhaman (1183.90 mm) in 2015. The monthly rainfall in June, July, August, and September 2015 were 21.48 mm, 146.73 mm, 398.72 mm, and 318.922 mm in Murshidabad; 57.35 mm, 220.91 mm, 841.54 mm, and 241.48 mm in Nadia; and 28.98 mm, 142.25 mm, 459.08 mm and 248.95 mm, respectively in Purba Bardhaman. A positive value of the standardized rainfall has been found in July, August, and September (2015) in each of the districts. The annual rainfall shows a higher deviation from the average annual rainfall in Nadia than in Murshidabad and Purba Bardhaman in 2015. In this situation, the excessive flow of water discharged from the check dams originated in the flood in a large area of the districts of West Bengal including parts of Murshidabad, Nadia, and Purba Bardhaman (Former Bardhaman or Burdwan). According to the annual flood report (Irrigation and Waterways Department, 2015, p. 49), an atmospheric disturbance that originated over the Bay of Bengal affected the flood-prone areas from July 24 onwards. The peak level of water above “extreme danger level (EDL)” in Bhagirathi-Hugli was 9.97 m near Swarupganj and 14.85 m near Katwa from July 27 to August 7 (2015) within a certain period. Figures 21.11 and 21.12 show the surface water extension during August–September, 2015, based on OCM, surface water layer product (NRSC, 2014), from August 3–4 to September 27–28. The most affected blocks by the flood in 2015 were Kandi, Bharatpur I and II, Khargram, and Burwan in Murshidabad district; Nabadwip and Nakashipara in Nadia district; and Jamalpur and Memari in Burdwan district (Irrigation and Waterways Department, 2015, p. 52). Along with the eastern tributaries of the Bhagirathi-Hugli River, a part flow of the Ganges River in Murshidabad and Damodar River in Purba Bardhaman district had influenced the occurrences of the flood in 2015. The accuracy flood susceptibility map and normalized difference flood index (NDFI3) map have been validated using the AUC-ROC (area under the ROC curve-receiver operating characteristic) representation. Rehman et al. (2022, p. 11) analyzed that area (%) under “predicted” and “actual” flood susceptibility represented a high (>9.0) “success” and “prediction” rates in Bhagirathi sub-basin in West Bengal, India. Present study represented the AUC-ROC curve for the accuracy of NDFI using the data of surface

extension of floodwater during monsoon flood of 2015 in Bhagirathi-Hugli River in the study area. Figure 21.13 (13.1–13.2) shows the AUC-ROC accuracy model which represents 84% of accuracy with the fitted ROC area 0.905. Thus, flood of 2015 highly supports the accuracy of the results produced by NDFI.

To eradicate the severe damage and restore the damage, several plans and programs have been initiated by the government including river dredging, embankment management, channel restoration, reservoir controlling, accurate weather forecasting, disaster preparedness, training, mitigation, and management.

## 5 Conclusion

Flood as a quasi-natural hazard has a severe impact on people, property, and the environment. In the present study, flood vulnerability and occurrences have been discussed in the Bhagirathi-Hugli sub-basin in the districts of Murshidabad, Nadia, and Purba Bardhamana. The study area has a record of previous floods including its vulnerable occurrence in 1999, 2000, and 2015. Several geometric, morphometric, hydrological, and climatic factors impact the occurrences and vulnerability of flood hazards in the study area of Bhagirathi-Hugli River basin. A meandering shape of the main river channel and its tributaries like Jalangi and Churni has existed in the study area under the influence of relief, slope, slope aspect, streamflow direction, sink flow, flow length, flow length density, normalized difference indices, vegetation, water (modified), built-up areas, flood situation, turbidity, and soil. The topographic wetness index, terrain ruggedness index, sediment transport index, standardized annual rainfall, and rainfall erosivity index also impact the situation of flood in the study area. The rainfall situation in the years 2000 and 2015 indicates that the monsoon season, i.e., the month of June to September, has the highest rainfall distribution among the other months of the year which accumulate extended the surface flow in the Bhagirathi-Hugli and its tributaries in Murshidabad, Nadia, and Purba Bardhamana. Besides, a large amount of erosion has been occurring during the years by the intensity of rainfall which decreases the navigability of the rivers. As a consequence, the rivers have a low capacity to carry a discharge of large amount of water from the check dams during heavy rainfall of monsoonal depression which ultimately causes flood situations in several areas of the respective study area. Satellite images show the channel conditions of Bhagirathi-Hugli and its tributaries in Murshidabad, Nadia, and Purba Bardhamana which are extensively flood-prone zones. The basin geometry and stream-related factors, such as basin length, basin area, basin perimeter, mean bifurcation ratio, basin circulatory ratio, elongation ratio, sinuosity index, drainage length ratio, drainage density, drainage texture, compactness coefficient, form factor, and shape factor, are also associated with the seasonal changes of the flow of the stream network of the Bhagirathi-Hugli River in the study area. In the study, MNDWI, NDTI, and REI significantly predict the normalized difference flood index (NDFI3) which indicates a positive relationship between NDFI3 with MNDWI and REI and a negative relationship between NDFI3 and



NDTI. The extracted layers from the OCM surface water raster indicate the surface extension of waters in the days of August and September 2015. Significant flood vulnerability zones have been prepared using the GIS application and statistical techniques that are composite flood vulnerability index (CFVI) and mean composite vulnerability index (MCFVI) in 2000. A very high CFVI (0.68–2.80) has existed in most of the Nadia and Purba Bardhaman districts influenced by the extended main river channel of Bhagirathi-Hugli in Nadia district and across the boundary of Nadia and Purba Bardhaman along with the eastern tributaries of Bhagirathi-Hugli River as Jalangi and Churni and Ajay and Damodar River in Purba Bardhaman. Murshidabad district is included in the high flood vulnerability zone (CFVI is  $-1.4$  to  $0.67$ ) influenced by the Bhagirathi River bifurcated from Farakka and some other tributary rivers. Overall, most of the C.D. Blocks of the three districts are included in very high to a high flood-prone zone. The overlapping isolines of normalized difference flood index and Z-score of annual rainfall on the mean composite flood vulnerability index (MCFVI) map indicate that the areas included in high NDFI3 and Z-score of annual rainfall also comprised high flood vulnerability zones in the study area. To eradicate the severe impact of the flood vulnerability and occurrences, integrated preparedness, training, mitigation measures, and sustainable management planning and procedures need to be implemented in the study area by the initiatives of public and private bodies including the local inhabitants.

**Acknowledgments** The authors would like to thank Indian Council of Social Science Research (ICSSR) for providing the supportive research funding and Netaji Subhas Open University for the essential support.

**Funding** This research work is supported by the research funding provided by the Indian Council of Social Science Research [ICSSR-MOST (Taiwan)/RP-1/2022-1C], New Delhi, India.

# Appendices

## Appendix A

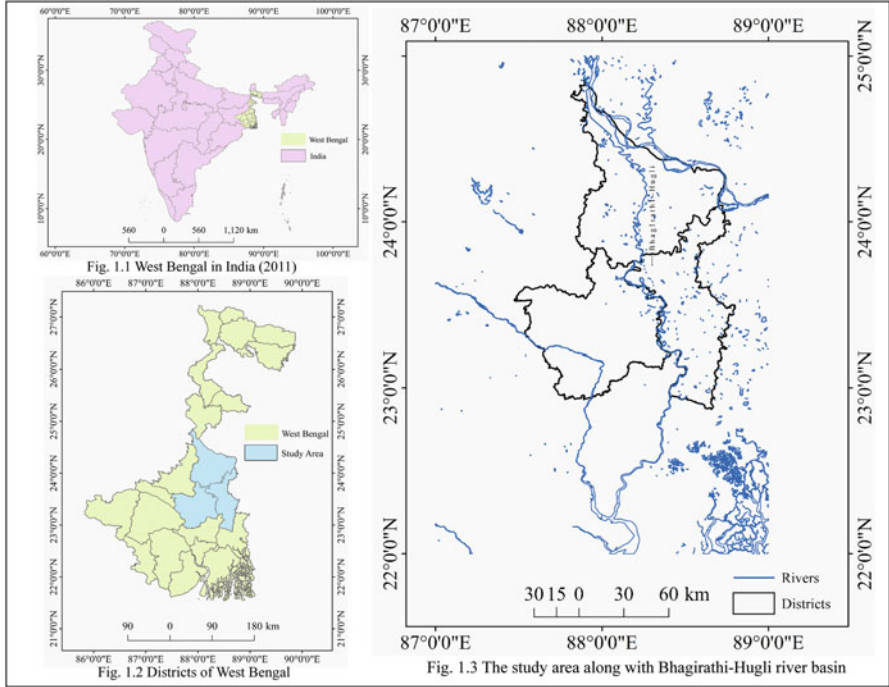


**Fig. 21.1** (1.1–1.3) Location map of the study area

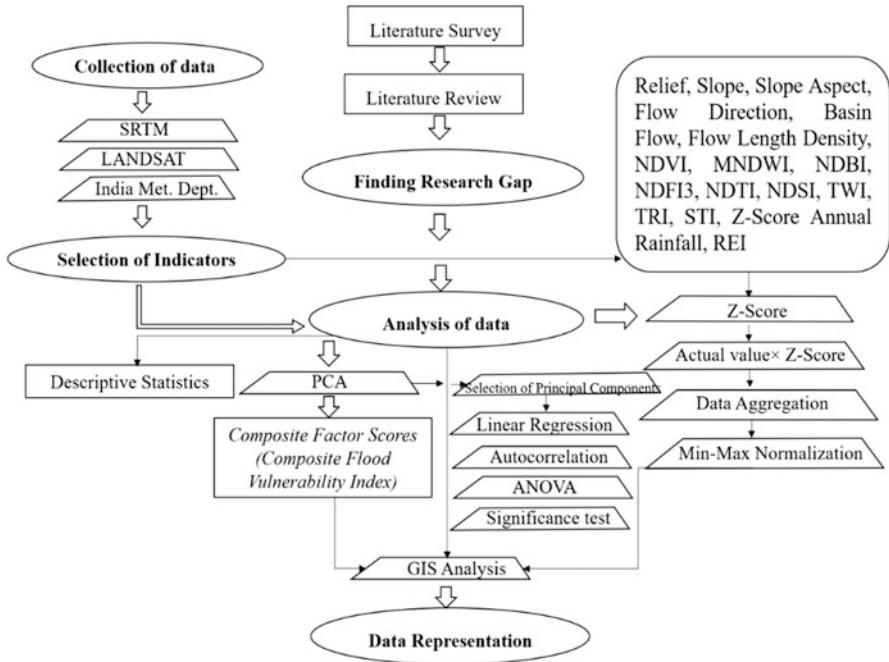


Fig. 21.2 A general methodological framework of the study

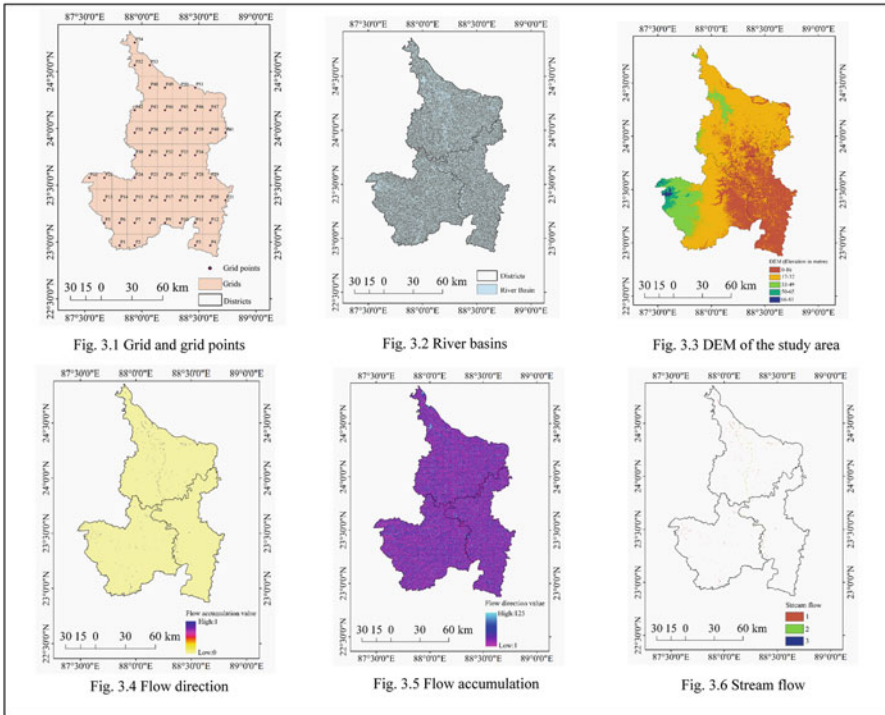
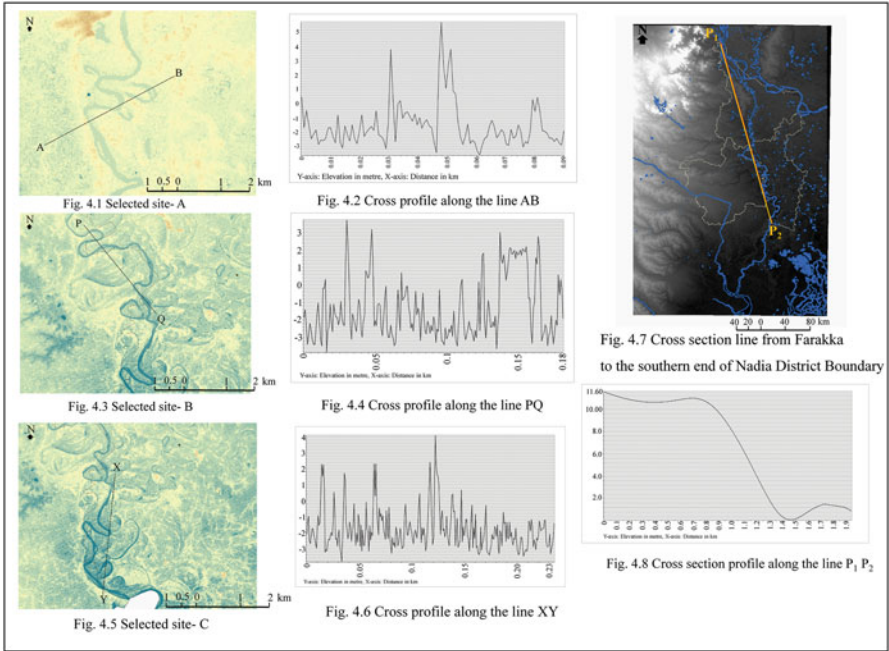
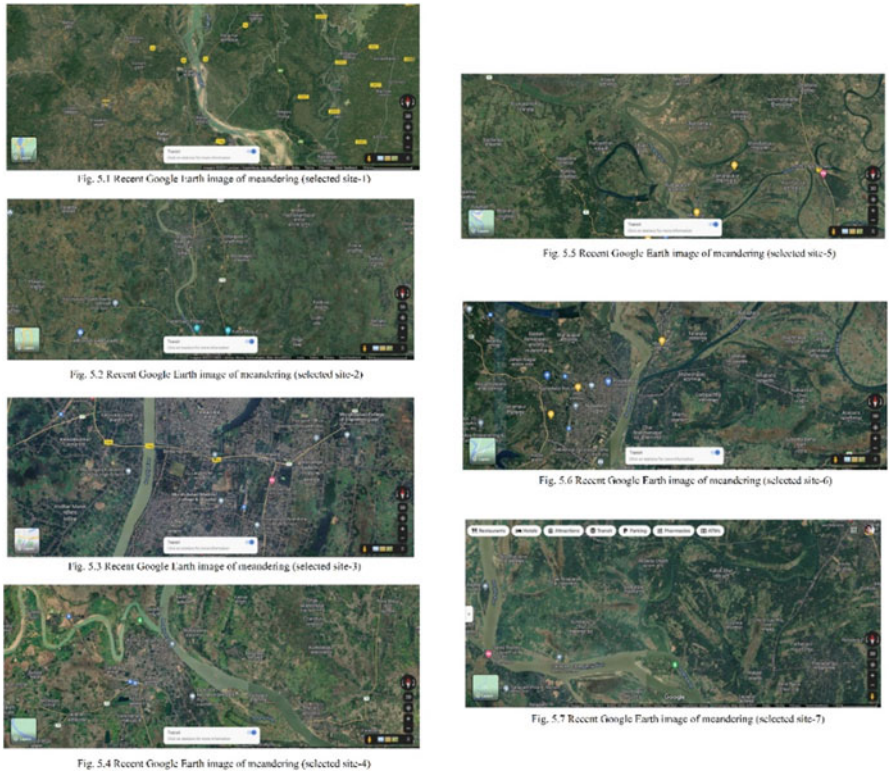


Fig. 21.3 (3.1–3.6) Extraction of the drainage basin, DEM, and streamflow



**Fig. 21.4** (4.1–4.8) Cross section along the lines in different observation sites



**Fig. 21.5** (5.1–5.7) Recent Google Earth image of meandering (selected sites 1–7)

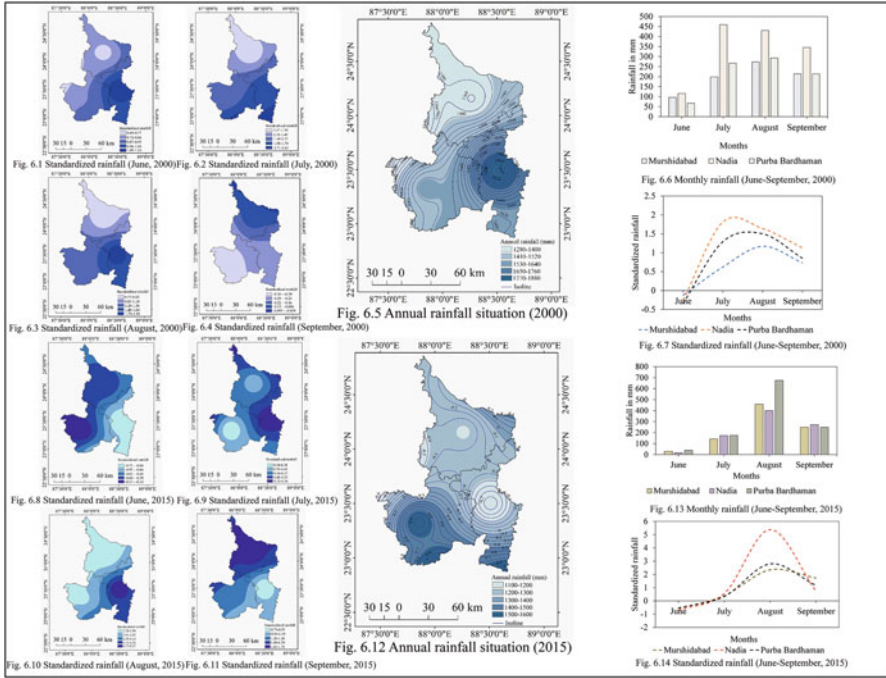


**Fig. 21.6** (6.1–6.14) Standardized rainfall (June–August 2000 and 2015) and annual rainfall (2000 and 2015)

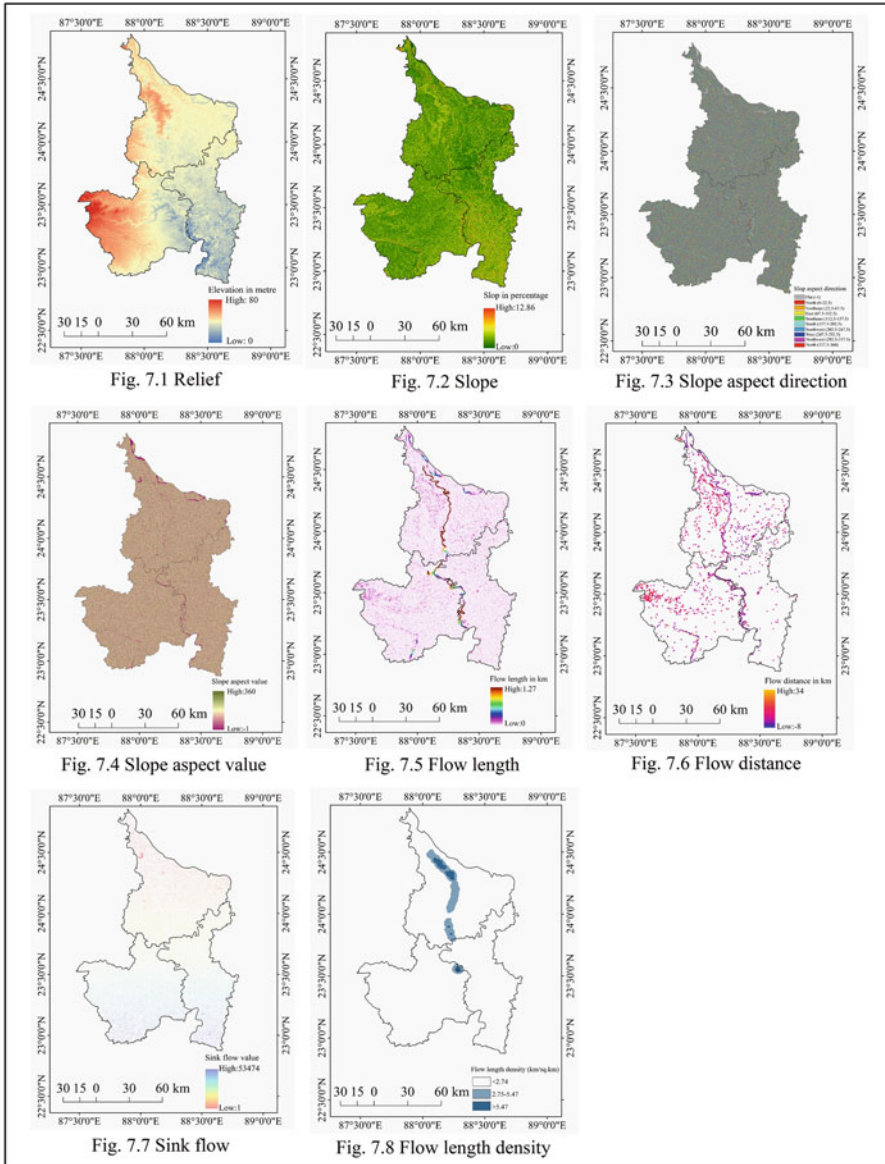
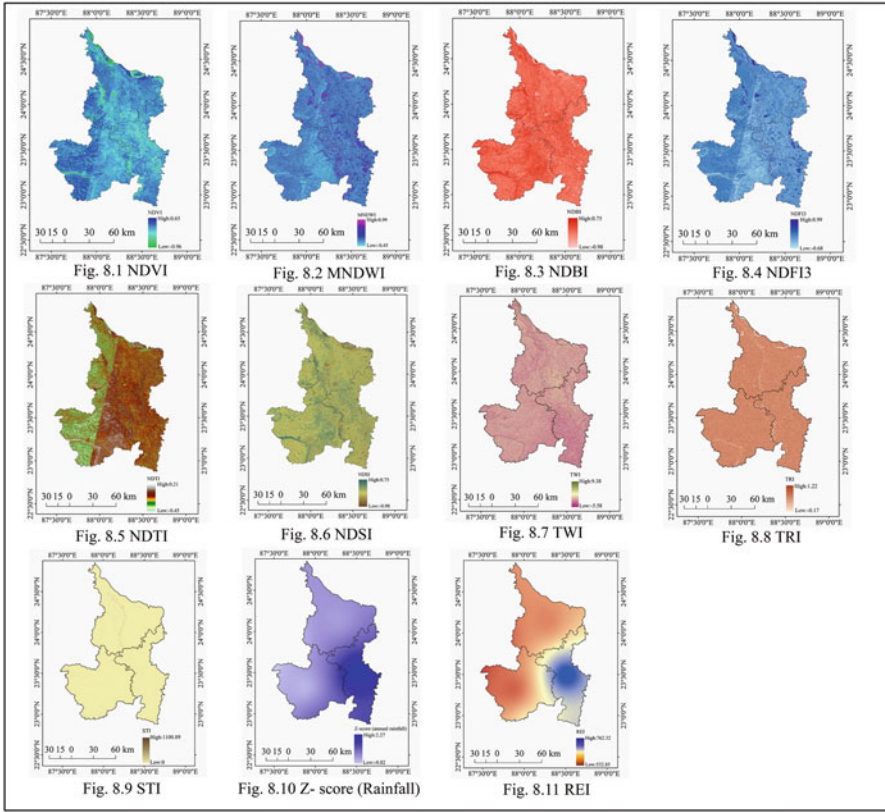
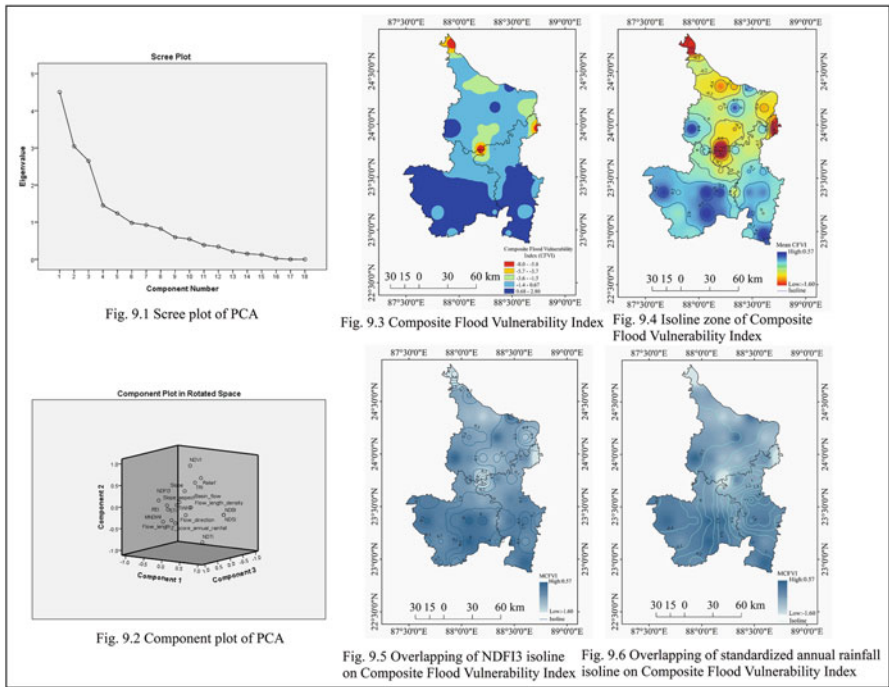


Fig. 21.7 (7.1–7.8) Different analyses of the selected indicators based on DEM



**Fig. 21.8** (8.1–8.11) Raster analysis of the selected indicators; Z-score of annual rainfall and rainfall erosivity index map



**Fig. 21.9** (9.1–9.6) Analysis of flood vulnerability in the study area

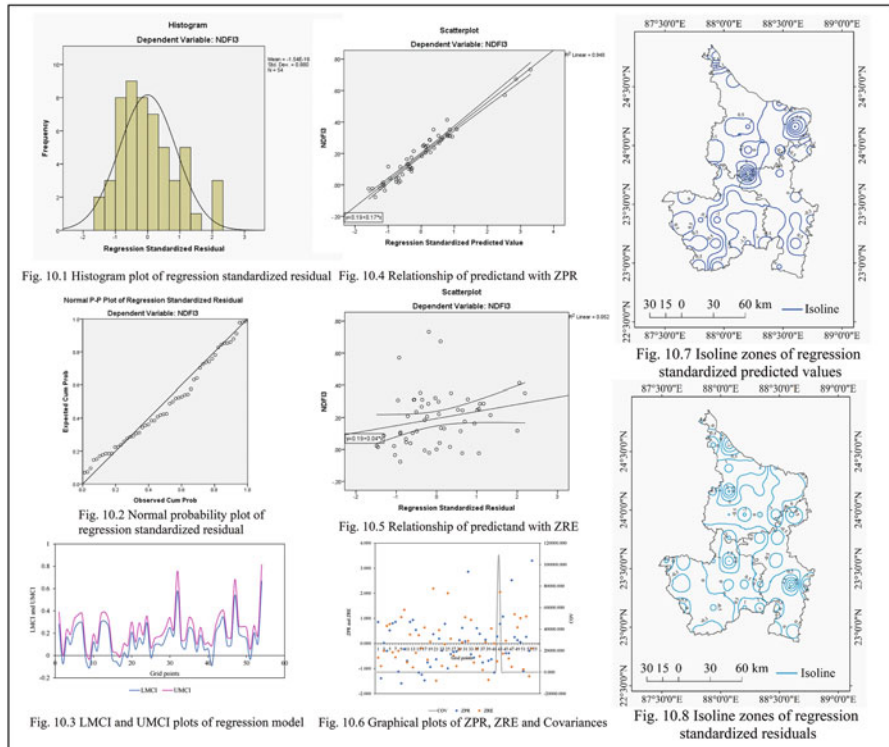


**Fig. 21.10** (10.1–10.8) Graphical plots of ZPR and ZRE (multiple linear regression model)



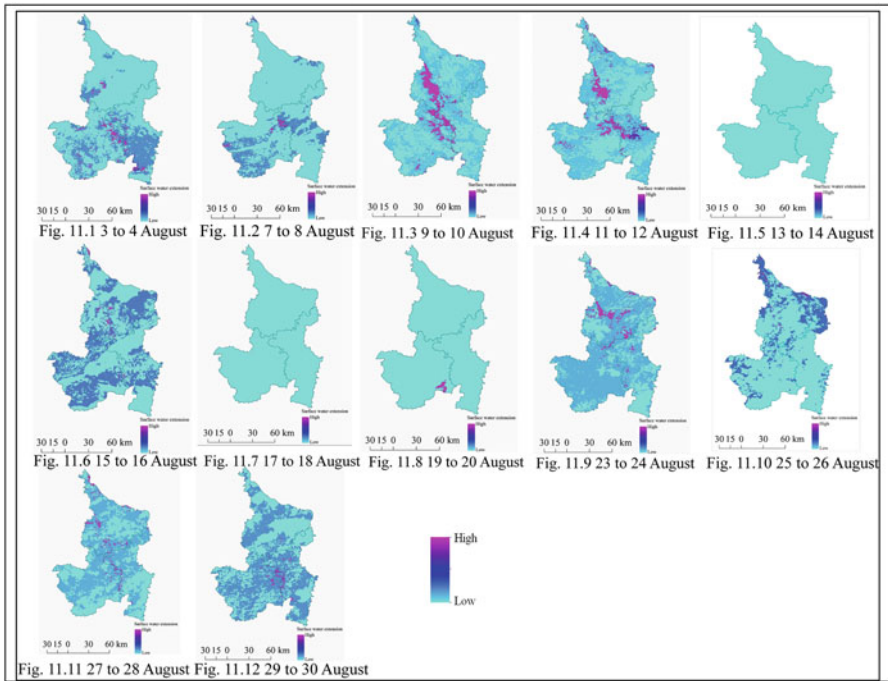


**Fig. 21.11** (11.1–11.12) Surface water extension during August, 2015. (OCM: Surface Water Layer Product)

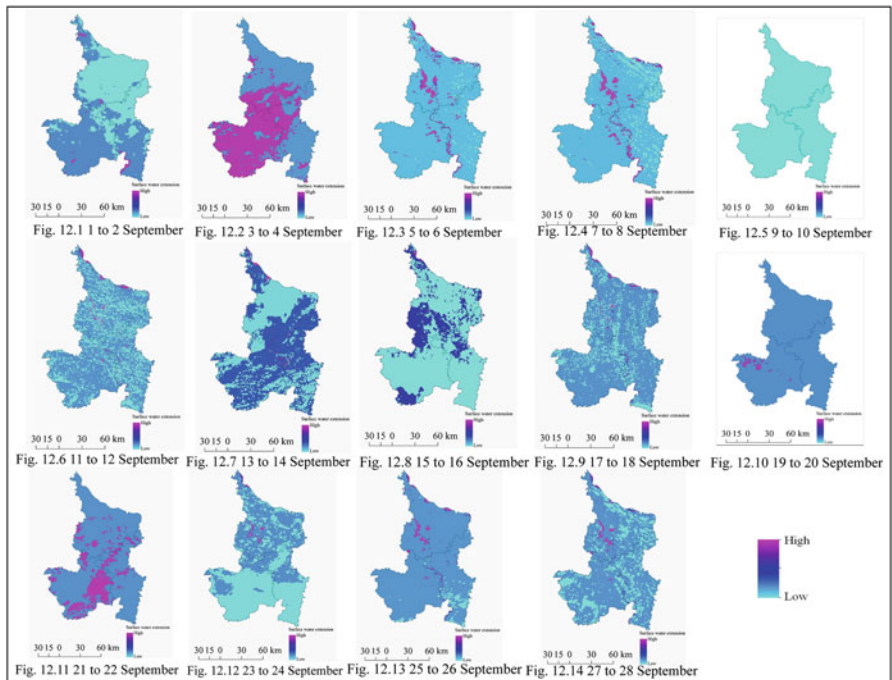


**Fig. 21.12** (12.1–12.14) Surface water extension during September, 2015 (OCM: Surface Water Layer Product)

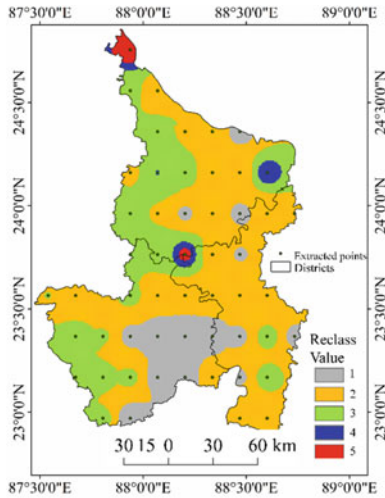


Fig. 13.1 Reclassified NDFI map

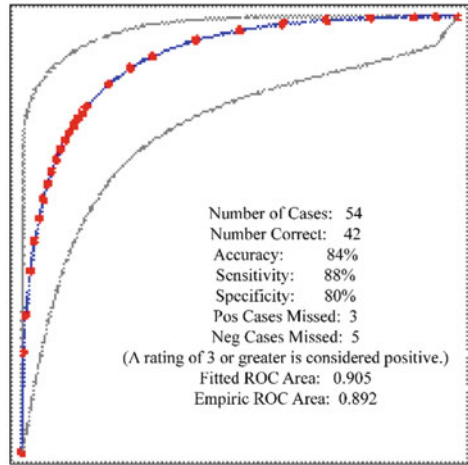


Fig. 13.2 AUC-ROC curve

Fig. 21.13 (13.1–13.2) AUC-ROC accuracy model

## Appendix B

Table 21.1 Sources and use of available data

Sl. No.	Available data	Year(s)	Source(s)	Methods and techniques	Web links
1	SRTM-DEM: SRTM1 arc-second global	2000	USGS (2000)	Digital elevation model (DEM), relief and slope analysis, drainage analysis, stream ordering	<a href="https://earthexplorer.usgs.gov/">https://earthexplorer.usgs.gov/</a>
2	LANDSAT ETM <sup>+</sup>	2001	USGS (2001)	Normalized difference spectral indices	<a href="https://earthexplorer.usgs.gov/">https://earthexplorer.usgs.gov/</a>
3	OCM: Surface water layer product	2015 (august and September)	NRSC (2014)	Extension of surface water	<a href="https://bhuvan-app3.nrsc.gov.in/data/download/index.php">https://bhuvan-app3.nrsc.gov.in/data/download/index.php</a>
4	Rainfall (mm)	2000, 2015 (January to December)	India Meteorological Department (2000, 2015)	Standardized annual rainfall, rainfall erosivity index	<a href="https://mausam.imd.gov.in/">https://mausam.imd.gov.in/</a>

Source: Selected by the authors

**Table 21.2** Details of the parameters and indicators used in the present study

Sl. No.	Parameters	Measurement	Source(s)	Justification for selection
1	Basin length (L) in km	Measurement tool in GIS	GIS analysis	Associated with linear aspect of drainage basin geometry
2	Basin area (A) in sq. km	Calculate geometry in GIS	GIS analysis	Associated with areal aspect of drainage basin geometry
3	Basin perimeter (P) in km	Vector measurement in the GIS environment	GIS analysis	Associated with drainage basin geometry
4	Basin circulatory ratio (Rc)	$Rc = 4 \Pi A/P^2$ (A = basin area, P = basin perimeter)	Strahler (1964)	Associated with watershed geometry
5	Elongation ratio (Re)	$Re = D/L = 1.128 \sqrt{A/L}$ (A = basin area, L = basin length)	Schumm (1956)	Associated with basin length geometry
6	Form factor (Ff)	$Ff = A/L^2$ (A = basin area, L = basin length)	Horton (1945)	Associated with basin shape parameter
7	Sinuosity index (Si)	$S = SI/\sqrt{L}$ (SI = stream length, $\sqrt{L}$ = valley length)	Mueller (1968)	Associated with length of channel and length of meandering axis
8	Stream length ratio (RL)	$RL = Lu/(Lu - 1)$ ; Lu = total length of the streams (km) in one order, (Lu - 1) = total length of the streams (km) in the next lower order of the stream segments. The mean can be estimated if the stream segment has more than two orders.	Horton (1945)	Associated with linear aspect of drainage basin geometry
9	Drainage density (Dd) in km/sq. km	$Dd = Lu/A$ (Lu = Total length of the streams in km, A = basin area in sq. km)	Horton (1945)	Associated with areal aspect of drainage basin morphometry
10	Drainage texture (T)	$T = Dd \times fs$ (Dd = drainage density, fs = stream frequency)	Smith (1950)	Associated the stream orders (linear aspect) and basin perimeter
11	Compactness coefficient (Cc)	$Cc = 0.2821 P/A^{0.5}$ (P = basin perimeter, A = basin area)	Horton (1945)	Associated with the geometry of watershed perimeter
12	Shape factor (Bs)	$Lb^2/A$ (Lb = basin length, A = basin area)	Horton (1945)	Associated with shape of the drainage basin
Sl. No.	Indicators	Measurement	Source(s)	Justification for selection
1	Relief (R) in m	Derived from digital elevation model (DEM)	Smith (1950) and Schumm (1956)	Terrain analysis and relief aspect of the morphometry of drainage basin

(continued)

**Table 21.2** (continued)

2	Slope (S) in %	$S = (Z \times (Ct/H)) / (10 \times A)$ , basin area (A), total basin relief (H), the maximum height of the basin (Z) and total contour length, the average angle of slope ( $\tan \bar{O}$ ) = average no. of contour crossing per mile (A) $\times$ contour interval (I) 3361 (constant)	Wentworth (1930)	Terrain analysis and relief aspect of the morphometry of drainage basin
3	Slope aspect (As)	The direction of maximum slope	Skidmore (1989)	Terrain analysis and relief aspect of the morphometry of drainage basin
4	Flow direction (Fdir)	Derived from DEM	Lemenkova, (2016) and Martz and Garbrecht (1992)	Linear aspect of the flow of drainage basin
5	Sink flow	Derived from flow direction raster	Spatial analyst in GIS	Aspect of the flow of drainage basin
6	Flow length in km (Fl)	Derived from stream raster	Lemenkova (2016)	Linear aspect of the flow of drainage basin
7	Flow length density (Fld)	Derived from stream raster using line density feature in GIS analysis	Spatial analyst in GIS	Areal aspect of the flow of drainage basin
8	Normalized difference vegetation index (NDVI)	$NDVI = \frac{NIR - RED}{NIR + RED}$	Rouse et al. (1973)	Satellite imagery based differential index of vegetation conditions
9	Modified normalized difference water index (MNDWI)	$MNDWI = \frac{Green - SWIR}{Green + SWIR}$	Xu (2005)	Satellite imagery based differential index of surface water conditions
10	Normalized difference built-up index (NDBI)	$NDBI = (SWIR - NIR) / (SWIR + NIR)$	Zha et al. (2003)	Satellite imagery based differential index of habitation conditions
11	Normalized difference flood index <sub>3</sub> (NDFI <sub>3</sub> )	$NDFI_3 = \frac{Blue - SWIR\_2}{Blue + SWIR\_2}$	Wan and Billa (2018) and Boschetti et al. (2014)	Satellite imagery based differential index of flood conditions
12	Normalized difference turbidity index (NDTI)	$NDTI = \frac{Red - Green}{Red + Green}$	Elhag et al. (2019) and Lacaux et al. (2007)	Satellite imagery based differential index of the relative clarity conditions of rivers

(continued)

**Table 21.2** (continued)

13	Normalized difference soil index (NDSI)	$\text{NDSI} = \frac{(\text{Band7} - \text{Band2})}{(\text{Band7} + \text{Band2})}$ (for ETM <sup>+</sup> Band7 = SWIR2 and Band2 = green.)	Deng et al. (2015)	Satellite imagery based differential index of soil conditions
14	Topographic wetness index (TWI)	$\text{TWI} = \ln \left( \frac{A_s}{\tan \beta} \right)$ where $A_s$ is the specific catchment area ( $\text{m}^2 \text{m}^{-1}$ ), $\beta$ is the slope gradient ( $^\circ$ )	Moore et al. (1991)	Terrain analysis as controlling factor of hydrological process by topography
15	Terrain ruggedness index (TRI)	$\text{TRI} = (\Sigma(z_c - z_i)^2)^2$ where, $z_c$ is the elevation of a central cell and $z_i$ is the elevation of one of the eight neighbouring cells ( $i = 1, 2, \dots, 8$ ). (in the present study it is derived from DEM).	Różycka et al. (2017) and Riley et al. (1999)	Terrain analysis as controlling factor of hydrological process by topography
16	Sediment transport index (STI)	$\text{STI} = (A_s / 22.13)^{0.6} \times \sin(\beta / 0.0896)^{1.3}$ where: $A_s$ is the unit contributing area (in $\text{m}^2/\text{m}$ ) and $\beta$ is the slope angle (in degrees) at a given pixel	Burrough et al. (2015)	Relative measurement of the sediment transportation index of river
17	Standardized annual rainfall (Z-score)	$Z = (x - M) / \text{SD}$ where Z is the standard score, x denotes the original value, M denotes the mean (simple arithmetic mean), and SD denotes the standard deviation	Andrade (2021) and Raha and Gayen (2021)	Standardized deviation of annual rainfall from the mean annual rainfall to analyze the drought conditions.
18	Rainfall erosivity index (REI)	$R = 79 + 0.363Xa$ where, R is the rainfall erosivity, Xa is the average annual rainfall in mm over the study area	Choudhury and Nayak (2003)	Relative erosivity factor of soil originated by the rainfall intensity which produces sediment materials into the river flow

Source: Selected by the authors

**Table 21.3** Descriptive statistics of the selected variables

Descriptive statistics			
Variables	Mean		Std. deviation
	Statistic	Std. error	Statistic
Relief	21.6163	1.47410	10.83239
Slope	1.6366	.11785	.86604
Slope_aspect	169.4490	11.82231	86.87589
Flow_direction	33.7961	5.07267	37.27639
Sink_flow	31519.5692	2641.65968	19412.15484
Flow_length	.0086	.00436	.03206
Flow_length_density	.3153	.11938	.87724
NDVI	.0970	.02293	.16851
MNDWI	-.0302	.02413	.17730
NDBI	-.0279	.01770	.13005
NDFI3	.1934	.02323	.17068
NDTI	-.0444	.00770	.05658
NDSI	-.0279	.01770	.13005
TWI	-1.8668	.11820	.86858
TRI	.4719	.01677	.12323
STI	1.3756	.18434	1.35462
Z_score_annual_rainfall	.2545	.09513	.69906
REI	601.7098	13.35755	98.15756
Valid N (listwise) 54			

Source: Calculated by the authors

**Table 21.4** Rotated component matrix and composite scores of factor analysis

Factors	Rotated component matrix <sup>a</sup>				
	Component				
	1	2	3	4	5
Relief		.540	-.545	.389	
Slope	.191	.411	.477		.404
Slope_aspect			.584		.422
Flow_direction	-.179	-.264		.475	.437
Sink_flow	.125	.164	.593	.150	.122
Flow_length	-.495	-.399			-.395
Flow_length_density					-.794
NDVI		.924			
MNDWI	-.828	-.489	-.118		
NDBI	.955	-.126			
NDFI3	-.947		-.113		
NDTI	.466	-.788	.168		
NDSI	.955	-.126			
TWI	-.110		-.144	-.848	

(continued)

**Table 21.4** (continued)

Factors	Rotated component matrix <sup>a</sup>				
	Component				
	1	2	3	4	5
TRI	.289	.579	.207	.388	
STI	-.331		.438	-.303	.276
Z_score_annual_rainfall	.128	-.299	.762	-.200	-.128
REI			.811	.297	-.158

Extraction method: Principal component analysis

Rotation method: Varimax with Kaiser normalization<sup>a</sup>

Composite scores of flood vulnerability

Points	Latitude	Longitude	Composite	Mean composite
P1	22.97	87.81	0.874	0.175
P2	22.97	87.94	0.405	0.081
P3	22.97	88.47	0.551	0.110
P4	22.97	88.60	2.582	0.516
P5	23.17	87.67	0.844	0.169
P6	23.17	87.81	0.030	0.006
P7	23.17	87.94	1.304	0.261
P8	23.17	88.07	2.791	0.558
P9	23.17	88.20	1.853	0.371
P10	23.17	88.34	0.556	0.111
P11	23.17	88.47	1.972	0.394
P12	23.17	88.60	-0.028	-0.006
P13	23.37	87.67	2.437	0.487
P14	23.37	87.81	0.949	0.190
P15	23.37	87.94	1.205	0.241
P16	23.37	88.07	2.840	0.568
P17	23.37	88.20	2.426	0.485
P18	23.37	88.34	-1.013	-0.203
P19	23.37	88.47	1.686	0.337
P20	23.37	88.60	1.635	0.327
P21	23.37	88.73	0.176	0.035
P22	23.57	87.54	1.278	0.256
P23	23.57	87.67	1.320	0.264
P24	23.57	87.94	0.099	0.020
P25	23.57	88.07	0.071	0.014
P26	23.57	88.20	-1.070	-0.214
P27	23.57	88.34	-0.766	-0.153
P28	23.57	88.47	1.061	0.212
P29	23.57	88.60	1.073	0.215
P30	23.76	87.94	-0.162	-0.032
P31	23.76	88.07	0.705	0.141
P32	23.76	88.20	-7.994	-1.599
P33	23.76	88.34	0.703	0.141

(continued)

**Table 21.4** (continued)

Composite scores of flood vulnerability				
Points	Latitude	Longitude	Composite	Mean composite
P34	23.76	88.47	-0.815	-0.163
P35	23.96	87.94	2.686	0.537
P36	23.96	88.07	0.638	0.128
P37	23.96	88.20	-1.822	-0.364
P38	23.96	88.34	-2.068	-0.414
P39	23.96	88.47	-0.396	-0.079
P40	23.96	88.60	0.675	0.135
P41	23.96	88.73	-6.828	-1.366
P42	24.16	87.94	-0.188	-0.038
P43	24.16	88.07	-0.261	-0.052
P44	24.16	88.20	-1.061	-0.212
P45	24.16	88.34	2.059	0.412
P46	24.16	88.47	-0.092	-0.018
P47	24.16	88.60	-2.345	-0.469
P48	24.36	88.07	-1.629	-0.326
P49	24.36	88.20	-2.824	-0.565
P50	24.36	88.34	-2.317	-0.463
P51	24.36	88.47	1.740	0.348
P52	24.56	87.94	-0.457	-0.091
P53	24.56	88.07	-0.412	-0.082
P54	24.76	87.94	-6.680	-1.336

Source: Calculated by the authors

<sup>a</sup>Rotation converged in 8 iterations

**Table 21.5** Results of multiple linear regressions

Model summary <sup>a</sup>									
Model	<i>R</i>	<i>R</i> square	Adjusted <i>R</i> square	Std. error of the estimate		Durbin-Watson			
1	0.974 <sup>b</sup>	0.948	0.933	0.04427		2.417			
ANOVA <sup>a</sup>									
Model	Sum of squares		<i>Df</i>	Mean square	<i>F</i>	Sig.			
1	Regression		1.464	12	0.122	62.246		0.000	
	Residual		0.080	41	0.002				
	Total		1.544	53					
Coefficients <sup>a</sup>									
Model	Unstandardized coefficients		Standardized coefficients	<i>t</i>	Sig.	95.0% confidence interval for B		Collinearity statistics	
	B	Std. error	Beta			Lower bound	Upper bound	Tolerance	VIF
1	(constant)	-0.028	0.047		-0.610	0.545	-0.123	0.066	

(continued)



**Table 21.5** (continued)

Coefficients <sup>a</sup>										
Model	Unstandardized coefficients		Standardized coefficients		t	Sig.	95.0% confidence interval for B		Collinearity statistics	
	B	Std. error	Beta				Lower bound	Upper bound	Tolerance	VIF
	Relief	0.002	0.001	0.115	2.007	0.051	0.000	0.004	0.384	2.607
	Slope	0.014	0.009	0.073	1.530	0.134	– 0.005	0.033	0.561	1.784
	Flow_direction	0.000	0.000	– 0.078	– 1.901	0.064	– 0.001	0.000	0.760	1.315
	Sink_flow	4.240E- 7	0.000	0.048	1.047	0.301	0.000	0.000	0.599	1.670
	Flow_length	–0.026	0.246	– 0.005	– 0.105	0.917	– 0.522	0.470	0.596	1.678
	MNDWI	0.891	0.058	0.926	15.317	0.000	0.774	1.009	0.347	2.880
	NDTI	–1.000	0.138	– 0.332	– 7.257	0.000	– 1.278	–0.722	0.608	1.644
	TWI	0.008	0.010	0.038	0.789	0.435	– 0.012	0.027	0.535	1.870
	TRI	0.042	0.083	0.031	0.508	0.614	– 0.126	0.211	0.349	2.864
	STI	0.001	0.006	0.007	0.127	0.899	– 0.012	0.014	0.479	2.088
	Z_score_annual_rainfall	–0.025	0.016	– 0.102	– 1.571	0.124	– 0.057	0.007	0.303	3.301
	REI	0.000	0.000	0.134	2.244	0.030	0.000	0.000	0.359	2.789

Source: Calculated by the authors

<sup>a</sup>Dependent variable: NDFI3

<sup>b</sup>Predictors: (constant), REI, flow\_length, flow\_direction, NDTI, TWI, sink\_flow, slope, TRI, STI, relief, MNDWI, Z\_score\_annual\_rainfall

## References

- Andrade, C. (2021). Z scores, standard scores, and composite test scores explained. *Indian Journal of Psychological Medicine*, 43(6), 555–557. <https://doi.org/10.1177/02537176211046525>
- Biswas, A., Das Majumdar, D., & Banerjee, S. (2014). Morphometry governs the dynamics of a drainage basin: Analysis and implications. *Geography Journal*, 2014, 1. <https://doi.org/10.1155/2014/927176>
- Boschetti, M., Nutini, F., Manfron, G., Brivio, P. A., & Nelson, A. (2014). Comparative analysis of normalised difference spectral indices derived from MODIS for detecting surface water in flooded rice cropping systems. *PLoS One*, 9(2), e88741. <https://doi.org/10.1371/journal.pone.0088741>
- Burrough, P. A., McDonnell, R. A., & Lloyd, C. D. (2015). *Principles of geographical information systems*. Oxford University Press.
- Carlin, J. B., & Doyle, L. W. (2000). 3: Basic concepts of statistical reasoning: Standard errors and confidence intervals. *Journal of Paediatrics and Child Health*, 36(5), 502–505. <https://doi.org/10.1046/j.1440-1754.2000.00588.x>

- Choudhury, M. K., & Nayak, T. (2003). *Estimation of soil erosion in Sagar Lake catchment of Central India* (pp. 387–392). Proceedings of the International Conference on Water and Environment. Dec 15–18, 2003.
- Danumah, J. H., Odai, S. N., Saley, B. M., Szarzynski, J., Thiel, M., Kwaku, A., et al. (2016). Flood risk assessment and mapping in Abidjan district using multi-criteria analysis (AHP) model and geoinformation techniques, (cote d'ivoire). *Geoenvironmental Disasters*, 3(1), 1–13. <https://doi.org/10.1186/s40677-016-0044-y>
- Das, S., Adak, K., & Samanta, K. (2014). Hydrodynamic changes of river course of part of Bhagirathi–Hugli in Nadia district-A Geoinformatics appraisal. *International Journal of Geomatics and Geosciences*, 5(2), 284–299.
- Das, B. C., Ghosh, S., Islam, A., & Roy, S. (Eds.). (2020). *Anthropogeomorphology of Bhagirathi-Hooghly River system in India*. CRC Press.
- Demir, V., & Kisi, O. (2016). Flood hazard mapping by using geographic information system and hydraulic model: Mert River, Samsun, Turkey. *Advances in Meteorology*, 2016, 1.
- Deng, Y., Wu, C., Li, M., & Chen, R. (2015). RNDSI: A ratio normalized difference soil index for remote sensing of urban/suburban environments. *International Journal of Applied Earth Observation and Geoinformation*, 39, 40–48.
- Durbin, J., & Watson, G. S. (1971). Testing for serial correlation in least squares regression. III. *Biometrika*, 58(1), 1–19. <https://doi.org/10.2307/2334313>
- Dutta, R. (2022). Floodplain dynamics in part of the Bhagirathi river near Karkaria and Jagannathpur villages, Nakashipara block, Nadia district, West Bengal. *IJRCS*, 6, 111–122. <https://doi.org/10.2017/IJRCS/202201023>
- Elhag, M., Gitas, I., Othman, A., Bahrawi, J., & Gikas, P. (2019). Assessment of water quality parameters using temporal remote sensing spectral reflectance in arid environments, Saudi Arabia. *Water*, 11(3), 556.
- Farebrother, R. W. (1980). The Durbin-Watson test for serial correlation when there is no intercept in the regression. *Econometrica: Journal of the Econometric Society*, 48(6), 1553–1563. <https://doi.org/10.2307/1912825>
- Fisher, R. A. (1934). *Statistical methods for research workers*. Oliver and Boyd, London and Edinburgh (§4 and §42 (Ex. 41), Reproduced.
- Ghosh, A., Roy, M. B., & Roy, P. K. (2020). Estimation and prediction of the oscillation pattern of meandering geometry in a sub-catchment basin of Bhagirathi-Hooghly river, West Bengal, India. *SN Applied Sciences*, 2(9), 1–24.
- Holt, W., & Refenes, P. (1998). The Durbin-Watson test for neural regression models. In *Risk measurement, econometrics and neural networks* (pp. 57–68). Physica.
- Horton, R. E. (1945). Erosional development of streams and their drainage basins; hydrological approach to quantitative morphology. *Geological Society of American Bulletin*, 56, 275–370.
- India Meteorological Department. (2000). *Climatological table*. Ministry of Earth Sciences. Government of India.
- India Meteorological Department. (2015). *Climatological table*. Ministry of Earth Sciences. Government of India.
- Irrigation and Waterways Department. (2015). Annual flood report 2015. *Government of West Bengal*, 1–57.
- Islam, A., Das, B. C., Maji, N. K., & Barman, S. D. (2020). Assessing meander belt width of Bhagirathi-Jalangi river system in lower Ganga delta, India. *European Journal of Geography*, 11(1), 140–162. <https://doi.org/10.48088/ejg.a.isl.11.1.140.162>
- Jha, C. V., & Bairagya, H. (2013). Flood and flood plains of West Bengal, India: A comparative analysis. *Revista Geoaraguaia*, 1, 1–10.
- Joint Research Centre-European Commission. (2008). *Handbook on constructing composite indicators: Methodology and user guide* (pp. 1–158). OECD Publishing. <https://www.oecd.org/sdd/42495745.pdf>

- Lacaux, J. P., Tourre, Y. M., Vignolles, C., Ndione, J. A., & Lafaye, M. (2007). Classification of ponds from high-spatial resolution remote sensing: Application to Rift Valley fever epidemics in Senegal. *Remote Sensing of Environment*, 106, 66–67.
- Lemenkova, P. (2016). *Flow direction and length determined by ArcGIS spatial analyst and terrain elevation data sets*. Proceedings of the Conference ‘Priority directions of the development of young research farmers in modern science’. 25th anniversary of Caspian Research Institute of Arid Agriculture RAAS.
- Leopold, L. B. (1994). *A view of the river*. Harvard University Press.
- Mandal, S. P., Kayet, N., Chakraborty, A. & Rahaman, G. (2016). Morphometric analysis of Bhagirathi river in Murshidabad district, West Bengal: using geospatial and statistical techniques. *Conference Paper*, <https://www.researchgate.net/publication/303365322>
- Mallick, S. (2016). Identification of Fluvio geomorphological changes and bank line shifting of river Bhagirathi-Hugli using remote sensing technique in and around of Mayapur Nabadwip area, West Bengal. *International Journal of Science and Research (IJSR)*, 5(3), 1130–1134.
- Martz, L. W., & Garbrecht, J. (1992). Numerical definition of drainage network and subcatchment areas from digital elevation models. *Computers and Geosciences.*, 18(6), 747–761. [https://doi.org/10.1016/0098-3004\(92\)90007-E](https://doi.org/10.1016/0098-3004(92)90007-E)
- Merz, B., Hall, J., Disse, M., & Schumann, A. (2010). Fluvial flood risk management in a changing world. *Natural Hazards and Earth System Sciences*, 10(3), 509–527.
- Misra, S. (2018). Changing morphometry of Bhagirathi River; A case study of eastern part of Burdwan District. *International Journal of Scientific Research and Review.*, 7(8), 493–502.
- Misra, S., & Roy, T. (2019). The impact of land use land cover on the flood plain of Bhagirathi River, Purba Bardhaman District, West Bengal, India. *Journal of Geography, Environment and Earth Science International*, 19(2), 1–10.
- Mollah, S. (2013). Regional flood hazard mapping in Murshidabad, West Bengal. *International Journal of Scientific Research*, 2(2), 391–393.
- Mollah, S. (2016). Causes of flood hazard in Murshidabad District of West Bengal: Victims’ perceptions. In *Neo-thinking on Ganges-Brahmaputra Basin geomorphology* (pp. 99–113). Springer.
- Moore, I. D., Grayson, R. B., & Ladson, A. R. (1991). Digital terrain modeling: A review of hydrological, geomorphological, and biological applications. *Hydrological Processes*, 5, 3–30.
- Mueller, J. E. (1968). An introduction to the hydraulic and topographic sinuosity indexes. *Annals of the Association of American Geographers*, 58(2), 371–385. <https://doi.org/10.1111/j.1467-8306.1968.tb00650.x>
- Nandargi, S. S., & Shelar, A. (2018). Rainfall and flood studies of the Ganga River basin in India. *Annals of Geographical Studies*, 1(1), 34–50.
- Nardo, M., Saisana, M., Saltelli, A., Tarantola, S., Hoffman, H., & Giovannini, E. (2009). *Handbook on constructing composite indicators: Methodology and user guide*. Organisation for Economic Co-operation and Development.
- Nath, S. K., Roy, D., & Thingbaijam, K. K. S. (2008). Disaster mitigation and management for West Bengal, India-An appraisal. *Current Science*, 858–864.
- National Remote Sensing Centre (NRSC). (2014). *Surface water layer products from OCM2 for BHUVAN NOEDA* (pp. 1–7). Geospatial and Spatial Products, SDAPSA.
- Pal, R., Biswas, S. S., Pramanik, M. K., & Mondal, B. (2016). Bank vulnerability and avulsion modeling of the Bhagirathi-Hugli river between Ajay and Jalangi confluences in lower Ganga Plain, India. *Modeling Earth Systems and Environment*, 2(2), 1–10.
- Pal, S. C., Das, B., Malik, S., Shit, M., & Chakraborty, R. (2021). Flood frequency analysis and its management in selected part of Bardhaman district, West Bengal. In *Habitat, ecology and estistics* (pp. 225–246). Springer.
- Pearson, K. (1897). Mathematical contributions to the theory of evolution. -on a form of spurious correlation which may arise when indices are used in the measurement of organs. *Proceedings of the Royal Society of London*, 60(359–367), 489–498. <https://doi.org/10.1098/rspl.1896.0076>

- Pearson, K. (1901). LIII. On lines and planes of closest fit to systems of points in space. *The London, Edinburgh, and Dublin Philosophical Magazine and Journal of Science*, 2(11), 559–572. <https://doi.org/10.1080/14786440109462720>
- Pearson, K. (1914). On certain errors with regard to multiple correlation occasionally made by those who have not adequately studied this subject. *Biometrika*, 10(1), 181–187. <https://doi.org/10.2307/2331747>
- Raha, S., & Gayen, S. K. (2021). Drought-induced human mobility in Purulia District of West Bengal. In *Habitat, ecology and ekistics* (pp. 263–277). Springer.
- Rehman, S., Hasan, M. S. U., Rai, A. K., Rahaman, M. H., Avtar, R., & Sajjad, H. (2022). *Integrated approach for spatial flood susceptibility assessment in Bhagirathi sub-basin, India using entropy information theory and geospatial technology*. Risk Analysis.
- Rouse, J. W., Jr., Haas, R. H., Schell, J. A., & Deering, D. W. (1973). Paper a 20. In *Third earth resources technology satellite-1 symposium: Section AB*. Technical presentations. 1, 309. Scientific and Technical Information Office, National Aeronautics and Space Administration.
- Riley, S. J., DeGloria, S. D., & Elliot, R. (1999). Index that quantifies topographic heterogeneity. *Intermountain Journal of Sciences*, 5(1–4), 23–27.
- Różycka, M., Migoń, P., & Michniewicz, A. (2017). Topographic Wetness Index and Terrain Ruggedness Index in geomorphic characterisation of landslide terrains, on examples from the Sudetes, SW Poland. *Zeitschrift für Geomorphologie, Supplementary issues*, 61, 61–80.
- Rudra, K. (2018). The Bhagirathi-Hugli River system. In *Rivers of the Ganga-Brahmaputra-Meghna Delta* (pp. 77–93). Springer.
- Saha, A., & Praneeth, D. V. S. (2016). Flood vulnerability assessment by remote sensing and GIS based applications in West Bengal: A review. *IRJET*, 3, 1654–1657.
- Samal, N. R., Roy, P. K., Majumadar, M., Bhattacharya, S., & Biswasroy, M. (2014). Six years major historical urban floods in West Bengal state in India: Comparative analysis using neuro-genetic model. *American Journal of Water Resources*, 2(2), 41–53.
- Sanyal, J., & Lu, X. X. (2003). *Application of GIS in flood hazard mapping: A case study of Gangetic West Bengal, India*. Proceedings of map Asia conference, GIS development. net.
- Sanyal, J., & Lu, X. X. (2005). Remote sensing and GIS-based flood vulnerability assessment of human settlements: A case study of Gangetic West Bengal, India. *Hydrological Processes: An International Journal*, 19(18), 3699–3716.
- Sanyal, J., & Lu, X. X. (2006). GIS-based flood hazard mapping at different administrative scales: A case study in Gangetic West Bengal, India. *Singapore Journal of Tropical Geography*, 27(2), 207–220.
- Schumm, S. A. (1956). Evolution of drainage systems and slopes in badlands at Perth Amboy, New Jersey. *Geological Society of America Bulletin*, 67, 597–646.
- Skidmore, A. K. (1989). A comparison of techniques for calculating gradient and aspect from a gridded digital elevation model. *International Journal of Geographical Information System*, 3(4), 323–334. <https://doi.org/10.1080/02693798908941519>
- Smith, K. G. (1950). Standards for grading texture of erosional topography. *American Journal of Science*, 248, 655–668.
- Strahler, A. N. (1957). Quantitative analysis of watershed geomorphology. *Eos, Transactions American Geophysical Union*, 38(6), 913–920. <https://doi.org/10.1029/TR038i006p00913>
- Strahler, A. N. (1964). Quantitative geomorphology of drainage basin and channel network. In V. T. Chow (Ed.), *Handbook of applied hydrology*. McGraw Hill Book Company.
- Student. (1908). *The probable error of a mean* (Vol. 6, p. 1). Biometrika, 6, 25, Reproduced by the kind permission the Biometrika Trustees. <https://doi.org/10.2307/2331554>
- United States Geological Survey. (USGS). (2000). *Shuttle USGS EROS archive – Digital elevation – Shuttle Radar Topography Mission (SRTM) non-void filled*. Department of the Interior.
- United States Geological Survey. (USGS). (2001). *Landsat data access*. Department of Interior.
- Uyanik, G. K., & Güler, N. (2013). A study on multiple linear regression analysis. *Procedia-Social and Behavioral Sciences*, 106, 234–240. <https://doi.org/10.1016/j.sbspro.2013.12.027>

- Wan, K. M., & Billa, L. (2018). Post-flood land use damage estimation using improved Normalized Difference Flood Index (NDFI3) on Landsat 8 datasets: December 2014 floods, Kelantan, Malaysia. *Arabian Journal of Geosciences*, *11*(15), 1–12.
- Wentworth, C. K. (1930). A simplified method of determining the average slope of land surfaces. *American Journal of Science*, *117*, 184–194. <https://doi.org/10.2475/ajs.s5-20.117.184>
- Xu, H. (2005). A study on information extraction of water body with the Modified Normalized Difference Water Index (MNDWI). *Journal of Remote Sensing*, *9*, 589–595.
- Zha, Y., Gao, J., & Ni, S. (2003). Use of normalized difference built-up index in automatically mapping urban areas from TM imagery. *International Journal of Remote Sensing*, *24*(3), 583–594.

## Chapter 22

# Floods of Gorai-Madhumati and Arial Khan Rivers, Bangladesh



Al Artat Bin Ali, Nazmoon Nahar Sumiya, and M. Shahidul Islam

**Abstract** The very seasonal climate of Bangladesh, along with the monsoon runoff that comes from the country's three most important Himalayan rivers, makes it prone to floods. As a consequence of the historically eastward movement of the Ganges mouth and the significant local rainfall, the whole Ganges Dependent Area (GDA) river system was developed. Arial Khan and the Gorai-Madhumati remain linked to the Ganges-Padma, serving the southwest and south central regions, respectively. The Gorai, a meandering alluvial perennial river, is the principal Ganges River distributary. A significant portion of Bangladesh's freshwater supply comes from the Ganges River near Gorai. The key concerns related to the Gorai-Madhumati River are the diversion of river flow in the upstream, as well as the degradation of the riverbed, the infiltration of salt water, the disturbance caused by excessive sedimentation, and the resulting flooding. These attributes have made the river a source of anxiety since it affects the agriculture, biodiversity, and freshwater supply of the southwest area. The upper portions of the Arial Khan River, which is a significant river running south and east and is a distributary of either the Ganges or the Padma, have been weakened by the monsoon flood. The water level of the Upper Arial Khan River has been recorded to have surpassed the danger threshold during prior flood occurrences in Bangladesh, causing significant flooding in the floodplain. Flood control continues to be a difficult task in Bangladesh despite the fact that the country has been hit by a number of disastrous floods in recent years. Due to its complexity, breadth, and interdisciplinary character, flood control is a cross-sectoral endeavor. This research used a number of secondary sources, such as national and international newspapers, books, journals, and relevant articles, and aims to understand the environmental and human causes of the Gorai-Madhumati and Arial Khan River floods, as well as to analyze flood vulnerability, consequences, and coping techniques in Bangladesh to propose a long-standing mitigation strategy.

**Keywords** Flooding · Vulnerability · Sedimentation · Flood management

---

A. A. B. Ali (✉) · N. N. Sumiya · M. S. Islam

Department of Geography and Environment, University of Dhaka, Dhaka, Bangladesh

## 1 Introduction

The majority of Bangladesh is made up of low-lying floodplains, with just a few hills situated in the country's northeast and southeast corners. The country's topography varies in elevation from 1 m to 60 m above mean sea level from north to south (BWDB, 2014). The Ganges, the Brahmaputra, and the Meghna are the three major rivers in this region, each of which has a number of smaller rivers that flow into and out of it. When the Ganges and Brahmaputra converge around Aricha-Gomundo, the Padma River is created. The Padma and Meghna rivers merge near Chandpur and discharge their waters into the Bay of Bengal. The Ganges, Brahmaputra, and Meghna rivers comprise the GBM basin, which encompasses practically the whole country and drains the huge runoff from these three river systems. During the monsoon season, over 100,900 million m<sup>3</sup> of water flow through this river system, which has a catchment area of around 1,721,300 km<sup>2</sup>, of which only about 7% is in Bangladesh and the remainder is outside the nation (BWDB, 2014; JRCB, 2016). The bulk of rivers have sandy bottoms, low slopes, considerable meandering, and erodible, channel-shifting banks. The three basins have precipitation regimes that range from very low to extremely high precipitation (Ahmed & Mirza, 2000). As a result of the region's very intense monsoon rains, an enormous volume of runoff pours through Bangladesh and into the Bay of Bengal. The local precipitation in Bangladesh contributes to the severity of the flooding that occurs there, which in turn causes overbank spills. Snow and glacier melt, siltation of major distributaries, backwater impact, unplanned infrastructure development, deforestation, El Nino-Southern Oscillation (ENSO) conditions, and the timing of flood maxima of major rivers are other variables that may contribute to flooding (Ahmed & Mirza, 2000).

The Ganges River is the primary source of water for most of Bangladesh's southwestern region (SWR) rivers. One of SWR's most significant sources of freshwater is the Gorai-Madhumati River, a Ganges River distributary, while the Arial Khan River is one of the Lower Ganges or Padma's most important southeastward outflows. Bangladesh, being a riverine nation, enjoys the plethora of resources offered by the rivers. Rivers have long been a vital component of the country's infrastructure but only lately have they become a problem due to natural and human forces. The primary issues associated with rivers in the country include upstream diversion of river flow, saltwater intrusion, excessive sedimentation that disrupts navigability, and subsequent flooding (Shamsad et al., 2014). In Bangladesh, the flood damage and records set by previous years are consistently topped by those set by subsequent years. Intense monsoons, melting Himalayan snows, and geophysical instability in the northern areas are only a few of the causes of these devastating floods. Nevertheless, human-caused floods may be traced back to activities such as overuse of depleted soils, deforestation, and other forms of uncontrolled growth. It's impossible for a developing country like Bangladesh to withstand the long-term effects of continuous floods.

## 2 Study Area

One of Bangladesh’s longest rivers, the Gorai-Madhumati, flows through this area. Madhumati and Gorai are the names of the river’s upper and lower reaches, respectively (Ahmed & Islam, 2003). Ganges River right bank distributary, Gorai-Madhumati, is an important waterway (Adams, 1919). The length of the Gorai-Madhumati River is 199 km, and its catchment area is about 15,160 km<sup>2</sup>. It runs across the Bangladeshi districts of Barguna, Bagerhat, Chuadanga, Faridpur, Gopalganj, Jessore, Jhenaidah, Khulna, Kushtia, Magura, Narail, Pabna, Pirojpur, Rajbari, and Sathkhira, with some or all of these districts being affected (Fig. 22.1; Islam, 2003). Both the Passur River and the Sibsa River empty into the Bay of Bengal, making them the entrance points for the Gorai-Madhumati River. Approximately 15 million people are within the boundaries of the catchment region based on the 2011 population census (BBS, 2016). In comparison, the southeast receives an annual average of 2478 mm of precipitation, whereas the northeast only receives an average of 1516 mm.

In the winter, temperatures in the catchment region range from 22 to 23 °C, while in the summer, they range from 23 to 32 °C (EGIS, 2000). The Gorai-Madhumati River serves as the most important supply of freshwater for the Sundarbans mangrove forest and the southwest part of Bangladesh (Islam & Gnauck, 2011). The river’s bed load consists of fine sand to silts, which are found in abundance in the

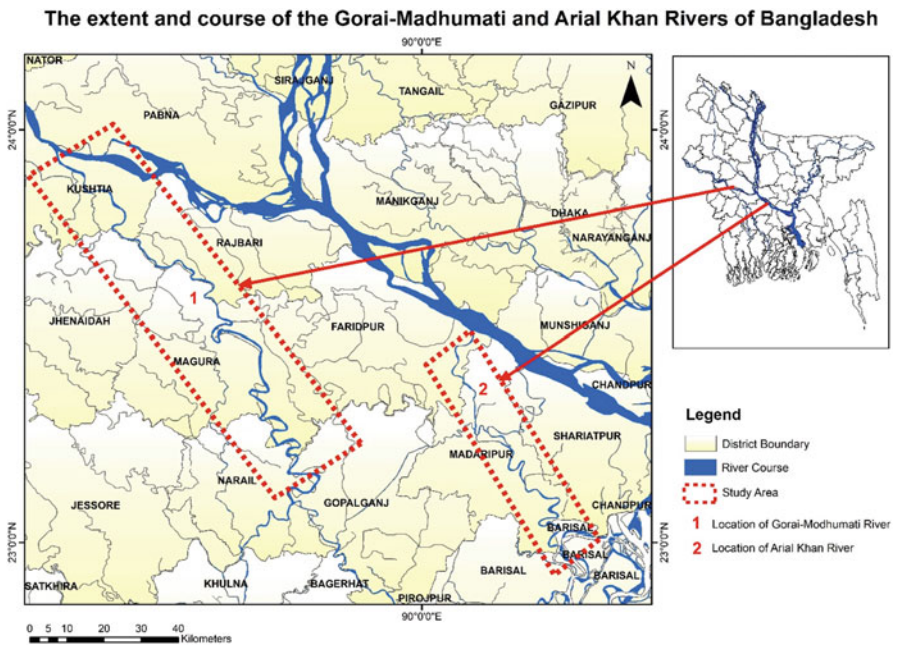


Fig. 22.1 Location of the study area



river. Bed load materials account for 40% of sediment transported annually, with silt and clay accounting for the remaining 60% (Halcrow et al., 1993). The Gorai-Madhumati deltaic river system, which is separated between deep depressions and large valley bottoms, saw substantial structural alterations as a consequence of the monsoon season's high rainfall. A flood flow of over 7000 m<sup>3</sup> in the Gorai-Madhumati River system during the monsoon season reduces to nearly nothing in the winter (Khanam & Navera, 2016). India's Farakka Barrage is located 272.4 km from the Gorai-Madhumati River in the upstream part of the Ganges River.

The Arial Khan River is one of the major distributaries of the lower Ganges that run southeast. Khan (2000) says that the Padma only has one branch, the Arial Khan, which is about 64 km east of where the Ganges and the Jamuna meet. In reality, the river connects the drainage basins of the Ganges and the Meghna. Madaripur is located on the right bank of the Arial Khan River. Brammer (1991) says that the bank sediments are mostly calcareous and may have been put there before 1840, when the Ganges moved from the Arial Khan channel to the lower Meghna channel. Rashid (1991) says that the Arial Khan was one of the primary rivers that came out of the Padma in the late 1800s. At the point where it went out, it was clogged up. Over the past 100 years, the mouth of the Ganges River has moved eastward. This has helped the evolution of river systems in the southwest, causing many small rivers to split off from the Ganges main channel; however, Gorai and Arial Khan are still two of Bangladesh's major rivers that feed into the Ganges (The World Bank, 2005). The river's overall length is 120 km. The point at which this river meets the Dhubaldia River marks the beginning of the upper segment of the river. The middle section, which starts with the confluence of the Dhubaldia, is about 35 km long. Through the estuaries between the Tentulia and Biskhali rivers, the river's downstream flows into the Bay of Bengal. Normal river flow ranges between 2500 and 4000 m<sup>3</sup>/s. The river is meandering, with recent bank movement and the formation of meandering loops that undergo occasional cutting. These occurrences have made the river very unstable (SWMC, 2001). The Padma's Arial Khan is a busy river with a vast corridor and many tributaries around its head. The river is one of the most significant rivers in the region, and it plays a significant part in assuring the well-being and continued vitality of the surrounding area (FAP4, 1993).

### 3 Materials and Methods

The study's emphasis allowed for a review of the research conducted on various aspects of Bangladesh's floods in the Gorai-Madhumati and Arial Khan Rivers, as well as their catchment areas. The study focuses on a review of Bangladesh's current flood research from 1987 to 2019. The data for this study was acquired from a variety of secondary sources using an exploratory research approach. This work is based on secondary datasets mostly from censuses, government and international organization reports, books, electronic journals, and pertinent publications.

## 4 The Changing Nature of the Delta over the Past Few Centuries

Following the formation of the river network during the Holocene epoch, rivers have changed their courses many times throughout the course of the previous few millennia. More than 250 years ago, the Brahmaputra River traveled from its current location in Bangladesh to its mouth in the Bay of Bengal through the east side of Madhupur tract, where it met the Meghna River. The Padma River was just the Ganges River's downstream extension prior to that time. The Ganges, which is now called the Padma, flowed into the Bay of Bengal about where the Arial Khan River is presently located, and Bhola Island was to the east (Fig. 22.1). During that period, the Ganges River and all of the distributaries in this area were flowing southeast. The Chandana-Barasia River, which flows southeast and has a little connection to the Gorai River, was the primary supply of sweet water for the southwest. A tiny channel linked the Kabodak and Ganges rivers. A single alteration in a natural system might result in a cascade of subsequent modifications. When the Brahmaputra avulsed into the present-day Jamuna and united with the Ganges in the early nineteenth century, it had a profound influence on the river systems in the southwestern region of Bangladesh.

According to Tassin's map from 1840, a big part of the Brahmaputra's water flowed into what is now the Jamuna in order to reach the Ganges. The combined flow went through a passage called "Kirtinasha" to get to the Meghna in Chandpur. The original path of the Ganges was the Arial Khan River, which is now a right bank distributary of the Ganges. It is believed that the Jamuna's link to the Ganges contributed to an increase in the water level of the Ganges River, which in turn led to the formation of the Gorai River (Fergusson, 1863). The Gorai-Madhumati and Chandana-Barasia rivers divide the southeast-flowing Kumar River. At this point, the eastern bank of the Meghna estuary had started to create a southeast-moving delta. Lower Meghna was discovered to be much larger than the Shahbajpur canal in the estuary. Beginning in the twentieth century, the majority of the Brahmaputra's water was diverted to the Jamuna. As a result, the majority of the Padma's water flow was diverted to the Meghna River, and the river abandoned its previous course. The primary current of the lower Meghna River has begun to move downstream in the direction of the Shahbajpur canal. The widths of the Meghna and Shahbajpur rivers were made equivalent, and a few fresh branches from the right bank started to flow southwestward. During this period, the Chandana River shrunk substantially, while the Gorai became an important distributary.

A number of river-related projects were constructed during the turn of the twentieth century, including the Halifax cut and the Madaripur Beel Route (MBR). In 1910, the Halifax cut was constructed to link the Madhumati and Nabaganga rivers. This action was taken to reduce the distance between Dhaka and Khulna. Because of this, a considerable volume of water from the Madhumati River ended up flowing into the Nabaganga River rather than its original destination. During the construction of the 23-km MBR between 1910 and 1912, water from the Arial Khan River was diverted into the Madhumati River.

There have been major changes to rivers and distributaries during the previous several decades. Due to dwindling water supplies, Shahbajpur canal (the Meghna estuary's western distributary) grew in size. This southwesterly course gave rise to several right bank distributaries, including Belua, Bisarkand-Bagda, Nunda, Tarki, Khal, and Shyandha rivers, as well as a few other small ones. At this point, most of the Gorai River's water was being diverted to the Nabaganga River.

Changes in the Bengal delta during the previous 250 years include the Brahmaputra River's avulsion from east of the Madhupur tract to its present route, and the Ganges River's confluence with it near Aricha. In this period, it became a delta-forming estuary rather than two discrete estuaries and traveled to its easternmost course. It was common for the Ganges' tributaries and main course to flow southeast in the late eighteenth and early nineteenth centuries.

Human activity was a major factor in many of the changes that occurred in the twentieth century. Once again, the Gorai-Madhumati River had shifted its course; this time toward the southwest and the Nabaganga River. As a result of the Arial Khan River's flow, a portion of it reached the MBR. Both of these changes were a result of human activity, but the delta's structure also had a role. Other notable natural changes include a shift in the delta's growing estuary to its west and an increase in delta depth by tens of kilometers to its south (Sarker et al., 2013).

## 5 The Process of Delta Formation

The silt transported downstream by the Ganges, Brahmaputra, and Meghna rivers is substantially responsible for the Bengal delta's current size, which exceeds 100,000 km<sup>2</sup> and makes it among the largest deltas in the world. The Himalayan mountain ranges that generate the highest sand and silt are drained by the Brahmaputra and Ganges rivers, respectively, on the north and south sides of the range.

The Gorai is a distributary that branches off of the Ganges River's right bank and eventually discharges its water into the bay on an annual basis. It transports 30 billion m<sup>3</sup> of water and 30 million tons of sediment at any one time (EGIS, 2001). Both the Bhairab and the Kabodak rivers, which are considered to be very large distributaries, had a key role in the formation of the delta back in the distant past. Nevertheless, a few centuries ago, the unbroken connection that had existed between these distributaries and the Ganges, the river that was their parent river, was disrupted (Williams, 1919). The Padma River is formed at the confluence of the Ganges River and the Jamuna River, while the Arial Khan River is a right bank distributary of the Padma River. On an annual basis, the Arial Khan River contributed around 30 billion m<sup>3</sup> of flow and 25 million tons of debris to the Padma River (EGIS, 2001).

In the Meghna estuary region, delta-building activities are now ongoing. Shabajpur, Hatiya, and Tetulia are the three principal distributary waterways through which the bulk of water and sediment enters the system. There are also several right bank distributary canals that deliver freshwater and sediment to the center of the

delta and are oriented to the southwest. One of these distributary canals is the Shandhya, which begins at the junction of the lower Meghna and Arial Khan Rivers and ultimately flows into the huge Baleswar estuary. It is the estuary's principal fluvial source at now. The Tetulia Channel is also linked to the Bishkhali and the Burishwar along the southwest-oriented distributary channels (Sarker et al., 2013).

## 6 Historical Perspective of Floods

Bangladesh was struck by three severe floods in the years 1987, 1988, and 1998 which, in ascending percentages, submerged 36, 63, and 69% of the nation, respectively (Mirza et al., 2003). As a consequence of monsoon rainfall, Bangladesh and cross-border basin regions experienced flooding in various months. In late June 1987, extreme rainfall in the northeastern regions of Sylhet and Sunamganj triggered flash floods (BWDB, 1987). The Brahmaputra and Ganges Rivers breached their respective danger thresholds in Chilmari and Goalundo in late July. The Meghna reached a perilous level at Bhairab Bazar at the beginning of August.

The floods of 1988 started in early May, when various rivers in the hill basins of the southeast surpassed their danger thresholds. Prior to the August–September devastation, the Brahmaputra River had been at flood level since early July and had reached many peaks. The late severe peak of the Brahmaputra River occurred at the same time as the moderately high peak of the Ganges River, which was separated by 3 days. Around the end of the first week of September, the Meghna flood reached its highest point. The 1998 flood started in the late second week of July and continued until the middle of September and, in some parts, the whole month (Chowdhury, 2000). The deluge of floodwaters from India wreaked havoc on the northern and central regions of Bangladesh, in addition to a section of the southwestern region of the nation. The flooding situation in the three river basins worsened during the first week of September. Throughout the 3 years of flooding, the peak flow of the major rivers fluctuated in size. In both the upstream and downstream areas, the flood depths and durations varied.

## 7 Hydro-Morphological Characteristics of Gorai-Madhumati River

The Gorai-Madhumati River is the largest perennial distributary of the Ganges in Bangladesh. Despite the fact that they supplied potable water during the dry seasons, they were not connected to the Ganges River, which was historically the sole supply of water for this region. The degradation of distributaries was part of a natural process that happened when the Ganges changed its route. The dry-season hydrology of the Ganges River and platform development are additional factors that impact

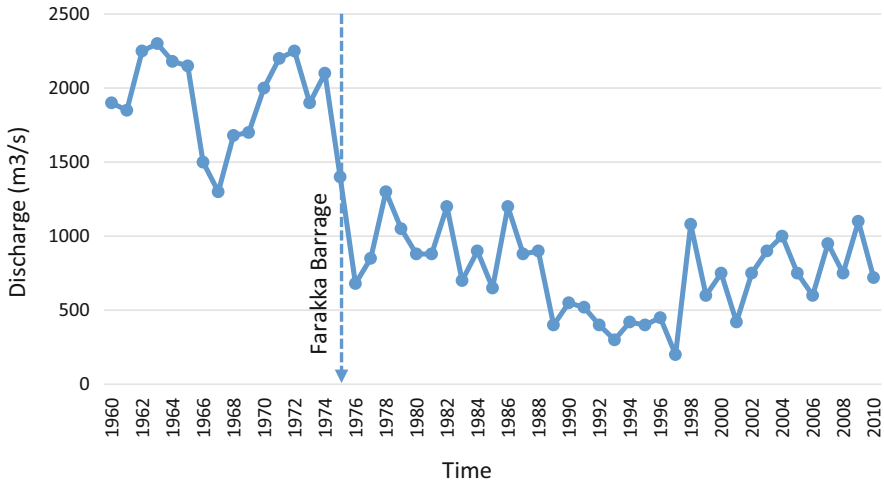


**Fig. 22.2** Discharge with time at Hardinge Bridge from 1960 to 2010. The construction of the Farakka Barrage in the river's upstream portion in India in 1975 resulted in a decrease in discharge

the flow of the Gorai River during the dry season. The dry-season flow of the Ganges River has been reduced as a result of the establishment of the Farakka Barrage. Since 1975, the Gorai River has not had any dry season flow since water has been diverted from the Farakka Barrage, and since 1988, there has been no dry season flow (Islam & Gnauck, 2008, 2009; EGIS, 2000).

Saline freshwater balance was disrupted in one area of the Sundarbans during the early nineteenth century when the intake mouths of many rivers that brought freshwater from the Ganges to the south region were silted up and lost their connection. More than half of the water from the Ganges River was diverted to India's Hoogly River in the early 1970s when India built a barrage 17 km upstream from Bangladesh's border. Historical discharge data analysis from the year 1960 up to 2010 at a station located on Hardinge Bridge in Bangladesh shows that the Gorai-Madhumati River and its downstream distributaries had experienced considerable decreases after the Farakka periods (Gazi et al., 2020) (Fig. 22.2).

It obstructs the Ganges' perennial flow and diverts its water into the Bhagirathi-Hoogly River through a feeder canal in order to improve Calcutta port navigation. The Gorai at Bardia is the only source of freshwater for the estuary, and it also prevents salt intrusion. Historically, upstream flows were usual, such as the Ganges River flows at the Hardinge Bridge in 1962, when the discharge was 3700 m<sup>3</sup>/s and, in 1968, when the Ganges' average monthly flow in the dry season was 3600 m<sup>3</sup>/s; however, the Ganges and the Gorai's flows decreased after 1976 (Ben et al., 1995). With the construction of the Farakka Barrage, the flow in the downstream was significantly reduced. The Ganges recorded its lowest flow of 9437 cusecs in April 1993, compared to its pre-diversion flow of 65,000 cusecs.

Since 1995, the flows have consistently been at a level that is lower than 500 m<sup>3</sup>/s in each year. In September of 2012–2013, the flow discharge in the upper Gorai

River, which extends from the Gorai offtake to the Gorai Railway Bridge, was 3343 m<sup>3</sup>/s, although during the dry season at the same time period, the flow discharge was just 250 m<sup>3</sup>/s (Rahman & Yunus, 2016). The Farakka Barrage not only reduced the amount of water that could flow through it, but it also caused substantial changes in the width of the river section, the morpho-dynamics of the sandbar, the shifting trend, and the history of erosion and accumulation. The decrease in the flow of the Ganges in the southwestern part of Bangladesh, which is entirely dependent on the river, has had catastrophic effects on a wide variety of ecosystems and industries, including hydro-morphology, forest ecosystems, navigation, drinking water, agriculture, fisheries, salt intrusion, and industrial goods (Hoque & Alam, 1995).

## 8 Hydro-Morphological Characteristics of Arial Khan River

The Arial Khan River has a significant variance in its discharge both throughout the year and during the seasons. The location of the rivers offtake and the flow direction departure from the Padma, which is its parent river, are the two factors that most heavily influence the river's hydro-morphology. A number of alterations have been made to the position and contour of the offtake in the most recent decades (CEGIS, 2010).

The perennial outflow of the Arial Khan River is Chowdhury Char. According to recent research, the amount of water flowing through the Arial Khan River saw a considerable drop during the first decade of the twenty-first century. The flow of the Arial Khan River is susceptible to change depending on the season. The average flow during the months of February and March is less than 50 m<sup>3</sup>/s, while during the months of August and September, the average flow is more than 2000 m<sup>3</sup>/s. This illustrates that the mean monthly flow is very diverse.

The average discharge in February, which represents the lowest flow of the year, reveals a rise until 1973, followed by a decline to almost nothing. However, minimum flow started to increase in the middle of the 1980s and continued to increase substantially until the middle of the 1990s. After then, it again started to decrease. In contrast, the average flow in August, which reflects the river's flood flow, closely resembles the flow pattern in February. CEGIS (2011, 2012) discovered a significant relationship between the discharge in the Arial Khan River and the plan form of the Padma River. The river's flow was observed to have increased when the Arial Khan's discharge was located on the Padma's outer bank. Until the 1970s, the Arial Khan River had many offtakes in addition to the present one at Chowdhury Char. Later, only the Arial Khan's current offtake at Chowdhury Char remained as a permanent source, and until the late 1990s, the flow increased.

The highest annual water levels of the Arial Khan River have remained relatively constant throughout time; however, the lowest annual water levels have declined

dramatically. The water levels at the offtake and in Madaripur town show a decline of around 1 m since the late 1970s, when the Padma's main flow was on the left bank and the Arial Khan Rivers offtake was practically isolated during the dry season. After the 1970s, there was a reduction in the amount of water being discharged, and a corresponding drop in water level also occurred (Akter & Sarker, 2013).

The riverbed material of the Arial Khan is fine sand. For the bulk of bed material transfer, suspension transport is used. According to studies undertaken by FAP 24 between 1993 and 1996, the silt load in the Arial Khan River increased dramatically throughout the late 1980s. The fortunate location of the Arial Khan River's outflow undoubtedly contributed to the increase in bed load. In the 1990s, the decadal average bed material load in the Arial Khan River was more than 6 million tons per year, and the average annual discharge volume was around 30 billion m<sup>3</sup> (Akter & Sarker, 2013).

## 9 Scenario of the Ganges Basin

During the monsoon of 2019, some areas of lower Brahmaputra and lower Ganges basins had a catastrophic flood that lasted longer than normal. There was a temporary flooding of the Meghna and South Eastern Hills basins. The Meghna basin was inundated in June and July, but the Brahmaputra, Ganges, and South Eastern Hill basins were only affected in July. In October, however, a few areas near the Ganges River experienced temporary flooding.

The 2019 annual flood report indicates that during the monsoon, the water level (WL) at 6 of the Ganges basin's 25 monitoring sites surpassed their respective danger levels (DL). The Padma at Goalundo, Bhagyakul, and Sureswar stations operated over DL for 7–17 days. As a consequence, low-lying parts in the districts of Rajbari, Faridpur, Dhaka, Munshiganj, Madaripur, and Shariatpur were predominantly inundated for a medium to slightly longer than average length of time in July of this year. Five days in October, the Ganges at Hardinge Bridge, flowed over DL. Throughout the season, the Pashure near Khulna flowed over DL for 28 days due mostly to tidal influences. The table compares WL for the current year, 2019, with historical occurrences for the Ganges basin between 2017 and 1998. Table 22.1 details the river's WL status at important places within this basin.

### 9.1 *The Gorai at Gorai Railway Bridge and Kamarkhali*

The water level of the Gorai River at Gorai Railway Bridge and Kamarkhali displayed a consistent rise and fall during the monsoon season in July and August of 2018. When the Gorai Railway Bridge was built, the WL of the Gorai River did not pass over the DL. When compared to the DL at Gorai Rail Bridge, the river's WL reached its annual high point of 12.47 mPWD on October 3, which represented a

**Table 22.1** Comparison of 2019 water level (in mPWD) to historical events of 2017 and 1998 at several important Ganges basin stations

River	Station	Previous highest value recorded	Danger level	Peak of the year			No. of days above danger level		
				1998	2017	2019	1998	2017	2019
Ganges	Pankha	24.14	22.50	24.14	21.48	22.23	66	0	0
Ganges	Rajshahi	20.00	18.50	19.68	17.54	18.19	28	0	0
Ganges	Hardinge Bridge	15.19	14.25	15.19	13.85	14.33	27	0	5
Gorai	Kamarkhali	9.48	8.20	NA	8.24	8.47	NA	3	6
Gorai	Gorai Rail Bridge	13.65	12.75	13.45	12.21	12.47	25	0	0
Arial Khan	Madaripur	5.80	4.17	NA	3.89	3.55	NA	0	0
Padma	Goalundo	10.21	8.65	10.21	9.71	9.33	68	20	17
Padma	Bhagyakul	7.50	6.30	7.50	6.81	6.70	72	20	7
Padma	Sureswar	7.50	4.45	–	5.04	4.56	–	13	11

Source: Annual Flood Report (2019)

difference of 28 cm (12.75 m). During that period of time, the DL in Kamarkhali was submerged in water from the Gorai River. On October 3, the river's WL reached its greatest yearly level of 8.47 mPWD, which was 27 cm higher than the DL at Kamarkhali station. This was the river's highest level ever recorded (8.20 m).

## 9.2 The Arial Khan at Madaripur

The water level of the river Arial Khan at Madaripur followed the same pattern of increasing and decreasing as the water level of the Padma River. The WL in the area of Arial Khan that is close to Madaripur was lower than the DL, while the monsoon was in effect. On the July 23, the WL reached its maximum height of 3.55 m, which was 62 cm less than the DL (4.17 m).

## 10 Human Dimensions of Flooding in Bangladesh

In developing nations, where there is often less protection from natural catastrophes and inadequately constructed infrastructure, the danger of flood-related damage is greater (Khan, 2008). Floods accounted for 40% of all natural catastrophes that occurred between 1985 and 2009, and they caused tremendous economic damage and human suffering (Jonkman & Vrijling, 2008).



Flooding caused by catastrophic hydro- and meteorological events with unexpected magnitudes and frequency has the potential to cause environmental damage in addition to the loss of lives, livelihoods, and infrastructure. There were more than 4000 major floods that occurred between the years 1900 and 2012, and they were responsible for the deaths of 6.9 million people. More than 3.6 billion people were forced to leave their homes, and \$550 billion worth of damage was done to the economy (Khan, 2008; Kugler, 2007; Kundzewicz et al., 2014).

In addition, economic losses caused by damaging floods are enormous and have been gradually increasing worldwide. In addition to the terrible loss of life, households, communities, and societies endure economic hardship as a result of the destruction of standing crops, residences, infrastructure, equipment, and buildings. This results in a decrease in the value of their assets. In many instances, extreme flooding has a devastating impact not just on individual houses but also on the nation as a whole (Chanda, 2010).

Bangladesh is one of the nations where flooding happens in a distinctive setting. Because the bulk of the country is low-lying and 80% of the land is in a floodplain, the nation is very susceptible to flooding. In the previous 50 years, Bangladesh has undergone at least seven severe floods, according to historical and current records. The nation's flooding patterns also indicate an increase in the frequency of flooding. Bangladesh endures frequent and strong floods as a consequence of its geographical location and poor economic standing. Due to the fact that Bangladesh is situated in the low-lying deltaic floodplain of the Ganges–Brahmaputra–Meghna (GBM) river basin, it is subject to annual flooding. Up to 34% of Bangladesh's land area is submerged in water for between 5 and 7 months each year, while floodplains make up over 80% of the topography of the country.

The floods of 1988, 1998, 2004, and 2007 were the worst in Bangladesh's history. The nation is rapidly becoming more susceptible to flood catastrophes, not only because of natural changes but also because of the fast population expansion in floodplains and widespread poverty, which drives people to live in floodplains. Significantly, living in poverty increases a person's vulnerability to flooding, and recurrent flooding makes people's financial situations more precarious and, as a result, more vulnerable (Chanda, 2010). As there is a shortage of land in this highly crowded country, many individuals, particularly those who are impoverished in rural areas, are forced to live in areas that are prone to flooding.

Homesteads, agricultural lands, everyday routines, water supply and sanitation, and the economy all suffer when floods occur. Flooding not only poses a significant threat to life and property but also poses significant challenges to public health, sanitation systems, and water supply. When there is flooding, the water and sanitation systems are placed at danger, which raises the probability that waterborne diseases may spread and cause significant health issues. The urbanization of a region has an effect not only on the hydrological and hydraulic processes that might result in flooding but also on societal issues, such as an increased risk of exposure. The quantity of surface runoff grows as a consequence of changes in land use and human activities, which in turn leads to larger flood regions and deeper flooding.

## 11 Flood Vulnerabilities in Bangladesh

Many people believe that Bangladesh is particularly susceptible to flooding. When a flood occurs, it has a devastating effect on the country's physical and social infrastructure, as well as its transportation system, assets, harvest, and lives of its residents. Flooding has an impact on the social and economic lives of those affected. This calamity has a severe effect on a variety of social amenities, including but not limited to houses, standing crops, poultry, livestock, transportation and communication networks, educational and institutional sectors, and other social amenities. Flooding poses a greater threat to human life, health, and well-being in less developed countries than it does in more developed nations. Drowning is responsible for two-thirds of flood-related fatalities, while physical trauma, heart attacks, and electrocution each account for one-third of the overall number of fatalities.

Among other things, flooding has an impact on dwellings, agricultural land, daily activities, water supply, hygiene, and the economy (Jonkman & Vrijling, 2008; Parvin et al., 2016). The floods of 1954, 1955, 1974, 1987, 1988, 1998, 2004, and 2007 caused devastating destruction and the loss of lives. During the years of 1987, 1988, 1998, 2004, and 2007, floods caused a significant amount of damage. Bangladesh has had the highest number of people killed each flood between 1971 and 2014 of any nation.

### 11.1 *Economic Effects of Flooding*

It's possible to determine the entire flood risk in Bangladesh using the strong correlation between economic losses and flood-affected regions. Floods in Bangladesh are estimated to cost the country an average of \$2.2 billion in 2014 USD – 1.5% of its GDP – per year. Several devastating floods have struck Bangladesh during the last several decades, notably those that occurred in 1987, 1988, 1998, and 2004. More than a quarter of Bangladesh's GDP (approximately \$12 billion in 2014 USD) was lost as a consequence of the severe floods in 1988 and 1998 (Ozaki, 2016a, b).

### 11.2 *Effect on Personal Safety*

In the view of the general public, the loss of human life is the most catastrophic kind of consequence that may result from a disaster (Jonkman & Vrijling, 2008). Flooding caused 15,033 fatalities in Bangladesh between 1972 and 2013, an average of 358 each year (Paul & Mahmood, 2016). The bulk of flood-related deaths in Bangladesh are attributable to factors including but not limited to drowning, snake-bites, waterborne diseases, and diarrhea. It was anticipated that drowning would be

the leading cause of death in Bangladesh during the 2007 monsoon floods; instead, the number of deaths caused by snakebites exceeded the number of deaths caused by both diarrhea and respiratory infections combined (Kunii et al., 2002; Morshed & Sobhan, 2010; Uddin, 2018). Due to the disaster, many people have had to change careers and migrate (Lu et al., 2016). In developing countries, both acts of violence and injuries are often underreported, especially in the wake of natural catastrophes like floods. Incidents of violence against children and women, as well as injuries, have been reported in areas of our country that have been impacted by flooding (Biswas et al., 2010).

### ***11.3 Impacts of Flooding on Buildings and Infrastructures***

According to research, flooding may have a substantial effect on property and households (Ozaki, 2016a, b). Floods that move quickly may destroy whole slums, but floodwaters that move slowly can inflict structural damage. In the rural districts of Bangladesh, crumbling “mud walls,” “coconut leaf walls,” and “tin walls” leave people and property vulnerable and unprotected. Slums are home to around one-third of the population of Bangladesh, meaning that a sizeable proportion inhabitants of the country are without homes and may be stranded for many days as a consequence of flooding (Braun & Abheuer, 2011; Dewan, 2015). In a similar vein, the ability to provide both immediate and long-term healthcare as well as assistance has considerably decreased (Younus, 2012; Thiele-Eich et al., 2015). The debris that was left behind after floods has caused damage to the city’s waste management system, which in turn impedes drainage systems and has a negative impact on the environment (Braun & Abheuer, 2011; Haque & Jahan, 2015).

### ***11.4 Impacts of Flooding on Crops and Animals***

The economy of Bangladesh is mostly dependent on agriculture. Agriculture accounts for 18.6% of Bangladesh’s gross domestic product and provides employment for almost half of the country’s labor force (Shaw, 2018). The most of the poor people reside in flood- and landslide-prone regions, making them more reliant on natural resources in this country. Bangladesh’s “Aman” kind of rain-fed rice is very susceptible to river flooding and has been destroyed in every flood year. As a result of the floods that occurred in Bangladesh in 1998, 69% of the country’s Aus rice supply, 91% of transplanted Aman, and 82% of deepwater Aman were destroyed, which left the whole nation without a reliable source of food (Alexander et al., 1998; Ali et al., 2002; Khan et al., 2012).

The flooding in Bangladesh is having a negative effect on Bangladesh’s small agricultural enterprises, such as mushroom farms. The 1998 and 2007 floods wrecked devastation on the mushroom industry, causing enormous foreign currency

losses (Ozaki, 2016a, b). The devastating impact of flooding in rural and semi-urban regions on domestic animals, such as chickens and dairy cows, which are key sources of income for both Bangladesh and India, can be seen in both countries. Financial hardship for fishing export business in Bangladesh is caused by the loss of cultured fish due to erosion of embankments and the edges of lakes and ponds. Agriculture contributes substantially to Bangladesh's food supply. These nations are now reliant on assistance from other countries as a result of the damage that flooding has caused to their agriculture, dairy, fisheries, and poultry industries (Braun & Abheuer, 2011; Brouwer et al., 2007; Ozaki, 2016b; Parvin et al., 2016; Islam et al., 2016). Another big consequence is the loss of trees. Floods and waterlogging have killed millions of trees as a consequence of the increasing trend of climate-induced floods. This problem has significantly impacted Bangladesh's socioeconomic standing. Major investment, biodiversity, and reforestation program losses were the results (Basak et al., 2015).

## 12 Possible Solutions to the Issue of Flooding

There are two fundamental sorts of solutions to the issue of flooding in Bangladesh, structural solutions and geologic solutions.

### 12.1 *Structural Solutions*

Riverbank embankments, dams, reservoirs, sewers, and other constructions that are meant to control the natural flow of rivers are some examples of structural solutions. In most cases, structural solutions investigate a problematic section of a river basin in isolation, and they do not take geology into consideration. As part of an effort to reduce the risk of flooding, Bangladesh is putting into action a number of structural solutions on a smaller scale (Rashid & Paul, 1987).

Fundamental to the development of a delta is the river-borne sediment deposition. The proposed berms will prevent sedimentation from exacerbating riverbeds and cause the area behind the berms to be inundated by the rising sea. Other concerns that may develop as a consequence of the execution of such a megaproject including flash floods, the loss of a substantial area of land to this project, considerable river channel alterations, the loss of soil fertility, and perhaps population relocation. Building such embankments will necessitate decades of maintenance, posing a formidable challenge for Bangladesh (Kabir & Hossen, 2019).

## ***12.2 Geologic Solutions***

Understanding the underlying geologic processes responsible for flooding is necessary for developing a solution to the flooding issue (Ali et al., 2002). Inundation in Bangladesh is just one aspect of a wider hydrodynamic process at work in the region. Only solutions consistent with natural processes have a possibility of success.

For preventative measures or development plans to be successful in reducing the impact of flooding, a comprehensive study of geologic processes, including river and channel hydrodynamics, sedimentation dynamics, amount of accumulated sediment and sedimentation rate, erosion and deposition rate, and the rate at which the local sea level is rising, is required. It's impossible to solve the problem of floods and protect the environment at the same time until we have a comprehensive knowledge of all geologic processes (Mirza, 2002, 2003; Karim & Mimura, 2008; Brammer, 2014; Ikeuchi et al., 2015; Khan et al., 2019). When examining geologic solutions to the flood issue, the two most crucial aspects to take into consideration are the elevation of the land, as well as the basin's ability to convey water. The likelihood of flooding in Bangladesh will decrease as a result of increases in land elevation as well as river water capacity (Khalequzzaman, 1994). It is going to be necessary to make use of techniques such as dredging, building of dams, sluice gates, and sediment dispersion in order to achieve the objective of increasing the capacity of drainage basins and the land elevation.

## ***12.3 Dredging and Re-excavation***

Dredging of the river and its channels, followed by the spread of the dredged material throughout the plain of the delta, would not only increase the carrying capacity of the river, but it would also raise the height of the delta. As a consequence of these factors, the severity of the annual floods will be mitigated to some degree. To ensure that the Ganges-Brahmaputra delta is able to adapt to rising sea levels, it is imperative that adequate supplies of sediment, as well as accumulation and dispersion, be maintained (Kabir & Hossen, 2019).

## ***12.4 Prevention of Land Degradation***

Suspension of particles surrounds the plant stems. Farmers should leave a few inches of stem on their rice crops prior to the start of the rainy season. Besides that, people need to be educated on the issue of soil erosion. Ploughing increases the soil's susceptibility to surface runoff-caused erosion. For example, strong earthen barriers between large farmlands and contour tilling may prevent sediments from being swept into streams by runoff.

### ***12.5 Flood Preparedness***

Innovative and less costly approaches to mitigating flood damage might arise from an understanding of how people have evolved to and been influenced by floods. It is also necessary to consider indigenous solutions, such as the creation of suitable dwelling units as well as other forms of support infrastructure (Rashid & Paul, 1987; Islam et al., 2016).

### ***12.6 Cooperation Within the Basin***

There is just 7% of the river basin under Bangladesh's jurisdiction. Without regional coordination with co-riparian nations, significant interbasin development projects are practically impossible to realize. In order to be effective, any interbasin flood control project has to be built to serve the shared interests of the people of the nations that are involved (Rashid & Paul, 1987; Paul, 1997; Khan, 2008; Pal et al., 2011).

## **13 Gorai River Restoration and Management**

The seasonal flow of the Gorai River (November to May) has decreased over the last two decades, and rapid siltation will be caused due to decrease in dry season flow near the river's mouth. The Government of Bangladesh (GoB) signed the Ganges Water Treaty (GWT) with the Government of India (GoI). After the signing the agreement, the Government of Bangladesh (GoB) sought help from the Government of the Netherlands, the World Bank (WB), and other donor organizations. As a result, between September 1997 and March 1998, a mission was launched.

The Gorai River Restoration Project GRRP comprises more than 1600 million hectares of land. The Ganges River tributaries form the northern limit of the GRRP zone, while the southern boundary is the southern edge of the Sundarbans. Under the auspices of the Bangladesh Water Development Board (BWDB) and with financing from the governments of Bangladesh, West Bengal, and Nigeria, the GRRP was scheduled to commence in 2001 (DHV-Haskoning and Associates., 2000).

The proposed GRRP's overarching goals are to prevent environmental degradation in the southwest region, the coastal belt. The project's major goals also include saving the Sundarbans by restoring the Gorai River and ensuring freshwater flow during the wet season while augmenting flow during the dry season.

An overriding objective of proposed GRRP is to protect the coastal belt and the southwest region from environmental deterioration. It is also one of the project's main objectives to ensure freshwater flow in the Gorai River during the rainy season and to increase the amount of water flowing during the dry season in order to save Sundarbans (BWDB, 1998). The proposed project would increase agricultural and

fisheries output, as well as navigation, by lessening the negative environmental effects of salt intrusion. Restoration of the river's distribution system, river training at the Gorai mouth and the Ganges approach to the Gorai offtake, as well as community development, participation, and the building of institutional capacity are the primary focuses of the GRRP, which aims to ensure the long-term sustainability of the Gorai River distribution system. The assessment of the river training works, a maintenance dredging program, and a design to improve the flows of the Gorai River are all included in the preparatory phase of the GRRP. The planned GRRP would update and expand technical, environmental, social, and economic studies, as well as include lessons gained from the repeated dredging attempts of the Government of Bangladesh's priority work program. The intended GRRP will be implemented based on project evaluations by the Government of Bangladesh, the World Bank, and other bilateral funders (BWDB, 1998).

## 14 Arial Khan River Management

The Arial Khan River is a swift-moving river, and its eroding bend is unlikely to stay in the same location for more than 5 years. Due to the time necessary for planning, fund approval, design, bidding, and contract awarding, it might take 3–4 years to install bank security measures in Bangladesh. Consequently, permanent constructions such as revetments may not be useful for erosion prevention, since the river's erosion activity would have most likely shifted to another place during the preparation operations, resulting in significant socioeconomic loss. As a result, activities like deploying sand-filled geo-bags at erosion-prone areas along the river, are less expensive. Moreover, funds can be collected from the local government in an emergency basis (Akter & Sarker, 2013).

Elements of river morphology and planform should be included into long-term river management programs. The flow pattern of the Arial Khan River is altering as a result of the changing topography of the Padma River adjacent to where it meets the Arial Khan offtake. Consequently, this river has become unstable, necessitating training measures. Successful river training schemes may be implemented if the Arial Khan's outflow is stabilized.

For a solution that will be effective over the long term, the river training activities should have a strong similarity to the natural forms of rivers while the outline is being designed. Although the entire Arial Khan River may be trained to minimize riverbank erosion, this may not be economically or ecologically possible. Because of the dynamic nature of the Arial Khan River in an active delta, some leeway must be provided for it in terms of the creation of land and the development of the area (Akter & Sarker, 2013).

## 15 Conclusion

Almost every year, several forms of floods hit Bangladesh, wreaking havoc on the people, livelihoods, and property of the nation. There is a long-held belief that Bangladesh's rivers are the country's lifelines, providing affordable transit for people and freight, water for agriculture, and fish for human sustenance. The problem arises when these rivers breach their banks and flood the region. Both the Bangladeshi government and nongovernmental groups have taken several measures to lessen the detrimental consequences of flooding. Flood management is primarily concerned with reducing the amount of damage that floods inflict. Flood warning and flood forecasting might be an effective nonstructural technique for attaining this goal. It would be simpler to take precautions to lessen the damage if notification was provided far enough in advance. A long-term plan must be developed by the authorities of the riparian nations in order to protect Bangladesh against forthcoming flood events. A regional solution is necessary since rivers are a part of the landscape. Comprehensive flood management plans and a coordinated approach among flood control agents will help Bangladesh reduce its risk of flooding in Gorai-Madhumati and Arial Khan River.

## References

- Adams, W. C. (1919). *History of the rivers in the genetic delta, 1750–1918*. Bengal Secretariat Press.
- Ahmed, S. J., & Islam, S. (2003). *Banglapedia: National Encyclopedia of Bangladesh* (Available at Banglapedia website).
- Ahmed, A. U., & Mirza, M. M. Q. (2000). Review of causes and dimensions of floods with particular reference to flood'98: National perspectives. In Q. K. Ahmad, A. K. A. Chowdhury, S. H. Imam, & M. Sarker (Eds.), *Perspectives on flood 1998*. University Press Ltd.
- Akter, J., & Sarker, M. H. (2013). Morphological processes and effective river erosion management: A case study of the Arial Khan River in Bangladesh. In *4th International Conference on Water & Flood Management (ICWFM-2013)*.
- Alexander, M. J., Rashid, M. S., Shamsuddin, S. D., & Alam, M. S. (1998). Flood control, drainage and irrigation projects in Bangladesh and their impact on soils: An empirical study. *Land Degradation and Development*, 9(3), 233–246. [https://doi.org/10.1002/\(SICI\)1099-145X\(199805/06\)9:3<233::AID-LDR277>3.0.CO;2-W](https://doi.org/10.1002/(SICI)1099-145X(199805/06)9:3<233::AID-LDR277>3.0.CO;2-W)
- Ali, M. A., Seraj, S. M., & Ahmad, S. (2002). *Engineering concerns of flood, 1998 perspective*. Bangladesh University of Engineering and Technology.
- Bangladesh Bureau of Statistics (BBS). (2016). *Statistical year book of Bangladesh*
- Basak, S. R., Basak, A. C., & Rahman, M. A. (2015). Impacts of floods on forest trees and their coping strategies in Bangladesh. *Weather and Climate Extremes*, 7, 43–48. <https://doi.org/10.1016/j.wace.2014.12.002>
- Ben, C., Lindquist, A., & Wilson, D. (1995). *Sharing the Ganges-the politics and technology of river development* (p. 272). University Press Limited.
- Biswas, A., Rahman, A., Mashreky, S., Rahman, F., & Dalal, K. (2010). Unintentional injuries and parental violence against children during flood: A study in rural Bangladesh. *Rural and Remote Health*, 10(1), 1199.



- Brammer, H. (1991). *Geology of Bangladesh*. University Press Limited.
- Brammer, H. (2014). Bangladesh's dynamic coastal regions and sea-level rise. *Climate Risk Management*, 1, 51–62. <https://doi.org/10.1016/j.crm.2013.10.001>
- Braun, B., & Abheuer, T. (2011). Floods in megacity environments: Vulnerability and coping strategies of slum dwellers in Dhaka/Bangladesh. *Natural Hazards*, 58(2), 771–787. <https://doi.org/10.1007/s11069-011-9752-5>
- Brouwer, R., Akter, S., Brander, L., & Haque, E. (2007). Socioeconomic vulnerability and adaptation to environmental risk: A case study of climate change and flooding in Bangladesh. *Risk Analysis*, 27(2), 313–326. <https://doi.org/10.1111/j.1539-6924.2007.00884.x>
- BWDB. (1987). *Flood in Bangladesh – 1987*. BWDB.
- BWDB. (1998). *Terms of reference for environmental and geographical information system support project on Gorai river restoration project*. Government of the People's Republic of Bangladesh, Bangladesh Water Development Board (BWDB).
- BWDB. (2014). *Annual flood report 2013*. Bangladesh Water Development Board.
- Chowdhury, A. M. (2000). Flood, 98: Oceanic perspective. In Q. K. Ahmad, A. K. A. Chowdhury, S. H. Imam, & M. Sarker (Eds.), *Perspectives on flood 1998*. University Press Ltd..
- CEGIS. (2010). Padma Multipurpose Bridge Design Project. River Training Works, Updated Scheme Design Report, Annex C: Morphological Analysis of Padma River, Volume II, prepared for Bangladesh Bridge Authority
- CEGIS. (2011). Bank erosion and navigability problem in the river Arial Khan from Madaripur launch ghat to Kalikapur-Habiganj-Rajarhat-Srinadi via Tekerhat river route. Final report prepared for BIWTA, Ministry of Shipping, Government of Bangladesh
- CEGIS. (2012). Morphological Processes of the Arial Khan River and Outline of the River Training Works. Technical Report: 4, prepared for BWDB under the project of Capital Dredging, Ministry of Water Resources, Government of Bangladesh
- Chanda, S. A., Ara, P. G., Biswas, C., & Shaw, R. (2010). Impact and adaptation to flood: A focus on water supply, sanitation and health problems of rural community in Bangladesh. *Disaster Prevention and Management: An International Journal*, 19(3), 298–313. <https://doi.org/10.1108/09653561011052484>
- Dewan, T. H. (2015). Societal impacts and vulnerability to floods in Bangladesh and Nepal. *Weather and Climate Extremes*, 7, 36–42. <https://doi.org/10.1016/j.wace.2014.11.001>
- DHV-Haskoning and Associates. (2000). *Feasibility report. Volume III, Annex-C. Gorai River restoration project, prepared for Bangladesh Water Development Board, Government of the People's Republic of Bangladesh*.
- EGIS. (2000). *Environmental baseline of Gorai river restoration project, EGIS-II* (p. 150). Bangladesh Water Development Board, Ministry of Water Resources, Government of Bangladesh.
- EGIS. (2001). *Remote sensing, GIS and morphological analyses of the Jamuna River, 2000. Part II, prepared for river bank protection project (RBPP)* (p. 66). BWDB.
- FAP4. (1993). *Southwest area water resources management project, final report*, Volume 1, Main Report.
- Fergusson, J. (1863). On recent changes in the Delta of the Ganges. *Proceedings of the Geological Society, Quarterly Journal, London*, 19, 321–353.
- Gazi, M. Y., Hossain, F., Sadek, S., & Uddin, M. M. (2020). Spatiotemporal variability of channel and bar morphodynamics in the Gorai-Madhumati River, Bangladesh using remote sensing and GIS techniques. *Frontiers in Earth Science*, 14(4), 828–841.
- Halcrow and Partners Ltd., DHI, EPC Ltd., Sthapati Sangshad Ltd. (FAP 4) (1993). *Morphological studies: Southwest area water resources management project*. In Report produced for flood plan coordination organization (FPCO).
- Haque, A., & Jahan, S. (2015). Impact of flood disasters in Bangladesh: A multi-sector regional analysis. *International Journal of Disaster Risk Reduction*, 13, 266–275. <https://doi.org/10.1016/j.ijdr.2015.07.001>

- Hoque, M. M., & Alam, S. M. K. (1995). Post Farakka dry season surface and ground water conditions in the Ganges and vicinity. In J. M. Hasna (Ed.), *Women for water sharing*. Academic Publishers.
- Ikeuchi, H., Hirabayashi, Y., Yamazaki, D., Kiguchi, M., Koirala, S., Nagano, T., & Kanae, S. (2015). Modeling complex flow dynamics of fluvial floods exacerbated by sea level rise in the Ganges–Brahmaputra–Meghna Delta. *Environmental Research Letters*, 10(12). <https://doi.org/10.1088/1748-9326/10/12/124011>
- Islam, S. (2003). *Banglapedia: National Encyclopedia of Bangladesh*. Asiatic Society of Bangladesh.
- Islam, S. N., & Gnauck, A. (2008). Mangrove wetland ecosystems in Ganges Brahmaputra delta in Bangladesh. *Frontiers of Earth Science in China*, 2, 439–448. <https://doi.org/10.1007/s11707-008-0049-2>
- Islam, S. N., & Gnauck, A. (2009). Threats to the Sundarbans mangrove wetland ecosystems from transboundary water allocation in the Ganges basin: A preliminary problem analysis. *International Journal of Ecological Economics & Statistics (IJEES)*, 13(W09), 64–78.
- Islam, S. N., & Gnauck, A. (2011). Water shortage in the Gorai River basin and damage of mangrove wetland ecosystems in Sundarbans, Bangladesh. In *3rd International Conference on Water & Food Management (ICWFM-2011)*.
- Islam, M. S., Solaiman, I. M. M., Tusher, T., & Kabir, M. (2016). Impacts of flood on Char livelihoods and its adaptation techniques by the local people. *Bangladesh Journal of Scientific Research*, 28(2), 123–135. <https://doi.org/10.3329/bjsr.v28i2.26783>
- Jonkman, S. N., & Vrijling, J. K. (2008). Loss of life due to floods: Loss of life due to floods. *Journal of Flood Risk Management*, 1(1), 43–56.
- JRCB. (2016). *Joint Rivers Commission Bangladesh*. Retrieved from [http://www.jrcb.gov.bd/basin\\_map.html](http://www.jrcb.gov.bd/basin_map.html)
- Kabir, M., & Hossen, M. N. (2019). Impacts of flood and its possible solution in Bangladesh. *Disaster Advances*, 12(10).
- Karim, M., & Mimura, N. (2008). Impacts of climate change and sea-level rise on cyclonic storm surge floods in Bangladesh. *Global Environmental Change*, 18(3), 490–500. <https://doi.org/10.1016/j.gloenvcha.2008.05.002>
- Khalequzzaman, M. (1994). Recent floods in Bangladesh: Possible causes and solutions. *Natural Hazards*, 9(1–2), 65–80. <https://doi.org/10.1007/BF00662591>
- Khan, F. H. (2000). *Geology of Bangladesh*. University Press Limited.
- Khan, M. S. A. (2008). Disaster preparedness for sustainable development in Bangladesh. *Disaster Prevention and Management: An International Journal*, 17(5), 662–671. <https://doi.org/10.1108/09653560810918667>
- Khan, M., Mia, M., & Hossain, M. (2012). Impacts of flood on crop production in Haor areas of two Upazillas in Kishoregonj. *Journal of Environmental Science and Natural Resources*, 5(1), 193–198. <https://doi.org/10.3329/jesnr.v5i1.11581>
- Khan, S. I., Flamig, Z., & Hong, Y. (2019). Flood monitoring system using distributed hydrologic modeling for Indus River Basin. In S. Khan & T. Adams (Eds.), *Indus River Basin* (pp. 335–355). Elsevier. <https://doi.org/10.1016/B978-0-12-812782-7.00015-1>
- Khanam, M., & Navera, U. K. (2016). Hydrodynamic and morphological analysis of Gorai River using delft 3d mathematical model. In: *Proceedings of the 3rd International Conference on Civil Engineering for Sustainable Development (ICCESD)*.
- Kugler Z. (2007). *The global flood detection system*, 45.
- Kundzewicz, Z. W., Kanae, S., Seneviratne, S. I., Handmer, J., Nicholls, N., Peduzzi, P., & Sherstyukov, B. (2014). Flood risk and climate change: Global and regional perspectives. *Hydrological Sciences Journal*, 59(1), 1–28.
- Kunii, O., Nakamura, S., Abdur, R., & Wakai, S. (2002). The impact on health and risk factors of the diarrhoea epidemics in the 1998 Bangladesh floods. *Public Health*, 116(2), 68–74. <https://doi.org/10.1038/sj.ph.1900828>
- Lu, Q. C., Zhang, J., Wu, L., & Rahman, A. B. M. S. (2016). Job and residential location changes responding to floods and cyclones: An analysis based on a cross-nested logit model. *Climatic Change*, 138(3–4), 453–469. <https://doi.org/10.1007/s10584-016-1740-z>

- Mirza, M. K. (2002). Global warming and changes in the probability of occurrence of floods in Bangladesh and implications. *Global Environmental Change*, 12(2), 127–138. [https://doi.org/10.1016/S0959-3780\(02\)00002-X](https://doi.org/10.1016/S0959-3780(02)00002-X)
- Mirza, M. M. Q. (2003). Three recent extreme floods in Bangladesh: A hydro-meteorological analysis. *Natural Hazards*, 28, 35–64.
- Mirza, M. M. Q., Warrick, R. A., & Ericksen, N. J. (2003). The implications of climate change on floods of the Ganges, Brahmaputra and Meghna Rivers in Bangladesh. *Climatic Change*, 57(3), 287–318. <https://doi.org/10.1023/A:1022825915791>
- Morshed, G., & Sobhan, A. (2010). The search for appropriate latrine solutions for flood-prone areas of Bangladesh. *Waterlines*, 29(3), 236–245. <https://doi.org/10.3362/1756-3488.2010.024>
- Ozaki, M. (2016a). Disaster risk financing in Bangladesh. *SSRN Electronic Journal*. <https://doi.org/10.2139/ssrn.2941319>
- Ozaki M., (2016b). Disaster risk financing in Bangladesh, Asian Development Bank. *SSRN Electronic Journal*. Retrieved from <https://www.adb.org/publications/disaster-risk-financingbangladesh>
- Pal, S. K., Adeloje, A. J., Babel, M. S., & Das, G. A. (2011). Evaluation of the effectiveness of water management policies in Bangladesh. *International Journal of Water Resources Development*, 27(2), 401–417. <https://doi.org/10.1080/07900627.2011.564973>
- Parvin, G., Shimi, A., Shaw, R., & Biswas, C. (2016). Flood in a changing climate: The impact on livelihood and how the rural poor cope in Bangladesh. *Climate*, 4(4), 60. <https://doi.org/10.3390/cli4040060>
- Paul, B. K. (1997). Flood research in Bangladesh in retrospect and prospect: A review. *Geoforum*, 28(2), 121–131. [https://doi.org/10.1016/S0016-7185\(97\)00004-3](https://doi.org/10.1016/S0016-7185(97)00004-3)
- Paul, B. K., & Mahmood, S. (2016). Selected physical parameters as determinants of flood fatalities in Bangladesh, 1972–2013. *Natural Hazards*, 83(3), 1703–1715. <https://doi.org/10.1007/s11069-016-2384-z>
- Rahman, A., & Yunus, A. (2016). Analysis on hydrodynamic and morphological characteristics of upper Gorai River using DELFT3D. *Technical Journal River Research Institute*, 13(1), 136–152.
- Rashid, H. E. (1991). *Geography of Bangladesh* (Second Revised Edition). University Press Limited.
- Rashid, H., & Paul, B. K. (1987). Flood problems in Bangladesh: Is there an indigenous solution? *Environmental Management*, 11(2), 155–173. <https://doi.org/10.1007/BF01867195>
- Sarker, M. H., Akter, J., & Rahman, M. (2013). Century-scale dynamics of the Bengal delta and future development. In *4th International Conference on Water & Flood Management (ICWFM-2013)*.
- Shamsad, S. Z. K. M., Islam, K. Z., & Mahmud, M. S. (2014). Surface water quality of Gorai River of Bangladesh. *Journal of Water Resources and Ocean Science*, 3(1), 10–16.
- Shaw, R. (2018). Flood and sustainable agriculture in the Haor Basin of Bangladesh: A review paper. *Universal Journal of Agricultural Research*, 6(1), 40–49.
- Surface Water Modelling Center. (2001). *Hydraulic mathematical modelling study, southwest road network development project: Construction of bridge over Arial Khan River, Final Report*, Volume-I, Main Report.
- The World Bank. (2005). *Bangladesh Country water resources assistance strategy*, Bangladesh development series-paper no. 3. Retrieved from <http://www.worldbank.org.bd/bds>
- Thiele-Eich, I., Burkart, K., & Simmer, C. (2015). Trends in water level and flooding in Dhaka, Bangladesh and their impact on mortality. *International Journal of Environmental Research and Public Health*, 12(2), 1196–1215. <https://doi.org/10.3390/ijerph120201196>
- Uddin, K. N. (2018). Health hazard after natural disasters in Bangladesh. *Bangladesh Journal of Medicine*, 28(2), 81–90. <https://doi.org/10.3329/bjmed.v28i2.33357>
- Williams, C. A. (1919). *History of the rivers in the Ganges Delta 1750–1918*. Bengal Secretariat Press. Reprinted by East Pakistan Inland Water Transport Authority, 1966, pp. 96.
- Younus, M. A. F. (2012). *Community-based autonomous adaptation and vulnerability to extreme floods in Bangladesh*, 416.

# Index

## A

Absolute relief, 290, 297  
Accessibility, 64, 130, 135, 248–250, 254, 262  
Accretion, 3, 8, 93, 97, 103, 106–112, 115, 120, 121, 405, 426, 436  
Advanced Spaceborne Thermal Emission and Reflection Radiometer (ASTER), 22, 23, 26, 30, 68, 288  
Aggradation, 3, 6, 47, 55, 57, 59, 270, 304, 455  
Agricultural production, 268, 367, 376, 443  
Agro-ecological zones (AEZ), 435, 436  
Ajay River Basin (ARB), 14, 267–283  
Alluvium, 213, 287, 295, 306, 307  
ALOS, 132, 184, 187, 198, 307, 310  
Analytical hierarchy process (AHP), 64, 70, 80, 98, 178, 205, 214–216, 218, 221, 226, 369  
Annual hydrograph, 325  
ANOVA, 409, 499, 500, 522  
Anthropogenic factor, 455–456, 477–478  
ArcGIS, 68, 97, 98, 130, 133, 165, 178, 190, 191, 237, 288, 306, 311, 328, 369, 474, 475  
Ariyal Khan River, 529–547  
Artificial Neural Networks, 310  
Autocorrelation, 43, 499–501, 504

## B

Back swamp, 426, 435  
Bangladesh Water Development Board (BWDB), 95–97, 100, 103, 104, 390, 391, 406–408, 428, 450, 452, 454, 458–461, 530, 535, 545, 546

Bank erosion, 8, 49, 83, 92–95, 109–111, 277, 353, 355, 422, 482, 502  
Bank toe scouring, 355  
Barind tracts, 8, 404  
Basin morphology, 93, 304, 426, 435–438  
Basin morphometry, 286, 498, 502, 517  
Basin slope, 189, 196, 197  
Bay of Bengal, 6, 9, 10, 26, 186, 319, 424, 426, 430, 437, 440, 450, 467, 492, 505, 530, 532, 533  
Beel, 96, 436, 442, 482, 483  
Bhagirathi-Hooghly River (BHR), 7, 269, 307, 341, 471, 483, 484  
Bhagirathi River, 234, 235, 467, 471, 477, 493, 495, 501, 507  
Bhairab Bazar, 428–430, 535  
Bhukosh GSI, 208, 209  
Bifurcation ratio, 189, 289, 290, 293, 497, 502, 506  
Biodiversity, 8, 269, 424, 442, 443, 543  
Boro cultivation, 443  
Brahmaputra-Jamuna Floodplain, 403–422, 442  
Brahmaputra River, 7, 8, 15, 93, 119, 120, 164, 385–399, 405, 430, 438, 450, 533, 535  
Braiding Index (BI), 54, 55, 134, 135, 140–145, 149  
Buriganga, 15, 353, 449–461

## C

Catastrophic, 49, 65, 81, 100, 112, 119, 184, 226, 299, 300, 420, 424, 428, 457, 537, 538, 540, 541

- Catchment, 9, 12, 22, 28, 39, 49, 50, 52, 59, 65, 91–122, 139, 306, 308, 309, 317, 318, 320–324, 326, 328, 329, 340–342, 367, 373–374, 404, 406, 420, 424–429, 433, 435, 438, 439, 442, 444, 454, 466, 467, 469, 471, 473, 492–494, 519, 530–532  
 areas, 65, 92, 95, 96, 98, 100–103, 109, 113–115, 117–121, 139, 309, 328, 404, 406, 420, 424, 427, 433, 442–444, 467, 469, 471, 492, 519, 530–531  
 shape, 374  
 Chandraswar khal, 367  
 Channel geomorphology, 277–278, 282  
 Channel planform, 128–130, 133–136, 141, 142, 144, 145, 147, 149, 151–153, 155, 308  
 Chars, 405, 406, 435, 437, 438, 482  
 Chittagong Hill Tracts, 404  
 Circularity Ratio, 189, 289  
 Climate change, 8, 12, 26, 64, 92–94, 162, 232, 269, 271, 278, 304, 318, 319, 341, 352, 386–388, 390, 391, 394, 395, 404, 438–440, 443, 444  
 CMIP6, 15, 385–399  
 Compactness coefficient, 289, 297, 497, 517  
 Confluence, 7, 46, 49, 65, 174, 207–210, 212, 217–219, 267–269, 273, 278, 315, 353, 404, 426, 450, 467, 474, 482, 493, 495, 502, 532, 534  
 Consistency ratio, 70, 71, 215, 216  
 Constant of channel maintenance, 290, 297  
 Coping strategies, 120, 357, 404, 406, 407, 413, 415, 417–420, 458  
 Cordon, 459  
 Co-riparian, 398, 444, 545  
 Correlation coefficient, 37, 48, 55, 196, 197, 476, 499, 500  
 Cost-effective, 64  
 Crop diversity, 239, 243–245  
 Cropping intensity, 239–240, 243  
 Curve number, 317, 326, 329  
 Cut-off, 435, 482, 483  
 Cyclone, 8, 9, 20, 92, 162, 204, 246, 286, 319, 320, 340, 428, 440–442
- D**  
 Dam, 12, 14, 15, 103, 119, 128, 129, 162–165, 168, 170, 174–176, 179, 243, 245, 269, 304–306, 308, 309, 321, 325–326, 328, 330–333, 337, 339, 340, 342, 343, 374, 378, 444, 456, 458, 461, 471, 472, 478, 492, 495, 502, 504, 505, 543, 544  
 Damodar fan-delta, 340, 341, 343  
 Damodar River Basin (DRB), 14, 303–343  
 Damodar Valley Corporation (DVC), 304, 308, 324, 326, 328, 330, 332, 336, 339–343, 374, 376  
 Darakeswar, 353, 354, 361, 374, 376, 382  
 Deforestation, 64, 85, 103, 129, 162, 478, 493, 504, 530  
 Delta, vii, 1–15, 20, 25, 26, 30, 120, 269, 270, 287, 305–308, 340–343, 352, 404, 424, 426, 437, 453, 466, 467, 471, 478, 480–481, 493, 533–535, 544, 546  
 Deltaic Rarh Bengal (DRB), 286  
 Delta plain, 5, 6, 404  
 Dhaka City, 15, 26, 445, 449–461  
 Dhaka Narayanganj and Demra (DND), 436, 452, 456, 458, 459, 461  
 Dharla, 91–122  
 Digital elevation model (DEM), 22–24, 27, 28, 68, 91, 130, 184, 187, 190, 207, 271, 312, 315, 409, 430, 431, 474, 496–498, 509, 512, 516–519  
 Digital surface model (DSM), 311  
 Digital terrain model (DTM), 315  
 Disaster reduction, 121, 411  
 Discharge, 8, 22, 38, 65, 93, 128, 166, 196, 204, 269, 288, 303, 353, 367, 386, 406, 424, 454, 471, 493, 530  
 Diyaras, 405  
 Drainage density, 99, 115, 165, 189, 195, 289, 290, 294, 295, 297, 502, 506, 517  
 Drainage pattern, 147, 192, 374, 375  
 Drainage texture, 294, 492, 497, 501, 502, 506, 517  
 Dredging and re-excavation, 544  
 Dudhkumar River, 91–122
- E**  
 Economic effect, 541  
 Economy, 13, 92, 204, 232, 233, 239, 243–246, 262, 304, 422, 442–445, 466, 540–542  
 Ecosystem, 8, 130, 153, 162, 164, 388, 398, 422, 440–442, 445, 461, 537  
 Education system, 254  
 El Nino Southern Oscillation (ENSO), 319, 530  
 Elongation Ratio, 189, 195, 197, 289, 294, 497, 502, 506, 517

- Embankment, 12, 15, 20, 24, 27, 47, 49, 51,  
 83, 103, 119, 127, 128, 133, 135, 139,  
 146, 147, 149, 150, 153, 188, 207, 213,  
 219, 224, 225, 246, 268, 269, 272–277,  
 282, 304, 306, 320, 338, 339, 342,  
 352–356, 358, 359, 361, 370, 371, 376,  
 378, 421, 430, 452, 456, 459, 471, 484,  
 485, 506, 543  
 Embankment circuit, 354  
 ERDAS Imagine, 311  
 Estuary, 8, 425, 427, 430, 436, 437, 440, 443,  
 533–536  
 Extreme precipitation, 286, 386, 387, 392,  
 394–395, 398, 399
- F**
- Farakka Barrage, 7, 224, 472, 477, 481, 532,  
 536, 537  
 Fixed effects model, 136  
 Flash flood, 45, 50, 188, 196, 204, 234, 306,  
 319, 320, 424, 428, 429, 433, 434, 439,  
 443, 474, 535, 543  
 Flashiness, 37, 38, 46, 49, 50, 57  
 Flood, 1–15, 19–30, 37–58, 63–85, 91–122,  
 127–155, 161–179, 183–199, 203–226,  
 267–283, 285–299, 303–343, 351–361,  
 365–383, 385–399, 403–445, 449–461,  
 465–486, 491–523, 529–547  
 forecasting, 48, 59, 120, 282, 305, 366, 421,  
 444, 459, 547  
 frequency, 38, 43–46, 113, 115, 163,  
 165–166, 237, 241, 242, 268, 272, 278,  
 303, 315, 330–333, 497  
 hazard, 29, 64, 67, 69, 71, 78, 81–83, 85, 94,  
 118, 129, 204, 205, 212, 213, 221, 222,  
 234, 237–239, 242–244, 271, 305, 352,  
 408, 413, 420, 492–494, 497  
 hazard map, 29, 205, 408, 414, 497  
 height, 278–282, 340  
 inundation, 14, 19–30, 49, 64, 65, 94, 167,  
 168, 190, 212, 213, 242, 243, 272, 279,  
 283, 298, 299, 314–315, 355–358, 369,  
 430, 435, 439, 443  
 level, 49, 131, 132, 136, 150, 171, 278, 407,  
 430, 435, 452, 459, 472, 474, 476, 535  
 magnitude, 173, 257, 330, 476  
 management, 25, 38, 64, 83, 95, 120–122,  
 163, 177, 269, 305, 306, 333, 357, 366,  
 420, 444, 459, 460, 477, 547  
 prioritization, 191, 197–198  
 recurrence map, 358  
 simulation, 14, 38, 165, 167, 303–343, 444  
 stage, 259, 308, 390, 397, 409  
 vulnerability, 15, 93–95, 98–100, 113–122,  
 214, 216, 225, 239, 254, 300, 338, 366,  
 371, 406, 409, 420, 457, 491–507, 514,  
 521, 522, 541–543  
 Flood-contaminated water, 252  
 Flood Danger Level (FDL), 398  
 Flood Forecasting and Warning Centre, 390,  
 398, 460  
 Flood frequency analysis (FFA), 51, 163,  
 315–316, 330, 331, 333  
 Flooding, 2, 19, 49, 65, 92, 127, 162, 184, 204,  
 233, 267, 271, 286, 304, 352, 366, 386,  
 404, 424, 449, 466, 494, 530  
 Floodplain, 8, 20, 38, 83, 92, 128, 162, 206,  
 232, 269, 285, 304, 353, 366, 404, 424,  
 450, 466, 495, 530  
 inundation maps, 338, 340  
 management, 449–461  
 morphology, 304, 435–438  
 Flood-prone, 20–26, 29, 30, 49, 65, 115,  
 119, 177, 199, 205, 214, 216, 220,  
 221, 223, 225, 243, 244, 247, 255,  
 257, 259, 262, 263, 267, 268, 306,  
 334, 352, 355, 358, 367, 376, 377,  
 404, 420, 449, 473, 474, 493, 495,  
 497, 502, 505–507  
 Flood risk, 26, 29, 63–85, 101, 102, 121, 122,  
 190, 197, 205, 207, 225, 234, 240, 271,  
 272, 303–343, 386, 387, 392, 403–422,  
 453, 541  
 assessment, 63–85, 234, 303–343, 404, 405,  
 420, 421  
 possibility, 190  
 zonation, 64, 65, 453  
 Flood susceptibility, 64, 65, 67–69, 78–81, 83,  
 85, 163, 169, 177–178, 183–199,  
 203–226, 243, 494, 505  
 Flood susceptibility mapping, 64, 69, 78–81,  
 85, 169, 184, 216, 220  
 Flood susceptibility zone (FSZ), 64, 65, 67,  
 214–218, 221, 222, 226  
 Floodwall, 417, 418, 459  
 Fluvial architecture, 480  
 Fluvio-tidal, 425, 428  
 Focus group, 407, 408  
 Foothill, 11, 14, 38, 39, 63–85, 95, 129, 184,  
 185, 199, 307  
 Foreland, 65, 69, 83  
 Form factor, 289, 294, 497, 502, 506, 517  
 Freshwater, 427, 428, 430, 440, 530, 531, 534,  
 536, 545

**G**

- Ganga, 1–15, 20, 26, 83, 164, 205–207, 213, 223, 224, 269, 270, 287, 319, 352, 404, 466, 479, 481, 492, 493, 495
- GBM delta, 2–6, 8–12, 14, 15, 424, 426, 437
- General Hazard Index, 411
- Generalized Pareto Distribution (GPD), 391, 394
- Geologic solutions, 543, 544
- Geospatial technology, 494, 496
- Ghatal Block, 352–358, 367, 374–376, 381
- Ghatal floods, 361, 366, 382
- Ghatal Master Plan (GMP), 355, 356, 359
- Gibbs-Martin (GM) index, 240, 244
- GIS-based model, 417
- GIS-aided multi-criteria analysis (GIS-MCA), 98, 115
- GIS technique, 97, 98, 205, 226, 366, 369, 409
- Global Circulation Models (GCMs), 387–390, 392–397
- Global warming, 8, 102, 318, 386–388, 391
- Gorai-Madhumati, 529–547
- Grain size, 438, 455
- Ground control points (GCPs), 23, 24, 26, 134
- Gumbel's extreme value, 38, 51–53, 171

**H**

- Haors, 424, 426, 435, 441, 442, 445
- Hazard, 8, 19, 38, 63, 92, 128, 169, 184, 204, 232, 271, 286, 304, 352, 376, 404, 458, 492
- Health problems, 83, 250–254, 457
- Highest Water Level (HWL), 398
- High flood level (HFL), 49, 131, 136, 149, 150, 152, 472–474, 476
- Himalayan belt, 388
- Holocene, 3, 5, 308, 426, 533
- Household damage, 378–379
- Human dimension, 457–458
- Human intervention, 64, 130, 134, 143–145, 162, 299, 427, 437, 444
- Hydro-geomorphology, 93, 95, 103–109, 113, 120, 278, 457
- Hydrological alternation, 164
- Hydrological floods, 304
- Hydrological risk, 308, 315, 330–333
- Hydrological variability, 325–329
- Hydrologic Engineering Center's River Analysis System (HEC-RAS), 26, 27, 167, 305, 306, 311, 313–315, 333, 334, 336–340, 342
- Hydrology, 44, 135, 169, 190, 295, 304, 305, 308, 317, 320, 352, 417, 435, 439
- Hydro-meteorology, 47, 424, 439, 444

Hydro-morphology, 535–538

Hypsometric integral, 196

**I**

- Immature delta, 471
- Indigenous knowledge, 120, 407, 410, 413–417
- Industrialization, 20, 25, 26, 455
- Infrastructural vulnerability, 234, 239, 263
- In situ uncertainty, 306
- Instability index, 166
- Intergovernmental Panel on Climate Change (IPCC), 94, 115, 118, 120, 232, 233, 387, 388, 390, 404, 411
- Inundation, 11, 14, 19–30, 49, 53, 64–67, 92–94, 100, 103, 121, 167, 168, 175, 190, 205, 207, 210, 212, 213, 225, 226, 237, 241–243, 271, 272, 279, 282, 283, 298, 299, 305, 306, 308, 314, 315, 320, 334, 336–343, 354–361, 366, 369, 400, 407, 424, 428, 430, 432, 435, 439, 443, 466, 471, 485, 505, 544

**J**

- Jalangi, 15, 465–486, 492, 493, 495, 497, 502, 504–507
- Jaldhaka river, 6, 9, 11, 12, 14, 63–85, 95, 130, 234
- Jamuna river, 5, 12, 13, 95, 403–422, 428, 429, 437, 438, 442, 450, 532–534
- Japan Aerospace Exploration Agency (JAXA), 311, 312

**K**

- Kaljani Basin, 39, 46, 49, 66, 130, 184–188, 191, 192, 195–199
- Kangsabati, 12, 286, 353, 361, 382
- Khal, 353, 367, 469, 534
- Kharif crops, 357
- Khari River Basin, 14, 285–300
- Konar, 306, 308, 309, 342
- Kunur River Basin (KRB), 269, 271, 273, 286–300
- Kushyara River, 433

**L**

- Land degradation, 175, 544
- Landfall, 440, 442
- Land grabbing, 456
- Landslide, 13, 65, 128, 132, 162, 176, 188, 197, 204, 542

- Land use/land cover (LULC), 28, 71, 72, 84, 97, 99, 115, 133, 134, 137–138, 145, 169, 178, 207–209, 211, 214, 217, 218, 220, 225, 269, 270, 295, 310, 317, 326, 328, 478, 479
- Laterites, 307
- Length of overland flow, 189, 195, 290, 397
- LiDAR, 20–22, 24, 26
- Livelihood, 3, 13, 14, 66, 92–94, 96, 102, 111–115, 118, 146, 163, 187, 233, 304, 365–383, 398, 440, 443, 445, 457, 494, 540, 547
- Living with flood, 13, 458, 485
- Local Government Engineering Department (LGED), 97, 409, 460, 461
- Local knowledge system, 413
- Log-pearson type III (LP III/LPT3), 38, 44, 51–53, 173, 315, 316, 324, 330–332, 337–339
- Lower meghna channel, 532
- M**
- Machine learning, 64, 163, 169, 184, 305
- Madaripur Beel Route (MBR), 533, 534
- Mahananda, 6, 9, 129, 130, 140, 144, 145, 205–207, 222, 224
- Mahananda-Balason system (MBS), 127–156
- Maithon, 308, 309, 322, 324, 326, 328, 340–342, 472
- Malda District, 9, 14, 163, 165, 203–226, 471
- Mann-Kendall test, 317, 322
- Mathabhanga-Churni, 465–486, 495, 505
- Mayurakshi River basin, 13, 14, 231–263
- Mean bifurcation ratio, 289, 290, 293, 497, 506
- Meandering, 72, 73, 81, 141, 366, 370, 373, 424, 492–495, 501, 502, 506, 510, 517, 530, 532
- Mean hazard index (MHI), 409
- Meghna river, 7, 15, 404–406, 422–445, 450, 530, 532–535, 538
- Memari fan-delta, 308
- Modelling, 19–30, 282, 303–343, 444
- Modified normalized difference water index (MNDWI), 46, 168, 503, 504, 506, 518, 520, 523
- Monsoon  
floods, 9–14, 65, 248, 304, 319, 387, 430, 432, 435, 506, 542  
rainfall, 15, 65, 187, 212, 304, 322, 333, 341, 376, 431, 449, 481, 535
- Morphological units, 206, 213
- Morphology, 7, 25, 46, 53–55, 59, 93, 134, 304, 366, 405, 426, 435–438, 493, 546
- Morphometric parameters, 187, 189–191, 196, 197, 289–290, 293, 296, 300, 492, 496
- Morphometric parameters sub-watershed prioritization (MPSWP), 184, 191, 197–199
- Mud-flats, 6–8, 426
- Multi-criteria decision-making (MCDM), 64, 79, 203–226
- Multi-model ensemble, 15, 385–399
- N**
- Natural disaster, 65, 95, 120, 162, 176, 204, 352, 375, 418, 460, 492
- Natural hazards, 8, 19–20, 25, 63, 64, 93, 113, 169, 184, 204, 232, 233, 286, 404, 413, 418, 506
- Neotectonic, 164, 477–480
- Non-structural approach, 93, 94, 118–120, 458–459, 485
- Normalized difference built-up index (NDBI), 169, 175, 503, 504, 518, 520
- Normalized difference moisture index (NDMI), 169
- Normalized difference turbidity index (NDTI), 503, 504, 506, 507, 518, 520, 523
- Normalized difference vegetation index (NDVI), 68–70, 75–77, 168, 169, 503, 504, 518, 520
- Normalized difference water index (NDWI), 168, 169, 504
- NRCS-CN, 317, 326, 329, 341
- O**
- Old Brahmaputra, 8, 15, 405
- 1D hydrodynamic model, 24, 311–314, 334, 339, 342, 343
- Oxbow lake, 6, 426, 435, 466, 467, 482, 483, 495, 502
- P**
- Padma, 6, 7, 9, 10, 404, 406, 424, 426, 450, 466, 467, 469, 471, 474, 477, 479–481, 486, 530, 532–534, 537–539, 546
- Palaeochannel, 305, 306, 342, 343, 356, 467
- PALSAR DEM, 132, 184, 187, 198
- Panagarh fan-delta, 308



- Panchet, 308, 309, 322, 324, 326, 328, 340–342, 472, 477
- Peak over threshold (PoT), 49, 391
- Peak streamflow, 311, 316, 387, 395–398
- Personal safety, 541–542
- Physico-environmental, 101
- Physiographic zone, 39, 269, 388
- Piedmont, 39, 47, 49, 50, 55, 57, 59, 388
- Political stability, 444
- Population density, 8, 99, 115, 162, 232, 271, 407, 410, 456
- Potential, 21, 66, 93, 100, 116–119, 129, 130, 147, 226, 286, 288–290, 297–300, 317, 329, 337–341, 386, 387, 420, 477, 540
- Pressure, state, and response (PSR) model, 168
- Principal component analysis (PCA), 498, 499, 504, 521
- Progradation, 3
- Public Works Datum (PWD), 102, 103, 397, 398, 452
- Punarbhaba river, 161–179
- Q**
- Quasi-natural hazard, 184, 204, 506
- Questionnaire survey, 239, 369, 407, 408
- R**
- Rabi crops, 357
- RADARSAT, 21
- Rainfall, 2, 38, 65, 92, 129, 162, 186, 204, 243, 270, 288, 304, 352, 366, 404, 424, 449, 471, 492, 532
- Rain-fed paddies, 369, 377
- Random forest, 169
- Rarh plain, 9, 12, 235
- RAS Mapper, 314
- Raster clipping methods, 409
- Regional Climate Models, 399
- Relative importance index (RII), 240, 260
- Relative relief, 189, 196, 212, 290, 297, 298
- Relief ratio, 189, 196, 197
- Remote sensing (RS), 64, 94, 98, 184, 205, 226, 271, 310, 312, 366, 461, 496, 497
- Return period, 26, 43–45, 51, 53, 167, 171, 173, 174, 271, 272, 278–283, 303, 306, 315, 316, 331, 332, 439
- Riparian corridor, 177, 179, 361
- Riparian ecosystem, 164
- Risk assessment, 14, 234, 403–422, 444
- Risk model, 413
- Riverbank, 9, 49, 83, 92, 97, 103, 119, 128, 129, 134, 135, 146, 151, 162, 188, 197, 298, 408, 428, 438, 456, 460, 474, 477, 493–495, 503, 543
- River bank erosion, 92, 94, 95, 109–111, 120, 205, 259, 354, 355, 359, 361, 421, 437–438, 492, 493, 495, 496, 504, 546
- Riverine floods, 30, 211, 424, 428, 440
- River management, 94, 129, 545–546
- River management programmes, 352
- River system, 9, 15, 21, 28, 29, 127–156, 162, 204, 223–225, 235, 277, 278, 287, 307, 314, 366, 404, 408, 426, 430, 437, 461, 466, 467, 471, 484, 492, 495, 530, 532
- Road damage, 113, 378, 379
- Root-Zone Soil Moisture map (RZSM), 341
- Ruggedness number, 189, 196
- Rupnarayan, 353, 361, 367, 373, 374, 376
- S**
- Saaty's scale, 208, 214, 216, 217
- Sand extraction, 461
- Sediment, 3–5, 8, 9, 12, 38, 39, 49, 59, 65, 93, 128–130, 132–135, 139, 145–147, 149, 151–153, 162, 187, 197, 224, 244, 245, 269, 278, 295, 305, 307, 308, 314, 353, 358, 366, 367, 373, 381, 382, 387, 422, 424, 426, 437, 439, 440, 455, 456, 480, 481, 492, 495, 503, 504, 506, 519, 532, 534, 543, 544
- Sedimentation, 14, 37–59, 83, 102, 103, 119, 269, 300, 342, 374, 437, 440, 455, 461, 480, 496, 530, 543, 544
- Sediment transport index (STI), 503, 504, 506, 519–521, 523
- Shape factor, 189, 195, 197, 297, 497, 502, 506, 517
- Shared Socioeconomic Pathways (SSPs), 388, 390, 392–399
- Shifting of river course, 370–372
- Shillong Plateau, 9, 424
- Shitalakhya, 15, 449–461
- Shuttle Radar Topography Mission (SRTM), 21–24, 26, 27, 30, 97, 98, 165, 177, 237, 407, 409, 410, 473, 474
- Silaboti river, 365–383
- Silai-Darakeswar interfluvium, 354
- Silt extraction, 461
- Simulation, 14, 30, 38, 51–53, 64, 165, 167, 271, 303–343, 406, 444

- Sinuosity index (SI), 370, 373, 493, 497, 501, 502, 506, 517
- Skewness, 44, 45, 241, 253, 260, 330, 331
- Small river, 14, 164, 286, 290, 429, 450, 530, 532
- Social vulnerability, 95, 99, 100, 115–118, 120, 232, 234, 239, 404
- Soil category map, 213
- SPSS, 409
- Steady flow, 305, 311–315, 333–340
- Stream frequency, 189, 195, 289, 294, 517
- Stream gradient ratio, 289, 293
- Stream length ratio, 189, 289, 293, 497, 517
- Stream order, 189, 192, 195, 207, 289–293, 496, 502, 516, 517
- Structural approach, 94, 118, 119, 458, 484–485
- Structural solutions, 93, 119, 543
- Student's t-test, 240, 255, 258, 501
- Sunamganj, 433, 435, 436, 535
- Sundarbans, 3, 6, 8, 269, 531, 536, 545
- Support vector machine (SVM), 133
- Surface slope, 212, 287, 290, 297, 298, 300
- Surface water occurrence (SWO), 311, 312
- Sylhet, 5, 8, 9, 424, 429, 430, 433–436, 535
- T**
- Tail index, 391, 394, 395, 399
- Teesta, 6, 9, 11, 12, 14, 39, 65, 66, 119, 130, 131, 164, 234, 305, 442
- Tennessee Valley Authority (TVA), 308, 320
- Terai, 39, 129, 131
- TerraSAR-X, 21
- Tertiary sediments, 307
- Threshold, 69, 70, 162, 168, 175, 211, 310, 391, 480, 535
- Tidal flooding, 430
- Tidal floods, 15, 234, 428
- Tilaiya, 308, 309, 324, 342
- Tilpara, 243, 245, 472, 477, 478
- Topographic wetness index (TWI), 68, 70–72, 77–78, 503, 504, 506, 519, 520, 523
- Torsa, 6, 9, 11, 12, 14, 37–59, 66, 130, 234
- Trans-boundary, 38, 47, 93, 95, 103, 163, 444, 450
- Transport system, 247, 435
- U**
- Unsteady flow, 305, 306, 312, 314, 315, 333–339
- Urbanization, 64, 94, 102, 128, 129, 137, 145, 146, 151, 176, 179, 352, 455, 478, 540
- V**
- Vulnerability
- assessment, 94, 99, 168, 232–234, 411–417
  - index, 98, 100, 118, 411, 415, 417, 420, 496, 498–499, 503
  - map, 416
- W**
- Water-borne diseases, 111, 113, 250, 252, 379, 421, 457, 540, 541
- Water level (WL), 11, 22, 24, 42, 49, 53, 55, 65, 67, 93, 96, 97, 102–104, 106, 119, 151, 165, 170–173, 177, 179, 187, 207, 235, 313, 406, 408, 409, 429, 430, 434, 452, 454, 458, 477, 480, 481, 486, 493, 533, 537–539
- Water surface elevations (WSE), 22, 26, 27, 30, 313, 315, 337
- Weighed overlay model (WOM), 216–218
- Wetland, 11, 22, 162–165, 168–170, 174–179, 361, 442, 466, 482, 483
- World Resources Institute (WRI), 271, 278, 282
- X**
- XLSTAT, 43, 311